ADIPOSE TISSUE IN THE CARDIOVASCULAR HOMEOSTASIS AND DISEASE

EDITED BY: Thiago Bruder, Ana Paula Davel and Joshua Thomas Butcher
PUBLISHED IN: Frontiers in Pharmacology and Frontiers in Physiology

frontiers Research Topics

ISSN 1664-8714
ISBN 978-2-88974-052-9
DOI 10.3389/978-2-88974-052-9

About Frontiers

Frontiers is more than just an open-access publisher of scholarly articles: it is a pioneering approach to the world of academia, radically improving the way scholarly research is managed. The grand vision of Frontiers is a world where all people have an equal opportunity to seek, share and generate knowledge. Frontiers provides immediate and permanent online open access to all its publications, but this alone is not enough to realize our grand goals.

Frontiers Journal Series

The Frontiers Journal Series is a multi-tier and interdisciplinary set of open-access, online journals, promising a paradigm shift from the current review, selection and dissemination processes in academic publishing. All Frontiers journals are driven by researchers for researchers; therefore, they constitute a service to the scholarly community. At the same time, the Frontiers Journal Series operates on a revolutionary invention, the tiered publishing system, initially addressing specific communities of scholars, and gradually climbing up to broader public understanding, thus serving the interests of the lay society, too.

Dedication to Quality

Each Frontiers article is a landmark of the highest quality, thanks to genuinely collaborative interactions between authors and review editors, who include some of the world's best academicians. Research must be certified by peers before entering a stream of knowledge that may eventually reach the public - and shape society; therefore, Frontiers only applies the most rigorous and unbiased reviews.
Frontiers revolutionizes research publishing by freely delivering the most outstanding research, evaluated with no bias from both the academic and social point of view. By applying the most advanced information technologies, Frontiers is catapulting scholarly publishing into a new generation.

What are Frontiers Research Topics?

Frontiers Research Topics are very popular trademarks of the Frontiers Journals Series: they are collections of at least ten articles, all centered on a particular subject. With their unique mix of varied contributions from Original Research to Review Articles, Frontiers Research Topics unify the most influential researchers, the latest key findings and historical advances in a hot research area! Find out more on how to host your own Frontiers Research Topic or contribute to one as an author by contacting the Frontiers Editorial Office: frontiersin.org/about/contact

ADIPOSE TISSUE IN THE CARDIOVASCULAR HOMEOSTASIS AND DISEASE

Topic Editors:
Thiago Bruder, University of Pittsburgh, United States
Ana Paula Davel, State University of Campinas, Brazil
Joshua Thomas Butcher, Oklahoma State University, United States

Citation: Bruder, T., Davel, A. P., Butcher, J. T., eds. (2022). Adipose Tissue in the Cardiovascular Homeostasis and Disease. Lausanne: Frontiers Media SA.
doi: 10.3389/978-2-88974-052-9

Table of Contents

frontiers in Pharmacology

EDITORIAL
published: 24 November 2021
doi: 10.3389/fphar.2021.803199

Editorial: Adipose Tissue in the Cardiovascular Homeostasis and Disease

Joshua T. Butcher[1], *Ana P. Davel*[2] *and Thiago Bruder-Nascimento*[3]*

[1]*Department of Physiological Sciences, College of Veterinary Medicine, Oklahoma State University, Stillwater, OK, United States,* [2]*Department of Structural and Functional Biology, Institute of Biology, University of Campinas–UNICAMP, Campinas, Brazil,* [3]*Department of Pediatrics, Center for Pediatrics Research in Obesity and Metabolism (CPROM), Vascular Medicine Institute (VMI), University of Pittsburgh, Pittsburgh, PA, United States*

Keywords: adipose tissue, cardiovascular, adipokines, lipid, vascular

Editorial on the Research Topic

Adipose Tissue in the Cardiovascular Homeostasis and Disease

From an evolutionary perspective, adipocyte signaling would not have been a significant priority until the past 40 years, when the increased availability of a diet high in carbohydrates and fats (the Western Diet) dramatically pushed obesity-derived cardiovascular dysfunction to the forefront of health concerns. As the body's largest endocrine organ, adipose tissue is predominantly composed of adipocytes as well as containing a small fraction of other cell types (ex: fibroblasts, vascular and immune cells). However, due to the broad dispersion of adipose tissue throughout the body and intra-organ location, its ability to contribute to and alter signaling cascades via adipokines magnify its importance in cardiovascular homeostasis. Indeed, adipose tissue plays a crucial role in health and disease, whether through expansion (obesity), or contraction (lipodystrophy) or dysfunction. This Research Topic was designed to highlight the multi-dimensional impact that adipose tissue has on systemic signaling throughout the body, with a focus on the cardiovascular system.

A highlight of the work enclosed in this Research Topic is the comprehensive models used to focus on the crosstalk of adipose and cardiovascular function, including human coronary arterioles, meta-analysis, and rodent models. A direct examination in humans of how epicardial adipose tissue (EAT) is altered in coronary artery disease (CAD) was shown by Wang et al. They determined that EAT in CAD patients possessed altered/dysfunctional transcriptomes and increased adipocyte size, likely contributing to the overall progression and development of CAD. Differentially expressed genes were used to construct a protein-protein interaction network and hub genes identified and validated, revealing a crucial interaction between inflammatory cells and chemokine signaling. Stephen T. O'Rourke's group explored the effect of apelin on BK_{Ca} channels in the coronary vasculature. Importantly, using patch clamping and wire myography, they showed that apelin does not inhibit BK_{Ca} currents or nitric oxide-induced relaxation, an effect that contrasts with cerebral vasculature (Mughal et al.). Han et al. performed a meta-analysis focused on to establish the effectiveness of beta-blockers in preventing cardiac events in long QT syndrome patients according to gender, age, and QTc interval.

Importantly, work enclosed in this Research Topic also highlighted compounds that could be used to alter advanced disease states, like atherosclerosis. *Astragalus membranaceus* is a low cost medicinal herb normally used in several herbal formulations in the practice of traditional Chinese medicine and major components include polysaccharides, saponins, and flavone. In a clinically relevant study led by Dr. Fan's group, the authors investigated the effects of total flavone of *Astragalus membranaceus* (TFA) treatment on atherosclerosis and hepatic steatosis in ApoE deficient mouse (ApoE KO, a well-established mouse model to study atherosclerosis). The authors observed that long-term TFA

OPEN ACCESS

Edited and reviewed by:
Francesco Rossi,
University of Campania Luigi Vanvitelli, Italy

***Correspondence:**
Thiago Bruder-Nascimento
bruder@pitt.edu

Received: *27 October 2021*
Accepted: *08 November 2021*
Published: *24 November 2021*

Citation:
Butcher JT, Davel AP and Bruder-Nascimento T (2021) Editorial: Adipose Tissue in the Cardiovascular Homeostasis and Disease. Front. Pharmacol. 12:803199. doi: 10.3389/fphar.2021.803199

supplementation attenuates atherosclerosis development in high fat diet (HFD) treated ApoE KO mice, which was associated with a striking improvement of lipid disorder and hepatic outcomes (Ma et al.). In addition, TFA reduces lipid retention and uptake, as well as increases lipid efflux in isolated macrophages. Taken together, this study shows that TFA supplementation has multiple beneficial effects on cardiovascular readout by regulating lipid metabolism, hepatic outcomes, and by modulating macrophages and endothelial cells directly.

Pivoting away from the negative role of adipocyte tissue, Liu et al., examined the role of adiponectin in protecting against cardiomyocyte apoptosis, which plays a role in the development and progression of heart failure. Adiponectin can be found in the heart and skeletal muscle, but it is best known and explored in adipocytes, therefore is recognized as an adipokine (molecule produced by adipose tissue). In this interesting manuscript, the authors observed that LPS treatment induced immune cells infiltration and myocardial cell necrosis, which was abrogated by pre-treating the mice with adiponectin. Such changes were associated with a regulation of connexin 43 expression, an abundant cardiac protein that plays major role on cardiomyocyte apoptosis. To understand the signaling pathways by which adiponectin confers cardiac protection in LPS-treated mice, rat cardiomyocytes were treated with LPS in presence of adiponectin and the authors found that adiponectin blocks LPS-induced apoptosis via regulating PI3K/AKT pathways. This set of data has many clinical implications by demonstrating the positive effects of adiponectin on controlling sepsis severity, but also it has valuable implications in understanding why obese subjects (with lower levels of circulating adiponectin) present with a larger risk of death in sepsis conditions.

This Research Topic also contains reviews that highlight the distinctive role that perivascular adipose tissue (PVAT) can play, not only through diverse adipocytes (brown, white, beige), but also in its secretome and anatomical distribution (Li et al.). Further reviews focus on specific microenvironments, such as the prostate (Passos et al.) and atherosclerosis (Liu et al.) and how targeting PVAT via intermittent fasting can reduce inflammation and drive remodeling of adipocyte tissues (Dwaib et al.). Uniquely, a review by Dr. Jennifer Thompson's group drew attention to the role of plasticizers, which certainly play a ubiquitous role in our society today, but yet have a poorly defined role as endocrine disruptors (Callaghan et al.). The pervasive role of these compounds, whether it is bisphenols (the most commonly known is BPA) or phthalates, is highlighted in the review, along with their impacts on adipogenesis, adipokine production, and inflammation. The protective role of PVAT is also impacted in the setting of obesity. Victorio et al. investigated whether the effect of obesogenic diets on PVAT function is dependent on sex. The authors found that PVAT dysfunction in response to two obesogenic HFD occurs early in females compared to age-matched males, suggesting a susceptibility of the female sex to obesity-induced PVAT dysfunction. The data illustrate the importance of the duration and composition of obesogenic diets for investigating sex-specific treatments and pharmacological targets for obesity-induced vascular complications.

Taken together, the enclosed work advances and clarifies our understanding of the cross-talk between adipose tissue and the cardiovascular system. This research informs on the foundational understanding of adipose tissue and its role in cardiovascular homeostasis, highlights new directions, and hopefully guides therapeutic targets in pathophysiological conditions driven by lipid disorders.

AUTHOR CONTRIBUTIONS

JB, AD, and TB-N contributed equally on discussion, writing, and review of this editorial.

Conflict of Interest: The authors declare that the research was conducted in the absence of any commercial or financial relationships that could be construed as a potential conflict of interest.

Publisher's Note: All claims expressed in this article are solely those of the authors and do not necessarily represent those of their affiliated organizations, or those of the publisher, the editors and the reviewers. Any product that may be evaluated in this article, or claim that may be made by its manufacturer, is not guaranteed or endorsed by the publisher.

frontiers in Pharmacology

ORIGINAL RESEARCH
published: 14 December 2020
doi: 10.3389/fphar.2020.610550

Astragalus Flavone Ameliorates Atherosclerosis and Hepatic Steatosis Via Inhibiting Lipid-Disorder and Inflammation in apoE$^{-/-}$ Mice

Chuanrui Ma[1,2†], Jing Zhang[1,2†], Shu Yang[3,4†], Yunqing Hua[1,2], Jing Su[5], Yuna Shang[6], Zhongyan Wang[7], Ke Feng[6], Jian Zhang[8], Xiaoxiao Yang[9], Hao Zhang[1,2], Jingyuan Mao[1,2] and Guanwei Fan[1,2]**

[1]First Teaching Hospital of Tianjin University of Traditional Chinese Medicine, Tianjin, China, [2]Tianjin Key Laboratory of Translational Research of TCM Prescription and Syndrome, Tianjin, China, [3]Department of Endocrinology, The Second Clinical Medical College, Shenzhen People's Hospital, Jinan University, Shenzhen, China, [4]Integrated Chinese and Western Medicine Postdoctoral Research Station, Jinan University, Guangzhou, China, [5]Tianjin State Key Laboratory of Component-Based Chinese Medicine, Tianjin University of Traditional Chinese Medicine, Tianjin, China, [6]College of Life Sciences, Nankai University, Tianjin, China, [7]Tianjin Key Laboratory of Radiation Medicine and Molecular Nuclear Medicine, Institute of Radiation Medicine, Chinese Academy of Medical Sciences and Peking Union Medical College, Tianjin, China, [8]Department of Pharmacology, College of Basic Medical Sciences, Tianjin Medical University, Tianjin, China, [9]Key Laboratory of Metabolism and Regulation for Major Diseases of Anhui Higher Education Institutes, College of Food and Biological Engineering, Hefei University of Technology, Hefei, China

Atherosclerosis is a major pathogenic driver of cardiovascular diseases. Foam cell formation plays a key role in atherogenesis, which is affected by lipid disorder and inflammation. Therefore, inhibition of foam cell formation is a therapeutic approach for atherosclerosis treatment. Total flavone of *Astragalus membranaceus* (TFA) is extracted from *A. membranaceus* that has protective effect on cardiovascular disease. However, the effect of TFA on atherosclerosis and the underlying mechanism remains unknown. In this study, we determined whether TFA could inhibit atherosclerosis and uncovered the underlying mechanism. *In vivo*, ApoE deficient mice were treated with TFA and high-fat diet for 16 weeks. Subsequently, atherosclerotic lesions, hepatic steatosis and associated genes expression *in vitro* and *in vivo* were determined. We found that TFA reduced atherosclerotic lesion size and enhanced plaque stability, which might be attributed to improved lipid disorder, reduced inflammation and decreased monocyte adhesion. Mechanistically, TFA inhibited hepatic steatosis via regulating the genes responsible for lipid metabolism, by which ameliorating the lipid disorder. Moreover, in macrophage, TFA reduced the expression of scavenger receptors such as CD36 and SRA; and promoted

OPEN ACCESS

Edited by:
Thiago Bruder Do Nascimento, University of Pittsburgh, United States

Reviewed by:
Gustavo H. Oliveira-Paula, Albert Einstein College of Medicine, United States
Bhupesh Singla, Augusta University, United States

***Correspondence:**
Jingyuan Mao
jymao@126.com
Guanwei Fan
guanwei.fan@tjutcm.edu.cn

†These authors have contributed equally to this work

Specialty section:
This article was submitted to Cardiovascular and Smooth Muscle Pharmacology, a section of the journal Frontiers in Pharmacology

Received: 26 September 2020
Accepted: 16 November 2020
Published: 14 December 2020

Citation:
Ma C, Zhang J, Yang S, Hua Y, Su J, Shang Y, Wang Z, Feng K, Zhang J, Yang X, Zhang H, Mao J and Fan G (2020) Astragalus Flavone Ameliorates Atherosclerosis and Hepatic Steatosis Via Inhibiting Lipid-Disorder and Inflammation in apoE$^{-/-}$ Mice. Front. Pharmacol. 11:610550. doi: 10.3389/fphar.2020.610550

Abbreviations: Arg1, arginase 1; CPT1α, carnitine palmitoyl transferase 1 alpha; CXCL1, C-X-C motif chemokine ligand 1; IFN-γ, Interferon gamma; Mgl2, macrophage lectin 2; Mrc1, mannose receptor C-type 1; NOS2, nitric oxide synthase 2; SREBP1c, sterol regulatory element-binding protein 1c; TGF-β1, transforming growth factor β1; FASN, fatty acid synthase; SR-BI, scavenger receptor class B type 1; RCT, reverse cholesterol transport; IL, interleukin; TNFα, tumor necrosis factor α; iNOS, inducible nitric oxide synthase; GAPDH, glyceraldehyde-3-phosphate dehydrogenase; COX2, prostaglandin-endoperoxide synthase 2; TLR4, toll like receptor 4; MCP-1, monocyte chemotactic protein 1; NLRP3, NLR family pyrin domain containing 3; VCAM-1, vascular cell adhesion molecule 1; ICAM-1, intercellular adhesion molecule 1; PECAM1, platelet and endothelial cell adhesion molecule 1; NF-κB, nuclear factor kappa B; CCL, C-C motif chemokine ligand; eNOS, endothelia NO synthase; PPARγ, peroxisome proliferator activated receptor gamma; Chi3I3, chitinase-like 3; FOXP3, fork head box P3; VEGF, vascular endothelial growth factor; MMP, matrix metallopeptidase; MERTK, MER proto-oncogene tyrosine kinase; HMGCR, 3-hydroxy-3-methylglutaryl-CoA reductase; LXRα/β, Liver X receptor α/β

the expression of ATP-binding cassette transporter A1 and G1 (ABCA1/G1). More importantly, TFA reduced miR-33 expression and dampened NFκB activity, by which de-repressing ABCA1/G1 activity and inhibiting the inflammation. Collectively, TFA can attenuate atherosclerosis via dual suppression of miR-33 and NFκB pathway, and partially through inhibition of scavenger receptors in macrophage. In addition, TFA ameliorates the hepatic steatosis and lipid disorder, which in turn contributes to the amelioration of atherosclerosis, suggesting that TFA might be a novel therapeutic approach for inhibition of atherosclerosis and hepatic steatosis.

Keywords: Astragalus flavone, inflammation, atherosclerosis, hepatic steatosis, lipid disorder

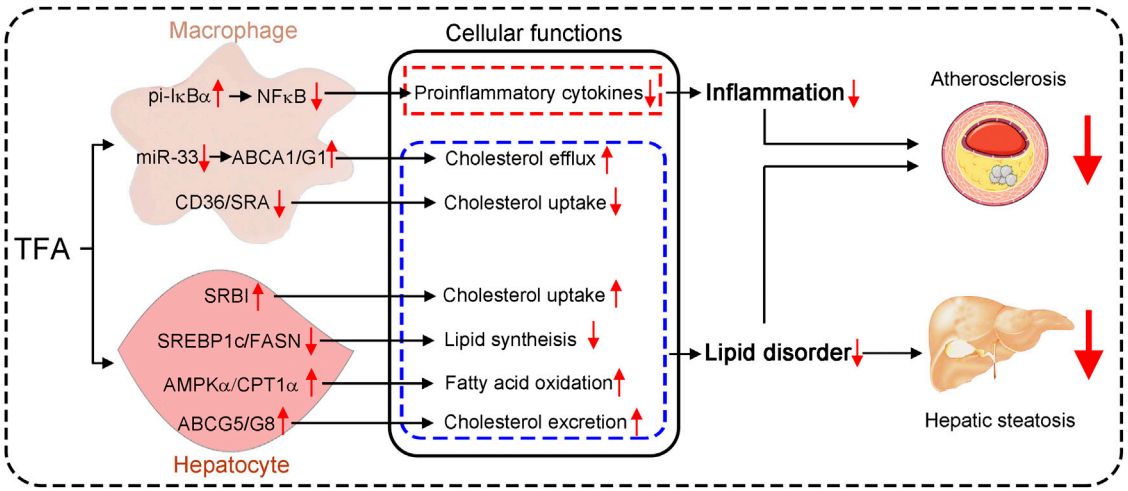

GRAPHICAL ABSTRACT | Astragalus flavone with different molecular weights have different effects on inflammation and lipid metabolism.

INTRODUCTION

Atherosclerosis is the principal risk factor of cardiovascular diseases, which is mainly driven by lipid disorder and inflammation. Although the introduction of lipid-lowering therapies, such as 3-hydroxy-3-methylglutaryl coenzyme A reductase (HMGCR) inhibitors and proprotein convertase subtilisin-kexin type 9 (PCSK9) inhibitors have lowered the risk of cardiovascular disease. The atherosclerosis-driven cardiovascular disease remains the major causes of morbidity and mortality worldwide (de Winther and Lutgens, 2019). Thereby, new strategies to lower the risk of cardiovascular disease are still in need.

Lipid-enriched foam cells are the hallmark of atherosclerotic plaques (Moore and Tabas, 2011). Lipid accumulation in the cytoplasm can induce macrophages to transform into detrimental foam cells, thereby accelerating atherosclerotic plaque destabilization, rupture, and even thrombogenesis (Yang et al., 2018). Therefore, inhibition of foam cell formation is a key target for retarding atherogenic progression. High cholesterol uptake and low efflux in macrophage can lead to cellular lipid accumulation and the following foam cell formation (Yu et al., 2013), which is mainly determined by the transporters responsible for cholesterol efflux, such as ABCA1 and ABCG1 (Tall et al., 2008); and scavenger receptors in charge of cholesterol uptake, such as, SRA and CD36 (Crucet et al., 2013; de Winther et al., 2000; Nakata et al., 1999). Therefore, inhibition of cholesterol uptake or promotion of efflux is a promising antiatherogenic strategy (Tall, 2018; Ouimet et al., 2019). Liver is a critical organ that regulates lipid metabolism, which mainly determines the cholesterol metabolism and lipid profile in serum, thereby affecting the atherogenesis (Lee et al., 2018). Importantly, ABCA1/G1-mediated cholesterol efflux is the initial step of reverse cholesterol transport (RCT), by which cholesterol moves out of foam cells in atherosclerotic plaques into liver and finally into the feces.

Atherosclerosis is driven not only by dyslipidemia but also by inflammation. Chronic inflammation can coordinate with lipid dysfunction. More specifically, hyperlipidemia can skew plaque macrophages toward an atherogenic M1 phenotype instead of toward the antiatherogenic M2 phenotype (Barrett et al., 2019). Importantly, NF-κB is a critical signaling regulator that controls inflammation. In the unstimulated state, the IκB binds to NF-κB dimers in the cytoplasm to render NF-κB inactive. However, upon stimulation, IκB proteins are phosphorylated and subsequently degraded, which leads to release of active NF-κB

dimers for nuclear translocation and target gene induction (Baeuerle and Baltimore, 1988). In addition, miRNAs can act as fine-tuners of genes expression, including genes responsible for lipid metabolism and inflammation (Feinberg and Moore, 2016). Among these miRNAs, miR-33 can regulate macrophage polarizaiton and inflammation (Ouimet et al., 2015). Moreover, miR-33 can limit cholesterol efflux capacity by restricting ABCA1/G1 activity in foam cells (Price et al., 2019). In contrast, inhibition of miR-33 can enhance RCT, raise plasma HDL, and lower VLDL (Rayner et al., 2010; Horie et al., 2012; Rayner et al., 2011a; Rayner et al., 2011b). Therefore, inhibition of miR-33 and NF-κB holds therapeutic promise for atherosclerosis treatment.

Flavone has shown the potential to improve HDL function through the effects on antioxidant status and anti-inflammation (Millar et al., 2017). Noticeable, the current study showed that higher intake of flavone was associated with a lower risk of coronary heart disease (Ma L. et al., 2020). Intriguingly, studies have shown that flavone can exert protective effect by modulating miRNAs expression in different model of diseases (Lam et al., 2012; Sun et al., 2015; Yin et al., 2015; Huang et al., 2016; Rigalli et al., 2016). Total flavone of *Astragalus membranaceus* (TFA) is extracted from *A. membranaceus* which is a traditional Chinese medicine that has protective effects on cardiovascular disease (Su et al., 2009; Liu et al., 2016). Moreover, TFA is easily available in technology and low-cost in economics. Therefore, in this study, we determined whether TFA could attenuate atherosclerosis and further uncovered the underlying mechanism. Given the important role of miR-33 and NF-κB pathway in cholesterol metabolism and inflammation, we postulated that TFA may inhibit atherosclerosis through regulating miR-33 expression and NF-κB pathway. In the current study, TFA reduced atherosclerosis and enhanced plaque stability in apoE deficient mice, which may be attributed to the improvement of lipid metabolism and inhibition of inflammation in liver and macrophage. Moreover, TFA suppressed the adhesion of monocytes to inflammatory endothelial cells. Mechanistically, these effects are associated with inactivation of miR-33 expression and NFκB activity as well as orchestrating genes responsible for lipid metabolism. Collectively, TFA may be a possible therapeutic intervention for atherosclerosis.

MATERIALS AND METHODS

Reagents

Mouse anti-ICAM-1(Cat#: sc107), VCAM-1(Cat#: sc13160), GAPDH (Cat#: sc365062) SRA (Cat#: sc56777), αSMA (Cat#: sc130617), CD36 (Cat#: sc70644), and CD68 (Cat#: sc20060) monoclonal antibodies were purchased from Santa Cruz Biotechnology, Inc (Santa Cruz, CA). Rabbit anti-ABCG1 (Cat#: NB400-132), ABCA1(Cat#: NB400-105) and SRBI (Cat#: NB400-104) polyclonal antibodies were purchased from Novus Biologicals (Littleton, CO). Mouse anti-IL-1β (Cat#: #12242) monoclonal antibody was purchased from Cell Signaling Technology. Mouse anti-Arg (Cat#: ab239731) monoclonal antibody were purchased from Abcam (Cambridge, MA). Mouse anti-rabbit IgG-R (Cat#: sc2492), mouse anti-rabbit IgG-FITC (Cat#: sc2359) and m-IgGκ BP-FITC (Cat#: sc516140) antibodies were purchased from Santa Cruz Biotechnology, Inc (Santa Cruz, CA). Astragalus flavone (Cat#: SA9780) was purchased from Solarbio (Beijing, China).

Cell Culture

Human umbilical vein endothelial cells (HUVECs) were cultured in VascuLife basal medium containing VEGF lifeFactors Kit (Lifeline Cell Technology, Frederick, MD). RAW264.7, THP-1 cells and peritoneal macrophages were cultured in complete RPMI1640 medium containing 10% FBS, 50 $\mu g\,mL^{-1}$ penicillin/streptomycin and 2 mM glutamine.

miR-33 Mimic Transfection in Macrophages

Macrophages were seeded into plate and cultured to 60% confluence. Cells were then transfected with 50 nM miR-33 mimic or miR-33 control (Guangzhou RiboBio Co., Ltd.) using Lipofectamine RNAiMAX (Invitrogen, Grand Island, NE) according to the manufacturer's instructions. The medium was replaced with fresh medium after 6 h transfection.

Animals and Treatment Schedule

The protocol for *in vivo* studies was approved by the Ethics Committee of Tianjin University of Traditional Chinese Medicine and conforms to the Guide for the Care and Use of Laboratory Animals published by the NIH (NIH publication, eighth edition, updated 2011). Eight weeks old, male $ApoE^{-/-}$ mice were purchased from Beijing Vital River Laboratory Animal Technology Co., Ltd. The animals were housed in SPF units of the Animal Center at Tianjin University of Traditional Chinese Medicine in the environment with 60–70% humidity at temperature 22 ± 1 C and 12 h light-dark cycle. The mice can freely access to water and high-fat diet (41% fat plus 0.5% cholesterol, MD12015A, Medicience Ltd., China). The $ApoE^{-/-}$ mice were randomly divided into three groups and fed HFD, HFD containing high dose TFA [low dose TFA-L, 10 $mg\,day^{-1}\,kg^{-1}$ bodyweight (mpk)], high dose TFA (TFA-L, 20 mpk) for 16 weeks. The mice were daily checked for food intake, water drink and bodyweight gain during the treatment. At the end of experiment, all mice were anesthetized and euthanized as we previously reported (Ma C. et al., 2020; Ma et al., 2018), following by collection of aortas, peritoneal macrophages, blood samples and other tissues. Serum was prepared to determine lipid profile, including total cholesterol (Total-C, TC), high-density lipoprotein (HDL)-C, low-density lipoprotein (LDL)-C, and triglycerides (TG) (Ma et al., 2018). Mouse ox-LDL level was evaluated by the commercially provided ELISA kit.

Atherosclerotic Lesion Analysis

The aortas were collected and used to prepare aortic root cross sections followed by determination of *en face* and sinus lesions with Oil Red O staining (Ma et al., 2018). All the images were obtained with a microscope and quantified lesion areas in *en face* aorta and aortic root cross sections, respectively. The lesion areas were expressed as μm^2 or % of the total surface area. Necrotic

core, fibrous cap, cellular apoptosis, collagen content, and expression of CD68, αSMA, Arg1, and IL-1β in lesion within aortic root cross sections were determined by Haematoxylin and eosin (H&E), sirius red staining, TUNEL staining, and immunofluorescent staining, respectively (Ma et al., 2018). The vulnerability index of plaques was calculated as (macrophage staining% + lipid staining%)/(SMCs% + collagen fiber%), according to a previous report (Williams et al., 2002).

Hepatic Steatosis Analysis

The hepatic steatosis was evaluated as previously described (Ma et al., 2018; Ma C. et al., 2020; Wang et al., 2020). Briefly, after sacrifice, the liver was isolated and photographed to exhibit the color and size. In addition, 5μm frozen section of liver was prepared to perform HE and Oil red O staining. Furthermore, total cholesterol and triglyceride was detected using commercially provided kit.

Determination of Foam Cell Formation *in vitro* and *in vivo*

Foam cell formation *in vitro* and *in vivo* was determined by Oil Red O staining as we previously described (Ma et al., 2018; Ma C. et al., 2020). Briefly, *in vivo*, peritoneal macrophages were isolated from TFA-treated apoE$^{-/-}$ mice and seeded on cover slips in 24-well plates, and then stained with Oil Red O solution. *In vitro*, RAW264.7 cells were seeded on cover slips in 24-well plates. Cells were incubated with oxLDL for 3 h following by TFA treatment for 16 h. Cells containing lipid droplets (>10/cell) were considered as foam cells, and >10 fields/sample were counted.

Cholesterol Uptake and Efflux Assay

Macrophages were incubated in medium containing DiI-oxLDL or 3-dodecanoyl-NBD cholesterol to evaluate ability of cholesterol uptake and efflux as previously studied (Ma C. et al., 2020). Briefly, in 12-well plates, macrophages (1.0×10^6 cells/well) pretreated with TFA at different doses were incubated with 10 μg/mL Dil-oxLDL (Introvegen) in RPMI 1,640 at 37°C for 6 h. Fluorescence intensity was examined by a fluorescence microscopy.

The ability of macrophage cholesterol efflux was determined as we previous study (Ma C. et al., 2020). In brief, macrophage was firstly incubated with 3-dodecanoyl-NBD cholesterol (1 μg/mL, Cayman Chemical) for 6 h. And then cells were switched into serum-free medium containing both apo-AI (5 μg/mL) and HDL (20 μg/mL) as cholesterol acceptor in the presence or absence of TFA for 5 h. The fluorescence-tagged cholesterol in the medium and cells lysate was determined by the automatic microplate reader (Thermo Scientific, Varioskan Lux, USA). Cholesterol efflux was expressed as a ratio of fluorescence in the medium to the total amount of fluorescence in cells together with medium.

Western Blot and Quantitative Real-Time PCR

Total cellular proteins were extracted from cells or liver tissue. Protein expression of ABCA1, ABCG1, CD36, GAPDH, FASN, SREBP1c, SRBI, IκBα, pi-IκBα, p65, pi-p65, and SRA were determined by Western blot (Yang et al., 2020).

Total RNA was isolated and purified, and cDNA was synthesized from 1 μg of total RNA using a reverse transcription kit (Vazyme bioteck co., ltd.). For quantitative real-time PCR (q-RT-PCR), specific genes were amplified by 40 cycles using SYBR green PCR master mix (DBI, Bioscience). Gene-specific primers are listed in Table S1. Expression of mRNA was normalized to the housekeeping gene GAPDH. miR-33 was normalized by U6 snRNA expression.

Monocyte Adhesion Assay

The HUVECs were seeded and incubated in 24-well dishes. After reaching 85% confluence, HUVECs were preincubated with oxLDL (100 μg/ml), or a combination of different dose of TFA (6, 12, 24 μg/ml) with oxLDL (100 μg/ml) for 24 h. The THP-1 cells were then added to the 24-well dishes and incubated with HUVECs for 1h. Subsequently, unbound monocytes were removed by 3 times of washes with warm PBS. After washout, the adherent THP-1 cells to HUVECs were captured with a microscope and counted with ImageJ.

Statistical Analysis

The data and statistical analysis complys with the recommendations on experimental design and analysis in pharmacology (Curtis et al., 2015). Data was expressed as means ± SEM and analyzed by using Graph Pad Prism software. One-way ANOVA for comparisons between multiple groups followed by Turkey's method. The value of $p < 0.05$ was considered statistically significant.

RESULTS

TFA Attenuates Atherosclerotic Development in apoE$^{-/-}$ Mice

Total flavone of *A. membranaceus* (TFA) is extracted from *A. membranaceus* and the main ingredient of TFA includes calycosin, kaempferol, isoliquiritigenin, siorhamnetin, formononetin, methylnissolin, isomucronulatol, and quercetin(Lin et al., 2000; Zhao et al., 2008; Li et al., 2019) (**Figure 1A**). To test the hypothesis that long-term administration with TFA would protect against atherosclerosis, we treated atherogenic apoE$^{-/-}$ mice with TFA and HFD for 16 weeks. After treatment, we evaluated atherosclerotic lesions. Analysis of atherosclerosis was assessed by Oil red O staining, which was followed by quantification as lesion area and the ratio of lesion area to total area of aorta or aortic root cross sections. Compared with mice that fed HFD alone, *en face* aortic lesions were markedly inhibited by TFA (**Supplementary Figures S1A, B**). Meanwhile, atherosclerotic lesion was assessed in four different vascular sites, including the ascending aorta, descending aorta, thoracic aorta, and abdominal aorta. The results showed that TFA reduced lesions in the above four sites of aorta (**Supplementary Figures S1C**). Moreover, TFA resulted in significant reduction in the aortic root (**Figures 1B,C**). Taken together, these data suggests that TFA can retard the atherosclerotic lesion development.

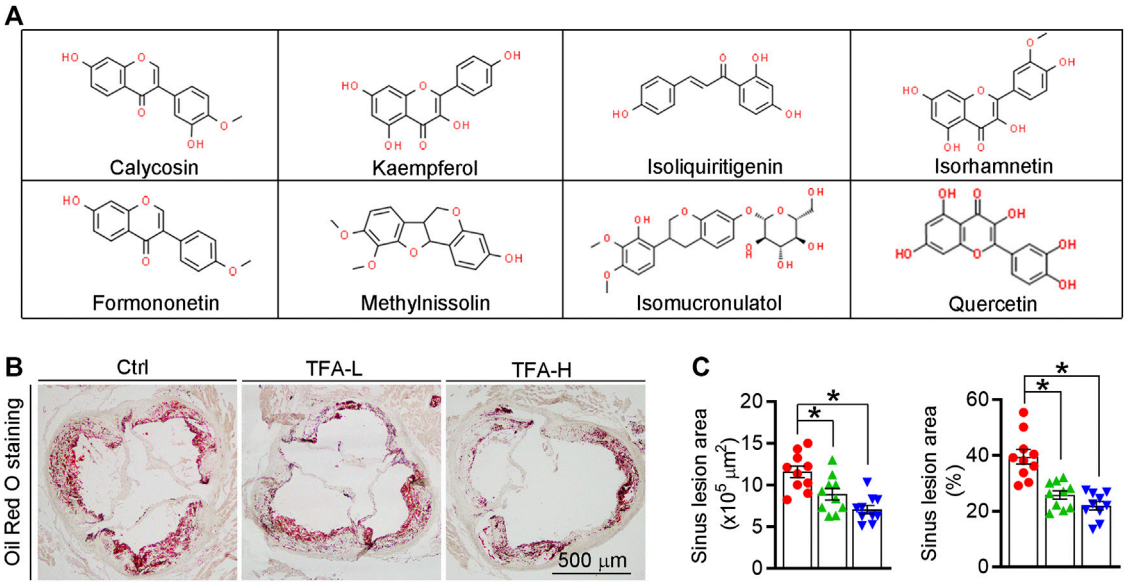

FIGURE 1 | TFA reduces atherosclerotic lesion size in apoE$^{-/-}$ mice. **(A)** The main ingredient of TFA. **(B, C)** Lesions in aortic root cross sections were determined by Oil Red O staining **(B)**, and quantified **(C)**. Lesion areas were expressed as μm^2 and the ratio of lesion area to total area of aortic root cross sections, $n = 10$. Data are presented as mean ± SEM, $^*p < 0.05$, significantly different from control; ns: not significantly different. TFA enhances atherosclerotic plaque stability by changing the plaque composition in apoE$^{-/-}$ mice.

The high necrotic core size and low fibrous cap area can increase plaque vulnerability and even lead to plaque rupture, which can result in myocardial infarction, stroke, and even sudden death. On aortic cross sections, we found that necrotic core area within the lesions was significantly smaller while the fibrous cap area was larger in TFA treated mice compared to control mice (**Figure 2A**). In addition, TFA increased the collagen positive area (**Figure 2B**). Moreover, we observed significant increase in percentages of αSMA$^+$ smooth muscle cells and reduction of CD68$^+$ foam cells/macrophages in TFA group compared to control group (**Figures 2C,D**). Dying cells in the plaque can lead to the formation of prothrombotic necrotic core and vulnerable fibrous cap. Therefore, we detected the apoptosis in the plaque by TUNEL staining and immunofluorescent staining with caspase1 antibody; and observed that TFA significantly reduced the cell apoptosis *in situ* (**Figure 2E** and **Supplementary Figures S2**). The quantification of **Figures 2B–E** was represented in **Figure 2F**. Moreover, the vulnerability index of plaque was reduced by TFA (**Figure 2G**). Taken together, the data suggests that the stability of atherosclerotic plaque can be enhanced by TFA, by which TFA may reduce the risk of plaque rupture and the following cardiovascular events.

Foam cell is predominant cells in atherosclerotic plaque, inhibition of which can retard the progression of atherosclerosis. In this study, TFA significantly reduced lipid accumulation in peritoneal macrophages from HFD-treated apoE$^{-/-}$ mice (**Figures 3A,B**), suggesting the inhibitory effect of TFA on foam cell formation. In addition, TFA markedly reduced the lipid retention in RAW264.7 cells by Oil red O staining (**Figure 3C**), which was followed by quantification of cellular cholesterol (**Figure 3D**). Furthermore, we assessed the capacity of cholesterol uptake and efflux, and observed that TFA significantly reduced lipid uptake and enhanced the cholesterol efflux (**Figures 3E,F**). To delineate the mechanism by which TFA inhibited foam cell formation, we examined the alterations of scavenger receptors (SRA and CD36) and transporters (ABCA1/G1) which are regarded as key mediators in cholesterol homeostasis during foam cell formation. Intriguingly, TFA markedly promoted the ABCA1/G1 expression whereas inhibited the expression of SRA and CD36 (**Figures 3G,H**). We further disclose the mechanism of TFA on ABCA1/G1 expression. Liver X receptors (LXRs) are the upstream genes of ABCA1/G1. Subsequently, we determined whether TFA could affect the expression of LXRα/β and found that TFA did not affect the expression of LXRα/β in transcriptional level (**Figure 3I**), indicating that other molecules may mediate the effect of TFA on ABCA1/G1 expression. Moreover, TFA did not change the expression of HMGCR, indicating that TFA did not affect the cholesterol synthesis (**Figure 3I**). It is well documented that miR-33 is a post-transcriptional regulator of genes involved in cholesterol homeostasis. Noteworthy, miR-33 is a negative regulator of ABCA1/G1. Therefore, we determined whether the TFA-induced ABCA1/G1 expression was involved in miR-33. Intriguingly, TFA significantly reduced the expression of miR-33 (**Figure 3J**), and miR-33 mimics treatment almost disrupted the promoting effect of TFA on cholesterol efflux (**Figure S3**), indicating that miR-33 plays a key role in TFA-mediated inhibitory effect on foam cell formation. In addition, we determined the effect of miR-33 mimic on expression of CD36 and SRA1. After transfection of miR-33 mimic in RAW264.7 cells, the expression of CD36 and SRA was evaluated by q-RT-PCR. miR-33 mimic did not affect the expression of either CD36 or SRA (**Supplementary Figures S7**), indicating that the regulation on CD36 and SRA1 expression by TFA was not miR-

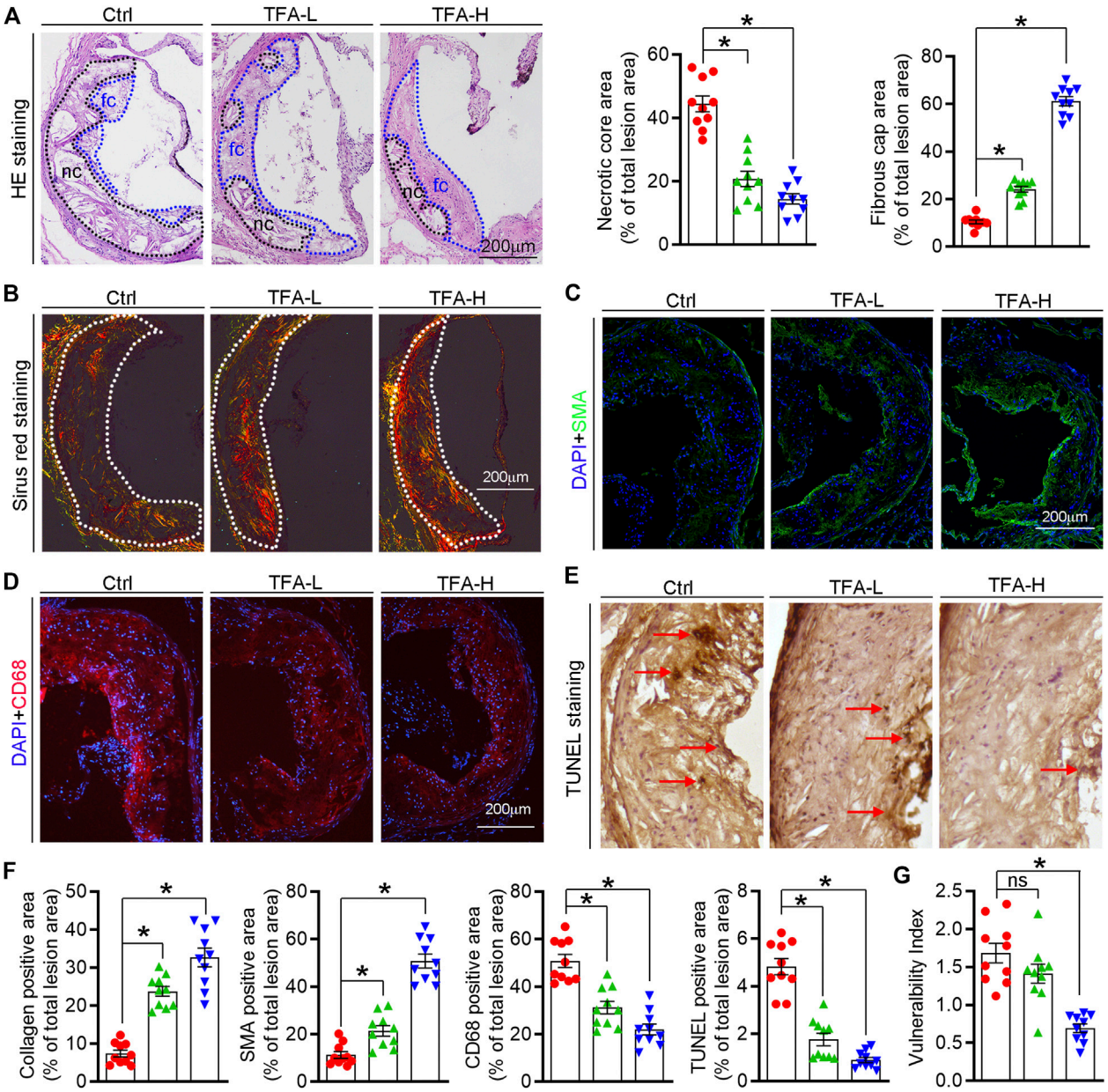

FIGURE 2 | TFA changes the plaque composition and enhances plaque stability. **(A)** Haematoxylin and eosin staining followed by quantitative analysis of sinus lesions, necrotic core area, and fibrous cap area in aortic root cross sections. nc: necrotic cores; fc: fibrous cap, $n = 10$. **(B–F)** Representative photomicrographs of aortic root sections stained with sirus red staining **(B)**, αSMA **(C)**, CD68 **(D)**, and TUNEL staining **(E)** in atherosclerotic plaque followed by the quantification **(F)**, $n = 10$. **(G)** The vulnerability index of plaques was calculated as (macrophage% + lipid staining%)/(SMCs% + collagen fiber%), $n = 10$. Data are presented as mean ± SEM, $^*p < 0.05$, significantly different from control; ns: not significantly different. TFA inhibits foam cell formation by regulating expression of transporters and scavenger receptors that orchestrating cholesterol efflux and uptake.

33-mediated and other underlying mechanism may exist. Collectively, these results demonstrate that TFA can suppress foam cell formation, mechanistically, through inhibiting scavenger receptor-meditated cholesterol uptake and de-repressing miR-33-mediated restriction on cholesterol efflux.

Inflammation is an important driver of atherogenesis. Therefore, we assessed the expression of proinflammatory cytokines in aorta; and found that TFA significantly reduced the proinflammatory cytokines whereas promoted the anti-inflammatory cytokines (**Figure 4A**). We further quantified the levels of representative pro- and anti-inflammatory factors in atherosclerotic lesions and found the expressions of proinflammatory cytokine IL-1β was downregulated while the anti-inflammatory cytokine Arg1 was upregulated in TFA-treated mice (**Figure 4B**), indicating that TFA ameliorated the inflammation during the lesion formation. Macrophages, as the

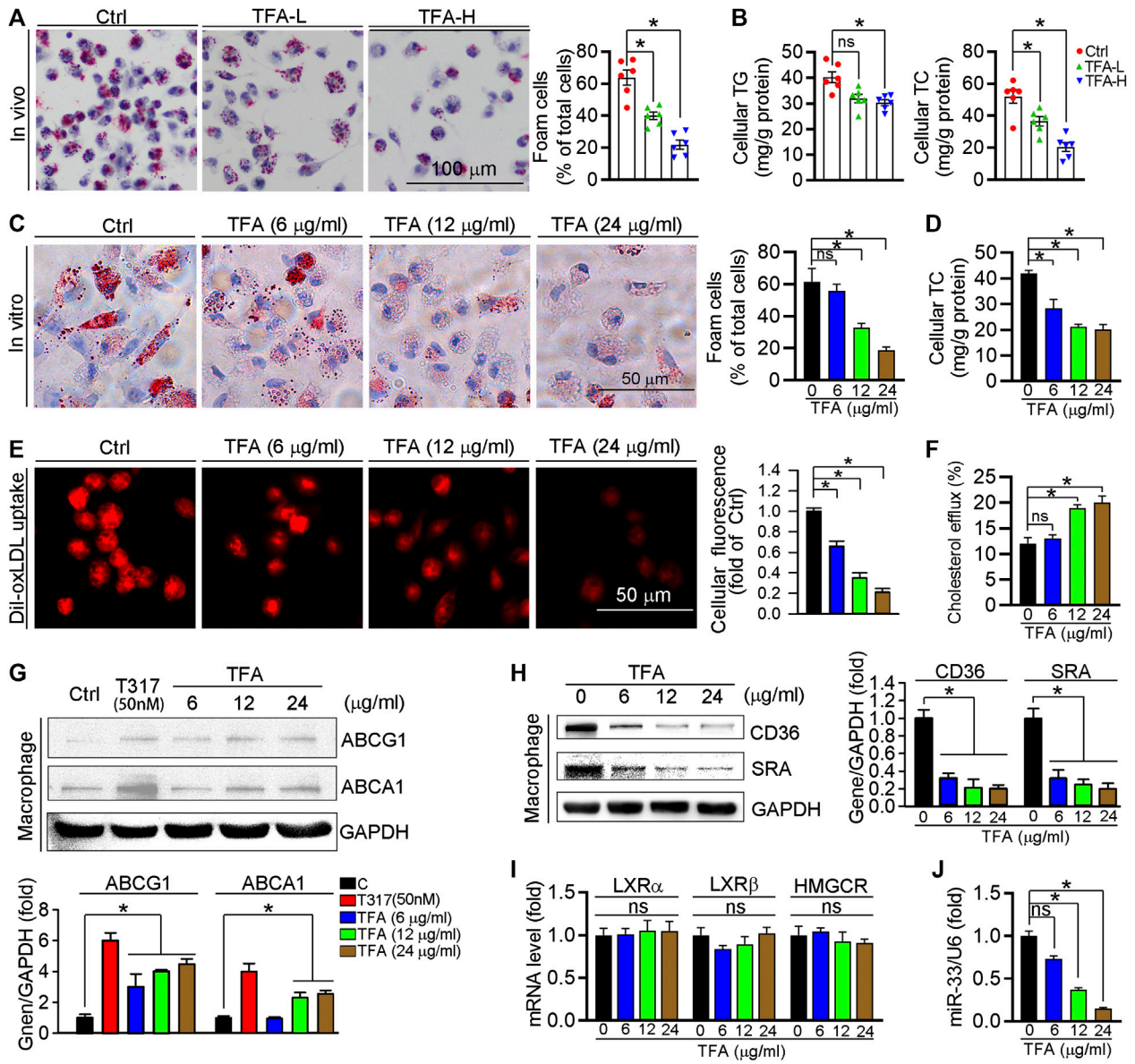

FIGURE 3 | TFA inhibits lipid accumulation and reduces expression of miR-33, CD36 and SRA in macrophage. **(A)** Inhibitory effect of TFA on foam cell formation using Oil Red O staining, $n = 5$. **(B)** Determination of cellular TG and TC in peritoneal macrophage from apoE$^{-/-}$ mice, $n = 5$. **(C)** Inhibitory effect of TFA on lipid accumulation using Oil Red O staining *in vitro* RAW264.7 cells, $n = 5$. **(D)**. Determination of cellular TC in RAW264.7 cells, $n = 5$. **(E)** LDL uptake assay in peritoneal macrophage, $n = 5$. **(F)** Cholesterol efflux assay in peritoneal macrophage, $n = 5$. **(G, H)** After 12 h treatment, expression of ABCA1, ABCG1, CD36, and SRA in peritoneal macrophage was determined by western blot, $n = 5$. **(I)** After 12 h treatment, expression of LXRα, LXRβ, and HMGCR in peritoneal macrophage was determined by q-RT-PCR, $n = 5$. **(J)** After 12 h treatment, expression of miR-33 in peritoneal macrophage was determined by q-RT-PCR, $n = 5$. Data are presented as mean ± SEM, $^*p < 0.05$, significantly different from control; ns: not significantly different. TC: total cholesterol; TG: triglyceride; T317: T0901317, a synthetic ligand of LXR as a positive control. TFA attenuates the inflammatory response in plaque via dual inactivation of NFκB and miR-33.

key mediators of inflammatory response, can affect the progression of atherosclerosis. M1 macrophages are present mainly in unstable plaques and can boost the production of pro-atherogenic inflammatory cytokines, thereby contributing to sustained inflammation and plaque vulnerability. Therefore, we further determined the effect of TFA on macrophage polarization and observed that the peritoneal macrophage from TFA-treated mice are prone to M2 transition but not M1 polarization (**Figures 4C,D**). To uncover the underlying mechanism of anti-inflammatory effect, we assessed NFκB pathway, the key regulator of inflammation. Noticeable, TFA significantly increased the expression of IκBα and reduced the phosphorylation of IκBα and p65 (**Figure 4E**), indicating that NFκB pathway was markedly inactivated. Moreover, miR-33 is a post-transcriptional regulator of genes involved in inflammation, and inhibition of which can reduce plaque macrophage

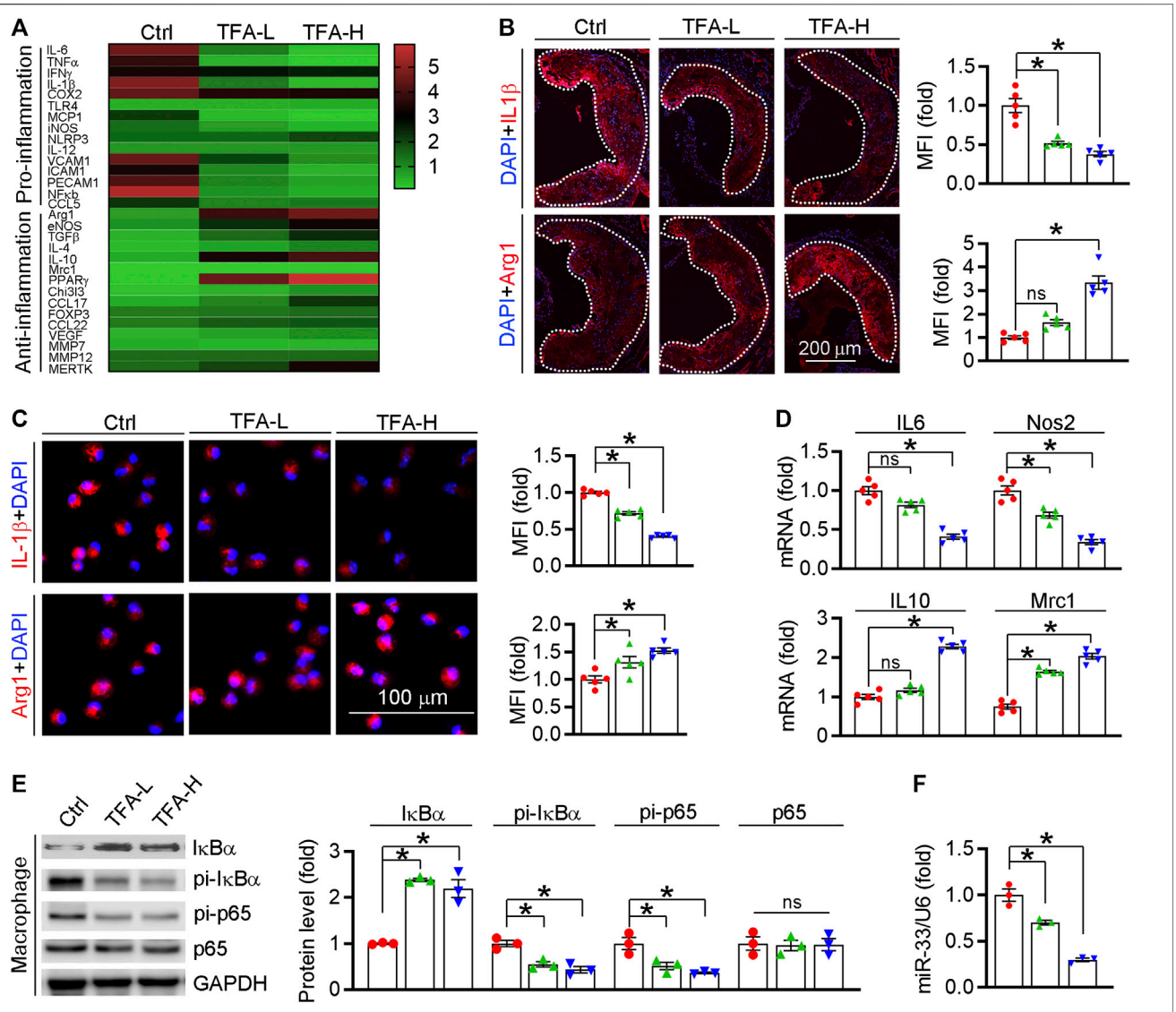

FIGURE 4 | TFA reduces inflammatory response *in vivo*. **(A)** Transcriptional level of atherosclerosis-associated factors was shown in heatmap, $n = 3$. **(B)** Representative pro- and anti-inflammatory factors in the plaque was assessed by immunofluorescent staining, $n = 5$. **(C)** Representative pro- and anti-inflammatory factors in peritoneal macrophage were assessed by immunofluorescent staining, $n = 5$. **(D)** After 12 h treatment, expression of IL10, Nos2, Mrc1, and IL6 in peritoneal macrophage was determined by q-RT-PCR, $n = 3$. **(E)** After 12 h treatment, expression of IκBα, pi- IκBα, pi-p65, and p65 in peritoneal macrophage was determined by western blot, $n = 3$. **(F)** After 12 h treatment, expression of miR-33 in peritoneal macrophage was determined by q-RT-PCR, $n = 3$. Data are presented as mean ± SEM, $^*p < 0.05$, significantly different from control; ns: not significantly different. TFA promotes macrophage phenotypic transition to anti-inflammatory M2 type *in vitro*

inflammation (Distel et al., 2014). Intriguingly, in peritoneal macrophage isolated from TFA-treated mice, expression of miR-33 was markedly reduced (**Figure 4F**), indicating that the anti-inflammatory effect of TFA may be partially associated with reduction of miR-33 expression. Taken together, we demonstrate that TFA reduced inflammation *in vivo* through inactivation of NFκB and negative regulation of miR-33 expression, by which contributing to its anti-atherogenic function.

We further detected effect of TFA on the inflammatory factor generation *in vitro* macrophage. The proinflammatory cytokines IL1β and TNFα were downregulated, whereas the anti-inflammatory cytokines Arg1 and IL10 were upregulated (**Figures 5A,B**). To uncover the underlying mechanism, we assessed NFκB pathway *in vitro* as we did *in vivo*. Indeed, TFA significantly reduced the activity of NFκB pathway (**Figure 5C**). To prove the contribution of NFκB to the anti-inflammatory proprieties of TFA, LPS was used to treat peritoneal macrophage to induce the NFκB activation in presence of TFA treatment. After treatment by LPS, the protective effects of TFA on inflammation was significantly abolished (**Figure 5D**), suggesting that TFA treatment is associated with inactivation of NFκB. Moreover, we further determined whether the anti-inflammatory effect of TFA was associated miR-33. As the data shown, TFA significantly reduced miR-33 expression *in vitro and*

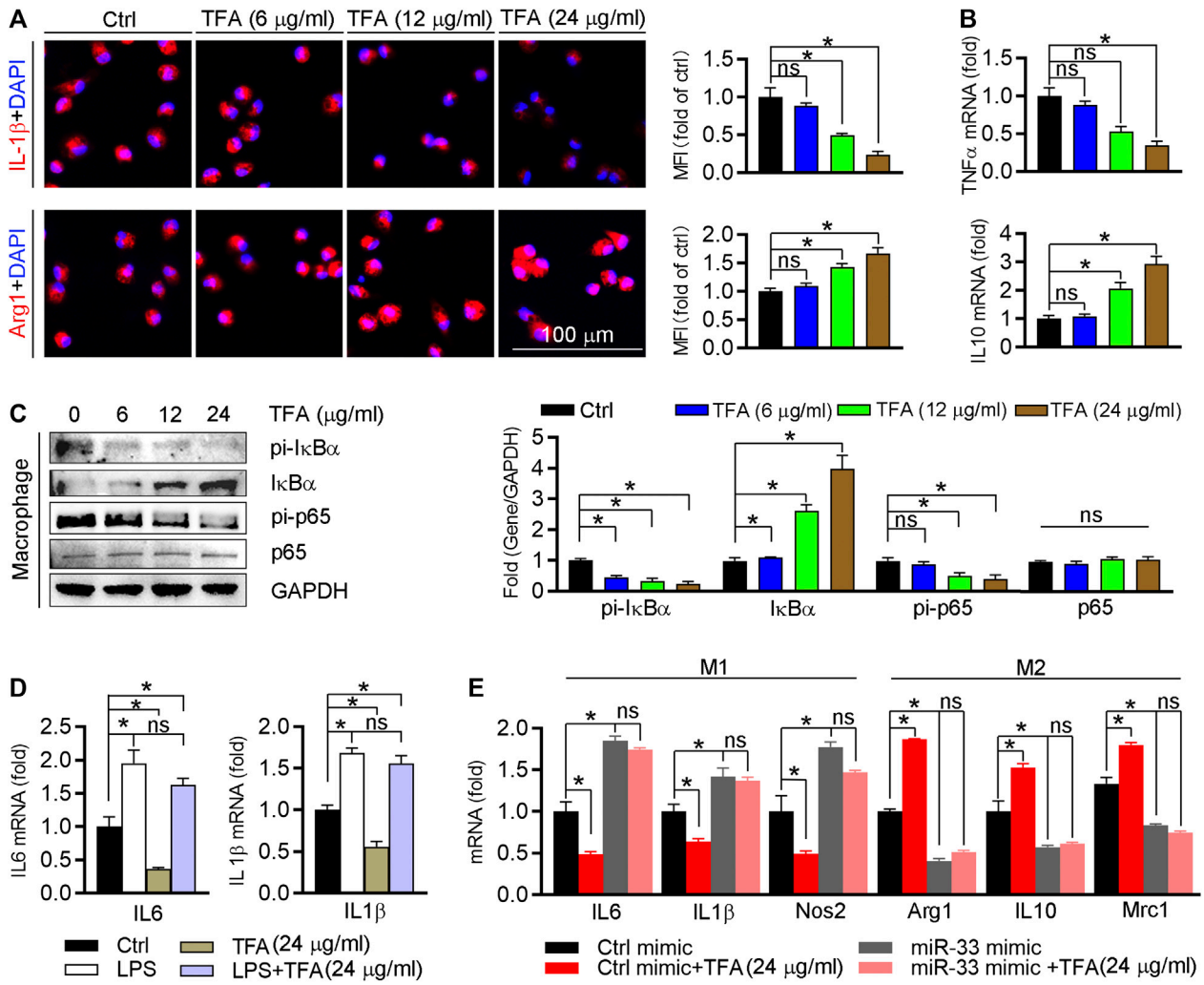

FIGURE 5 | TFA inhibits inflammation and promotes the macrophage M2 transition. **(A)** After TFA treatment in peritoneal macrophage, expression of Arg1 and IL-1β was determined by immunofluorescent staining, $n = 5$. **(B)** After 12 h TFA treatment, expression of TNFα and IL-10 mRNA in peritoneal macrophage was determined by q-RT-PCR, $n = 5$. **(C)** After 12 h TFA treatment, expression of IκBα, pi-IκBα, pi-p65, and p65 in peritoneal macrophage was determined by western blot, $n = 5$. **(D)** After treatment with LPS (100 ng/ml) and TFA, expression of M1 markers in peritoneal macrophage was determined by q-RT-PCR, $n = 5$. **(E)** After 12 h treatment by miR-33 mimics and TFA, expression of M1 or M2 markers in peritoneal macrophage was determined by q-RT-PCR, $n = 5$. Data are presented as mean ± SEM, $^*p < 0.05$, significantly different as indicated; ns: not significantly different. TFA inhibits endothelial activation and monocyte recruitment to endothelial cells.

in vivo (**Figures 3J** and **4F**), which partially accounted for the anti-inflammatory effect of TFA. Furthermore, we treated macrophages with TFA in presence or absence of miR-33 mimics. Noticeable, TFA promoted the macrophage toward M2 phenotype, which was markedly abolished by miR-33 mimics (**Figure 5E**), indicating that the regulatory effect on macrophage phenotypic transition is partially miR-33-mediated. Taken together, TFA can inhibit inflammatory *in vitro*, which was associated inactivation of NFκB pathway and negative regulation of miR-33 expression.

Circulating monocytes are recruited by inflammatory cytokines to the endothelium in the aorta, and then transform into foam cells under LDL or oxLDL stimulation, which contributes to aortic lesions formation. We determined whether TFA could inhibit the monocyte adhesion to endothelial cells and observed that TFA significantly reduced the number of THP-1 cells adhering to human umbilical vein endothelial cells (HUVECs) (**Figures 6A,B**). Pro-inflammatory cytokines can induce the expression of adhesion molecules in endothelial cells, such as ICAM-1 and VCAM-1, which provide a scaffold for leukocyte migration in endothelial cells. Mechanistically, TFA decreased expression of ICAM-1 and VCAM-1 in HUVEC (**Figure 6C**). Noteworthy, in THP-1 cells, TFA markedly reduced expression of proinflammatory cytokines, including TNFα, IL1β, and IL-6 (**Figure 6F**), which contributed to inactivation of the ICAM-1 and VCAM-1 expression in endothelial cells. Due to the important role of miR-33 and NFκB in inflammatory response, we evaluated their role in monocyte adhesion. To prove the contribution of NFκB to inhibition of monocyte recruitment by TFA, LPS was used to treat

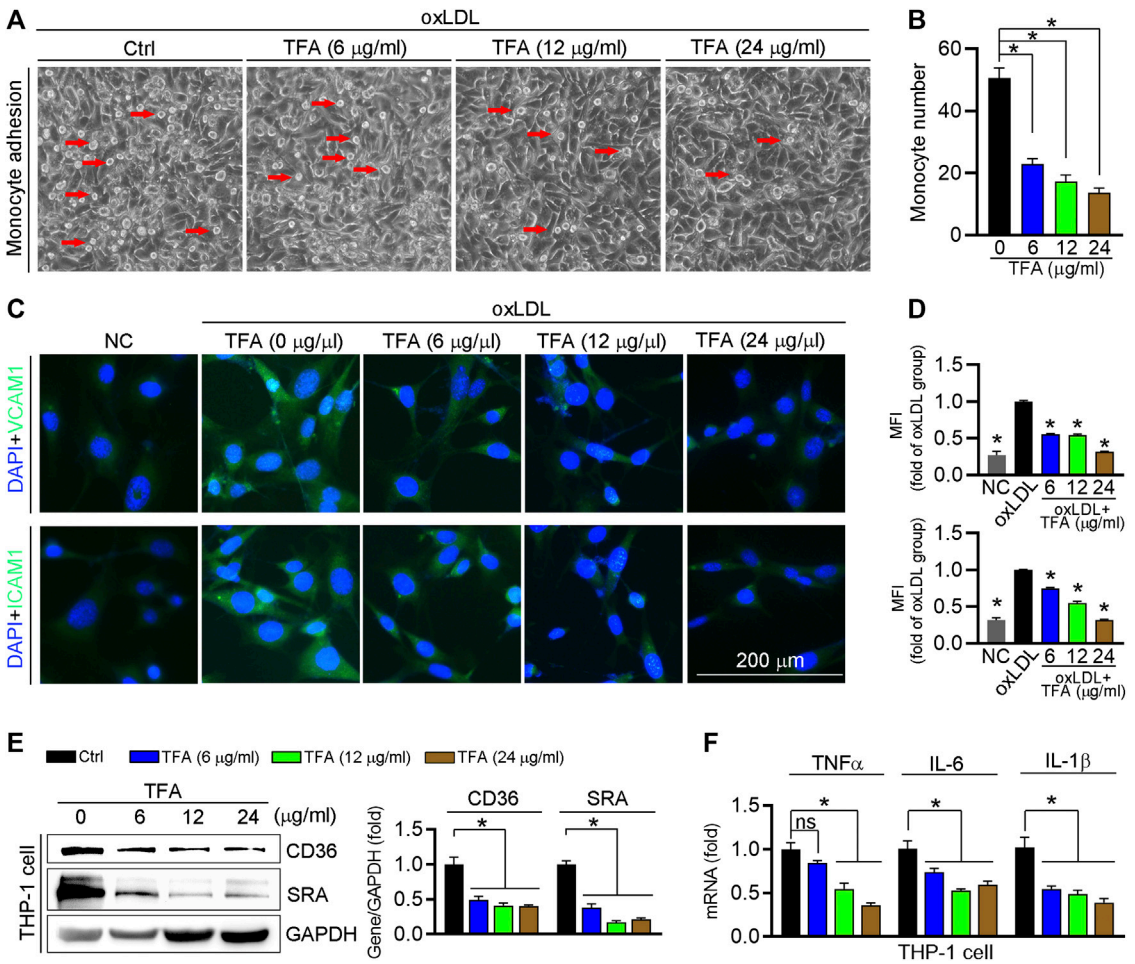

FIGURE 6 | TFA inhibits monocyte adhesion to endothelial cells. **(A, B)** HUVECs in 24-well plates and THP-1 cells were pretreated with oxLDL (100 μg mL^{-1}) for 12 h. After incubation with oxLDL, THP-1 cells were added to HUVECs and co-incubated for 1 h. The image of adherent THP-1 cells were captured with a microscope and the number of adherent THP-1 cells was calculated, $n = 5$. **(C, D)** After 12 h TFA treatment in HUVECs, expression of ICAM-1 and VCAM-1 was determined by immunofluorescent staining, $n = 5$. **(E)** Expression of CD36 and SRA protein in THP-1 cells was determined by western blot after 12 h TFA treatment, $n = 3$. **(F)** Expression of proinflammatory cytokines in THP-1 cells was determined by q-RT-PCR after 12 h TFA treatment, $n = 5$. Data are presented as mean ± SEM, $^*p < 0.05$, significantly different as indicated. TFA improves the HFD-induced dyslipidemia in $apoE^{-/-}$ mice and reduces the oxidant stress *in vitro*.

HUVEC to induce the activation of NFκB in presence of TFA treatment. In addition, HUVEC was treated with miR-33 mimic. After treatment by LPS or miR-33 mimic, the protective effects of TFA on monocyte recruitment was significantly abolished (**Supplementary Figures S5**), suggesting that TFA treatment is associated with inactivation of NFκB and miR-33. Moreover, adhesion molecules from endothelial cells can bind to specific ligands expressed by monocytes, such as CD36 and SRA, resulting in the increased leukocyte-endothelial interactions (Santiago-García et al., 2003; Trinh-Trang-Tan et al., 2010). Therefore, we further assessed the expression of CD36 and SRA in THP-1 cells and found that both were reduced by TFA (**Figure 6E**), indicating that the monocyte binding ligand was decreased, which contributed not only to the inhibition of lipid uptake (**Figure 3E**) but also to the reduction in monocyte adhesion to HUVEC. Collectively, TFA reduced monocyte recruitment to endothelial cells by reducing binding ligands (CD36 and SRA) in monocyte and adhesion molecules (ICAM-1 and VCAM-1) expression in endothelial cells, partially by which exerting the antiatherogenic function.

Lipid dysfunction is a critical contributor to atherosclerosis development. The influx of LDL into the arterial intima, the site of atherogenesis, is closely associated with their plasma concentration because high concentrations of LDL lead to higher LDL uptake by macrophages. In addition, infiltrated LDL are oxidized to turn into highly atherogenic form, such as ox-LDL. Macrophages ingest the modified LDL particles via scavenger receptors and thereby transformed into foam cells. In contrast, HDL is considered antiatherogenic lipoproteins because it can initiate the reverse cholesterol transport, by which transfering cholesterol from foam cells to the liver, and ultimately to the gut for excretion. In this study, the body weight of mice was not changed by TFA (**Figure 7A**). Of note, TFA significantly reduced level of total cholesterol (T-CHO), LDL, TG, and VLDL, whereas increased the

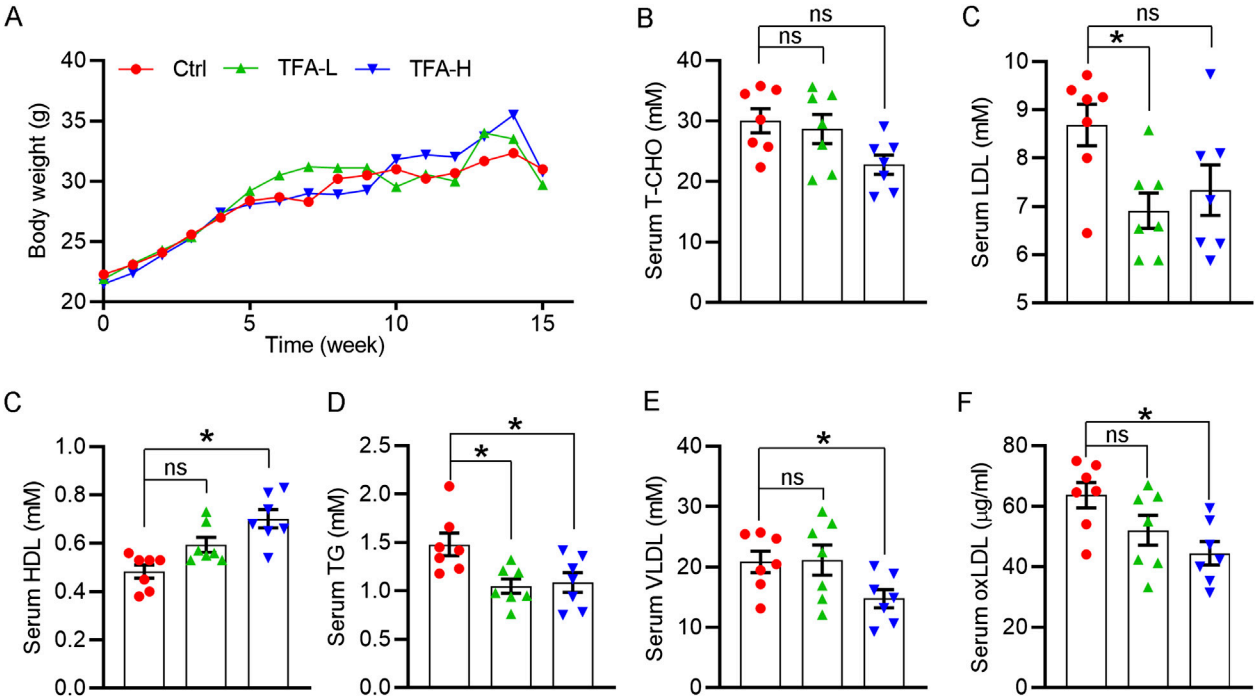

FIGURE 7 | TFA improves the lipid disorder *in vivo* under HFD condition. **(A)** Body weight was recorded weekly. Date are presented as mean ± SEM (n = 10). **(B–F)** Serum levels of total cholesterol (T-CHO), LDL- and HDL-C, VLDL, TG (mM) and oxLDL (μg/ml) were determined by biochemical analyzer or ELISA assay. Date are presented as mean ± SEM (n = 7), $^*p < 0.05$, significantly different from control; ns: not significantly different. TFA ameliorates the HFD-induced hepatic steatosis in apoE$^{-/-}$ mice.

HDL level (**Figures 7B–E**). In addition, we quantified the level of ox-LDL, a modified LDL that contributed to atherogenesis, and observed that ox-LDL level was downregulated in TFA-treated mice compared with control mice (**Figure 7F**), suggesting that the atherogenic form of LDL was reduced and oxidant stress may be attenuated by TFA. Therefore, we further determined the cellular ROS levels by DCF staining. Intriguingly, DCF fluorescent intensity was reduced by TFA in dose-dependent manner (**Supplementary Figures S6**), indicating that TFA reduced the production of cellular ROS. Collectively, TFA improved the lipid profile and restrained the transformation of LDL to atherogenic form during the atherosclerosis development, partially by which TFA exerted the anti-atherogenic function.

Hepatic steatosis facilitates atherogenesis because the liver plays an important role in lipid metabolism, such as RCT, lipid synthesis, and fatty acid oxidation (Patel and Siddiqui, 2019; Stols-Gonçalves et al., 2019; Jiang et al., 2020). As shown in **Figure 8A**, liver color and weight were changed to almost normal condition, which was accompanied by reduced ratio of liver weight to body weight (**Figure 8B**). Moreover, H&E and Oil Red O staining revealed that hepatic steatosis was attenuated in TFA-treated mice compared to control mice (**Figures 8C,F**). Furthermore, TFA significantly reduced the hepatic TC and TG content (**Figures 8D,E**), indicating that hepatic steatosis was attenuated by TFA. Hepatic steatosis can lead to the liver injury. Noticeable, chronic treatment with TFA did not cause hepatic toxicity as measured by plasma AST and ALT enzyme levels. In contrast, TFA markedly reduced the HFD-induced liver injury, which was shown by the reduced levels of AST and ALT (**Figures 8G,H**). To further determine the mechanism of TFA on hepatic lipid metabolism, we assessed the expression of genes involved lipid oxidation and genesis. Intriguingly, TFA markedly promoted the expression of SRBI, the gene in charge of cholesterol uptake in liver; and simultaneously promoted the expression of ABCG5/G8, the genes responsible for cholesterol transportation to intestine (**Figures 8I,J**), by which enhanced the RCT and then reduced the hepatic retention of cholesterol. In addition, TFA significantly reduced expression of genes responsible for lipid genesis, including FASN and SREBP1c (**Figure 8K**), indicating that TFA inhibited hepatic lipid synthesis. Consistent with this observation, the protein or mRNA expression of genes involved in fatty acid oxidation (AMPKα and CPT1α) were upregulated in TFA-treated mice (**Figures 8L,M**), which indicated that TFA promoted the lipid consumption. Taken together, TFA attenuated the hepatic steatosis by promoting RCT, enhancing fatty acid oxidation, and downregulating lipid synthesis, by which improving the lipid metabolism and thereby partially accounting for its antiatherogenic function.

DISCUSSION

Atherosclerosis, a major pathogen of coronary heart disease (CHD), is closely associated with lipid disorder and chronic

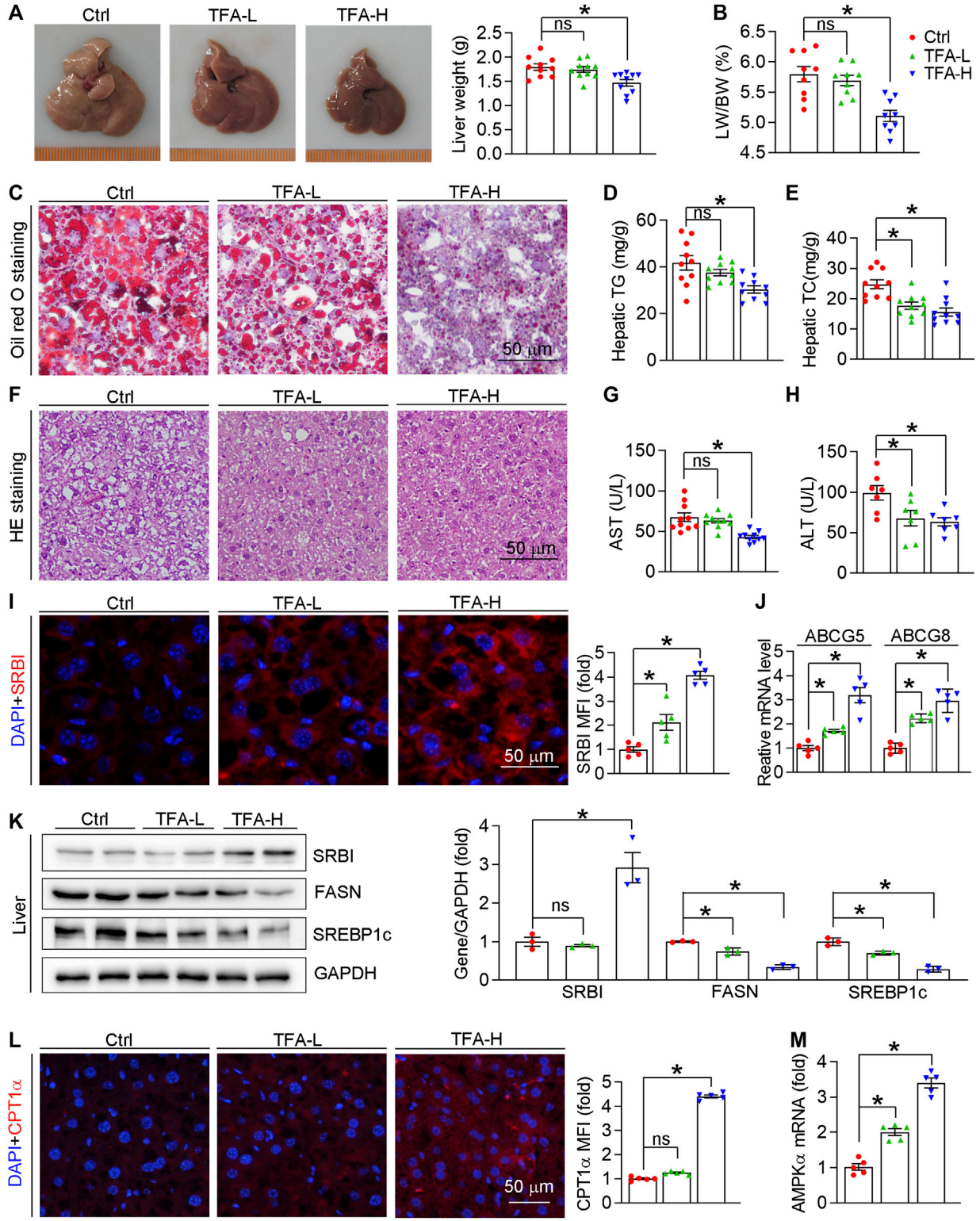

FIGURE 8 | TFA ameliorates hepatic steatosis *in vivo*. **(A)** Liver photos and weight, $n = 10$. **(B)** Ratio of liver to body weight, $n = 10$. **(C)** Oil Red O staining on liver frozen sections, $n = 10$. **(D, E)** Quantitative analysis of hepatic TG and TC. **(F)** Haematoxylin and eosin staining of liver frozen sections, $n = 10$. **(G,H)** Serum levels of AST ($n = 10$) and ALT ($n = 7$). **(I)** Expression of SRBI in liver was determined by immunofluorescent staining, $n = 5$. **(J)** Expression of ABCG5 and ABCG8 in liver was determined by q-RT-PCR, $n = 5$. **(K)** Expression of SRBI, FASN, and SREBP1c in liver was determined by western blot, $n = 3$. (**L**) Expression of CPT1α in liver was determined by immunofluorescent staining, $n = 5$. (**M**) Expression of AMPKα in liver was determined by q-RT-PCR, $n = 5$. Data are presented as mean ± SEM, $^*p < 0.05$, significantly different as indicated.

inflammation. TFA is the flavone component from *A. membranaceus* which is the long-term used traditional Chinese medicine for CHD treatment in clinic. Noticeable, the current study showed that higher intake of flavone was associated with a lower risk of CHD (Ma L. et al., 2020). In this study, we determined whether TFA could inhibit atherosclerosis, and attempted to uncover the underlying mechanism. Intriguingly, TFA treatment substantially reduced the atherosclerotic development, enhanced the plaque stability, and reduced monocyte recruitment, which may be attributed to the inhibition of lipid disorder and inflammation. Mechanistically, we found that miR-33 is a critical signaling mediator of TFA on promoting ABCA1/G1 expression as well as inhibiting inflammation in macrophages, which coordinated the anti-inflammatory effect of TFA by inactivating NFκB signaling pathway.

Increased vulnerability is prone to plaque rupture, which can result in severe cardiovascular event (Seneviratne et al., 2017). Of note, composition of plaque markedly affects the lesion stability (Naghavi et al., 2003). In this study, TFA significantly reduced atherosclerotic plaque size and promoted a more favorable plaque composition with increased fibrous cap, plaque collagen and SMC content; and reduced necrotic core area and macrophage accumulation, indicating that TFA significantly reduced the plaque vulnerability. Moreover, TFA markedly promoted the expression of ABCA1/G1 and inhibited the CD36 and SRA expression (**Figures 3G,H**), by which enhancing cholesterol efflux, reducing cholesterol uptake and thereby inhibiting foam cell formation. However, as the upstream regulatory gene of ABCA1/G1, liver X receptor (LXR) was not activated by TFA (**Figure 3I**). Moreover, the key gene for cholesterol synthesis, HMGCR, was also not affected by TFA (**Figure 3I**). These results indicated that other molecule may mediate the TFA-induced of ABCA1/G1 expression.

To gain further insight into the effect of TFA on ABCA1/G1 expression, we investigated the mechanism. Noticeable, miRNAs, a group of small endogenous non-coding RNAs, can regulate gene expression at posttranscriptional levels. Functionally, miRNAs can serve as important regulators of atherogenic process, such as cellular adhesion, lipid uptake and efflux, and generation of inflammatory mediators (Feinberg and Moore, 2016). Therefore, we hypothesized that miRNAs may participate in the protective effect of TFA on lipid metabolism and inflammation. Noticeable, miR-33 is a negative regulator of ABCA1/G1 and thereby promoting foam cell formation via inhibiting macrophage cholesterol efflux (Rayner et al., 2011b). We further postulated that the enhancement of ABCA1/G1 and the inhibition of inflammation by TFA may be through suppression of miR-33, by which removing the restriction on expression of ABCA1/G1. To test the hypothesis, we evaluated miR-33 expression *in vitro* and *in vivo*, and found that miR-33 was reduced by TFA (**Figure 3J**), which accounted for the upregulation of ABCA1/G1 expression.

Atherosclerosis is characterized with the predominance of an M1 macrophage phenotype within the plaque, whereas plaques undergoing regression are rich in M2 macrophages (Lutgens et al., 2019; Tunon et al., 2019). Intriguingly, in this study, TFA significantly inhibited M1 macrophage polarization, whereas promoted M2 macrophage phenotype *in vivo* and *in vitro*, as indicated by the reduced levels of proinflammatory cytokines and increased anti-inflammatory cytokines (**Figures 4A–D** and **5A**). NFκB signaling pathway plays important role in regulating macrophage polarization and inflammation (Song et al., 2019). In addition, miR-33 can sustain the inflammatory M1 macrophage phenotype, and inhibition of which can reduce plaque inflammation (Distel et al., 2014; Ouimet et al., 2015). Therefore, we determined whether the anti-inflammatory effect of TFA was involved in NFκB and miR-33. We assessed not only the activity of NFκB pathway but also the expression of miR-33, and observed that TFA markedly inactivated the NFκB activity (**Figures 4E** and **5C**) and reduced the expression of miR-33 (Figure 4F). Intriguingly, miR-33 mimic or LPS almost abolished the effect of TFA on macrophage inflammation (Figure 5D, E). These results indicated that anti-inflammatory effect of TFA may be attributed to dual suppression of miR-33 and NFκB pathway.

Atherogenic endothelial activation enhances circulating monocytes adhesion, and especially in the context of hypercholesterolemia. These monocytes uptake excessive lipid to drive early plaque formation (Tabas et al., 2015). In the monocyte attachment assay, TFA markedly suppressed the monocyte recruitment to HUVECs, and mechanistically reduced the expression of VCAM-1 and ICAM-1 (**Figures 6A–D**), the major molecules that expressed in the activated ECs (Gerhardt and Ley, 2015), indicating that TFA can attenuate the endothelial activation and the following monocyte adhesion. Moreover, TFA significantly reduced the HFD-induced the lipid disorder (**Figures 7A–F**), which favored the reduction in cellular lipid accumulation in monocyte and thereby retarding the initiation and development of atherosclerosis.

Liver is a critical organ that regulates lipid metabolism, which mainly determines the cholesterol metabolism and lipid profile in serum, thereby affecting the atherogenesis. Despite no significant differences were observed in body weight over the 16 weeks of HFD along with TFA feeding, the serum lipid profile was significantly improved by TFA (**Figure 7**). Mechanistically, SREBP-1c can activate transcription of genes involved in lipid synthesis, such as fatty acid synthase (FASN) (Shimano, 2009). Noteworthy, in the liver, TFA markedly damped the expression of SREBP-1c and FASN while increased the expression of CPT1α and AMPKα (**Figures 8K–M**), indicating that lipid synthesis was decreased, and fatty acid oxidation (FAO) was increased. Noticeable, miR-33, an intronic miRNA that co-expressed with its host gene SREBP1 (Najafi-Shoushtari et al., 2010), can balance cellular lipid levels by increasing genes that oppose SREBP-regulated pathways, including those involved in cholesterol efflux and FAO. For instance, in non-human primate model, miR-33 antagonism increased FAO and reduced fatty acid synthesis (Rayner et al., 2011a). In this study, hepatic miR-33 expression was reduced by TFA (**Supplementary Figures S4**), which may be attributed to repression of SREBP1 (**Figure 8K**). In addition, scavenger receptor class B member 1 (SR-BI) is key molecule for RCT, loss of which in people are associated with

increased cardiovascular risk (Zanoni et al., 2016). After ABCA1/G1-mediated cholesterol efflux to HDL, mature HDL can directly deliver cholesterol to the liver via SR-BI, by which mediates RCT and are thereby anti-atherogenic (Rader et al., 2009; Rosenson et al., 2012; Shen et al., 2018). In this study, TFA significantly enhanced SRBI expression (**Figures 8I,K**), which may promote RCT and thereby inhibit atherogenesis. Additionally, the TFA-induced promotion in efflux capacity was significantly correlated with plasma HDL concentrations (**Figure 7C**). Moreover, the biliary cholesterol excretion rate is mainly dependent on the expression of ABCG5/G8 (Nijstad et al., 2011; Lee-Rueckert et al., 2016); and it should be noted that the RCT rate in the mice can be promoted by increasing the hepatic expression of ABCG5/G8 (Escolà-Gil et al., 2011). In the present study, TFA markedly increased the expression of the ABCG5/G8 (**Figure. 8J**), indicating that TFA may contribute to the cholesterol excretion into bile and thereby increasing RCT, by which inhibiting the foam cell formation in the atherogenic plaque.

This study explored a broad variety of potential downstream mechanisms that could be associated with TFA effects. However, the limitation of the study is that upstream mechanisms need to be further investigated. Oxidant stress is a factor of atherogenesis (Förstermann et al., 2017). Previous study has reported the antioxidant effect of TFA *in vitro* (Xu et al., 2014). In our study, TFA reduced the oxLDL level in the serum (**Figure 7F**) and reduced the ROS generation *in vitro* (**Supplementary Figures S6**), indicating that oxidant stress may be attenuated by TFA. These data indicate that TFA may react with reactive oxygen species associated with atherosclerosis, which then triggers the observed downstream mechanisms.

CONCLUSION

Taken together, TFA can attenuate the atherosclerotic development via inhibiting foam cell formation and inflammation, which is through negative regulation of miR-33, CD36, and SRA expression; and NF-κB pathway. Simultaneously, TFA markedly ameliorates hepatic steatosis via improving the hepatic lipid metabolism, and thereby reduces proatherogenic lipid disorder, which is through promoting reverse cholesterol transport, enhancing fatty acid oxidation, and downregulating lipid synthesis. Therefore, TFA may act as a very promising anti-atherosclerotic drug by activating multiple signaling pathways that regulating lipid metabolism and inflammation.

DATA AVAILABILITY STATEMENT

The original contributions presented in the study are included in the article/**Supplementary Material**, further inquiries can be directed to the corresponding authors.

ETHICS STATEMENT

The animal study was reviewed and approved by Ethics Committee of Tianjin University of Traditional Chinese Medicine.

AUTHOR CONTRIBUTIONS

JZ, SY, and YH conducted the experiment; CM wrote the article; JS, YS, ZW, KF, JZ, XY, and HZ offered the advice; JM and GF designed the experiment.

FUNDING

This work was supported by Grants from National Major Scientific and Technological Special Project for "Significant New Drugs Development" (2019ZX09201005-007-001); National Natural Science Foundation of China (81774050, 82003747, 82000824); Tianjin Outstanding Youth Science Foundation (17JCJQJC46200); Natural Science Foundation of Tianjin (19JCQNJC12600, 20JCQNJC00260); Research project of Tianjin education commission (2019KJ044); Training Program Foundation for Innovative Research Team of Higher Education in Tianjin during the 13th Five-Year Plan Period (No. TD13-5050).

ACKNOWLEDGEMENTS

This manuscript has been released as a pre-print at https://www.researchsquare.com/article/rs-50056/v1. (CM et al.)

SUPPLEMENTARY MATERIAL

The Supplementary Material for this article can be found online at: https://www.frontiersin.org/articles/10.3389/fphar.2020.610550/full#supplementary-material.

REFERENCES

Baeuerle, P. A., and Baltimore, D. (1988). I kappa B: a specific inhibitor of the NF-kappa B transcription factor. *Science* 242 (4878), 540–546. doi:10.1126/science.3140380

Barrett, T. J., Distel, E., Murphy, A. J., Hu, J., Garshick, M. S., Ogando, Y., et al. (2019). Apolipoprotein AI) promotes atherosclerosis regression in diabetic mice by suppressing myelopoiesis and plaque inflammation. *Circulation* 140 (14), 1170–1184. doi:10.1161/circulationaha.119.039476

Crucet, M., Wust, S. J., Spielmann, P., Luscher, T. F., Wenger, R. H., and Matter, C. M. (2013). Hypoxia enhances lipid uptake in macrophages: role of the scavenger receptors Lox1, SRA, and CD36. *Atherosclerosis* 229 (1), 110–117. doi:10.1016/j.atherosclerosis.2013.04.034

Curtis, M. J., Bond, R. A., Spina, D., Ahluwalia, A., Alexander, S. P., Giembycz, M. A., et al. (2015). Experimental design and analysis and their reporting: new guidance for publication in BJP. *Br. J. Pharmacol.* 172 (14), 3461–3471. doi:10.1111/bph.12856

de Winther, M. P. J., and Lutgens, E. (2019). The link between hematopoiesis and atherosclerosis. *N. Engl. J. Med.* 380 (19), 1869–1871. doi:10.1056/NEJMcibr1901397

de Winther, M. P., van Dijk, K. W., Havekes, L. M., and Hofker, M. H. (2000). Macrophage scavenger receptor class A: a multifunctional receptor in atherosclerosis. *Arterioscler. Thromb. Vasc. Biol.* 20 (2), 290–297. doi:10.1161/01.atv.20.2.290

Distel, E., Barrett, T. J., Chung, K., Girgis, N. M., Parathath, S., Essau, C. C., et al. (2014). miR33 inhibition overcomes deleterious effects of diabetes mellitus on atherosclerosis plaque regression in mice. *Circ. Res.* 115 (9), 759–769. doi:10.1161/circresaha.115.304164

Escolà-Gil, J. C., Llaverias, G., Julve, J., Jauhiainen, M., Méndez-González, J., and Blanco-Vaca, F. (2011). The cholesterol content of Western diets plays a major role in the paradoxical increase in high-density lipoprotein cholesterol and upregulates the macrophage reverse cholesterol transport pathway. *Arterioscler. Thromb. Vasc. Biol.* 31 (11), 2493–2499. doi:10.1161/atvbaha.111.236075

Feinberg, M. W., and Moore, K. J. (2016). MicroRNA regulation of atherosclerosis. *Circ. Res.* 118 (4), 703–720. doi:10.1161/circresaha.115.306300

Förstermann, U., Xia, N., and Li, H. (2017). Roles of vascular oxidative stress and nitric oxide in the pathogenesis of atherosclerosis. *Circ. Res.* 120 (4), 713–735. doi:10.1161/circresaha.116.309326

Gerhardt, T., and Ley, K. (2015). Monocyte trafficking across the vessel wall. *Cardiovasc. Res.* 107 (3), 321–330. doi:10.1093/cvr/cvv147

Horie, T., Baba, O., Kuwabara, Y., Chujo, Y., Watanabe, S., Kinoshita, M., et al. (2012). MicroRNA-33 deficiency reduces the progression of atherosclerotic plaque in ApoE$^{-/-}$ mice. *J Am Heart Assoc* 1 (6), e003376. doi:10.1161/jaha.112.003376

Huang, Z., Huang, Q., Ji, L., Wang, Y., Qi, X., Liu, L., et al. (2016). Epigenetic regulation of active Chinese herbal components for cancer prevention and treatment: a follow-up review. *Pharmacol. Res.* 114, 1–12. doi:10.1016/j.phrs.2016.09.023

Jiang, F., Chen, Q., Wang, W., Ling, Y., Yan, Y., and Xia, P. (2020). Hepatocyte-derived extracellular vesicles promote endothelial inflammation and atherogenesis via microRNA-1. *J. Hepatol.* 72 (1), 156–166. doi:10.1016/j.jhep.2019.09.014

Lam, T. K., Shao, S., Zhao, Y., Marincola, F., Pesatori, A., Bertazzi, P. A., et al. (2012). Influence of quercetin-rich food intake on microRNA expression in lung cancer tissues. *Cancer Epidemiol. Biomark. Prev.* 21 (12), 2176–2184. doi:10.1158/1055-9965.Epi-12-0745

Lee, S. B., Park, G. M., Lee, J. Y., Lee, B. U., Park, J. H., Kim, B. G., et al. (2018). Association between non-alcoholic fatty liver disease and subclinical coronary atherosclerosis: an observational cohort study. *J. Hepatol.* 68 (5), 1018–1024. doi:10.1016/j.jhep.2017.12.012

Lee-Rueckert, M., Escola-Gil, J. C., and Kovanen, P. T. (2016). HDL functionality in reverse cholesterol transport--Challenges in translating data emerging from mouse models to human disease. *Biochim. Biophys. Acta* 1861 (7), 566–583. doi:10.1016/j.bbalip.2016.03.004

Li, Y., Guo, S., Zhu, Y., Yan, H., Qian, D. W., Wang, H. Q., et al. (2019). Flowers of *Astragalus membranaceus* var. mongholicus as a novel high potential by-product: phytochemical characterization and antioxidant activity. *Molecules* 24 (3), 28. doi:10.3390/molecules24030434

Lin, L. Z., He, X. G., Lindenmaier, M., Nolan, G., Yang, J., Cleary, M., et al. (2000). Liquid chromatography-electrospray ionization mass spectrometry study of the flavonoids of the roots of Astragalus mongholicus and *Astragalus membranaceus*. *J. Chromatogr. A* 876 (1–2), 87–95. doi:10.1016/s0021-9673(00)00149-7

Liu, C. H., Tsai, C. H., Li, T. C., Yang, Y. W., Huang, W. S., Lu, M. K., et al. (2016). Effects of the traditional Chinese herb *Astragalus membranaceus* in patients with poststroke fatigue: a double-blind, randomized, controlled preliminary study. *J. Ethnopharmacol.* 194, 954–962. doi:10.1016/j.jep.2016.10.058

Lutgens, E., Atzler, D., Doring, Y., Duchene, J., Steffens, S., and Weber, C. (2019). Immunotherapy for cardiovascular disease. *Eur. Heart J.* 9, 24–33. doi:10.1093/eurheartj/ehz283

Ma, C., Zhang, W., Yang, X., Liu, Y., Liu, L., Feng, K., et al. (2018). Functional interplay between liver X receptor and AMP-activated protein kinase alpha inhibits atherosclerosis in apolipoprotein E-deficient mice—a new anti-atherogenic strategy. *Br. J. Pharmacol.* 175 (9), 1486–1503. doi:10.1111/bph.14156

Ma, C., Xia, R., Yang, S., Liu, L., Zhang, J., Feng, K., et al. (2020). Formononetin attenuates atherosclerosis via regulating interaction between KLF4 and SRA in apoE(-/-) mice. *Theranostics* 10 (3), 1090–1106. doi:10.7150/thno.38115

Ma, L., Liu, G., Ding, M., Zong, G., Hu, F. B., Willett, W. C., et al. (2020). Isoflavone intake and the risk of coronary heart disease in US men and women: results from 3 prospective cohort studies. *Circulation* 141 (14), 1127–1137. doi:10.1161/circulationaha.119.041306

Millar, C. L., Duclos, Q., and Blesso, C. N. (2017). Effects of dietary flavonoids on reverse cholesterol transport, HDL metabolism, and HDL function. *Adv. Nutr.* 8 (2), 226–239. doi:10.3945/an.116.014050

Moore, K. J., and Tabas, I. (2011). Macrophages in the pathogenesis of atherosclerosis. *Cell* 145 (3), 341–355. doi:10.1016/j.cell.2011.04.005

Naghavi, M., Libby, P., Falk, E., Casscells, S. W., Litovsky, S., Rumberger, J., et al. (2003). From vulnerable plaque to vulnerable patient: a call for new definitions and risk assessment strategies: Part II. *Circulation* 108 (15), 1772–1778. doi:10.1161/01.cir.0000087481.55887.c9

Najafi-Shoushtari, S. H., Kristo, F., Li, Y., Shioda, T., Cohen, D. E., Gerszten, R. E., et al. (2010). MicroRNA-33 and the SREBP host genes cooperate to control cholesterol homeostasis. *Science* 328 (5985), 1566–1569. doi:10.1126/science.1189123

Nakata, A., Nakagawa, Y., Nishida, M., Nozaki, S., Miyagawa, J., Nakagawa, T., et al. (1999). CD36, a novel receptor for oxidized low-density lipoproteins, is highly expressed on lipid-laden macrophages in human atherosclerotic aorta. *Arterioscler. Thromb. Vasc. Biol.* 19 (5), 1333–1339. doi:10.1161/01.atv.19.5.1333

Nijstad, N., Gautier, T., Briand, F., Rader, D. J., and Tietge, U. J. (2011). Biliary sterol secretion is required for functional *in vivo* reverse cholesterol transport in mice. *Gastroenterology* 140 (3), 1043–1051. doi:10.1053/j.gastro.2010.11.055

Ouimet, M., Barrett, T. J., and Fisher, E. A. (2019). HDL and reverse cholesterol transport. *Circ. Res.* 124 (10), 1505–1518. doi:10.1161/circresaha.119.312617

Ouimet, M., Ediriweera, H. N., Gundra, U. M., Sheedy, F. J., Ramkhelawon, B., Hutchison, S. B., et al. (2015). MicroRNA-33-dependent regulation of macrophage metabolism directs immune cell polarization in atherosclerosis. *J. Clin. Invest.* 125 (12), 4334–4348. doi:10.1172/jci81676

Patel, S. S., and Siddiqui, M. S. (2019). The interplay between nonalcoholic fatty liver disease and atherosclerotic heart disease. *Hepatology* 69 (4), 1372–1374. doi:10.1002/hep.30410

Price, N. L., Rotllan, N., Zhang, X., Canfrán-Duque, A., Nottoli, T., Suarez, Y., et al. (2019). Specific disruption of Abca1 targeting largely mimics the effects of miR-33 knockout on macrophage cholesterol efflux and atherosclerotic plaque development. *Circ. Res.* 124 (6), 874–880. doi:10.1161/circresaha.118.314415

Rader, D. J., Alexander, E. T., Weibel, G. L., Billheimer, J., and Rothblat, G. H. (2009). The role of reverse cholesterol transport in animals and humans and relationship to atherosclerosis. *J. Lipid Res.* 50 (Suppl. l), S189–194. doi:10.1194/jlr.R800088-JLR200

Rayner, K. J., Esau, C. C., Hussain, F. N., McDaniel, A. L., Marshall, S. M., van Gils, J. M., et al. (2011a). Inhibition of miR-33a/b in non-human primates raises plasma HDL and lowers VLDL triglycerides. *Nature* 478 (7369), 404–407. doi:10.1038/nature10486

Rayner, K. J., Sheedy, F. J., Esau, C. C., Hussain, F. N., Temel, R. E., Parathath, S., et al. (2011b). Antagonism of miR-33 in mice promotes reverse cholesterol transport and regression of atherosclerosis. *J. Clin. Invest.* 121 (7), 2921–2931. doi:10.1172/jci57275

Rayner, K. J., Suárez, Y., Dávalos, A., Parathath, S., Fitzgerald, M. L., Tamehiro, N., et al. (2010). MiR-33 contributes to the regulation of cholesterol homeostasis. *Science* 328 (5985), 1570–1573. doi:10.1126/science.1189862

Rigalli, J. P., Tocchetti, G. N., Arana, M. R., Villanueva, S. S., Catania, V. A., Theile, D., et al. (2016). The phytoestrogen genistein enhances multidrug resistance in breast cancer cell lines by translational regulation of ABC transporters. *Canc. Lett.* 376 (1), 165–172. doi:10.1016/j.canlet.2016.03.040

Rosenson, R. S., Brewer, H. B., Jr., Davidson, W. S., Fayad, Z. A., Fuster, V., Goldstein, J., et al. (2012). Cholesterol efflux and atheroprotection: advancing the concept of reverse cholesterol transport. *Circulation* 125 (15), 1905–1919. doi:10.1161/circulationaha.111.066589

Santiago-García, J., Kodama, T., and Pitas, R. E. (2003). The class A scavenger receptor binds to proteoglycans and mediates adhesion of macrophages to the extracellular matrix. *J. Biol. Chem.* 278 (9), 6942–6946. doi:10.1074/jbc.M208358200

Seneviratne, A. N., Edsfeldt, A., Cole, J. E., Kassiteridi, C., Swart, M., Park, I., et al. (2017). Interferon regulatory factor 5 controls necrotic core formation in atherosclerotic lesions by impairing efferocytosis. *Circulation* 136 (12), 1140–1154. doi:10.1161/circulationaha.117.027844

Shen, W. J., Azhar, S., and Kraemer, F. B. (2018). SR-B1: a unique multifunctional receptor for cholesterol influx and efflux. *Annu. Rev. Physiol.* 80, 95–116. doi:10.1146/annurev-physiol-021317-121550

Shimano, H. (2009). SREBPs: physiology and pathophysiology of the SREBP family. *FEBS J.* 276 (3), 616–621. doi:10.1111/j.1742-4658.2008.06806.x

Song, W., Zhang, C. L., Gou, L., He, L., Gong, Y. Y., Qu, D., et al. (2019). Endothelial TFEB (transcription factor EB) restrains IKK (IκB kinase)-p65 pathway to attenuate vascular inflammation in diabetic db/db mice. *Arterioscler. Thromb. Vasc. Biol.* 39 (4), 719–730. doi:10.1161/atvbaha.119.312316

Stols-Gonçalves, D., Hovingh, G. K., Nieuwdorp, M., and Holleboom, A. G. (2019). NAFLD and atherosclerosis: two sides of the same dysmetabolic coin?. *Trends Endocrinol. Metabol.: TEM (Trends Endocrinol. Metab.* 30 (12), 891–902. doi:10.1016/j.tem.2019.08.008

Su, D., Li, H. Y., Yan, H. R., Liu, P. F., Zhang, L., and Cheng, J. H. (2009). Astragalus improved cardiac function of adriamycin-injured rat hearts by upregulation of SERCA2a expression. *Am. J. Chin. Med.* 37 (3), 519–529. doi:10.1142/s0192415x09007028

Sun, D. W., Zhang, H. D., Mao, L., Mao, C. F., Chen, W., Cui, M., et al. (2015). Luteolin inhibits breast cancer development and progression in vitro and in vivo by suppressing notch signaling and regulating MiRNAs. *Cell. Physiol. Biochem.* 37 (5), 1693–1711. doi:10.1159/000438535

Tabas, I., García-Cardeña, G., and Owens, G. K. (2015). Recent insights into the cellular biology of atherosclerosis. *J. Cell Biol.* 209 (1), 13–22. doi:10.1083/jcb.201412052

Tall, A. R. (2018). Plasma high density lipoproteins: therapeutic targeting and links to atherogenic inflammation. *Atherosclerosis* 276, 39–43. doi:10.1016/j.atherosclerosis.2018.07.004

Tall, A. R., Yvan-Charvet, L., Terasaka, N., Pagler, T., and Wang, N. (2008). HDL, ABC transporters, and cholesterol efflux: implications for the treatment of atherosclerosis. *Cell Metabol.* 7 (5), 365–375. doi:10.1016/j.cmet.2008.03.001

Trinh-Trang-Tan, M. M., Vilela-Lamego, C., Picot, J., Wautier, M. P., and Cartron, J. P. (2010). Intercellular adhesion molecule-4 and CD36 are implicated in the abnormal adhesiveness of sickle cell SAD mouse erythrocytes to endothelium. *Haematologica* 95 (5), 730–737. doi:10.3324/haematol.2009.017392

Tunon, J., Badimon, L., Bochaton-Piallat, M. L., Cariou, B., Daemen, M. J., Egido, J., et al. (2019). Identifying the anti-inflammatory response to lipid lowering therapy: a position paper from the working group on atherosclerosis and vascular biology of the European Society of Cardiology. *Cardiovasc. Res.* 115 (1), 10–19. doi:10.1093/cvr/cvy293

Wang, Z., Ma, C., Shang, Y., Yang, L., Zhang, J., Yang, C., et al. (2020). Simultaneous co-assembly of fenofibrate and ketoprofen peptide for the dual-targeted treatment of nonalcoholic fatty liver disease (NAFLD). *Chem. Commun.* 56 (36), 4922–4925. doi:10.1039/d0cc00513d

Williams, H., Johnson, J. L., Carson, K. G., and Jackson, C. L. (2002). Characteristics of intact and ruptured atherosclerotic plaques in brachiocephalic arteries of apolipoprotein E knockout mice. *Arterioscler. Thromb. Vasc. Biol.* 22 (5), 788–792.

Xu, X., Li, F., Zhang, X., Li, P., Zhang, X., Wu, Z., et al. (2014). *In vitro* synergistic antioxidant activity and identification of antioxidant components from *Astragalus membranaceus* and Paeonia lactiflora. *PloS One* 9 (5), e96780. doi:10.1371/journal.pone.0096780

Yang, S., Ma, C., Wu, H., Zhang, H., Yuan, F., Yang, G., et al. (2020). Tectorigenin attenuates diabetic nephropathy by improving vascular endothelium dysfunction through activating AdipoR1/2 pathway. *Pharmacol. Res.* 153, 104678. doi:10.1016/j.phrs.2020.104678

Yang, Y., Li, X., Peng, L., An, L., Sun, N., Hu, X., et al. (2018). Tanshindiol C inhibits oxidized low-density lipoprotein induced macrophage foam cell formation via a peroxiredoxin 1 dependent pathway. *Biochim. Biophys. Acta (BBA)—Mol. Basis Dis.* 1864 (3), 882–890. doi:10.1016/j.bbadis.2017.12.033

Yin, M., Yuan, Y., Cui, Y., Hong, X., Luo, H., Hu, X., et al. (2015). Puerarin suppresses the self-renewal of murine embryonic stem cells by inhibition of REST-MiR-21 regulatory pathway. *Cell. Physiol. Biochem.* 37 (2), 527–536. doi:10.1159/000430374

Yu, X. H., Fu, Y. C., Zhang, D. W., Yin, K., and Tang, C. K. (2013). Foam cells in atherosclerosis. *Clin. Chim. Acta* 424, 245–252. doi:10.1016/j.cca.2013.06.006

Zanoni, P., Khetarpal, S. A., Larach, D. B., Hancock-Cerutti, W. F., Millar, J. S., Cuchel, M., et al. (2016). Rare variant in scavenger receptor BI raises HDL cholesterol and increases risk of coronary heart disease. *Science* 351 (6278), 1166–1171. doi:10.1126/science.aad3517

Zhao, J., Yu, Q. T., Li, P., Zhou, P., Zhang, Y. J., and Wang, W. (2008). Determination of nine active components in Radix Hedysari and Radix Astragali using capillary HPLC with diode array detection and MS detection. *J. Separ. Sci.* 31 (2), 255–261. doi:10.1002/jssc.200700379

Conflict of Interest: The authors declare that the research was conducted in the absence of any commercial or financial relationships that could be construed as a potential conflict of interest.

frontiers in Pharmacology

REVIEW
published: 14 December 2020
doi: 10.3389/fphar.2020.579525

The Efficacy of Beta-Blockers in Patients With Long QT Syndrome 1–3 According to Individuals' Gender, Age, and QTc Intervals: A Network Meta-analysis

*Lu Han, Fuxiang Liu, Qing Li, Tao Qing, Zhenyu Zhai, Zirong Xia and Juxiang Li**

Department of Cardiovascular Medicine, The Second Affiliated Hospital of Nanchang University, Nanchang, China

Long QT syndrome (LQTS) is an arrhythmic heart disease caused by congenital genetic mutations, and results in increased occurrence rates of polymorphic ventricular tachyarrhythmias and sudden cardiac death (SCD). Clinical evidence from numerous previous studies suggested that beta blockers (BBs), including atenolol, propranolol, metoprolol, and nadolol, exhibit different efficacies for reducing the risk of cardiac events (CEs), such as syncope, arrest cardiac arrest (ACA), and SCD, in patients with LQTS. In this study, we identified relevant studies in MEDLINE, PubMed, embase, and Cochrane databases and performed a meta-analysis to assess the relationship between the rate of CEs and LQTS individuals with confounding variables, including different gender, age, and QTc intervals. Moreover, a network meta-analysis was not only established to evaluate the effectiveness of different BBs, but also to provide the ranked efficacies of BBs treatment for preventing the recurrence of CEs in LQT1 and LQT2 patients. In conclusion, nadolol was recommended as a relatively effective strategy for LQT2 in order to improve the prognosis of patients during a long follow-up period.

Keywords: beta-blockers, atenolol, propranolol, metoprolol, nadolol, cardiac events

OPEN ACCESS

Edited by:
Joshua Thomas Butcher, Oklahoma State University, United States

Reviewed by:
Cees Korstanje, Consultant, Nieuw-Vennep, Netherlands
Thiago Bruder Do Nascimento, University of Pittsburgh, United States

****Correspondence:***
Juxiang Li
ljx912@126.com

Specialty section:
This article was submitted to Cardiovascular and Smooth Muscle Pharmacology, a section of the journal Frontiers in Pharmacology

Received: *02 July 2020*
Accepted: *13 November 2020*
Published: *14 December 2020*

Citation:
Han L, Liu F, Li Q, Qing T, Zhai Z, Xia Z and Li J (2020) The Efficacy of Beta-Blockers in Patients With Long QT Syndrome 1–3 According to Individuals' Gender, Age, and QTc Intervals: A Network Meta-analysis. Front. Pharmacol.11:579525. doi: 10.3389/fphar.2020.579525

INTRODUCTION

Congenital long QT syndrome (LQTS) is characterized by a prolonged QT interval and action potential duration (APD). Patients with LQTS have a propensity to develop ventricular tachycardia (VT) and also have a higher rate of cardiac events (CEs) (Arking et al., 2014). The three major genotypes of LQTS, LQT1, LQT2, and LQT3, account for 80–90% of all 15 gene-mutations identified in LQTS patients (Tester and Ackerman, 2014). LQT1, as the prevailing inherited genotype of LQTS, results from gain-of-function mutations in a slow potassium (K^+) outward current channel encoded by KCNQ1. LQT2 is associated with dysfunction of a rapid K^+ channel encoded by the KCNH2 gene. Mutations in the SCN5A gene trigger enhanced levels of late sodium (Na^+) inward current, which is the pathomechanism of LQT3 (Maguy et al., 2020).

Although there are a few novel targeted treatments for LQTS, such as peptide/antibody-based antiarrhythmic approaches, RNA interference, and immunotherapy (Lumley, 2002; Salanti et al., 2011; Boutjdir and Lazzerini, 2020), beta blockers (BBs) are regarded as first-line therapy for LQTS patients in the absence of obvious contraindications. The most common BBs include atenolol, propranolol, metoprolol, and nadolol, all of which are efficient at reducing the risk of cardiac events

TABLE 1 | Characteristics of included studies according to the effective of BBs on CEs.

Study (Ref. no)	Study design	No. of participant (female,%)	The percentage of treated with BBs, %	Prescribed BBs and dose	Follow-up duration, yrs	Mean QTc value	Definition of CEs	Mean ages, yrs	Included LQTS genotype(s)
Moss et al. (2000)	ITS	869 (62.3)	100	Atenolol: 1.36 ± 0.8 (mg/kg/day) Metoprolol: 1.8 ± 1.1 (mg/kg/day) Nadolol: 1.4 ± 1.0 (mg/kg/day) Propranolol: 2.9 ± 1.8 (mg/kg/day)	5	Probands: 520 ± 60 Affected family members: 500 ± 40	Syncope, ACA,SCD	15.7	LQT1, LQT2, LQT3
Conrath et al. (2002)	ITS	87 (females: 55.2, girls: 13.8, males: 16.0, boys: 15.0)	100	NS	5.5 ± 5.7	Boys, LQT1: 504 ± 10 LQT2: 488 ± 9 Girls, LQT1: 485 ± 9 LQT2: 461 ± 19 Males, LQT1: 472 ± 10 LQT2: 494 ± 12 Females, LQT1: 502 ± 19 LQT2: 493 ± 8	NS	NS	LQT1, LQT2
Chatrath et al. (2004)	Cohort	28 (71.4)	100	Atenolol, metoprolol, Nadolol: 0.75–1.25 mg/kg/day Propranolol: 2.5–4 mg/kg/day	4	507 ± 67	Syncope, ACA	19.8 ± 11.9	LQT1, LQT2, LQT3
Priori et al. (2004)	ITS	335 (62)	100	Nadolol: 1.2 ± 0.5 mg/kg/day Propranolol: 2.2 ± 1.04 mg/kg/day	4.7 (0.6–36)	492 ± 47	ACA, SCD	26 ± 17	LQT1, LQT2, LQT3
Wang and Wu (2004)	ITS	26 (65.3)	84.6	Metoprolol: 67.5 ± 39.1 mg/day Propranolol: 60.0 ± 5.5 mg/day	3.1 ± 1	560 ± 60	Syncope	19 ± 10	LQT1, LQT2
Goldenberg et al. (2008)	Cohort	3,015 children (girls: 63)	21.3	Atenolol, female: 75 ± 51 mg/day Male: 85 ± 61 mg/day Metoprolol, female: 119 ± 72 mg/day Male: 89 ± 55 mg/day Nadolol, female: 57 ± 49 mg/day Male: 50 ± 35 mg/day Propranolol, female: 51 ± 35 mg/day Male: 51 ± 34 mg/day	Female: 11.6 ± 1.7 Male: 489 ± 48	Female: 493 ± 49 Male: 489 ± 48	Syncope, ACA, SCD	7.5 ± 5.4	LQT1, LQT2, LQT3
Vincent et al. (2009)	ITS	216 (64)	100	Nadolol, 2.2 ± 1.1 mg/kg/day Propranolol, 1.7 ± 0.79 mg/kg/day	12.5 (7–26)	495 ± 46	Syncope, ACA, SCD	26 (18–42)	LQT1
Shimizu et al. (2009)	Cohort	858 (27.8)	23.4	NS	41	Rochester: 490 ± 60 Netherlands: 470 ± 50 Japan: 490 ± 50 Mayo: 470 ± 50	Syncope, ACA, SCD	Rochester: 25 ± 20 Netherlands: 33 ± 21 Japan: 30 ± 18 Mayo: 22 ± 16	LQT2
Goldenberg et al. (2010)	Cohort	971 (58.7)	57.2	Atenolol: 49 ± 32 mg/day Metoprolol: 67 ± 55 mg/day Nadolol: 58 ± 45 mg/day Propranolol: 96 ± 71 mg/day	LQT1: 5.0 ± 6.8 LQT2: 6.1 ± 7	QTc ≥ 500 (34.5%)	Syncope, ACA, SCD	31 ± 12	LQT1, LQT2

(Continued on following page)

TABLE 1 | (*Continued*) Characteristics of included studies according to the effective of BBs on CEs.

Study (Ref. no)	Study design	No. of participant (female,%)	The percentage of treated with BBs, %	Prescribed BBs and dose	Follow-up duration, yrs	Mean QTc value	Definition of CEs	Mean ages, yrs	Included LQTS genotype(s)
Goldenberg et al. (2012)	Cohort	721 (45.3)	43.8	NS	NS	CE triggered by four factor or no event Exercise: 504 ± 52 Acute arousal: 491 ± 49 Sleep/rest nonarousal: 486 ± 58 Other triggers: 480 ± 48 No event: 471 ± 43	Syncope, ACA, SCD	30 ± 12	LQT1
Chockalingam et al. (2012)	Cohort	382 (56)	100	Metoprolol: 1.4 (0.9–2.5) Nadolol: 0.8 Propranolol: 2.5 (1.3–3)	Propranolol: 2 (1–6) Metoprolol: 4 (2–8) Nadolol: 3 (2–5)	472 ± 46	Syncope, ACA, SCD	14 (8–32)	LQT1, LQT2
Abu-zaitone et al. (2014)	Cohort	1,530 (60.1)	45.1	Atenolol, Age>18 years: 0.7 ± 0.3 Age<18 years: 1.0 ± 0.7 Metoprolol, Age>18 years: 1.2 ± 0.9 Age<18 years: 1.4 ± 1.0 Nadolol, Age>18 years: 1.0 ± 0.8 Age<18 years: 1.0 ± 0.8 Propranolol, Age>18 years: 2.1 ± 2.3 Age<18 years: 2.3 ± 1.5	5	Atenolol: 492 ± 49 Metoprolol: 496 ± 52 Nadolol: 490 ± 51 Propranolol: 500 ± 58	Syncope, ACA, SCD	14.9	LQT1, LQT2
Koponen et al. (2015)	Cohort	316 (53.1)	77.2	Metoprolol: 1.3 ± 0.4 (mg/kg/day) Bisoprolol: 0.1 ± 0.1 (mg/kg/day) Atenolol: 1.2 ± 1.5 (mg/kg/day) Propranolol: 2.4 ± 0.8 (mg/kg/day)	5.8	LQT1 mutation (G589D): 454 ± 35 Mutation (c.1129–2A > G): 465 ± 37 Non-mutation: 475 ± 43 LQT2 Mutation (L552S): 448 ± 32 Mutation (R176W): 436 ± 31 Non-mutation: 480 ± 39	Syncope, ACA, SCD	12.0 ± 5.5	LQT1, LQT2
Steinberg et al. (2016)	Cohort	114 (58.7)	100	Atenolol: 53 ± 30 mg/day Nadolol: 74 ± 47 mg/day	Atenolol: 6 (3–10) Nadolol: 3 (1–5)	Atenolol: 466 ± 23 Nadolol: 469 ± 32	Syncope, ACA, VT	Atenolol: 37 ± 19 Nadolol: 27 ± 13	LQT1, LQT2
Wilde et al. (2016)	Cohort	391 (55)	29	ND	7.25	476 ± 57	Syncope, ACA, SCD	28 ± 20	LQT3
Mazzanti et al. (2018)	Cohort	1710 (52)	ND	Nadolol: >0.5 mg/kg/day Propranolol: >1.5 mg/kg/day Metoprolol: >1.0 mg/kd/day	9 ± 7	471 ± 45	Syncope,ACA, SCD	ND	LQT1, LQT2, LQT3

BBs: beta-blockers; LQTS: long-QT syndromes; ITS: interrupted time series; ACA: aborted cardiac death; SCD:sudden cardiac death; VT: ventricular tachycardia.

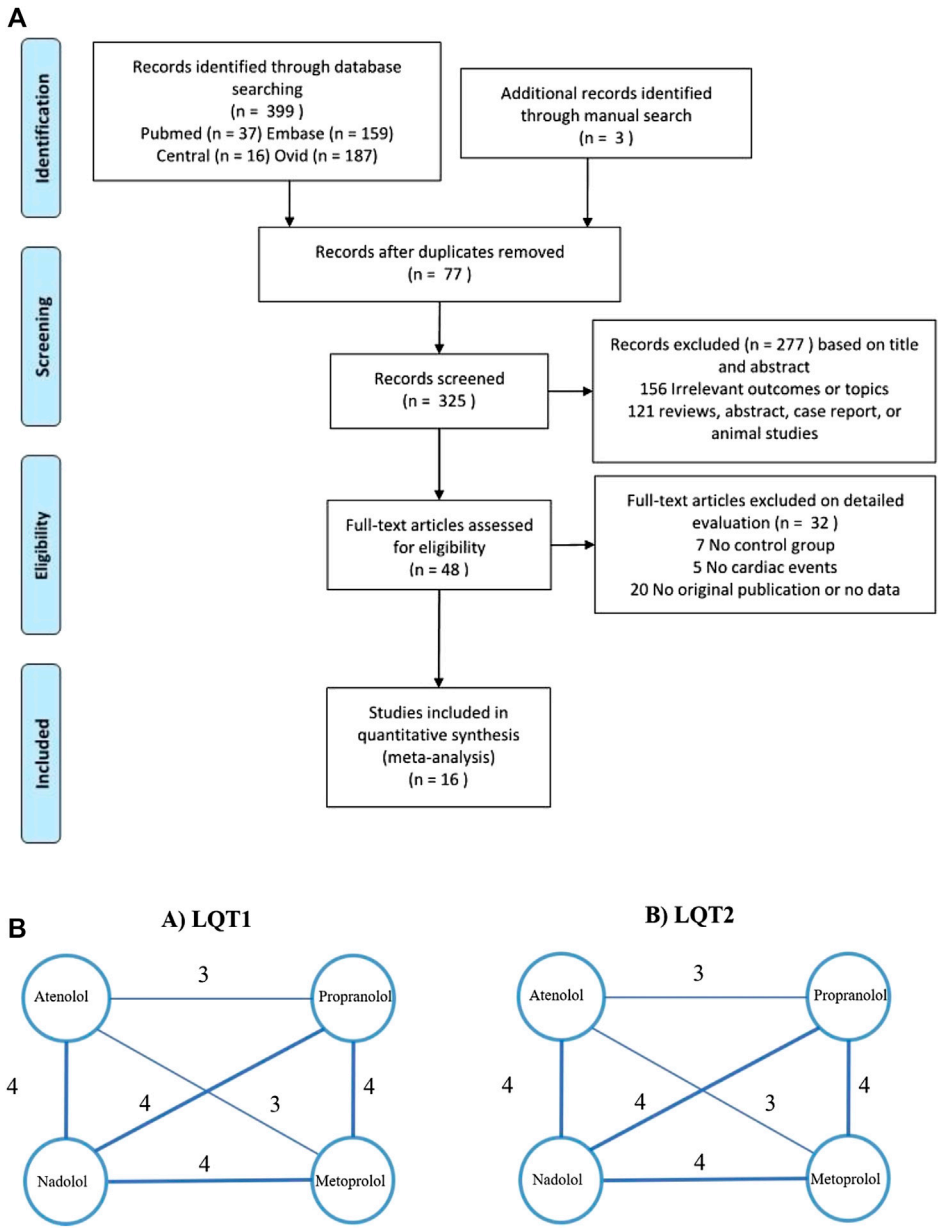

FIGURE 1 | (A), Flow diagram showing the identification of literatures according to the PRISMA format. **(B)**, Evidence of eligible comparisons for network meta-analysis. Numbers by the lines indicates the cumulative number of enrolled studies for each indirect comparison.

[CEs, e.g., syncope, aborted cardiac arrest (ACA), and sudden cardiac death (SCD)] in LQTS patients (Chatrath et al., 2004). However, a previous study has shown that different BBs exhibit various pharmacodynamic and pharmacokinetics, which may explain why nadolol is superior to its counterparts in the treating of LQT2 patients (Wilde and Ackerman, 2014). Out of the above-mentioned BBs, propranolol has furthermore been found to be the least efficient in preventing the recurrence of CEs (Abu-Zeitone et al., 2014). In addition, the effectiveness of BBs can be affected by different genotype of LQTS. The protective effect of BBs has been proposed to be highest in LQT1 patients, lower (albeit present) in LQT2 patients, and completely absent in LQT3 (Priori et al., 2004). Interestingly, the efficacy of BBs has also been shown to be associated with individual factors, such as gender, age, and corrected QT (QTc) intervals. Previous research has demonstrated that QTc, gender, and age are indispensable factors influencing the clinical course of LQTS patients (Vincent et al., 2009; Mazzanti et al., 2018). We therefore performed a network meta-analysis to assess how epidemiological factors influence the efficacy of BBs for CE risk reduction in LQT1-3 patients, in order to define more beneficial therapeutic strategies in these patients.

METHODS

Search Strategy and Selection Criteria

This meta-analysis was carried out in accordance with the Preferred Reporting Items for Systematic Reviews and Meta-Analyses (PRISMA) Statement. The article protocol was registered on the PROSPERO International Prospective Register of Systematic Reviews (CRD42020179454). We searched for and collected relevant studies published between Jan 1, 1990, and April 30, 2020, from MEDLINE, PubMed, embase, and Cochrane Library (CENTRAL) databases. The keywords applied for computerized searching were atenolol, propranolol, metoprolol, nadolol, long QT syndromes, and beta-blockers. Additionally, manual searches were also carried out to identify potentially relevant literatures (**Supplementary Table S1**).

Study Selection and Data Extraction

Studies included in this meta-analysis had to meet the following criteria: 1) The study selected participants with LQT1-3 genotypes. 2) Primary CEs included syncope, ACA, and SCD. 3) The studies needed to discuss the efficacy of different BBs on reducing the rate of CEs. 4) Articles needed to contain at least two of the following BBs: atenolol, propranolol, metoprolol, and nadolol. 5) The effectiveness of four BBs needed to be analyzed by comparing patients before and after BB therapy. 6) The data should be available for our analysis.

If papers met any of the following criteria, they were excluded: 1) Duplicated studies and reviews, conference papers, abstracts, and case reports. 2) Studies of subjects who received two or more BBs in combination therapy. 3) Studies that did not involve a comparison of efficacy among the four BBs. 4) Studies that provided insufficient and unqualified data (**Figure 1A**) (Moss et al., 2000; Conrath et al., 2002; Chatrath et al., 2004; Priori et al., 2004; Wang and Wu, 2004; Goldenberg et al., 2008; Shimizu et al., 2009; Vincent et al., 2009; Goldenberg et al., 2010; Chockalingam et al., 2012; Goldenberg et al., 2012; Abu-Zeitone et al., 2014; Koponen et al., 2015; Steinberg et al., 2016; Wilde et al., 2016; Mazzanti et al., 2018).

Data Extraction and Quality Assessment

We extracted information from selected studies, including authors, study type, year of publication, race, number of participants with or without BBs, age, types of BBs, clinical CEs, the period of follow-up, gender, and the length of QTc interval (**Table 1**). Quality assessment was carried out by two independent reviewers using a standardized data collection form (Stang et al., 2018), as presented in **Supplementary Figure S1**. Discrepancies were addressed and resolved by a third reviewer. Sensitivity analysis was conducted to verify the robustness of the above results and to evaluate the deviational degree of each study; sensitivity analysis was performed using the command metaninf in STATA 12.0 (Stata Corp, College Station, TX). Rank probabilities were calculated via the surface under the cumulative ranking curve (SUCRA) (Fabritz et al., 2010). The SUCRA line shows the effectiveness of each treatment accounting for all possible rankings.

Statistical Analysis

Hazard ratios (HRs) with 95% confidence intervals (CIs) of CEs were extracted or analyzed. We conducted our meta-analysis by applying random-effects models. HRs were assessed using the Inverse-Variance method, as well as the calculation of subgroups. Heterogeneity among these comparisons was evaluated using the I^2 test, with an $I^2 > 75\%$ considered as a series of comparisons with unacceptable heterogeneity. Statistical calculations in traditional meta-analyses were performed using RevMan 5.3 (Cochrane Collaboration, Oxford, United Kingdom) and STATA 12.0 software. Moreover, a network meta-analysis was evaluated using a random-effects model within a Bayesian framework (Lumley, 2002). HRs and corresponding 95% credible intervals (CrIs) were analyzed using gemtc package (https://drugis.org/software/r-packages/gemtc) in R (x64 3.6.0) for all statistical analyses. Publication bias was evaluated using the command metabias with the Egger's linear regression test in STATA 12.0. When the number of studies was less than 10, the Egger's linear regression test was used to measure the publication bias by performing a quantitative test on the funnel chart.

RESULTS

Correlation Between Gender, Age, Corrected QT, and CEs Risk in Long QT Syndrome Patients

Our analysis showed that before puberty, male and female LQTS patients had a similar likelihood of experiencing CEs (girls vs. boys in group of 10-years-old: HR 1.01, 95% CI 0.45–2.23; I^2 = 0%, p for heterogeneity 0.78; **Figure 2A**). However, the risk of CEs between female and male LQTS patients after the onset of puberty was not compared due to a lack of data. Individuals with a QTc ≥ 500 ms had a higher risk of CEs than individuals with QTc < 500 ms during childhood (HR 4.20, 95% CI 2.47–7.14, I^2 = 0%, p = 0.96; **Figure 2B**). On the other hand, CE risk was higher in LQT1 patients than in LQT2 patients at the age of 10 (HR 1.52, 95% CI 1.08–2.14; I^2 = 0%, p = 0.79; **Figure 2C**). Due to the lack of sufficient data throughout the adolescent period, there was no assessment of different QTc intervals and genotypes on CE risk in this age group.

The Efficacy of Beta Blockers in Long QT Syndrome Patients Based on the Different Gender, Age, and Corrected QT Intervals

Overall, BBs treatments showed a significant risk reduction for CEs in LQTS patients. Throughout preadolescence, boys were more likely to be affected by CEs than girls when both were treated with BBs (boys vs. girls: HR 1.75, 95% CI 1.17–2.62; I^2 = 52%, p = 0.1; **Figure 3A**). Interestingly, after puberty, females had a higher likelihood of developing CEs than male patients, despite BB therapy (males vs. females, ages 13–40: HR 0.43, 95% CI 0.26–0.72 I^2 = 42%, p = 0.16; **Figure 3A**). Thus, we observed that

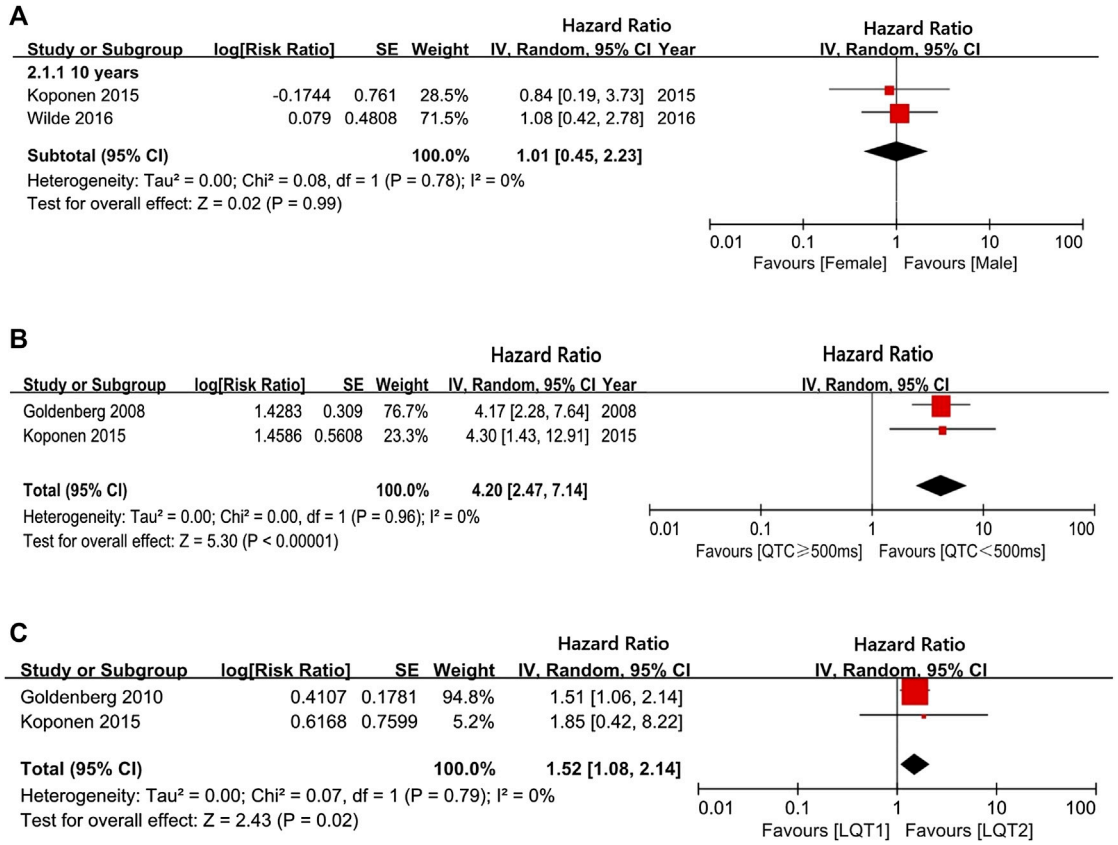

FIGURE 2 | The risk of CEs in a long follow-up period. **(A)**, the hazard ratio (HR) values in comparing females/males at 10-years-old; **(B)**, the HR values in comparing QTc ≥ 500 ms/QTc < 500 ms at 10-years-old; **(C)**, the HR values in comparing LQT1/LQT2 at 10-years-old.

age and gender could synergistically influence the efficacy of BB therapy on the risk reduction of CEs.

Our findings showed that BBs therapy efficiently decreased QTc intervals lengths by an average of 17.8 ms (95% CI 14.51–21.09 ms; **Figure 3B**). Under BBs treatments, patients with the LQT1 genotype had a significantly higher reduction in QTc-length than LQT2 patients (95% CI 2.24–14.19 ms, I^2 = 6%, p = 0.30; **Figure 3C**). Furthermore, similarly to the above findings, even after BBs therapy, LQTS patients with QTc ≥ 500 ms had a greater risk of experiencing CEs than subjects with QTc < 500 ms (HR 2.28, 95% CI 1.46–3.55; I^2 = 17%, p = 0.31, **Figure 3D**).

Comparison of the Efficiency of Different Beta Blockers in the Three Main LQT Genotypes

We observed a significant reduction of CEs in LQT1 and LQT2 following BBs management, but not in LQT3 (LQT1: HR 0.32, 95% CI 0.24–0.47; I^2 = 17%, p = 0.3; LQT2: HR 0.44, 95% CI 0.33–0.59; I^2 = 8%, p = 0.34; LQT3: HR 0.63, 95% CI 0.36–1.10; I^2 = 0%, p = 0.43; **Figure 4A**). Upon intervention with BBs, LQT2 patients tended to have a greater propensity of suffering CEs compared to LQT1 patients, although this was not statistically significant (LQT2 vs. LQT1: HR 1.64, 95% CI 0.97–2.78; I^2 = 33%, p = 0.19; **Figure 4B**). Interestingly, when the effect of BBs in LQT3 was respectively compared with LQT2 or LQT1 alone, it revealed a similar efficacy for controlling CE risk (LQT3 vs. LQT1: HR 2.17, 95% CI 0.62–7.58; I^2 = 40%, p = 0.19 and LQT3 vs. LQT2: HR 1.99, 95% CI 0.76–5.24; I^2 = 0%, p = 0.73; **Figure 4B**).

Atenolol appeared to reduce the risk of CEs in LQT1, but not in LQT2 patients (HR 0.49, 95% CI 0.31–0.76; I^2 = 0%, p = 0.59 in LQT1 and HR 0.51, 95% CI 0.24–1.11; I^2 = 15%, p = 0.31 in LQT2; **Figure 4C**). However, comparing these groups directly, we found in significant differences in the efficacy of atenolol between LQT1 and LQT2 patients (LQT2 vs. LQT1, HR 1.13, 95% CI 0.71–1.83; I^2 = 0%, p = 0.44; **Figure 4D**). Propranolol also attenuated the rate of CEs in patients with LQTS (HR 0.44, 95% CI 0.28–0.67; I^2 = 0%, p = 0.73; **Figure 4C**). Although the efficiency of propranolol appeared to be somewhat higher in LQT2 than in LQT1 patients, these results also did not reach significance (LQT2 vs. LQT1, HR 0.80, 95% CI 0.53–1.23; I^2 = 0%, p = 0.73; **Figure 4D**). Metoprolol exhibited an obvious risk-reducing effect in LQT1 (HR 0.30, 95% CI 0.12–0.72; I^2 = 0%, p = 0.37; **Figure 4C**), but not in LQT2 (HR 0.73, 95% CI 0.30–1.77; I^2 = 0%, p = 0.51; **Figure 4C**), although a direct comparison of the efficacy of this BB in LQT1 and LQT2 patients was not statistically significant (LQT2 vs. LQT1, HR 2.17, 95% CI 0.67–7.07; I^2 = 19%, p = 0.27; **Figure 4D**). Nadolol provided a strong risk reduction for CEs in LQTS patients (HR

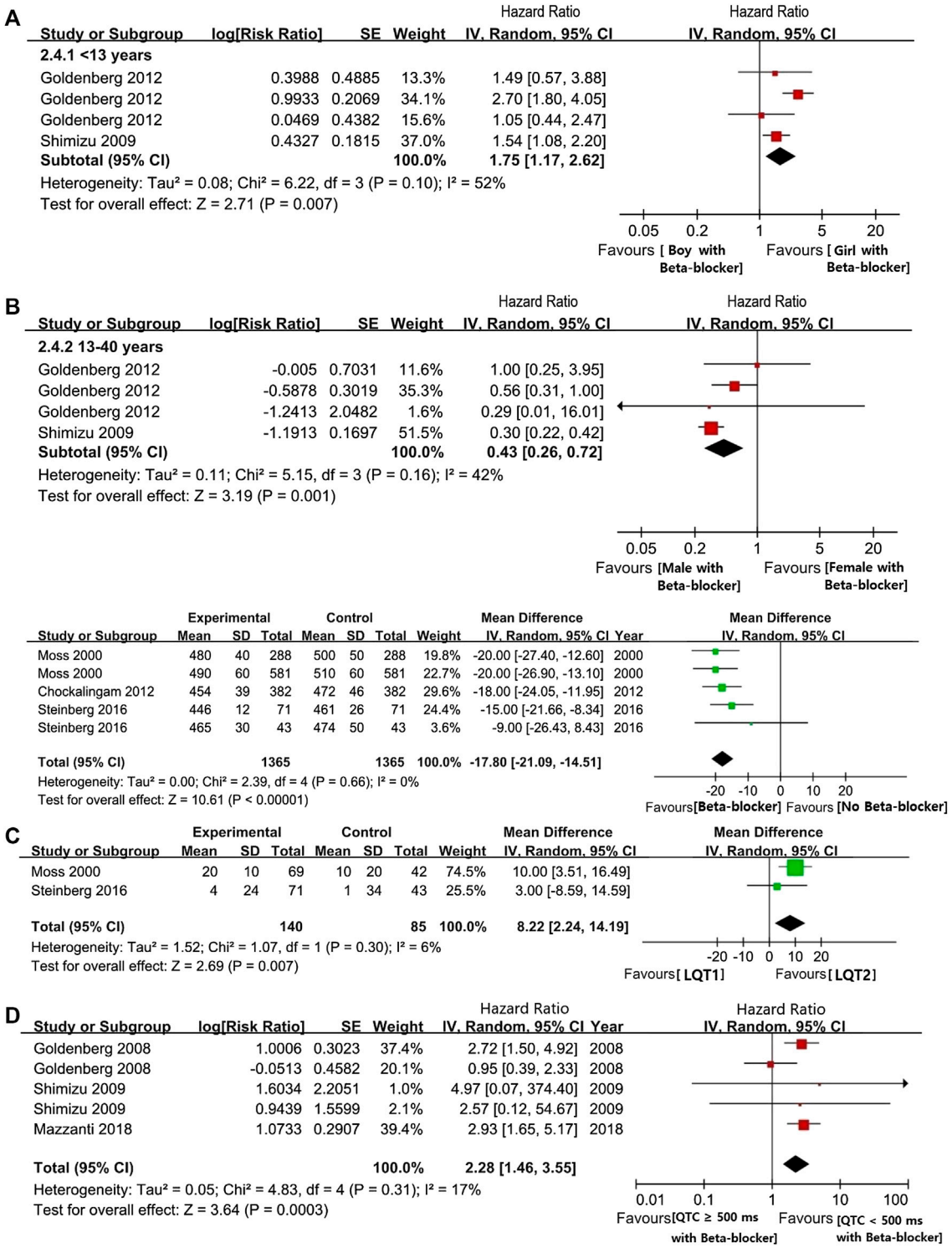

FIGURE 3 | (A), The HR value of CEs in LQTs patients with female and male. **(B)**, the HR value of CEs via comparsing female and male patients during pre-adolescent or post-adolescent periods (males vs. females). **(C)**, The efficacy of BBs on shorting the length of QTc intervals. **(D)**, The efficacy of BB on shorting the length of QTc intervals in comparison with LQT1 and LQT2 (LQT1 vs. LQT2). **(E)**, The HR value of the possibility of CEs in the comparsion between LQTs patients with QTc ≥ 500 ms or QTc < 500 ms (QTc ≥ 500 ms vs. QTc < 500 ms).

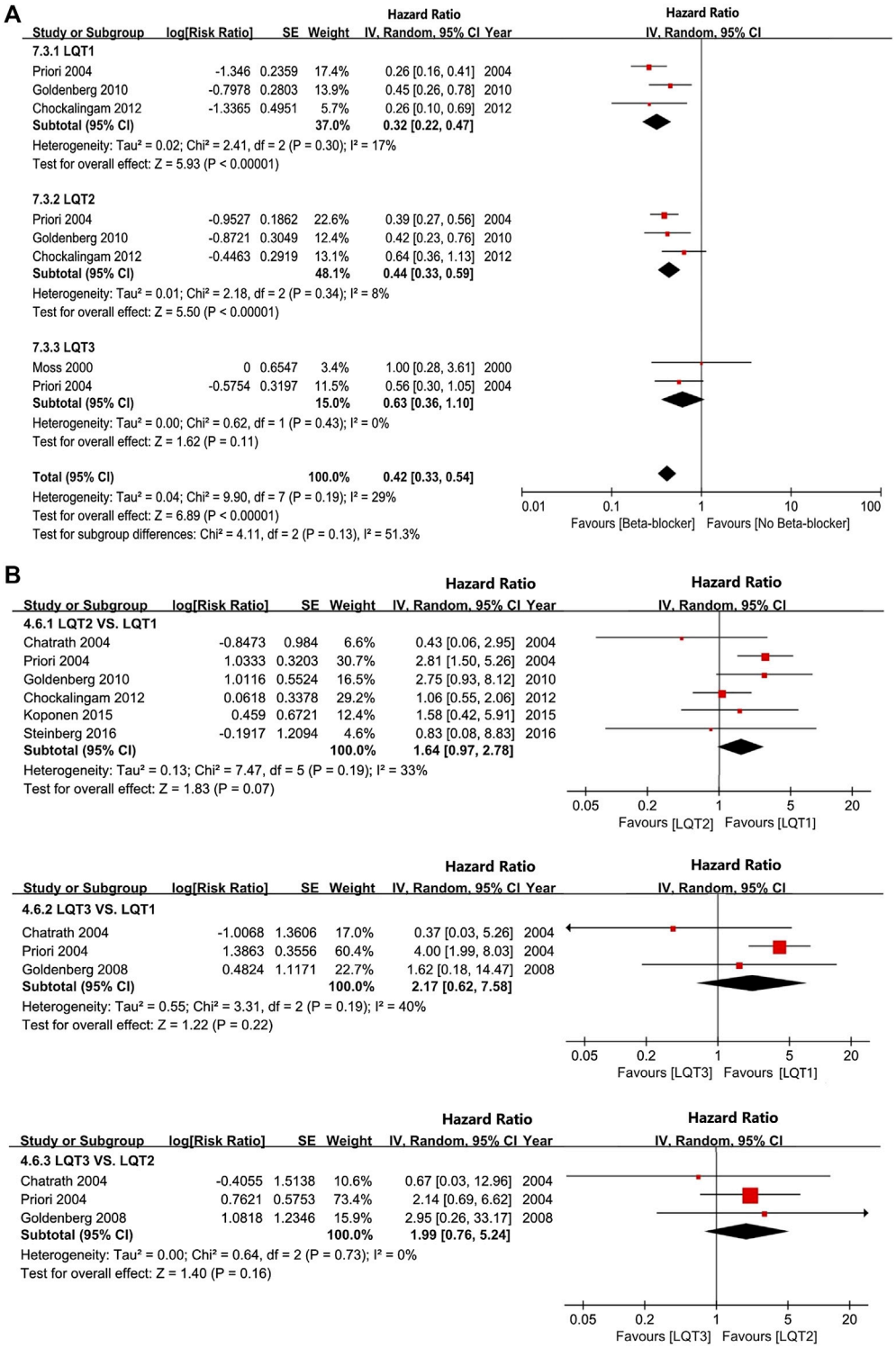

FIGURE 4 | (A), The HR value of CEs in comparing the two different LQT genotypes, including LQT2 vs. LQT1, LQT3 vs. LQT1, and LQT3 vs. LQT2. **(B)**, the effectiveness of BBs in reducing the occur of CEs via comparsing LQT2 and LQT1 (LQT2 vs. LQT1). **(C)**, The efficacy of different BBs on the risk reduction of CEs in LQT1 and LQT2. **(D)**, The efficacy of BBs therapy on managing of CEs in different LQTs genotypes, including LQT1, LQT2, LQT3. **(E)**, The efficacy of BBs therapy in reducing the incidence of syncope or ACA respectively.

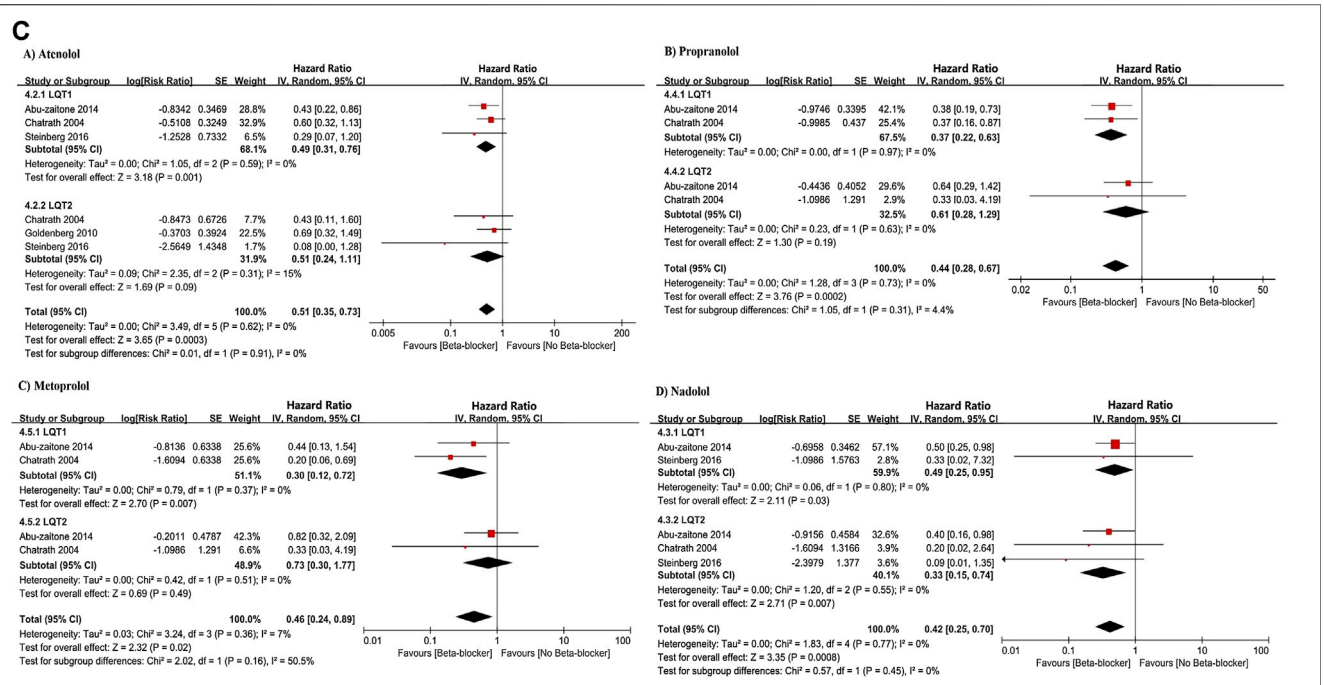

FIGURE 4 | (Continued).

0.42, 95% CI 0.25–0.70; $I^2 = 0\%$, $p = 0.77$; **Figure 4C**). This effect was more pronounced in LQT2 than in LQT1 patients, and a direct comparison between the groups revealed that this was statistically significant (LQT2 vs. LQT1, HR 0.53, 95% CI 0.27–1.04; $I^2 = 0\%$, $p = 0.92$; **Figure 4D**). We observed a different efficacy of these BBs for risk reduction of different types of CEs. BBs seemed to be more effective at preventing syncope than decreasing the rate of ACA (HR 0.13, 95% CI 0.08–0.22; $I^2 = 5\%$, $p = 0.37$ in syncope and HR 0.32, 95% CI 0.16–0.64; $I^2 = 0\%$, $p = 0.46$ in ACA; **Figure 4E**).

Joint Comparison of the Effectiveness of Different Beta Blockers

For LQT1 patients, the CrIs value was too wide to show significance for the difference observed for atenolol over propranolol and metoprolol (atenolol vs. propranolol, HR 0.73, 95% CrIs 0.37–1.5, and atenolol vs. Metoprolol, HR = 0.71, 95% CrIs 0.33–1.7; **Figure 5A**, **Table 2**). Conversely, atenolol efficacy for risk reduction seemed somewhat lower than for nadolol (atenolol vs. nadolol, HR = 1.2, 95% CrIs 0.56–2.4; **Figure 5A**; **Table 2**). Propranolol and metoprolol had similar efficacy for risk reduction (propranolol vs. Metoprolol, HR 0.98, 95% CrIs 0.49–2.1; **Figure 5A**; **Table 2**). All four BBs interventions had an almost equal effect in LQT1 patients via pairwise comparisons (nadolol vs. propranolol: HR 0.63, 95% CrIs 0.32–1.3; and nadolol vs. Metoprolol: HR 0.61, 95% CrIs 0.3–1.4; **Figure 5A**; **Table 2**). In addition, we found that LQT2 patients treated with nadolol showed the greatest decrease in the risk of CEs compared to the other three BBs (nadolol vs. atenolol: HR 0.35, 95% CrIs 0.22–0.55; nadolol vs. propranolol: HR 0.36, 95% CrIs 0.23–0.58 and nadolol vs. Metoprolol: HR 0.35, 95% CrIs 0.21–0.57; **Figure 5A**; **Table 2**). With the exception of nadolol, pairwise comparisons among the other three BBs exhibited no superiority to any others in managing LQT2 patients (atenolol vs. propranolol: HR 1.0, 95% CrIs 0.7–1.6; atenolol vs. Metoprolol: HR 1.0, 95% CrIs 0.65–1.6 and propranolol vs. Metoprolol: HR 0.98, 95% CrIs 0.62–1.5; **Figure 5A**; **Table 2**). Due to a lack of sufficient data, we were unable to assess the effectiveness of different BBs for LQT3 patients.

Relative Ranking of Four Beta Blockers

Next, we used SUCRA to analyze rank probability of different BBs on the risk reduction for CEs based on LQTS genotype, as shown in **Table 3** and **Figures 5C–F**. For LQT1 patients, nadolol ranked first with a higher efficacy for reducing CEs risk (**Figures 5C,E**). Interestingly, we noticed that atenolol was the second-most effective treatment of the four BBs for patients with LQT1. Propranolol was ranked third, and metoprolol was ranked last. In LQT2 patients, nadolol was further verified to be a first-line therapy with minimal risk of CEs. The other three BBs treatments displayed no benefit for managing the CEs risk (**Figures 5D,F**).

DISCUSSION

The aim of this study was to assess the relationship between epidemiological variables (gender, age, and QTc intervals) and CE risk in LQTS patients using a meta-analysis. We furthermore systematically evaluated the efficacy of BBs therapy in LQTS with different ages, genders, and QTc intervals, as well as genetic subtypes (Bohnen et al., 2017). It is well-established that the rate

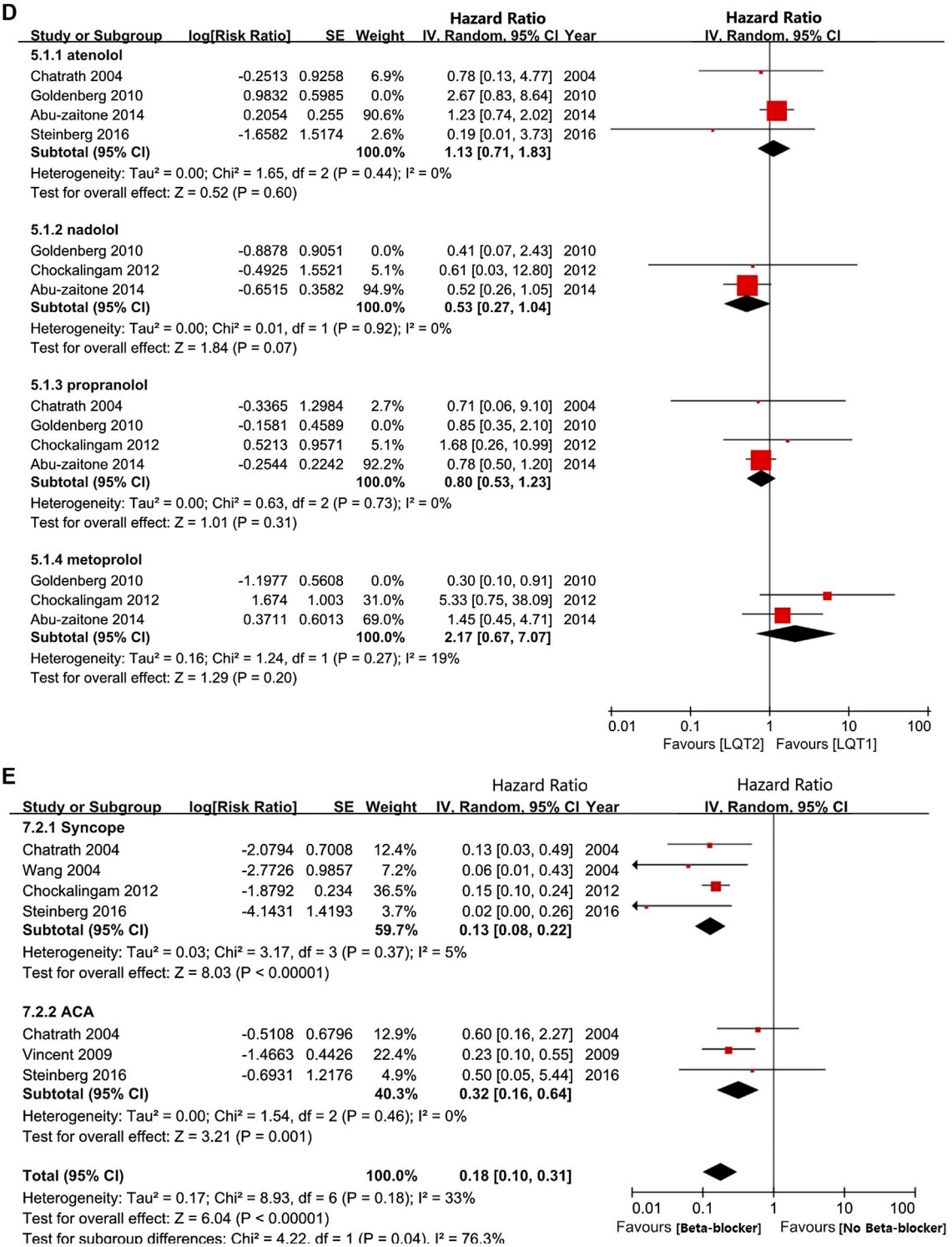

FIGURE 4 | (Continued).

of CEs in LQTS patients is closely correlated with age and sex (Wang and Wu, 2004). Previous reports have indicated that the risk of fatal events in LQTS is higher in boys than girls during childhood (Goldenberg et al., 2008). After adolescence, gender-related risk is reversed, and a greater risk of CEs is observed in the group of female patients (Goldenberg et al., 2012). This might be due to longer QTc intervals in LQTS female patients than in male patients in adulthood (Conrath et al., 2002). However, we showed

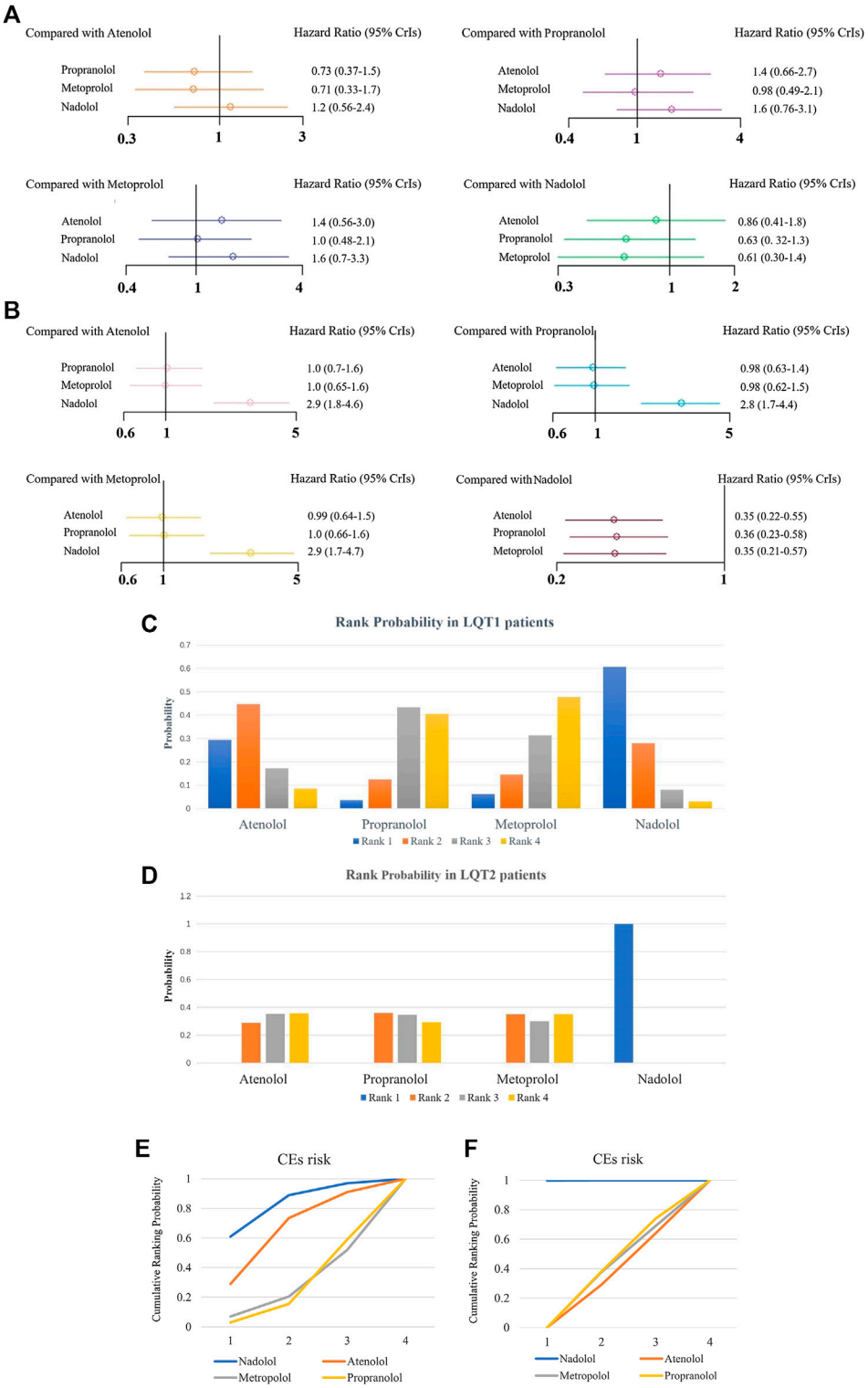

FIGURE 5 | (A, B), The effect of different BBs on risk reduction of CEs in patients with LQT1 **(A)** or LQT2 **(B)**. **(C, D)**, The rank probability of BBs therapy for reducing the occurrence of CEs in LQT1 **(C)** and LQT2 **(D)** patients. E-F, SUCRAs between 0 and 1 represent the probability of being ranked highest. For the CEs risk, higher score corresponds to higher proportion achieving at least 5% CEs risk reduction with a most effective therapy in LQT1 **(E)** and LQT2 **(F)** patients.

TABLE 2 | The efficacy of different BB therapies on reducing the occurrence of CEs (syncope, SCD, ACA) in patients with LQT1 and LQT2 by the network meta-analysis using HR and 95% CrIs.

		LQT1		
Cardiac events	Atenolol	1.4 (0.66–2.7)	1.4 (0.56–3.0)	0.86 (0.41–1.8)
	0.73 (0.37–1.5)	Propranolol	1.0 (0.48–2.1)	0.63 (0.32–1.3)
	0.71 (0.33–1.7)	0.98 (0.49–2.1)	Metoprolol	0.61 (0.3–1.4)
	1.2 (0.56–2.4)	1.6 (0.76–3.1)	1.6 (0.7–3.3)	nadolol
		LQT2		
Cardiac events	Atenolol	0.98 (0.63–1.4)	0.99 (0.64–1.5)	0.35 (0.22–0.55)
	1.0 (0.7–1.6)	Propranolol	1.0 (0.66–1.6)	0.36 (0.23–0.58)
	1.0 (0.65–1.6)	0.98 (0.62–1.5)	Metoprolol	0.35 (0.21–0.57)
	2.9 (1.8–4.6)	2.8 (1.7–4.4)	2.9 (1.7–4.7)	nadolol

that boys and girls with LQTS have a similar risk of CEs during pre-adolescence. After the onset of puberty, there was no result concerning the risk of CEs among females' and males' patients due to a lack of data (**Figure 2A**). Strikingly, although there was a decreased risk for CEs in both males and females after BBs treatment regardless of age, girls were less likely to experience CEs than boys in pre-puberty (<13-year-old). After the onset of adolescence, BBs were more efficient at reducing CEs in males than in females (13–40-year-old) (**Figure 3A**).

Recent studies have suggested that both genotype and QTc duration are independent risk factors influencing the risk of CEs in patients with LQTS (Mazzanti et al., 2018; Priori et al., 2004; Ebbehøj et al., 2004). Furthermore, a 3.3-times lower risk for CEs were detected in LQTS patients with shorted QTc duration compared to patients with prolonged QTc duration (Koponen et al., 2015). Consistent with this view, our result indicates that LQTS patients with QTc intervals ≥500 ms had a higher risk of experiencing CEs compared to patients with QTc < 500 ms during childhood (at 10-years-old) (**Figure 2B**). Unfortunately, due to insufficient data in the present studies, we were unable to assess the effect of QTc duration on the risk of CEs in adulthood. The efficacy of BBs in patients with QTc ≥ 500 ms was lower than in patients with QTc < 500 ms (**Figure 3D**). Our study found that BBs reduce the QTc interval in LQTS patients by an average of 17.8 ms (**Figure 3B**). We also observed that this effect of decreasing QTc was more pronounced in LQT1 patients than in LQT2 patients (**Figure 2C**). A previous study showed a 3-fold increased risk for CEs in LQT2 patients compared to LQT1 during adulthood, regardless of BBs therapy (Goldenberg et al., 2010). Interestingly, we summarized that, in the pre-adolescent period, LQT1 patients were reported to have more CEs than LQT2 patients. The rate of CEs among LQT1 and LQT2 patients in post-adolescence was not presented due to a lack of sufficient evidence (**Figure 2C**). Thus, appropriate stratification in terms of the above factors should be performed, in order to guide clinical decision-making for BBs therapy and improve the prognosis of LQTS with the minimum adverse-events (Migdalovich et al., 2011; Westphal et al., 2020).

BBs are considered the most effective therapy for alleviating CEs in LQTS patients (Moss et al., 2000). Notably, although BB treatments may be applied to LQT1 patients with a minimum risk of CEs during a long follow-up period, this does not mean that it is inherently safe for treating patients with other LQT subtypes with the same BB (Postema et al., 2013). Therefore, it is important to investigate which BBs perform best for controlling CEs in different LQTS genotypes. In our study, we found that after BBs therapy, patients with LQT1 had a relatively lower rate of CEs than patients with LQT2 (**Figure 4B**). BBs therapy had no apparent function in decreasing CEs risk for LQT3 patients, but the risk of CEs in LQT3 patients was generally higher than in other LQTS genotypes (Priori et al., 2004). This phenomenon could be explained by the incorrect notion that BBs therapy has no effect on LQT3 patients (Schwartz et al., 2012) (**Figure 4A**). Strikingly, the blocking effect of BBs is observed among LQT3 female patients but absent in male patients (Wilde et al., 2016). We confirmed a protective effect of BBs therapy for LQT2 and LQT3 patients was somewhat lower than for LQT1 patients, which was consistent with prevailing findings (Shimizu et al., 2009), although there was no statistically significant difference on the risk of CEs via the pairwise comparisons between the LQT1-3 genotypes (**Figure 4B**). Among the four BBs, we investigated that nadolol exhibited a pronounced risk reduction in both LQT1 and LQT2 (HR 0.49 and HR 0.33, respectively; **Figure 4C**). However, atenolol, propranolol, and metoprolol only prevented LQT1 patients from CEs (HR 0.49, 0.37 and 0.30, respectively), but did not prevent them in LQT2 patients (HR 0.51, 0.61 and 0.73, respectively). Nadolol, a hydrophilic long-acting nonselective drug with the longest elimination half-life of these four BBs, could maintain high pharmacodynamic levels, which might be the main reason why it is regarded as the most effective BB therapy for LQTS patients (Abu-Zeitone et al., 2014). In addition, it could be because of the membrane-stabilizing effect of nadolol, which was attributed to its effect of shorting QTc intervals when compared to atenolol, propranolol and metoprolol in LQT2 patients (Chockalingam et al., 2012). On the other hand, nadolol exhibited a significant effect of reducing the CEs in LQT2. Compared to the effect of BBs between LQT1 and

TABLE 3 | Relative ranking of different BBs assessed by using SUCRA values.

	Rank 1	**Rank 2**	**Rank 3**	**Rank 4**
LQT1				
Atenolol	0.294350	0.447550	0.17180	0.0863
Propranolol	0.035675	0.124925	0.43360	0.4058
Metoprolol	0.062550	0.146400	0.31355	0.4775
Nadolol	0.607425	0.281125	0.08105	0.0304
LQT2				
Atenolol	0.000250	0.289075	0.352525	0.358375
Propranolol	0.000150	0.36075	0.347125	0.291975
Metoprolol	0.000100	0.349900	0.300350	0.349650
Nadolol	0.999725	0.000275	0.000000	0.000000

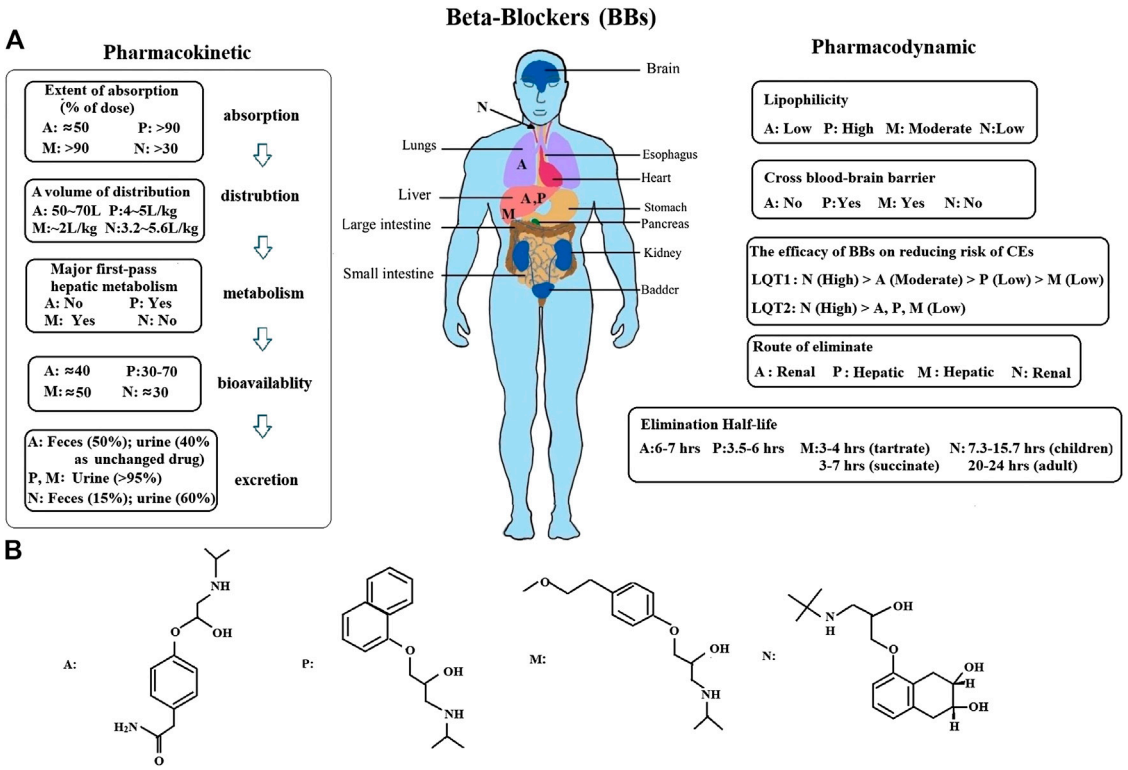

FIGURE 6 | (A), An overview of the pharmacokinetic and pharmacodynamic of BBs was presented. Atenolol is mainly concentrated in the lungs and liver. Propranolol and metoprolol are almost totally metabolized in the liver. Nadolol is absorpted by the gastrointestinal tract, and primarily appears in blood serum. However, it is not metabolized by the liver in humans, only excreted in an unchanged form by the kidney (75%) (A: atenolol, P: propranolol, M: metoprolol, N: nadolol). **(B)**, The structural formula of BBs.

LQT2 patients, there was no superiority in controlling the recurrence of CEs among other three BBs, including atenolol, propranolol, and metoprolol (**Figure 4D**). Lastly, we also observed that BBs seemed to be somewhat more effective in preventing syncope than ACA in LQTS patients (**Figure 4E**).

Furthermore, we conducted a network meta-analysis to assess the efficacy of different BBs in LQT1 and LQT2 via pairwise comparisons, and then joint ranked those results using cluster analysis. Steinberg et al. suggested that all four BBs had a similar effect in preventing the rate of CEs in LQT1, but nadolol was regarded as the most effective drug with the minimum risk of CEs in LQT2 (Steinberg et al., 2016). Our study also showed that nadolol had the best efficacy for reducing the risk of CEs in LQT2. Interestingly, it also ranked first for LQT1 with the lowest possibility of CEs. A previous article suggested that metoprolol had a greater risk of CEs in symptomatic patients than a combined therapy of propranolol and nadolol (Chockalingam et al., 2012). We retrieved various studies and our results have demonstrated that metoprolol is the least effective of the four studied BBs in decreasing the risk of CEs in LQTS (**Figures 5A,B**). The therapeutic effect of atenolol seemed somewhat superior compared to propranolol for LQT1 patients, but neither of them were beneficial in LQT2 (**Figures 5A,B**). Interestingly, there has been a controversial view on whether propranolol is inferior to its counterparts in high-risk LQTS patients (Steinberg et al., 2016; Kwok et al., 2017). It is well-known that the discrepancy of BBs efficacy in monitoring LQTS could be attributed to inadequate dosage and/or patients' noncompliance in earlier research (Moss et al., 2000). In summary, our results propose that the ranked effectiveness of BBs in reducing CEs risk in LQT1 patients is the following: nadolol, atenolol, propranolol, and metoprolol. For LQT2 patients, nadolol showed a protective effect, while other BBs did not significantly prevent the occurrence of CEs, including atenolol, propranolol, and metoprolol (**Figures 5C,D**). These findings are consistent with previous reports (Ahn et al., 2017; Wallace et al., 2019). As described earlier, atenolol had fewer neuropsychiatric side effects, which was attributed to its lower lipid solubility and permeability of the blood-brain barrier (Chatrath et al., 2004). The above results indicate that if patients do not tolerate nadolol, atenolol could represent an alternative therapy for controlling CEs in LQT1 patients. However, for LQT2, propranolol might be a relatively better choice. The different efficacies of BBs was primarily due to the pharmacological and pharmacokinetic characteristics of each blocker (Ågesen et al., 2019) (**Figure 6**). Generally, long-term safety and effectiveness have to be considered for BB treatments in the clinical management of LQTS patients.

CONCLUSION

In the present study, we investigated the relationship between the risk of CEs in LQTS patients and their age, gender, and QTc length. We also clarified different efficacies of BBs for CE risk reduction based on patients with LQTS genotypes. Our analysis did not only induce a pairwise comparison to reveal the efficacy of four BBs in LQTS patients, but also provided the ranked efficacies of BBs treatment for preventing the recurrence of CEs in LQT1 and LQT2 patients. Our results demonstrated that nadolol was the most effective therapy for LQT2 patients. However, in LQT1 patients, the effect of nadolol was also relatively superior to treatment with the three other BBs. In the future, we will investigate which BB is to be preferred for the management of LQTS patients with increased risk factors, such as QTc > 500 ms, male gender in pre-puberty, female gender in adulthood, and LQT2/LQT3 genotypes.

LIMITATIONS

We only included sixteen studies, which was due to a lack of sufficient evidence reflecting the efficiency of BB treatments in LQTS patients based on randomized controlled trials. The results of sensitivity analysis indicated that studies had comparable bias and heterogeneities (Goldenberg et al., 2008). In addition, we will continue to retrieve new studies in order to further investigate the effectiveness of different BBs treatments in relation to other characteristics of LQTS patients, such as ethnicity. Finally, the BBs dosage and the follow-up years of patients plays a pivotal role in their efficacy (Ahrens-Nicklas et al., 2009). How those factors affect their efficacy in LQTS patients warrants further study.

AUTHOR CONTRIBUTIONS

LH and JL designed and performed this study. LH and FL independently used the inclusion disciplines to select identified and qualified literature, and extracted the data from it. QL, QT, and ZZ contributed to the process of double identifying and retrieving the studies from collected literatures. LH conducted traditional meta-analysis and network analysis. LH and JL. wrote and reviewed the draft. LH and ZX critically revised the manuscript.

FUNDING

This work was supported in part by grants from the National Natural Science Foundation of China (No: 81760065), the Natural Science Foundation of Jiangxi Province (No: 20152ACB20025), and the Science and Technology Support of Jiangxi Province (No: 20151BB-G70166).

ACKNOWLEDGMENTS

We are grateful to JL for careful reading and revision of the manuscript.

SUPPLEMENTARY MATERIAL

The Supplementary Material for this article can be found online at: https://www.frontiersin.org/articles/10.3389/fphar.2020.579525/full#supplementary-material

REFERENCES

Abu-Zeitone, A., Peterson, D. R., Polonsky, B., McNitt, S., and Moss, A. J. (2014). Efficacy of different beta-blockers in the treatment of long QT syndrome. *J. Am. Coll. Cardiol.* 64, 1352–1358. doi:10.1016/j.jacc.2014.05.068

Ågesen, F. N., Weeke, P. E., Tfelt-Hansen, P., and Tfelt-Hansen, J. (2019). Pharmacokinetic variability of beta-adrenergic blocking agents used in cardiology. *Pharmacol Res Perspect* 12, e00496. doi:10.1002/prp2.496

Ahn, J., Kim, H. J., Choi, J. I., Lee, K. N., Shim, J., Ahn, H. S., et al. (2017). Effectiveness of beta-blockers depending on the genotype of congenital long-QT syndrome: a meta-analysis. *PLoS One* 12, e0185680. doi:10.1371/journal.pone.0185680

Ahrens-Nicklas, R. C., Clancy, C. E., and Christini, D. J. (2009). Re-evaluating the efficacy of beta-adrenergic agonists and antagonists in long QT-3 syndrome through computational modelling. *Cardiovasc. Res.* 82, 439–447. doi:10.1093/cvr/cvp083

Arking, D. E., Pulit, S. L., Crotti, L., van der Harst, P., Munroe, P. B., Koopmann, T. T., et al. (2014). Genetic association study of QT interval highlights role for calcium signaling pathways in myocardial repolarization. *Nat. Genet.* 46, 826–836. doi:10.1038/ng.3014

Bohnen, M. S., Peng, G., Robey, S. H., Terrenoire, C., Iyer, V., Sampson, K. J., et al. (2017). Molecular pathophysiology of congenital long QT syndrome. *Physiol. Rev.* 97, 89–134. doi:10.1152/physrev.00008.2016

Boutjdir, M., and Lazzerini, P. E. (2020). A novel peptide/antibody-based antiarrhythmic approach to long QT syndrome and beyond. *J. Am. Coll. Cardiol.* 75, 2153–2155. doi:10.1016/j.jacc.2020.03.027

Chatrath, R., Bell, C. M., and Ackerman, M. J. (2004). Beta-blocker therapy failures in symptomatic probands with genotyped long-QT syndrome. *Pediatr. Cardiol.* 25, 459–465. doi:10.1007/s00246-003-0567-3

Chockalingam, P., Crotti, L., Girardengo, G., Johnson, J. N., Harris, K. M., van der Heijden, J. F., et al. (2012). Not all beta-blockers are equal in the management of long QT syndrome types 1 and 2: higher recurrence of events under metoprolol. *J. Am. Coll. Cardiol.* 60, 2092–2099. doi:10.1016/j.jacc.2012.07.046

Conrath, C. E., Wilde, A. A., Jongbloed, R. J., Alders, M., van Langen, I. M., van Tintelen, J. P., et al. (2002). Gender differences in the long QT syndrome: effects of beta-adrenoceptor blockade. *Cardiovasc. Res.* 53, 770–776. doi:10.1016/s0008-6363(01)00477-1

Ebbehøj, E., Arildsen, H., Hansen, K. W., Mogensen, C. E., Mølgaard, H., and Poulsen, P. L. (2004). Effects of metoprolol on QT interval and QT dispersion in type 1 diabetic patients with abnormal albuminuria. *Diabetologia* 47, 1009–1015. doi:10.1007/s00125-004-1422-7

Fabritz, L., Damke, D., Emmerich, M., Kaufmann, S. G., Theis, K., Blana, A., et al. (2010). Autonomic modulation and antiarrhythmic therapy in a model of long QT syndrome type 3. *Cardiovasc. Res.* 87, 60–72. doi:10.1093/cvr/cvq029

Goldenberg, I., Zareba, W., and Moss, A. J. (2008). Long QT syndrome. *Curr. Probl. Cardiol.* 33, 629–694. doi:10.1016/j.cpcardiol.2008.07.002

Goldenberg, I., Bradley, J., Moss, A., McNitt, S., Polonsky, S., Robinson, J. L., et al. (2010). Beta-blocker efficacy in high-risk patients with the congenital long-QT syndrome types 1 and 2: implications for patient management. *J. Cardiovasc. Electrophysiol.* 21, 893–901. doi:10.1111/j.1540-8167.2010.01737.x

Goldenberg, I., Thottathil, P., Lopes, C. M., Moss, A. J., McNitt, S., O-Uchi, J., et al. (2012). Trigger-specific ion-channel mechanisms, risk factors, and response to therapy in type 1 long QT syndrome. *Heart Rhythm* 9, 49–56. doi:10.1016/j.hrthm.2011.08.020

Koponen, M., Marjamaa, A., Hiippala, A., Happonen, J. M., Havulinna, A. S., Salomaa, V., et al. (2015). Follow-up of 316 molecularly defined pediatric long-QT syndrome patients: clinical course, treatments, and side effects. *Circ. Arrhythm. Electrophysiol.* 8, 815–823. doi:10.1161/CIRCEP.114.002654

Kwok, S. Y., Pflaumer, A., Pantaleo, S. J., Date, E., Jadhav, M., and Davis, A. M. (2017). Ten-year experience in atenolol use and exercise evaluation in children with genetically proven long QT syndrome. *J Arrhythm* 33, 624–629. doi:10.1016/j.joa.2017.08.004

Lumley, T. (2002). Network meta-analysis for indirect treatment comparisons. *Stat. Med.* 21, 2313–2324. doi:10.1002/sim.1201

Maguy, A., Kucera, J. P., Wepfer, J. P., Forest, V., Charpentier, F., and Li, J. (2020). KCNQ1 antibodies for immunotherapy of long QT syndrome type 2. *J. Am. Coll. Cardiol.* 75, 2140–2152. doi:10.1016/j.jacc.2020.02.067

Mazzanti, A., Maragna, R., Vacanti, G., Monteforte, N., Bloise, R., Marino, M., et al. (2018). Interplay between genetic substrate, QTc duration, and arrhythmia risk in patients with long QT syndrome. *J. Am. Coll. Cardiol.* 71, 1663–1671. doi:10.1016/j.jacc.2018.01.078

Migdalovich, D., Moss, A. J., Lopes, C. M., Costa, J., Ouellet, G., Barsheshet, A., et al. (2011). Mutation and gender-specific risk in type 2 long QT syndrome: implications for risk stratification for life-threatening cardiac events in patients with long QT syndrome. *Heart Rhythm* 8, 1537–1543. doi:10.1016/j.hrthm.2011.03.049

Moss, A. J., Zareba, W., Hall, W. J., Schwartz, P. J., Crampton, R. S., Benhorin, J., et al. (2000). Effectiveness and limitations of beta-blocker therapy in congenital long-QT syndrome. *Circulation* 101, 616–623. doi:10.1161/01.cir.101.6.616

Postema, P. G., Neville, J., de Jong, J. S., Romero, K., Wilde, A. A., and Woosley, R. L. (2013). Safe drug use in long QT syndrome and Brugada syndrome: comparison of website statistics. *Europace* 15, 1042–1049. doi:10.1093/europace/eut018

Priori, S. G., Napolitano, C., Schwartz, P. J., Grillo, M., Bloise, R., Ronchetti, E., et al. (2004). Association of long QT syndrome loci and cardiac events among patients treated with beta-blockers. *J. Am. Med. Assoc.* 292, 1341–1344. doi:10.1001/jama.292.11.1341

Salanti, G., Ades, A. E., and Ioannidis, J. P. (2011). Graphical methods and numerical summaries for presenting results from multiple-treatment meta-analysis: an overview and tutorial. *J. Clin. Epidemiol.* 64, 163–171. doi:10.1016/j.jclinepi.2010.03.016

Schwartz, P. J., Crotti, L., and Insolia, R. (2012). Long-QT syndrome: from genetics to management. *Circ Arrhythm Electrophysiol* 5, 868–877. doi:10.1161/CIRCEP.111.962019

Shimizu, W., Moss, A. J., Wilde, A. A., Towbin, J. A., Ackerman, M. J., January, C. T., et al. (2009). Genotype-phenotype aspects of type 2 long QT syndrome. *J. Am. Coll. Cardiol.* 54, 2052–2062. doi:10.1016/j.jacc.2009.08.028

Stang, A., Jonas, S., and Poole, C. (2018). Case study in major quotation errors: a critical commentary on the Newcastle-Ottawa scale. *Eur. J. Epidemiol.* 33, 1025–1031. doi:10.1007/s10654-018-0443-3

Steinberg, C., Padfield, G. J., Al-Sabeq, B., Adler, A., Yeung-Lai-Wah, J. A., Kerr, C. R., et al. (2016). Experience with bisoprolol in long-QT1 and long-QT2 syndrome. *J. Intervent. Card Electrophysiol.* 47, 163–170. doi:10.1007/s10840-016-0161-2

Tester, D. J., and Ackerman, M. J. (2014). Genetics of long QT syndrome. *Methodist. Debakey. Cardiovasc. J.* 10, 29–33. doi:10.14797/mdcj-10-1-29

Vincent, G. M., Schwartz, P. J., Denjoy, I., Swan, H., Bithell, C., Spazzolini, C., et al. (2009). High efficacy of beta-blockers in long-QT syndrome type 1: contribution of noncompliance and QT-prolonging drugs to the occurrence of beta-blocker treatment "failures". *Circulation* 119, 215–221. doi:10.1161/CIRCULATIONAHA.108.772533

Wallace, E., Howard, L., Liu, M., O'Brien, T., Ward, D., Shen, S., et al. (2019). Long QT syndrome: genetics and future perspective. *Pediatr. Cardiol.* 40, 1419–1430. doi:10.1007/s00246-019-02151-x

Wang, L., and Wu, T. (2004). Predictive factors for an effective beta-blocker therapy in Chinese patients with congenital long QT syndrome: a multivariate regression analysis. *Exp. Clin. Cardiol.* 9 (3), 193–195.

Westphal, D. S., Burkard, T., Moscu-Gregor, A., Gebauer, R., Hessling, G., and Wolf, C. M. (2020). Reclassification of genetic variants in children with long QT syndrome. *Mol. Genet. Genomic Med.* 8, e1300. doi:10.1002/mgg3.1300

Wilde, A., and Ackerman, M. J. (2014). Beta-blockers in the treatment of congenital long QT syndrome: is one beta-blocker superior to another?. *J. Am. Coll. Cardiol.* 64, 1359–1361. doi:10.1016/j.jacc.2014.06.1192

Wilde, A. A., Moss, A. J., Kaufman, E. S., Shimizu, W., Peterson, D. R., Benhorin, J., et al. (2016). Clinical aspects of type 3 long-QT syndrome: an international multicenter study. *Circulation* 134, 872–882. doi:10.1161/CIRCULATIONAHA.116.021823

Conflict of Interest: The authors declare that the research was conducted in the absence of any commercial or financial relationships that could be construed as a potential conflict of interest.

frontiers in Physiology

REVIEW
published: 18 December 2020
doi: 10.3389/fphys.2020.615503

Perivascular Adipose Tissue as an Indication, Contributor to, and Therapeutic Target for Atherosclerosis

*Yan Liu, Yan Sun, Chengping Hu, Jinxing Liu, Ang Gao, Hongya Han, Meng Chai, Jianwei Zhang, Yujie Zhou and Yingxin Zhao**

Department of Cardiology, Beijing Anzhen Hospital, Capital Medical University, Beijing Institute of Heart Lung and Blood Vessel Disease, Beijing, China

Perivascular adipose tissue (PVAT) has been identified to have significant endocrine and paracrine functions, such as releasing bioactive adipokines, cytokines, and chemokines, rather than a non-physiological structural tissue. Considering the contiguity with the vascular wall, PVAT could play a crucial role in the pathogenic microenvironment of atherosclerosis. Growing clinical evidence has shown an association between PVAT and atherosclerosis. Moreover, based on computed tomography, the fat attenuation index of PVAT was verified as an indication of vulnerable atherosclerotic plaques. Under pathological conditions, such as obesity and diabetes, PVAT shows a proatherogenic phenotype by increasing the release of factors that induce endothelial dysfunction and inflammatory cell infiltration, thus contributing to atherosclerosis. Growing animal and human studies have investigated the mechanism of the above process, which has yet to be fully elucidated. Furthermore, traditional treatments for atherosclerosis have been proven to act on PVAT, and we found several studies focused on novel drugs that target PVAT for the prevention of atherosclerosis. Emerging as an indication, contributor to, and therapeutic target for atherosclerosis, PVAT warrants further investigation.

Keywords: perivascular adipose tissue, atherosclerosis, inflammation, imaging, adipocytokines

OPEN ACCESS

Edited by:
Joshua Thomas Butcher, Oklahoma State University, United States

Reviewed by:
Jessica Faulkner, Augusta University, United States
Eliana Hiromi Akamine, University of São Paulo, Brazil
Ibra Fancher, University of Delaware, United States

****Correspondence:***
Yingxin Zhao
zyingxinmi@163.com

Specialty section:
This article was submitted to Vascular Physiology, a section of the journal Frontiers in Physiology

Received: *09 October 2020*
Accepted: *30 November 2020*
Published: *18 December 2020*

Citation:
Liu Y, Sun Y, Hu C, Liu J, Gao A, Han H, Chai M, Zhang J, Zhou Y and Zhao Y (2020) Perivascular Adipose Tissue as an Indication, Contributor to, and Therapeutic Target for Atherosclerosis. Front. Physiol. 11:615503. doi: 10.3389/fphys.2020.615503

INTRODUCTION

Atherosclerosis is a process in which the formation and buildup of lipid, cells, as well as matrix, and represents a major stage of atheromatous plaque formation. Atherosclerosis can cause myocardial infarction, stroke, and disabling peripheral artery disease, leading to high morbidity and mortality worldwide (Libby et al., 2019). The pathogenesis of atherosclerosis including endothelial dysfunction, inflammatory cells recruitment, vascular smooth muscle cells (VSMCs)

Abbreviations: 10,12 CLA, 10,12 conjugated linoleic acid; AMPK, AMP-activated protein kinase; AT1, angiotensin II type 1 receptor; CA, coronary artery; CAD, atherosclerotic coronary artery disease; CRP, C-reactive protein; CT, computed tomography; DPP-4, dipeptidyl peptidase-4; EMT, extramedial thickness; eNOS, endothelial nitric oxide synthase; FAI, fat attenuation index; GLP-1, glucagon like peptide-1; GM-CSF, granulocyte macrophage colony stimulating factor; HFD, high-fat diet; IL, interleukin; IMT, intima-media thickness; ITA, internal thoracic artery; MB, myocardial bridge; MCP-1, monocyte chemoattractant protein-1; mitoNEET, CDGSH iron sulfur domain 1 protein; MMP-9, matrix metalloprotein-9; MRI, magnetic resonance imaging; mRNA, messenger RNA; Nh, native human; PIAS1, inhibiting protein of activated STAT1; PPARγ, peroxisome proliferator-activated receptor-γ; PPD, pseudoprotodioscin; Psgl-1, P-selectin glycoprotein ligand-1; PVAT, perivascular adipose tissue; SGLT2, sodium glucose cotransporter 2; SLE, systemic lupus erythematosus; SOCS3, suppressor of cytokine signaling 3; TGF, transforming growth factor; TNF, tumor necrosis factor; VCAM-1, vascular cell adhesion molecule-1; VEGF, vascular endothelial growth factor; VSMCs, vascular smooth muscle cells.

proliferation and migration. During the process, cytokines are released by different types of cells and exert multiple effects, such as crosstalk among endothelial cells, vascular smooth muscle cells, inflammatory cells, and adipocytes (Tousoulis et al., 2016). The dynamic microenvironment plays a fundamental role in the pathogenesis of atherosclerosis.

The perivascular adipose tissue (PVAT) has long been considered a non-physiological structural tissue, but in the last decade, an increasing number of studies have identified it to have significant endocrine and paracrine functions, including the release of bioactive adipokines, cytokines, and chemokines (Szasz and Webb, 2012). Given the anatomical proximity between PVAT and the vascular wall, PVAT could play a crucial role in the pathogenic processes of atherosclerosis, mainly toward endothelial dysfunction (Virdis, 2016) and inflammatory cell recruitment (Omar et al., 2014). However, the pathophysiological characteristics of PVAT seem to be distinct in different anatomical locations (Gil-Ortega et al., 2015) and metabolic statuses (Molica et al., 2015; Ferrara et al., 2019), which remains to be clarified. In this review, we discuss the PVAT imaging features from the latest clinical evidence, the proatherogenic and antiatherogenic phenotypes of PVAT, the underlying molecular mechanisms and pathways, and potential therapeutic measures.

IMAGING FEATURES OF PVAT

Ultrasound

Carotid intima-media thickness (IMT) is an index measure derived from high-resolution carotid ultrasound to assess the burden of atherosclerosis. As a complement, carotid extramedial thickness (EMT) focuses on the adventitial structure of arteries, which is mainly attributed to PVAT (Falk et al., 2009). Haberka et al. (2019) reported that EMT is an independent and strong predictor of significant internal carotid artery stenosis instead of obesity measurements. In addition, the combination of ultrasound indexes related to PVAT and the vascular wall was associated with more complex atherosclerotic coronary artery disease (CAD) in patients with high risk (Haberka et al., 2018). Carotid EMT is a promising index for early assessment of the clinical risk of atherosclerosis (Skilton, 2019). Similarly, intravascular photoacoustic ultrasound detected increased iliac arteries-PVAT in Ossabaw swine with metabolic syndrome, which was verified by histology as early-stage atherosclerotic changes (Kole et al., 2019).

Computed Tomography

CT-based volumetric quantification of PVAT is feasible and highly reproducible (Schlett et al., 2009). Recent evidence has demonstrated that coronary artery-PVAT transforms from the lipid to aqueous phase during vascular inflammation, resulting in increased CT attenuation around the inflamed coronary artery (Antonopoulos et al., 2017). A novel non-invasive biomarker, the fat attenuation index (FAI), was designed to predict vulnerable atherosclerotic plaques and cardiac mortality (Antonopoulos et al., 2017; Antoniades et al., 2019; Lin et al., 2019). Moreover, the FAI was validated in a clinical cohort to show significant reduction around the culprit lesion; by contrast, there was no change around the stable atherosclerotic plaques (Antonopoulos et al., 2017). In CT imaging, we can identify adipose tissue with voxels between -190 and -30HU, and perform quantitative evaluation by calculating FAI or volume of PVAT, which helps the prediction of atherosclerosis.

Magnetic Resonance Imaging

Due to its high cost and time consumption, studies based on MRI are limited and controversial. Randrianarisoa et al. (2018) showed a correlation between brachial artery PVAT and insulin resistance, while aorta PVAT is associated with carotid IMT, indicating that brachial artery PVAT and aorta PVAT may act differently as possible modulators of insulin resistance and subclinical atherosclerosis. However, Alkhalil et al. (2018) demonstrated the dissociation between the spatial distribution of PVAT and arterial wall thickening in the aorta and carotid arteries, which does not support that PVAT promotes atherosclerotic plaque through the paracrine route. The quantitative evaluations were implemented with different special software. Further research focusing on the assessment of PVAT with MRI is warranted.

PVAT and Vascular Calcification

Vascular calcification was found to be associated with PVAT as a surrogate measure of atherosclerosis. The coronary artery segment covered by a myocardial bridge (MB) was isolated from the influence of PVAT. Verhagen et al. (2013) revealed that segments without an MB have a higher calcium score than segments covered with an MB. The association between calcium scores and MBs was influenced by local PVAT thickness (Verhagen et al., 2013). Moreover, women with systemic lupus erythematosus (SLE) were demonstrated to have greater aortic PVAT, which correlated with the calcification of different vascular beds (Shields et al., 2013). The summary of clinical imaging studies of PVAT and atherosclerosis is presented in **Table 1**. Based on above studies, it can be concluded that the increased volume or thickness of PVAT is associated with atherosclerosis. The enlargement of PVAT may indicates the transition from anti-atherogenic to pro-atherogenic phenotypes, which mediating the progression of atherosclerosis. The imaging features and pathological characteristics of PVAT needs further investigations.

REGIONAL AND SEX DIFFERENCES IN PVAT

Regional Differences in PVAT

Several rodents and human studies found regional differences in PVAT impacting vascular function. Mouse abdominal aorta-PVAT is more inflamed than thoracic aorta-PVAT, which is independent of aging (Padilla et al., 2013). The phenotypic differences in PVAT between the regions of the aorta may account for the evidence that the abdominal aorta is more vulnerable to atherosclerosis than the thoracic aorta (Padilla et al., 2013; Victorio et al., 2016). A study based on multimodal

TABLE 1 | Overview of clinical imaging studies of perivascular adipose tissue (PVAT) and atherosclerosis.

Authors	Study design	Number of subjects	Imaging technology	Imaging index	Main findings
Haberka et al., 2019	Cross-sectional	391	Ultrasound	Carotid EMT	Carotid EMT was an independent and strong predictor of significant internal carotid artery stenosis
Haberka et al., 2018	Cross-sectional	215	Ultrasound	PATIMA index	The PATIMA index was associated with more complex CAD in high- and very-high-risk patients
Antonopoulos et al., 2017	Cross-sectional	273	CT	FAI	The FAI gradient around coronary arteries identified early subclinical coronary artery disease and vulnerable atherosclerotic plaques
Randrianarisoa et al., 2018	Cross-sectional	95	MRI	Volume	Brachial artery-PVAT was associated with insulin sensitivity, while aorta-PVAT was associated with carotid IMT
Alkhalil et al., 2018	Cross-sectional	29	MRI	Thickness	The spatial distribution of PVAT was uncorrelated with arterial wall thickening in the aorta and carotid arteries
Verhagen et al., 2013	Cross-sectional	128	CT	Thickness	The coronary artery segments without an MB have a higher calcium score than segments covered with an MB. The association between calcium scores and MBs was influenced by local PVAT thickness
Shields et al., 2013	Cross-sectional	135	CT	Volume	Women with SLE had greater aortic-PVAT, which correlated with calcification of different vascular beds

EMT, extramedial thickness; PATIMA, periarterial adipose tissue intima media adventitia; CT, computed tomography; FAI, fat attenuation index; MRI, magnetic resonance imaging; IMT, intima-media thickness; MB, myocardial bridge; SLE, systemic lupus erythematosus.

non-linear optical imaging reported that mouse thoracic PVAT changes differentially from the initial stages to advanced stages of atherosclerosis and undergoes spatial impairment focused on atherosclerotic plaques (Kim et al., 2019). In humans, the phenotype of internal thoracic artery (ITA)-PVAT is closer to that of subcutaneous adipose tissue than that of coronary artery (CA)-PVAT (Numaguchi et al., 2019). ITA-PVAT appears to be protected from inflammation and consecutive adipose tissue remodeling, which may explain the decreased atherosclerotic plaque burden in the ITA (Numaguchi et al., 2019). Similarly, in patients with CAD, the genes related to inflammation, lipid metabolism and myocardial processes are differentially expressed in CA-PVAT and ITA-PVAT, demonstrating that PVAT is the key determinant in the development of atherosclerosis (Lu et al., 2017). In a community-based sample, individuals with high thoracic aorta-PVAT in the absence of high visceral adipose tissue were characterized by adverse cardiometabolic profiles, such as smoking and reduced high-density lipoprotein cholesterol (Britton et al., 2012). Therefore, compared with thoracic aorta and ITA, the vulnerability of abdominal aorta and CA to atherosclerosis may be explained by the regional differences of PVAT.

Sex Differences in PVAT

Abdominal aortic aneurysm is a fatal disease with significant sexual dimorphism. Testosterone was verified to increase aneurysm rupture rates in female, which suggest the aortic vascular biology is regulated by sex chromosome (Alsiraj et al., 2017). Similarly, male is a risk factor of CAD, and estrogen could protect vascular from atherosclerosis. El Khoudary et al. (2015) demonstrated women gain cardiovascular fat after menopause, and the aortic PVAT volume is positively associated with estradiol reduction. Therefore, sex and sex hormones could play an important role in PVAT-mediated vascular atherosclerosis. Thromboxane and PGF2α mediate PVAT-induced vasoconstriction of porcine coronary artery in male and female pigs, respectively (Ahmad et al., 2017b). PVAT from female pigs inhibit contraction of porcine coronary artery, not male pigs (Ahmad et al., 2017a). Sex differences in PVAT have been reviewed in detail recently (Victorio et al., 2020), while the sex differences in PVAT-mediated atherosclerosis remains to be verified.

Inflammation and Immunity of PVAT

Genome-wide expression analyses identified that the genes associated with the regulation of inflammation, angiogenesis, blood clotting, and vascular morphology were differentially expressed in human perivascular adipocytes and subcutaneous adipocytes (Chatterjee et al., 2013). Perivascular adipocytes signal to both inflammatory cells and endothelial cells, thus significantly modulating vascular inflammatory crosstalk in atherogenesis (Chatterjee et al., 2013).

Proinflammatory and Anti-inflammatory Phenotypes of PVAT

Under physiological conditions, PVAT protects the artery against atherosclerosis by counteracting inflammation. Ren et al. (2019) founded that PVAT was formed around the disturbed blood flow-induced carotid atherosclerosis, and transplantation of thoracic PVAT from wild-type mice, which showed lower messenger RNA (mRNA) levels of inflammatory cytokines than thoracic PVAT from $ApoE^{-/-}$ mice, decreased plaque macrophage content. Similarly, wild-type mouse periaortic PVAT transplantation inhibited atherosclerosis development by exerting TGF (transforming growth factor)-β1-mediated anti-inflammatory activity, which might involve M2 macrophages (Terada et al., 2018). Under pathological conditions, PVAT contributes to the formation process of atherosclerosis. Transplantation of abdominal aortic PVAT from high-fat diet (HFD)-fed mice increased aortic atherosclerosis and inhibited

endothelium-dependent relaxation (Horimatsu et al., 2018). In the transplanted abdominal aortic PVAT tissue, MCP-1 (monocyte chemoattractant protein-1) and TNF (tumor necrosis factor)-α expression was elevated, while adiponectin expression was reduced (Horimatsu et al., 2018). Moreover, compared with PVAT surrounding a normal vessel (internal mammary artery), human PVAT of atherosclerotic arteries (coronary artery) showed more extensive inflammation, lymphangiogenesis, and fibrosis, probably due to local VEGF (vascular endothelial growth factor)-C, VEGF-D, and angiopoietin-2 overexpression (Drosos et al., 2019).

Similarly, the proinflammatory state of PVAT was identified with cardiovascular risk factors, such as hypertension, diabetes mellitus and peripheral arterial disease. In a hypertensive mouse model, T cells preferentially accumulated in aortic PVAT and could be increased by angiotensin II (Guzik et al., 2007). Accordingly, aortic PVAT-specific renin-angiotensin system activation contributes to accelerating atherosclerotic development in uninephrectomized mice (Kawahito et al., 2013). Angiotensin II type 1 receptor (AT1) plays an important role in the HFD-induced phenotypic alteration of aortic PVAT in $ApoE^{-/-}$ mice, identified as higher expression of proinflammatory cytokines and inflammatory cell infiltration, and modulation of AT1 may exert beneficial effects on atherosclerosis (Irie et al., 2015). In patients with diabetes, carotid PVAT surrounding the atheromatous plaques showed an increase in the mRNA levels of TNF-a, MCP-1, and IL (interleukin)-6 (Hamlat-Khennaf et al., 2017). Patients with peripheral arterial disease showed higher gene expression of TNF-α in renal artery-PVAT (Cejkova et al., 2017). According to Wakana et al. (2015), maternal HFD accelerated atherosclerosis development in offspring, as the increasing thoracic aorta-PVAT specific inflammatory response mediated by higher expression of macrophage colony-stimulating factor. In contrast, an Ossabaw pig experiment exhibited disconnection between left anterior descending coronary artery-PVAT inflammation and HFD-induced cardiometabolic dysfunction (Vieira-Potter et al., 2015).

Inflammatory Cells of PVAT

Human aortic PVAT produces different chemokines, such as IL-8 and MCP-1, which induce the chemotaxis of granulocytes, monocytes, and activated T cells (Henrichot et al., 2005). In patients with CAD, the ratio of macrophages was significantly higher in the coronary arterial wall, and a close relationship was identified between the ratio of macrophages in the arterial wall and PVAT (Verhagen et al., 2012; Kralova Lesna et al., 2015). Coronary PVAT macrophages were associated with stenosis of the adjacent vessel, and M2 macrophages were more abundant than M1 macrophages in PVAT (Verhagen et al., 2014). The inflammatory cells in PVAT seem to play a crucial role in atherogenesis. A postmortem study revealed that the plaque/media ratio increased with the area and macrophages of coronary PVAT (Verhagen et al., 2012). The area of coronary PVAT was related to the presence of a lipid core and the infiltration of macrophages and lymphocytes in atherosclerotic plaques (Verhagen et al., 2012). Similarly, Farias-Itao et al. (2019) identified the correlation between inflammatory cells in coronary PVAT and atherosclerotic plaque features. In periplaque coronary PVAT, the density of $CD68^+$ macrophages and $CD20^+$ B lymphocytes increased with the size of the plaque, and coronary PVAT surrounding unstable atherosclerotic plaques exhibited greater $CD68^+$ macrophages than surrounding stable lesions (Farias-Itao et al., 2019). In addition, in the development of atherogenesis, commensal microbes activate B2 cells in PVAT through lipid metabolism-independent mechanisms (Chen et al., 2016). B1 cells in PVAT were found to produce immunoglobulin type M antibodies to limit atherosclerosis development (Srikakulapu et al., 2017).

PVAT and Immunity

Both rodents and human experiments suggested that PVAT produced complement proteins C3 and C4, which bind to elastin fibers and collagen within the adventitia, leading to increased vascular atherosclerosis and vascular calcification (Shields et al., 2011; Nagaraj et al., 2015). In rats, immunization intracutaneously with native human (nh)-LDL or nh-HDL induced increased PVAT volume and atherosclerosis-like changes in the aortic wall: leukocytes accumulation, intima destruction and media structure disruption (Fomina et al., 2017). Therefore, the immune response toward native lipoproteins might be adipogenic and atherogenic.

Taken together, the inflammation and immunity of PVAT are key determinants in the pathogenesis of atherosclerosis, which deserve further exploration.

Endothelial Function and PVAT-Derived Adipocytokines

Endothelial function is largely based on endothelial nitric oxide synthase (eNOS) function and activity (Daiber et al., 2019). PVAT may regulate arterial tone by releasing diffusible vasorelaxation factors, which, through endothelium-derived NO production, compensate for impaired vasodilatation in metabolic disorders (Kagota et al., 2017; Baltieri et al., 2018). On the other hand, factors released from PVAT may inhibit endothelial NO production and induce vasocontraction by increasing the expression of Cav-1 protein (Lee et al., 2014). AMP-activated protein kinase (AMPK) was revealed to regulate adipocyte metabolism, adipose biology and vascular function (Almabrouk et al., 2014). Activation of AMPK restrains the production of PVAT-released adipokines and prevents endothelial dysfunction by increasing the bioavailability of NO (Gao et al., 2018). Compared with the PVAT of the thoracic aorta, eNOS-derived NO production decreased in the PVAT of the abdominal aorta, suggesting the susceptibility of the abdominal aorta to vascular injury (Victorio et al., 2016). It is now well accepted that adiponectin, as a protective adipocytokine secreted by PVAT, possesses anti-inflammatory, insulin-sensitizing, and vasodilating properties (Milutinovic et al., 2019). In HFD mice, endothelium-mediated vascular relaxation was impaired, and subcutaneously pumped adiponectin was demonstrated to increase eNOS phosphorylation and decrease PVAT inflammation, thereby restoring endothelial cell function (Sena et al., 2017). Consistently, endothelium-dependent

relaxation was reduced in obese patients (Virdis, 2016; Cybularz et al., 2017). Endogenous adiponectin expression was increased in PVAT to maintain endothelial function (Cybularz et al., 2017). Moreover, in patients with atherosclerosis, peroxidation products produced in the vascular wall promote adiponectin gene expression in PVAT through a peroxisome proliferator-activated receptor-γ (PPARγ)-dependent mechanism (Margaritis et al., 2013). Then, adiponectin restores eNOS coupling to improve the redox state (Margaritis et al., 2013). In addition, PPARγ deficiency in PVAT enhances atherosclerosis and results in vascular and systemic inflammation (Xiong et al., 2018). Additionally, PVAT-secreted adiponectin promotes macrophage autophagy by suppressing the Akt/FOXO3a signaling pathway, subsequently suppressing plaque formation (Li et al., 2015). Growing studies focus on glucose metabolism of endothelial and VSMCs. Diabetes restrains glycolysis upregulation in endothelial cells under hypoxia conditions (Primer et al., 2020). High concentration of glucose promotes P. gingivalis invasion of human aortic SMCs, then initiates osteogenic phenotype switch, which results in calcification (Chen et al., 2018). Adiponectin also participates in the regulation of related process. High glucose leads to vascular adiponectin resistance, and contributes to diabetic endothelial dysfunction (Liu et al., 2015). High glucose could reduce adiponectin expression of stromal cells in epicardial adipose tissue, which induce an inflammatory paracrine process in endothelial cells (Fernández-Trasancos et al., 2016). Besides, adiponectin could reduce VSMCs proliferation and migration which induced by high glucose (Cersosimo et al., 2020). Leptin was perceived as a risk factor in atherosclerosis progression, which promote endothelial dysfunction, PVAT inflammation and vascular smooth muscle cell phenotypic switching (Dib et al., 2014; Li et al., 2014; Payne et al., 2014). Circulating plasma leptin negatively correlates with endothelial dependent vasodilation (Gonzalez et al., 2013). In Ossabaw with metabolic syndrome, the increased epicardial PVAT leptin was revealed to exacerbate coronary endothelial dysfunction via a protein kinase C-β-dependent pathway (Payne et al., 2010). In female mice, leptin was found to induce endothelial dysfunction through aldosterone-dependent mechanisms (Huby et al., 2016). In addition, patients with coronary artery disease were identified to have more severe hypoxia in local tissue and higher expression of leptin in PVAT, as well as increased inflammation, vascularization, and fibrosis, accounting for the increased atherosclerotic plaque burden within the coronary arteries (Drosos et al., 2016). A study of ewes showed that leptin increased IL-1B and TNF-a gene expression, which may moderate the inflammatory reaction progress in PVAT (Krawczynska et al., 2019).

Perivascular adipose tissue dysfunction is characterized by its inflammatory state, reduced production of vasoprotective adipocyte-derived relaxing factors such as adiponectin and omentin (Van de Voorde et al., 2013) and augmented production of proinflammatory factors such as leptin, resistin, cytokines (TNF-α and IL-6) and chemokines (MCP-1 and RANTES) (Nosalski and Guzik, 2017). These factors promote inflammatory cell infiltration and induce eNOS dysfunction, ultimately leading to the development of atherosclerotic diseases (Van de Voorde et al., 2013; Nosalski and Guzik, 2017; Aroor et al., 2018).

PVAT and Thermoregulation

Perivascular adipose tissue is similar to brown adipose tissue and is essential for intravascular thermoregulation upon cold acclimation, which plays a protective role in the pathogenesis of atherosclerosis (Chang et al., 2012). Proteomics analysis of PVAT from mice identified that cold exposure improves endothelial function and inhibits atherosclerosis (Chang et al., 2012). Moreover, an experiment in ferrets found that cold exposure downregulated gene expression in aortic PVAT, which was associated with the immune response, cell cycle and gene expression regulation (Reynes et al., 2017). Aortic PVAT exhibited an anti-inflammatory response to cold acclimation and demonstrated a protective effect against atherogenesis (Reynes et al., 2017). Different proteins mediated the thermoregulatory response of PVAT. As a mitochondrial outer membrane protein, the CDGSH iron sulfur domain 1 protein (referred to as mitoNEET) could regulate oxidative capacity and the browning of adipose tissue (Xiong et al., 2017). MitoNEET in PVAT contributes to PVAT-dependent thermogenesis, thereby preventing atherosclerosis development (Xiong et al., 2017). In addition, Tang et al. (2018) demonstrated ribosomal protein S3A as a key factor in modulating the brown fat-specific gene uncoupling protein 1 and carbon metabolic enzymes in epicardial adipose tissue to prevent CAD. These findings suggested that the thermogenic capacity of PVAT is beneficial to the protection of atherosclerosis.

Proatherogenesis-Related Molecular Mechanisms and Pathways

With respect to the proatherogenic role of PVAT, different proteins, bioactive factors and pathways have been investigated. Coronary PVAT of Ossabaw swine was identified to attenuate vasodilation through the inhibitions of vascular smooth muscle K + channels (Noblet et al., 2015). Carotid PVAT transplantation leads to endothelial dysfunction and accelerated atherosclerosis in $ApoE^{-/-}$ mice, and it could be blocked by neutralization of Psgl-1 (P-selectin glycoprotein ligand-1) (Ohman et al., 2011). Consistently, Psgl-1 deficiency was revealed to prevent mesenteric PVAT inflammation and endothelial dysfunction in obese mice (Wang et al., 2012). Thus, Psgl-1 may play a crucial role in the formation of atherosclerotic lesions. Moreover, in HFD-fed rabbits, especially in carotid PVAT(+) groups, CRP (C-reactive protein) significantly promoted endothelial dysfunction, which might be mediated by activating the inflammatory response of adipose tissue (Chen et al., 2013). CRP was also found to contribute to vasa vasorum growth by activating the proangiogenic activity of adipose-derived stem cells (Chen et al., 2016), which promote the pathogenesis of atherosclerosis.

Xpr1 and Taf3, a regulator of macrophage differentiation and a core transcription factor, which were detected in mouse PVAT, were significantly upregulated during atherosclerosis, suggesting a role in the pathogenesis of atherosclerosis (Hueso et al., 2016). Interestingly, hepatokine fibroblast growth factor

21 exerts secretome-modulating responses in human perivascular adipocytes, establishing a novel liver-PVAT-blood vessel axis that possibly accounts for vascular inflammation and atherosclerosis (Berti et al., 2016). Moreover, miR-19b in endothelial cell-derived microvesicles promotes atherosclerosis progression by increasing PVAT-specific inflammation by diminishing SOCS3 (suppressor of cytokine signaling 3) expression (Li et al., 2018). In addition, endoplasmic reticulum stress in PVAT destabilizes atherosclerotic plaques by increasing GM-CSF (granulocyte macrophage colony stimulating factor) in a paracrine manner via the transcription factor NF-κB (Ying et al., 2018). In addition, higher levels of inhibiting protein of activated STAT1 (PIAS1) and diminished expression of NF-κB- or STAT1-regulated genes involved in adipocyte inflammation, differentiation, senescence and apoptosis were present in mouse PVAT, while PIAS1 was decreased in the PVAT of patients with atherosclerosis (Schutz et al., 2019), suggesting that STAT1- or NF-κB-regulated genes may mediate the proatherogenesis effects of PVAT. Taken together, PVAT may contribute to atherosclerosis through promoting endothelial dysfunction, accelerating inflammation reaction, and motivating vasa vasorum growth. The underlining molecular mechanism warrants further clarification.

THERAPEUTIC TARGETS

Smoking Cessation

Nicotine, as the key active component of cigarette smoke, was proven to correlate with PVAT inflammation and contribute to endothelial dysfunction. The PVAT of smokers showed higher expression and activity of the P2 × 7 receptor-inflammasome complex, which contributed to the proinflammatory status (Rossi et al., 2014). Nicotine induced mature adipocyte dysfunction, thus leading to the abnormal secretion of adiponectin and inflammatory adipokines and exacerbating endothelial inflammation (Wang et al., 2016). In addition, adipocytes promote nicotine-induced apoptosis of endothelial cells through the NF-κB pathway (Liu et al., 2017). Smoking cessation could prevent vascular atherosclerosis induced by PVAT dysfunction.

Antidiabetic Drugs

Pioglitazone, an insulin sensitizer, alleviated PVAT oxidative damage induced by fructose treatment and prominently diminished proinflammatory markers in $ApoE^{-/-}$ mice (Quesada et al., 2018). Additionally, pioglitazone dramatically downregulated the expression of vascular cell adhesion molecule-1 (VCAM-1) and matrix metalloprotein-9 (MMP-9), as well as the activity of MMP-9 in the aortic media wall, and markedly decreased the accumulation of macrophages and lipids in atheroma plaques (Quesada et al., 2018). Pioglitazone treatment increased adiponectin serum level (Negrotto et al., 2016), which enhance endothelial mediated vasodilation (Quinn et al., 2010) and increase the number and function of endothelial progenitor cells (Werner et al., 2007), thereby improve vascular dysfunction (Fernandez et al., 2008).

It was reported that glucagon-like peptide-1 (GLP-1)-based therapeutic methods may positively affect autophagy in PVAT, thus improving endothelial dysfunction caused by obesity (Costantino and Paneni, 2019). Both dipeptidyl peptidase-4 (DPP-4) inhibitors and GLP-1 receptor agonists are modulators of this process. In addition, PVAT is a source of DPP-4, and its biology could be influenced by DPP-4 inhibition (Akoumianakis and Antoniades, 2017). DPP-4 inhibition was associated with diminished oxidative stress and local inflammation both in the PVAT and the vascular wall, potentially regulating atherogenesis progression *in vivo* (Akoumianakis and Antoniades, 2017). For instance, teneligliptin could decrease the expression of a major NADPH oxidase subunit, Nox-4, and a macrophage marker in perivascular adipocytes of normoglycemic $ApoE^{-/-}$ mice (Salim et al., 2017).

Sodium glucose cotransporter 2 (SGLT2) inhibitors were revealed to suppress the inflammation of PVAT and attenuate atherogenesis in an *in vivo* mouse model. Empagliflozin ameliorated the RNA expression of inflammatory factors in PVAT, attenuated diabetes-induced endothelial dysfunction, and decreased the atherosclerotic lesion area in the aortic arch of diabetic $ApoE^{-/-}$ mice (Ganbaatar et al., 2020). Empagliflozin suppressed the expression of PDGF-B in PVAT macrophages, thereby attenuating neointimal hyperplasia after wire injury in HFD-fed mice (Mori et al., 2019).

Other Drugs

Short-term intensive atorvastatin therapy attenuates PVAT inflammation by inhibiting the 5-lipoxygenase pathway, thus significantly ameliorating endothelial dysfunction in HFD rabbits (Wang et al., 2014). The selective Mas receptor agonist AVE0991 (angiotensin 1-7 mimetic) affected macrophage differentiation and recruitment into the perivascular space, exhibiting anti-inflammatory and antiatherosclerotic actions during the early stages of atherosclerosis in $ApoE^{-/-}$ mice (Skiba et al., 2017).

Morinda citrifolia leaf extract was shown to reduce PVAT deposition while preventing atherosclerosis through lipid elimination and anti-inflammatory reactions in ovariectomized HFD-fed mice (Chong et al., 2018). Similarly, pseudoprotodioscin (PPD), a phytoestrogen isolated from Dioscorea nipponica Makino, alleviated atherosclerotic lesions and exerted estrogenic and anti-inflammatory properties in ovariectomized HFD-fed $ApoE^{-/-}$ mice (Sun et al., 2020).

Polysaccharide peptide from Ganoderma lucidum, as one source of antioxidant, had a significant effect in decreasing H_2O_2 levels, PVAT thickness, the number of foam cells, and atherosclerotic plaque width in mice (Andri Wihastuti et al., 2015). 10,12 Conjugated linoleic acid (10,12 CLA)-supplemented mice were characterized by enrichment of M2 macrophages in artery lesions and surrounding PVAT, which contributed to the antiatherosclerotic role of 10,12 CLA (Kanter et al., 2018). Dietary ethanolic extract of mangosteen pericarp significantly diminished the expression of VCAM-1 and decreased the thickness of PVAT and IMT in HFD-fed mice (Wihastuti et al., 2019).

Smoking, antidiabetic drugs and other drugs have been verified to act on PVAT, reducing inflammation reaction and endothelial dysfunction, thus preventing atherosclerosis. PVAT is emerging as the therapeutic target of atherosclerosis.

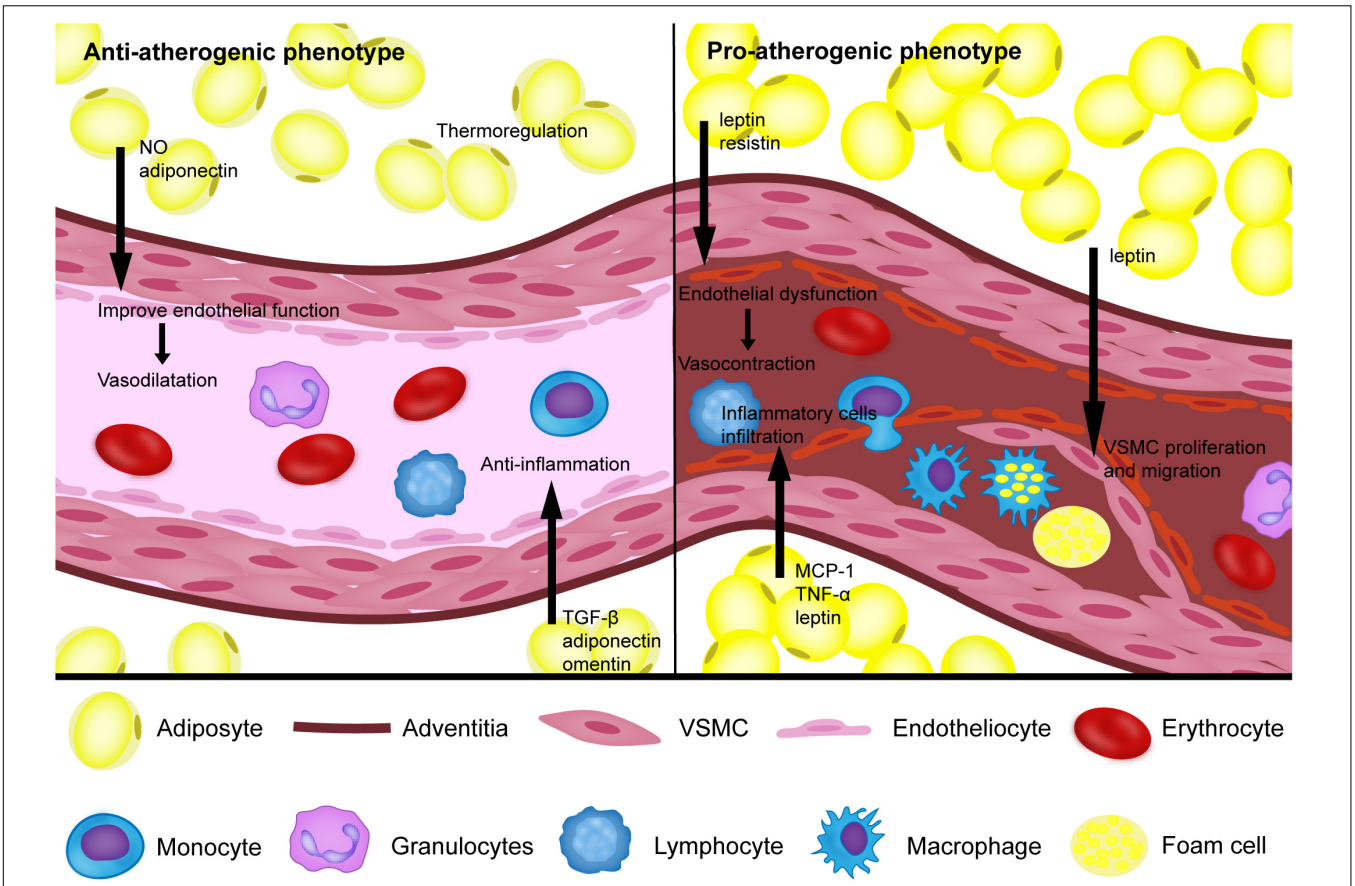

FIGURE 1 | The proatherogenic and antiatherogenic phenotypes of perivascular adipose tissue. Under physiological conditions, perivascular adipose tissue (PVAT) can secrete NO, TGF-β, adiponectin, omentin, and other bioactive factors to reduce the inflammatory response and improve endothelial function, which helps vasodilation. In addition, PVAT also acts as an antiatherogenic phenotype through thermoregulation. Under pathological conditions, such as obesity and diabetes, PVAT shows a proatherogenic phenotype by increasing the release of MCP-1, TNF-a, leptin, resistin and other bioactive factors to induce endothelial dysfunction, inflammatory cell infiltration, vascular smooth cell (VSMC) proliferation and migration.

CONCLUSION

Growing clinical evidence based on imaging technology suggests that the phenotype of PVAT is associated with inflammation and the metabolic profile of the corresponding vasculature as the key determinants for the pathogenesis of atherosclerosis. Under physiological conditions, PVAT acts as an antiatherogenic phenotype by releasing vasodilating factors, exerting an anti-inflammatory response, and thermoregulation. Under pathological conditions, such as obesity and diabetes, PVAT shows the proatherogenic phenotype by increasing the release of adipocytokines and chemokines, which induce endothelial dysfunction, inflammatory cell infiltration, VSMC proliferation and migration, thus contributing to the augmented atherosclerotic plaque burden of the arteries (**Figure 1**). Improving cardiovascular risk stratification based on PVAT imaging could help identify individuals with unstable lesions. Furthermore, the traditional treatments for atherosclerosis, such as smoking cessation, atorvastatin and antidiabetic drugs, have been proven to act on PVAT. Rapid progress in pharmaceutical research has led to the identification of novel drugs targeting PVAT for the prevention of atherosclerosis. Defining the mechanism of PVAT regulation of vascular homeostasis warrants more and better controlled investigations.

AUTHOR CONTRIBUTIONS

YL and YXZ conceived the original scope of this manuscript. YL, YS, CH, JL, and AG wrote specific sections. HH, MC, JZ, YJZ, and YXZ critically reviewed and revised the final manuscript. All authors read and approved the final manuscript.

FUNDING

This work was supported by grants from the National Key Research and Development Program of China (2017YFC0908800), the Beijing Municipal Administration of Hospitals' Ascent Plan (DFL20150601) and Mission plan (SML20180601), and the Beijing Municipal Health Commission "Project of Science and Technology Innovation Center" (PXM2019_026272_000006) (PXM2019_026272_000005).

REFERENCES

Ahmad, A. A., Randall, M. D., and Roberts, R. E. (2017a). Sex differences in the regulation of porcine coronary artery tone by perivascular adipose tissue: a role of adiponectin? *Br. J. Pharmacol.* 174, 2773–2783. doi: 10.1111/bph.13902

Ahmad, A. A., Randall, M. D., and Roberts, R. E. (2017b). Sex differences in the role of phospholipase A(2) -dependent arachidonic acid pathway in the perivascular adipose tissue function in pigs. *J. Physiol.* 595, 6623–6634. doi: 10.1113/jp274831

Akoumianakis, I., and Antoniades, C. (2017). Dipeptidyl peptidase IV inhibitors as novel regulators of vascular disease. *Vascul. Pharmacol.* 9, 1–4. doi: 10.1016/j.vph.2017.07.001

Alkhalil, M., Edmond, E., Edgar, L., Digby, J. E., Omar, O., Robson, M. D., et al. (2018). The relationship of perivascular adipose tissue and atherosclerosis in the aorta and carotid arteries, determined by magnetic resonance imaging. *Diab. Vasc. Dis. Res.* 15, 286–293. doi: 10.1177/1479164118757923

Almabrouk, T. A., Ewart, M. A., Salt, I. P., and Kennedy, S. (2014). Perivascular fat, AMP-activated protein kinase and vascular diseases. *Br. J. Pharmacol.* 171, 595–617. doi: 10.1111/bph.12479

Alsiraj, Y., Thatcher, S. E., Charnigo, R., Chen, K., Blalock, E., Daugherty, A., et al. (2017). Female mice with an XY sex chromosome complement develop severe angiotensin II-induced abdominal aortic aneurysms. *Circulation* 135, 379–391. doi: 10.1161/circulationaha.116.023789

Andri Wihastuti, T., Sargowo, D., Heriansyah, T., Eka Aziza, Y., Puspitarini, D., Nur Iwana, A., et al. (2015). The reduction of aorta histopathological images through inhibition of reactive oxygen species formation in hypercholesterolemia rattus norvegicus treated with polysaccharide peptide of *Ganoderma lucidum*. *Iran. J. Basic Med. Sci.* 18, 514–519.

Antoniades, C., Kotanidis, C. P., and Berman, D. S. (2019). State-of-the-art review article. Atherosclerosis affecting fat: what can we learn by imaging perivascular adipose tissue? *J. Cardiovasc. Comput. Tomogr.* 13, 288–296. doi: 10.1016/j.jcct.2019.03.006

Antonopoulos, A. S., Sanna, F., Sabharwal, N., Thomas, S., and Antoniades, C. (2017). Detecting human coronary inflammation by imaging perivascular fat. *Sci. Transl. Med.* 9:eaal2658. doi: 10.1126/scitranslmed.aal2658

Aroor, A. R., Jia, G., and Sowers, J. R. (2018). Cellular mechanisms underlying obesity-induced arterial stiffness. *Am. J. Physiol. Regul. Integr. Comp. Physiol.* 314, R387–R398. doi: 10.1152/ajpregu.00235.2016

Baltieri, N., Guizoni, D. M., Victorio, J. A., and Davel, A. P. (2018). Protective role of perivascular adipose tissue in endothelial dysfunction and insulin-induced vasodilatation of hypercholesterolemic LDL receptor-deficient mice. *Front. Physiol.* 9:229. doi: 10.3389/fphys.2018.00229

Berti, L., Hartwig, S., Irmler, M., Radle, B., Siegel-Axel, D., Beckers, J., et al. (2016). Impact of fibroblast growth factor 21 on the secretome of human perivascular preadipocytes and adipocytes: a targeted proteomics approach. *Arch. Physiol. Biochem.* 122, 281–288. doi: 10.1080/13813455.2016.1212898

Britton, K. A., Pedley, A., Massaro, J. M., Corsini, E. M., Murabito, J. M., Hoffmann, U., et al. (2012). Prevalence, distribution, and risk factor correlates of high thoracic periaortic fat in the Framingham Heart Study. *J. Am. Heart Assoc.* 1:e004200. doi: 10.1161/jaha.112.004200

Cejkova, S., Kralova Lesna, I., Fronek, J., Janousek, L., Kralova, A., Zdychova, J., et al. (2017). Pro-inflammatory gene expression in adipose tissue of patients with atherosclerosis. *Physiol. Res.* 66, 633–640. doi: 10.33549/physiolres.933352

Cersosimo, E., Xu, X., Terasawa, T., and Dong, L. Q. (2020). Anti-inflammatory and anti-proliferative action of adiponectin mediated by insulin signaling cascade in human vascular smooth muscle cells. *Mol. Biol. Rep.* 47, 6561–6572. doi: 10.1007/s11033-020-05707-w

Chang, L., Villacorta, L., Li, R., Hamblin, M., Xu, W., Dou, C., et al. (2012). Loss of perivascular adipose tissue on peroxisome proliferator-activated receptor-gamma deletion in smooth muscle cells impairs intravascular thermoregulation and enhances atherosclerosis. *Circulation* 126, 1067–1078. doi: 10.1161/circulationaha.112.104489

Chatterjee, T. K., Aronow, B. J., Tong, W. S., Manka, D., Tang, Y., Bogdanov, V. Y., et al. (2013). Human coronary artery perivascular adipocytes overexpress genes responsible for regulating vascular morphology, inflammation, and hemostasis. *Physiol. Genomics* 45, 697–709. doi: 10.1152/physiolgenomics.00042.2013

Chen, J., Gu, Z., Wu, M., Yang, Y., Zhang, J., Ou, J., et al. (2016). C-reactive protein can upregulate VEGF expression to promote ADSC-induced angiogenesis by activating HIF-1alpha via CD64/PI3k/Akt and MAPK/ERK signaling pathways. *Stem Cell Res. Ther.* 7:114. doi: 10.1186/s13287-016-0377-1

Chen, L., Ishigami, T., Nakashima-Sasaki, R., Kino, T., Doi, H., Minegishi, S., et al. (2016). Commensal microbe-specific activation of B2 cell subsets contributes to atherosclerosis development independently of lipid metabolism. *EBioMedicine* 13, 237–247. doi: 10.1016/j.ebiom.2016.10.030

Chen, T. C., Lin, C. T., Chien, S. J., Chang, S. F., and Chen, C. N. (2018). Regulation of calcification in human aortic smooth muscle cells infected with high-glucose-treated *Porphyromonas gingivalis*. *J. Cell. Physiol.* 233, 4759–4769. doi: 10.1002/jcp.26268

Chen, Y., Wang, X., Mai, J., Zhao, X., Liang, Y., Gu, M., et al. (2013). C-reactive protein promotes vascular endothelial dysfunction partly via activating adipose tissue inflammation in hyperlipidemic rabbits. *Int. J. Cardiol.* 168, 2397–2403. doi: 10.1016/j.ijcard.2013.01.158

Chong, C. L. G., Othman, F., and Hussan, F. (2018). Vascular protective effects of *Morinda citrifolia* leaf extract on postmenopausal rats fed with thermoxidized palm oil diet: evidence at microscopic level. *Int. J. Vasc. Med.* 2018:6317434. doi: 10.1155/2018/6317434

Costantino, S., and Paneni, F. (2019). GLP-1-based therapies to boost autophagy in cardiometabolic patients: from experimental evidence to clinical trials. *Vascul. Pharmacol.* 115, 64–68. doi: 10.1016/j.vph.2019.03.003

Cybularz, M., Langbein, H., Zatschler, B., Brunssen, C., Deussen, A., Matschke, K., et al. (2017). Endothelial function and gene expression in perivascular adipose tissue from internal mammary arteries of obese patients with coronary artery disease. *Atheroscler. Suppl.* 30, 149–158. doi: 10.1016/j.atherosclerosissup.2017.05.042

Daiber, A., Xia, N., Steven, S., Oelze, M., Hanf, A., Kroller-Schon, S., et al. (2019). New therapeutic implications of endothelial nitric oxide synthase (eNOS) function/dysfunction in cardiovascular disease. *Int. J. Mol. Sci.* 20:187. doi: 10.3390/ijms20010187

Dib, L. H., Ortega, M. T., Fleming, S. D., Chapes, S. K., and Melgarejo, T. (2014). Bone marrow leptin signaling mediates obesity-associated adipose tissue inflammation in male mice. *Endocrinology* 155, 40–46. doi: 10.1210/en.2013-1607

Drosos, I., Chalikias, G., Pavlaki, M., Kareli, D., Epitropou, G., Bougioukas, G., et al. (2016). Differences between perivascular adipose tissue surrounding the heart and the internal mammary artery: possible role for the leptin-inflammation-fibrosis-hypoxia axis. *Clin. Res. Cardiol.* 105, 887–900. doi: 10.1007/s00392-016-0996-7

Drosos, I., Pavlaki, M., Ortega Carrillo, M. D. P., Kourkouli, A., Buschmann, K., Konstantinou, F., et al. (2019). Increased lymphangiogenesis and lymphangiogenic growth factor expression in perivascular adipose tissue of patients with coronary artery disease. *J. Clin. Med.* 8:1000. doi: 10.3390/jcm8071000

El Khoudary, S. R., Shields, K. J., Janssen, I., Hanley, C., Budoff, M. J., Barinas-Mitchell, E., et al. (2015). Cardiovascular fat, menopause, and sex hormones in women: the SWAN cardiovascular fat ancillary study. *J. Clin. Endocrinol. Metab.* 100, 3304–3312. doi: 10.1210/jc.2015-2110

Falk, E., Thim, T., and Kristensen, I. B. (2009). Atherosclerotic plaque, adventitia, perivascular fat, and carotid imaging. *JACC Cardiovasc. Imaging* 2, 183–186. doi: 10.1016/j.jcmg.2008.11.005

Farias-Itao, D. S., Pasqualucci, C. A., Nishizawa, A., da Silva, L. F. F., Campos, F. M., Bittencourt, M. S., et al. (2019). B lymphocytes and macrophages in the perivascular adipose tissue are associated with coronary atherosclerosis: an autopsy study. *J. Am. Heart Assoc.* 8:e013793. doi: 10.1161/jaha.119.013793

Fernandez, M., Triplitt, C., Wajcberg, E., Sriwijilkamol, A. A., Musi, N., Cusi, K., et al. (2008). Addition of pioglitazone and ramipril to intensive insulin therapy in type 2 diabetic patients improves vascular dysfunction by different mechanisms. *Diabetes Care* 31, 121–127. doi: 10.2337/dc07-0711

Fernández-Trasancos, Á, Guerola-Segura, R., Paradela-Dobarro, B., Álvarez, E., García-Acuña, J. M., Fernández, ÁL., et al. (2016). Glucose and inflammatory cells decrease adiponectin in epicardial adipose tissue cells: paracrine consequences on vascular endothelium. *J. Cell. Physiol.* 231, 1015–1023. doi: 10.1002/jcp.25189

Ferrara, D., Montecucco, F., Dallegri, F., and Carbone, F. (2019). Impact of different ectopic fat depots on cardiovascular and metabolic diseases. *J. Cell. Physiol.* 234, 21630–21641. doi: 10.1002/jcp.28821

Fomina, K., Beduleva, L., Menshikov, I., Anikaeva, M. M., Suntsova, D., Sidorov, A., et al. (2017). Immune response to native lipoproteins induces visceral obesity and aortic wall injury in rats: the role of testosterone. *Endocr. Metab. Immune Disord. Drug Targets* 17, 125–133. doi: 10.2174/1871530317666170711154825

Ganbaatar, B., Fukuda, D., Shinohara, M., Yagi, S., Kusunose, K., Yamada, H., et al. (2020). Empagliflozin ameliorates endothelial dysfunction and suppresses atherogenesis in diabetic apolipoprotein E-deficient mice. *Eur. J. Pharmacol.* 875:173040. doi: 10.1016/j.ejphar.2020.173040

Gao, F., Chen, J., and Zhu, H. (2018). A potential strategy for treating atherosclerosis: improving endothelial function via AMP-activated protein kinase. *Sci. China Life Sci.* 61, 1024–1029. doi: 10.1007/s11427-017-9285-1

Gil-Ortega, M., Somoza, B., Huang, Y., Gollasch, M., and Fernandez-Alfonso, M. S. (2015). Regional differences in perivascular adipose tissue impacting vascular homeostasis. *Trends Endocrinol. Metab.* 26, 367–375. doi: 10.1016/j.tem.2015.04.003

Gonzalez, M., Lind, L., and Söderberg, S. (2013). Leptin and endothelial function in the elderly: the prospective investigation of the vasculature in uppsala seniors (PIVUS) study. *Atherosclerosis* 228, 485–490. doi: 10.1016/j.atherosclerosis.2013.03.018

Guzik, T. J., Hoch, N. E., Brown, K. A., McCann, L. A., Rahman, A., Dikalov, S., et al. (2007). Role of the T cell in the genesis of angiotensin II induced hypertension and vascular dysfunction. *J. Exp. Med.* 204, 2449–2460. doi: 10.1084/jem.20070657

Haberka, M., Lelek, M., Bochenek, T., Kowalowka, A., Mlynarski, R., Mizia-Stec, K., et al. (2018). Novel combined index of cardiometabolic risk related to periarterial fat improves the clinical prediction for coronary artery disease complexity. *Atherosclerosis* 268, 76–83. doi: 10.1016/j.atherosclerosis.2017.09.015

Haberka, M., Skilton, M., Biedron, M., Szostak-Janiak, K., Partyka, M., Matla, M., et al. (2019). Obesity, visceral adiposity and carotid atherosclerosis. *J. Diabetes Complications* 33, 302–306. doi: 10.1016/j.jdiacomp.2019.01.002

Hamlat-Khennaf, N., Neggazi, S., Ayari, H., Feugier, P., Bricca, G., Aouichat-Bouguerra, S., et al. (2017). Inflammation in the perivascular adipose tissue and atherosclerosis. *C. R. Biol.* 340, 156–163. doi: 10.1016/j.crvi.2017.01.001

Henrichot, E., Juge-Aubry, C. E., Pernin, A., Pache, J. C., Velebit, V., Dayer, J. M., et al. (2005). Production of chemokines by perivascular adipose tissue: a role in the pathogenesis of atherosclerosis? *Arterioscler. Thromb. Vasc. Biol.* 25, 2594–2599. doi: 10.1161/01.atv.0000188508.40052.35

Horimatsu, T., Patel, A. S., Prasad, R., Reid, L. E., Benson, T. W., Zarzour, A., et al. (2018). Remote effects of transplanted perivascular adipose tissue on endothelial function and atherosclerosis. *Cardiovasc. Drugs Ther.* 32, 503–510. doi: 10.1007/s10557-018-6821-y

Huby, A. C., Otvos, L. Jr., and Belin de Chantemèle, E. J. (2016). Leptin induces hypertension and endothelial dysfunction via aldosterone-dependent mechanisms in obese female mice. *Hypertension* 67, 1020–1028. doi: 10.1161/hypertensionaha.115.06642

Hueso, M., De Ramon, L., Navarro, E., Ripoll, E., Cruzado, J. M., Grinyo, J. M., et al. (2016). Silencing of CD40 in vivo reduces progression of experimental atherogenesis through an NF-kappaB/miR-125b axis and reveals new potential mediators in the pathogenesis of atherosclerosis. *Atherosclerosis* 255, 80–89. doi: 10.1016/j.atherosclerosis.2016.11.002

Irie, D., Kawahito, H., Wakana, N., Kato, T., Kishida, S., Kikai, M., et al. (2015). Transplantation of periaortic adipose tissue from angiotensin receptor blocker-treated mice markedly ameliorates atherosclerosis development in apoE-/- mice. *J. Renin Angiotensin Aldosterone Syst.* 16, 67–78. doi: 10.1177/1470320314552434

Kagota, S., Iwata, S., Maruyama, K., McGuire, J. J., and Shinozuka, K. (2017). Time-dependent differences in the influence of perivascular adipose tissue on vasomotor functions in metabolic syndrome. *Metab. Syndr. Relat. Disord.* 15, 233–239. doi: 10.1089/met.2016.0146

Kanter, J. E., Goodspeed, L., Wang, S., Kramer, F., Wietecha, T., Gomes-Kjerulf, D., et al. (2018). 10,12 conjugated linoleic acid-driven weight loss is protective against atherosclerosis in mice and is associated with alternative macrophage enrichment in perivascular adipose tissue. *Nutrients* 10:1416. doi: 10.3390/nu10101416

Kawahito, H., Yamada, H., Irie, D., Kato, T., Akakabe, Y., Kishida, S., et al. (2013). Periaortic adipose tissue-specific activation of the renin-angiotensin system contributes to atherosclerosis development in uninephrectomized apoE-/- mice. *Am. J. Physiol. Heart Circ. Physiol.* 305, H667–H675. doi: 10.1152/ajpheart.00053.2013

Kim, S., Lee, E. S., Lee, S. W., Kim, Y. H., Lee, C. H., Jo, D. G., et al. (2019). Site-specific impairment of perivascular adipose tissue on advanced atherosclerotic plaques using multimodal nonlinear optical imaging. *Proc. Natl. Acad. Sci. U.S.A.* 116, 17765–17774. doi: 10.1073/pnas.1902007116

Kole, A., Cao, Y., Hui, J., Bolad, I. A., Alloosh, M., Cheng, J. X., et al. (2019). Comparative quantification of arterial lipid by intravascular photoacoustic-ultrasound imaging and near-infrared spectroscopy-intravascular ultrasound. *J. Cardiovasc. Transl. Res.* 12, 211–220. doi: 10.1007/s12265-018-9849-2

Kralova Lesna, I., Tonar, Z., Malek, I., Maluskova, J., Nedorost, L., Pirk, J., et al. (2015). Is the amount of coronary perivascular fat related to atherosclerosis? *Physiol. Res.* 64(Suppl. 3), S435–S443.

Krawczynska, A., Herman, A. P., Antushevich, H., Bochenek, J., Wojtulewicz, K., and Zieba, D. A. (2019). The influence of photoperiod on the action of exogenous leptin on gene expression of proinflammatory cytokines and their receptors in the thoracic perivascular adipose tissue (PVAT) in ewes. *Mediators Inflamm.* 2019:7129476. doi: 10.1155/2019/7129476

Lee, M. H., Chen, S. J., Tsao, C. M., and Wu, C. C. (2014). Perivascular adipose tissue inhibits endothelial function of rat aortas via caveolin-1. *PLoS One* 9:e99947. doi: 10.1371/journal.pone.0099947

Li, C., Li, S., Zhang, F., Wu, M., Liang, H., Song, J., et al. (2018). Endothelial microparticles-mediated transfer of microRNA-19b promotes atherosclerosis via activating perivascular adipose tissue inflammation in apoE(-/-) mice. *Biochem. Biophys. Res. Commun.* 495, 1922–1929. doi: 10.1016/j.bbrc.2017.11.195

Li, C., Wang, Z., Wang, C., Ma, Q., and Zhao, Y. (2015). Perivascular adipose tissue-derived adiponectin inhibits collar-induced carotid atherosclerosis by promoting macrophage autophagy. *PLoS One* 10:e0124031. doi: 10.1371/journal.pone.0124031

Li, H., Wang, Y. P., Zhang, L. N., and Tian, G. (2014). Perivascular adipose tissue-derived leptin promotes vascular smooth muscle cell phenotypic switching via p38 mitogen-activated protein kinase in metabolic syndrome rats. *Exp. Biol. Med. (Maywood)* 239, 954–965. doi: 10.1177/1535370214527903

Libby, P., Buring, J. E., Badimon, L., Hansson, G. K., Deanfield, J., Bittencourt, M. S., et al. (2019). Atherosclerosis. *Nat. Rev. Dis. Primers* 5:56. doi: 10.1038/s41572-019-0106-z

Lin, A., Dey, D., Wong, D. T. L., and Nerlekar, N. (2019). Perivascular adipose tissue and coronary atherosclerosis: from biology to Imaging phenotyping. *Curr. Atheroscler. Rep.* 21:47. doi: 10.1007/s11883-019-0817-3

Liu, G. Z., Liang, B., Lau, W. B., Wang, Y., Zhao, J., Li, R., et al. (2015). High glucose/high lipids impair vascular adiponectin function via inhibition of caveolin-1/AdipoR1 signalsome formation. *Free Radic. Biol. Med.* 89, 473–485. doi: 10.1016/j.freeradbiomed.2015.09.005

Liu, X., Wang, C. N., Qiu, C. Y., Song, W., Wang, L. F., and Liu, B. (2017). Adipocytes promote nicotine-induced injury of endothelial cells via the NF-kappaB pathway. *Exp. Cell. Res.* 359, 251–256. doi: 10.1016/j.yexcr.2017.07.022

Lu, D., Wang, W., Xia, L., Xia, P., and Yan, Y. (2017). Gene expression profiling reveals heterogeneity of perivascular adipose tissues surrounding coronary and internal thoracic arteries. *Acta Biochim. Biophys. Sin. (Shanghai)* 49, 1075–1082. doi: 10.1093/abbs/gmx113

Margaritis, M., Antonopoulos, A. S., Digby, J., Lee, R., Reilly, S., Coutinho, P., et al. (2013). Interactions between vascular wall and perivascular adipose tissue reveal novel roles for adiponectin in the regulation of endothelial nitric oxide synthase function in human vessels. *Circulation* 127, 2209–2221. doi: 10.1161/circulationaha.112.001133

Milutinovic, A., Suput, D., and Zorc-Pleskovic, R. (2019). Pathogenesis of atherosclerosis in the tunica intima, media, and adventitia of coronary arteries: an updated review. *Bosn. J. Basic Med. Sci.* 20, 21–30. doi: 10.17305/bjbms.2019.4320

Molica, F., Morel, S., Kwak, B. R., Rohner-Jeanrenaud, F., and Steffens, S. (2015). Adipokines at the crossroad between obesity and cardiovascular disease. *Thromb. Haemost.* 113, 553–566. doi: 10.1160/th14-06-0513

Mori, Y., Terasaki, M., Hiromura, M., Saito, T., Kushima, H., Koshibu, M., et al. (2019). Luseogliflozin attenuates neointimal hyperplasia after wire injury in

high-fat diet-fed mice via inhibition of perivascular adipose tissue remodeling. *Cardiovasc. Diabetol.* 18:143. doi: 10.1186/s12933-019-0947-5

Nagaraj, N., Matthews, K. A., Shields, K. J., Barinas-Mitchell, E., Budoff, M. J., and El Khoudary, S. R. (2015). Complement proteins and arterial calcification in middle aged women: cross-sectional effect of cardiovascular fat. The SWAN cardiovascular fat ancillary study. *Atherosclerosis* 243, 533–539. doi: 10.1016/j.atherosclerosis.2015.10.095

Negrotto, L., Farez, M. F., and Correale, J. (2016). Immunologic effects of metformin and pioglitazone treatment on metabolic syndrome and multiple sclerosis. *JAMA Neurol.* 73, 520–528. doi: 10.1001/jamaneurol.2015.4807

Noblet, J. N., Owen, M. K., Goodwill, A. G., Sassoon, D. J., and Tune, J. D. (2015). Lean and obese coronary perivascular adipose tissue impairs vasodilation via differential inhibition of vascular smooth muscle K+ channels. *Arterioscler. Thromb. Vasc. Biol.* 35, 1393–1400. doi: 10.1161/atvbaha.115.305500

Nosalski, R., and Guzik, T. J. (2017). Perivascular adipose tissue inflammation in vascular disease. *Br. J. Pharmacol.* 174, 3496–3513. doi: 10.1111/bph.13705

Numaguchi, R., Furuhashi, M., Matsumoto, M., Sato, H., Yanase, Y., Kuroda, Y., et al. (2019). Differential phenotypes in perivascular adipose tissue surrounding the internal thoracic artery and diseased coronary artery. *J. Am. Heart Assoc.* 8:e011147. doi: 10.1161/jaha.118.011147

Ohman, M. K., Luo, W., Wang, H., Guo, C., Abdallah, W., Russo, H. M., et al. (2011). Perivascular visceral adipose tissue induces atherosclerosis in apolipoprotein E deficient mice. *Atherosclerosis* 219, 33–39. doi: 10.1016/j.atherosclerosis.2011.07.012

Omar, A., Chatterjee, T. K., Tang, Y., Hui, D. Y., and Weintraub, N. L. (2014). Proinflammatory phenotype of perivascular adipocytes. *Arterioscler. Thromb. Vasc. Biol.* 34, 1631–1636. doi: 10.1161/atvbaha.114.303030

Padilla, J., Jenkins, N. T., Vieira-Potter, V. J., and Laughlin, M. H. (2013). Divergent phenotype of rat thoracic and abdominal perivascular adipose tissues. *Am. J. Physiol. Regul. Integr. Comp. Physiol.* 304, R543–R552. doi: 10.1152/ajpregu.00567.2012

Payne, G. A., Borbouse, L., Kumar, S., Neeb, Z., Alloosh, M., Sturek, M., et al. (2010). Epicardial perivascular adipose-derived leptin exacerbates coronary endothelial dysfunction in metabolic syndrome via a protein kinase C-beta pathway. *Arterioscler. Thromb. Vasc. Biol.* 30, 1711–1717. doi: 10.1161/atvbaha.110.210070

Payne, G. A., Tune, J. D., and Knudson, J. D. (2014). Leptin-induced endothelial dysfunction: a target for therapeutic interventions. *Curr. Pharm. Des.* 20, 603–608. doi: 10.2174/13816128113199990017

Primer, K. R., Psaltis, P. J., Tan, J. T. M., and Bursill, C. A. (2020). The role of high-density lipoproteins in endothelial cell metabolism and diabetes-impaired angiogenesis. *Int. J. Mol. Sci.* 21:3633. doi: 10.3390/ijms21103633

Quesada, I., Cejas, J., Garcia, R., Cannizzo, B., Redondo, A., and Castro, C. (2018). Vascular dysfunction elicited by a cross talk between periaortic adipose tissue and the vascular wall is reversed by pioglitazone. *Cardiovasc. Ther.* 36:e12322. doi: 10.1111/1755-5922.12322

Quinn, C. E., Lockhart, C. J., Hamilton, P. K., Loughrey, C. M., and McVeigh, G. E. (2010). Effect of pioglitazone on endothelial function in impaired glucose tolerance. *Diabetes Obes. Metab.* 12, 709–715. doi: 10.1111/j.1463-1326.2010.01224.x

Randrianarisoa, E., Stefan, N., Fritsche, A., Reis-Damaschk, N., Hieronimus, A., Balletshofer, B., et al. (2018). Periaortic adipose tissue compared with peribrachial adipose tissue mass as markers and possible modulators of cardiometabolic risk. *Angiology* 69, 854–860. doi: 10.1177/0003319718755581

Ren, L., Wang, L., You, T., Liu, Y., Wu, F., Zhu, L., et al. (2019). Perivascular adipose tissue modulates carotid plaque formation induced by disturbed flow in mice. *J. Vasc. Surg.* 70, 927–936.e924. doi: 10.1016/j.jvs.2018.09.064

Reynes, B., van Schothorst, E. M., Garcia-Ruiz, E., Keijer, J., Palou, A., and Oliver, P. (2017). Cold exposure down-regulates immune response pathways in ferret aortic perivascular adipose tissue. *Thromb. Haemost.* 117, 981–991. doi: 10.1160/th16-12-0931

Rossi, C., Santini, E., Chiarugi, M., Salvati, A., Comassi, M., Vitolo, E., et al. (2014). The complex P2X7 receptor/inflammasome in perivascular fat tissue of heavy smokers. *Eur. J. Clin. Invest.* 44, 295–302. doi: 10.1111/eci.12232

Salim, H. M., Fukuda, D., Higashikuni, Y., Tanaka, K., Hirata, Y., Yagi, S., et al. (2017). Teneligliptin, a dipeptidyl peptidase-4 inhibitor, attenuated pro-inflammatory phenotype of perivascular adipose tissue and inhibited atherogenesis in normoglycemic apolipoprotein-E-deficient mice. *Vascul. Pharmacol.* 9, 19–25. doi: 10.1016/j.vph.2017.03.003

Schlett, C. L., Massaro, J. M., Lehman, S. J., Bamberg, F., O'Donnell, C. J., Fox, C. S., et al. (2009). Novel measurements of periaortic adipose tissue in comparison to anthropometric measures of obesity, and abdominal adipose tissue. *Int. J. Obes. (Lond.)* 33, 226–232. doi: 10.1038/ijo.2008.267

Schutz, E., Gogiraju, R., Pavlaki, M., Drosos, I., Georgiadis, G. S., Argyriou, C., et al. (2019). Age-dependent and -independent effects of perivascular adipose tissue and its paracrine activities during neointima formation. *Int. J. Mol. Sci.* 21:282. doi: 10.3390/ijms21010282

Sena, C. M., Pereira, A., Fernandes, R., Letra, L., and Seica, R. M. (2017). Adiponectin improves endothelial function in mesenteric arteries of rats fed a high-fat diet: role of perivascular adipose tissue. *Br. J. Pharmacol.* 174, 3514–3526. doi: 10.1111/bph.13756

Shields, K. J., Barinas-Mitchell, E., Gingo, M. R., Tepper, P., Goodpaster, B. H., Kao, A. H., et al. (2013). Perivascular adipose tissue of the descending thoracic aorta is associated with systemic lupus erythematosus and vascular calcification in women. *Atherosclerosis* 231, 129–135. doi: 10.1016/j.atherosclerosis.2013.09.004

Shields, K. J., Stolz, D., Watkins, S. C., and Ahearn, J. M. (2011). Complement proteins C3 and C4 bind to collagen and elastin in the vascular wall: a potential role in vascular stiffness and atherosclerosis. *Clin. Transl. Sci.* 4, 146–152. doi: 10.1111/j.1752-8062.2011.00304.x

Skiba, D. S., Nosalski, R., Mikolajczyk, T. P., Siedlinski, M., Rios, F. J., Montezano, A. C., et al. (2017). Anti-atherosclerotic effect of the angiotensin 1-7 mimetic AVE0991 is mediated by inhibition of perivascular and plaque inflammation in early atherosclerosis. *Br. J. Pharmacol.* 174, 4055–4069. doi: 10.1111/bph.13685

Skilton, M. R. (2019). Revisiting carotid imaging: integrating atherosclerosis, the adventitia, and perivascular adipose tissue. *Kardiol. Pol.* 77, 1005–1006. doi: 10.33963/kp.15066

Srikakulapu, P., Upadhye, A., Rosenfeld, S. M., Marshall, M. A., McSkimming, C., Hickman, A. W., et al. (2017). Perivascular adipose tissue harbors atheroprotective IgM-producing B cells. *Front. Physiol.* 8:719. doi: 10.3389/fphys.2017.00719

Sun, B., Yang, D., Yin, Y. Z., and Xiao, J. (2020). Estrogenic and anti-inflammatory effects of pseudoprotodioscin in atherosclerosis-prone mice: insights into endothelial cells and perivascular adipose tissues. *Eur. J. Pharmacol.* 869:172887. doi: 10.1016/j.ejphar.2019.172887

Szasz, T., and Webb, R. C. (2012). Perivascular adipose tissue: more than just structural support. *Clin. Sci. (Lond.)* 122, 1–12. doi: 10.1042/cs20110151

Tang, Y., He, Y., Li, C., Mu, W., Zou, Y., Liu, C., et al. (2018). RPS3A positively regulates the mitochondrial function of human periaortic adipose tissue and is associated with coronary artery diseases. *Cell Discov.* 4:52. doi: 10.1038/s41421-018-0041-2

Terada, K., Yamada, H., Kikai, M., Wakana, N., Yamamoto, K., Wada, N., et al. (2018). Transplantation of periaortic adipose tissue inhibits atherosclerosis in apoE(-/-) mice by evoking TGF-beta1-mediated anti-inflammatory response in transplanted graft. *Biochem. Biophys. Res. Commun.* 501, 145–151. doi: 10.1016/j.bbrc.2018.04.196

Tousoulis, D., Oikonomou, E., Economou, E. K., Crea, F., and Kaski, J. C. (2016). Inflammatory cytokines in atherosclerosis: current therapeutic approaches. *Eur. Heart J.* 37, 1723–1732. doi: 10.1093/eurheartj/ehv759

Van de Voorde, J., Pauwels, B., Boydens, C., and Decaluwe, K. (2013). Adipocytokines in relation to cardiovascular disease. *Metabolism* 62, 1513–1521. doi: 10.1016/j.metabol.2013.06.004

Verhagen, S. N., Buijsrogge, M. P., Vink, A., van Herwerden, L. A., van der Graaf, Y., and Visseren, F. L. (2014). Secretion of adipocytokines by perivascular adipose tissue near stenotic and non-stenotic coronary artery segments in patients undergoing CABG. *Atherosclerosis* 233, 242–247. doi: 10.1016/j.atherosclerosis.2013.12.005

Verhagen, S. N., Rutten, A., Meijs, M. F., Isgum, I., Cramer, M. J., van der Graaf, Y., et al. (2013). Relationship between myocardial bridges and reduced coronary atherosclerosis in patients with angina pectoris. *Int. J. Cardiol.* 167, 883–888. doi: 10.1016/j.ijcard.2012.01.091

Verhagen, S. N., Vink, A., van der Graaf, Y., and Visseren, F. L. (2012). Coronary perivascular adipose tissue characteristics are related to atherosclerotic plaque size and composition. A post-mortem study. *Atherosclerosis* 225, 99–104. doi: 10.1016/j.atherosclerosis.2012.08.031

Victorio, J. A., da Costa, R. M., Tostes, R. C., and Davel, A. P. (2020). Modulation of vascular function by perivascular adipose tissue: sex differences. *Curr. Pharm. Des.* 26, 3768–3777. doi: 10.2174/1381612826666200701211912

Victorio, J. A., Fontes, M. T., Rossoni, L. V., and Davel, A. P. (2016). Different anti-contractile function and nitric oxide production of thoracic and abdominal perivascular adipose tissues. *Front. Physiol.* 7:295. doi: 10.3389/fphys.2016.00295

Vieira-Potter, V. J., Lee, S., Bayless, D. S., Scroggins, R. J., Welly, R. J., Fleming, N. J., et al. (2015). Disconnect between adipose tissue inflammation and cardiometabolic dysfunction in Ossabaw pigs. *Obesity (Silver Spring)* 23, 2421–2429. doi: 10.1002/oby.21252

Virdis, A. (2016). Endothelial dysfunction in obesity: role of inflammation. *High Blood Press. Cardiovasc. Prev.* 23, 83–85. doi: 10.1007/s40292-016-0133-8

Wakana, N., Irie, D., Kikai, M., Terada, K., Yamamoto, K., Kawahito, H., et al. (2015). Maternal high-fat diet exaggerates atherosclerosis in adult offspring by augmenting periaortic adipose tissue-specific proinflammatory response. *Arterioscler. Thromb. Vasc. Biol.* 35, 558–569. doi: 10.1161/atvbaha.114.305122

Wang, C. N., Yang, G. H., Wang, Z. Q., Liu, C. W., Li, T. J., Lai, Z. C., et al. (2016). Role of perivascular adipose tissue in nicotineinduced endothelial cell inflammatory responses. *Mol. Med. Rep.* 14, 5713–5718. doi: 10.3892/mmr.2016.5934

Wang, H., Luo, W., Wang, J., Guo, C., Wang, X., Wolffe, S. L., et al. (2012). Obesity-induced endothelial dysfunction is prevented by deficiency of P-selectin glycoprotein ligand-1. *Diabetes* 61, 3219–3227. doi: 10.2337/db12-0162

Wang, X., Lin, Y., Luo, N., Chen, Z., Gu, M., Wang, J., et al. (2014). Short-term intensive atorvastatin therapy improves endothelial function partly via attenuating perivascular adipose tissue inflammation through 5-lipoxygenase pathway in hyperlipidemic rabbits. *Chin. Med. J. (Engl.)* 127, 2953–2959.

Werner, C., Kamani, C. H., Gensch, C., Böhm, M., and Laufs, U. (2007). The peroxisome proliferator-activated receptor-gamma agonist pioglitazone increases number and function of endothelial progenitor cells in patients with coronary artery disease and normal glucose tolerance. *Diabetes* 56, 2609–2615. doi: 10.2337/db07-0069

Wihastuti, T. A., Aini, F. N., Tjahjono, C. T., and Heriansyah, T. (2019). Dietary ethanolic extract of *Mangosteen* pericarp reduces VCAM-1, perivascular adipose tissue and aortic intimal medial thickness in hypercholesterolemic rat model. *Open Access Maced. J. Med. Sci.* 7, 3158–3163. doi: 10.3889/oamjms.2019.717

Xiong, W., Zhao, X., Garcia-Barrio, M. T., Zhang, J., Lin, J., Chen, Y. E., et al. (2017). MitoNEET in perivascular adipose tissue blunts atherosclerosis under mild cold condition in mice. *Front. Physiol.* 8:1032. doi: 10.3389/fphys.2017.01032

Xiong, W., Zhao, X., Villacorta, L., Rom, O., Garcia-Barrio, M. T., Guo, Y., et al. (2018). Brown adipocyte-specific PPARgamma (peroxisome proliferator-activated receptor gamma) deletion impairs perivascular adipose tissue development and enhances atherosclerosis in mice. *Arterioscler. Thromb. Vasc. Biol.* 38, 1738–1747. doi: 10.1161/atvbaha.118.311367

Ying, R., Li, S. W., Chen, J. Y., Zhang, H. F., Yang, Y., Gu, Z. J., et al. (2018). Endoplasmic reticulum stress in perivascular adipose tissue promotes destabilization of atherosclerotic plaque by regulating GM-CSF paracrine. *J. Transl. Med.* 16:105. doi: 10.1186/s12967-018-1481-z

Conflict of Interest: The authors declare that the research was conducted in the absence of any commercial or financial relationships that could be construed as a potential conflict of interest.

frontiers in Pharmacology

MINI REVIEW
published: 12 February 2021
doi: 10.3389/fphar.2021.626155

The Role of Periprostatic Adipose Tissue on Prostate Function in Vascular-Related Disorders

Gabriela Reolon Passos[‡], *Ana Carolina Ghezzi*[‡], *Edson Antunes, Mariana Gonçalves de Oliveira and Fabiola Zakia Mónica*[*†]

Department of Pharmacology, Faculty of Medical Sciences, University of Campinas (UNICAMP), Campinas, Brazil

The lower urinary tract symptoms (LUTS) secondary to benign prostatic hyperplasia (BPH) are highly prevalent worldwide. Clinical and experimental data suggest that the incidence of LUTS-BPH is higher in patients with vascular-related disorders such as in pelvic ischemia, obesity and diabetes as well as in the ageing population. Obesity is an important risk factor that predisposes to glucose intolerance, insulin resistance, dyslipidemia, type 2 diabetes mellitus and cardiovascular disorders. Prospective studies showed that obese men are more likely to develop LUTS-BPH than non-obese men. Yet, men with greater waist circumferences were also at a greater risk of increased prostate volume and prostate-specific antigen than men with lower waist circumference. BPH is characterized by an enlarged prostate and increased smooth muscle tone, thus causing urinary symptoms. Data from experimental studies showed a significant increase in prostate and epididymal adipose tissue weight of obese mice when compared with lean mice. Adipose tissues that are in direct contact with specific organs have gained attention due to their potential paracrine role. The prostate gland is surrounded by periprostatic adipose tissue (PPAT), which is believed to play a paracrine role by releasing growth factors, pro-inflammatory, pro-oxidant, contractile and anti-contractile substances that interfere in prostate reactivity and growth. Therefore, this review is divided into two main parts, one focusing on the role of adipokines in the context of obesity that can lead to LUTS/BPH and the second part focusing on the mediators released from PPAT and the possible pathways that may interfere in the prostate microenvironment.

Keywords: prostate, periprostatic adipose tissue, obesity, adipokines, benign prostate hyperplasia

OPEN ACCESS

Edited by:
Thiago Bruder Do Nascimento, University of Pittsburgh, United States

Reviewed by:
Martin Hennenberg, Hospital of the University of Munich, Germany
Cees Korstanje, Consultant, Nieuw-Vennep, Netherlands

***Correspondence:**
Fabiola Zakia Mónica
fabiolataufic@gmail.com

[†]***ORCID:***
Fabiola Zakia Mónica
orcid.org/0000-0002-8449-6677

[‡]*These authors have contributed equally to this work*

Specialty section:
This article was submitted to Cardiovascular and Smooth Muscle Pharmacology, a section of the journal Frontiers in Pharmacology

Received: *05 November 2020*
Accepted: *11 January 2021*
Published: *12 February 2021*

Citation:
Passos GR, Ghezzi AC, Antunes E, de Oliveira MG and Mónica FZ (2021) The Role of Periprostatic Adipose Tissue on Prostate Function in Vascular-Related Disorders. Front. Pharmacol. 12:626155. doi: 10.3389/fphar.2021.626155

INTRODUCTION

The prostate gland is a reproductive organ whose main function is to secrete an alkaline fluid that, along with sperm cells from the testicles and fluids from other glands, makes up the semen (Verze et al., 2016). The human prostate is divided into three zones, according to John McNeal (McNeal 1984), namely the peripheral zone (contains the majority of glandular tissue), the central zone (surrounds the ejaculatory ducts) and the transition zone (surrounds the urethra just beneath the bladder). The enlargement of the transition zone is considered the main cause of benign prostatic hyperplasia (BPH) in ageing men and is one of the main causes of lower urinary tract symptoms (LUTS) (Roehrborn 2008; D'Ancona et al., 2019).

LUTS refer to a group of clinical symptoms that involve the bladder, urinary sphincter, urethra and, in men, prostate. LUTS are divided into three main groups that are storage, voiding and post

micturition symptoms. *Storage symptoms* are observed during the storage phase of the bladder and can be classified into i) general storage symptoms, ii) sensory symptoms and iii) incontinence symptoms. *Voiding symptoms* are LUTS experienced during micturition (hesitancy, episodic inability to void, straining to void, slow stream, intermittency, terminal dribbling, spraying, dysuria, hematuria, pneumaturia and urinary retention) (**Figure 1A**). Post-micturition symptoms are experienced after voiding ceases and are characterized by a feeling of incomplete bladder emptying, a need to immediately re-void, post-void incontinence and post-micturition urgency (D'Ancona et al., 2019). The prevalence of LUTS is over 60% in men and women aged > 40 years (Irwin et al., 2006; Coyne et al., 2009) and are also associated with various modifiable risk factors such as obesity, diabetes, and metabolic syndrome (Gacci et al., 2015; Chughtai et al., 2016). LUTS interfere in the quality of life, sexual quality, social functioning and productivity at work. The therapeutic management of LUTS secondary to BPH is aimed at relaxing the bladder (antimuscarinics, beta-3 adrenoceptors agonist) and/or prostatic smooth muscle (alpha-1 antagonists, phosphodiesterase type 5 inhibitors) and to inhibit prostate proliferation (5-alpha reductase inhibitors) (Morelli et al., 2011; Mónica and De Nucci, 2019).

The overproduction of testicular androgens is considered a key step in the development of BPH. The enzyme 5-alpha reductase type 2 converts testosterone into dihydrotestosterone (DHT), the main intraprostatic androgen. The imbalance between cell proliferation and cell death is a proposed mechanism for BPH progression (Carson and Rittmaster, 2003). DHT, which is more potent than testosterone, translocates to the nucleus and favors the transcription of several growth factors such as keratinocyte growth factor, epidermal growth factor and insulin-like growth factor (Chughtai et al., 2016).

Clinical and experimental data show a greater prevalence of LUTS in patients who present metabolic disorders that predispose to various diseases including obesity and BPH. The prostate gland is surrounded by the periprostatic adipose tissue (PPAT), which is believed to play a paracrine role by releasing anti-and pro-inflammatory substances, growth factors, contractile and anti-contractile substances. Therefore, this review is divided into two main parts, one highlighting the role of adipokines in the context of obesity that can lead to LUTS/BPH and the second part the role of substances released from PPAT that may facilitate the development of prostate growth.

OBESITY AS RISK FACTOR

Obesity is an epidemic health problem worldwide. A 20% increase in body weight increases significantly the risk of developing insulin resistance, dyslipidemia, type 2 diabetes mellitus and other cardiovascular diseases (World Health Organization, 2002). A strong association between heritability and obesity (Friedman, 2016; Chiurazzi et al., 2020; Lan et al., 2020) and low-grade systemic inflammation (Xu et al., 2003; Hotamisligil 2006) also exist. Adipokines which are released from adipose tissue, may also engage cells of the immune system that can also contribute to the chronic inflammatory state seen in obesity (Bouloumié et al., 2005).

Mice and rats fed with a high fat diet showed marked increases in the body and prostate weights (Silva et al., 2015; Calmasini et al., 2018), along with larger number of cells and blood vessels in the ventral prostate when compared to the prostates from lean animals (Silva, et al., 2015). *In vitro* studies reported a hypercontractile state of the prostate smooth muscle from obese animals as characterized by greater contraction induced by transmural stimulation or by direct activation of alpha-1-adrenoceptors (Silva, et al., 2015; Calmasini, et al., 2018). Another study has identified increased levels of phosphorylated-ERK (Extracellular Signal-Regulated Kinases) in the prostate from hyperinsulinemic rats fed with a high fat diet, suggesting an involvement of the MERK/ERK (Mitogen-activated protein kinases/Extracellular signal-regulated kinases) pathway in the prostate growth (Vikram et al., 2010).

The inflammatory microenvironment favors the proliferation of epithelial and stromal cells in BPH pathogenesis. Meng et al., 2020, included 77 patients (±69 years) with BPH who underwent transurethral prostatic resection and no report of LUTS complaint. In all biopsy samples, inflammatory infiltrates were identified. The predominant cell type was T lymphocytes, which were identified in 96% of samples, followed by B lymphocytes (77%) and macrophages (52.6%). Individuals with a waist circumference more than 100 cm had a higher incidence of moderate/severe LUTS, evaluated by an International Prostate Symptoms Score (IPSS) greater than eight for the initiation of the treatment of BPH, erectile and ejaculatory dysfunction, as well as a greater propensity to increased prostate volume (Penson et al., 2011). In Sweden, a survey with 27,858 men showed that participants exhibiting the highest abdominal obesity ratio were 22% more likely to suffer moderate to severe LUTS. Furthermore, for every 5-unit increase in BMI the risk of developing severe LUTS secondary to BPH increased by 13% as evaluated by IPSS (Laven et al., 2008).

THE ADIPOSE TISSUE

Three types of adipocytes are identified, commonly classified based on their morphology and function. The White Adipose Tissue (WAT), composed by a unilocular lipid droplet that occupies > 95% of the adipocyte, is composed of non-thermogenic and energy-storing type of fat cells. Brown Adipose Tissue (BAT), composed of multilocular lipid droplets dispersed in a mitochondrial rich cytoplasm, acts in thermogenesis, which is mediated by uncoupling protein 1 (UCP-1) (Jeremic et al., 2017; Lu et al., 2020). Beige adipose tissue has now been identified as a cluster in WAT, with multilocular/unilocular morphology and able to both store and spend energy (Cheng et al., 2019; Mao et al., 2020).

The stimulation of beta-adrenoceptors (ARs) in the WAT and BAT is crucial for the activation of thermogenic pathways. The beta- ARs are the main adrenergic receptors involved in pathways related to WAT browning and BAT thermogenesis, although the

subtypes involved differ between species. For example, in rodents, beta3-AR agonists increase lipolysis, fat oxidation and energy expenditure (Galitzky et al., 1993; Uehling et al., 2006; Michel and Korstanje, 2016; Hao et al., 2019), thus leading to the belief that this class of substances would be effective in the treatment of diabetes and obesity. However, in humans, lipolysis occurs mainly via beta-1AR (Rosenbaum et al., 1993; Barbe et al., 1996; Michel and Korstanje, 2016). The differences between species (rodents vs human), the lack of selective tools (antibodies, agonists and antagonists) to differentiate beta3-AR over beta1-/beta2-ARs and the absence of clinical data make beta3-AR agonists ineffective in the treatment of obesity and type 2 diabetes. On the other hand, in the human bladder, beta3-AR is the main subtype that induces smooth muscle relaxation (Nomiya and Yamaguchi, 2003). To date, mirabegron, a beta3-AR agonist is used to treating patients with overactive bladder.

ADIPOSE TISSUE IN OBESITY

Under conditions of over-nutrition, an expansion of WAT, a remodeling of extracellular matrix components and blood vasculature, along with an enhanced secretion of pro-inflammatory mediators all contribute to local and systemic inflammation (Vgontzas et al., 2000). Adipose tissue is mainly formed by adipocytes, but other cell types also contribute to its growth and function such as pre-adipocytes, lymphocytes, macrophages, fibroblasts and vascular cells (Tilg and Moschen, 2006; Ouchi et al., 2011). WAT exerts endocrine and paracrine functions by releasing peptides, non-peptides and cytokines called adipokines. Adipokines have highly diverse chemical structures and physiological functions. For example, some adipokines are involved in inflammation such as the cytokines; Tumor Necrosis Factor - alpha (TNF-α), interleukin-1 [IL-1], IL-6, monocyte chemoattractant protein-1 (MCP-1) while others regulate feeding behaviour through the central nervous system (leptin), sensitize insulin (adiponectin) or have anti-inflammatory properties (adiponectin, secreted frizzled-related proteins) (Ouchi et al., 2011). In humans, leptin, adiponectin, resistin and visfatin are key adipokines that work as hormones to interfere in energy haemostasis and to regulate neuroendocrine function. Adipokines that have cytokine properties interfere mainly in immunological and inflammatory processes, both locally and systemically (La Cava and Matarese, 2004; Kusminski et al., 2007; Tilg and Moschen, 2006; Carr and Rodeo, 2019; Smith et al., 2020).

Leptin, along with adiponectin, are the main adipokines released from the adipose tissue, although they are not all exclusively derived from this organ. In mammals, the action of leptin in the central nervous system reduces food intake and increases energy expenditure, in addition to regulating neuroendocrine function and glucose and fat metabolism (Friedman, 1997). Animals that are leptin-deficient present defects in the neuroendocrine axis, are infertile or subfertile and present greater levels of corticosterone. Male ob/ob mice treated with leptin for 15 and 75 days were used to evaluate energy expenditure thorough food intake and body composition. The body mass of ob/ob mice decreased around 30% in 15 days of leptin treatment and the food consumption of the animals was reduced by about 95%. Leptin-induced reduction of food intake ceased during treatment with leptin over 75 days, when the lipid reserves of the mice were depleted and energy expenditure became similar to that in control mice (Rafael and Herling 2000). In mice, the activation of sympathetic efferent nerves to adipose tissue was seen to be involved in the leptin-induced lipolysis in WAT (Zeng et al., 2015). While in mice a defect in leptin axis promotes hyperphagia and a decrease in energy expenditure, in humans, leptin acts mainly on appetite (Friedman, 2016). However, obese individuals have elevated plasma leptin in comparison with non-obese individuals. The hyperleptinemia found in obese individuals is attributed to alterations in the leptin receptor or a deficiency in its transport, a phenomenon called leptin resistance (Considine et al., 1996). The beneficial effects of the treatment with leptin in obese patients are controversial. Four weeks treatment of exogenous leptin in both eutrophic and obese individuals reduced body weight (Friedman and Hallas, 1998), however, this effect was only observed in those individuals who did not present hyperleptinemia, as the administration of leptin in obese patients resistant to leptin did not produce a significant weight loss (Maffei et al., 1995; Lee et al., 2002). Leptin receptors are also found in endothelial cells and may induce reactive oxidative stress, which can aggravate cardiometabolic problems (Bouloumie et al., 1999; Yamagishi et al., 2001).

Adiponectin, in turn, has a cardioprotective role (Matsubara et al., 2002). He et al., 2016 showed that TNF-α impairs adiponectin multimerization and, consequently, decreases adiponectin secretion both *in vitro* and *in vivo*. Adiponectin overexpression in leptin-deficient *ob/ob* mice induces the redirection of adipose tissue deposits from the visceral region to the subcutaneous region, promoting an improvement in blood glucose, systemic insulin sensitivity, dyslipidemia and inflammation (Kim et al., 2007). The cardioprotective effect promoted by adiponectin has been partially explained by its anti-inflammatory role. In co-culture of human skeletal muscle cells with human adipocytes adiponectin negatively modulates the release of IL-6, IL-8 TNF-α and MCP-1 in the adipose tissue, which are linked to insulin resistance (Dietze-Schroeder et al., 2005). Adiponectin also releases IL-10 secretion, an anti-inflammatory cytokine that plays an important role in the polarization of macrophages to the M2 profile (Kumada et al., 2004).

ROLE OF ADIPOKINES IN PROSTATE GROWTH

Inflammatory cells release cytokines and growth factors that may contribute to prostate growth (Steiner et al., 2003; Delongchamps et al., 2008). For instance, in primary culture of prostatic epithelial cells, IL-8 increased the expression of the fibroblast growth factor (FGF) and its blockade reduced the production of FGF. In specimens from patients with BPH, the expression of IL-8 was greater in epithelial cells than in normal prostate (Giri and

Ittmann, 2001). The levels of IL-8 and its receptors were up-regulated in BPH tissues when compared to normal tissues. In BPH-1 cells, the IL-8 axis was increased in comparison with normal epithelial cells and the deletion of its receptor, CXR7 inhibited the growth (Smith et al., 2020). A study with normal, BPH and PCa prostate tissue found greater expression of IL-1 and IL-6 in specimens from BPH and PC samples in the epithelial and stromal compartments, thus suggesting that these cytokines may play a role in epithelial hyperplasia (Mechergui et al., 2009).

Prostates removed from leptin-deficient ob/ob male mice that received testosterone (3 mg/kg for 14 days) to induce BPH, showed a smaller proportion of glandular lumen and reduced collagen deposition in comparison to prostates from control and ob/ob mice. Because extracellular deposition and glandular hyperplasia are typical patterns of BPH, these results suggest that leptin deficiency attenuated morphological changes and collagen deposition. Yet, prostates from ob/ob + testosterone exhibited greater levels of E-cadherin and lower levels of vimentin in comparison to the testosterone control group. These results suggested that leptin may function as a facilitator of the epithelial-mesenchymal transition (EMT) to favor BPH progression (Zhang et al., 2020).

The receptors for adiponectin; AdipoR1 and AdipoR2 are expressed in normal epithelial and stromal cells lines (RPWE and WPMY1), as well as in the stroma and epithelium in specimens from BPH. *In vitro* addition of adiponectin in RPWE and WPMY1 cells arrested cells in G0 phase and induced apoptosis by increasing the expression of caspase-3. In obese mice fed with a high-fat diet, treatment with recombinant adiponectin for 14 days protected the prostate from histologic BPH, thus showing that adiponectin reduced prostate growth (Fu et al., 2017).

RELATIONSHIP BETWEEN PERIPROSTATIC ADIPOSE TISSUE AND PROSTATE GROWTH

Adipose tissues that are in direct contact with specific organs have gained attention due to their potential paracrine role. Among them are perivascular adipose tissue (PVAT), which comprises 3% of all adipose tissue mass and surrounds the vessels (Szasz et al., 2013), and PPAT, which surrounds the prostate and the prostatic urethra. The anatomic distribution of PPAT was evaluated in radical prostatectomy specimens. The presence of PPAT was along 48% of the prostate surface, of that 57-59% present PPAT on the right and lateral surface and 44% and 36% along the anterior and posterior region, respectively (Hong et al., 2003). PPAT can have similar characteristics to PVAT by releasing pro-inflammatory cytokines (resistin, IL-6, TNF-α, MCP-1, chemerin, progranulin) (Blüher 2013; Alexandre et al., 2018), growth factors (progranulin and chemerin) (Klöting et al., 2010), contractile (angiotensin II, superoxide generation) (Lu et al., 2010) and anti-contractile (leptin, adiponectin, H_2O_2, ADRF and NO) (Victorio et al., 2016; Araujo et al., 2018) substances (**Figure 1B**).

Most studies that have evaluated the role of substances released from PPAT on prostate focused on cancer. Although that there is no evidence to suggest that men with LUTS due to BPH are at an increased risk of prostate cancer, in this section we focused only on experimental studies that evaluated the possible interplay between PPAT and BPH due to word limit. More information about PPAT in cancer can be seen in the studies conducted by Finley et al., 2009 and Ribeiro et al., 2012 (**Table 1**).

In obese mice, the area of PPAT and the gene expression for NADPH oxidase 2 (NOX 2) and TNF-α were all higher than in the lean mice. Although this study did not evaluate the impact of PPAT on the prostate, it strongly suggests that PPAT may release pro-inflammatory and pro-oxidant substances that could interfere in prostate contractility (Alexandre et al., 2018).

The secretome derived from conditioned media from PPAT (PPAT-CM) obtained from patients with prostate cancer and BPH were assessed. The authors observed that the amount of protein in PPAT-CM derived from patients with prostate cancer stage 3 (PCa-T3) were significantly higher, relative to CM-PCaT2 and CM-BPH. Proteins related to lipid transport and adipogenesis were detected in all three CM. Regarding pathways related to biological functions, the integrin family cell surface interaction, homeostatic pathway and TNF-related apoptosis-inducing ligand/Apo-2L (TRAIL) signaling pathway were the most enriched pathways for CM-T3, CM-T2 and CM-BPH, respectively, which means that in the case of cancer cells, overexpression of these biological pathways is related to cell adhesion, migration and invasiveness (Sacca et al., 2019). In this study it is not possible to know the source of these proteins, as in PPAT-CM there are different cell types. According to the study above, TRAIL was the most enriched biological pathway observed in CM-BPH. In a cell line from the epithelium of a hyperplasic prostate, BPH-1 cells, which express low abundance of the protein DJ-1 (a protein involved in transcriptional regulation, antioxidative stress reaction and chaperone) in comparison with cancer cells (LNCaP, Du145, PC-3), the addition of increasing concentrations of TRAIL correlated with an increased the expression of DJ-1. Yet the accumulation of TRAIL increased DJ-1 in treated BPH-1 cells, occurred in a time-dependent manner, reaching its peak after 25 min. These results suggest that DJ-1 plays a role in the control of apoptosis (Hod, 2004).

FINAL REMARKS: POTENTIAL THERAPIES TARGETING ADIPOSE TISSUE

Cardiometabolic risk factors affect the function of different adipose tissue deposits. Ageing, sex steroid hormones, metabolic syndrome, cardiovascular diseases, inflammation and obesity are modifiable and non-modifiable risk factors that contribute to the pathogenesis of BPH. Obesity is a component of metabolic syndrome and both are associated with systemic and local inflammation. PPAT, which surrounds part of the prostate surface, has been implicated in the release

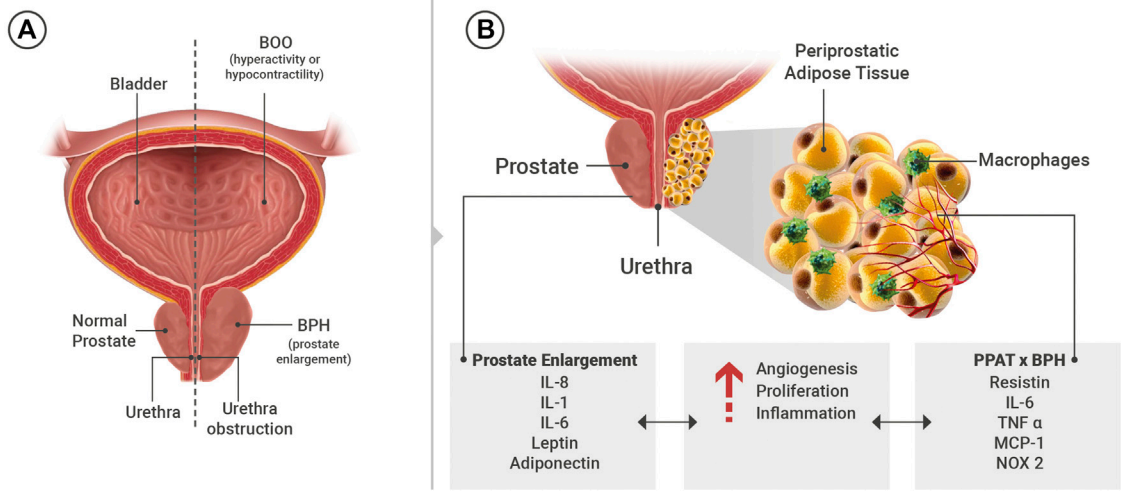

FIGURE 1 | (A) General scheme showing the organs of the lower urinary tract. **(B)** Substances present in the systemic circulation and/or released from periprostatic adipose tissue (PPAT) that may interfere in the prostate microenvironment such as angiogenesis, proliferation and inflammation. IL: interleukins, TNF: tumor necrosis factor-α, NADPH oxidase 2 (NOX 2), MCP-1: monocyte chemoattractant protein-1.

TABLE 1 | Major pre-clinical and clinical findings linking the role of PPAT, adipokines and lower urinary tract dysfunction.

Specie	Protocol design	Key results	Reference
Human	Specimens from patients with BPH	The inflammation associated with BPH is characterized by greater number of T-cells and greater expression of the cytokine IL-1.	Steiner et al. (2003)
Human	PPAT anatomic distribution	Presence of PPAT was along the 48% of prostate surface, of that 57-59% represent the PPAT on the right and lateral surface, 44% and 36% along the anterior and posterior region, respectively.	Hong et al. (2003)
Human	Normal, BPH and PCa prostate tissue	Greater expression of IL-1 and IL-6 in specimens from BPH and PC sample in the epithelial and stromal compartments in comparison with normal prostate.	Mechergui et al. (2009)
Human	PPAT explants from patients with prostate cancer	Higher secretion of IL-6 from PPAT, which was correlated with higher tumor grade. Increased phosphorilation in Jak/Stat, Akt/mTOR and NFκB pathways identified as IL-6 downstream.	Finley et al. (2009)
Human	Cultured PPAT and stromal vascular fraction (SVF) from BPH patients	In PPAT explants increased proteolitic activities and up-regulation of MMP2 and MMP9 in comparison with SVF	Ribeiro et al. 2012
Human	Prostate cancer cells lines	PPAT supernatants-derived factors increased migration of both PC3 and LNCaP cells, while PPAT had a strong proliferative effect on PC3.	Ribeiro et al. (2012)
Human and mice	RPWE and WPMY1 and in specimens from patients with BPH.	Addition of adiponectin in RPWE and WPMY1 cells arrested cells in G_0 phase and induced apoptosis. Long-term treatment with adiponectin protected the prostate from histologic BPH in obese mice	Fu et al. (2017)
Mouse	Urethral smooth muscle from high fat diet-induced obesity	Obese mice exhibited urethral hypercontractility and reduced NO-induced relaxation response along with increased PPAT size, higher ROS generation besides NOX2 and TNFα overexpression.	Alexandre et al. (2018)
Human	Conditioned media from PPAT obtained from patients with prostate cancer and BPH	The integrin family cells surface interaction, homeostasis pathway and TRAIL signaling pathway were the most enriched pathway for CM-T3, CM-T2 and CM-BPH, respectively.	Sacca et al. (2019)
Human	BPH patients and BPH-1 cells	The levels of IL-8 and its receptors were up-regulated in BPH tissues when compared to normal tissues. In BPH-1 cells the IL-8 axis was increased in comparison with normal epithelial cells and the deletion of its receptor, CXR7 inhibited the growth by 50%	Smith et al. (2020)
Human and mice	Prostates from ob/ob mice that received testosterone and BPH-1 cells	Leptin deficiency attenuated morphological changes and collagen deposition. In BPH-1 cells treated with leptin a decrease and increase protein expression of E-cadherin and vimentin, respectively, were observed.	Zhang et al. (2020)

of paracrine factors that may lead to the development of BPH. The therapeutic aim in BPH is to improve symptoms and lower the risk of progression to improve patient quality of life. Different pharmacological classes of drugs are used in LUTS-BPH including those to reduce outlet obstruction and to treat bladder overactivity. The role of PPAT dysfunction as a

trigger of BPH, especially in cases of obesity, is a new area of investigation and more studies are needed to find key mediators directly involved in the pathogenesis of prostatic hyperplasia.

AUTHOR CONTRIBUTIONS

All authors contributed to the writing and have made intellectual contribution to this study. GP, AG and MO: Organized and edited the manuscript. MO, EA and FM: provided critical revisions. All authors approved it for publication.

FUNDING

This work was supported by the Sao Paulo Research Foundation (FAPESP, grants n 2017/15175-1; 2018/09765-3; 2018/05956-9; 2018/21880-2; 2019/19490-4).

ACKNOWLEDGMENTS

The authors acknowledge Charles Serpellone Nash for english editing services.

REFERENCES

Alexandre, E. C., Calmasini, F. B., Sponton, A. C. D. S., de Oliveira, M. G., André, D. M., Silva, F. H., et al. (2018). Influence of the periprostatic adipose tissue in obesity-associated mouse urethral dysfunction and oxidative stress: effect of resveratrol treatment. *Eur. J. Pharmacol.* 836, 25–33. doi:10.1016/j.ejphar.2018.08.010

Araujo, H. N., Victório, J. A., Valgas da Silva, C. P., Sponton, A. C. S., Vettorazzi, J. F., de Moraes, C., et al. (2018). Anti-contractile effects of perivascular adipose tissue in thoracic aorta from rats fed a high-fat diet: role of aerobic exercise training. *Clin. Exp. Pharmacol. Physiol.* 45, 293–302. doi:10.1111/1440-1681.12882

Barbe, P., Millet, L., Galitzky, J., Lafontan, M., and Berlan, M. (1996). *In situ* assessment of the role of the β1, β2- and β3-adrenoceptors in the control of lipolysis and nutritive blood flow in human subcutaneous adipose tissue. *Br. J. Pharmacol.* 117, 907–913. doi:10.1111/j.1476-5381.1996.tb15279.x

Blüher, M. (2013). Adipose tissue dysfunction contributes to obesity related metabolic diseases. *Best Pract. Res. Clin. Endocrinol. Metabol.* 27, 163–177. doi:10.1016/j.beem.2013.02.005

Bouloumie, A., Marumo, T., Lafontan, M., and Busse, R. (1999). Leptin induces oxidative stress in human endothelial cells. *Faseb. J.* 13, 1231–1238. doi:10.1096/fasebj.13.10.1231

Bouloumié, A., Curat, C. A., Sengenès, C., Lolmède, K., Miranville, A., and Busse, R. (2005). Role of macrophage tissue infiltration in metabolic diseases. *Curr. Opin. Clin. Nutr. Metab. Care* 8, 347–354. doi:10.1097/01.mco.0000172571.41149.52

Calmasini, F. B., de Oliveira, M. G., Alexandre, E. C., Silva, F. H., Tavares, E. B. G., André, D. M., et al. (2018). Obesity-induced mouse benign prostatic hyperplasia (BPH) is improved by treatment with resveratrol: implication of oxidative stress, insulin sensitivity and neuronal growth factor. *J. Nutr. Biochem.* 55, 53–58. doi:10.1016/j.jnutbio.2017.12.009

Carr, J. B., and Rodeo, S. A. (2019). The role of biologic agents in the management of common shoulder pathologies: current state and future directions. *J. Shoulder Elbow Surg.* 28, 2041–2052. doi:10.1016/j.jse.2019.07.025

Carson, C., and Rittmaster, R. (2003). The role of dihydrotestosterone in benign prostatic hyperplasia. *Urology* 61, 2–7. doi:10.1016/s0090-4295(03)00045-1

Cheng, C. F., Ku, H. C., Cheng, J. J., Chao, S. W., Li, H. F., Lai, P. F., et al. (2019). Adipocyte browning and resistance to obesity in mice is induced by expression of ATF3. *Commun Biol* 2, 389. doi:10.1038/s42003-019-0624-y

Cheng, G. S. (2006). Inflammation and metabolic disorders. *Nature* 444, 860–867. doi:10.1038/nature05485

Chiurazzi, M., Cozzolino, M., Orsini, R. C., Di Maro, M., Di Minno, M. N. D., and Colantuoni, A. (2020). Impact of genetic variations and epigenetic mechanisms on the risk of obesity. *Int. J. Mol. Sci.* 21. 9035. doi:10.3390/ijms21239035

Chughtai, B., Forde, J. C., Thomas, D. D., Laor, L., Hossack, T., Woo, H. H., et al. (2016). Benign prostatic hyperplasia. *Nat Rev Dis Primers* 2 (2), 16031. doi:10.1038/nrdp.2016.31

Considine, R. V., Sinha, M. K., Heiman, M. L., Kriauciunas, A., Stephens, T. W., Nyce, M. R., et al. (1996). Serum immunoreactive-leptin concentrations in normal-weight and obese humans. *N. Engl. J. Med.* 334, 292–295. doi:10.1056/NEJM199602013340503

Coyne, K. S., Sexton, C. C., Thompson, C. L., Milsom, I., Irwin, D., Kopp, Z. S., et al. (2009). The prevalence of lower urinary tract symptoms (LUTS) in the United States, the United Kingdom and Sweden: results from the Epidemiology of LUTS (EpiLUTS) study. *BJU Int.* 104, 352–360. doi:10.1111/j.1464-410X.2009.08427.x

D'Ancona, C., Haylen, B., Oelke, M., Abranches-Monteiro, L., Arnold, E., Goldman, H., et al. (2019). The International Continence Society (ICS) report on the terminology for adult male lower urinary tract and pelvic floor symptoms and dysfunction. *Neurourol. Urodyn.* 38, 433–477. ddoi:10.1002/nau.23897

Delongchamps, N. B., de la Roza, G., Chandan, V., Jones, R., Sunheimer, R., Threatte, G., et al. (2008). Evaluation of prostatitis in autopsied prostates--is chronic inflammation more associated with benign prostatic hyperplasia or cancer?. *J. Urol.* 179, 1736–1740. doi:10.1016/j.juro.2008.01.034

Dietze-Schroeder, D., Sell, H., Uhlig, M., Koenen, M., and Eckel, J. (2005). Autocrine action of adiponectin on human fat cells prevents the release of insulin resistance-inducing factors. *Diabetes* 54, 2003–2011. doi:10.2337/diabetes.54.7.2003

Finley, D. S., Calvert, V. S., Inokuchi, J., Lau, A., Narula, N., Petricoin, E. F., et al. (2009). Periprostatic adipose tissue as a modulator of prostate cancer aggressiveness. *J. Urol.* 182, 1621–1627. doi:10.1016/j.juro.2009.06.015

Friedman, J. M., and Halaas, J. L. (1998). Leptin and the regulation of body weight in mammals. *Nature* 395, 763–770. doi:10.1038/27376

Friedman, J. M. (1997). The alphabet of weight control. *Nature* 385, 119–120. doi:10.1038/385119a0

Fu, S., Xu, H., Gu, M., Liu, C., Wang, Q., Wan, X., et al. (2017). Adiponectin deficiency contributes to the development and progression of benign prostatic hyperplasia in obesity. *Sci. Rep.* 7, 43771. doi:10.1038/srep43771

Gacci, M., Sebastianelli, A., Salvi, M., De Nunzio, C., Tubaro, A., Vignozzi, L., et al. (2015). Central obesity is predictive of persistent storage lower urinary tract symptoms (LUTS) after surgery for benign prostatic enlargement: results of a multicentre prospective study. *BJU Int.* 116, 271–277. doi:10.1111/bju.13038

Galitzky, J., Lafontan, M., Nordenström, J., and Arner, P. (1993). Role of vascular alpha-2 adrenoceptors in regulating lipid mobilization from human adipose tissue. *J. Clin. Invest.* 91, 1997–2003. doi:10.1172/JCI116421

Giri, D., and Ittmann, M. (2001). Interleukin-8 is a paracrine inducer of fibroblast growth factor 2, a stromal and epithelial growth factor in benign prostatic hyperplasia. *Am. J. Pathol.* 159, 139–147. doi:10.1016/S0002-9440(10)61681-1

Hao, L., Scott, S., Abbasi, M., Zu, Y., Khan, M. S. H., Yang, Y., et al. (2019). Beneficial metabolic effects of mirabegron in vitro and in high-fat diet-induced obese mice. *J. Pharmacol. Exp. Therapeut.* 369, 419–427. doi:10.1124/jpet.118.255778

He, Y., Lu, L., Wei, X., Jin, D., Qian, T., Yu, A., et al. (2016). The multimerization and secretion of adiponectin are regulated by TNF-alpha. *Endocrine* 51, 456–468. doi:10.1007/s12020-015-0741-4

Hong, H., Koch, M. O., Foster, R. S., Bihrle, R., Gardner, T. A., Fyffe, J., et al. (2003). Anatomic distribution of periprostatic adipose tissue: a mapping study of 100 radical prostatectomy specimens. *Cancer* 97, 1639–1643. doi:10.1002/cncr.11231

Irwin, D. E., Milsom, I., Hunskaar, S., Reilly, K., Kopp, Z., Herschorn, S., et al. (2006). Population-based survey of urinary incontinence, overactive bladder, and other lower urinary tract symptoms in five countries: results of the EPIC study. *Eur. Urol.* 50, 1306–1315. doi:10.1016/j.eururo.2006.09.019

Jeremic, N., Chaturvedi, P., and Tyagi, S. C. (2017). Browning of white fat: novel insight into factors, mechanisms, and therapeutics. *J. Cell. Physiol.* 232, 61–68. doi:10.1002/jcp.25450

Kim, J. Y., van de Wall, E., Laplante, M., Azzara, A., Trujillo, M. E., Hofmann, S. M., et al. (2007). Obesity-associated improvements in metabolic profile through expansion of adipose tissue. *J. Clin. Invest.* 117, 2621–2637. doi:10.1172/JCI31021

Klöting, N., Fasshauer, M., Dietrich, A., Kovacs, P., Schön, M. R., and Kern, M. (2010). Insulin-sensitive obesity. *Am. J. Physiol. Endocrinol. Metab.* 299, E506–E515. doi:10.1152/ajpendo.00586.2009

Kumada, M., Kihara, S., Ouchi, N., Kobayashi, H., Okamoto, Y., Ohashi, K., et al. (2004). Adiponectin specifically increased tissue inhibitor of metalloproteinase-1 through interleukin-10 expression in human macrophages. *Circulation* 109, 2046–2049. doi:10.1161/01.CIR.0000127953.9813110.1161/01.CIR.0000127953.98131.ED

Kusminski, C. M., McTernan, P. G., Schraw, T., Kos, K., O'Hare, J. P., Ahima, R., et al. (2007). Adiponectin complexes in human cerebrospinal fluid: distinct complex distribution from serum. *Diabetologia* 50, 634–642. doi:10.1007/s00125-006-0577-9

La Cava, A., and Matarese, G. (2004). The weight of leptin in immunity. *Nat. Rev. Immunol.* 4, 371–379. doi:10.1038/nri1350

Lan, N., Lu, Y., Zhang, Y., Pu, S., Xi, H., Nie, X., et al. (2020). FTO-a common genetic basis for obesity and cancer. *Front. Genet.* 11, 559138. doi:10.3389/fgene.2020.559138

Laven, B. A., Orsini, N., Andersson, S. O., Johansson, J. E., Gerber, G. S., and Wolk, A. (2008). Birth weight, abdominal obesity and the risk of lower urinary tract symptoms in a population based study of Swedish men. *J. Urol.* 179, 1891–1896. doi:10.1016/j.juro.2008.01.029

Lee, D. W., Leinung, M. C., Rozhavskaya-Arena, M., and Grasso, P. (2002). Leptin and the treatment of obesity: its current status. *Eur. J. Pharmacol.* 440, 129–139. doi:10.1016/s0014-2999(02)01424-3

Lu, C., Su, L. Y., Lee, R. M., and Gao, Y. J. (2010). Mechanisms for perivascular adipose tissue-mediated potentiation of vascular contraction to perivascular neuronal stimulation: the role of adipocyte-derived angiotensin II. *Eur. J. Pharmacol.* 634, 107–112. doi:10.1016/j.ejphar.2010.02.006

Lu, K. Y., Primus Dass, K. T., Lin, S. Z., Harn, H. J., and Liu, S. P. (2020). The application of stem cell therapy and brown adipose tissue transplantation in metabolic disorders. *Cytotherapy* 22, 521–528. doi:10.1016/j.jcyt.2020.06.004

Maffei, M., Halaas, J., Ravussin, E., Pratley, R. E., Lee, G. H., and Zhang, Y. (1995). Leptin levels in human and rodent: measurement of plasma leptin and ob RNA in obese and weight-reduced subjects. *Nat. Med.* 1, 1155–1161. doi:10.1038/nm1195-1155

Mao, X., Huang, D., Rao, C., Du, M., Liang, M., Li, F., et al. (2020). Enoyl coenzyme A hydratase 1 combats obesity and related metabolic disorders by promoting adipose tissue browning. *Am. J. Physiol. Endocrinol. Metab.* 318 (318), E318–E329. doi:10.1152/ajpendo.00424.2019

Matsubara, M., Maruoka, S., and Katayose, S. (2002). Inverse relationship between plasma adiponectin and leptin concentrations in normal-weight and obese women. *Eur. J. Endocrinol.* 147, 173–180. doi:10.1530/eje.0.1470173

McNeal, J. E. (1984). Anatomy of the prostate and morphogenesis of BPH. *Prog. Clin. Biol. Res.* 145, 27–53. doi:10.1016/j.ucl.2016.04.012

Mechergui, Y. B., Ben Jemaa, A., Mezigh, C., Fraile, B., Ben Rais, N., Paniagua, R., et al. (2009). The profile of prostate epithelial cytokines and its impact on sera prostate specific antigen levels. *Inflammation* 32, 202–210. doi:10.1007/s10753-009-9121-7

Meng, Y., Yu, W., Liu, Z., Zhang, M., Chen, Y., Li, S., et al. (2020). The inflammation patterns of different inflammatory cells in histological structures of hyperplasic prostatic tissues. *Transl. Androl. Urol.* 9, 1639–1649. doi:10.21037/tau-20-448

Michel, M. C., and Korstanje, C. (2016). β3-Adrenoceptor agonists for overactive bladder syndrome: role of translational pharmacology in a repositioning clinical drug development project. *Pharmacol. Ther.* 159, 66–82. doi:10.1016/j.pharmthera.2016.01.007

Mónica, F. Z., and De Nucci, G. (2019). Tadalafil for the treatment of benign prostatic hyperplasia. *Expet Opin. Pharmacother.* 20, 929–937. doi:10.1080/14656566.2019.1589452

Morelli, A., Sarchielli, E., Comeglio, P., Filippi, S., Mancina, R., Gacci, M., et al. (2011). Phosphodiesterase type 5 expression in human and rat lower urinary tract tissues and the effect of tadalafil on prostate gland oxygenation in spontaneously hypertensive rats. *J. Sex. Med.* 8, 2746–2760. doi:10.1111/j.1743-6109.2011.02416.x

Nomiya, M., and Yamaguchi, O. (2003). A quantitative analysis of mRNA expression of alpha 1 and beta-adrenoceptor subtypes and their functional roles in human normal and obstructed bladders. *J. Urol.* 170, 649–653. doi:10.1097/01.ju.0000067621.62736.7c

Ornstein, J. (2016). The long road to leptin. *J. Clin. Invest.* 126, 4727–4734. doi:10.1172/JCI91578

Ouchi, N., Parker, J., Lugus, J. J., and Walsh, K. (2011). Adipokines in inflammation and metabolic disease. *Nat. Rev. Immunol.* 11, 85–97. doi:10.1038/nri2921

Penson, D. F., Munro, H. M., Signorello, L. B., Blot, W. J., Fowke, J. H., and Project, U. D. A. (2011). Obesity, physical activity and lower urinary tract symptoms: results from the Southern Community Cohort Study. *J. Urol.* 186, 2316–2322. doi:10.1016/j.juro.2011.07.067

Rafael, J., and Herling, A. W. (2000). Leptin effect in ob/ob mice under thermoneutral conditions depends not necessarily on central satiation. *Am. J. Physiol. Regul. Integr. Comp. Physiol.* 278, R790–R795. doi:10.1152/ajpregu.2000.278.3.R790

Ribeiro, R., Monteiro, C., Cunha, V., Oliveira, M. J., Freitas, M., Fraga, A., et al. (2012). Human periprostatic adipose tissue promotes prostate cancer aggressiveness *in vitro*. *J. Exp. Clin. Canc. Res.* 31, 32. doi:10.1186/1756-9966-31-32

Roehrborn, C. G. (2008). Pathology of benign prostatic hyperplasia. *Int. J. Impot. Res.* 20 (3), S11–S18. doi:10.1038/ijir.2008.55

Rosenbaum, M., Malbon, C. C., Hirsch, J., and Leibel, R. L. (1993). Lack of beta 3-adrenergic effect on lipolysis in human subcutaneous adipose tissue. *J. Clin. Endocrinol. Metab.* 77, 352–355. doi:10.1210/jcem.77.2.8393882

Sacca, P. A., Mazza, O. N., Scorticati, C., Vitagliano, G., Casas, G., and Calvo, J. C. (2019). Human periprostatic adipose tissue: secretome from patients with prostate cancer or benign prostate hyperplasia. *Cancer Genom. Proteom.* 16, 29–58. doi:10.21873/cgp.20110

Silva, S. A., Gobbo, M. G., Pinto-Fochi, M. E., Rafacho, A., Taboga, S. R., Almeida, E. A., et al. (2015). Prostate hyperplasia caused by long-term obesity is characterized by high deposition of extracellular matrix and increased content of MMP-9 and VEGF. *Int. J. Exp. Pathol.* 96, 21–30. doi:10.1111/iep.12107

Smith, C. J., Perfetti, T. A., Hayes, A. W., and Berry, S. C. (2020). Obesity as a source of endogenous compounds associated with chronic disease: a review. *Toxicol. Sci.* 175, 149–155. doi:10.1093/toxsci/kfaa042

Steiner, G. E., Stix, U., Handisurya, A., Willheim, M., Haitel, A., Reithmayr, F., et al. (2003). Cytokine expression pattern in benign prostatic hyperplasia infiltrating T cells and impact of lymphocytic infiltration on cytokine mRNA profile in prostatic tissue. *Lab. Invest.* 83, 1131–1146. doi:10.1097/01.lab.0000081388.40145.65

Szasz, T., Bomfim, G. F., and Webb, R. C. (2013). The influence of perivascular adipose tissue on vascular homeostasis. *Vasc. Health Risk Manag.* 9, 105–116. doi:10.2147/VHRM.S33760

Tilg, H., and Moschen, A. R. (2006). Adipocytokines: mediators linking adipose tissue, inflammation and immunity. *Nat. Rev. Immunol.* 6, 772–783. doi:10.1038/nri1937

Uehling, D. E., Shearer, B. G., Donaldson, K. H., Chao, E. Y., Deaton, D. N., Adkison, K. K., et al. (2006). Biarylaniline phenethanolamines as potent and selective beta3 adrenergic receptor agonists. *J. Med. Chem.* 49, 2758–2771. doi:10.1021/jm0509445

Verze, P., Cai, T., and Lorenzetti, S. (2016). The role of the prostate in male fertility, health and disease. *Nat. Rev. Urol.* 13, 379–386. doi:10.1038/nrurol.2016.89

Vgontzas, A. N., Bixler, E. O., Papanicolaou, D. A., and Chrousos, G. P. (2000). Chronic systemic inflammation in overweight and obese adults. *J. Am. Med. Assoc.* 283, 2235. doi:10.1001/jama.283.17.2235

Victorio, J. A., Fontes, M. T., Rossoni, L. V., and Davel, A. P. (2016). Different anti-contractile function and nitric oxide production of thoracic and abdominal perivascular adipose tissues. *Front. Physiol.* 7, 295. doi:10.3389/fphys.2016.00295

Vikram, A., Jena, G. B., and Ramarao, P. (2010). Increased cell proliferation and contractility of prostate in insulin resistant rats: linking hyperinsulinemia with benign prostate hyperplasia. *Prostate* 70, 79–89. doi:10.1002/pros.21041

World Health Organization (2002). Obesity:preventing and managing the global epidemic. Available at: https://www.who.int/nutrition/publications/obesity/WHO_TRS_894/en/ (Accessed September 15, 2020).

Xu, H., Barnes, G. T., Yang, Q., Tan, G., Yang, D., Chou, C. C. J., et al. (2003). Chronic inflammation in fat plays a crucial role in the development of

obesity-related insulin resistance. *J. Clin. Invest.* 112, 1821–1830. doi:10.1172/JCI19451

Yamagishi, S. I., Edelstein, D., Du, X. L., Kaneda, Y., Guzmán, M., and Brownlee, M. (2001). Leptin induces mitochondrial superoxide production and monocyte chemoattractant protein-1 expression in aortic endothelial cells by increasing fatty acid oxidation via protein kinase A. *J. Biol. Chem.* 276, 25096–25100. doi:10.1074/jbc.M007383200

Yang, Y. (2004). Differential control of apoptosis by DJ-1 in prostate benign and cancer cells. *J. Cell. Biochem.* 92, 1221–1233. doi:10.1002/jcb.20159

Zeng, W., Pirzgalska, R. M., Pereira, M. M. A., Kubasova, N., Barateiro, A., and Seixas, E. (2015). Sympathetic neuro-adipose connections mediate leptin-driven lipolysis. *Cell* 163, 84–94. doi:10.1016/j.cell.2015.08.055

Zhang, B., Chen, X., Xie, C., Chen, Z., Liu, Y., Ru, F., et al. (2020). Leptin promotes epithelial-mesenchymal transition in benign prostatic hyperplasia through downregulation of BAMBI. *Exp. Cell Res.* 387, 111754. doi:10.1016/j.yexcr.2019.111754

Conflict of Interest: The authors declare that the research was conducted in the absence of any commercial or financial relationships that could be constructed as a potential conflict of interest.

frontiers in Pharmacology

REVIEW
published: 25 February 2021
doi: 10.3389/fphar.2020.626448

Plasticizers and Cardiovascular Health: Role of Adipose Tissue Dysfunction

Mikyla A. Callaghan[1,2], *Samuel Alatorre-Hinojosa*[1], *Liam T. Connors*[1,2], *Radha D. Singh*[1,2] *and Jennifer A. Thompson*[1,2,3]*

[1]Department of Physiology and Pharmacology, University of Calgary, Calgary, AB, Canada, [2]Libin Cardiovascular Institute, Calgary, AB, Canada, [3]Alberta Children's Health Research Institute, Calgary, AB, Canada

Since the 1950s, the production of plastics has increased 200-fold, reaching 360 million tonnes in 2019. Plasticizers, additives that modify the flexibility and rigidity of the product, are ingested as they migrate into food and beverages. Human exposure is continuous and widespread; between 75 and 97% of urine samples contain detectable levels of bisphenols and phthalates, the most common plasticizers. Concern over the toxicity of plasticizers arose in the late 1990s, largely focused around adverse developmental and reproductive effects. More recently, many studies have demonstrated that exposure to plasticizers increases the risk for obesity, type 2 diabetes, and cardiovascular disease (CVD). In the 2000s, many governments including Canada, the United States and European countries restricted the use of certain plasticizers in products targeted towards infants and children. Resultant consumer pressure motivated manufacturers to substitute plasticizers with analogues, which have been marketed as safe. However, data on the effects of these new substitutes are limited and data available to-date suggest that many exhibit similar properties to the chemicals they replaced. The adverse effects of plasticizers have largely been attributed to their endocrine disrupting properties, which modulate hormone signaling. Adipose tissue has been well-documented to be a target of the disrupting effects of both bisphenols and phthalates. Since adipose tissue function is a key determinant of cardiovascular health, adverse effects of plasticizers on adipocyte signaling and function may underlie their link to cardiovascular disease. Herein, we discuss the current evidence linking bisphenols and phthalates to obesity and CVD and consider how documented impacts of these plasticizers on adipocyte function may contribute to the development of CVD.

Keywords: bisphenols (BPs), phthalates (PAEs), adipogenesis, adipose tissue, cardiovascular disease

OPEN ACCESS

Edited by:
Joshua Thomas Butcher, Oklahoma State University, United States

Reviewed by:
Sara Fournier, Rutgers, The State University of New Jersey, United States
Carlos F Sánchez-Ferrer, Autonomous University of Madrid, Spain

***Correspondence:**
Jennifer A. Thompson
jennifer.thompson2@ucalgary.ca

Specialty section:
This article was submitted to Cardiovascular and Smooth Muscle Pharmacology, a section of the journal Frontiers in Pharmacology

Received: *05 November 2020*
Accepted: *22 December 2020*
Published: *25 February 2021*

Citation:
Callaghan MA, Alatorre-Hinojosa S, Connors LT, Singh RD and Thompson JA (2021) Plasticizers and Cardiovascular Health: Role of Adipose Tissue Dysfunction. Front. Pharmacol. 11:626448. doi: 10.3389/fphar.2020.626448

INTRODUCTION

Cardiovascular diseases (CVD) lead to an estimated 17.9 million deaths annually, making them one of the leading causes of death worldwide.[1] The substantial global impact of CVD is one of the most critical public health issues of our time. One of the strongest predictors of CVD is obesity. While obesity is considered an independent risk factor for CVD, it frequently occurs in conjunction with

[1]https://www.who.int/health-topics/cardiovascular-diseases#tab=tab_1.

other risk factors, including hypertension, insulin resistance and dyslipidemia (Kachur et al., 2017), in what is known as the metabolic syndrome (MetS). Presence of the MetS increases the risk of death from CVD by approximately 2-fold (Ju et al., 2017).

Given that obesity is a major driver of CVD, preventative strategies depend on an understanding of the environmental and socioeconomic factors that underpin worldwide trends in obesity rates. According to the World Health Organization (WHO), over 1.9 billion adults were overweight (BMI > 20) and 650 million adults were obese (BMI > 30) in 2016, representing 39 and 13% of the world population, respectively. If trends continue, approximately half of U.S. adults will be obese by 2030, with one in four experiencing severe conditions (Ward et al., 2019). Over the past decades, the rates of obesity have risen faster in children than in adults (Biro et al., 2016), leading to the present reality that one third of North American children suffer from one or more risk factors for CVD (Tremblay and Willms, 2000; Biro et al., 2016). Approximately three-quarters of overweight or obese children will be obese as adults and at risk for cardiovascular complications (Ward et al., 2019).

The high incidence of obesity is attributable to multiple environmental and lifestyle factors, most notably changes in food production and supply and reductions in physical activity. While consumption of high caloric foods and sedentary behaviour are indeed driving forces in the pathogenesis of cardiometabolic disease, there is some evidence to suggest that they do not fully explain the obesity epidemic (Huo et al., 2016). In the early 2000s, Paula Baillie Hamilton synthesized ecological data to reveal a correlation between increasing rates of obesity in the United States and increasing production of synthetic chemicals (Baillie-Hamilton, 2002). This observation coincided with the emerging theory of endocrine disruption that attributes the homeostasis-disrupting effects of exogenous chemicals to an interference with the synthesis, release, transportation, metabolism, or elimination of endogenous bodily hormones. In 2006, Grun and Blumberg coined the "environmental obesogen hypothesis", proposing a causal link between environmental toxins and the obesity epidemic (Grün and Blumberg, 2006).

Endocrine disrupting chemicals (EDCs) interfere with hormone signaling by mimicking endogenous ligands to nuclear receptors and acting as agonists or antagonists depending on the dose, species, and cell-type. Plasticizers are among the most pervasive EDCs owing to their high production, slow degradation and leaching into the environment. There are two main groups of plasticizers: 1) bisphenols, which confer rigidity to hard polycarbonate plastics and 2) phthalates, which provide flexibility to soft plastics and polyvinyl chloride (PVC) products. A large body of evidence indicates that these plastics interfere with adipocyte differentiation and adipose tissue function. Since adipose tissue is a critical regulator of cardiovascular health, the effects of plasticizers on adipocyte biology may underlie their association with obesity and CVD. Thus, this review will discuss bisphenols and phthalates, their relationship with MetS, and their impact on adipose tissue development and function.

PLASTICIZERS

Bisphenols

Bisphenols are one of the most commonly produced synthetic chemicals worldwide. They are used in the manufacturing of polycarbonate plastics and epoxy resin coatings in food and beverage containers. Additional products containing bisphenols include medical and dental devices, building materials, thermal receipt paper, and children's toys (Chen et al., 2016). The most common and well-known bisphenol is 2,2-bis(4-hydroxyphenyl) propane or bisphenol A (BPA). Worldwide production of BPA increased by approximately 2.3 million tons between 2003 and 2011 (Flint et al., 2012) and its consumption is expected to increase at a rate of 3.6% per year through 2023[2]. Human exposure primarily occurs through the ingestion of food, beverages and drinking water that have been contaminated through leaching due to incomplete polymerization or polymer degradation. A study conducted on Harvard students found that after a washout period during which BPA exposure was limited, 1 week of drinking from polycarbonate water bottles increased urinary BPA levels by almost 70% (Carwile et al., 2009). In National Health and Nutrition Examination Survey (NHANES) participants that consumed one or more canned foods over a 24 h period, urinary BPA levels were over 50% higher than those who consumed no canned goods (Hartle et al., 2016). Bisphenols can enter the body through routes other than ingestion (Stojanoska et al., 2017) as they are ubiquitous in our environment, detected in surface water, biosolids, soil and air (Corrales et al., 2015).

Ingested BPA is quickly conjugated in the liver and excreted in bile or urine, with an approximate half-life of 6 h (Völkel et al., 2008; Genuis et al., 2012). Despite its rapid metabolism and clearance, BPA is persistent in our environment and detected in over 92% of urine samples (Calafat et al., 2008). Findings of a recent study that employed a new direct method of measuring levels of BPA and its conjugated metabolites suggest that traditional indirect methods used by regulatory bodies to estimate health risk in humans may have underestimated exposure by over 40-fold (Gerona et al., 2020). Studies show that bisphenols cross the placenta and accumulate in fetal tissues at levels higher than maternal serum (Ikezuki et al., 2002; Gerona et al., 2013). This may be due to immature detoxification defences, leading to slower clearance of bisphenols from the fetal compartment, as demonstrated by studies in pregnant sheep (Corbel et al., 2015; Gingrich et al., 2019). The fetus is particularly vulnerable to the endocrine disrupting effects of bisphenols and other xenobiotics as it is undergoing critical developmental stages of organ maturation and setting of endocrine axes.

By 2005, there were over 100 studies showing adverse effects of BPA at or below the safety standard, conducted by dozens of laboratories in the United States, Japan, and Europe. In 2008, the Government of Canada declared BPA a toxic substance and in

[2]https://ihsmarkit.com/products/bisphenol-chemical-economicshandbook.html

2010 banned all import and sales of baby products containing BPA[3], actions that were followed by the European Union in 2011 and the FDA in 2012. These policies, founded on developments in toxicology and toxicokinetic data, prompted consumer concern that pressured industries to replace BPA with chemical substitutes. BPA analogues share two hydroxyphenol functionalities (Chen et al., 2016). Bisphenol S (BPS), bisphenol F (BPF) and bisphenol AF (BPAF), are the most common analogues and are found in products labeled "BPA-free" (Rochester and Bolden, 2015). Increased production and consumption of BPA analogues have resulted in a rise in environmental and human exposure. Based on data from NHANES, BPA, BPS, and BPF, were detected in 96, 84, and 67% of U.S. adult urine samples, respectively (Lehmler et al., 2018). Another study by Liao et al. reported the presence of BPS in 81% of urine samples collected in the United States (Lehmler et al., 2018). Wang et al. determined that exposure levels of BPA analogues vary across countries, likely a reflection of manufacturing practices or sources of exposure. Human BPS daily intake was highest in Saudi Arabia, France, and Vietnam, whereas human BPF daily intake was highest in Saudi Arabia, the Netherlands and Canada (Wang et al., 2020). Canada, the country that first restricted the use of BPA, had the lowest intake of BPA, but the highest intake of BPF (Wang et al., 2020). While there has been extensive investigation into the health effects of BPA, relatively few studies have explored the analogues that have replaced it. The toxicity of BPA analogues was not investigated sufficiently before introduction to the market, and the data that is available indicate that they exhibit similar endocrine disrupting properties and may lead to the same adverse health effects.

Phthalates

Phthalates are diesters of 1,2-benzendicarboxylic acid that are used as plasticizers in polymer products, softeners in PVC plastics and fragrance stabilizers in hygiene and cosmetic products (Stojanoska et al., 2017; Wang et al., 2019). Exposure to phthalates is pervasive as they are found in numerous consumer products ranging from adhesives, detergents, automotive plastics, clothing, storage containers, and personal-care products. Human exposure primarily occurs through ingestion, inhalation, or by skin absorption as phthalates can migrate out of products into food, air, dust, and water (Wang et al., 2019). Approximately 60% of ingested phthalates are metabolized within 24 h and excreted in urine; however, metabolites have been detected in blood, saliva, amniotic fluid, and breast milk (Stojanoska et al., 2017).

Di(2-ethylhexyl)phthalate (DEHP) is a high molecular weight phthalate that is most commonly found in plastics and is transformed into several different metabolites after entering the body. Primary monoester metabolites of DEHP include: mono(2-ethylhexyl)phthalate (MEHP), di-n-octyl phthalate (DnOP), di-n-butyl phthalate (DnBP), benzyl butyl phthalate (BBzP), and diethyl phthalate (Lang et al., 2008). Secondary oxidation metabolites include: mono-2-ethyl-5-hydroxyhexyl phthalate (MEHHP), mono-2-ethyl-5-oxohexyl phthalate (MEOHP), and mono-2-ethyl-5-carboxypentyl phthalate (MECPP) amongst many others (Meeker et al., 2012). According to NHANES 1999–2000 data, MEHP was detectable in the urine of >75% participants, and MEP, MBP, and MBzP were detectable in >97% of participants in the USA (Silva et al., 2004). In the Canadian Health Measures Survey 2007–2009, 11 metabolites were monitored, and results indicated that MEP, MnBP, MBzP, MCPP, MEHP, MEOHP, and MEHHP were detected in >90% of Canadians (Saravanabhavan et al., 2013).

In the late 1990s, concerns arose about adverse effects of phthalates in humans, originally focused on DEHP and DINP and their possible reproductive and developmental toxicity. Panels formed by the American Council on Science and Health (ACSH) and the NTP Center for the Evaluation of Risk to Human Reproduction (NTP-CERHR) evaluated the toxicity of a number of phthalates (Kamrin, 2009). In 2008, the US Consumer Product Safety Improvement Act (CPSIA) named limits on the use of six phthalates in children's products. Under this act DEHP, DBP, and BBP are restricted to an individual concentration limit of 1000 ppm in children's toys and products for those under the age of 3 (Smith et al., 2020). Whereas, DINP, DIOP, and DnOP are limited to concentrations no greater than 1000 ppm in children's toys that are small enough to enter a child's mouth, and in products for those under the age of three (Smith et al., 2020). Canadian and European governments have implemented similar restrictions on these six phthalates. The Chronic Hazard Advisory Panel convened in 2010 recommended further action by US agencies to widen restrictions for DBP, BBP, and DEHP to include additional consumer products. These regulations initiated a push toward safer alternatives, motivating some companies to voluntarily use substitutes with presumed lower toxicity.

EXPOSURE TO PLASTICIZERS AND RISK FOR METABOLIC SYNDROME: EPIDEMIOLOGICAL EVIDENCE

Bisphenols

To-date epidemiological research examining the association between urinary bisphenol concentrations and the development of obesity and other risk factors for CVD have primarily focused on BPA. Many of these studies have been conducted in a cross-sectional design, mainly utilizing data from NHANES (LaKind et al., 2012). Using 2003–2008 data, researchers determined that higher urinary BPA levels were strongly associated with weight circumference (WC) and BMI in males and females over 20 years of age (Shankar et al., 2012). Cai et al. used NHANES 2003–2014 data to determine that higher levels of BPA were associated with increased total CVD burden in males; however, no results were determined in female groups (Cai et al., 2020). Through analysis of 2003–2004 data, Lang et al., similarly demonstrated that CVD was associated with relatively high levels of BPA compared to lower quartiles and that an

[3]https://www.canada.ca/en/health-canada/services/chemical-substances/challenge/batch-2/bisphenol-a.html

increase in CVD was associated with a one standard deviation increase of BPA (Lang et al., 2008). While the above findings indicate a relationship between bisphenols and MetS, there has been debate regarding analytical methods and suitability of NHANES data to determine associations. By applying different inclusion criteria, methods and case definitions, Lankind et al. was unable to find associations between BPA concentrations and CVD in multiple NHANES datasets (LaKind et al., 2012).

Data obtained from cohorts other than NHANES provide further evidence to support a relationship between bisphenol exposure and MetS. In a cross-sectional study, Wang et al. analyzed a population of adults over the age of 40 from a community in Shanghai, China (n = 3,390). Positive associations between the highest quartiles of BPA exposure and insulin resistance, as well as both general and abdominal obesity were determined (Wang et al., 2012). A case-control study performed by Duan et al. revealed a positive correlation between urinary BPS or BPAF concentrations and type 2 diabetes (T2D) (Duan et al., 2018). Another study aimed to determine the risk of developing T2D over a 9-year period in the French cohort called "Data from an Epidemiological Study on the Insulin Resistance Syndrome" (D.E.S.I.R). Of 755 participants, 201 cases of diabetes were diagnosed, and results suggested that participants in higher quartiles of BPA exposure had nearly double the risk of developing T2D (Rancière et al., 2019). Overall, available data provide strong evidence supporting a link between bisphenol exposure and MetS.

Phthalates

Several epidemiological studies have explored the relationship between phthalates exposure and the risk for obesity and related metabolic disorders. Using data from NHANES (1992–2002), two studies highlighted a relationship between urinary phthalate metabolites and obesity. Hatch et al. found that BMI and WC were positively associated with exposure to six phthalates in males aged 20–59: the strongest associations occurring with MBzP, MEHHP, and MEOHP (Hatch et al., 2008). However, only MEP significantly predicted BMI and WC in adolescent females, but not in adult females. Stahlhut et al. reported links between MBzP, MEHHP, MEOHP, and MEP and WC (Stahlhut et al., 2007). Both studies determined that MEHP was not significantly correlated with WC, with a possible explanation being its shorter half-life compared to the other studied metabolites.

A cross-sectional study using data from the 2012–2014 Korean National Environmental Health Survey II (n = 5,251) reported a significant association between urine MEHHP levels and MetS, defined by NCEP ATP III criteria (Shim et al., 2019). In agreement with these results, James-Todd et al., used NHANES data from 2001 to 2010 (n = 2,719) and found that higher concentrations of DEHP metabolites, including MEHP, MEHHP, and MEOHP, increased the odds of developing MetS in males (Shim et al., 2019). Similar to findings revealed by Hatch et al., (2008), no correlations were found in adult females. Gaston and Tulve performed a cross-sectional study with NHANES data from 2003 to 2013 in U.S. adolescents (n = 918) and discovered a strong association between MnBP and MetS (Gaston and Tulve, 2019). A smaller study examining MetS patients in a hospital in Prague (n = 168) revealed significantly higher urine levels of four phthalate metabolites (MnBP, MEHHP, MEOHP, MECPP) in T2D patients compared to non-diabetic patients, but no relationship with hypertension or dyslipidemia (Piecha et al., 2016). Similarly, another study noted significantly elevated concentrations of DEHP and MECPP in T2D Mexican women; however, correlations between DEHP and IR were only noted for non-diabetic patients (Svensson et al., 2011). Lastly, Huang et al. (2014) determined there was a significant correlation between MnBP, MiBP, MCPP, and DEHP with IR, glycemia, and insulinemia (Huang et al., 2014). In summary, current literature supports a relationship between phthalate exposure and MetS.

UNDERSTANDING THE LINK BETWEEN PLASTICIZERS AND CVD: ROLE OF ADIPOSE TISSUE

Adipose tissue is thought to be a major target for the adverse developmental and functional effects of plasticizers and other EDC as it tends to sequester lipophilic toxins. Numerous investigations have implicated adipose tissue dysfunction as central in the development of obesity-associated CVD. The metabolic consequences of adipose tissue dysfunction, which include insulin resistance, dyslipidemia and increased visceral adiposity among others, are defining features of MetS.

Adipogenesis

Adipose tissue is the body's largest endocrine organ and major energy reservoir (Berry et al., 2013). There is growing appreciation for the importance of the "quality" of adipose tissue, over its mass-based quantity, in carrying out its role in regulating systemic metabolic homeostasis (Ikeoka et al., 2010; Akoumianakis et al., 2017). As the body's main energy reserve, adipose tissue undergoes dynamic remodeling to expand or contract in response to fluctuations in energy balance (Chait and den Hartigh, 2020). In a state of prolonged positive energy balance, subcutaneous fat depots serve as a "metabolic sink" that buffers the excess energy. Healthy expansion of adipose tissue depends on a dynamic balance between hypertrophic growth of existing adipocytes and hyperplastic growth that increases the number of adipocytes through adipogenesis (Chatterjee et al., 2014; Choe et al., 2016; Jeffery et al., 2016). Adipogenesis is the process by which adipocyte stem cells commit and differentiate into mature, lipid-storing adipocytes. When adipogenesis is insufficient, expansion relies on hypertrophy, which beyond a threshold leads to lipid spillover into the circulation and engorged adipocytes that are hypoxic, inflamed and resistant to the anti-lipolytic effects of insulin (Kim et al., 2015; Jang et al., 2016). Thus, failed expansion of adipose tissue underlies the insulin resistance, hyperlipidemia and low-grade inflammation that triggers obesity-induced onset of CVD (Medina-Gomez et al., 2007; Chatterjee et al., 2014).

In adult depots, new adipocytes are recruited from a resident population of progenitors that are committed *in utero*, as revealed

by seminal studies by the Gaffe group (Jiang et al., 2014). Therefore, a perturbation in the critical *in utero* window of adipocyte lineage commitment will not only influence postnatal fat mass but may also have later-life consequences for availability of preadipocytes for differentiation and thereby the buffering capacity of adipose tissue. Adipogenesis *in vitro* is increased in response to BPA, as supported by a large body of evidence (Sargis et al., 2010; Boucher et al., 2014; Ohlstein et al., 2014; Ariemma et al., 2016). Much less is known regarding the effect of BPA substitutes on *in vitro* adipogenesis, but the evidence to-date points to similar pro-adipogenic properties. A non-monotonic response to BPS exposure, where increased adipogenesis was observed at lower doses, was reported in stem cells isolated from the subcutaneous depots of female donors (Boucher et al., 2016). In 3T3-L1 murine fibroblasts, pro-adipogenic effects were more pronounced after treatment with BPS compared to BPA (Ahmed and Atlas, 2016). Using the same cell line, a recently published study showed that the adipogenic response of BPS, BPF and BPB occurred at lower doses than that of BPA (Ramskov Tetzlaff et al., 2020). The molecular pathways mediating bisphenol-induced potentiation of adipogenesis are unclear, although a few studies have demonstrated the involvement of estrogen (Boucher et al., 2014) or glucocorticoid (Sargis et al., 2010) signaling.

Phthalates and their metabolites have been studied far less compared to BPA with respect to their effect on preadipocyte differentiation; however, existing evidence indicate similar pro-adipogenic properties. Feige et al. showed increased differentiation via PPARγ activation in 3T3-L1 cells exposed to MEHP, a monoester metabolite of DEHP (Feige et al., 2007). In agreement, a more recent study reported that MEHP promoted differentiation in the same cell line (Qi et al., 2019). Work by Pomatto et al. assessed four plasticizers (DiNP, DiDP, DEGDB, and TMCP) commonly used in the manufacture of food packaging as substitutes for the phthalate DEHP. All DEHP substitutes increased adipogenesis in 3T3-L1 cells, albeit with a maximal response lower than BPA (Pomatto et al., 2018). Another study reported an increase in 3T3-L1 differentiation in response to prolonged exposure to the DEHP substitute, DiNP, an effect that was prevented by PPARγ antagonism (Zhang et al., 2019). Overall, these findings suggest that phthalates and their substitutes augment *in vitro* differentiation of adipocyte progenitors.

While the pro-adipogenic effects of plasticizers in isolated stem cells are well-documented, whether this translates to increased *in vivo* adipogenesis during critical developmental windows of adipose tissue development remains unclear. In offspring born to pregnant rats treated with a low dose of BPA during pregnancy, body weight of both sexes was increased at birth and at weaning total mass and adipocyte size was increased in fat depots of females only (Somm et al., 2009). However, the authors studied only visceral fat, which contributes negligibly to total fat mass in rodents at weaning, as these secondary depots develop primarily after birth (Wang and Scherer, 2014). Later in postnatal life, there were no differences in body weight between offspring born to BPA or vehicle treated dams; however, BPS-exposed offspring were more vulnerable to diet-induced weight gain (Somm et al., 2009). Mice and rats are not ideal species to study the effect of *in utero* exposures on adipogenesis as they are born with very little fat compared to humans, sheep, and guinea pigs. In ovine fetuses of BPA-exposed, but not BPS-exposed dams, there was a sex-dependent increase in differentiation of isolated preadipocytes, without changes in body weight and perirenal adipocyte size (Pu et al., 2017). However, exposure was restricted to mid-gestation (Gd 30–100) despite the accumulation of fat mass occurring predominately in late gestation in sheep and other precocious species. While some studies have examined prenatal bisphenol exposure, fewer have investigated the impact of intrauterine phthalate exposure on early life fat accumulation. One study found higher body weight and visceral adiposity in 8-week old offspring born to pregnant C57BL/6J mice dams exposed to a low dose of the DEHP metabolite, MEHP (Hao et al., 2012).

In humans, studies regarding the relationship between plasticizer exposure and early-life fat mass have yielded inconsistent results. As far as bisphenols, some studies have reported a negative association between maternal exposure and birth weight (Miao et al., 2011; Troisi et al., 2014), while others have found a positive association (Lee et al., 2014). A study by Vafeiadi et al. studied a cohort of 1,363 pregnancies in Greece and showed maternal urinary BPA levels in the first trimester to be negatively associated with BMI in girls between the ages of 1–4, but positively associated with BMI in boys (Vafeiadi et al., 2016). The same study showed that urinary BPA levels were lower in mothers compared to their children and that BPA levels in children at 4 years of age predicted higher BMI and prevalence of obesity. BPA levels in spot urine samples collected from a smaller cohort of pregnant women were negatively associated with BMI in 9 year old girls, with no effect on boys, while BPA levels in children of both sexes were higher in those with greater BMI (Harley et al., 2013). In a Spanish cohort, prenatal BPA levels had no effect on growth in the first 6-months, but was correlated to higher WC and BMI at 4 years of age (Valvi et al., 2013). Overall, these findings suggest that obesity is associated with postnatal rather than prenatal exposure to bisphenols.

Similar to data on bisphenols, current evidence does not support a relationship between prenatal phthalate exposure and birth weight (Shoaff et al., 2016; Chiu et al., 2018). Weight gain in the first 6 months and BMI between ages 1 and 7 were positively associated with maternal DEHP metabolites measured in the first and third trimester, while higher *in utero* exposure decreased early life weight gain in boys (Valvi et al. 2015). No relationship between maternal exposure to DEHP metabolites and fat mass in children aged 4–9 was reported by Buckley et al., (2016b). In a pooled analysis of three cohorts, prenatal exposure to MCPP, a non-specific metabolite of high molecular weight phthalates, was associated with a 2-fold increase in childhood obesity, while exposure to metabolites specific to DEHP was inversely related to childhood obesity (Buckley et al., 2016a). The effect of childhood exposure on adiposity is clearer, with studies showing high levels, particularly in low molecular weight phthalates, to predict childhood obesity (Hatch et al., 2008; Trasande et al., 2013;

Deierlein et al., 2016). Together, the above studies underscore the importance of timing of exposure in relation to stages of development. Slower clearance in the fetus due to immature detoxification defences may shift the non-monotonic dose response curve to the right and additionally, toxic effects on the placenta may adversely affect fetal growth. Further, low dose effects are difficult to extract from epidemiological studies due to ubiquitous exposure. As well, studies typically treat EDCs in isolation when human exposure occurs in mixtures. In summary, while *in vitro* studies demonstrate a pro-adipogenic effect of plasticizers, more studies are needed to determine if accelerated fat accumulation due to early life exposure leads to the development of obesity and its cardiometabolic complications.

Production of Adipokines

Adipose tissue regulates systemic metabolic homeostasis in part through secreting adipokines, a group of adipocyte-derived hormones, proteins, and cytokines with autocrine, paracrine and endocrine effects on energy balance, lipid and glucose metabolism, appetite, insulin sensitivity and inflammation (Ahima and Lazar, 2008). Dysregulated adipokine secretion is a hallmark of hypertrophic adipocyte dysfunction and contributes to the pathogenesis of obesity-associated CVD.

Many plasticizers can alter adipose function by disrupting endocrine signaling in adipose tissue. Obesogenic effects leading to adipocyte hypertrophy and dysfunction may account for dysregulated adipokine release, or EDC may directly influence the endocrine function of adipose tissue. In human adipose tissue explants, treatment with BPA inhibited the release of the hormone adiponectin when present at nanomolar concentrations (Hugo et al., 2008). Adiponectin itself is a 30 kDa protein with the capacity to form several multimers, the synthesis of which is regulated by PPARγ receptors (Trujillo and Scherer, 2006). Once released from adipocytes, the physiological effects of adiponectin vary based on the specific adiponectin multimer and tissue-specific receptor to which the protein binds. For example, adiponectin increases fatty acid oxidation and glucose metabolism in muscle when bound to skeletal AdipoR1. When bound to hepatic AdipoR2, however, adiponectin stimulates increased insulin sensitivity. Adiponectin also has the potential to stimulate anti-inflammatory and antiatherogenic effects and is considered to be a key regulator of insulin sensitivity (Trujillo and Scherer, 2006). BADGE, a synthesis product of BPA, has been shown to antagonize PPARγ receptors, potentially inhibiting adiponectin expression through this mechanism (Wright et al., 2000). Moreover, BPA may directly inhibit adiponectin synthesis by disrupting the action of protein disulfide isomerase, an enzyme crucial to the assembly and retention of adiponectin (Hiroi et al., 2006). Other bisphenols, including BPF, have also been shown to inhibit adiponectin production (Rochester and Bolden, 2015). Further, the phthalate DEHP has been shown to inhibit the expression of adiponectin in female mice (Schmidt et al., 2012; Klöting et al., 2015). Similarly to bisphenols, this phthalate and its metabolites suppress expression of PPARγ receptors (Schmidt et al., 2012).

Plasticizers have also been shown to disrupt the production of the adipokine leptin in adipose tissue, which is a signaling protein involved in regulating feelings of hunger and satiety. BPA exposure was positively associated with serum leptin levels in both humans and rats, although this increase was not correlated with a change in fat mass in human subjects (Wei et al., 2011). Elevation of leptin in these studies was shown to be attributable, in part, to neonatal exposure to BPA (Rönn et al., 2014). The plasticizer, DEHP, a phthalate, has also been shown to increase leptin levels in human pre-adipocytes, although decreased lipid accumulation was observed in this study (Wei et al., 2011; Rönn et al., 2014; Haq et al., 2020). In contrast to the anti-inflammatory properties of adiponectin, leptin stimulates the production of pro-inflammatory cytokines, and an imbalance in the ratio of leptin-to-adiponectin secretion has been associated with obesity and its cardiovascular outcomes (López-Jaramillo et al., 2014).

Adipocytes are responsible for the production of a number of other adipokines, although the effects of plasticizers on these compounds is less studied. Chemerin is a protein produced by adipocytes that is associated with inflammation, metabolic dysfunction and carcinogenesis (Hoffmann et al., 2018). BPA and its halogenated derivatives have been shown to decrease the mRNA expression levels of this peptide in a cancer cell model (Hoffmann et al., 2018). Resistin, an adipokine that interferes with insulin signaling, also shows increased expression *in vitro* in the presence of BPA (Jamaluddin et al., 2012; Menale et al., 2017). The phthalate DEHP did not affect resistin levels in rats, while increases in circulating resistin were observed in female mice after perinatal DEHP exposure (Campioli et al., 2014; Neier et al., 2019). The plasticizer dibutyl phthalate (DBP) has also been negatively correlated with the serum levels of the adipokine omentin (Zhang et al., 2017). The effects of plasticizers on other adipokines such as visfatin and dipeptidyl peptidase 4 have been insufficiently studied. Visfatin, however, is regulated by PPARγ signalling (Choi et al., 2005). Given the previously discussed effects of plasticizers on these receptors, it is possible to speculate that plasticizers may impact visfatin expression.

Adipose Tissue Inflammation and Oxidative Stress

Inflammation and oxidative stress are core underlying mechanisms in the progression of adipose tissue dysfunction and CVD. BPA has been shown to stimulate the release of inflammatory adipocytokines, including IL-6 and TNF-α from preadipocytes, adipocytes and macrophages within adipose tissue (Heinrich et al., 2003; Ben-Jonathan et al., 2009). Phthalates such as DEHP have also been shown to stimulate TNF-α in adipose tissue (Campioli et al., 2014). While both cytokines exhibit potent inflammatory effects, IL-6 is a pleiotropic cytokine that has been known to stimulate lipolysis, inhibit lipoprotein lipase, and reduce glucose uptake in the adipose tissue. This cytokine furthermore suppresses adiponectin release (Kamimura et al., 2003). TNF-α stimulates lipolysis in the adipose tissue and suppresses

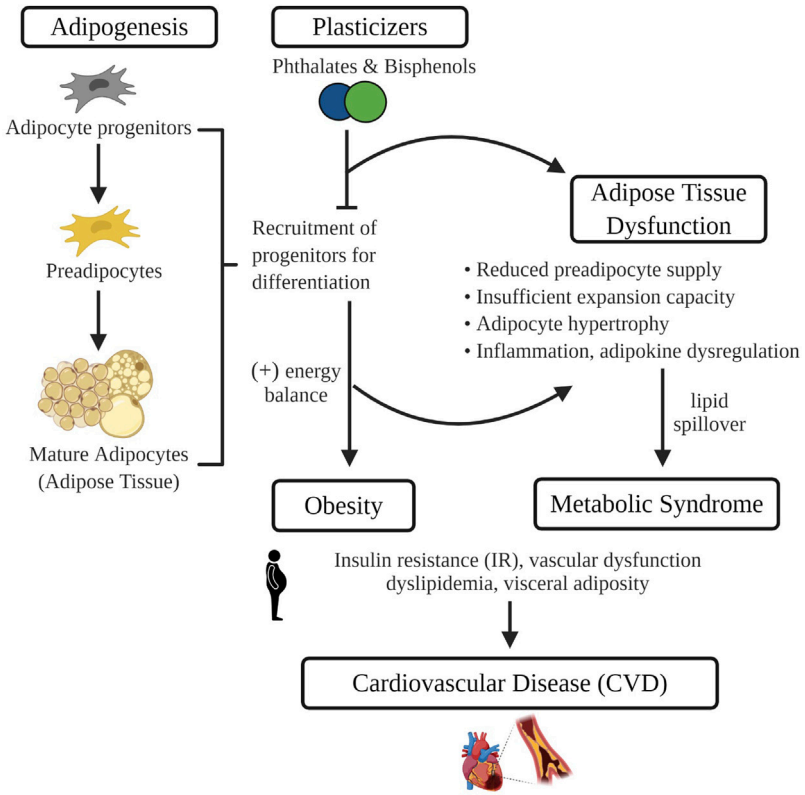

FIGURE 1 | In isolated adipocyte progenitors, differentiation is enhanced with exposure to common plasticizers, phthalates and bisphenols. Therefore, exposure to plasticizers during critical developmental windows of adipogenesis may recruit a greater number of progenitors towards terminal differentiation. Increased adipogenesis during early life leads to the development of obesity and may prematurely deplete the progenitor pool that protects against obesity-associated adipose tissue dysfunction. Adipose tissue dysfunction characterized by an impaired energy buffering capacity, adipocyte hypertrophy and inflammation, is a pivotal pathogenic event in the development of CVD risk factors such as dyslipidemia and insulin resistance. Image made in Biorender.

insulin sensitivity by downregulating glucose transporter expression, interfering with insulin signaling, and by inhibiting transcription factors involved in insulin sensitivity (Ben-Jonathan et al., 2009).

An increase in oxidative stress in response to BPA has been reported in several cell types (Gassman, 2017). A relationship between the inflammation induced by BPA and oxidative stress has been demonstrated (Ferguson et al., 2016). In an inflammatory state, immune cells such as macrophages are recruited to the adipose tissue; these cells generate reactive oxygen species (ROS) and nitrogen species that both contribute to chronic inflammation and damage cells. Furthermore, oxidative stress induced by BPA was shown to be essential in the activation of the NOD-like receptor protein 3 (NLRP3) inflammasome in adipose cells (Ahmed and Atlas, 2016). The activation of an inflammatory response by BPA-induced oxidative stress causes the recruitment of additional ROS-generating immune cells to the adipose tissue, leading to a sustained cycle of inflammation and oxidative stress (Meli et al., 2020). Alternatively, BPA may induce the production of ROS directly by inhibiting the action of antioxidant enzymes, including superoxide dismutase, catalase, glutathione reductase (GR), and glutathione peroxidase (GSH-Px) (Meli et al., 2020). Further, BPA exposure leads to ATP depletion, cytochrome c release, loss of mitochondrial mass, and loss membrane potential (Lin et al., 2013). Thus, mitochondrial dysfunction may be both a cause and consequence of BPA-induced oxidative stress. Phthalate exposure has also been associated with oxidative stress in adipose tissue (Schaedlich et al., 2018). It has been hypothesized that phthalate-induced oxidative stress is mediated through the activation of PPAR receptors or through changes in mitochondrial function (Trasande and Attina, 2015). The above evidence highlights oxidative stress and inflammation as important pathogenic mechanisms linking plasticizer exposure to adipose tissue dysfunction and CVD.

CONCLUSION

Commonly used plasticizers, bisphenols and phthalates, are among the most pervasive environmental toxins in our environment. Numerous studies have revealed that exposure to these synthetic chemicals can lead to

reproductive and developmental disorders including infertility and early puberty. More recently, exposure has been linked to the pathogenesis of cardiometabolic diseases such as obesity, diabetes and CVD. Given that adipose tissue sequesters environmental toxins and is central to the development of obesity-associated CVD, it may play a critical role in mediating the impact of plasticizers on cardiovascular health (**Figure 1**). Herein we highlight current evidence surrounding potential mechanisms by which plasticizer exposure modulates adipose tissue development and function. Data described include those from recent studies revealing that synthetic analogues marketed as safer alternatives have similar effects on adipogenesis, oxidative stress and adipose tissue function. These findings emphasize the need for further scientific inquiry into synthetic analogues and their purported safety and continued efforts to limit environmental exposure or develop safer alternatives such as the emerging bio-polymers.

AUTHOR CONTRIBUTIONS

All authors contributed to the literature search, analysis and writing of the manuscript. JT edited all sections of the manuscript. Small components of an undergraduate thesis written by SA-H were incorporated into the manuscript, with permission provided by SA-H.

FUNDING

JT, MC, LC, and RS are funded by the Libin Cardiovascular Institute. LC is funded by a Graduate Scholarship in Women's Cardiovascular Health, RS is funded by a Kertland Fellowship. MC was funded by a summer studentship from the National Sciences and Engineering Research Council of Canada (NSERC). MC also supported by a studentship from Alberta Children's Hospital Research Institute (ACHRI).

REFERENCES

Ahima, R. S., and Lazar, M. A. (2008). Adipokines and the peripheral and neural control of energy balance. *Mol. Endocrinol.* 22, 1023–1031. doi:10.1210/me.2007-0529

Ahmed, S., and Atlas, E. (2016). Bisphenol S- and bisphenol A-induced adipogenesis of murine preadipocytes occurs through direct peroxisome proliferator-activated receptor gamma activation. *Int. J. Obes.* 40, 1566–1573. doi:10.1038/ijo.2016.95

Akoumianakis, I., Akawi, N., and Antoniades, C. (2017). Exploring the crosstalk between adipose tissue and the cardiovascular system. *Korean Circ. J.* 47, 670–685. doi:10.4070/kcj.2017.0041

Ariemma, F., D'esposito, V., Liguoro, D., Oriente, F., Cabaro, S., Liotti, A., et al. (2016). Low-dose bisphenol-A impairs adipogenesis and generates dysfunctional 3T3-L1 adipocytes. *PLoS One* 11, e0150762. doi:10.1371/journal.pone.0150762

Baillie-Hamilton, P. F. (2002). Chemical toxins: a hypothesis to explain the global obesity epidemic. *J. Alternative Compl. Med.* 8, 185–192. doi:10.1089/107555302317371479

Ben-Jonathan, N., Hugo, E. R., and Brandebourg, T. D. (2009). Effects of bisphenol A on adipokine release from human adipose tissue: implications for the metabolic syndrome. *Mol. Cell. Endocrinol.* 304, 49–54. doi:10.1016/j.mce.2009.02.022

Berry, D. C., Stenesen, D., Zeve, D., and Graff, J. M. (2013). The developmental origins of adipose tissue. *Development* 140, 3939–3949. doi:10.1242/dev.080549

Biro, S., Barber, D., Williamson, T., Morkem, R., Khan, S., and Janssen, I. (2016). Prevalence of toddler, child and adolescent overweight and obesity derived from primary care electronic medical records: an observational study. *CMAJ Open* 4, E538–e544. doi:10.9778/cmajo.20150108

Boucher, J. G., Ahmed, S., and Atlas, E. (2016). Bisphenol S induces adipogenesis in primary human preadipocytes from female donors. *Endocrinology* 157, 1397–1407. doi:10.1210/en.2015-1872

Boucher, J. G., Boudreau, A., and Atlas, E. (2014). Bisphenol A induces differentiation of human preadipocytes in the absence of glucocorticoid and is inhibited by an estrogen-receptor antagonist. *Nutr. Diabetes* 4, e102. doi:10.1038/nutd.2013.43

Buckley, J. P., Engel, S. M., Braun, J. M., Whyatt, R. M., Daniels, J. L., Mendez, M. A., et al. (2016a). Prenatal phthalate exposures and body mass index among 4- to 7-Year-old children: a pooled analysis. *Epidemiology* 27, 449–458. doi:10.1097/EDE.0000000000000436

Buckley, J. P., Engel, S. M., Mendez, M. A., Richardson, D. B., Daniels, J. L., Calafat, A. M., et al. (2016b). Prenatal phthalate exposures and childhood fat mass in a New York city cohort. *Environ. Health Perspect.* 124, 507–513. doi:10.1289/ehp.1509788

Cai, S., Rao, X., Ye, J., Ling, Y., Mi, S., Chen, H., et al. (2020). Relationship between urinary bisphenol a levels and cardiovascular diseases in the U.S. adult population, 2003-2014. *Ecotoxicol. Environ. Saf.* 192, 110300. doi:10.1016/j.ecoenv.2020.110300

Calafat, A. M., Ye, X., Wong, L. Y., Reidy, J. A., and Needham, L. L. (2008). Exposure of the U.S. population to bisphenol A and 4-tertiary-octylphenol: 2003-2004. *Environ. Health Perspect.* 116, 39–44. doi:10.1289/ehp.10753

Campioli, E., Martinez-Arguelles, D. B., and Papadopoulos, V. (2014). In utero exposure to the endocrine disruptor di-(2-ethylhexyl) phthalate promotes local adipose and systemic inflammation in adult male offspring. *Nutr. Diabetes* 4, e115. doi:10.1038/nutd.2014.13

Carwile, J. L., Luu, H. T., Bassett, L. S., Driscoll, D. A., Yuan, C., Chang, J. Y., et al. (2009). Polycarbonate bottle use and urinary bisphenol A concentrations. *Environ. Health Perspect.* 117, 1368–1372. doi:10.1289/ehp.0900604

Chait, A., and Den Hartigh, L. J. (2020). Adipose tissue distribution, inflammation and its metabolic consequences, including diabetes and cardiovascular disease. *Front Cardiovasc. Med.* 7, 22. doi:10.3389/fcvm.2020.00022

Chatterjee, T. K., Basford, J. E., Knoll, E., Tong, W. S., Blanco, V., Blomkalns, A. L., et al. (2014). HDAC9 knockout mice are protected from adipose tissue dysfunction and systemic metabolic disease during high-fat feeding. *Diabetes* 63, 176–187. doi:10.2337/db13-1148

Chen, D., Kannan, K., Tan, H., Zheng, Z., Feng, Y. L., Wu, Y., et al. (2016). Bisphenol analogues other than BPA: environmental occurrence, human exposure, and toxicity-A review. *Environ. Sci. Technol.* 50, 5438–5453. doi:10.1021/acs.est.5b05387

Chiu, Y. H., Bellavia, A., James-Todd, T., Correia, K. F., Valeri, L., Messerlian, C., et al. (2018). Evaluating effects of prenatal exposure to phthalate mixtures on birth weight: a comparison of three statistical approaches. *Environ. Int.* 113, 231–239. doi:10.1016/j.envint.2018.02.005

Choe, S. S., Huh, J. Y., Hwang, I. J., Kim, J. I., and Kim, J. B. (2016). Adipose tissue remodeling: its role in energy metabolism and metabolic disorders. *Front. Endocrinol.* 7, 30. doi:10.3389/fendo.2016.00030

Choi, K. C., Ryu, O. H., Lee, K. W., Kim, H. Y., Seo, J. A., Kim, S. G., et al. (2005). Effect of PPAR-alpha and -gamma agonist on the expression of visfatin, adiponectin, and TNF-alpha in visceral fat of OLETF rats. *Biochem. Biophys. Res. Commun.* 336, 747–753. doi:10.1016/j.bbrc.2005.08.203

Corbel, T., Perdu, E., Gayrard, V., Puel, S., Lacroix, M. Z., Viguié, C., et al. (2015). Conjugation and deconjugation reactions within the fetoplacental compartment in a sheep model: a key factor determining bisphenol A fetal exposure. *Drug Metab. Dispos.* 43, 467–476. doi:10.1124/dmd.114.061291

Corrales, J., Kristofco, L. A., Steele, W. B., Yates, B. S., Breed, C. S., Williams, E. S., et al. (2015). Global assessment of bisphenol A in the environment: review and

analysis of its occurrence and bioaccumulation. *Dose Response* 13, 1559325815598308. doi:10.1177/1559325815598308

Deierlein, A. L., Wolff, M. S., Pajak, A., Pinney, S. M., Windham, G. C., Galvez, M. P., et al. (2016). Longitudinal associations of phthalate exposures during childhood and body size measurements in young girls. *Epidemiology* 27, 492–499. doi:10.1097/EDE.0000000000000489

Duan, Y., Yao, Y., Wang, B., Han, L., Wang, L., Sun, H., et al. (2018). Association of urinary concentrations of bisphenols with type 2 diabetes mellitus: a case-control study. *Environ. Pollut.* 243, 1719–1726. doi:10.1016/j.envpol.2018.09.093

Feige, J. N., Gelman, L., Rossi, D., Zoete, V., Métivier, R., Tudor, C., et al. (2007). The endocrine disruptor monoethyl-hexyl-phthalate is a selective peroxisome proliferator-activated receptor gamma modulator that promotes adipogenesis. *J. Biol. Chem.* 282, 19152–19166. doi:10.1074/jbc.M702724200

Ferguson, K. K., Cantonwine, D. E., Mcelrath, T. F., Mukherjee, B., and Meeker, J. D. (2016). Repeated measures analysis of associations between urinary bisphenol-A concentrations and biomarkers of inflammation and oxidative stress in pregnancy. *Reprod. Toxicol.* 66, 93–98. doi:10.1016/j.reprotox.2016.10.002

Flint, S., Markle, T., Thompson, S., and Wallace, E. (2012). Bisphenol A exposure, effects, and policy: a wildlife perspective. *J. Environ. Manag.* 104, 19–34. doi:10.1016/j.jenvman.2012.03.021

Gassman, N. R. (2017). Induction of oxidative stress by bisphenol A and its pleiotropic effects. *Environ. Mol. Mutagen.* 58, 60–71. doi:10.1002/em.22072

Gaston, S. A., and Tulve, N. S. (2019). Urinary phthalate metabolites and metabolic syndrome in U.S. adolescents: cross-sectional results from the National Health and Nutrition Examination Survey (2003-2014) data. *Int. J. Hyg Environ. Health* 222, 195–204. doi:10.1016/j.ijheh.2018.09.005

Genuis, S. J., Beesoon, S., Birkholz, D., and Lobo, R. A. (2012). Human excretion of bisphenol A: blood, urine, and sweat (BUS) study. *J Environ Public Health*, 2012, 185731. doi:10.1155/2012/185731

Gerona, R., Vom Saal, F. S., and Hunt, P. A. (2020). BPA: have flawed analytical techniques compromised risk assessments? *Lancet Diabetes Endocrinol* 8, 11–13. doi:10.1016/S2213-8587(19)30381-X

Gerona, R. R., Woodruff, T. J., Dickenson, C. A., Pan, J., Schwartz, J. M., Sen, S., et al. (2013). Bisphenol-A (BPA), BPA glucuronide, and BPA sulfate in midgestation umbilical cord serum in a northern and central California population. *Environ. Sci. Technol.* 47, 12477–12485. doi:10.1021/es402764d

Gingrich, J., Pu, Y., Ehrhardt, R., Karthikraj, R., Kannan, K., and Veiga-Lopez, A. (2019). Toxicokinetics of bisphenol A, bisphenol S, and bisphenol F in a pregnancy sheep model. *Chemosphere* 220, 185–194. doi:10.1016/j.chemosphere.2018.12.109

Grün, F., and Blumberg, B. (2006). Environmental obesogens: organotins and endocrine disruption via nuclear receptor signaling. *Endocrinology* 147, S50–S55. doi:10.1210/en.2005-1129

Hao, C., Cheng, X., Xia, H., and Ma, X. (2012). The endocrine disruptor mono-(2-ethylhexyl) phthalate promotes adipocyte differentiation and induces obesity in mice. *Biosci. Rep.* 32, 619–629. doi:10.1042/BSR20120042

Haq, M. E. U., Akash, M. S. H., Rehman, K., and Mahmood, M. H. (2020). Chronic exposure of bisphenol A impairs carbohydrate and lipid metabolism by altering corresponding enzymatic and metabolic pathways. *Environ. Toxicol. Pharmacol.* 78, 103387. doi:10.1016/j.etap.2020.103387

Harley, K. G., Aguilar Schall, R., Chevrier, J., Tyler, K., Aguirre, H., Bradman, A., et al. (2013). Prenatal and postnatal bisphenol A exposure and body mass index in childhood in the CHAMACOS cohort. *Environ. Health Perspect.* 121, 514–520. doi:10.1289/ehp.1205548

Hartle, J. C., Navas-Acien, A., and Lawrence, R. S. (2016). The consumption of canned food and beverages and urinary Bisphenol A concentrations in NHANES 2003-2008. *Environ. Res.* 150, 375–382. doi:10.1016/j.envres.2016.06.008

Hatch, E. E., Nelson, J. W., Qureshi, M. M., Weinberg, J., Moore, L. L., Singer, M., et al. (2008). Association of urinary phthalate metabolite concentrations with body mass index and waist circumference: a cross-sectional study of NHANES data, 1999-2002. *Environ. Health* 7, 27. doi:10.1186/1476-069X-7-27

Heinrich, P. C., Behrmann, I., Haan, S., Hermanns, H. M., Müller-Newen, G., and Schaper, F. (2003). Principles of interleukin (IL)-6-type cytokine signalling and its regulation. *Biochem. J.* 374, 1–20. doi:10.1042/BJ20030407

Hiroi, T., Okada, K., Imaoka, S., Osada, M., and Funae, Y. (2006). Bisphenol A binds to protein disulfide isomerase and inhibits its enzymatic and hormone-binding activities. *Endocrinology* 147, 2773–2780. doi:10.1210/en.2005-1235

Hoffmann, M., Rak, A., and Ptak, A. (2018). Bisphenol A and its derivatives decrease expression of chemerin, which reverses its stimulatory action in ovarian cancer cells. *Toxicol. Lett.* 291, 61–69. doi:10.1016/j.toxlet.2018.04.004

Huang, T., Saxena, A. R., Isganaitis, E., and James-Todd, T. (2014). Gender and racial/ethnic differences in the associations of urinary phthalate metabolites with markers of diabetes risk: national Health and Nutrition Examination Survey 2001-2008. *Environ. Health* 13, 6. doi:10.1186/1476-069X-13-6

Hugo, E. R., Brandebourg, T. D., Woo, J. G., Loftus, J., Alexander, J. W., and Ben-Jonathan, N. (2008). Bisphenol A at environmentally relevant doses inhibits adiponectin release from human adipose tissue explants and adipocytes. *Environ. Health Perspect.* 116, 1642–1647. doi:10.1289/ehp.11537

Huo, L., Lyons, J., and Magliano, D. J. (2016). Infectious and environmental influences on the obesity epidemic. *Curr. Obes. Rep.* 5, 375–382. doi:10.1007/s13679-016-0224-9

Ikeoka, D., Mader, J. K., and Pieber, T. R. (2010). Adipose tissue, inflammation and cardiovascular disease. *Rev. Assoc. Med. Bras. (1992)* 56, 116–121. doi:10.1590/s0104-42302010000100026

Ikezuki, Y., Tsutsumi, O., Takai, Y., Kamei, Y., and Taketani, Y. (2002). Determination of bisphenol A concentrations in human biological fluids reveals significant early prenatal exposure. *Hum. Reprod.* 17, 2839–2841. doi:10.1093/humrep/17.11.2839

Jamaluddin, M. S., Weakley, S. M., Yao, Q., and Chen, C. (2012). Resistin: functional roles and therapeutic considerations for cardiovascular disease. *Br. J. Pharmacol.* 165, 622–632. doi:10.1111/j.1476-5381.2011.01369.x

Jang, H., Kim, M., Lee, S., Kim, J., Woo, D. C., Kim, K. W., et al. (2016). Adipose tissue hyperplasia with enhanced adipocyte-derived stem cell activity in Tc1(C8orf4)-deleted mice. *Sci. Rep.* 6, 35884. doi:10.1038/srep35884

Jeffery, E., Wing, A., Holtrup, B., Sebo, Z., Kaplan, J. L., Saavedra-Peña, R., et al. (2016). The adipose tissue microenvironment regulates depot-specific adipogenesis in obesity. *Cell Metab.* 24, 142–150. doi:10.1016/j.cmet.2016.05.012

Jiang, Y., Berry, D. C., Tang, W., and Graff, J. M. (2014). Independent stem cell lineages regulate adipose organogenesis and adipose homeostasis. *Cell Rep.* 9, 1007–1022. doi:10.1016/j.celrep.2014.09.049

Ju, S. Y., Lee, J. Y., and Kim, D. H. (2017). Association of metabolic syndrome and its components with all-cause and cardiovascular mortality in the elderly: a meta-analysis of prospective cohort studies. *Medicine (Baltim.)* 96, e8491. doi:10.1097/MD.0000000000008491

Kachur, S., Lavie, C. J., De Schutter, A., Milani, R. V., and Ventura, H. O. (2017). Obesity and cardiovascular diseases. *Minerva Med.* 108, 212–228. doi:10.23736/S0026-4806.17.05022-4

Kamimura, D., Ishihara, K., and Hirano, T. (2003). IL-6 signal transduction and its physiological roles: the signal orchestration model. *Rev. Physiol. Biochem. Pharmacol.* 149, 1–38. doi:10.1007/s10254-003-0012-2

Kamrin, M. A. (2009). Phthalate risks, phthalate regulation, and public health: a review. *J. Toxicol. Environ. Health B Crit. Rev.* 12, 157–174. doi:10.1080/10937400902729226

Kim, J. I., Huh, J. Y., Sohn, J. H., Choe, S. S., Lee, Y. S., Lim, C. Y., et al. (2015). Lipid-overloaded enlarged adipocytes provoke insulin resistance independent of inflammation. *Mol. Cell Biol.* 35, 1686–1699. doi:10.1128/MCB.01321-14

Klöting, N., Hesselbarth, N., Gericke, M., Kunath, A., Biemann, R., Chakaroun, R., et al. (2015). Di-(2-Ethylhexyl)-Phthalate (DEHP) causes impaired adipocyte function and alters serum metabolites. *PLoS One* 10, e0143190. doi:10.1371/journal.pone.0143190

López-Jaramillo, P., Gómez-Arbeláez, D., López-López, J., López-López, C., Martínez-Ortega, J., Gómez-Rodríguez, A., et al. (2014). The role of leptin/adiponectin ratio in metabolic syndrome and diabetes. *Horm. Mol. Biol. Clin. Invest.* 18, 37–45. doi:10.1515/hmbci-2013-0053

Lakind, J. S., Goodman, M., and Naiman, D. Q. (2012). Use of NHANES data to link chemical exposures to chronic diseases: a cautionary tale. *PLoS One* 7, e51086. doi:10.1371/journal.pone.0051086

Lang, I. A., Galloway, T. S., Scarlett, A., Henley, W. E., Depledge, M., Wallace, R. B., et al. (2008). Association of urinary bisphenol A concentration with medical disorders and laboratory abnormalities in adults. *JAMA* 300, 1303–1310. doi:10.1001/jama.300.11.1303

Lee, B. E., Park, H., Hong, Y. C., Ha, M., Kim, Y., Chang, N., et al. (2014). Prenatal bisphenol A and birth outcomes: MOCEH (mothers and children's environmental health) study. *Int. J. Hyg. Environ. Health* 217, 328–334. doi:10.1016/j.ijheh.2013.07.005

Lehmler, H. J., Liu, B., Gadogbe, M., and Bao, W. (2018). Exposure to bisphenol A, bisphenol F, and bisphenol S in U.S. Adults and children: the national health and nutrition examination survey 2013-2014. *ACS Omega* 3, 6523–6532. doi:10.1021/acsomega.8b00824

Lin, Y., Sun, X., Qiu, L., Wei, J., Huang, Q., Fang, C., et al. (2013). Exposure to bisphenol A induces dysfunction of insulin secretion and apoptosis through the damage of mitochondria in rat insulinoma (INS-1) cells. *Cell Death Dis.* 4, e460. doi:10.1038/cddis.2012.206

Medina-Gomez, G., Gray, S. L., Yetukuri, L., Shimomura, K., Virtue, S., Campbell, M., et al. (2007). PPAR gamma 2 prevents lipotoxicity by controlling adipose tissue expandability and peripheral lipid metabolism. *PLoS Genet.* 3, e64. doi:10.1371/journal.pgen.0030064

Meeker, J. D., Calafat, A. M., and Hauser, R. (2012). Urinary phthalate metabolites and their biotransformation products: predictors and temporal variability among men and women. *J. Expo. Sci. Environ. Epidemiol.* 22, 376–385. doi:10.1038/jes.2012.7

Meli, R., Monnolo, A., Annunziata, C., Pirozzi, C., and Ferrante, M. C. (2020). Oxidative stress and BPA toxicity: an antioxidant approach for male and female reproductive dysfunction. *Antioxidants* 9, 405. doi:10.3390/antiox9050405

Menale, C., Grandone, A., Nicolucci, C., Cirillo, G., Crispi, S., Di Sessa, A., et al. (2017). Bisphenol A is associated with insulin resistance and modulates adiponectin and resistin gene expression in obese children. *Pediatr Obes* 12, 380–387. doi:10.1111/ijpo.12154

Miao, M., Yuan, W., Zhu, G., He, X., and Li, D. K. (2011). In utero exposure to bisphenol-A and its effect on birth weight of offspring. *Reprod. Toxicol.* 32, 64–68. doi:10.1016/j.reprotox.2011.03.002

Neier, K., Cheatham, D., Bedrosian, L. D., Gregg, B. E., Song, P. X. K., and Dolinoy, D. C. (2019). Longitudinal metabolic impacts of perinatal exposure to phthalates and phthalate mixtures in mice. *Endocrinology* 160, 1613–1630. doi:10.1210/en.2019-00287

Ohlstein, J. F., Strong, A. L., Mclachlan, J. A., Gimble, J. M., Burow, M. E., and Bunnell, B. A. (2014). Bisphenol A enhances adipogenic differentiation of human adipose stromal/stem cells. *J. Mol. Endocrinol.* 53, 345–353. doi:10.1530/JME-14-0052

Piecha, R., Svačina, Š., Malý, M., Vrbík, K., Lacinová, Z., Haluzík, M., et al. (2016). Urine levels of phthalate metabolites and bisphenol A in relation to main metabolic syndrome components: dyslipidemia, hypertension and type 2 diabetes. A pilot study. *Cent. Eur. J. Publ. Health* 24, 297–301. doi:10.21101/cejph.a4704

Pomatto, V., Cottone, E., Cocci, P., Mozzicafreddo, M., Mosconi, G., Nelson, E. R., et al. (2018). Plasticizers used in food-contact materials affect adipogenesis in 3T3-L1 cells. *J. Steroid Biochem. Mol. Biol.* 178, 322–332. doi:10.1016/j.jsbmb.2018.01.014

Pu, Y., Gingrich, J. D., Steibel, J. P., and Veiga-Lopez, A. (2017). Sex-specific modulation of fetal adipogenesis by gestational bisphenol A and bisphenol S exposure. *Endocrinology* 158, 3844–3858. doi:10.1210/en.2017-00615

Qi, W., Zhou, L., Zhao, T., Ding, S., Xu, Q., Han, X., et al. (2019). Effect of the TYK-2/STAT-3 pathway on lipid accumulation induced by mono-2-ethylhexyl phthalate. *Mol. Cell. Endocrinol.* 484, 52–58. doi:10.1016/j.mce.2019.01.012

Rönn, M., Lind, L., Örberg, J., Kullberg, J., Söderberg, S., Larsson, A., et al. (2014). Bisphenol A is related to circulating levels of adiponectin, leptin and ghrelin, but not to fat mass or fat distribution in humans. *Chemosphere* 112, 42–48. doi:10.1016/j.chemosphere.2014.03.042

Ramskov Tetzlaff, C. N., Svingen, T., Vinggaard, A. M., Rosenmai, A. K., and Taxvig, C. (2020). Bisphenols B, E, F, and S and 4-cumylphenol induce lipid accumulation in mouse adipocytes similarly to bisphenol A. *Environ. Toxicol.* 35, 543–552. doi:10.1002/tox.22889

Rancière, F., Botton, J., Slama, R., Lacroix, M. Z., Debrauwer, L., Charles, M. A., et al. (2019). Exposure to bisphenol A and bisphenol S and incident type 2 diabetes: a case-cohort study in the French cohort D.E.S.I.R. *Environ. Health Perspect.* 127, 107013. doi:10.1289/EHP5159

Rochester, J. R., and Bolden, A. L. (2015). Bisphenol S and F: a systematic review and comparison of the hormonal activity of bisphenol A substitutes. *Environ. Health Perspect.* 123, 643–650. doi:10.1289/ehp.1408989

Saravanabhavan, G., Guay, M., Langlois, É., Giroux, S., Murray, J., and Haines, D. (2013). Biomonitoring of phthalate metabolites in the Canadian population through the Canadian health measures survey (2007-2009). *Int. J. Hyg Environ. Health* 216, 652–661. doi:10.1016/j.ijheh.2012.12.009

Sargis, R. M., Johnson, D. N., Choudhury, R. A., and Brady, M. J. (2010). Environmental endocrine disruptors promote adipogenesis in the 3T3-L1 cell line through glucocorticoid receptor activation. *Obesity* 18, 1283–1288. doi:10.1038/oby.2009.419

Schaedlich, K., Gebauer, S., Hunger, L., Beier, L. S., Koch, H. M., Wabitsch, M., et al. (2018). DEHP deregulates adipokine levels and impairs fatty acid storage in human SGBS-adipocytes. *Sci. Rep.* 8, 3447. doi:10.1038/s41598-018-21800-4

Schmidt, J. S., Schaedlich, K., Fiandanese, N., Pocar, P., and Fischer, B. (2012). Effects of di(2-ethylhexyl) phthalate (DEHP) on female fertility and adipogenesis in C3H/N mice. *Environ. Health Perspect.* 120, 1123–1129. doi:10.1289/ehp.1104016

Shankar, A., Teppala, S., and Sabanayagam, C. (2012). Urinary bisphenol a levels and measures of obesity: results from the national health and nutrition examination survey 2003-2008. *ISRN Endocrinol.* 2012, 965243. doi:10.5402/2012/965243

Shim, Y. H., Ock, J. W., Kim, Y. J., Kim, Y., Kim, S. Y., and Kang, D. (2019). Association between heavy metals, bisphenol A, volatile organic compounds and phthalates and metabolic syndrome. *Int. J. Environ. Res. Publ. Health* 16, 671. doi:10.3390/ijerph16040671

Shoaff, J. R., Romano, M. E., Yolton, K., Lanphear, B. P., Calafat, A. M., and Braun, J. M. (2016). Prenatal phthalate exposure and infant size at birth and gestational duration. *Environ. Res.* 150, 52–58. doi:10.1016/j.envres.2016.05.033

Silva, M. J., Barr, D. B., Reidy, J. A., Malek, N. A., Hodge, C. C., Caudill, S. P., et al. (2004). Urinary levels of seven phthalate metabolites in the U.S. population from the national health and nutrition examination survey (NHANES) 1999-2000. *Environ. Health Perspect.* 112, 331–338. doi:10.1289/ehp.6723

Smith, M. N., Cohen Hubal, E. A., and Faustman, E. M. (2020). A Case study on the utility of predictive toxicology tools in alternatives assessments for hazardous chemicals in children's consumer products. *J. Expo. Sci. Environ. Epidemiol.* 30, 160–170. doi:10.1038/s41370-019-0165-y

Somm, E., Schwitzgebel, V. M., Toulotte, A., Cederroth, C. R., Combescure, C., Nef, S., et al. (2009). Perinatal exposure to bisphenol a alters early adipogenesis in the rat. *Environ. Health Perspect.* 117, 1549–1555. doi:10.1289/ehp.11342

Stahlhut, R. W., Van Wijngaarden, E., Dye, T. D., Cook, S., and Swan, S. H. (2007). Concentrations of urinary phthalate metabolites are associated with increased waist circumference and insulin resistance in adult U.S. males. *Environ. Health Perspect.* 115, 876–882. doi:10.1289/ehp.9882

Stojanoska, M. M., Milosevic, N., Milic, N., and Abenavoli, L. (2017). The influence of phthalates and bisphenol A on the obesity development and glucose metabolism disorders. *Endocrine* 55, 666–681. doi:10.1007/s12020-016-1158-4

Svensson, K., Hernández-Ramírez, R. U., Burguete-García, A., Cebrián, M. E., Calafat, A. M., Needham, L. L., et al. (2011). Phthalate exposure associated with self-reported diabetes among Mexican women. *Environ. Res.* 111, 792–796. doi:10.1016/j.envres.2011.05.015

Trasande, L., and Attina, T. M. (2015). Association of exposure to di-2-ethylhexylphthalate replacements with increased blood pressure in children and adolescents. *Hypertension* 66, 301–308. doi:10.1161/HYPERTENSIONAHA.115.05603

Trasande, L., Attina, T. M., Sathyanarayana, S., Spanier, A. J., and Blustein, J. (2013). Race/ethnicity-specific associations of urinary phthalates with childhood body mass in a nationally representative sample. *Environ. Health Perspect.* 121, 501–506. doi:10.1289/ehp.1205526

Tremblay, M. S., and Willms, J. D (2000). Secular trends in the body mass index of Canadian children. *CMAJ* 163(11), 1429–1433.

Troisi, J., Mikelson, C., Richards, S., Symes, S., Adair, D., Zullo, F., et al. (2014). Placental concentrations of bisphenol A and birth weight from births in the Southeastern U.S *Placenta* 35, 947–952. doi:10.1016/j.placenta.2014.08.091

Trujillo, M. E., and Scherer, P. E. (2006). Adipose tissue-derived factors: impact on health and disease. *Endocr. Rev.* 27, 762–778. doi:10.1210/er.2006-0033

Völkel, W., Kiranoglu, M., and Fromme, H. (2008). Determination of free and total bisphenol A in human urine to assess daily uptake as a basis for a valid risk assessment. *Toxicol. Lett.* 179, 155–162. doi:10.1016/j.toxlet.2008.05.002

Vafeiadi, M., Roumeliotaki, T., Myridakis, A., Chalkiadaki, G., Fthenou, E., Dermitzaki, E., et al. (2016). Association of early life exposure to bisphenol A with obesity and cardiometabolic traits in childhood. *Environ. Res.* 146, 379–387. doi:10.1016/j.envres.2016.01.017

Valvi, D., Casas, M., Mendez, M. A., Ballesteros-Gómez, A., Luque, N., Rubio, S., et al. (2013). Prenatal bisphenol a urine concentrations and early rapid growth

and overweight risk in the offspring. *Epidemiology* 24, 791–799. doi:10.1097/EDE.0b013e3182a67822

Valvi, D., Casas, M., Romaguera, D., Monfort, N., Ventura, R., Martinez, D., et al. (2015). Prenatal phthalate exposure and childhood growth and blood pressure: evidence from the Spanish INMA-sabadell birth cohort study. *Environ. Health Perspect.* 123, 1022–1029. doi:10.1289/ehp.1408887

Wang, H., Liu, Z. H., Zhang, J., Huang, R. P., Yin, H., and Dang, Z. (2020). Human exposure of bisphenol A and its analogues: understandings from human urinary excretion data and wastewater-based epidemiology. *Environ. Sci. Pollut. Res. Int.* 27, 3247–3256. doi:10.1007/s11356-019-07111-9

Wang, Q. A., and Scherer, P. E. (2014). The AdipoChaser mouse: a model tracking adipogenesis *in vivo*. *Adipocyte* 3, 146–150. doi:10.4161/adip.27656

Wang, T., Li, M., Chen, B., Xu, M., Xu, Y., Huang, Y., et al. (2012). Urinary bisphenol A (BPA) concentration associates with obesity and insulin resistance. *J. Clin. Endocrinol. Metab.* 97, E223–E227. doi:10.1210/jc.2011-1989

Wang, Y., Zhu, H., and Kannan, K. (2019). A review of biomonitoring of phthalate exposures. *Toxics* 7, 21. doi:10.3390/toxics7020021

Ward, Z. J., Bleich, S. N., Cradock, A. L., Barrett, J. L., Giles, C. M., Flax, C., et al. (2019). Projected U.S. State-level prevalence of adult obesity and severe obesity. *N. Engl. J. Med.* 381, 2440–2450. doi:10.1056/NEJMsa1909301

Wei, J., Lin, Y., Li, Y., Ying, C., Chen, J., Song, L., et al. (2011). Perinatal exposure to bisphenol A at reference dose predisposes offspring to metabolic syndrome in adult rats on a high-fat diet. *Endocrinology* 152, 3049–3061. doi:10.1210/en.2011-0045

Wright, H. M., Clish, C. B., Mikami, T., Hauser, S., Yanagi, K., Hiramatsu, R., et al. (2000). A synthetic antagonist for the peroxisome proliferator-activated receptor gamma inhibits adipocyte differentiation. *J. Biol. Chem.* 275, 1873–1877. doi:10.1074/jbc.275.3.1873

Zhang, L., Sun, W., Duan, X., Duan, Y., and Sun, H. (2019). Promoting differentiation and lipid metabolism are the primary effects for DINP exposure on 3T3-L1 preadipocytes. *Environ. Pollut.* 255, 113154. doi:10.1016/j.envpol.2019.113154

Zhang, M., Tan, X., Yin, C., Wang, L., Tie, Y., and Xiao, Y. (2017). Serum levels of omentin-1 are increased after weight loss and are particularly associated with increases in obese children with metabolic syndrome. *Acta Paediatr.* 106, 1851–1856. doi:10.1111/apa.14026

Conflict of Interest: The authors declare that the research was conducted in the absence of any commercial or financial relationships that could be construed as a potential conflict of interest.

frontiers in Physiology

ORIGINAL RESEARCH
published: 30 March 2021
doi: 10.3389/fphys.2021.605811

Exploring the Role of Epicardial Adipose Tissue in Coronary Artery Disease From the Difference of Gene Expression

Qian-Chen Wang[1], Zhen-Yu Wang[2], Qian Xu[3], Ruo-Bing Li[1], Guo-Gang Zhang[1] and Rui-Zheng Shi[1]**

[1] Department of Cardiovascular Medicine, Xiangya Hospital, Central South University, Changsha, China, [2] Department of Cardiovascular Medicine, The Second Xiangya Hospital, Central South University, Changsha, China, [3] Department of Cardiovascular Surgery, Xiangya Hospital, Central South University, Changsha, China

Objectives: Epicardial adipose tissue (EAT) is closely adjacent to the coronary arteries and myocardium, its role as an endocrine organ to affect the pathophysiological processes of the coronary arteries and myocardium has been increasingly recognized. However, the specific gene expression profiles of EAT in coronary artery disease (CAD) has not been well characterized. Our aim was to investigate the role of EAT in CAD at the gene level.

Methods: Here, we compared the histological and gene expression difference of EAT between CAD and non-CAD. We investigated the gene expression profiles in the EAT of patients with CAD through the high-throughput RNA sequencing. We performed bioinformatics analysis such as functional enrichment analysis and protein-protein interaction network construction to obtain and verify the hub differentially expressed genes (DEGs) in the EAT of CAD.

Results: Our results showed that the size of epicardial adipocytes in the CAD group was larger than in the control group. Our findings on the EAT gene expression profiles of CAD showed a total of 747 DEGs (fold change >2, p value <0.05). The enrichment analysis of DEGs showed that more pro-inflammatory and immunological genes and pathways were involved in CAD. Ten hub DEGs (*GNG3*, *MCHR1*, *BDKRB1*, *MCHR2*, *CXCL8*, *CXCR5*, *CCR8*, *CCL4L1*, *TAS2R10,* and *TAS2R41*) were identified.

Conclusion: Epicardial adipose tissue in CAD shows unique gene expression profiles and may act as key regulators in the CAD pathological process.

Keywords: epicardial adipose tissue, coronary artery disease, gene expression profiles, bioinformatics analysis, mRNA

OPEN ACCESS

Edited by:
Joshua Thomas Butcher, Oklahoma State University, United States

Reviewed by:
Michael Sturek, Indiana University Bloomington School of Medicine, United States
Ellen Gillis, Augusta University Medical College of Georgia, United States

****Correspondence:***
Guo-Gang Zhang
zhangguogang@csu.edu.cn
Rui-Zheng Shi
xyshiruizheng@csu.edu.cn

Specialty section:
This article was submitted to Vascular Physiology, a section of the journal Frontiers in Physiology

Received: *13 September 2020*
Accepted: *24 February 2021*
Published: *30 March 2021*

Citation:
Wang Q-C, Wang Z-Y, Xu Q, Li R-B, Zhang G-G and Shi R-Z (2021) Exploring the Role of Epicardial Adipose Tissue in Coronary Artery Disease From the Difference of Gene Expression. Front. Physiol. 12:605811. doi: 10.3389/fphys.2021.605811

INTRODUCTION

Obesity, hypertension, type 2 diabetes, hyperlipidemia, and other pathogenic factors are all associated with coronary artery disease (Gensini et al., 1998; Zengin et al., 2015; Messerli et al., 2019). Recent studies have found that in addition to the accumulation of peripheral fat, the increase in local epicardial fat is also one of the important risk factors for coronary artery disease (CAD)

(Franssens et al., 2017). In addition to storing fat, adipose tissue has been increasingly recognized as an endocrine organ, particularly because it is related to glucose and lipid homeostasis (Chong et al., 2017; Wong et al., 2017; Gruzdeva et al., 2019). Excessive calorie intake will trigger chronic inflammatory changes in adipose tissue (Sekimoto et al., 2015), and the link between adipose tissue inflammation and CAD has been gradually attracting attention.

Adipose tissue mainly includes two types, white adipose tissue (WAT) and brown adipose tissue (BAT). In terms of morphology and distribution, WAT containing unilocular lipid droplets is the main body fat, which contains less cytoplasm and mitochondria. BAT containing polylocular lipid droplets is mainly distributed in the inside of the scapula or around the kidney. Its mitochondria express abundant uncoupling protein 1 (UCP1), and are rich in blood vessels and innervation. Cold and β3 receptor stimulation can trigger the yielding of UCP1-positive cells in WAT, which are similar in shape to BAT adipocytes, with multilocular lipid droplets and abundant mitochondria, and are named as "browning" adipocytes (Alipoor et al., 2020; Reinisch et al., 2020). Under physiological conditions, Epicardial adipose tissue (EAT) belongs to WAT, but under pathological conditions, UCP1 expression increases in EAT which then presents "browning" changes (Chechi et al., 2017). Clinical studies have found that EAT deposition is positively correlated with increased metabolic abnormalities and CAD (Milanese et al., 2020).

Epicardial adipose tissue covers almost all coronary arteries anatomically (Iacobellis, 2015). By wrapping around and directly contacting the coronary arteries without fascia separation, EAT is able to affect the pathophysiological process of coronary arteries. EAT is mainly located in the atrioventricular and ventricular sulcus. It is regarded as a unique adipose depot with unique metabolic characteristics, which has a higher ability to absorb and release fatty acid (FFA) than other visceral fats and is an effective source of FFA that fuels the energy-intensive myocardial tissue (Kankaanpää et al., 2006; Pezeshkian and Mahtabipour, 2013). Many studies have shown that CAD patients have more expressions and pro-inflammatory cytokines production in the EAT than in the subcutaneous adipose tissue (SAT) (Vacca et al., 2016; Mráz et al., 2019). The EAT in CAD patients expresses pro-inflammatory adipokines and is accompanied by the infiltration of various immune cells (Nomura et al., 2020). However, most studies only compare the difference between EAT and SAT in an individual with CAD and lack the comparison with the EAT in subjects with normal coronary arteries. Therefore, it is difficult to estimate the scale of the EAT pro-inflammatory effect on coronary arteries in CAD.

In this study, we first directly compared the gene expression in the EAT of subjects with and without CAD through RNA sequencing (RNA-Seq), and obtained the gene expression profiles of EAT in CAD, and then performed bioinformatics analysis such as functional enrichment analysis and protein-protein interaction (PPI) network construction, etc., and obtained and verified differentially expressed genes with research value.

MATERIALS AND METHODS

Study Population

The study subjects were 11 patients with CAD who underwent coronary artery bypass surgery and 11 patients without CAD who underwent valve replacement in the Department of Cardiovascular Surgery of Xiangya Hospital of Central South University. The selective and exclusive criteria were as follows: (1) CAD group were patients with CAD who underwent coronary artery bypass surgery (confirmed by coronary angiography); (2) Control group (CTRL group) were patients with valvular disease who matched the age, gender, and body mass index (BMI) of the CAD group and underwent valve replacement with no evidence of CAD syndrome and negative findings in coronary angiography; (3) The main exclusive criteria included a previous PCI history, history of diabetes mellitus, previous thoracotomy history, tumor, severe infection, and autoimmune diseases. We selected five pairs from the two groups matched in age, gender, BMI, and abdominal circumference (AC), and RNA-seq was performed on the selected pairs. All patients underwent a preoperative risk assessment and signed informed consent forms. This study was approved by the Ethics Committee of Xiangya Hospital of Central South University. Trial registration: Chinese Clinical Trial Registry, No. ChiCTR1900024782.

Sample Collection

Before starting the extracorporeal circulation, the samples of EAT were taken from uninjured areas near the anterior descending coronary artery or along the atrioventricular sulcus near the right coronary artery. The samples were quickly frozen with liquid nitrogen for molecular biology experiments and stored at -80°C.

Histology

The EAT samples were fixed in 4% paraformaldehyde, embedded in paraffin, and cut into 4 μm thick slices. The size of the adipocyte was determined by calculating the Feret's diameter of the H&E stained slices (Lin et al., 2013). For each slice, we used the Image-Pro 6.2 software to check five fields of view and calculated the average.

RNA Sequencing

Total RNA was extracted from the samples using TRIzol. RNase H method was used to remove rRNA. After RNA fragmentation, cDNA synthesis, A-Tailing Mix, and adapters were added to establish a library. An Agilent 2100 Bioanalyzer (Agilent DNA 1000 Reagents) was used to detect the inserted fragments of the library, and HiSeq4000 (BGI-Shenzhen, China) was used to sequence the library qualified for detection.

Functional Enrichment Analysis of DEGs

The database for annotation, visualization, and integrated discovery (DAVID 6.8[1]) (Huang da et al., 2009) was used to analyze the functional enrichment of key differentially expressed genes (DEGs) in the GO Terms and KEGG Pathways. The threshold was $p < 0.05$.

[1]http://david.ncifcrf.gov

PPI Network Construction and Analysis

Studying the interaction between the encoded proteins will help us to discover the core regulatory genes. Thus, in order to explore the DEGs with a research value, a search tool (STRING 10.5[2]) (Szklarczyk et al., 2019) was used to establish a PPI network, and Cytoscape (Shannon et al., 2003) was used to plot the network. Interactions with a score >0.4 were set as the cutoff point. The most important modules in the PPI network were identified using MCODE in Cytoscape, which clustered a given network through topology. The threshold was set as: MCODE scores > 5, degree cut-off = 2, node score cut-off = 0.2, max depth = 100, and *k*-score = 2. Subsequently, the maximal clique centrality (MCC) algorithm of CytoHubba was used to explore the hub genes of the PPI network.

Real-Time Quantitative PCR

Total RNA was extracted from the samples using TRIzol (Takara) according to the manufacturer's instruction. We used the cDNA synthesis kit (Takara) to conduct reverse transcription. Real-time quantitative PCR (RT-qPCR) was performed by the FastStart Universal SYBR Green Master (ROX) (Takara). $2^{-\Delta\Delta Ct}$ relative quantification method was used for relative expression. β-actin was used as the internal reference (Sangon Biotech). The primer sequences were as following: *UCP1* forward CGACGTCCAGTGTTATTAGGTA, *UCP1* reverse GTAGAGTTTCATCCGCCCTTC, *GNG3* forward CGGTGAACAGCACTATGAGTAT, *GNG3* reverse TCACAGTA AGTCATCAGGTCTG, *MCHR1* forward CGCTTGGTCC TGTCGGTGAAG, *MCHR1* reverse GCCTTTGCTTTCTG TCCTCTCCTC, *BDKRB1* forward CTTTTTGTCCTGTTGG TCTTCC, *BDKRB1* reverse CTGATGAACAAATTGGCCTTGA, *MCHR2* forward AACCTGGCTGTGGCTGATTTGG, *MCHR2* reverse GGGATGTGATGATGGTGCAGAGAG, *CXCL8* forward AACTGAGAGTGATTGAGAGTGG, *CXCL8* reverse ATGA ATTCTCAGCCCTCTTCAA, *CXCR5* forward CGGCAG ACACGCAGTTCCAC, *CXCR5* reverse ACGGCAAAGGGCAA GATGAAGAC, *CCR8* forward TGGCCCTGTCTGACCT GCTTT, *CCR8* reverse GGCATAAGTCAGCTGTTGGCT, *CCL4L1* forward CTCAGTATCAGCACAGGACACAGC, *CCL 4L1* reverse AGAGACAGGACAGTCACGCAGAG, *TAS2R10* forward AGTGTTTGGGGTTTTGGGGAATGG, *TAS2R10* reverse AGCCGGTGAGAATAAAGCCAATCG, *TAS2R41* forward ACTCAGCCACCTTCTGGTTTTGC, and *TAS2R41* reverse ATCAGGACAGAGCCCAACAGGAG.

Statistical Analysis

The statistical analysis was performed by SPSS25.0 (IBM). All values were expressed as mean ± SD. Statistically significant differences were assessed by ANOVA and Chi-squared test for comparisons between two groups. Two-tailed *p* value <0.05 was considered statistically significant.

[2]http://string-db.org

TABLE 1 | Patient characteristics.

	CTRL (*n* = 11)	CAD (*n* = 11)	*p* values
Age (years)	56.0 ± 8.0	58.8 ± 7.0	0.392
Sex, male (%)	6 (54.5)	5 (45.5)	0.748
BMI (Kg/m^2)	22.5 ± 2.4	23.8 ± 2.1	0.197
AC (cm)	86.1 ± 10.3	87.2 ± 6.6	0.779
Complications			
Diabetes mellitus (%)	0 (0.0)	0 (0.0)	1.000
Hypertension (%)	3 (27.2)	5 (45.5)	0.478
CAD			
1-Vessel disease	0 (0.0)	1 (9.1)	
2-Vessel disease	0 (0.0)	4 (36.4)	
3-Vessel disease	0 (0.0)	6 (54.5)	
Gensini score	3.6 ± 1.4	88.4 ± 43.7	<0.001
Laboratory measurements			
WBC (×10^9/L)	5.9 ± 2.7	6.5 ± 1.4	0.513
TG (mmol/L)	1.6 (0.6–2.6)	1.6 (1.2–2.0)	0.997
TC (mmol/L)	4.2 ± 0.8	4.6 ± 1.7	0.411
LDL-c (mmol/L)	2.6 ± 0.5	2.9 ± 1.3	0.472
Left heart function			
EF (%)	55.6 ± 9.9	58.0 ± 12.6	0.636

Data are presented as mean ± SD or the number (%) of patients.
BMI, body mass index; AC, abdominal circumference; WBC, white blood cell; TGs, triglycerides; TC, total cholesterol; LDL-c, low-density lipoprotein cholesterol; EF, ejection fraction.

RESULTS

Study Population

The clinical characteristics of the study subjects are listed in **Table 1**. There was no significant difference in age, gender, body mass index (BMI), abdominal circumference (AC), comorbidities, and plasma lipid levels between the two groups. The average age of the control subjects was 56.0 ± 8.0 years and the CAD subjects was 58.8 ± 7.0 years (p = 0.392). Therefore, our research groups were well matched except for the presence of CAD.

Comparison of EAT in Histology

The EAT samples of both groups were mainly unilocular white adipocytes (**Figure 1A**). The sizes of EAT adipocytes in the CAD group were significantly larger than those in the control group (126.59 ± 23.27 μm^2 and 66.45 ± 14.90 μm^2, $p < 0.001$) (**Figure 1B**). Then, we compared the "browning" of fat in each group by detecting the expression of UCP1 (**Figure 1C**) and found that the level UCP1 was not different in the two groups ($p > 0.05$).

EAT Gene Expression Profiles in CAD

In order to compare the difference of gene expression in EAT between the CAD and non-CAD groups, we used the high-throughput RNA sequencing. The thresholds of differentially expressed genes (DEGs) were fold change > 2 and adjusted p value < 0.05. In total, there were 747 DEGs, of which, 301 were significantly up-regulated in the CAD group and 446 genes were significantly down-regulated (**Figure 2A**). Enrichment

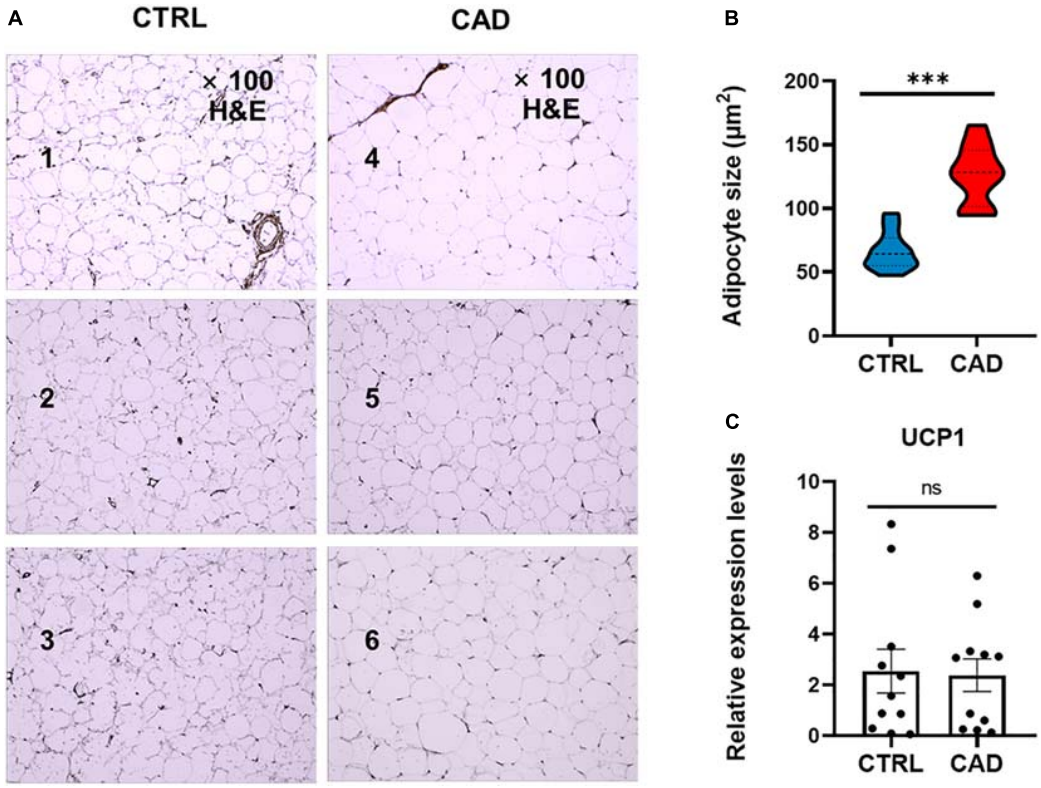

FIGURE 1 | Comparison of EAT in histology. **(A)** H&E staining of epicardial adipose tissue (EAT) in the control and coronary artery disease (CAD) groups (100× magnification). Numbers 1–3 were EAT samples of three control subjects, while numbers 4–6 were EAT samples of three CAD patients. **(B)** The mean adipocyte size was larger in CAD group (***$p < 0.001$). **(C)** Expression levels of uncoupling protein 1 (UCP1) in the CTRL and CAD group (ns, $p > 0.05$).

analysis of 301 up-regulated differential genes showed that the KEGG pathways were significantly enriched in cytokine-cytokine receptor interaction, jak-STAT signaling pathway, nicotine addiction, chemokine signaling pathway, hematopoietic cell lineage, steroid hormone biosynthesis, butanoate metabolism, and neuroactive ligand-receptor interaction (**Figure 2B**). The top eight GO analysis results were listed in **Table 2**. The biological processes (BP) of GO analysis showed that genes were mainly enriched in epidermis development, cytoskeleton organization, cellular calcium ion homeostasis, chemokine-mediated signaling pathway, chemotaxis, neutrophil chemotaxis, steroid metabolic process, and lymphocyte chemotaxis.

PPI Network Construction and Hub Genes Verification

To further identify the key genes with research value, 301 up-regulated DEGs were submitted to the STRING database to predict the interaction between proteins. DEGs' PPI network was constructed with a comprehensive score greater than 0.4 (**Figure 3A**), and the most important module was obtained using MCODE in Cytoscape. The first module included 14 nodes and 67 edges; the second module included eight nodes and 28 edges; and the third module included six nodes and 15 edges. The hub genes were selected from the PPI network using the maximal clique centrality (MCC) algorithm of CytoHubba (**Figure 3B**). The top 10 hub genes identified by MCC were *GNG3, MCHR1, BDKRB1, MCHR2, CXCL8, CXCR5, CCR8, CCL4L1, TAS2R10,* and *TAS2R41*. RT-qPCR was performed using the total RNA extracted from 11 pairs of EAT to verify the expression levels of the hub genes. The results of the RT-qPCR showed significant changes in the expression levels of hub genes such as *GNG3, MCHR1, BDKRB1, CCR8,* and *TAS2R41* in **Figure 4** (p value < 0.05).

DISCUSSION

Epicardial adipose tissue directly contacts with the coronary arteries without fascia isolation, which provides an important anatomical basis for the interaction between them. EAT can be used as a target for drugs targeting adipose tissue. New hypoglycemic drugs, such as glucagon-like peptide-1 receptor (GLP-1R) agonists and glucose-sodium co-transporter 2 inhibitors (SGLT2i) (Bouchi et al., 2017; Iacobellis et al., 2017), and lipid-lowering drugs such as atorvastatin (Raggi et al., 2019), have been shown to directly target the EAT and reduce its volume. GLP-1R's regulation of EAT promotes fatty acid β-oxidation and white-to-brown adipocyte differentiation, promoting favorable metabolic changes. Clinical studies have shown that EAT is remarkably correlated with the presence

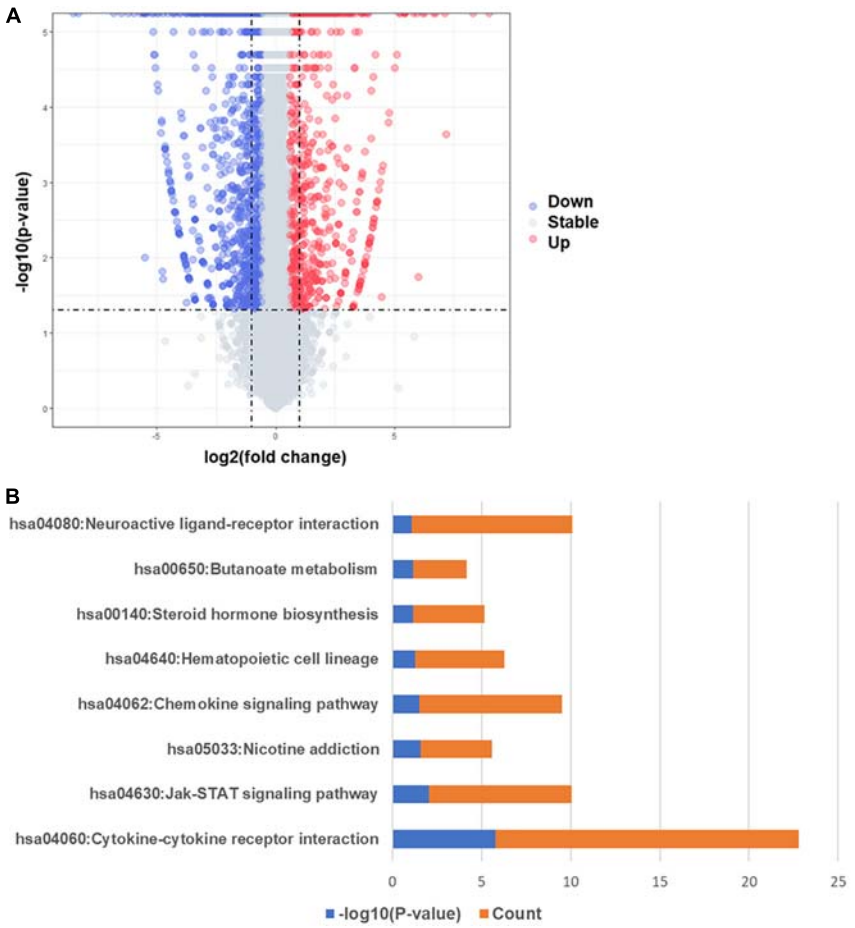

FIGURE 2 | Differentially expressed genes and KEGG pathway enrichment analysis. **(A)** Volcano map of differentially expressed genes, red spots represent up-regulated genes and blue spots represent down-regulated genes. **(B)** KEGG pathways significantly associated with the upregulated genes.

of CAD (Le Jemtel et al., 2019; Liu et al., 2019; Nappi et al., 2019). Previous studies have focused on comparing the difference between EAT and SAT. Different from previous studies, we directly compared the differences in EAT gene expression profiles between CAD and non-CAD subjects, providing novel information to describe the genomic characteristics of EAT in healthy and diseased subjects. Then, we provided evidence that, compared with the control group, EAT in CAD was characterized by enhanced inflammatory genes, metabolic remodeling, and fat remodeling. These results might help us discover the key genes and therapeutic targets in CAD, which might provide a more theoretical basis for exploring the pathogenesis of CAD.

Our research confirmed the findings of some previous studies and suggested some potentially novel discoveries. Our results showed that the size of epicardial adipocytes in the CAD group was larger than the control group, which was consistent with the results of previous studies (Vianello et al., 2016). However, we found that the "browning" marker UCP1 was not significantly different in the two groups. Our findings of the EAT gene expression profiles of CAD showed a total of 747 DEGs, of which, 301 DEGs were up-regulated and 446 DEGs were down-regulated. It was notable that the enrichment analysis of DEGs showed that more pro-inflammatory and immunological genes and pathways were involved in CAD, including chemokine-mediated signaling pathway, chemotaxis, neutrophil chemotaxis, lymphocyte chemotaxis, chemokine activity, cytokine activity, cytokine-cytokine receptor interaction, and chemokine signaling pathway. This suggested that inflammatory factors and immune cell activation might play an important role in the regulation of CAD. We constructed the DEG's PPI network in which three key modules and 10 central genes were explored, including *GNG3, MCHR1, BDKRB1, MCHR2, CXCL8, CXCR5, CCR8, CCL4L1, TAS2R10,* and *TAS2R41*. In addition, we used RT-qPCR to further verify the results.

A meta-analysis focusing on the transcriptome assessment of EAT in CAD patients confirmed the activation of inflammatory, immune, and metabolic pathways in CAD–EAT, and highlighted interleukin-6 (IL-6) and tumor protein p53 (TP53) as core genes (Maghbooli and Hossein-Nezhad, 2015). McKenney et al. (2014) demonstrated in a porcine model that the resection of local EAT can prevent CAD progression. These results suggest that EAT dysfunction may lead to changes in

TABLE 2 | The significant GO enriched analysis of differentially expressed genes in CAD.

Category	Term	Count	*p*-value	Genes
GO_BP	GO:0008544	11	0.000000129	*PTHLH, EVPLL, ELF3, CST6, KRT5, KRT16, POU2F3, KRT15, SPRR2F, LAMC2,* and *EDAR*
	Epidermis development			
	GO:0007010	13	0.00000145	*BUB1B-PAK6, ARC, CCL2, BLK, CTNNA2, CCL24, CCL11, KISS1, DES,* and *KRT5*
	Cytoskeleton organization			
	GO:0006874	8	0.0000854	*CCL11, CCL2, SLC8A2, TRPM8, GRIN1, CHRFAM7A, ATP13A5,* and *ATP13A4*
	Cellular calcium ion homeostasis			
	GO:0070098	7	0.001093	*CCL24, CCL11, CCR8, CCL2, CXCR5, CXCL8,* and *CCL4L2*
	Chemokine-mediated signaling pathway			
	GO:0006935	8	0.004041	*CCL24, CCL11, CCR8, CCL2, CXCR5, CXCL8, SERPIND1,* and *FOSL1*
	Chemotaxis			
	GO:0030593	6	0.004568	*CCL24, CCL11, CCL2, EDN2, CXCL8,* and *CCL4L2*
	Neutrophil chemotaxis			
	GO:0008202	5	0.005327	*AKR1C4, CYP3A7, CYP1A1, AKR1B10,* and *SULT1A3*
	Steroid metabolic process			
	GO:0048247	4	0.010621	*CCL24, CCL11, CCL2,* and *CCL4L2*
	Lymphocyte chemotaxis			
GO_CC	GO:0005615	52	1.95E-08	*HMSD, NOG, LYPD3, KERA, MASP1, EDN2, FAM3B, IL13, DLK1, IL11,...*
	Extracellular space			
	GO:0005576	50	0.00000209	*LYPD2, NOG, KERA, CNDP1, MASP1, EDN2, FAM3B, BCAN, IL13, IL11,...*
	Extracellular region			
	GO:0005882	9	0.0000576	*KRT72, KRT6A, DES, KRT5, KRT16, KRT15, KRT7, BFSP2,* and *KRT86*
	Intermediate filament			
	GO:0005886	88	0.00618	*LYPD2, CYP24A1, MCHR1, MCHR2, SYT4, OR4F21, LYPD5, PRSS41, SLC6A4,* and *SYT3,*
	Plasma membrane			
	GO:0045095	6	0.025111	*KRT72, KRT6A, KRT5, KRT7, KRT86,* and *KRT71*
	Keratin filament			
	GO:0005887	34	0.028064	*MCHR1, MCHR2, SLC6A4, AQP4, MFSD2A, BDKRB1, AQP6, GCGR, GPRC5A, CXCR5,...*
	Integral component of plasma membrane			
	GO:0005578	10	0.034652	*WNT10A, COL9A2, CPA6, ZP2, KERA, IMPG1, DGCR6, ENAM, BCAN,* and *MUC4*
	Proteinaceous extracellular matrix			
	GO:0016021	100	0.045498	*LYPD3, SYT4, SERTM1, OR4F21, B3GALT5, SLC9A2, SYT3, SLC6A4, AQP4, OR1E1,...*
	Integral component of membrane			
GO_MF	GO:0005200	9	0.000397	*KRT6A, DES, KRT5, KRT16, KRT15, TUBAL3, BFSP2, NEFH,* and *CTNNA2*
	Structural constituent of cytoskeleton			
	GO:0005198	13	0.000673	*KRT72, EVPLL, KRT6A, DES, KRT5, KRT16, KRT15, KRT7, NEFH, SPRR2F,...*
	Structural molecule activity			
	GO:0008009	5	0.007812	*CCL24, CCL11, CCL2, CXCL8,* and *CCL4L2*
	Chemokine activity			
	GO:0005544	5	0.01399	*SYT4, SYT3, SYTL5, SYT13,* and *PLA2G4B*
	Calcium-dependent phospholipid binding			
	GO:0005509	20	0.022734	*S100A5, MASP1, SYT4, GRIN1, SYT3, CAPN9, RCVRN, CDH2, DLK1, CLGN,...*
	Calcium ion binding			
	GO:0005125	8	0.023818	*LIF, CSF3, FAM3B, LEFTY2, IL13, IL24, IL11,* and *IL20*
	Cytokine activity			
	GO:0005328	3	0.033172	*SLC6A4, SLC6A15,* and *SLC6A17*
	Neurotransmitter: sodium symporter activity			

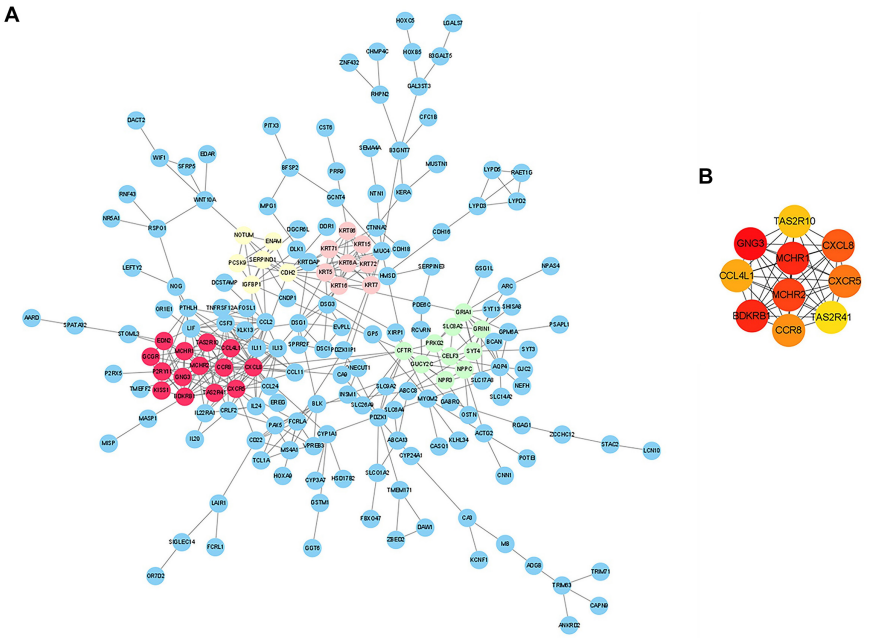

FIGURE 3 | Analysis of protein-protein interaction (PPI) network of CAD-related differentially expressed genes (DEGs) in EAT. **(A)** Edges represented protein-protein associations which were meant to be specific and meaningful. The colored nodes (red, green, pink, and yellow) represented the top four modules in the PPI network. **(B)** Top 10 hub genes identified by CytoHubba in Cytoscape.

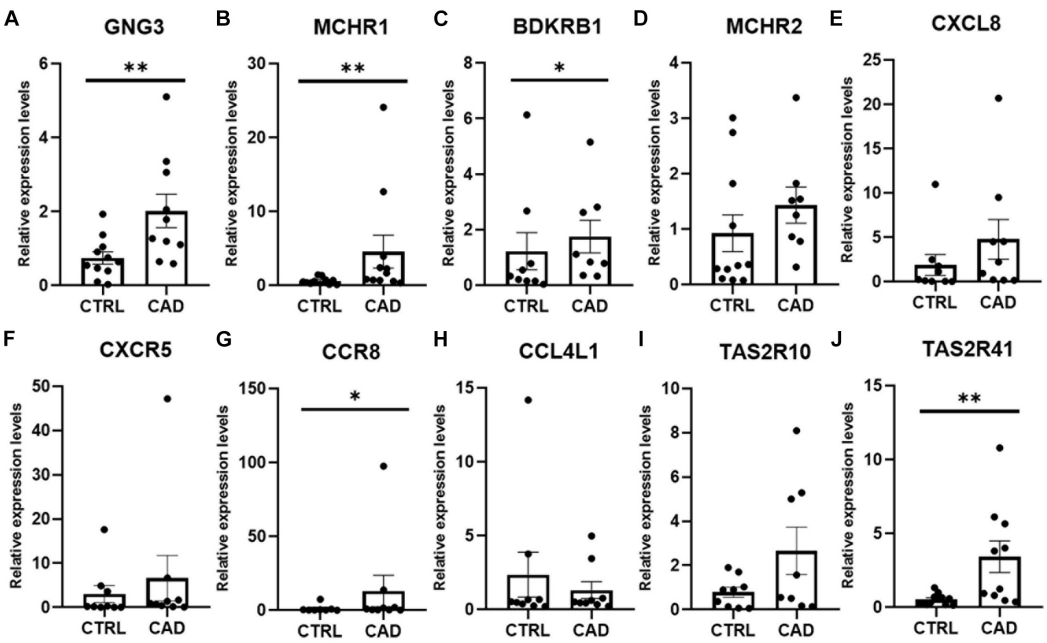

FIGURE 4 | Real-time quantitative PCR (RT-qPCR) verification of 10 hub genes in EAT of CAD. **(A)** GNG3 expression was significantly increased in the CAD group. **(B)** MCHR1 expression was significantly higher in the CAD group. **(C)** BDKRB1 expression was greater in the CAD group. **(D)** MCHR2 was increased in the CAD group, although the difference was not statistically significant. **(E)** CXCL8 expression was not statistically different between the two groups. **(F)** CXCR5 expression was higher in the CAD group, although the difference was not statistically significant. **(G)** CCR8 expression was significantly higher in the CAD group. **(H)** CCL4L1 expression was not different in the two groups. **(I)** TAS2R10 expression was increased in the CAD group, although the difference was not statistically significant. **(J)** TAS2R41 expression was significantly increased in EAT of CAD. $^{*}p < 0.05$, $^{**}p < 0.01$. In each column, error bars show the mean and standard deviation per group.

inflammation and metabolic microenvironment, thereby affecting vascular homeostasis, and may trigger coronary atherosclerosis. We found that the salient features of EAT in CAD include an enhanced communication between the inflammatory cells and chemokine signaling (*CXCL8*, *CXCR5*, *CCR8,* and *CCL4L1*). Studies have confirmed that many CC and CXC chemokines are involved in cardiovascular diseases (Frangogiannis and Entman, 2005; Frangogiannis, 2014). Cytokines in the EAT of CAD are also gradually attracting attention. Immunocyte like monocytes and neutrophils infiltrate the intima and activate endothelial cells, which induce the differentiation of monocytes into macrophages and formation of foam cells. CXC chemokines like *CXCL8* was reported to control neutrophil infiltration (Dyer et al., 2014) and CXCR5 + T cells was found to contribute to inflammatory reactions in CAD (Ding et al., 2017). *CCR8* can recruit IL-5 + T(H)2 cells (Islam et al., 2011) and act as a driver of atherosclerosis (Gast et al., 2019). *CCL4L1* may play a role in aortic aneurysm (Gäbel et al., 2017) though its involvement in CAD has yet to be clarified. Overall, our findings indicate that the immunological function of *CXCL8*, *CXCR5*, *CCR8,* and *CCL4L1* in the pathogenesis of EAT in CAD may be the focus of future investigations.

The other six hub genes had been rarely studied in the field of cardiovascular research. *GNG3* has not been reported in CAD. However, Schwindinger et al. (2004) reported that the mice which were lacking *GNG3* had a significantly reduced weight. Balber et al. (2019) reported that *MCHR1* expression was increased in BAT, and the use of *MCHR1* antagonists in rodents was able to reduce adipogenesis. It is well known that obesity is a risk factor of CAD and the findings of these genes may suggest that they may be indirectly involved in CAD pathogenesis. The discovery of the melanin-concentrating hormone (MCH) and its receptors (*MCHR1* and *MCHR2*) secreted by the hypothalamus may provide a new target for the research on the mechanism of obesity and therefore may contribute to the prevention of CAD. Schulze-Topphoff et al. (2009) provided evidence that Bdkrb1 may be a therapeutic target for chronic inflammation. TAS2R10 and *TAS2R41* can stimulate the secretion of ghrelin in gastric fundic cells (Wang et al., 2019), yet they have not been studied in the cardiovascular system. These newly discovered genes in EAT that we have discovered may provide new targets for CAD research.

However, there are some limitations in our study. The main limitation of the study could be the ethical (quantity of total adipose tissue) limitation. Many CAD patients undergoing coronary artery bypass grafting have diabetes, which our study needs to exclude, making it even more difficult to obtain the samples. In addition, the present study stopped short of validating and further exploring the related mechanisms because of the limitation of culturing human epicardial adipocytes. Further studies are required to gain insight into the pathogenesis.

In summary, in this study, we explored the gene expression profiles of EAT in CAD. We found that EAT may participate in CAD through key genes including *GNG3, MCHR1, BDKRB1, MCHR2, CXCL8, CXCR5, CCR8, CCL4L1, TAS2R10,* and *TAS2R41*, and some novel pathways, including cytokine-cytokine receptor interaction, jak-STAT signaling pathway, nicotine addiction, chemokine signaling pathway, hematopoietic cell lineage, steroid hormone biosynthesis, butanoate metabolism, and neuroactive ligand-receptor interaction. These results may help us explore the role of EAT in CAD from a new and deeper perspective.

DATA AVAILABILITY STATEMENT

The datasets presented in this study can be found in online repositories. The names of the repository/repositories and accession number(s) can be found below: https://figshare.com/ and https://doi.org/10.6084/m9.figshare.12826109.v1.

ETHICS STATEMENT

The studies involving human participants were reviewed and approved by the Ethics Committee of Xiangya Hospital of Central South University. The patients/participants provided their written informed consent to participate in this study.

AUTHOR CONTRIBUTIONS

Q-CW and Z-YW designed the protocols and performed the experiments. QX and R-BL included the patients and collected the samples. G-GZ and R-ZS did the formal analysis. All the authors have contributed to the writing of the manuscript.

FUNDING

This work was supported by grants from the National Natural Science Foundation of China (Grant Nos. 81670267 and 81873479), the Outstanding Youth Foundation Project of Hunan Natural Science Foundation (Grant No. 2019JJ20036), and the Key R&D Program of Hunan Provincial Department of Science and technology (Grant No. 2018SK2137).

ACKNOWLEDGMENTS

We thank Professor Wan-Jun Luo for his expert advice and helpful suggestions.

REFERENCES

Alipoor, E., Hosseinzadeh-Attar, M. J., Rezaei, M., Jazayeri, S., and Chapman, M. (2020). White adipose tissue browning in critical illness: A review of the evidence, mechanisms and future perspectives. *Obes. Rev.* 21:e13085.

Balber, T., Benčurová, K., Kiefer, F. W., Kulterer, O. C., Klebermass, E. M., Egger, G., et al. (2019). In vitro Radiopharmaceutical Evidence for MCHR1 Binding Sites in Murine Brown Adipocytes. *Front. Endocrinol.* 10:324. doi: 10.3389/fendo.2019.00324

Bouchi, R., Terashima, M., Sasahara, Y., Asakawa, M., Fukuda, T., Takeuchi, T., et al. (2017). Luseogliflozin reduces epicardial fat accumulation in patients with type 2 diabetes: a pilot study. *Cardiovasc. Diabetol.* 16:32. doi: 10.1186/s12933-017-0516-8

Chechi, K., Voisine, P., Mathieu, P., Laplante, M., Bonnet, S., Picard, F., et al. (2017). Functional characterization of the Ucp1-associated oxidative phenotype of human epicardial adipose tissue. *Sci. Rep.* 7:15566. doi: 10.1038/s41598-017-15501-7

Chong, C. R., Clarke, K., and Levelt, E. (2017). Metabolic Remodeling in Diabetic Cardiomyopathy. *Cardiovasc. Res.* 113, 422–430. doi: 10.1093/cvr/cvx018

Ding, R., Gao, W., He, Z., Wu, F., Chu, Y., Wu, J., et al. (2017). Circulating CD4(+)CXCR5(+) T cells contribute to proinflammatory responses in multiple ways in coronary artery disease. *Int. Immunopharmacol.* 52, 318–323. doi: 10.1016/j.intimp.2017.09.028

Dyer, D. P., Thomson, J. M., Hermant, A., Jowitt, T. A., Handel, T. M., Proudfoot, A. E., et al. (2014). TSG-6 inhibits neutrophil migration via direct interaction with the chemokine CXCL8. *J. Immunol.* 192, 2177–2185. doi: 10.4049/jimmunol.1300194

Frangogiannis, N. G. (2014). The inflammatory response in myocardial injury, repair, and remodelling. *Nat. Rev. Cardiol.* 11, 255–265. doi: 10.1038/nrcardio.2014.28

Frangogiannis, N. G., and Entman, M. L. (2005). Chemokines in myocardial ischemia. *Trends Cardiovasc. Med.* 15, 163–169. doi: 10.1016/j.tcm.2005.06.005

Franssens, B. T., Nathoe, H. M., Leiner, T., van der Graaf, Y., and Visseren, F. L. (2017). Relation between cardiovascular disease risk factors and epicardial adipose tissue density on cardiac computed tomography in patients at high risk of cardiovascular events. *Eur. J. Prev. Cardiol.* 24, 660–670. doi: 10.1177/2047487316679524

Gäbel, G., Northoff, B. H., Weinzierl, I., Ludwig, S., Hinterseher, I., Wilfert, W., et al. (2017). Molecular Fingerprint for Terminal Abdominal Aortic Aneurysm Disease. *J. Am. Heart Assoc.* 6:6798. doi: 10.1161/jaha.117.006798

Gast, M., Rauch, B. H., Nakagawa, S., Haghikia, A., Jasina, A., Haas, J., et al. (2019). Immune system-mediated atherosclerosis caused by deficiency of long non-coding RNA MALAT1 in ApoE-/-mice. *Cardiovasc. Res.* 115, 302–314. doi: 10.1093/cvr/cvy202

Gensini, G. F., Comeglio, M., and Colella, A. (1998). Classical risk factors and emerging elements in the risk profile for coronary artery disease. *Eur. Heart J.* 19(Suppl. A), A53–A61.

Gruzdeva, O., Uchasova, E., Dyleva, Y., Borodkina, D., Akbasheva, O., Antonova, L., et al. (2019). Adipocytes Directly Affect Coronary Artery Disease Pathogenesis via Induction of Adipokine and Cytokine Imbalances. *Front. Immunol.* 10:2163. doi: 10.3389/fimmu.2019.02163

Huang da, W., Sherman, B. T., and Lempicki, R. A. (2009). Systematic and integrative analysis of large gene lists using DAVID bioinformatics resources. *Nat. Protoc.* 4, 44–57. doi: 10.1038/nprot.2008.211

Iacobellis, G. (2015). Local and systemic effects of the multifaceted epicardial adipose tissue depot. *Nat. Rev. Endocrinol.* 11, 363–371. doi: 10.1038/nrendo.2015.58

Iacobellis, G., Mohseni, M., Bianco, S. D., and Banga, P. K. (2017). Liraglutide causes large and rapid epicardial fat reduction. *Obesity* 25, 311–316. doi: 10.1002/oby.21718

Islam, S. A., Chang, D. S., Colvin, R. A., Byrne, M. H., McCully, M. L., Moser, B., et al. (2011). Mouse CCL8, a CCR8 agonist, promotes atopic dermatitis by recruiting IL-5+ T(H)2 cells. *Nat. Immunol.* 12, 167–177. doi: 10.1038/ni.1984

Kankaanpää, M., Lehto, H. R., Pärkkä, J. P., Komu, M., Viljanen, A., Ferrannini, E., et al. (2006). Myocardial triglyceride content and epicardial fat mass in human obesity: relationship to left ventricular function and serum free fatty acid levels. *J. Clin. Endocrinol. Metab.* 91, 4689–4695. doi: 10.1210/jc.2006-0584

Le Jemtel, T. H., Samson, R., Ayinapudi, K., Singh, T., and Oparil, S. (2019). Epicardial Adipose Tissue and Cardiovascular Disease. *Curr. Hypertens. Rep.* 21:36. doi: 10.1007/s11906-019-0939-6

Lin, Y. K., Chen, Y. C., Chang, S. L., Lin, Y. J., Chen, J. H., Yeh, Y. H., et al. (2013). Heart failure epicardial fat increases atrial arrhythmogenesis. *Int. J. Cardiol.* 167, 1979–1983. doi: 10.1016/j.ijcard.2012.05.009

Liu, Z., Wang, S., Wang, Y., Zhou, N., Shu, J., Stamm, C., et al. (2019). Association of epicardial adipose tissue attenuation with coronary atherosclerosis in patients with a high risk of coronary artery disease. *Atherosclerosis* 284, 230–236. doi: 10.1016/j.atherosclerosis.2019.01.033

Maghbooli, Z., and Hossein-Nezhad, A. (2015). Transcriptome and Molecular Endocrinology Aspects of Epicardial Adipose Tissue in Cardiovascular Diseases: A Systematic Review and Meta-Analysis of Observational Studies. *Biomed. Res. Int.* 2015:926567. doi: 10.1155/2015/926567

McKenney, M. L., Schultz, K. A., Boyd, J. H., Byrd, J. P., Alloosh, M., Teague, S. D., et al. (2014). Epicardial adipose excision slows the progression of porcine coronary atherosclerosis. *J. Cardiothorac. Surg.* 9:2. doi: 10.1186/1749-8090-9-2

Messerli, F. H., Hofstetter, L., Rimoldi, S. F., Rexhaj, E., and Bangalore, S. (2019). Risk Factor Variability and Cardiovascular Outcome: JACC Review Topic of the Week. *J. Am. Coll. Cardiol.* 73, 2596–2603. doi: 10.1016/j.jacc.2019.02.063

Milanese, G., Silva, M., Ledda, R. E., Goldoni, M., Nayak, S., Bruno, L., et al. (2020). Validity of epicardial fat volume as biomarker of coronary artery disease in symptomatic individuals: Results from the ALTER-BIO registry. *Int. J. Cardiol.* 314, 20–24. doi: 10.1016/j.ijcard.2020.04.031

Mráz, M., Cinkajzlová, A., Klouèková, J., Lacinová, Z., Kratochvílová, H., Lipš, M., et al. (2019). Dendritic Cells in Subcutaneous and Epicardial Adipose Tissue of Subjects with Type 2 Diabetes, Obesity, and Coronary Artery Disease. *Mediat. Inflamm.* 2019:5481725. doi: 10.1155/2019/5481725

Nappi, C., Ponsiglione, A., Acampa, W., Gaudieri, V., Zampella, E., Assante, R., et al. (2019). Relationship between epicardial adipose tissue and coronary vascular function in patients with suspected coronary artery disease and normal myocardial perfusion imaging. *Eur. Heart J. Cardiovasc. Imaging* 20, 1379–1387. doi: 10.1093/ehjci/jez182

Nomura, C. H., Assuncao-Jr, A. N., Guimarães, P. O., Liberato, G., Morais, T. C., Fahel, M. G., et al. (2020). Association between perivascular inflammation and downstream myocardial perfusion in patients with suspected coronary artery disease. *Eur. Heart J. Cardiovasc. Imaging* 21, 599–605. doi: 10.1093/ehjci/jeaa023

Pezeshkian, M., and Mahtabipour, M. R. (2013). Epicardial and subcutaneous adipose tissue Fatty acids profiles in diabetic and non-diabetic patients candidate for coronary artery bypass graft. *Bioimpacts* 3, 83–89. doi: 10.5681/bi.2013.004

Raggi, P., Gadiyaram, V., Zhang, C., Chen, Z., Lopaschuk, G., and Stillman, A. E. (2019). Statins Reduce Epicardial Adipose Tissue Attenuation Independent of Lipid Lowering: A Potential Pleiotropic Effect. *J. Am. Heart Assoc.* 8:e013104. doi: 10.1161/jaha.119.013104

Reinisch, I., Schreiber, R., and Prokesch, A. (2020). Regulation of thermogenic adipocytes during fasting and cold. *Mol. Cell Endocrinol.* 512:110869. doi: 10.1016/j.mce.2020.110869

Schulze-Topphoff, U., Prat, A., Prozorovski, T., Siffrin, V., Paterka, M., Herz, J., et al. (2009). Activation of kinin receptor B1 limits encephalitogenic T lymphocyte recruitment to the central nervous system. *Nat. Med.* 15, 788–793. doi: 10.1038/nm.1980

Schwindinger, W. F., Giger, K. E., Betz, K. S., Stauffer, A. M., Sunderlin, E. M., Sim-Selley, L. J., et al. (2004). Mice with deficiency of G protein gamma3 are lean and have seizures. *Mol. Cell Biol.* 24, 7758–7768. doi: 10.1128/mcb.24.17.7758-7768.2004

Sekimoto, R., Fukuda, S., Maeda, N., Tsushima, Y., Matsuda, K., Mori, T., et al. (2015). Visualized macrophage dynamics and significance of S100A8 in obese fat. *Proc. Natl. Acad. Sci. U S A.* 112, E2058–E2066. doi: 10.1073/pnas.1409480112

Shannon, P., Markiel, A., Ozier, O., Baliga, N. S., Wang, J. T., Ramage, D., et al. (2003). Cytoscape: a software environment for integrated models of biomolecular interaction networks. *Genome Res.* 13, 2498–2504. doi: 10.1101/gr.1239303

Szklarczyk, D., Gable, A. L., Lyon, D., Junge, A., Wyder, S., Huerta-Cepas, J., et al. (2019). STRING v11: protein-protein association networks with increased coverage, supporting functional discovery in genome-wide experimental datasets. *Nucleic Acids Res.* 47, D607–D613. doi: 10.1093/nar/gky1131

Vacca, M., Di Eusanio, M., Cariello, M., Graziano, G., D'Amore, S., Petridis, F. D., et al. (2016). Integrative miRNA and whole-genome analyses of epicardial adipose tissue in patients with coronary atherosclerosis. *Cardiovasc. Res.* 109, 228–239. doi: 10.1093/cvr/cvv266

Vianello, E., Dozio, E., Arnaboldi, F., Marazzi, M. G., Martinelli, C., Lamont, J., et al. (2016). Epicardial adipocyte hypertrophy: Association with M1-polarization and toll-like receptor pathways in coronary artery disease patients. *Nutr. Metab. Cardiovasc. Dis.* 26, 246–253. doi: 10.1016/j.numecd.2015.12.005

Wang, Q., Liszt, K. I., Deloose, E., Canovai, E., Thijs, T., Farré, R., et al. (2019). Obesity alters adrenergic and chemosensory signaling pathways that regulate ghrelin secretion in the human gut. *FASEB J.* 33, 4907–4920.

Wong, C. X., Ganesan, A. N., and Selvanayagam, J. B. (2017). Epicardial fat and atrial fibrillation: current evidence, potential mechanisms, clinical implications, and future directions. *Eur. Heart J.* 38, 1294–1302. doi: 10.1093/eurheartj/ehw045

Zengin, E., Bickel, C., Schnabel, R. B., Zeller, T., Lackner, K. J., Rupprecht, H. J., et al. (2015). Risk Factors of Coronary Artery Disease in Secondary Prevention–Results from the AtheroGene–Study. *PLoS One* 10:e0131434. doi: 10.1371/journal.pone.0131434

Conflict of Interest: The authors declare that the research was conducted in the absence of any commercial or financial relationships that could be construed as a potential conflict of interest.

frontiers in Pharmacology

MINI REVIEW
published: 09 April 2021
doi: 10.3389/fphar.2021.626313

Modulatory Effect of Intermittent Fasting on Adipose Tissue Inflammation: Amelioration of Cardiovascular Dysfunction in Early Metabolic Impairment

Haneen S. Dwaib[1,2], *Ibrahim AlZaim*[1,3], *Ali H. Eid*[4,5], *Omar Obeid*[2]* and *Ahmed F. El-Yazbi*[1,6,7]*

[1]Department of Pharmacology and Toxicology, Faculty of Medicine, American University of Beirut, Beirut, Lebanon, [2]Department of Nutrition and Food Sciences, Faculty of Agricultural and Food Sciences, American University of Beirut, Beirut, Lebanon, [3]Department of Biochemistry and Molecular Genetics, Faculty of Medicine, American University of Beirut, Beirut, Lebanon, [4]Department of Basic Medical Sciences, College of Medicine, QU Health, Qatar University, Doha, Qatar, [5]Biomedical and Pharmaceutical Research Unit, QU Health, Qatar University, Doha, Qatar, [6]Department of Pharmacology and Toxicology, Faculty of Pharmacy, Alexandria University, Alexandria, Egypt, [7]Faculty of Pharmacy, Al-Alamein International University, Alamein, Egypt

OPEN ACCESS

Edited by:
Joshua Thomas Butcher,
Oklahoma State University,
United States

Reviewed by:
Sarah B. Withers,
The University of Manchester,
United Kingdom
Fabiano Beraldi Calmasini,
State University of Campinas, Brazil
Fernanda Priviero,
University of South Carolina,
United States

***Correspondence:**
Ahmed F. El-Yazbi
ahmed.fawzy.aly@alexu.edu.eg
Omar Obeid
oo01@aub.edu.lb

Specialty section:
This article was submitted to Cardiovascular and Smooth Muscle Pharmacology, a section of the journal Frontiers in Pharmacology

Received: 05 November 2020
Accepted: 18 February 2021
Published: 09 April 2021

Citation:
Dwaib HS, AlZaim I, Eid AH, Obeid O and El-Yazbi AF (2021) Modulatory Effect of Intermittent Fasting on Adipose Tissue Inflammation: Amelioration of Cardiovascular Dysfunction in Early Metabolic Impairment. Front. Pharmacol. 12:626313. doi: 10.3389/fphar.2021.626313

Cardiometabolic syndrome (CMS) is a cluster of maladaptive cardiovascular, renal, thrombotic, inflammatory, and metabolic disorders. It confers a high risk of cardiovascular mortality and morbidity. CMS is triggered by major shifts in lifestyle and dietary habits with increased consumption of refined, calorie-dense diets. Evidence indicates that diet-induced CMS is linked to Adipose tissue (AT) inflammation. This led to the proposal that adipose inflammation may be involved in metabolic derangements, such as insulin resistance and poor glycemic control, as well as the contribution to the inflammatory process predisposing patients to increased cardiovascular risk. Therefore, in the absence of direct pharmacological interventions for the subclinical phase of CMS, time restricted feeding regimens were anticipated to alleviate early metabolic damage and subsequent comorbidities. These regimens, referred to as intermittent fasting (IF), showed a strong positive impact on the metabolic state of obese and non-obese human subjects and animal models, positive AT remodeling in face of overnutrition and high fat diet (HFD) consumption, and improved CV outcomes. Here, we summarize the available evidence on the role of adipose inflammation in triggering cardiovascular impairment in the context of diet induced CMS with an emphasis on the involvement of perivascular adipose tissue. As well, we propose some possible molecular pathways linking intermittent fasting to the ameliorative effect on adipose inflammation and cardiovascular dysfunction under such circumstances. We highlight a number of targets, whose function changes in perivascular adipose tissue inflammation and could be modified by intermittent fasting acting as a novel approach to ameliorate the inflammatory status.

Keywords: cardiometabolic syndrome, early metabolic dysfunction, prediabetes, perivascular adipose inflammation, therapeutic fasting

INTRODUCTION

Cardiometabolic syndrome (CMS) has long been recognized as a cluster of maladaptive cardiovascular, renal, thrombotic, inflammatory, and metabolic disorders by several global health authorities (Castro et al., 2003). At the core of the framework of processes resulting in this syndrome lies multi-organ insulin resistance (IR), especially adipose tissue (AT) IR, that is considered key in CMS pathogenesis and prognosis (Kirk and Klein, 2009). While CMS is typically considered a pre-morbid condition, it is associated with a high risk of cardiovascular mortality and morbidity due to ischemic heart disease, ischemic stroke, cardiac metabolic dysfunction, and heart failure (Ash-Bernal and Peterson, 2006; von Bibra et al., 2016). Although recent estimates indicate a 35% surge in prevalence of CMS over the past 20 years (Moore et al., 2017), the definition and the diagnostic criteria of CMS are still debatable (Kirk and Klein, 2009). While most authorities agree on the inclusion of abnormalities of blood pressure, HDL-cholesterol, triacylglycerol and glucose tolerance, in addition to central obesity, they use different cut-off values for diagnosis and non-identical rank order of importance (Simmons et al., 2010).

Metabolic disorders that could be considered a culmination of CMS, including diet-induced obesity (DIO) (WHO, 2019) and type 2 diabetes (International Diabetes Federation, 2019), have increased in prevalence over the past few decades together with their associated cardiovascular morbidities. This steep rise could be attributed to major shifts in lifestyle and dietary habits comprising overnutrition and increased consumption of refined, calorie-dense diets rich in saturated fats and simple sugars (Lutsey et al., 2008; Misra et al., 2010). The rising health and economic burden makes an early intervention with CMS prudent. Significantly, several challenges face pre-emptive mitigation of CMS complications, particularly that cardiovascular risk increases at early disease stages that do not meet established diagnostic criteria of overt metabolic disease (Grundy, 2012). Moreover, subtle forms of vascular dysfunction, including impaired microvascular vasodilation and blood flow auto-regulation leading to cardiac consequences can occur in absence of overt signs of atherosclerosis and other vascular disease in the context of early CMS (Tune et al., 2017). Thus, a detailed study of the underlying cardiometabolic pathophysiology is warranted.

In this regard, research in the past two decades highlighted the association of chronic excessive caloric intake triggering negative adipose tissue remodeling (ATR) with the development of obesity and type 2 diabetes (Choe et al., 2016). Given the long recognized relationship between insulin resistance and the pathophysiology of CMS (Reaven, 1988), ATR and inflammation is very likely to play a central role in this pathogenesis (Richardson et al., 2013; Shimizu et al., 2013; Kohlgruber and Lynch, 2015). Indeed, increased cardiovascular risk in patients with metabolic disorders is linked to inflammation (Festa et al., 2003), possibly initiating in the AT in response to insulin resistance and hyperinsulinemia (Pedersen et al., 2015), making such a pathology an attractive target for early alleviation of CMS. On the other hand, as overnutrition and positive energy balance being the key triggers of CMS, calorie restriction becomes an attractive intervention to study as a possible way to prevent, improve and even treat CMS cardiovascular manifestations. Intermittent fasting (IF) regimens hypothesized to impact metabolic health can adopt several patterns (Patterson et al., 2015; Antoni et al., 2017). Complete alternate-day fasting involves the alternation between fasting and eating days, while time-restricted feeding involves ad libitum energy intake within defined timeframes, allowing for the establishment of regular fasting intervals. Other IF regimens include modified fasting regimens which involve the consumption of 20–25% of energetic needs on scheduled fasting days and ad libitum feeding on other days. Religious fasting can take a variety of forms, the most practiced of which is Ramadan fasting which involves a sunrise-to-sunset fast for a month period yearly. Other religious fasts involve abstinence from food consumption for prolonged periods of time that can extend for days. Importantly, the different regimens of IF have been shown to improve the metabolic state of obese and non-obese animal models and human subjects (Patterson et al., 2015; St-Onge et al., 2017). In this context, it becomes necessary to understand the potential impact of such an intervention on the pathogenetic pathways linking early metabolic dysfunction to cardiovascular impairment. As such, in the present review, we summarize the available evidence on the role of negative adipose remodeling in triggering cardiovascular impairment in the context of CMS with an emphasis on the involvement of perivascular adipose tissue (PVAT). As well, the possible molecular pathways linking IF to the ameliorative effect on adipose inflammation and cardiovascular dysfunction under such circumstances are examined.

ADIPOSE TISSUE REMODELING IN RESPONSE TO INCREASED CALORIC INTAKE

AT is one of the major players in the pathophysiology of CMS. Over the past two decades, our traditional view of the AT as a mere storage pool of excess calories evolved to encompass its endocrine functions as an integral factor in the regulation of glucose and lipid homeostasis (Guilherme et al., 2008). Such an endocrine function arises from complex interactions between adipocytes and the cells of the stromal vascular fraction (SVF), which modulates AT functioning in homeostatic and pathological conditions. This endocrine function is ascribed to white adipose tissue (WAT), which comprises unilocular adipocytes that specialize in energy storage and production of several crucial protein factors collectively called adipokines. Brown adipose tissue (BAT), on the other hand, comprises mitochondria-rich multilocular adipocytes that specialize in energy dissipation through non-shivering thermogenesis (Chouchani et al., 2019). This evolving view led to a surge of interest in its role in mediating the pathogenesis of CMS (Bjørndal et al., 2011).

Adipose Tissue Hypertrophy vs. Hyperplasia

Upon an increased caloric intake, exemplified by the consumption of a high-fat diet (HFD) in experimental

settings, hypertrophic and hyperplastic AT expansion ensue. As the terms imply, the hypertrophic pathway involves an increase in the size of adipocytes (ACs), while hyperplastic expansion is the increase in the number of ACs. In both settings, these pathways ensures the adaptation of the AT to the positive energy balance, and hence an increased storage capacity of the AT (Choe et al., 2016).

Diet-induced hypertrophy is considered a failure of ACs normal proliferation (Bays, 2011), resulting in malfunctioning ACs that are typically accompanied with cardio-metabolic derangements (Berg and Scherer, 2005; Bays et al., 2008), like hyperinsulinemia, hyperlipidemia, hypertension and atherosclerosis (Gustafson and Smith, 2015). For example, subjects diagnosed with type 2 DM or dyslipidemia were found to have larger subcutaneous ACs than their control counterparts (Berg and Scherer, 2005). The failure of recruitment and differentiation of fat progenitor cells in obesity and prediabetes occurs due to a combination of factors including AT insulin resistance, which provokes the expansion of existing ACs (Gustafson and Smith, 2015). As insulin inhibits lipolysis, insulin resistance leads to increased circulating free fatty acids, which in turn fuels and exaggerates the insulin resistance tightly correlated with hypertension and CVDs at the core of CMS (Bays et al., 2008). In this context, nutrient excess triggers an increased demand for protein and lipid synthesis leading to endoplasmic reticulum stress, which in turn activates Jun kinase and nuclear factor-kB (NF-κB). These latter pathways impair the action of insulin by promoting the inhibitory phosphorylation of insulin receptor substrate 1 (IRS-1). Moreover, it could be plausible that compensatory hyperinsulinemia in obesity or HFD intake may augment AC glucose uptake eventually leading to abnormally hypertrophied ACs in a self-reinforcing vicious cycle (Bays et al., 2008). The vital role of insulin in white AC hypertrophy was confirmed in several animal models. A mouse model of AT-specific insulin receptor knockout showed a significant reduction in total fat mass, age related obesity, and other metabolic abnormalities (Bays, 2011). Moreover, an AT-specific insulin receptor knockout rat model was found to be resistant to diet-induced hypertrophy compared to their wild type littermates (Friesen et al., 2016).

Furthermore, animal studies showed that diet-induced hypertrophy in PVAT was associated with atherosclerosis (Horimatsu et al., 2018), and was correlated to increased vascular tone in aorta and cerebral arterioles (Elkhatib et al., 2019; Fakih et al., 2020). As will be discussed in more detail below, AC enlargement is often associated with reduced oxygen supply subsequently leading to elevated level of hypoxia inducible factor 1-α (HIF1-α), a transcriptional factor that is activated under hypoxic conditions, which promotes the production pro-inflammatory mediators, such as tumor necrosis factor α (TNFα) (van Dam et al., 2017; Agabiti-Rosei et al., 2018). Significantly, incubation of blood vessels obtained from healthy individuals with TNFα abolished the anticontractile effect of PVAT, while PVAT with hypertrophied ACs isolated from obese patients showed no dilator effect (Greenstein et al., 2009). Moreover, as observed in animal studies, hypertrophy is linked to increased production of other pro-inflammatory cytokines, such as Interleukins (IL)-6, IL-8, IL-1β and monocyte-chemoattractant protein 1 (MCP1) (Jernås et al., 2006).

On the other hand, hyperplastic AT expansion, also referred to as adipogenesis (Choe et al., 2016), requires the differentiation of adipose progenitor cells, which are pooled in the AT within the SVF, especially in the white AT (WAT) (Raajendiran et al., 2019). While some adipocyte progenitor cells were identified in murine models ($CD31^-$, $CD45^-$, $CD29^+$, $CD34^+$, $CD24^+$ and Sca-1+) (Rodeheffer et al., 2008) and in humans (CD44, CD73, CD29 among others) (Raajendiran et al., 2019), the mechanism of *de novo* adipogenesis remains uncertain (Raajendiran et al., 2019). One of the well-established transcriptional factors involved in adipogenesis is peroxisome proliferator-activated receptor-γ (PPARγ), which plays a crucial role in cellular metabolism and the regulation of fatty acids homeostasis (Rosen et al., 1999; Kershaw et al., 2007; Choe et al., 2016). Indeed, the activation of PPARγ2, which is mainly expressed in the AT, promotes adipogenesis by stimulating the differentiation of AC progenitor cells into mature ACs (Tontonoz et al., 1994; Zhang et al., 2004). Importantly, PPARγ expression was found to be higher in the visceral and mesenteric AT of obese diabetic individuals (Yang et al., 2008). Remarkably, obese rats exhibit a lower adipogenic activity in subcutaneous than visceral AT depots including perirenal and gonadal AT (Jamdar, 1978). Intriguingly, an AT-specific PPARγ knockout mouse model was found to be resistant to DIO and subsequent metabolic derangements. Unlike their genetic controls, these mice showed a total lack of brown AT (BAT) in addition to WAT abnormalities including increased fibrosis and vascularization. Yet, they demonstrated normal blood glucose levels, serum triglyceride levels, insulin sensitivity and reduced serum adipokines levels while freely feeding on a high-fat diet (Jones et al., 2005). On another note, deletion of PPARγ in vascular smooth muscle cells in HFD-fed mice, showed its various roles in different AT depots, as it lead to immature mesenteric and perirenal AT, while gonadal, sub-cutaneous, interscapular WAT, and BAT were fully mature (Chang et al., 2012).

Adipose Tissue Browning or Beiging

Browning or beiging of AT is a process that involves the increase of uncoupling Protein 1 (UCP1) expression. UCP1 is a thermogenic inner mitochondrial membrane protein that uncouples the activity of the electron transport chain from oxidative phosphorylation through the production of a proton leak, and thus dissipates energy in the form of heat in the AT (Ricquier and Bouillaud, 2000; Cannon and Nedergaard, 2017). UCP1 is abundantly expressed in BAT, which specializes in thermogenesis rather than energy storage (Foster and Frydman, 1978; Nedergaard et al., 2001; Kajimura et al., 2015). The regulation of UCP1 expression mainly occurs downstream of β-adrenergic receptors (AR) signaling, more specifically β_3-AR (Cannon and Nedergaard, 2017). Moreover the activation of β_3-AR induces lipolysis, which increases the levels of free fatty acids further enhancing the activity of UCP1 (Coman et al., 2009).

Browning usually occurs in WAT, in order to increase energy expenditure (Nedergaard and Cannon, 2014). Specifically, a

recent study showed that AC browning and increased expression of UCP1, among other BAT markers, were observed in several WAT depots in rats receiving a HFD (García-Ruiz et al., 2015). However, murine studies reported an increase in UCP1 expression in BAT as well, in response to HFD feeding (Bonet et al., 2017). Interestingly and from a different perspective, studies showed that inflammation, expected to occur in AT in association with increased caloric intake, downregulates UCP1 expression in WAT and hence, precludes browning (Bartelt and Heeren, 2014). When Adipocytes were challenged with macrophages activated by lipopolysaccharide (LPS) and TNF-α, UCP1 mRNA expression, UCP1 promoter and transcriptional factor binding to cAMP response element were suppressed in WAT in a process mediated by Erk kinase (Sakamoto et al., 2013). Similarly, other studies suggested that UCP1 is downregulated in BAT by low-grade inflammation as seen in mice chronically treated with LPS (Nøhr et al., 2017). In this study, it was proposed that BAT is immunologically naïve since *in vitro* LPS treatment was not able to induce inflammation and cause UCP1 downregulation, which was achieved by direct stimulation with IL-1β instead. A possible pathway for this IL-1β-evoked UCP1 downregulation was proposed to occur through the inhibition of Sirtuin-1 (SIRT1), which stimulates UCP1 expression (Nøhr et al., 2017). This is suggested to occur through upregulating the expression of the endogenous protein deleted in breast cancer-1, an inhibitor of SIRT1. In this regard, SIRT1 plays a crucial role in the AT as it suppresses PPARγ activity in ACs thus decreasing fat accumulation (Rahman and Islam, 2011). This is associated with an increase in lipolysis by inducing mitochondrial fatty acid oxidation, through the activation of the transcriptional factor PPARγ coactivator-1α (PGC-1α) (Gerhart-Hines et al., 1913). In a SIRT1 AC-specific knockout model, normal chow-fed mice exhibited low-grade AT inflammation, along with IR and glucose intolerance in comparison to their wild type littermates (Mayoral et al., 2015). Moreover, this phenotype was exacerbated by short-term HFD consumption. Intriguingly, wild type mice on chronic HFD developed a more pronounced metabolic dysfunction in comparison to their SIRT1 knockout counterparts (Mayoral et al., 2015). Indeed, this was associated with a hyperacetylated PPARγ in the ACs of SIRT1 knockout mice, which correlated with increased dephosphorylation of PPARγ, promoting its constitutive activity that enhances insulin sensitivity (Mayoral et al., 2015). Significantly, a lack of increase in UCP1-mediated energy dissipation in response to HFD consumption triggers BAT changes reminiscent of AT hypertrophy typically seen in WAT depots. Indeed, UCP1 knockout mice receiving HFD exhibited BAT whitening, which was accompanied by an increased AC size and macrophage infiltration (Winn et al., 2017). Additionally, reduced mitochondrial biogenesis, increased endoplasmic reticulum stress, and disrupted glucose tolerance were more pronounced in these mice upon HFD consumption. However, these mice did not show any alterations in visceral adiposity, body weight, energy intake or energy expenditure (Winn et al., 2017). Another important factor is the sympathetic overactivation that is usually triggered by cold exposure. Sympathetic stimulation augments PPARγ-mediated BAT recruitment and proliferation, which in turn was associated with increased expression of UCP1 and mitochondrial biogenesis. This was shown in an *in vivo* study comparing innervated and denervated BAT and demonstrating that PPARγ-mediated UCP1 activation was dependent on the sympathetic nervous system (Festuccia et al., 2010). This is in contrast to *in vitro* research findings, where treating BAT cells with Rosiglitazone, a selective PPARγ agonist, was enough to increase UCP1 and mitochondrial biogenesis in manner that does not involve sympathetic activation (Petrovic et al., 2008). Significantly, it has long been recognized that hyperinsulinemia in early metabolic dysfunction in humans and animals triggers increased sympathetic activity (Anderson et al., 1991; Thorp and Schlaich, 2015).

On the other hand, the increased oxygen consumption associated with browning of white ACs differentiated from human adipose-derived stem cells was correlated with increased mitochondria fission indicated by an increased Dynamin-Related Protein-1 (DRP-1) phosphorylation on serine 616 (Pisani et al., 2018). Moreover, other triggers leading to sub-cutaneous white AC browning were also associated with increased Erk-mediated ser616-DRP1 phosphorylation and mitochondrial fission (Velazquez-Villegas et al., 2018). In response to sympathetic stimulation, BAT adipocytes exhibit a protein kinase A-evoked DRP1 phosphorylation at the same site, enhancing DRP1-mediated mitochondrial fission in order to increase energy dissipation (Wikstrom et al., 2014). The exact molecular relationship between increased UCP1 expression and mitochondrial fission remains unclear. However, increased mitochondrial fission observed under these circumstances has recently been proposed to act as a feedback mechanism increasing the metabolic resilience and protecting against the deleterious effects of increased caloric intake (Rui, 2017). Yet, in the above situations, mitochondrial changes were seen under circumstances not perceived to contribute to AT pathologies. Interestingly, WAT inflammation in diabetic mice was associated with increased ser616-DRP1 phosphorylation. Both observations were reversed when animals received treatments increasing 5′AMP-Activated Protein kinase (AMPK) activity. However, this study did not examine the status of UCP1 expression (Li et al., 2016).

In addition to UCP1, creatine futile cycling is considered as an alternative thermogenic pathway in UCP1-expressing and UCP1-nonexpressing beige ACs (Bertholet et al., 2017). This cycle enhances energy expenditure in beige adipocytes when ADP is limiting, and thus results in a significantly higher oxygen consumption rate through the stimulation of ADP-limited cellular respiration (Kazak et al., 2015). The enzyme creatine kinase (CK) catalyzes the phosphorylation of creatine. Four different CK isoforms have been identified; two cytosolic isoforms, muscle-type creatine kinase (CKM) and brain-type creatine kinase (CKB), and two mitochondrial isoforms, CKMT1 and CKMT2 (Desjardins and Steinberg, 2018). Phosphatases then hydrolyze phosphocreatine into creatine and ATP. Indeed, creatine kinases and creatine phosphatases are compartmentalized within cells to sites of energy production and energy utilization. This uneven distribution of enzymes allows for intercompartmental energy buffering (Wallimann

et al., 1992). AC cellular creatine content is either endogenously biosynthesized or imported from the extracellular medium via the creatine transporter Slc6a8 (Kazak and Cohen, 2020). The influx of creatine through Slc6a8 is reduced in states of low energy charge in an AMPK-dependent manner (Li et al., 2010). Also, Slc6a8 expression in human subcutaneous adipocytes is negatively correlated with insulin resistance and BMI (Kazak et al., 2019). In a mouse knockout model of glycine amidinotransferase, the rate limiting enzyme in creatine biogenesis, mice were prone to DIO, had a significantly lower energy expenditure level and exhibited hyperinsulinemia. These metabolic dysfunctions were reversed following creatine administration (Kazak et al., 2017). On another note, intracellular creatine content was depleted following Slc6a8 AC-specific knockout (AdCrTKO). AdCrTKO mice displayed a metabolic response to HFD similar to that shown by glycine amidinotransferase knockouts including reduced energy expenditure and an enhanced weight gain further elucidating the important role of creatine in driving energy expenditure to combat the metabolic challenge (Kazak et al., 2019). Moreover, this type of thermogenesis co-exists with UCP1-dependent thermogenesis in UCP1-positive beige ACs, while it seems to be the only known thermogenic mechanism employed by UCP1-negative beige ones. In comparison to classical UCP1-mediated thermogenesis, creatine cycling seems not to be activated by an acute β_3-AR stimulation but it rather contributes to the modulation of the basal metabolic activity of adipocytes (Bertholet et al., 2017). Importantly, a recent study provided no evidence for creatine supplementation-mediated activation of BAT thermogenesis in acute cold-exposed young, healthy, lean, vegetarian adults, who are characterized by low creatine levels (Connell et al., 2021). This supports previous murine observations where the mere supplementation of creatine is not enough to show the physiological relevance of creatine futile cycling in thermogenesis, if it was not coupled with HFD consumption and β_3-AR stimulation. Moreover, the supplementation of creatine in these individuals does not guarantee an alteration of creatine levels in BAT, and thus, does not necessarily activates the futile cycle.

Another important player in AT remodeling and browning is AMPK (Rui*, 2017). As the deletion of either the *a* or *ß* subunits of AMPK resulted in an impaired WAT beiging with a resistance to β_3-AR stimulation (Mottillo et al., 2016; Wu et al., 2018). In another study, AMPK gain of function mutation induced subcutaneous AT browning. Strikingly, this browning was neither attributed to a detectable increase in UCP1 expression nor to an activated creatine cycling, despite the increase of oxygen consumption in this depot (Pollard et al., 2019). Nevertheless, this does not exclude a role of creatine cycling in enhancing energy expenditure and oxygen consumption in other adipose depots that have not yet been investigated.

Adipose Tissue Inflammation

As discussed above, increased caloric intake-induced hyperinsulinemia drives AC hypertrophy, promoting its diametric expansion beyond the diffusion potential of oxygen (Pedersen et al., 2015). Importantly, this occurs in the absence of compensatory AT vascularization creating a local hypoxic state that is associated with an increased expression of HIF-1α (Ye et al., 2007; He et al., 2011; Trayhurn, 2013). An extensive crosstalk between signaling pathways involving HIF-1α and other transcription factors implicated in the AT hypoxic response such as NF-κB occurs, where NF-κB was shown to regulate HIF-1α transcription (Rius et al., 2008; van Uden et al., 2008; Trayhurn, 2013). Additionally, it was shown that hypoxia-triggered expression of HIF-1α induces NF-κB-mediated cytokine production including IL-1β, which results in subsequent recruitment and accumulation of distinct populations of immune cells giving rise to a state of chronic AT inflammation (Jeong et al., 2005; Fitzgibbons and Czech, 2014; Dzhalilova et al., 2019; Saxton et al., 2019). Importantly, the dysfunction of adipose depots implicated in the pathogenesis of CMS, such as epicardial, perivascular, and perirenal adipose depots, is associated with a perturbed immune cell landscape and adipokine profiles in states of metabolic dysfunction (Alzaim et al., 2020).

Adipose tissue macrophages (ATMs) exhibit remarkable polarization-dependent transcriptomic heterogeneity that is highly dependent on microenvironmental factors (Thapa and Lee, 2019; Caslin et al., 2020). AT-resident or infiltrating macrophages can either adopt a classical, pro-inflammatory M1 polarization, or an anti-inflammatory M2 polarization. ATMs in lean AT are predominantly M2 polarized (Morris et al., 2011; Chylikova et al., 2018), while M1 macrophage infiltration into inflamed ATs as well as the phenotypic switch of resident M2 macrophages to M1 macrophages occur in response to HFD consumption (Lumeng et al., 2008; Kralova Lesna et al., 2016). As such, these macrophages associate with crown-like structures (CLS), which represent macrophages actively phagocytosing apoptotic adipocytes with the concurrent increased production of proinflammatory cytokines and chemokines as well as reactive oxygen species (ROS) (Sartipy and Loskutoff, 2003; Weisberg et al., 2003; Cinti et al., 2005; Lumeng et al., 2007; Wensveen et al., 2015; Chylikova et al., 2018).

Moreover, it was suggested that ATMs represent the primary source of the proinflammatory cytokines TNFα, IL-1, IL-6 and iNOS (Weisberg et al., 2003; Xu et al., 2003). Noteworthy, it was suggested that WAT preadipocytes can undergo a phenotypic switch, by which they transdifferentiate into macrophages *in vivo* in response to HFD under a contact-dependent macrophage-mediated stimulation (Charrière et al., 2003; Xu et al., 2003). Nevertheless, *in vitro* studies suggest that AC-macrophage crosstalk is mainly mediated by free fatty acids (FFA) and TNFα. Indeed, TNFα was shown to drive AT inflammation and to reduce adiponectin expression, while FFAs were found to increase macrophage cytokines production (Suganami et al., 2005). This crosstalk was found to be exaggerated upon the use of hypertrophied or obese ACs (Suganami et al., 2005). Accumulating evidence suggests a role for TNFα in inhibiting PPARγ activity through several pathways (Ye, 2008), among which is the activation of the classical NF-κB pathway, which prevents PPARγ binding to its response element, and hence blocks its downstream effect (Suzawa et al., 2014). As PPARγ represents a major promoter of adipogenesis, it is thought that

TNFα-mediated suppression of PPARγ signaling would increase levels of circulating FFAs and subsequently enhancing the proinflammatory polarization of ATMs (Ren et al., 2006). This is supported by evidence from PPARγ receptor agonist treated HFD-fed mice, which exhibited an enhanced overall insulin sensitivity and an increased M2 count in VAT (Fujisaka et al., 2011). Indeed, TNFα KO mice were protected from HFD-induced IR and exhibited reduced serum FFA levels (Uysal et al., 1997). Moreover, ATM-derived TNFα is suggested to be the leading promoter of adipose-specific insulin resistance through various mechanisms (Ruan et al., 2002; Xu et al., 2003; Cawthorn and Sethi, 2008). It was shown that TNFα downregulates the expression of insulin receptor substrate 1 (IRS-1) and glucose transporter type 4 (GLUT4) (Stephens et al., 1997; Engelman et al., 2000), and inhibits the activity of AMPK activity (Steinberg et al., 2006). In addition to AMPK energy sensing activity, and the crucial role of AMPK signaling dysfunction in the pathogenesis of IR, AMPK activation was shown to prime M2 macrophage polarization (Chan et al., 2015).

Although ATMs are considered the main contributors to HFD-induced AT inflammation (Weisberg et al., 2003), other distinct immune cell populations were also found to be involved (Alzaim et al., 2020). For example, dendritic cells were shown to regulate AT inflammation, where the accumulation of dendritic cells in the AT of HFD-fed mice promotes the recruitment of macrophages and the mounting of a Th17-driven inflammatory response (Bertola et al., 2012; Stefanovic-Racic et al., 2012; Chen et al., 2014). Moreover, the uptake of FFAs by dendritic cells and the formation of lipid droplets is suggested to promote dendritic cell immunogenicity, which likely occurs in states of metabolic dysfunction (den Brok et al., 2018). Moreover, neutrophils, which are relatively rare in the AT of lean mice, exhibit a maintained flux into the inflamed AT of HFD-fed mice, whereby they promote IR and the production of proinflammatory cytokines (Talukdar et al., 2012). Neutrophils accumulation in inflamed AT is thought to precede and subsequently enhance macrophage infiltration through the increased activity of NF-κB and production of IL-1β (Watanabe et al., 2019). Similarly, mast cells are enriched and further increase in VAT of mice and humans in states of obesity and T2D, where they drive macrophage infiltration and AT inflammation (Nishimura et al., 2009b; Liu et al., 2009; Żelechowska et al., 2018; Kumar et al., 2019). It was also suggested that mast cell accumulation in inflamed AT occurs prior to overt obesity and the genetic ablation or functional impairment of mast cells in HFD-fed mice decreased weight gain and reduced IR (Nishimura et al., 2009b; Liu et al., 2009). Alternatively, AT-resident eosinophils promote AT homeostasis through the secretion of IL-4 and IL-13 which promotes M2 macrophage polarization, triggers Th2 differentiation, and enhances B cell activation (Wu et al., 2011; Yoon et al., 2019). The homeostatic role of eosinophils is supported by the observation that eosinophil-deficient HFD-fed mice show pronounced IR while increasing eosinophil abundance in the AT reduced HFD-induced increased adiposity (Wu et al., 2011; Molofsky et al., 2013; Lee et al., 2018). Moreover, the forced increase of AT eosinophil abundance in different models enhanced metabolic homeostasis (Wu et al., 2011; Qiu et al., 2014; Berbudi et al., 2016).

T and B lymphocytes also play major immunoregulatory roles in AT homeostasis and dysfunction. Different subsets of proinflammatory T cells increase in visceral adipose depots of mice and humans including helper T cells, γδ T cells, and cytotoxic T cells and drive IR (Weinstock et al., 2020). Conversely, the abundance of anti-inflammatory T cells such as regulatory T cells and invariant killer T cells, decreases in obesity (Feuerer et al., 2009; Deiuliis et al., 2011). It was proposed that T cell infiltration into inflamed AT precedes that of macrophages with particular enrichment of $CD4^+$ T cells (Kintscher et al., 2008; Shen et al., 2015). Also, expanding regulatory T cells in HFD-fed mice was shown to alleviate HFD-induced metabolic dysfunction (Ilan et al., 2010). B cells accumulation in AT also modulates AT inflammation. For example, regulatory B cells suppress Th1 and Th2 polarization, as well as inhibit macrophage and dendritic cell activation (Alzaim et al., 2020). Moreover, different subpopulations of B cells such as B-2 cells are thought to promote AT inflammation (Winer et al., 2011; Defuria et al., 2013; Ying et al., 2017), while B-1 cells improve glucose tolerance and reduces AT inflammation through the induction of M2 macrophage polarization and IL-10 secretion with simultaneous reduction in the production of IL-6 and TNF-α (Wong et al., 2010; Wu et al., 2014; Shen et al., 2015; Harmon et al., 2016; Srikakulapu et al., 2017).

Of particular relevance to the pathogenesis of the CMS, PVAT was recently shown to harbor a plethora of basally activated immune cells under homeostatic conditions including $CD4^+$ and $CD8^+$ T cells, natural killer cells, B cells, macrophages, mast cells, and neutrophils (Kumar et al., 2020). Metabolically dysfunctional PVAT is infiltrated by macrophages, T cells, NK cells, and DCs that produce either pro-inflammatory or anti-inflammatory cytokines depending on PVAT adipokine profile shifts (Saxton et al., 2019). As such, accumulating evidence implicates local alterations of resident and infiltrating immune cell populations within the SVF in AT inflammation and the pathogenesis of insulin resistance, metabolic syndrome, and diabetes (Alzaim et al., 2020). Moreover, AT dysfunction is associated with an imbalanced adipokine profile that further promotes detrimental AT immune cell landscape shifts (Alzaim et al., 2020).

ADIPOSE TISSUE AND CARDIOMETABOLIC SYNDROME

AT affect cardiac health through paracrine and endocrine interactions with cardiovascular tissues making it prudent to study AT inflammation in the context of CMS (Berg and Scherer, 2005; Shah et al., 2008). Significantly, excessive calorie intake, DIO and T2DM are correlated with a wide range of CVDs while sharing a background of low-grade AT inflammation (Nishimura et al., 2009a; Klöting and Blüher, 2014). One example is the increase of proinflammatory macrophages, cytokines, and reactive oxygen species in epicardial AT in patients with coronary artery diseases (Eiras et al., 2008;

Salgado-Somoza et al., 2010; Hirata et al., 2011). Another important one is cardiac autonomic neuropathy (CAN) showing as reduced parasympathetic activity and endothelial dysfunction, both major risk factors predisposing to CVD associated with metabolic impairment (Bakkar et al., 2020a). CAN is known to occur early in the course of metabolic derangement exemplified by the prediabetic stage (Gonzalez and Selwyn, 2003; Vinik et al., 2013; Williams et al., 2019). In fact, obese patients with insulin resistance had systemic arterial dysfunction concurrent with high M1 ATMs and TNFα mRNA in SAT and elevated serum C reactive protein (CRP), indicating a proinflammatory state (Apovian et al., 2008). Interestingly, recent studies on a prediabetic rat model showed that mildly increased caloric intake led to clear cardiovascular manifestations even in absence of overt hyperglycemia, increased body weight, or high blood pressure (Al-Assi et al., 2018; Alaaeddine et al., 2019; Elkhatib et al., 2019). Significantly, the observed endothelial dysfunction and CAN were linked to localized PVAT inflammation with neither inflammatory changes in other adipose pool nor systemic involvement (Al-Assi et al., 2018; Alaaeddine et al., 2019; Elkhatib et al., 2019). This early PVAT involvement in the course of metabolic disease is of particular relevance given the close anatomical proximity between PVAT and the cardiovascular tissue. While the role of PVAT has been initially limited to vascular supportive and structural functions, its ability to modulate vascular contractility has long been recognized (Verlohren et al., 2004; Galvez et al., 2006; Gao et al., 2006; Gao et al., 2007; Greenstein et al., 2009). Mechanistic pathways by which PVAT secretes a complex array of factors to modulate vascular tone have been proposed. Indeed, as early as 1991, periaortic fat was shown to exert an anti-contractile effect (Soltis and Cassis, 1991) that persisted when vessels without AT were treated with PVAT-conditioned media (Lohn et al., 2002). In this regard, PVAT adipokines are highly likely to exert direct effects on the nearby vascular tissue. Of these, adiponectin was shown to mediate the anticontractile effect via eNOS stimulation (Sung et al., 2004; Ouchi et al., 2011). Additionally, animal models of deleted PPARγ that lacked the PVAT depot, showed endothelial dysfunction and increased cardiovascular diseases (Chang et al., 2012) supporting the fundamental role of PVAT in modulating cardiovascular health (Agabiti-Rosei et al., 2018; Qi et al., 2018). Of note, studies have shown that the anticontractile effect is lost in metabolic diseases like diabetes, as PVAT phenotype shifts into a proinflammatory state (Azul et al., 2019). This is accompanied by significant perturbation in the adipokine profile involving several of these products including adiponectin, leptin, chemerin, resistin, and visfatin as described previously in detail (Rafeh et al., 2020).

Noteworthy, PVAT in postmenopausal women was found to have a higher number of proinflammatory macrophages, compared to other depots, and it was suggested that this is associated with increased CV risk (Kralova Lesna et al., 2016). Another study indicated that upon the transplant of thoracic aortic PVAT from HFD fed mice to the carotid artery of HFD-fed ApoE$^{-/-}$ mice vascular injury was augmented, and it was mediated by MCP1 expression (Manka et al., 2014). It also was suggested that proinflammatory ATMs migration induces inflammation in the vascular bed and poses atherogenic effect (Britton and Fox, 2011). Furthermore, it appears that PVAT is especially sensitive to hypoxia-driven inflammation (Greenstein et al., 2009). Indeed, isolated PVAT inflammation, with significant implications on vascular structure and function, was observed in more than one animal model of metabolic challenge. Transplantation of inflamed PVAT from HFD-fed ApoE$^{-/-}$ mice increased the incidence of atherosclerosis and endothelial dysfunction in recipient animals on a control diet (Horimatsu et al., 2018). Moreover, prediabetic rats fed mild hypercaloric diet exhibited an increased expression of PVAT UCP1, DRP1 as well as HIF1-α, in addition to a hypertrophied inflamed morphology that were associated with vascular dysfunction in absence of similar changes in other adipose depots (Elkhatib et al., 2019). As such, one would assume that this peculiar nature, whereby several PVAT pools expressed brown adipose-specific genes (Chatterjee et al., 2009; Sacks et al., 2013; Gaborit et al., 2015), might be the cause of the observed early involvement and increased sensitivity to inflammation. In this context, an assumed exaggerated oxygen consumption triggered by increased UCP1 expression would be exacerbated by the observed adipocyte hypertrophy in a combination of events less likely to occur in other adipose depots. This model is illustrated in **Figure 1**. Importantly, another rat model on HFD showed increased UCP1 expression in PVAT, however this increase was not explained nor were its implications investigated (Winn et al., 2017). On the other hand, HFD reduced UCP1 in WAT and VAT, supporting the hypothesis indicating that AT depots act varyingly in response to the same energy stimuli (Winn et al., 2017). As for creatine cycling, it remains widely unknown if the creatine-mediated enhanced basal metabolic activity may predispose PVAT to hypoxia following HFD consumption, or if this enhancement will limit cellular thermogenic needs, and thus limit UCP1 induction. Indeed, it has been suggested that creatine cycling and UCP1-dependent thermogenesis represent parallel thermogenic pathways that are independently operational and potentially reciprocal (Kazak and Cohen, 2020). Of relevance to inflammatory changes, Slc6a8-mediated creatine uptake and accumulation stimulate macrophages reprograming by inhibiting the pro-inflammatory M1 and promoting the tissue repair-responsible M2 polarization in peritoneal macrophages via regulating cytokine responses (Ji et al., 2019). Moreover, accumulating evidence suggests the implication of creatine metabolism in mediating anti-inflammatory phenotypes in immune cells (Kazak and Cohen, 2020).

In the above rat model of early metabolic dysfunction, localized PVAT inflammation led to increased IL-1β and TGF-β1 production, which was associated with reduced AMPK activation, increased vascular Erk1/2 phosphorylation, medial hypertrophy, oxidative stress, increased rho-associated kinase (ROCK)-mediated calcium sensitization and a hypercontractile response (Elkhatib et al., 2019; Lefranc et al., 2019). This isolated PVAT inflammation model was also associated with impaired endothelial relaxing function due to reduced expression/function of inward rectifier K^+ channels (Alaaeddine et al., 2019). Treatment of the local PVAT inflammation ameliorated the

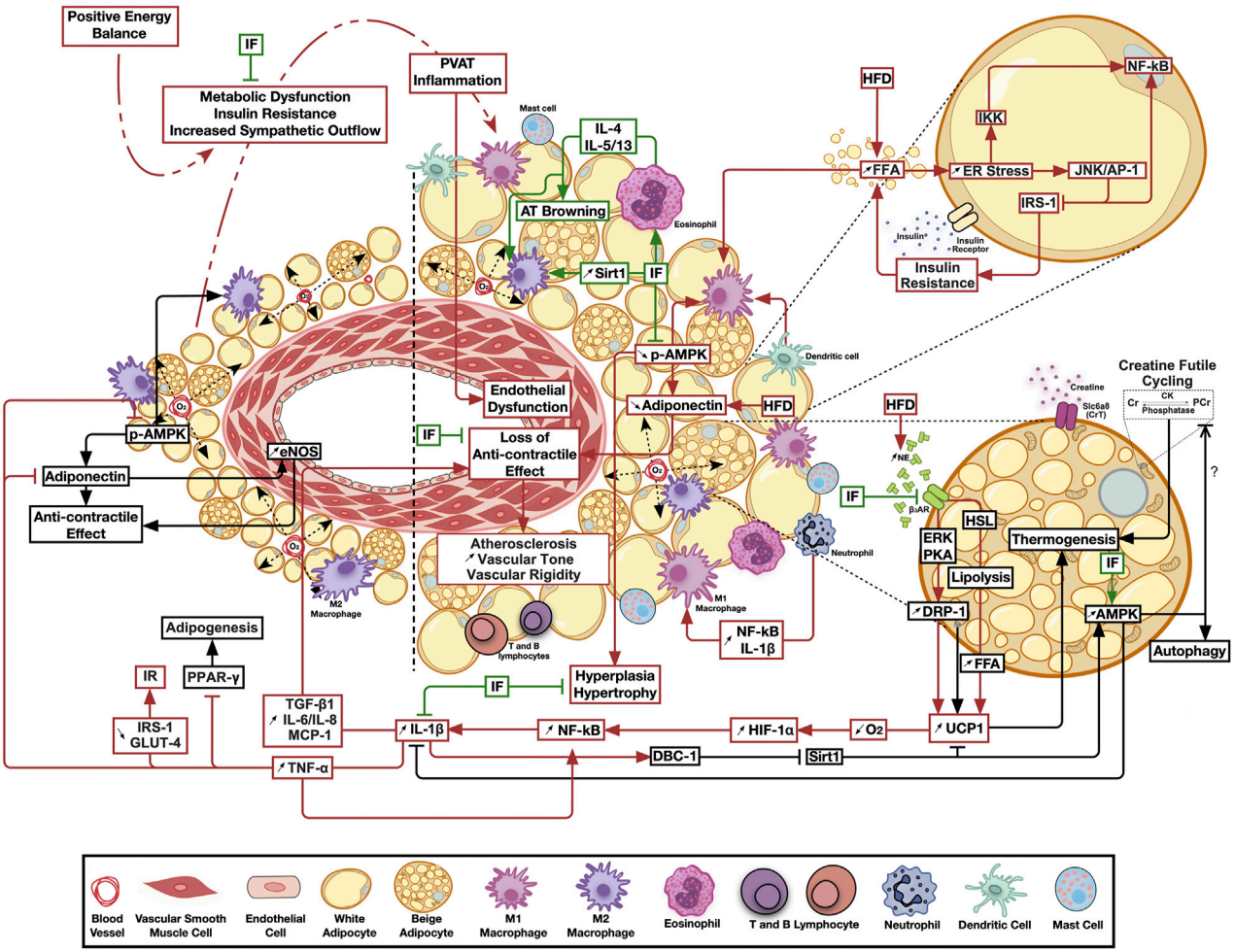

FIGURE 1 | The emerging ameliorative role of intermittent fasting on perivascular adipose tissue inflammation and thermogenesis. Calorie excess resulting in metabolic dysfunction triggers perivascular adipose tissue chronic low-grade inflammation, leading to the loss of its anticontractile effects and the subsequent negative paracrine modulation of vascular structure and function. Intermittent fasting ameliorates inflammatory, thermogenic and bioenergetic pathways favoring adipose tissue homeostasis. Pathways involved in adipose tissue homeostasis are shown in black, those activated by metabolic dysfunction in red, while those modulated by intermittent fasting in green arrows. AT, Adipose tissue; AMPK, AMP-activated protein kinase; β_3AR, Beta 3 adrenergic receptor; CK, Creatine kinase; Cr, Creatine; DBC-1, Deleted in bladder cancer protein 1; DRP-1, Dynamin related protein 1; eNOS, Endothelial nitric oxide synthase; ER, Endoplasmic reticulum; ERK, Extracellular signal-regulated kinase; FFA, Free fatty acids; HFD, High fat diet; HIF-1α, Hypoxia-inducible factor 1-alpha; HSL, Hormone sensitive lipase; IF, Intermittent fasting; IKK, IKβ kinase; IL, Interleukin; IRS-1, insulin receptor substrate 1; JNK/AP-1, c-jun N-terminal kinase/activator protein 1; MCP-1, Monocyte Chemoattractant protein 1; NE, Norepinephrine; NF-κB, Nuclear factor kappa B; O_2, Oxygen; PVAT, Perivascular adipose tissue; PCr, Phosphocreatine; PKA, Protein kinase A; Sirt1, Sirtuin 1; TGF-β1, Transforming growth factor beta 1; TNF-α, Tumor necrosis factor alpha; UCP1, Uncoupling protein 1.

contractile and endothelial manifestations. A different animal study using *AMPKα1* knockout mice assessed the impact of HFD on PVAT function. HFD in wild-type mice reduced P-AMPK and adiponectin levels, in addition to diminished anti-contractile involvement of PVAT accompanied by an infiltration of macrophage with M1 polarization, indicated by increase in iNOS and IL-1 *ß*. Yet in *AMPKα1* KO mice, PVAT of both HFD and control fed animals showed a massive reduction in P-AMPK, adiponectin and abolished vasorelaxation (Almabrouk et al., 2018). More recent investigation showed that not only is the occurrence of PVAT inflammation linked to the early incidence of cardiovascular manifestations associated with metabolic dysfunction, but is also necessary for the progression of cardiac autonomic insult as the metabolism deteriorates further ending up in overt hyperglycemia and diabetes (Bakkar et al., 2020b). Taken together, one can conclude that HFD-induced negative remodeling of PVAT lead to a state of cardiometabolic dysfunction.

ADIPOSE TISSUE REMODELING IN RESPONSE TO THERAPEUTIC OR INTERMITTENT FASTING

Intermittent Fasting was found to produce a positive impact on AT remodeling occurring in diet-induced metabolic dysfunction.

After eight weeks of treatment, not only did IF (24-h fast on three nonconsecutive days per week) improve glucose tolerance, and insulin resistance in HFD-fed mice, it also reduced adipocyte hypertrophy and markers of inflammation including macrophage infiltration and the NLRP3 inflammasome signaling components (Liu et al., 2018). Moreover, the same IF protocol as well as a complete alternate-day fasting protocol evoked an increased energy expenditure and UCP1 expression in WAT tissue in DIO mice in a manner that also involved reduction of inflammatory markers (Liu et al., 2019b; de Souza Marinho et al., 2020). Yet, while IF reduced WAT fat mass in both obese mice models and obese human subjects, no UCP1 upregulation was observed in humans (Liu et al., 2019b). Nevertheless, the exact mechanism of how these fasting regimens improve the metabolic state are still not fully understood. Specifically, despite the many desired outcomes reported for calorie restriction, isocaloric IF seems to have a prominent effect on the metabolic health, despite the fact in a lot of studies did not involve calorie restriction (Aksungar et al., 2017; Kim et al., 2017; St-Onge et al., 2017).

In murine models, HFD-induced hypertrophy was reported to be reversed by 24-h and 72-h IF in VAT; especially gonadal and subcutaneous inguinal AT depots (Tang et al., 2017). Interestingly, the change in fat pad size was found to be triggered by IF alone, regardless of the daily caloric intake, and independent of the change in body weight as animal studies showed a decrease in size and weight of adipose depots, with mild or no change in total body weight (Varady et al., 2007; Varady et al., 2009; Varady et al., 2010; Liu et al., 2019b). Certainly in our work, a calorie restricted regimen of a HFD failed to exert any corrective effect on CAN and PVAT inflammation involvement in rats (Al-Assi et al., 2018) as opposed to isocaloric IF (12-h feeding/12-h fasting) (Dwaib et al., 2020). In studies involving obese human subjects, IF appeared to reduce total fat mass with varying fasting protocols such as intermittent continuous energy restriction for 2 days a week and alternate day fasting (Harvie et al., 2011; Bhutani et al., 2013; Tinsley and La Bounty, 2015), and circulating markers of inflammation (Harvie et al., 2011; Wang et al., 2020), the latter effect being more marked in obese than in normal weight subjects (Wang et al., 2020).

In further confirmation of the observations in animal studies, IF regimens were better capable of reducing circulating markers of inflammation than calorie restricted regimens *per se* (Wang et al., 2020). Nonetheless, mixed results were found in human studies. In a study examining IF during the month of Ramadan, which is the religious fasting in Islam involving fasting from sunrise till sunset for 30 days, body weight and fat percentage decreased in both men and women in absence of calorie restriction (Faris et al., 2012). Meanwhile, others reported that the IF-induced weight loss was dependent on calorie restriction that mediated the metabolic benefit rather than the fasting regimen itself (Klempel et al., 2012; Patterson and Sears, 2017). Moreover, a recent clinical trial comparing the effects of calorie restriction to IF (24-h fast on three nonconsecutive days per week) showed a transient increase in inflammatory markers in AT after IF only, which was attributed to an ATM response to increased lipolysis (Liu et al., 2019a). Still in either case, a marked overall improvement in AT functioning was observed.

As such, IF might constitute an adequate intervention in the low-grade inflammatory state evoked in AT by DIO. Indeed, IF produced the previously mentioned anti-inflammatory effects in metabolically challenged mice alongside reduction of body weight and insulin resistance (Liu et al., 2018). Interestingly, isocaloric IF was shown to produce the same effects and trigger alternative activation of macrophages to the M2 polarization in mice (Kim et al., 2017). Another murine study involving IF in a calorie restriction protocol showed a shift in AT macrophages to the M2 polarization that was mediated by SIRT1 activity (Fabbiano et al., 2016). SIRT1 is a nutrient sensitive histone deacetylase that is thought to mediate the beneficial metabolic effects of fasting and calorie restriction including improved serum glucose and lipid levels, increased insulin sensitivity and reduced body weight (Bordone et al., 2007; Schenk et al., 2011). Specifically, mice mildly overexpressing SIRT1 were protected against HFD-induced inflammation through a reduction of NF-κB activation and pro-inflammatory cytokine production (Pfluger et al., 2008). Pertinent to the inflammatory context in AT, SIRT1 activation was shown to mitigate hypoxic cardiomyocyte damage through the augmentation of autophagic flux that was mediated by AMPK activation (Luo et al., 2019). Indeed, IF (15 or 39 h fast) was found to augment AMPK phosphorylation in rats (Kajita et al., 2008). Significantly, not only has our work shown a reduced AMPK activity in cardiovascular impairment associated with early metabolic dysfunction involving PVAT inflammation in HFD-fed rats (Al-Assi et al., 2018), our results also demonstrated autophagy suppression as a possible contributor to the observed phenotype (Bakkar et al., 2020b; Fakih et al., 2020). Moreover, a lack of AMPK activity was implicated in AC hypertrophy (Villena et al., 2004). As such, IF-mediated SIRT1 activation could offer a mechanistic link for the observed positive changes in AT remodeling. However, it is important to note that studies on human subjects reported inconsistent results where some studies showed increased SIRT1 expression in AT following 6 days of total fasting (Pedersen et al., 2008), and others have reported no change (Madkour et al., 2019). These observations could be related to a lack of consistency in the fasting regimens employed and warrant further investigation.

On the other hand, murine studies employing different IF regimens have been shown to strongly induce WAT browning and increase the expression of mitochondrial UCP1, which was linked to an improved metabolic state (Fabbiano et al., 2016; Kim et al., 2017; Kivelä and Alitalo, 2017; Liu et al., 2019b). Indeed, this could be related to SIRT1 activation that was shown to increase UCP1 expression as mentioned previously (Nøhr et al., 2017). Yet, data from mouse models, showed that caloric restriction induces browning in SAT and VAT, via eosinophils infiltration, M2 macrophage polarization and anti-inflammatory cytokines production. Genetic ablation of the effect of these cytokines (IL-4,-5 and -13) abolished AT browning along with the observed improvement of AT inflammation and metabolic parameters (Fabbiano et al., 2016). Significantly, another aspect of mitochondrial function involves AMPK activity. Evidence suggests that fasting-mediated AMPK activity has a role in

mitochondrial metabolism and homeostasis, where chronic activation of AMPK maintains the dynamic nature of mitochondrial networks together with their ability to interact with other organelles and increase fatty acid oxidation (Weir et al., 2017). Furthermore, AMPK phosphorylates and inhibits creatine kinase and thus impedes creatine cycling in skeletal muscle (Ponticos et al., 1998; Weir et al., 2017). Such an effect would reduce basal mitochondrial oxygen consumption and help mitigate AT hypoxia. However, though emerging evidence implicates AMPK in the modulation of AC phenotype plasticity, AMPK-mediated inhibition of creatine kinases in ACs has not yet been investigated (Desjardins and Steinberg, 2018). This further extends the mechanism by which the beneficial metabolic effect of IF may arise via AMPK-activation. Indeed, the increased AMPK activity is consistent with the effect of IF on adiponectin production. A localized increase in adiponectin in AT, especially WAT, was achieved by different IF protocols even in the presence of HFD. These observations were consistent in both human and animal studies (Barnosky et al., 2014a; Patterson et al., 2015; Lettieri-Barbato et al., 2016; Antoni et al., 2017; Kim et al., 2017). However, the effect of IF on adipokine profile alteration as well as its role in immune cell metabolic rewiring subsequent to such metabolic challenges warrant further investigation, especially that specific alterations in adipokine profile were shown to adversely affect immune cell recruitment and polarization.

On another note, fasting was suggested to activate autophagy as cells tend to recycle intracellular particles to produce energy in several tissues including AT (Bagherniya et al., 2018; Ferhat et al., 2019; Clemente-Postigo et al., 2020). IF has been linked to the upregulation of several autophagy-related genes, microtubule-associated protein 1 light chain 3 (LC3), Beclin1, lysosomal associated membrane protein, Unc-51-like kinases (ULK1), in addition to SIRT1 (Bagherniya et al., 2018), which are involved in different parts of the autophagy machinery; initiation, nucleation, autophagosome formation, maturation and cargo degradation (Ferhat et al., 2019; Clemente-Postigo et al., 2020). Significantly, a crossover randomized trial of 18 h daily fasting for 4 days found to improved glucose balance and lipid metabolism alongside with increased serum SIRT1 and LC3A in overweight adults (Jamshed et al., 2019). Indeed, the autophagy machinery is managed by the major nutrient sensing kinases mTORC1 and AMPK, which inhibit and activate autophagy, respectively (Ferhat et al., 2019; Lahiri et al., 2019; Clemente-Postigo et al., 2020). Persistent inhibition of autophagy in response to overnutrition has determinantal effects on the metabolic state (Singh et al., 2009a; Ro et al., 2019). As such, IF-mediated AMPK activation might be a possible pathway through which therapeutic fasting can alleviate metabolic dysfunction in adipose tissue by achieving autophagic homeostasis.

Data on the level of autophagy in adipose tissue have been conflicting. Some studies reported that autophagy is overactivated in obese WAT where autophagy suppression was suggested to inhibit WAT adiposity in DIO (Ro et al., 2019). On the other hand, acute starvation at different time points (12–72 h) after HFD feeding was found to induce lipophagy and lipolysis by increased ß-oxidation (Singh et al., 2009a). Another study reported that VAT of obese and insulin resistant indivduals had hypertrophied ACs and increased mRNA expression of autophagy genes compared to subcutaneous WAT (Kovsan et al., 2011). Moreover, autophagy inhibition or more specifically blocking of mitophagy in WAT leads to a state of browning, due to the accumulation of mitochondria (Altshuler-Keylin and Kajimura, 2017). A study on HFD-fed rats found that pharmacological inhibition of autophagy induced WAT browning and protected against DIO (Parray and Yun, 2017). On the contrary, it was suggested that obesity is correlated with increased dysfunctional mitochondria in WAT (Chattopadhyay et al., 2015), which might be a sign of impaired mitophagy in AT in response to DIO (Ro et al., 2019). Atg7 knockout mice demonstrated a lean phenotype with increased BAT, ß-oxidation and browner WAT (Singh et al., 2009b). While seemingly conflicting, these findings emphasize the vital role of autophagy in maintaining AT plasticity in terms of thermogenic activity (Cairó and Villarroya, 2020).

Importantly, one study examined the impact of short-term fasting for 24 h on genomic profile of WAT and BAT in male Wister rats. Autophagy gene expression increased in BAT of fasted rats (Nakai et al., 2008). Another mouse model fed an isocaloric fasting regimen, which provides food in 12-h inter-meal cycles, showed increased autophagy, improved body compositions, reduced AC size reduced adiposity and enhanced muscle mass compared to ad libitum fed controls. Interestingly, M2 polarization was observed in ATM (Martinez-Lopez et al., 2017). These changes were found to be autophagy dependent, as they were abolished in AT Atg7 knockout mice regardless of the dietary regimen. Moreover, the knockout mice had impaired glucose tolerance and insulin sensitivity in response to inter-meal fasting compared to the wild-type controls, suggesting the role of AT autophagy in modulating glucose homeostasis.

Nevertheless, all of the above observations were reported in large WAT pools including sub-cutaneous, gonadal, and other visceral AT depots. To the best of our knowledge, there is no direct investigation of the effect of IF on PVAT in situations of metabolic dysfunction. As such, a systematic examination of the impact of IF on PVAT remodeling and inflammation in early metabolic dysfunction and its impact on cardiovascular impairment is warranted. While several parallels among that responses of different WAT pools to IF can be drawn, one must be cautious in extrapolating these findings to PVAT given the peculiar nature of this adipose pool. In this context, prolonged periods of reduced caloric intake, as in case of IF, might, in addition to the previously observed effects in other AT depots, exert further benefit by relieving the UCP1-mediated exacerbation of oxygen deficiency, and hence ameliorate the early inflammatory response. This framework is depicted in **Figure 1**.

CARDIOMETABOLIC SYNDROME AND THERAPEUTIC OR INTERMITTENT FASTING

The positive impact of IF on AT is expected to ameliorate the cardiovascular manifestations of cardiometabolic syndrome.

Indeed, the American heart association (AHA) included IF as one of the dietary measures to prevent CVDs. Based on human studies, AHA concluded that IF, regardless of its effect on weight, improves lipid profile, lowers LDL and cholesterol and increases HDL, in addition to improving insulin sensitivity, indicated by reduced HOMA-IR, with no change in blood glucose level (St-Onge et al., 2017). As well, human and animal studies indicated that alternate day fasting and religious Ramadan fasting IF protocols reduced blood pressure (Wan et al., 2003; Lotfi et al., 2010; Erdem et al., 2018) and heart rate (Lotfi et al., 2010). Another study on a rat model found that both 40% calorie restriction and alternate day fasting reduced the low frequency component in the diastolic blood pressure variability, a marker of reduced sympathetic activity, and increased high frequency component in heart rate variability, which is reflective of the parasympathetic tone, both being indicative of positive modulation of cardiovascular state (Mager et al., 2006). Specifically, in the context of early metabolic dysfunction, preliminary data indicate that not only did IF (12-h feeding/12-h fasting) improve parasympathetic cardiac autonomic neuropathy, this was also associated with amelioration of PVAT inflammation in an HFD-fed rat model of metabolic dysfunction (Dwaib et al., 2020).

Furthermore, IF (19-h fast daily for 26 days) improved endothelial and non-endothelial dependent vasorelaxation in healthy men (Esmaeilzadeh and Van De Borne, 2016). Significantly, alternate day IF exerted a similar pattern in Wistar male rats, as it showed an improved aortic endothelial depend relaxation (Razzak et al., 2011). Moreover, IF is found to prevent atherosclerotic state by promoting an anti-inflammatory response (Malinowski et al., 2019). However, mechanistic data describing the impact of IF on cardiovascular remodeling is scarce. A recent study examined the effect of alternate day fasting on cardiac remodeling post-myocardial infarction (MI) in rats. While IF improved cardiac function and reduced left ventricular dilation, none of the fibrosis gene markers examined appeared to have been affected (Okoshi et al., 2019). Another study showed that alternate day fasting promoted cardiomyocyte survival post-MI in rats by increasing the expression of anti-apoptotic and angiogenic factors (Katare et al., 2009). Interestingly, the post-MI protective effect of alternate day fasting was suggested to be mediated by an increase in adiponectin (Wan et al., 2010) further implicating the normalization of AT homeostasis as a possible mediator of the observed beneficial effect. Noteworthy, prophylactic IF was found to be protective against tissue and neurological damage caused by ischemic stroke. It works mainly on reducing inflammatory cytokines (IL-1β, IL-6, TNFα among others), inflammasome activation in the stroke side of the brain and oxidative stress, while increasing autophagy, mitophagy and neuroprotective proteins like; neurotrophic factors (BDNF and bFGF), antioxidants enzymes (HO-1), UCP-2 and UCP-4 (Fann et al., 2017). In this context, it was also found the fasting mediates its beneficial effects by increasing neuronal and glial SIRT-1 and P-AMPK (Fann et al., 2017).

Literature summarizing the impact of various dietary interventions on cardiovascular disease makes little discrimination between the effect of intermittent fasting and calorie-restrictive diets on cardiovascular outcomes (Maugeri and Vinciguerra, 2020). However, a recent trial directly compared an eight-week protocol of intermittent calorie restriction (3 days/week of low-calorie intake) to chronic reduced calorie intake in humans with mild metabolic impairment (overweight with mild hypertriglyceridemia). The results showed that while both protocols had an equal impact on body weight, body composition, and blood lipid levels, intermittent lowered insulin resistance further possibly having a more profound impact on AT inflammation and cardiovascular risk (Maroofi and Nasrollahzadeh, 2020). Moreover, another clinical trial specifically comparing the post-prandial indices of cardiometabolic risk between intermittent calorie restriction for two days per week and chronic calorie restriction in protocols extending to 3 months found that intermittent restriction was more effective in reducing post-prandial lipemia and insulinemia (Antoni et al., 2018). Nevertheless, a recent systematic review of clinical studies comparing IF to chronic calorie restriction found intermittent fasting to be more effective in weight reduction without a clear effect on blood glucose levels (Allaf et al., 2021). Indeed, this confirms the view of earlier investigation that different fasting protocols were not clearly effective in reducing blood glucose levels, and hence effectiveness in diabetes (Barnosky et al., 2014b). Certainly, more investigation is required to ascertain the efficacy of the intermittent fasting on cardiovascular risk as well as determine if a certain protocol is associated with more benefit.

Significantly, there has been no structured effort to investigate whether any of these positive cardiovascular outcomes of IF were mediated by its impact on AT remodeling independent of other metabolic factors. Indeed, the cardiometabolic markers consistently reported to be improved by IF like serum lipid and insulin levels as well as insulin resistance are those closely linked to AT inflammation. AT depots in immediate contact with the cardiac and vascular tissue microenvironment, namely PVAT and epicardial AT, would be ideal targets to mediate such effects. Limited changes in the status of immune cell and adipokine secretome of these depots could be sufficient to exert profound effects on cardiovascular structure and function. Interestingly, this highlights the importance and potential utility of IF protocols in the cardiovascular outcome of early metabolic impairment where adipose inflammation plays a more important role vs. hyperglycemia being a more predominant factor in more advanced conditions of metabolic decompensation in diabetes (Elkhatib et al., 2019; Bakkar et al., 2020b).

CONCLUSION

Adipose tissue deleterious remodeling and CMS are tightly linked to positive energy balance and HFD intake (Bays et al., 2007). PVAT has been recently implicated as one of the integral components of CMS that is highly sensitive to energy imbalance (Almabrouk et al., 2018; Qi et al., 2018). Positive energy balance appears to induce PVAT inflammation preceding other AT depots, which in turn triggers cardiovascular dysfunction early in the course of metabolic impairment. IF alleviates the metabolic and AT derangements known to accompany CMS. As IF promotes beneficial AT

remodeling, the inflammatory state is ameliorated with the potential consequence of improved cardiovascular structural and functional status. Whereas the peculiar nature of PVAT and its localization in close proximity to vascular tissue has brought it to the forefront of investigation of CMS, the impact of IF on PVAT under these circumstances is not well-studied. We propose a framework whereby IF relieves PVAT inflammation and thus induces positive cardiovascular outcomes in such a way that makes IF a feasible intervention with the early manifestations of CMS. Indeed, this is supported by the fact that prolonged intermittent fasting elicits pro-longevity metabolic alterations. However, for such an intervention to be of relevance in the treatment or prevention of CMS, the safety of prolonged fasting must be assured (Longo and Panda, 2016). A recent study highlighted that healthy individuals who have undergone alternate day fasting for six months had reduced cholesterol levels, inflammatory markers, and CVD risk (Stekovic et al., 2019). In another study that employed the Buchinger fasting protocol (fasting period between 4 and 21 days), adverse effects were reported in less than 1% of the 1,422 study subjects (Wilhelmi De Toledo et al., 2019). A review of studies following patients for up to twelve months only reported mild headaches as adverse outcomes of intermittent fasting (Allaf et al., 2021). Indeed, this indicates that prolonged alternate day fasting and complete fasting protocols are safe and well tolerated, and provides clinical evidence for their feasible utilization.

AUTHOR CONTRIBUTIONS

HSD and IA participated in literature review and screening and contributed to manuscript writing. HSD and IA wrote the first draft of the manuscript. AHE and OO helped in overseeing and coordinating the work and participated in manuscript draft review. AFE developed the idea, supervised the work, reviewed and modified manuscript draft, and provided research funding support. All authors read and approved of the manuscript.

FUNDING

This study was supported by a Medical Practice Plan Research Grant #320148 offered by the Faculty of Medicine at the American University of Beirut to AFE. HSD is supported by a PhD Scholarship from the Faculty of Agriculture and Food Sciences at the American University of Beirut. HSD is also a l'Oreal-UNESCO For Women in Science Program Pre-doctoral Fellow.

REFERENCES

Agabiti-Rosei, C., Paini, A., De Ciuceis, C., Withers, S., Greenstein, A., Heagerty, A. M., et al. (2018). Modulation of vascular reactivity by perivascular adipose tissue (PVAT). *Curr. Hypertens. Rep.* 20, 44. doi:10.1007/s11906-018-0835-5

Aksungar, F. B., Sarıkaya, M., Coskun, A., Serteser, M., and Unsal, I. (2017). Comparison of intermittent fasting versus caloric restriction in obese subjects: a two year follow-up. *J. Nutr. Health Aging* 21, 681–685. doi:10.1007/s12603-016-0786-y

Al-Assi, O., Ghali, R., Mroueh, A., Kaplan, A., Mougharbil, N., Eid, A. H., et al. (2018). Cardiac autonomic neuropathy as a result of mild hypercaloric challenge in absence of signs of diabetes: modulation by antidiabetic drugs. *Oxidative Med. Cell. longev.* 2018, 9389784. doi:10.1155/2018/9389784

Alaaeddine, R., Elkhatib, M. A. W., Mroueh, A., Fouad, H., Saad, E. I., El-Sabban, M. E., et al. (2019). Impaired endothelium-dependent hyperpolarization underlies endothelial dysfunction during early metabolic challenge: increased ROS generation and possible interference with NO function. *J. Pharmacol. Exp. Ther.* 371, 567–582. doi:10.1124/jpet.119.262048

Allaf, M., Elghazaly, H., Mohamed, O. G., Fareen, M. F., Zaman, S., Salmasi, A. M., et al. (2021). Intermittent fasting for the prevention of cardiovascular disease. *Cochrane Database Syst. Rev.* 1, CD013496. doi:10.1002/14651858.cd013496.pub2

Almabrouk, T. A. M., White, A. D., Ugusman, A. B., Skiba, D. S., Katwan, O. J., Alganga, H., et al. (2018). High fat diet attenuates the anticontractile activity of aortic PVAT via a mechanism involving AMPK and reduced adiponectin secretion. *Front. Physiol.* 9, 51. doi:10.3389/fphys.2018.00051

Altshuler-Keylin, S., and Kajimura, S. (2017). Mitochondrial homeostasis in adipose tissue remodeling. *Sci. Signal.* 10. doi:10.1126/scisignal.aai9248

Alzaim, I., Hammoud, S. H., Al-Koussa, H., Ghazi, A., Eid, A. H., and El-Yazbi, A. F. (2020). Adipose tissue immunomodulation: a novel therapeutic approach in cardiovascular and metabolic diseases. *Front. Cardiovasc. Med.* 7, 602088. doi:10.3389/fcvm.2020.602088

Anderson, E. A., Hoffman, R. P., Balon, T. W., Sinkey, C. A., and Mark, A. L. (1991). Hyperinsulinemia produces both sympathetic neural activation and vasodilation in normal humans. *J. Clin. Invest.* 87, 2246–2252. doi:10.1172/JCI115260

Antoni, R., Johnston, K. L., Collins, A. L., and Robertson, M. D. (2017). Effects of intermittent fasting on glucose and lipid metabolism. *Proc. Nutr. Soc.* 76, 361–368. doi:10.1017/S0029665116002986

Antoni, R., Johnston, K. L., Collins, A. L., and Robertson, M. D. (2018). Intermittentv. continuous energy restriction: differential effects on postprandial glucose and lipid metabolism following matched weight loss in overweight/obese participants. *Br. J. Nutr.* 119, 507–516. doi:10.1017/s0007114517003890

Apovian, C. M., Bigornia, S., Mott, M., Meyers, M. R., Ulloor, J., Gagua, M., et al. (2008). Adipose macrophage infiltration is associated with insulin resistance and vascular endothelial dysfunction in obese subjects. *Arterioscler Thromb. Vasc. Biol.* 28, 1654–1659. doi:10.1161/ATVBAHA.108.170316

Ash-Bernal, R., and Peterson, L. R. (2006). The cardiometabolic syndrome and cardiovascular disease. *J. Cardiometab Syndr.* 1, 25–28. doi:10.1111/j.0197-3118.2006.05452.x

Azul, L., Leandro, A., Boroumand, P., Klip, A., Seica, R., and Sena, C. M. (2019). Increased inflammation, oxidative stress and a reduction in antioxidant defense enzymes in perivascular adipose tissue contribute to vascular dysfunction in type 2 diabetes. *Free Radic. Biol. Med.* 146, 264–274. doi:10.1016/j.freeradbiomed.2019.11.002

Bagherniya, M., Butler, A. E., Barreto, G. E., and Sahebkar, A. (2018). The effect of fasting or calorie restriction on autophagy induction: a review of the literature. *Ageing Res. Rev.* 47, 183–197. doi:10.1016/j.arr.2018.08.004

Bakkar, N. Z., Dwaib, H. S., Fares, S., Eid, A. H., Al-Dhaheri, Y., and El-Yazbi, A. F. (2020a). Cardiac autonomic neuropathy: a progressive consequence of chronic low-grade inflammation in type 2 diabetes and related metabolic disorders. *Int. J. Mol. Sci.* 21. doi:10.3390/ijms21239005

Bakkar, N. Z., Mougharbil, N., Mroueh, A., Kaplan, A., Eid, A. H., Fares, S., et al. (2020b). Worsening baroreflex sensitivity on progression to type 2 diabetes: localized vs. systemic inflammation and role of antidiabetic therapy. *Am. J. Physiol. Endocrinol. Metab.* 319, E835–e851. doi:10.1152/ajpendo.00145.2020

Barnosky, A. R., Hoddy, K. K., Unterman, T. G., and Varady, K. A. (2014a). Intermittent fasting vs daily calorie restriction for type 2 diabetes prevention: a

review of human findings. *Transl Res.* 164, 302–311. doi:10.1016/j.trsl.2014.05.013

Barnosky, A. R., Hoddy, K. K., Unterman, T. G., and Varady, K. A. (2014b). Intermittent fasting vs daily calorie restriction for type 2 diabetes prevention: a review of human findings. *Transl Res.* 164, 302–311. doi:10.1016/j.trsl.2014.05.013

Bartelt, A., and Heeren, J. (2014). Adipose tissue browning and metabolic health. *Nat. Rev. Endocrinol.* 10, 24. doi:10.1038/nrendo.2013.204

Bays, H., Rodbard, H. W., Schorr, A. B., and González-Campoy, J. M. (2007). Adiposopathy: treating pathogenic adipose tissue to reduce cardiovascular disease risk. *Curr. Treat. Options. Cardiovasc. Med.* 9, 259–271. doi:10.1007/s11936-007-0021-6

Bays, H. E., González-Campoy, J. M., Bray, G. A., Kitabchi, A. E., Bergman, D. A., Schorr, A. B., et al. (2008). Pathogenic potential of adipose tissue and metabolic consequences of adipocyte hypertrophy and increased visceral adiposity. *Expert Rev. Cardiovasc. Ther.* 6, 343–368. doi:10.1586/14779072.6.3.343

Bays, H. E. (2011). Adiposopathy is "sick fat" a cardiovascular disease?. *J. Am. Coll. Cardiol.* 57, 2461–2473. doi:10.1016/j.jacc.2011.02.038

Berbudi, A., Surendar, J., Ajendra, J., Gondorf, F., Schmidt, D., Neumann, A. L., et al. (2016). Filarial infection or antigen administration improves glucose tolerance in diet-induced obese mice. *J. Innate Immun.* 8, 601–616. doi:10.1159/000448401

Berg, A. H., and Scherer, P. E. (2005). Adipose tissue, inflammation, and cardiovascular disease. *Circ. Res.* 96, 939–949. doi:10.1161/01.RES.0000163635.62927.34

Bertholet, A. M., Kazak, L., Chouchani, E. T., Bogaczyńska, M. G., Paranjpe, I., Wainwright, G. L., et al. (2017). Mitochondrial patch clamp of beige adipocytes reveals UCP1-positive and UCP1-negative cells both exhibiting futile creatine cycling. *Cell Metab.* 25, 811–822. doi:10.1016/j.cmet.2017.03.002

Bertola, A., Ciucci, T., Rousseau, D., Bourlier, V., Duffaut, C., Bonnafous, S., et al. (2012). Identification of adipose tissue dendritic cells correlated with obesity-associated insulin-resistance and inducing Th17 responses in mice and patients. *Diabetes* 61, 2238–2247. doi:10.2337/db11-1274

Bhutani, S., Klempel, M. C., Kroeger, C. M., Trepanowski, J. F., and Varady, K. A. (2013). Alternate day fasting and endurance exercise combine to reduce body weight and favorably alter plasma lipids in obese humans. *Obesity (Silver Spring)* 21, 1370–1379. doi:10.1002/oby.20353

Bjørndal, B., Burri, L., Staalesen, V., Skorve, J., and Berge, R. K. (2011). Different adipose depots: their role in the development of metabolic syndrome and mitochondrial response to hypolipidemic agents. *J. Obes.* 2011, 490650. doi:10.1155/2011/490650

Bonet, M. L., Mercader, J., and Palou, A. (2017). A nutritional perspective on UCP1-dependent thermogenesis. *Biochimie* 134, 99–117. doi:10.1016/j.biochi.2016.12.014

Bordone, L., Cohen, D., Robinson, A., Motta, M. C., Van Veen, E., Czopik, A., et al. (2007). SIRT1 transgenic mice show phenotypes resembling calorie restriction. *Aging Cell* 6, 759–767. doi:10.1111/j.1474-9726.2007.00335.x

Britton, K., and Fox, C. (2011). Perivascular adipose tissue and vascular disease. *Clin. Lipidol.* 6, 79–91. doi:10.2217/clp.10.89

Cairó, M., and Villarroya, J. (2020). The role of autophagy in brown and beige adipose tissue plasticity. *J. Physiol. Biochem.* 76, 213–226. doi:10.1007/s13105-019-00708-1

Cannon, B., and Nedergaard, J. (2017). What ignites UCP1?. *Cell Metab.* 26, 697–698. doi:10.1016/j.cmet.2017.10.012

Caslin, H. L., Bhanot, M., Bolus, W. R., and Hasty, A. H. (2020). Adipose tissue macrophages: unique polarization and bioenergetics in obesity. *Immunol. Rev.* 295, 101–113. doi:10.1111/imr.12853

Castro, J. P., El-Atat, F. A., Mcfarlane, S. I., Aneja, A., and Sowers, J. R. (2003). Cardiometabolic syndrome: pathophysiology and treatment. *Curr. Hypertens. Rep.* 5, 393–401. doi:10.1007/s11906-003-0085-y

Cawthorn, W. P., and Sethi, J. K. (2008). TNF-alpha and adipocyte biology. *FEBS Lett.* 582, 117–131. doi:10.1016/j.febslet.2007.11.051

Chan, K. L., Pillon, N. J., Sivaloganathan, D. M., Costford, S. R., Liu, Z., Théret, M., et al. (2015). Palmitoleate reverses high fat-induced proinflammatory macrophage polarization via AMP-activated protein kinase (AMPK). *J. Biol. Chem.* 290, 16979–16988. doi:10.1074/jbc.M115.646992

Chang, L., Villacorta, L., Li, R., Hamblin, M., Xu, W., Dou, C., et al. (2012). Loss of perivascular adipose tissue on peroxisome proliferator-activated receptor-γ deletion in smooth muscle cells impairs intravascular thermoregulation and enhances atherosclerosis. *Circulation* 126, 1067–1078. doi:10.1161/CIRCULATIONAHA.112.104489

Charrière, G., Cousin, B., Arnaud, E., André, M., Bacou, F., Pénicaud, L., et al. (2003). Preadipocyte conversion to macrophage. Evidence of plasticity. *J. Biol. Chem.* 278, 9850–9855. doi:10.1074/jbc.M210811200

Chatterjee, T. K., Stoll, L. L., Denning, G. M., Harrelson, A., Blomkalns, A. L., Idelman, G., et al. (2009). Proinflammatory phenotype of perivascular adipocytes: influence of high-fat feeding. *Circ. Res.* 104, 541–549. doi:10.1161/CIRCRESAHA.108.182998

Chattopadhyay, M., Khemka, V. K., Chatterjee, G., Ganguly, A., Mukhopadhyay, S., and Chakrabarti, S. (2015). Enhanced ROS production and oxidative damage in subcutaneous white adipose tissue mitochondria in obese and type 2 diabetes subjects. *Mol. Cel Biochem.* 399, 95–103. doi:10.1007/s11010-014-2236-7

Chen, Y., Tian, J., Tian, X., Tang, X., Rui, K., Tong, J., et al. (2014). Adipose tissue dendritic cells enhances inflammation by prompting the generation of Th17 cells. *PloS one* 9, e92450. doi:10.1371/journal.pone.0092450

Choe, S. S., Huh, J. Y., Hwang, I. J., Kim, J. I., and Kim, J. B. (2016). Adipose tissue remodeling: its role in energy metabolism and metabolic disorders. *Front. Endocrinol. (Lausanne)* 7, 30. doi:10.3389/fendo.2016.00030

Chouchani, E. T., Kazak, L., and Spiegelman, B. M. (2019). New advances in adaptive thermogenesis: UCP1 and beyond. *Cell Metab.* 29, 27–37. doi:10.1016/j.cmet.2018.11.002

Chylikova, J., Dvorackova, J., Tauber, Z., and Kamarad, V. (2018). M1/M2 macrophage polarization in human obese adipose tissue. *Biomed. Pap. Med. Fac. Univ. Palacky Olomouc Czech Repub.* 162, 79–82. doi:10.5507/bp.2018.015

Cinti, S., Mitchell, G., Barbatelli, G., Murano, I., Ceresi, E., Faloia, E., et al. (2005). Adipocyte death defines macrophage localization and function in adipose tissue of obese mice and humans. *J. Lipid Res.* 46, 2347–2355. doi:10.1194/jlr.M500294-JLR200

Clemente-Postigo, M., Tinahones, A., El Bekay, R., Malagón, M. M., and Tinahones, F. J. (2020). The Role of autophagy in white adipose tissue function: implications for metabolic health. *Metabolites.* 10, 179. doi:10.3390/metabo10050179

Coman, O. A., Păunescu, H., Ghiță, I., Coman, L., Bădărău, A., and Fulga, I. (2009). Beta 3 adrenergic receptors: molecular, histological, functional and pharmacological approaches. *Rom. J. Morphol. Embryol.* 50, 169–179.

Connell, N. J., Doligkeit, D., Andriessen, C., Kornips-Moonen, E., Bruls, Y. M. H., Schrauwen-Hinderling, V. B., et al. (2021). No evidence for brown adipose tissue activation after creatine supplementation in adult vegetarians. *Nat. Metab.* 3, 107–117. doi:10.1038/s42255-020-00332-0

de Souza Marinho, T., Ornellas, F., Aguila, M. B., and Mandarim-De-Lacerda, C. A. (2020). Browning of the subcutaneous adipocytes in diet-induced obese mouse submitted to intermittent fasting. *Mol. Cell Endocrinol.* 513, 110872. doi:10.1016/j.mce.2020.110872

Defuria, J., Belkina, A. C., Jagannathan-Bogdan, M., Snyder-Cappione, J., Carr, J. D., Nersesova, Y. R., et al. (2013). B cells promote inflammation in obesity and type 2 diabetes through regulation of T-cell function and an inflammatory cytokine profile. *Proc. Natl. Acad. Sci. USA* 110, 5133–5138. doi:10.1073/pnas.1215840110

Deiuliis, J., Shah, Z., Shah, N., Needleman, B., Mikami, D., Narula, V., et al. (2011). Visceral adipose inflammation in obesity is associated with critical alterations in tregulatory cell numbers. *PLoS One* 6, e16376. doi:10.1371/journal.pone.0016376

den Brok, M. H., Raaijmakers, T. K., Collado-Camps, E., and Adema, G. J. (2018). Lipid droplets as immune modulators in myeloid cells. *Trends Immunol.* 39, 380–392. doi:10.1016/j.it.2018.01.012

Desjardins, E. M., and Steinberg, G. R. (2018). Emerging role of AMPK in Brown and Beige adipose tissue (BAT): implications for obesity, insulin resistance, and type 2 diabetes. *Curr. Diab Rep.* 18, 80. doi:10.1007/s11892-018-1049-6

Dwaib, H. S., Taher, M. F., Mougharbil, N., Obeid, O. F., and El-Yazbi, A. F. (2020). Therapeutic fasting mitigates metabolic and cardiovascular dysfunction in a prediabetic rat model: possible role of adipose inflammation. *FASEB j.* 34, 1. doi:10.1096/fasebj.2020.34.s1.05510

Dzhalilova, D. S., Kosyreva, A. M., Diatroptov, M. E., Ponomarenko, E. A., Tsvetkov, I. S., Zolotova, N. A., et al. (2019). Dependence of the severity of the systemic inflammatory response on resistance to hypoxia in male Wistar rats. *J. Inflamm. Res.* 12, 73–86. doi:10.2147/JIR.S194581

Eiras, S., Teijeira-Fernández, E., Shamagian, L. G., Fernandez, A. L., Vazquez-Boquete, A., and Gonzalez-Juanatey, J. R. (2008). Extension of coronary artery disease is associated with increased IL-6 and decreased adiponectin gene expression in epicardial adipose tissue. *Cytokine* 43, 174–180. doi:10.1016/j.cyto.2008.05.006

Elkhatib, M. A. W., Mroueh, A., Rafeh, R. W., Sleiman, F., Fouad, H., Saad, E. I., et al. (2019). Amelioration of perivascular adipose inflammation reverses vascular dysfunction in a model of nonobese prediabetic metabolic challenge: potential role of antidiabetic drugs. *Transl Res.* 214, 121–143. doi:10.1016/j.trsl.2019.07.009

Engelman, J. A., Berg, A. H., Lewis, R. Y., Lisanti, M. P., and Scherer, P. E. (2000). Tumor necrosis factor alpha-mediated insulin resistance, but not dedifferentiation, is abrogated by MEK1/2 inhibitors in 3T3-L1 adipocytes. *Mol. Endocrinol.* 14, 1557–1569. doi:10.1210/mend.14.10.0542

Erdem, Y., Özkan, G., Ulusoy, Ş., Arıcı, M., Derici, Ü., Şengül, Ş., et al. (2018). The effect of intermittent fasting on blood pressure variability in patients with newly diagnosed hypertension or prehypertension. *J. Am. Soc. Hypertens.* 12, 42–49. doi:10.1016/j.jash.2017.11.008

Esmaeilzadeh, F., and Van De Borne, P. (2016). Does intermittent fasting improve microvascular endothelial function in healthy middle-aged subjects?. *Biol. Med.* 8, 1. doi:10.4172/0974-8369.1000337

Fabbiano, S., Suárez-Zamorano, N., Rigo, D., Veyrat-Durebex, C., Stevanovic Dokic, A., Colin, D. J., et al. (2016). Caloric restriction leads to browning of white adipose tissue through type 2 immune signaling. *Cell Metab.* 24, 434–446. doi:10.1016/j.cmet.2016.07.023

Fakih, W., Mroueh, A., Salah, H., Eid, A. H., Obeid, M., Kobeissy, F., et al. (2020). Dysfunctional cerebrovascular tone contributes to cognitive impairment in a non-obese rat model of prediabetic challenge: role of suppression of autophagy and modulation by anti-diabetic drugs. *Biochem. Pharmacol.* 178, 114041. doi:10.1016/j.bcp.2020.114041

Fann, D. Y., Ng, G. Y., Poh, L., and Arumugam, T. V. (2017). Positive effects of intermittent fasting in ischemic stroke. *Exp. Gerontol.* 89, 93–102. doi:10.1016/j.exger.2017.01.014

Faris, M. A., Kacimi, S., Al-Kurd, R. A., Fararjeh, M. A., Bustanji, Y. K., Mohammad, M. K., et al. (2012). Intermittent fasting during Ramadan attenuates proinflammatory cytokines and immune cells in healthy subjects. *Nutr. Res.* 32, 947–955. doi:10.1016/j.nutres.2012.06.021

Ferhat, M., Funai, K., and Boudina, S. (2019). Autophagy in adipose tissue physiology and pathophysiology. *Antioxid. Redox Signaling* 31, 487–501. doi:10.1089/ars.2018.7626

Festa, A., Hanley, A. J., Tracy, R. P., D'agostino, R., Jr., and Haffner, S. M. (2003). Inflammation in the prediabetic state is related to increased insulin resistance rather than decreased insulin secretion. *Circulation* 108, 1822–1830. doi:10.1161/01.CIR.0000091339.70120.53

Festuccia, W. T., Blanchard, P. G., Richard, D., and Deshaies, Y. (2010). Basal adrenergic tone is required for maximal stimulation of rat brown adipose tissue UCP1 expression by chronic PPAR-gamma activation. *Am. J. Physiol. Regul. Integr. Comp. Physiol.* 299, R159–R167. doi:10.1152/ajpregu.00821.2009

Feuerer, M., Herrero, L., Cipolletta, D., Naaz, A., Wong, J., Nayer, A., et al. (2009). Lean, but not obese, fat is enriched for a unique population of regulatory T cells that affect metabolic parameters. *Nat. Med.* 15, 930–939. doi:10.1038/nm.2002

Fitzgibbons, T. P., and Czech, M. P. (2014). Epicardial and perivascular adipose tissues and their influence on cardiovascular disease: basic mechanisms and clinical associations. *J. Am. Heart Assoc.* 3, e000582. doi:10.1161/JAHA.113.000582

Foster, D. O., and Frydman, M. L. (1978). "Brown adipose tissue: the dominant site of nonshivering thermogenesis in the rat," in *Effectors of thermogenesis*. Springer, 147–151. doi:10.1007/978-3-0348-5559-4_16

Friesen, M., Hudak, C. S., Warren, C. R., Xia, F., and Cowan, C. A. (2016). Adipocyte insulin receptor activity maintains adipose tissue mass and lifespan. *Biochem. Biophys. Res. Commun.* 476, 487–492. doi:10.1016/j.bbrc.2016.05.151

Fujisaka, S., Usui, I., Kanatani, Y., Ikutani, M., Takasaki, I., Tsuneyama, K., et al. (2011). Telmisartan improves insulin resistance and modulates adipose tissue macrophage polarization in high-fat-fed mice. *Endocrinol.* 152, 1789–1799. doi:10.1210/en.2010-1312

Gaborit, B., Venteclef, N., Ancel, P., Pelloux, V., Gariboldi, V., Leprince, P., et al. (2015). Human epicardial adipose tissue has a specific transcriptomic signature depending on its anatomical peri-atrial, peri-ventricular, or peri-coronary location. *Cardiovasc. Res.* 108, 62–73. doi:10.1093/cvr/cvv208

Gálvez, B., De Castro, J., Herold, D., Dubrovska, G., Arribas, S., González, M. C., et al. (2006). Perivascular adipose tissue and mesenteric vascular function in spontaneously hypertensive rats. *Arterioscler Thromb. Vasc. Biol.* 26, 1297–1302. doi:10.1161/01.ATV.0000220381.40739.dd

Gao, Y. J., Lu, C., Su, L. Y., Sharma, A. M., and Lee, R. M. (2007). Modulation of vascular function by perivascular adipose tissue: the role of endothelium and hydrogen peroxide. *Br. J. Pharmacol.* 151, 323–331. doi:10.1038/sj.bjp.0707228

Gao, Y. J., Takemori, K., Su, L. Y., An, W. S., Lu, C., Sharma, A. M., et al. (2006). Perivascular adipose tissue promotes vasoconstriction: the role of superoxide anion. *Cardiovasc. Res.* 71, 363–373. doi:10.1016/j.cardiores.2006.03.013

García-Ruiz, E., Reynés, B., Díaz-Rúa, R., Ceresi, E., Oliver, P., and Palou, A. (2015). The intake of high-fat diets induces the acquisition of brown adipocyte gene expression features in white adipose tissue. *Int. J. Obes.* 39, 1619–1629. doi:10.1038/ijo.2015.112

Gerhart-Hines, Z., Rodgers, J., Bare, O., Lerin, C., Kim, S., Mostoslavsky, R., et al. (1913). Metabolic control of muscle mitochondrial function and fatty acid oxidation through SIRT1/PGC-1alpha. *EMBO J.* 26, 1913. doi:10.1038/sj.emboj.7601633

Gonzalez, M. A., and Selwyn, A. P. (2003). Endothelial function, inflammation, and prognosis in cardiovascular disease. *Am. J. Med.* 115 (Suppl 8A), 99S–106S. doi:10.1016/j.amjmed.2003.09.016

Greenstein, A. S., Khavandi, K., Withers, S. B., Sonoyama, K., Clancy, O., Jeziorska, M., et al. (2009). Local inflammation and hypoxia abolish the protective anticontractile properties of perivascular fat in obese patients. *Circulation* 119, 1661–1670. doi:10.1161/CIRCULATIONAHA.108.821181

Grundy, S. M. (2012). Pre-diabetes, metabolic syndrome, and cardiovascular risk. *J. Am. Coll. Cardiol.* 59, 635–643. doi:10.1016/j.jacc.2011.08.080

Guilherme, A., Virbasius, J. V., Puri, V., and Czech, M. P. (2008). Adipocyte dysfunctions linking obesity to insulin resistance and type 2 diabetes. *Nat. Rev. Mol. Cel Biol* 9, 367–377. doi:10.1038/nrm2391

Gustafson, B., and Smith, U. (2015). Regulation of white adipogenesis and its relation to ectopic fat accumulation and cardiovascular risk. *Atherosclerosis* 241, 27–35. doi:10.1016/j.atherosclerosis.2015.04.812

Harmon, D. B., Srikakulapu, P., Kaplan, J. L., Oldham, S. N., Mcskimming, C., Garmey, J. C., et al. (2016). Protective role for B-1b B cells and IgM in obesity-associated inflammation, glucose intolerance, and insulin resistance. *Arterioscler Thromb. Vasc. Biol.* 36, 682–691. doi:10.1161/ATVBAHA.116.307166

Harvie, M. N., Pegington, M., Mattson, M. P., Frystyk, J., Dillon, B., Evans, G., et al. (2011). The effects of intermittent or continuous energy restriction on weight loss and metabolic disease risk markers: a randomized trial in young overweight women. *Int. J. Obes. (Lond)* 35, 714–727. doi:10.1038/ijo.2010.171

He, Q., Gao, Z., Yin, J., Zhang, J., Yun, Z., and Ye, J. (2011). Regulation of HIF-1{alpha} activity in adipose tissue by obesity-associated factors: adipogenesis, insulin, and hypoxia. *Am. J. Physiol. Endocrinol. Metab.* 300, E877–E885. doi:10.1152/ajpendo.00626.2010

Hirata, Y., Tabata, M., Kurobe, H., Motoki, T., Akaike, M., Nishio, C., et al. (2011). Coronary atherosclerosis is associated with macrophage polarization in epicardial adipose tissue. *J. Am. Coll. Cardiol.* 58, 248–255. doi:10.1016/j.jacc.2011.01.048

Horimatsu, T., Patel, A. S., Prasad, R., Reid, L. E., Benson, T. W., Zarzour, A., et al. (2018). Remote effects of transplanted perivascular adipose tissue on endothelial function and atherosclerosis. *Cardiovasc. Drugs Ther.* 32, 503–510. doi:10.1007/s10557-018-6821-y

Ilan, Y., Maron, R., Tukpah, A. M., Maioli, T. U., Murugaiyan, G., Yang, K., et al. (2010). Induction of regulatory T cells decreases adipose inflammation and alleviates insulin resistance in ob/ob mice. *Proc. Natl. Acad. Sci. USA* 107, 9765–9770. doi:10.1073/pnas.0908771107

International Diabetes Federation (2019). "IDF diabetes atlas," in *Brussels, Belgium: international diabetes federation*. 9 ed..

Jamdar, S. C. (1978). Glycerolipid biosynthesis in rat adipose tissue. Influence of adipose-cell size and site of adipose tissue on triacylglycerol formation in lean and obese rats. *Biochem. J.* 170, 153–160. doi:10.1042/bj1700153

Jamshed, H., Beyl, R., Della Manna, D., Yang, E., Ravussin, E., and Peterson, C. (2019). Early time-restricted feeding improves 24-hour glucose levels and

affects markers of the circadian clock, aging, and autophagy in humans. *Nutrients* 11, 1234. doi:10.3390/nu11061234

Jeong, H. J., Hong, S. H., Park, R. K., Shin, T., An, N. H., and Kim, H. M. (2005). Hypoxia-induced IL-6 production is associated with activation of MAP kinase, HIF-1, and NF-kappaB on HEI-OC1 cells. *Hear. Res.* 207, 59–67. doi:10.1016/j.heares.2005.04.003

Jernås, M., Palming, J., SjöHolm, K., Jennische, E., Svensson, P.-A., Gabrielsson, B. G., et al. (2006). Separation of human adipocytes by size: hypertrophic fat cells display distinct gene expression. *FASEB J.* 20, 1540–1542. doi:10.1096/fj.05-5678fje

Ji, L., Zhao, X., Zhang, B., Kang, L., Song, W., Zhao, B., et al. (2019). Slc6a8-Mediated creatine uptake and accumulation reprogram macrophage polarization via regulating cytokine responses. *Immunity* 51, 272–e7. doi:10.1016/j.immuni.2019.06.007

Jones, J. R., Barrick, C., Kim, K. A., Lindner, J., Blondeau, B., Fujimoto, Y., et al. (2005). Deletion of PPARgamma in adipose tissues of mice protects against high fat diet-induced obesity and insulin resistance. *Proc. Natl. Acad. Sci. USA* 102, 6207–6212. doi:10.1073/pnas.0306743102

Kajimura, S., Spiegelman, B. M., and Seale, P. (2015). Brown and beige fat: physiological roles beyond heat generation. *Cell Metab.* 22, 546–559. doi:10.1016/j.cmet.2015.09.007

Kajita, K., Mune, T., Ikeda, T., Matsumoto, M., Uno, Y., Sugiyama, C., et al. (2008). Effect of fasting on PPARgamma and AMPK activity in adipocytes. *Diabetes Res. Clin. Pract.* 81, 144–149. doi:10.1016/j.diabres.2008.05.003

Katare, R. G., Kakinuma, Y., Arikawa, M., Yamasaki, F., and Sato, T. (2009). Chronic intermittent fasting improves the survival following large myocardial ischemia by activation of BDNF/VEGF/PI3K signaling pathway. *J. Mol. Cel Cardiol.* 46, 405–412. doi:10.1016/j.yjmcc.2008.10.027

Kazak, L., Chouchani, E. T., Jedrychowski, M. P., Erickson, B. K., Shinoda, K., Cohen, P., et al. (2015). A creatine-driven substrate cycle enhances energy expenditure and thermogenesis in beige fat. *Cell* 163, 643–655. doi:10.1016/j.cell.2015.09.035

Kazak, L., Chouchani, E. T., Lu, G. Z., Jedrychowski, M. P., Bare, C. J., Mina, A. I., et al. (2017). Genetic depletion of adipocyte creatine metabolism inhibits diet-induced thermogenesis and drives obesity. *Cell Metab.* 26, 660–663. doi:10.1016/j.cmet.2017.08.009e3

Kazak, L., and Cohen, P. (2020). Creatine metabolism: energy homeostasis, immunity and cancer biology. *Nat. Rev. Endocrinol.* 16, 421–436. doi:10.1038/s41574-020-0365-5

Kazak, L., Rahbani, J. F., Samborska, B., Lu, G. Z., Jedrychowski, M. P., Lajoie, M., et al. (2019). Ablation of adipocyte creatine transport impairs thermogenesis and causes diet-induced obesity. *Nat. Metab.* 1, 360–370. doi:10.1038/s42255-019-0035-x

Kershaw, E. E., Schupp, M., Guan, H. P., Gardner, N. P., Lazar, M. A., and Flier, J. S. (2007). PPARgamma regulates adipose triglyceride lipase in adipocytes *in vitro* and *in vivo*. *Am. J. Physiol. Endocrinol. Metab.* 293, E1736–E1745. doi:10.1152/ajpendo.00122.2007

Kim, K. H., Kim, Y. H., Son, J. E., Lee, J. H., Kim, S., Choe, M. S., et al. (2017). Intermittent fasting promotes adipose thermogenesis and metabolic homeostasis via VEGF-mediated alternative activation of macrophage. *Cell Res.* 27, 1309–1326. doi:10.1038/cr.2017.126

Kintscher, U., Hartge, M., Hess, K., Foryst-Ludwig, A., Clemenz, M., Wabitsch, M., et al. (2008). T-lymphocyte infiltration in visceral adipose tissue: a primary event in adipose tissue inflammation and the development of obesity-mediated insulin resistance. *Arterioscler Thromb. Vasc. Biol.* 28, 1304–1310. doi:10.1161/ATVBAHA.108.165100

Kirk, E. P., and Klein, S. (2009). Pathogenesis and pathophysiology of the cardiometabolic syndrome. *J. Clin. Hypertens. (Greenwich)* 11, 761–765. doi:10.1111/j.1559-4572.2009.00054.x

Kivelä, R., and Alitalo, K. (2017). White adipose tissue coloring by intermittent fasting. *Cel Res.* 27, 1300. doi:10.1038/cr.2017.130

Klempel, M. C., Kroeger, C. M., Bhutani, S., Trepanowski, J. F., and Varady, K. A. (2012). Intermittent fasting combined with calorie restriction is effective for weight loss and cardio-protection in obese women. *Nutr. J.* 11, 98. doi:10.1186/1475-2891-11-98

Klöting, N., and Blüher, M. (2014). Adipocyte dysfunction, inflammation and metabolic syndrome. *Rev. Endocr. Metab. Disord.* 15, 277–287. doi:10.1007/s11154-014-9301-0

Kohlgruber, A., and Lynch, L. (2015). Adipose tissue inflammation in the pathogenesis of type 2 diabetes. *Curr. Diab Rep.* 15, 92. doi:10.1007/s11892-015-0670-x

Kovsan, J., Blüher, M., Tarnovscki, T., Klöting, N., Kirshtein, B., Madar, L., et al. (2011). Altered autophagy in human adipose tissues in obesity. *J. Clin. Endocrinol. Metab.* 96, E268–E277. doi:10.1210/jc.2010-1681

Kralova Lesna, I., Kralova, A., Cejkova, S., Fronek, J., Petras, M., Sekerkova, A., et al. (2016). Characterisation and comparison of adipose tissue macrophages from human subcutaneous, visceral and perivascular adipose tissue. *J. Transl Med.* 14, 208. doi:10.1186/s12967-016-0962-1

Kumar, D., Pandya, S. K., Varshney, S., Shankar, K., Rajan, S., Srivastava, A., et al. (2019). Temporal immmunometabolic profiling of adipose tissue in HFD-induced obesity: manifestations of mast cells in fibrosis and senescence. *Int. J. Obes.* 43, 1281–1294. doi:10.1038/s41366-018-0228-5

Kumar, R. K., Jin, Y., Watts, S. W., and Rockwell, C. E. (2020). Naïve, regulatory, activated, and memory immune cells Co-exist in PVATs that are comparable in density to non-PVAT fats in health. *Front. Physiol.* 11, 58. doi:10.3389/fphys.2020.00058

Lahiri, V., Hawkins, W. D., and Klionsky, D. J. (2019). Watch what you (self-) eat: autophagic mechanisms that modulate metabolism. *Cell Metab.* 29, 803–826. doi:10.1016/j.cmet.2019.03.003

Lee, E.-H., Itan, M., Jang, J., Gu, H.-J., Rozenberg, P., Mingler, M. K., et al. (2018). Eosinophils support adipocyte maturation and promote glucose tolerance in obesity. *Scientific Rep.* 8, 1–12. doi:10.1038/s41598-018-28371-4

Lefranc, C., Friederich-Persson, M., Braud, L., Palacios-Ramirez, R., Karlsson, S., Boujardine, N., et al. (2019). MR (mineralocorticoid receptor) induces adipose tissue senescence and mitochondrial dysfunction leading to vascular dysfunction in obesity. *Hypertension* 73, 458–468. doi:10.1161/HYPERTENSIONAHA.118.11873

Lettieri-Barbato, D., Giovannetti, E., and Aquilano, K. (2016). Effects of dietary restriction on adipose mass and biomarkers of healthy aging in human. *Aging (Albany NY)* 8, 3341. doi:10.18632/aging.101122

Li, A., Zhang, S., Li, J., Liu, K., Huang, F., and Liu, B. (2016). Metformin and resveratrol inhibit Drp1-mediated mitochondrial fission and prevent ER stress-associated NLRP3 inflammasome activation in the adipose tissue of diabetic mice. *Mol. Cel Endocrinol.* 434, 36–47. doi:10.1016/j.mce.2016.06.008

Li, H., Thali, R. F., Smolak, C., Gong, F., Alzamora, R., Wallimann, T., et al. (2010). Regulation of the creatine transporter by AMP-activated protein kinase in kidney epithelial cells. *Am. J. Physiol. Ren. Physiol* 299, F167–F177. doi:10.1152/ajprenal.00162.2010

Liu, B., Hutchison, A. T., Thompson, C. H., Lange, K., and Heilbronn, L. K. (2019). Markers of adipose tissue inflammation are transiently elevated during intermittent fasting in women who are overweight or obese. *Obes. Res. Clin. Pract.* 13, 408–415. doi:10.1016/j.orcp.2019.07.001

Liu, B., Page, A. J., Hutchison, A. T., Wittert, G. A., and Heilbronn, L. K. (2019b). Intermittent fasting increases energy expenditure and promotes adipose tissue browning in mice. *Nutrition* 66, 38–43. doi:10.1016/j.nut.2019.03.015

Liu, B., Page, A. J., Hatzinikolas, G., Chen, M., Wittert, G. A., and Heilbronn, L. K. (2018). Intermittent fasting improves glucose tolerance and promotes adipose tissue remodeling in male mice fed a high-fat diet. *Endocrinol.* 160, 169–180. doi:10.1210/en.2018-00701

Liu, J., Divoux, A., Sun, J., Zhang, J., Clément, K., Glickman, J. N., et al. (2009). Genetic deficiency and pharmacological stabilization of mast cells reduce diet-induced obesity and diabetes in mice. *Nat. Med.* 15, 940–945. doi:10.1038/nm.1994

Löhn, M., Dubrovska, G., Lauterbach, B., Luft, F. C., Gollasch, M., and Sharma, A. M. (2002). Periadventitial fat releases a vascular relaxing factor. *Faseb j* 16, 1057–1063. doi:10.1096/fj.02-0024com

Longo, V. D., and Panda, S. (2016). Fasting, circadian rhythms, and time-restricted feeding in healthy lifespan. *Cell Metab.* 23, 1048–1059. doi:10.1016/j.cmet.2016.06.001

Lotfi, S., Madani, M., Abassi, A., Tazi, A., Boumahmaza, M., and Talbi, M. (2010). CNS activation, reaction time, blood pressure and heart rate variation during ramadan intermittent fasting and exercise. *World J. Sports Sci.* 3, 37–43.

Lumeng, C. N., Bodzin, J. L., and Saltiel, A. R. (2007). Obesity induces a phenotypic switch in adipose tissue macrophage polarization. *J. Clin. Invest.* 117, 175–184. doi:10.1172/JCI29881

Lumeng, C. N., Delproposto, J. B., Westcott, D. J., and Saltiel, A. R. (2008). Phenotypic switching of adipose tissue macrophages with obesity is generated by spatiotemporal differences in macrophage subtypes. *Diabetes* 57, 3239–3246. doi:10.2337/db08-0872

Luo, G., Jian, Z., Zhu, Y., Zhu, Y., Chen, B., Ma, R., et al. (2019). Sirt1 promotes autophagy and inhibits apoptosis to protect cardiomyocytes from hypoxic stress. *Int. J. Mol. Med.* 43, 2033–2043. doi:10.3892/ijmm.2019.4125

Lutsey, P. L., Steffen, L. M., and Stevens, J. (2008). Dietary intake and the development of the metabolic syndrome: the Atherosclerosis Risk in Communities study. *Circulation* 117, 754–761. doi:10.1161/CIRCULATIONAHA.107.716159

Madkour, M. I., T El-Serafi, A., Jahrami, H. A., Sherif, N. M., Hassan, R. E., Awadallah, S., et al. (2019). Ramadan diurnal intermittent fasting modulates SOD2, TFAM, Nrf2, and sirtuins (SIRT1, SIRT3) gene expressions in subjects with overweight and obesity. *Diabetes Res. Clin. Pract.* 155, 107801. doi:10.1016/j.diabres.2019.107801

Mager, D. E., Wan, R., Brown, M., Cheng, A., Wareski, P., Abernethy, D. R., et al. (2006). Caloric restriction and intermittent fasting alter spectral measures of heart rate and blood pressure variability in rats. *FASEB J.* 20, 631–637. doi:10.1096/fj.05-5263com

Malinowski, B., Zalewska, K., Węsierska, A., Sokołowska, M. M., Socha, M., Liczner, G., et al. (2019). Intermittent fasting in cardiovascular disorders-an overview. *Nutrients* 11, 673. doi:10.3390/nu11030673

Manka, D., Chatterjee, T. K., Stoll, L. L., Basford, J. E., Konaniah, E. S., Srinivasan, R., et al. (2014). Transplanted perivascular adipose tissue accelerates injury-induced neointimal hyperplasia: role of monocyte chemoattractant protein-1. *Arterioscler Thromb. Vasc. Biol.* 34, 1723–1730. doi:10.1161/ATVBAHA.114.303983

Maroofi, M., and Nasrollahzadeh, J. (2020). Effect of intermittent versus continuous calorie restriction on body weight and cardiometabolic risk markers in subjects with overweight or obesity and mild-to-moderate hypertriglyceridemia: a randomized trial. *Lipids Health Dis.* 19, 216. doi:10.1186/s12944-020-01399-0

Martinez-Lopez, N., Tarabra, E., Toledo, M., Garcia-Macia, M., Sahu, S., Coletto, L., et al. (2017). System-wide benefits of intermeal fasting by autophagy. *Cell Metab.* 26, 856–871. doi:10.1016/j.cmet.2017.09.020

Maugeri, A., and Vinciguerra, M. (2020). The effects of meal timing and frequency, caloric restriction, and fasting on cardiovascular health: an overview. *J. Lipid Atheroscler.* 9, 140–152. doi:10.12997/jla.2020.9.1.140

Mayoral, R., Osborn, O., Mcnelis, J., Johnson, A. M., Oh, D. Y., Izquierdo, C. L., et al. (2015). Adipocyte SIRT1 knockout promotes PPARγ activity, adipogenesis and insulin sensitivity in chronic-HFD and obesity. *Mol. Metab.* 4, 378–391. doi:10.1016/j.molmet.2015.02.007

Misra, A., Singhal, N., and Khurana, L. (2010). Obesity, the metabolic syndrome, and type 2 diabetes in developing countries: role of dietary fats and oils. *J. Am. Coll. Nutr.* 29, 289s–301s. doi:10.1080/07315724.2010.10719844

Molofsky, A. B., Nussbaum, J. C., Liang, H. E., Van Dyken, S. J., Cheng, L. E., Mohapatra, A., et al. (2013). Innate lymphoid type 2 cells sustain visceral adipose tissue eosinophils and alternatively activated macrophages. *J. Exp. Med.* 210, 535–549. doi:10.1084/jem.20121964

Moore, J. X., Chaudhary, N., and Akinyemiju, T. (2017). Metabolic syndrome prevalence by race/ethnicity and sex in the United States, national health and nutrition examination survey, 1988-2012. *Prev. Chronic Dis.* 14, E24. doi:10.5888/pcd14.160287

Morris, D. L., Singer, K., and Lumeng, C. N. (2011). Adipose tissue macrophages: phenotypic plasticity and diversity in lean and obese states. *Curr. Opin. Clin. Nutr. Metab. Care* 14, 341. doi:10.1097/MCO.0b013e328347970b

Mottillo, E. P., Desjardins, E. M., Crane, J. D., Smith, B. K., Green, A. E., Ducommun, S., et al. (2016). Lack of adipocyte AMPK exacerbates insulin resistance and hepatic steatosis through Brown and beige adipose tissue function. *Cell Metab.* 24, 118–129. doi:10.1016/j.cmet.2016.06.006

Nakai, Y., Hashida, H., Kadota, K., Minami, M., Shimizu, K., Matsumoto, I., et al. (2008). Up-regulation of genes related to the ubiquitin-proteasome system in the brown adipose tissue of 24-h-fasted rats. *Biosci. Biotechnol. Biochem.* 72, 139–148. doi:10.1271/bbb.70508

Nedergaard, J., and Cannon, B. (2014). The browning of white adipose tissue: some burning issues. *Cell Metab.* 20, 396–407. doi:10.1016/j.cmet.2014.07.005

Nedergaard, J., Golozoubova, V., Matthias, A., Asadi, A., Jacobsson, A., and Cannon, B. (2001). UCP1: the only protein able to mediate adaptive non-shivering thermogenesis and metabolic inefficiency. *Biochim. Biophys. Acta.* 1504, 82–106. doi:10.1016/s0005-2728(00)00247-4

Nishimura, S., Manabe, I., and Nagai, R. (2009a). Adipose tissue inflammation in obesity and metabolic syndrome. *Discov. Med.* 8, 55.

Nishimura, S., Manabe, I., Nagasaki, M., Eto, K., Yamashita, H., Ohsugi, M., et al. (2009b). CD8+ effector T cells contribute to macrophage recruitment and adipose tissue inflammation in obesity. *Nat. Med.* 15, 914–920. doi:10.1038/nm.1964

Nøhr, M. K., Bobba, N., Richelsen, B., Lund, S., and Pedersen, S. B. (2017). Inflammation downregulates UCP1 expression in brown adipocytes potentially via SIRT1 and DBC1 interaction. *Int. J. Mol. Sci.* 18, 1006. doi:10.3390/ijms18051006

Okoshi, K., Cezar, M. D. M., Polin, M. a. M., Paladino, J. R., Martinez, P. F., Oliveira, S. A., et al. (2019). Influence of intermittent fasting on myocardial infarction-induced cardiac remodeling. *BMC Cardiovasc. Disord.* 19, 126. doi:10.1186/s12872-019-1113-4

Ouchi, N., Parker, J. L., Lugus, J. J., and Walsh, K. (2011). Adipokines in inflammation and metabolic disease. *Nat. Rev. Immunol.* 11, 85. doi:10.1038/nri2921

Parray, H. A., and Yun, J. W. (2017). Combined inhibition of autophagy protein 5 and galectin-1 by thiodigalactoside reduces diet-induced obesity through induction of white fat browning. *IUBMB life* 69, 510–521. doi:10.1002/iub.1634

Patterson, R. E., Laughlin, G. A., Lacroix, A. Z., Hartman, S. J., Natarajan, L., Senger, C. M., et al. (2015). Intermittent fasting and human metabolic health. *J. Acad. Nutr. Diet.* 115, 1203–1212. doi:10.1016/j.jand.2015.02.018

Patterson, R. E., and Sears, D. D. (2017). Metabolic effects of intermittent fasting. *Annu. Rev. Nutr.* 37, 371. doi:10.1146/annurev-nutr-071816-064634

Pedersen, D. J., Guilherme, A., Danai, L. V., Heyda, L., Matevossian, A., Cohen, J., et al. (2015). A major role of insulin in promoting obesity-associated adipose tissue inflammation. *Mol. Metab.* 4, 507–518. doi:10.1016/j.molmet.2015.04.003

Pedersen, S. B., Ølholm, J., Paulsen, S. K., Bennetzen, M. F., and Richelsen, B. (2008). Low Sirt1 expression, which is upregulated by fasting, in human adipose tissue from obese women. *Int. J. Obes. (Lond)* 32, 1250–1255. doi:10.1038/ijo.2008.78

Petrovic, N., Shabalina, I. G., Timmons, J. A., Cannon, B., and Nedergaard, J. (2008). Thermogenically competent nonadrenergic recruitment in brown preadipocytes by a PPARgamma agonist. *Am. J. Physiol. Endocrinol. Metab.* 295, E287–E296. doi:10.1152/ajpendo.00035.2008

Pfluger, P. T., Herranz, D., Velasco-Miguel, S., Serrano, M., and Tschöp, M. H. (2008). Sirt1 protects against high-fat diet-induced metabolic damage. *Proc. Natl. Acad. Sci. USA* 105, 9793–9798. doi:10.1073/pnas.0802917105

Pisani, D. F., Barquissau, V., Chambard, J. C., Beuzelin, D., Ghandour, R. A., Giroud, M., et al. (2018). Mitochondrial fission is associated with UCP1 activity in human brite/beige adipocytes. *Mol. Metab.* 7, 35–44. doi:10.1016/j.molmet.2017.11.007

Pollard, A. E., Martins, L., Muckett, P. J., Khadayate, S., Bornot, A., Clausen, M., et al. (2019). AMPK activation protects against diet induced obesity through Ucp1-independent thermogenesis in subcutaneous white adipose tissue. *Nat. Metab.* 1, 340–349. doi:10.1038/s42255-019-0036-9

Ponticos, M., Lu, Q. L., Morgan, J. E., Hardie, D. G., Partridge, T. A., and Carling, D. (1998). Dual regulation of the AMP-activated protein kinase provides a novel mechanism for the control of creatine kinase in skeletal muscle. *EMBO J.* 17, 1688–1699. doi:10.1093/emboj/17.6.1688

Qi, X. Y., Qu, S. L., Xiong, W. H., Rom, O., Chang, L., and Jiang, Z. S. (2018). Perivascular adipose tissue (PVAT) in atherosclerosis: a double-edged sword. *Cardiovasc. Diabetol.* 17, 134–153. doi:10.1186/s12933-018-0777-x

Qiu, Y., Nguyen, K. D., Odegaard, J. I., Cui, X., Tian, X., Locksley, R. M., et al. (2014). Eosinophils and type 2 cytokine signaling in macrophages orchestrate development of functional beige fat. *Cell* 157, 1292–1308. doi:10.1016/j.cell.2014.03.066

Raajendiran, A., Ooi, G., Bayliss, J., O'Brien, P. E., Schittenhelm, R. B., Clark, A. K., et al. (2019). Identification of metabolically distinct adipocyte progenitor cells in human adipose tissues. *Cell Rep.* 27, 1528–1540. doi:10.1016/j.celrep.2019.04.010

Rafeh, R., Viveiros, A., Oudit, G. Y., and El-Yazbi, A. F. (2020). Targeting perivascular and epicardial adipose tissue inflammation: therapeutic opportunities for cardiovascular disease. *Clin. Sci. (Lond)* 134, 827–851. doi:10.1042/CS20190227

Rahman, S., and Islam, R. (2011). Mammalian Sirt1: insights on its biological functions. *Cell Commun Signal* 9, 11. doi:10.1186/1478-811X-9-11

Razzak, R., Abu-Hozaifa, B. M., Bamosa, A. O., and Ali, N. M. (2011). Assessment of enhanced endothelium-dependent vasodilation by intermittent fasting in Wistar albino rats. *Indian J. Physiol. Pharmacol.* 55, 336–342.

Reaven, G. M. (1988). Banting lecture 1988. Role of insulin resistance in human disease. *Diabetes* 37, 1595–1607. doi:10.2337/diab.37.12.1595

Ren, T., He, J., Jiang, H., Zu, L., Pu, S., Guo, X., et al. (2006). Metformin reduces lipolysis in primary rat adipocytes stimulated by tumor necrosis factor-alpha or isoproterenol. *J. Mol. Endocrinol.* 37, 175–183. doi:10.1677/jme.1.02061

Richardson, V. R., Smith, K. A., and Carter, A. M. (2013). Adipose tissue inflammation: feeding the development of type 2 diabetes mellitus. *Immunobiol.* 218, 1497–1504. doi:10.1016/j.imbio.2013.05.002

Ricquier, D., and Bouillaud, F. (2000). The uncoupling protein homologues: UCP1, UCP2, UCP3, StUCP and AtUCP. *Biochem. J.* 345 Pt 2, 161–179. doi:10.1042/bj3450161

Rius, J., Guma, M., Schachtrup, C., Akassoglou, K., Zinkernagel, A. S., Nizet, V., et al. (2008). NF-kappaB links innate immunity to the hypoxic response through transcriptional regulation of HIF-1alpha. *Nature* 453, 807–811. doi:10.1038/nature06905

Ro, S. H., Jang, Y., Bae, J., Kim, I. M., Schaecher, C., and Shomo, Z. D. (2019). Autophagy in adipocyte browning: emerging drug target for intervention in obesity. *Front. Physiol.* 10, 22. doi:10.3389/fphys.2019.00022

Rodeheffer, M. S., Birsoy, K., and Friedman, J. M. (2008). Identification of white adipocyte progenitor cells *in vivo*. *Cell* 135, 240–249. doi:10.1016/j.cell.2008.09.036

Rosen, E. D., Sarraf, P., Troy, A. E., Bradwin, G., Moore, K., Milstone, D. S., et al. (1999). PPAR gamma is required for the differentiation of adipose tissue *in vivo* and *in vitro*. *Mol. Cel.* 4, 611–617. doi:10.1016/s1097-2765(00)80211-7

Ruan, H., Miles, P. D., Ladd, C. M., Ross, K., Golub, T. R., Olefsky, J. M., et al. (2002). Profiling gene transcription *in vivo* reveals adipose tissue as an immediate target of tumor necrosis factor-alpha: implications for insulin resistance. *Diabetes* 51, 3176–3188. doi:10.2337/diabetes.51.11.3176

Rui, L. (2017). Brown and beige adipose tissues in health and disease. *Compr. Physiol.* 7, 1281–1306. doi:10.1002/cphy.c170001

Sacks, H. S., Fain, J. N., Bahouth, S. W., Ojha, S., Frontini, A., Budge, H., et al. (2013). Adult epicardial fat exhibits beige features. *J. Clin. Endocrinol. Metab.* 98, E1448–E1455. doi:10.1210/jc.2013-1265

Sakamoto, T., Takahashi, N., Sawaragi, Y., Naknukool, S., Yu, R., Goto, T., et al. (2013). Inflammation induced by RAW macrophages suppresses UCP1 mRNA induction via ERK activation in 10T1/2 adipocytes. *Am. J. Physiol. Cel Physiol* 304, C729–C738. doi:10.1152/ajpcell.00312.2012

Salgado-Somoza, A., Teijeira-Fernández, E., Fernández, A. L., González-Juanatey, J. R., and Eiras, S. (2010). Proteomic analysis of epicardial and subcutaneous adipose tissue reveals differences in proteins involved in oxidative stress. *Am. J. Physiol. Heart Circ. Physiol.* 299, H202–H209. doi:10.1152/ajpheart.00120.2010

Sartipy, P., and Loskutoff, D. J. (2003). Monocyte chemoattractant protein 1 in obesity and insulin resistance. *Proc. Natl. Acad. Sci. USA* 100, 7265–7270. doi:10.1073/pnas.1133870100

Saxton, S. N., Clark, B. J., Withers, S. B., Eringa, E. C., and Heagerty, A. M. (2019). Mechanistic links between obesity, diabetes, and blood pressure: role of perivascular adipose tissue. *Physiol. Rev.* 99, 1701–1763. doi:10.1152/physrev.00034.2018

Schenk, S., Mccurdy, C. E., Philp, A., Chen, M. Z., Holliday, M. J., Bandyopadhyay, G. K., et al. (2011). Sirt1 enhances skeletal muscle insulin sensitivity in mice during caloric restriction. *J. Clin. Invest.* 121, 4281–4288. doi:10.1172/JCI58554

Shah, A., Mehta, N., and Reilly, M. P. (2008). Adipose inflammation, insulin resistance, and cardiovascular disease. *JPEN J. Parenter. Enteral Nutr.* 32, 638–644. doi:10.1177/0148607108325251

Shen, L., Chng, M. H., Alonso, M. N., Yuan, R., Winer, D. A., and Engleman, E. G. (2015). B-1a lymphocytes attenuate insulin resistance. *Diabetes* 64, 593–603. doi:10.2337/db14-0554

Shimizu, I., Yoshida, Y., Katsuno, T., and Minamino, T. (2013). Adipose tissue inflammation in diabetes and heart failure. *Microbes Infect.* 15, 11–17. doi:10.1016/j.micinf.2012.10.012

Simmons, R. K., Alberti, K. G., Gale, E. A., Colagiuri, S., Tuomilehto, J., Qiao, Q., et al. (2010). The metabolic syndrome: useful concept or clinical tool? Report of a WHO Expert Consultation. *Diabetologia* 53, 600–605. doi:10.1007/s00125-009-1620-4

Singh, R., Kaushik, S., Wang, Y., Xiang, Y., Novak, I., Komatsu, M., et al. (2009a). Autophagy regulates lipid metabolism. *Nature* 458, 1131–1135. doi:10.1038/nature07976

Singh, R., Xiang, Y., Wang, Y., Baikati, K., Cuervo, A. M., Luu, Y. K., et al. (2009b). Autophagy regulates adipose mass and differentiation in mice. *J. Clin. Invest.* 119, 3329–3339. doi:10.1172/JCI39228

Soltis, E. E., and Cassis, L. A. (1991). Influence of perivascular adipose tissue on rat aortic smooth muscle responsiveness. *Clin. Exp. Hypertens. A.* 13, 277–296. doi:10.3109/10641969109042063

Srikakulapu, P., Upadhye, A., Rosenfeld, S. M., Marshall, M. A., Mcskimming, C., Hickman, A. W., et al. (2017). Perivascular adipose tissue harbors atheroprotective IgM-producing B cells. *Front. Physiol.* 8, 719. doi:10.3389/fphys.2017.00719

St-Onge, M. P., Ard, J., Baskin, M. L., Chiuve, S. E., Johnson, H. M., Kris-Etherton, P., et al. (2017). Meal timing and frequency: implications for cardiovascular disease prevention: a scientific statement from the American Heart Association. *Circulation* 135, e96–e121. doi:10.1161/CIR.0000000000000476

Stefanovic-Racic, M., Yang, X., Turner, M. S., Mantell, B. S., Stolz, D. B., Sumpter, T. L., et al. (2012). Dendritic cells promote macrophage infiltration and comprise a substantial proportion of obesity-associated increases in CD11c+ cells in adipose tissue and liver. *Diabetes* 61, 2330–2339. doi:10.2337/db11-1523

Steinberg, G. R., Michell, B. J., Van Denderen, B. J., Watt, M. J., Carey, A. L., Fam, B. C., et al. (2006). Tumor necrosis factor alpha-induced skeletal muscle insulin resistance involves suppression of AMP-kinase signaling. *Cel. Metab.* 4, 465–474. doi:10.1016/j.cmet.2006.11.005

Stekovic, S., Hofer, S. J., Tripolt, N., Aon, M. A., Royer, P., Pein, L., et al. (2019). Alternate day fasting improves physiological and molecular markers of aging in healthy, non-obese humans. *Cel. Metab.* 30, 462–e6. doi:10.1016/j.cmet.2019.07.016

Stephens, J. M., Lee, J., and Pilch, P. F. (1997). Tumor necrosis factor-alpha-induced insulin resistance in 3T3-L1 adipocytes is accompanied by a loss of insulin receptor substrate-1 and GLUT4 expression without a loss of insulin receptor-mediated signal transduction. *J. Biol. Chem.* 272, 971–976. doi:10.1074/jbc.272.2.971

Suganami, T., Nishida, J., and Ogawa, Y. (2005). A paracrine loop between adipocytes and macrophages aggravates inflammatory changes: role of free fatty acids and tumor necrosis factor alpha. *Arterioscler Thromb. Vasc. Biol.* 25, 2062–2068. doi:10.1161/01.ATV.0000183883.72263.13

Sung, B., Park, S., Yu, B. P., and Chung, H. Y. (2004). Modulation of PPAR in aging, inflammation, and calorie restriction. *J. Gerontol. A. Biol. Sci. Med. Sci.* 59, 997–1006. doi:10.1093/gerona/59.10.b997

Suzawa, M., Takada, I., Yanagisawa, J., Ohtake, F., Ogawa, S., Yamauchi, T., et al. (2014). Retraction: cytokines suppress adipogenesis and PPAR-γ function through the TAK1/TAB1/NIK cascade. *Nat. Cel Biol.* 16, 1126. doi:10.1038/ncb3068

Talukdar, S., Oh, D. Y., Bandyopadhyay, G., Li, D., Xu, J., Mcnelis, J., et al. (2012). Neutrophils mediate insulin resistance in mice fed a high-fat diet through secreted elastase. *Nat. Med.* 18, 1407–1412. doi:10.1038/nm.2885

Tang, H. N., Tang, C. Y., Man, X. F., Tan, S. W., Guo, Y., Tang, J., et al. (2017). Plasticity of adipose tissue in response to fasting and refeeding in male mice. *Nutr. Metab. (Lond)* 14, 3. doi:10.1186/s12986-016-0159-x

Thapa, B., and Lee, K. (2019). Metabolic influence on macrophage polarization and pathogenesis. *BMB Rep.* 52, 360. doi:10.5483/bmbrep.2019.52.6.140

Thorp, A. A., and Schlaich, M. P. (2015). Relevance of sympathetic nervous system Activation in obesity and metabolic syndrome. *J. Diabetes Res.* 2015, 341583. doi:10.1155/2015/341583

Tinsley, G. M., and La Bounty, P. M. (2015). Effects of intermittent fasting on body composition and clinical health markers in humans. *Nutr. Rev.* 73, 661–674. doi:10.1093/nutrit/nuv041

Tontonoz, P., Hu, E., and Spiegelman, B. M. (1994). Stimulation of adipogenesis in fibroblasts by PPAR gamma 2, a lipid-activated transcription factor. *Cell* 79, 1147–1156. doi:10.1016/0092-8674(94)90006-x

Trayhurn, P. (2013). Hypoxia and adipose tissue function and dysfunction in obesity. *Physiol. Rev.* 93, 1–21. doi:10.1152/physrev.00017.2012

Tune, J. D., Goodwill, A. G., Sassoon, D. J., and Mather, K. J. (2017). Cardiovascular consequences of metabolic syndrome. *Transl Res.* 183, 57–70. doi:10.1016/j.trsl.2017.01.001

Uysal, K. T., Wiesbrock, S. M., Marino, M. W., and Hotamisligil, G. S. (1997). Protection from obesity-induced insulin resistance in mice lacking TNF-alpha function. *Nature* 389, 610–614. doi:10.1038/39335

van Dam, A. D., Boon, M. R., Berbée, J. F. P., Rensen, P. C. N., and Van Harmelen, V. (2017). Targeting white, brown and perivascular adipose tissue in atherosclerosis development. *Eur. J. Pharmacol.* 816, 82–92. doi:10.1016/j.ejphar.2017.03.051

van Uden, P., Kenneth, N. S., and Rocha, S. (2008). Regulation of hypoxia-inducible factor-1alpha by NF-kappaB. *Biochem. J.* 412, 477–484. doi:10.1042/BJ20080476

Varady, K. A., Allister, C. A., Roohk, D. J., and Hellerstein, M. K. (2010). Improvements in body fat distribution and circulating adiponectin by alternate-day fasting versus calorie restriction. *J. Nutr. Biochem.* 21, 188–195. doi:10.1016/j.jnutbio.2008.11.001

Varady, K. A., Hudak, C. S., and Hellerstein, M. K. (2009). Modified alternate-day fasting and cardioprotection: relation to adipose tissue dynamics and dietary fat intake. *Metab. Clin. Exp.* 58, 803–811. doi:10.1016/j.metabol.2009.01.018

Varady, K., Roohk, D., Loe, Y., Mcevoy-Hein, B., and Hellerstein, M. (2007). Effects of modified alternate-day fasting regimens on adipocyte size, triglyceride metabolism, and plasma adiponectin levels in mice. *J. Lipid Res.* 48, 2212–2219. doi:10.1194/jlr.M700223-JLR200

Velazquez-Villegas, L. A., Perino, A., Lemos, V., Zietak, M., Nomura, M., Pols, T. W. H., et al. (2018). TGR5 signalling promotes mitochondrial fission and beige remodelling of white adipose tissue. *Nat. Commun.* 9, 245. doi:10.1038/s41467-017-02068-0

Verlohren, S., Dubrovska, G., Tsang, S. Y., Essin, K., Luft, F. C., Huang, Y., et al. (2004). Visceral periadventitial adipose tissue regulates arterial tone of mesenteric arteries. *Hypertension* 44, 271–276. doi:10.1161/01.HYP.0000140058.28994.ec

Villena, J. A., Viollet, B., Andreelli, F., Kahn, A., Vaulont, S., and Sul, H. S. (2004). Induced adiposity and adipocyte hypertrophy in mice lacking the AMP-activated protein kinase-alpha2 subunit. *Diabetes* 53, 2242–2249. doi:10.2337/diabetes.53.9.2242

Vinik, A. I., Erbas, T., and Casellini, C. M. (2013). Diabetic cardiac autonomic neuropathy, inflammation and cardiovascular disease. *J. Diabetes Investig.* 4, 4–18. doi:10.1111/jdi.12042

von Bibra, H., Paulus, W., and St John Sutton, M. (2016). Cardiometabolic syndrome and increased risk of heart failure. *Curr. Heart Fail. Rep.* 13, 219–229. doi:10.1007/s11897-016-0298-4

Wallimann, T., Wyss, M., Brdiczka, D., Nicolay, K., and Eppenberger, H. (1992). Intracellular compartmentation, structure and function of creatine kinase isoenzymes in tissues with high and fluctuating energy demands: the 'phosphocreatine circuit' for cellular energy homeostasis. *Biochem. J.* 281 (Pt 1), 21–40. doi:10.1042/bj2810021

Wan, R., Ahmet, I., Brown, M., Cheng, A., Kamimura, N., Talan, M., et al. (2010). Cardioprotective effect of intermittent fasting is associated with an elevation of adiponectin levels in rats. *J. Nutr. Biochem.* 21, 413–417. doi:10.1016/j.jnutbio.2009.01.020

Wan, R., Camandola, S., and Mattson, M. P. (2003). Intermittent fasting and dietary supplementation with 2-deoxy-D-glucose improve functional and metabolic cardiovascular risk factors in rats. *FASEB J.* 17, 1133–1134. doi:10.1096/fj.02-0996fje

Wang, X., Yang, Q., Liao, Q., Li, M., Zhang, P., Santos, H. O., et al. (2020). Effects of intermittent fasting diets on plasma concentrations of inflammatory biomarkers: a systematic review and meta-analysis of randomized controlled trials. *Nutrition* 79-80, 110974. doi:10.1016/j.nut.2020.110974

Watanabe, Y., Nagai, Y., Honda, H., Okamoto, N., Yanagibashi, T., Ogasawara, M., et al. (2019). Bidirectional crosstalk between neutrophils and adipocytes promotes adipose tissue inflammation. *FASEB J.* 33, 11821–11835. doi:10.1096/fj.201900477RR

Weinstock, A., Moura Silva, H., Moore, K. J., Schmidt, A. M., and Fisher, E. A. (2020). Leukocyte heterogeneity in adipose tissue, including in obesity. *Circ. Res.* 126, 1590–1612. doi:10.1161/CIRCRESAHA.120.316203

Weir, H. J., Yao, P., Huynh, F. K., Escoubas, C. C., Goncalves, R. L., Burkewitz, K., et al. (2017). Dietary restriction and AMPK increase lifespan via mitochondrial network and peroxisome remodeling. *Cell Metab.* 26, 884–896. doi:10.1016/j.cmet.2017.09.024

Weisberg, S. P., Mccann, D., Desai, M., Rosenbaum, M., Leibel, R. L., and Ferrante, A. W. (2003). Obesity is associated with macrophage accumulation in adipose tissue. *J. Clin. Invest.* 112, 1796–1808. doi:10.1172/JCI19246

Wensveen, F. M., Valentić, S., Šestan, M., Turk Wensveen, T., and Polić, B. (2015). The "Big Bang" in obese fat: events initiating obesity-induced adipose tissue inflammation. *Eur. J. Immunol.* 45, 2446–2456. doi:10.1002/eji.201545502

WHO (2019). *World health statistics 2019: monitoring health for the SDGs, sustainable development goals*.

Wikstrom, J. D., Mahdaviani, K., Liesa, M., Sereda, S. B., Si, Y., Las, G., et al. (2014). Hormone-induced mitochondrial fission is utilized by brown adipocytes as an amplification pathway for energy expenditure. *Embo J.* 33, 418–436. doi:10.1002/embj.201385014

Wilhelmi De Toledo, F., Grundler, F., Bergouignan, A., Drinda, S., and Michalsen, A. (2019). Safety, health improvement and well-being during a 4 to 21-day fasting period in an observational study including 1422 subjects. *PLoS One* 14, e0209353. doi:10.1371/journal.pone.0209353

Williams, S. M., Eleftheriadou, A., Alam, U., Cuthbertson, D. J., and Wilding, J. P. H. (2019). Cardiac autonomic neuropathy in obesity, the metabolic syndrome and prediabetes: a narrative review. *Diabetes Ther.* 10, 1995–2021. doi:10.1007/s13300-019-00693-0

Winer, D. A., Winer, S., Shen, L., Wadia, P. P., Yantha, J., Paltser, G., et al. (2011). B cells promote insulin resistance through modulation of T cells and production of pathogenic IgG antibodies. *Nat. Med.* 17, 610–617. doi:10.1038/nm.2353

Winn, N. C., Vieira-Potter, V. J., Gastecki, M. L., Welly, R. J., Scroggins, R. J., Zidon, T. M., et al. (2017). Loss of UCP1 exacerbates Western diet-induced glycemic dysregulation independent of changes in body weight in female mice. *Am. J. Physiol. Regul. Integr. Comp. Physiol.* 312, R74–R84. doi:10.1152/ajpregu.00425.2016

Wong, S. C., Puaux, A. L., Chittezhath, M., Shalova, I., Kajiji, T. S., Wang, X., et al. (2010). Macrophage polarization to a unique phenotype driven by B cells. *Eur. J. Immunol.* 40, 2296–2307. doi:10.1002/eji.200940288

Wu, D., Molofsky, A. B., Liang, H. E., Ricardo-Gonzalez, R. R., Jouihan, H. A., Bando, J. K., et al. (2011). Eosinophils sustain adipose alternatively activated macrophages associated with glucose homeostasis. *Science* 332, 243–247. doi:10.1126/science.1201475

Wu, L., Parekh, V. V., Hsiao, J., Kitamura, D., and Van Kaer, L. (2014). Spleen supports a pool of innate-like B cells in white adipose tissue that protects against obesity-associated insulin resistance. *Proc. Natl. Acad. Sci. USA* 111, E4638–E4647. doi:10.1073/pnas.1324052111

Wu, L., Zhang, L., Li, B., Jiang, H., Duan, Y., Xie, Z., et al. (2018). AMP-activated protein kinase (AMPK) regulates energy metabolism through modulating thermogenesis in adipose tissue. *Front. Physiol.* 9, 122. doi:10.3389/fphys.2018.00122

Xu, H., Barnes, G. T., Yang, Q., Tan, G., Yang, D., Chou, C. J., et al. (2003). Chronic inflammation in fat plays a crucial role in the development of obesity-related insulin resistance. *J. Clin. Invest.* 112, 1821–1830. doi:10.1172/JCI19451

Yang, Y. K., Chen, M., Clements, R. H., Abrams, G. A., Aprahamian, C. J., and Harmon, C. M. (2008). Human mesenteric adipose tissue plays unique role versus subcutaneous and omental fat in obesity related diabetes. *Cell Physiol Biochem* 22, 531–538. doi:10.1159/000185527

Ye, J., Gao, Z., Yin, J., and He, Q. (2007). Hypoxia is a potential risk factor for chronic inflammation and adiponectin reduction in adipose tissue of ob/ob and dietary obese mice. *Am. J. Physiol. Endocrinol. Metab.* 293, E1118–E1128. doi:10.1152/ajpendo.00435.2007

Ye, J. (2008). Regulation of PPARgamma function by TNF-alpha. *Biochem. Biophys. Res. Commun.* 374, 405–408. doi:10.1016/j.bbrc.2008.07.068

Ying, W., Wollam, J., Ofrecio, J. M., Bandyopadhyay, G., El Ouarrat, D., Lee, Y. S., et al. (2017). Adipose tissue B2 cells promote insulin resistance through

leukotriene LTB4/LTB4R1 signaling. *J. Clin. Invest.* 127, 1019–1030. doi:10.1172/JCI90350

Yoon, J., Um, H. N., Jang, J., Bae, Y. A., Park, W. J., Kim, H. J., et al. (2019). Eosinophil activation by toll-like receptor 4 ligands regulates macrophage polarization. *Front Cel Dev Biol* 7, 329. doi:10.3389/fcell.2019.00329

Żelechowska, P., Agier, J., Kozłowska, E., and Brzezińska-Błaszczyk, E. (2018). Mast cells participate in chronic low-grade inflammation within adipose tissue. *Obes. Rev.* 19, 686–697. doi:10.1111/obr.12670

Zhang, J., Fu, M., Cui, T., Xiong, C., Xu, K., Zhong, W., et al. (2004). Selective disruption of PPARgamma 2 impairs the development of adipose tissue and insulin sensitivity. *Proc. Natl. Acad. Sci. USA* 101, 10703–10708. doi:10.1073/pnas.0403652101

Conflict of Interest: The authors declare that the research was conducted in the absence of any commercial or financial relationships that could be construed as a potential conflict of interest.

frontiers in Pharmacology

ORIGINAL RESEARCH
published: 18 May 2021
doi: 10.3389/fphar.2021.644225

Adiponectin Attenuates Lipopolysaccharide-induced Apoptosis by Regulating the Cx43/PI3K/AKT Pathway

Luqian Liu[1,2,3†], *Meijuan Yan*[1,2,3†], *Rui Yang*[1,2,4], *Xuqing Qin*[1,2,4], *Ling Chen*[1,2], *Li Li*[1,2], *Junqiang Si*[1,2,4], *Xinzhi Li*[1,2,3*] *and Ketao Ma*[1,2,4*]

[1]*Key Laboratory of Xinjiang Endemic and Ethnic Diseases, Ministry of Education, Shihezi University School of Medicine, Shihezi, China,* [2]*NHC Key Laboratory of Prevention and Treatment of Central Asia High Incidence Diseases, First Affiliated Hospital, Shihezi University School of Medicine, Shihezi, China,* [3]*Department of Pathophysiology, Shihezi University School of Medicine, Shihezi, China,* [4]*Department of Physiology, Shihezi University School of Medicine, Shihezi, China*

Cardiomyocyte apoptosis is a crucial factor leading to myocardial dysfunction. Adiponectin (APN) has a cardiomyocyte-protective impact. Studies have shown that the connexin43 (Cx43) and phosphatidylinositol-3-kinase (PI3K)/protein kinase B (AKT) signaling pathways play an important role in the heart, but whether APN plays a protective role by regulating these pathways is unclear. Our study aimed to confirm whether APN protects against lipopolysaccharide (LPS)-induced cardiomyocyte apoptosis and to explore whether it plays an important role through regulating the Cx43 and PI3K/AKT signaling pathways. In addition, our research aimed to explore the relationship between the Cx43 and PI3K/AKT signaling pathways. *In vitro* experiments: Before H9c2 cells were treated with LPS for 24 h, they were pre-treated with APN for 2 h. The cytotoxic effect of APN on H9c2 cells was evaluated by a CCK-8 assay. The protein levels of Bax, Bcl2, cleaved caspase-3, cleaved caspase-9, Cx43, PI3K, p-PI3K, AKT and p-AKT were evaluated by Western blot analysis, and the apoptosis rate was evaluated by flow cytometry. APN attenuated the cytotoxicity induced by LPS. LPS upregulated Bax, cleaved caspase-3 and cleaved caspase-9 and downregulated Bcl2 in H9c2 cells; however, these effects were attenuated by APN. In addition, LPS upregulated Cx43 expression, and APN downregulated Cx43 expression and activated the PI3K/AKT signaling pathway. LPS induced apoptosis and inhibited PI3K/AKT signaling pathway in H9c2 cells, and these effects were attenuated by Gap26 (a Cx43 inhibitor). Moreover, the preservation of APN expression was reversed by LY294002 (a PI3K/AKT signaling pathway inhibitor). *In vivo* experiments: In C57BL/6J mice, a sepsis model was established by intraperitoneal injection of LPS, and APN was injected into enterocoelia. The protein levels of Bax, Bcl2, cleaved caspase-3, and Cx43 were evaluated by Western blot analysis, and immunohistochemistry was used to detect Cx43 expression and localization in myocardial tissue. LPS upregulated Bax and cleaved caspase-3 and downregulated Bcl2 in sepsis; however, these effects were attenuated by APN. In addition, the expression of Cx43 was upregulated in septic myocardial tissue, and APN downregulated Cx43 expression in septic myocardial tissue. In conclusion, both *in vitro* and *in vivo*, the data demonstrated that APN can protect against LPS-induced apoptosis during sepsis by modifying the Cx43 and PI3K/AKT signaling pathways.

Keywords: adiponectin, apoptosis, sepsis, PI3K/AKT, connexin43

OPEN ACCESS

Edited by:
Ana Paula Davel,
State University of Campinas, Brazil

Reviewed by:
Vesna Jaćević,
National Poison Control Center, Serbia
Thiago Bruder Do Nascimento,
University of Pittsburgh, United States

***Correspondence:**
Ketao Ma
maketao@hotmail.com
Xinzhi Li
lixinzhi@shzu.edu.cn

[†]These authors have contributed equally to this work

Specialty section:
This article was submitted to Cardiovascular and Smooth Muscle Pharmacology, a section of the journal Frontiers in Pharmacology

Received: *20 December 2020*
Accepted: *31 March 2021*
Published: *18 May 2021*

Citation:
Liu L, Yan M, Yang R, Qin X, Chen L, Li L, Si J, Li X and Ma K (2021) Adiponectin Attenuates Lipopolysaccharide-induced Apoptosis by Regulating the Cx43/PI3K/AKT Pathway. Front. Pharmacol. 12:644225. doi: 10.3389/fphar.2021.644225

INTRODUCTION

Numerous studies have shown that sepsis is a multiple organ dysfunction caused by the body's immune response to microbial infections. Sepsis is an extremely rapid and deadly disease with high morbidity and mortality (Merx and Weber, 2007; Sammon et al., 2015). Sepsis is often accompanied by organ damage and organ failure. Sepsis-induced myocardial dysfunction (SIMD) is a common complication in patients with sepsis. Many studies have shown that approximately 50% of patients with sepsis show signs of myocardial insufficiency, and the repair of myocardial function affects the prognosis of patients with sepsis (Poveda-Jaramillo, 2021). Compared with patients without cardiovascular dysfunction, sepsis patients with myocardial dysfunction have an increased mortality rate (by 3-fold), and these patients usually show myocarditis, abnormal contractility, increased interstitial collagen and mitochondrial damage (Blanco et al., 2008; Alvarez et al., 2016). Moreover, due to the complexity of myocardial injury in sepsis, its pathophysiological mechanism is not yet fully understood. Lipopolysaccharide (LPS), a major endotoxin derived from Gram-negative bacteria, has been widely used to induce sepsis myocardial injury models *in vivo* and *in vitro* (Luo et al., 2020). LPS induces cardiac dysfunction and the production of inflammatory factors (Fallach et al., 2010).

Adiponectin (APN) is widely expressed in myocardial tissues and has cardioprotective effects *in vivo* and *in vitro* (Dong et al., 2012; Essick Eric et al., 2013; Ghantous et al., 2015) through its anti-inflammatory and anti-atherosclerotic effects. It can protect the heart by reducing inflammation and preventing damage caused by various mediators (Han & Judd Robert, 2018). A study showed that APN can reduce the secretion of TNF-α and apoptosis induced by LPS in rat cardiomyocytes (Shibata et al., 2005). In addition, APN inhibits ROS-induced cardiac remodeling of rat ventricular myocytes by activating AMPK and inhibiting ERK signalling and NF-kB activation (Essick et al., 2011). Connexin43 (Cx43)-mediated gap junctions play a role increasingly recognized as important in the cardiovascular system. Cx43 protein abnormalities are associated with a variety of cardiovascular diseases. In addition, several studies have reported that Cx43 regulates various cellular activities. Cx43 is related to arrhythmia, ischemia-reperfusion and heart failure-related apoptosis (Zhang et al., 2017; Ostrakhovitch & Tabibzadeh, 2019; Yang et al., 2019). Previous research by our team showed that APN can protect smooth muscle cell apoptosis induced by CoCl2 by regulating Cx43 (Xiao et al., 2019). However, whether Cx43 modulates the cardioprotective effect of APN is currently unclear.

The phosphatidylinositol-3-kinase (PI3K)/protein kinase B (AKT) pathway is a classical signaling pathway that plays an important role in regulating cell growth, proliferation, autophagy, and apoptosis (Hamzehzadeh et al., 2018). Various growth factors and cytokines activate the PI3K/AKT signaling pathway, which ultimately phosphorylates AKT. Numerous studies have demonstrated that activated AKT1 has cardioprotective effects (Matsui et al., 2001; Matsui et al., 2002; DeBosch et al., 2006). Several studies have found that AKT2 gene knockout mice have more severe cardiomyocyte apoptosis than normal mice during myocardial ischemia, indicating that AKT2 also has a role in reducing cardiomyocyte apoptosis and protecting the heart (Roberts et al., 2013). A great deal of research has confirmed that the PI3K/AKT signalling pathway can decrease cardiomyocyte apoptosis and protect the heart through a variety of pathways after activation, but many mechanisms remain to be elucidated (Yu et al., 2019). Whether APN protects the myocardium by regulating the PI3K/AKT signaling pathway and whether Cx43 modulates the PI3K/AKT signaling pathway are questions worth exploring.

Our study aimed to establish a septic myocardial injury model to study whether APN preconditioning reduces myocardial injury in sepsis, to explore whether APN can protect myocardial injury through the Cx43 and PI3K/AKT signalling pathways and to investigate the relationship between Cx43 and PI3K/AKT signalling.

MATERIALS AND METHODS

Experimental Animals

C57BL/6J (age 6–8 W; weight 25 ± 5 g) mice were purchased from Beijing Weitong Lihua Experimental Animal Technology (Beijing, China; laboratory animal certificate number: SCXK (jing), 2016-0006). The mice were fostered in the Animal Experiment and Breeding Center of Shihezi University. The entire experiment was carried out in compliance with the requirements of the Animal Experiment Ethics Committee of Shihezi University (Animal Use Certificate SCXK (New) 2018-0001). All mice were housed in an environment with good light and a suitable temperature and humidity. After all mice were adaptively fed for 1 week, 40 mice were randomly divided into four groups, with ten in each group: sham operation (sham group), septic myocardial injury (LPS group), APN combined with LPS (LPS + APN group) and APN (APN group). Each mouse was injected intraperitoneally with 10 mg/kg LPS to establish the septic myocardial injury model. In the sham group, the same amount of normal saline was injected intraperitoneally. Mice in the LPS + APN group were injected intraperitoneally with 6 mg/kg APN 12 h before LPS injection, and mice in the APN group were injected with 6 mg/kg APN. After 12 h, the mice were sacrificed and used for experiments.

Cell Culture

H9c2 cells were purchased from The Shanghai Institute of Biological Sciences, Chinese Academy of Sciences. This cell line is currently used for screening molecular mechanisms *in vitro*. H9c2 cells were cultured in 10% FBS (Gibco, Carlsbad, CA, USA) and DMEM (Gibco, Thermo Fisher Scientific, Inc.). The control group did not undergo any processing. APN (PeproTech, Rocky Hill, NJ, United States) was added at three concentrations (0.5, 1 and 2 μg/ml) for 2 h, and 1 μg/ml LPS (Sigma, USA) was then added for 24 h. In addition, the Cx43 inhibitor Gap26 (APExBIO Technology LLC, 0.5 μmol/L, 30 min) was added to the preconditioned cells before LPS treatment. The cells were also pre-treated with LY294002 at a

concentration of 10 μM for 1 h and then treated with 2 μg/ml APN for 2 h before treatment with LPS for 24 h.

Cell Viability Assay

Cell viability was estimated by a CCK-8 assay (MultiSciences Lianke Biotech Co., Ltd. Hangzhou). H9c2 cells were cultured in 96-well plates with 1×10^4 cells/well, pre-treated with APN (0.5, 1 and 2 μg/ml) for 2 h, and then incubated with LPS at 37°C for 24 h. After 24 h, 10 μl of the CCK-8 solution was added to each well, and the cells were cultured in an incubator at 37°C for 2 h. The absorbance was measured at 450 nm using enzyme labelling (BioTek Instruments, Inc.).

Flow Cytometry

The Annexin V-fluorescein isothiocyanate/propidium iodide apoptosis kit (MultiSciences Lianke Biotech Co., Ltd. Hangzhou, China) was used to detect apoptosis. First, H9c2 cells were seeded at a quantity of 1×10^6 cells/ml in a six-well plate. After each group was treated according to the experimental protocol, the cells were detached with 0.25% trypsin, gently triturated, and then washed with PBS after centrifugation. Additionally, the H9c2 cells were combined with Annexin V-FITC, PI and 1× buffer, and the solution was fully mixed and incubated in a dark room at 4°C for 30 min. Quantitative analysis of apoptotic cells was performed by flow cytometry (Becton, Dickinson and Company).

Western Blot

Treated cells and myocardial tissue were lyzed on ice for at least 15 min. Total protein lysates were collected in 1.5 ml EP tubes, and the protein concentration was determined by the BCA method. Samples with equivalent amounts of protein were separated by SDS-PAGE in 5 × loading buffer. The separated proteins were transferred to PVDF membranes (EMD Millipore), which were subsequently blocked at room temperature with 5% skim milk or 5% BSA for 2 h. The proteins were incubated with antibodies specific for the following proteins overnight in a 4°C shaker: Cx43 (1:1000, Abcam), Bax (1:1000, Abcam), β-actin (1: 1000, Beijing Fir Jinqiao Biotechnology), GAPDH (1:1000, Abcam), Bcl2 (1:1000, Abcam), caspase-3 (1:1000, Abcam), caspase-9 (1:1000, Abcam), p-PI3K (1:1000, CST), PI3K (1: 1000, Proteintech), p-AKT (1:1000, Proteintech), and AKT (1: 1000, Bioworld). Then, the samples were incubated at room temperature for 2 h with the corresponding secondary antibody. The membranes were washed with TBST for 5 min three times, incubated with ECL reagent (GE Healthcare Life Sciences, United Kingdom) and developed. Quantity One software (Bio-Rad, Hercules, CA, United States) was used to analyse the collected images.

Immunofluorescence

H9c2 cells were evenly distributed in a six-well plate with aseptic slides at a density of 3×10^5 cells/ml. After 24 h, the treated cells were removed and discarded from the culture medium, washed with preheated PBS at 37°C 3 times, and then fixed with rewarmed 40 g/L paraformaldehyde for 10 min. The H9c2 cells were washed with PBS and permeabilized with Triton X-100 for 3 min. Then, the cells were washed with PBS 3 times and incubated with 5% BSA (Sigma-Aldrich, United States) at 37 °C for 30 min. The cells were again washed with PBS 3 times, 100 μL of the primary antibody [(Cx43 (1:100, Abcam)] was added, and the cells were placed in a 4°C wet box overnight. The following day, the cells were washed with PBS 3 times, and the corresponding secondary antibody was added to the wells for incubation at 37°C for 2 h. Subsequently, the cells were washed with PBS three times, the nuclei were stained with DAPI (Solarbio Science and Technology Co., Beijing, China) for 15 min, and the cells were again washed with PBS 3 times. A confocal microscope (Zeiss LSM 510 META, Carl Zeiss AG, Germany) was used to acquire images. Image-Pro Plus 6.0 software (Media Cybernetics, Rockville, MD, United States) was used for semiquantitative analysis of protein expression.

Hematoxylin-Eosin Staining

The myocardial tissue of each group was placed in 10% formalin overnight and was then dehydrated and embedded in paraffin. According to the instruction manual, the sections were immersed in a concentration gradient of xylene, ethanol and hematoxylin and sealed with neutral gum. An optical microscope (BX51; Olympus, 400×) was used to observe the morphology of cardiomyocytes, cardiac matrix and myofilaments.

Immunohistochemical Staining

Myocardial tissues were baked at 60°C for 2 h. The tissues were dewaxed and dehydrated with xylene and ethanol, washed with water, repaired with sodium citrate, and incubated with 3% hydrogen peroxide to inhibit the activity of endogenous peroxidase. Then, the tissues were incubated with 5% BSA at 37°C for 1 h. Then, 100 μL of the primary antibody [(Cx43 (1:100, Abcam)] was added, and the tissues were placed in a 4°C wet box overnight. The next day, the corresponding secondary antibody was added to the tissues for incubation at 37°C for 1 h. Signals were developed by using diaminobenzidine as a substrate for 2 min. Six samples were randomly selected from each group, and 5 fields of view were randomly selected from each sample. Images were then acquired under an optical microscope (400×).

Statistical Analysis

The statistical software SPSS20.0 (IBM Corp.) and GraphPad prism 8.0 (GraphPad Software, La Jolla, CA, United States) were used to analyse the results. The values were expressed as the means ± standard errors, and one-way analysis of variance (ANOVA) and the *t*-test were used to analyse the differences among groups. $p < 0.05$ indicates a significant difference.

RESULTS

APN Attenuated the Cytotoxicity Induced by LPS and Reversed LPS-Induced Apoptosis in H9c2 Rat Cardiomyocytes

The H9c2 cells were pre-treated with three concentrations of APN (0.5, 1 and 2 μg/ml) for 2 h and were then treated with LPS to observe the effect of APN on cardiomyocyte toxicity induced by LPS. The **Figure 1A** shows that 1 and 2 μg/ml APN had clear

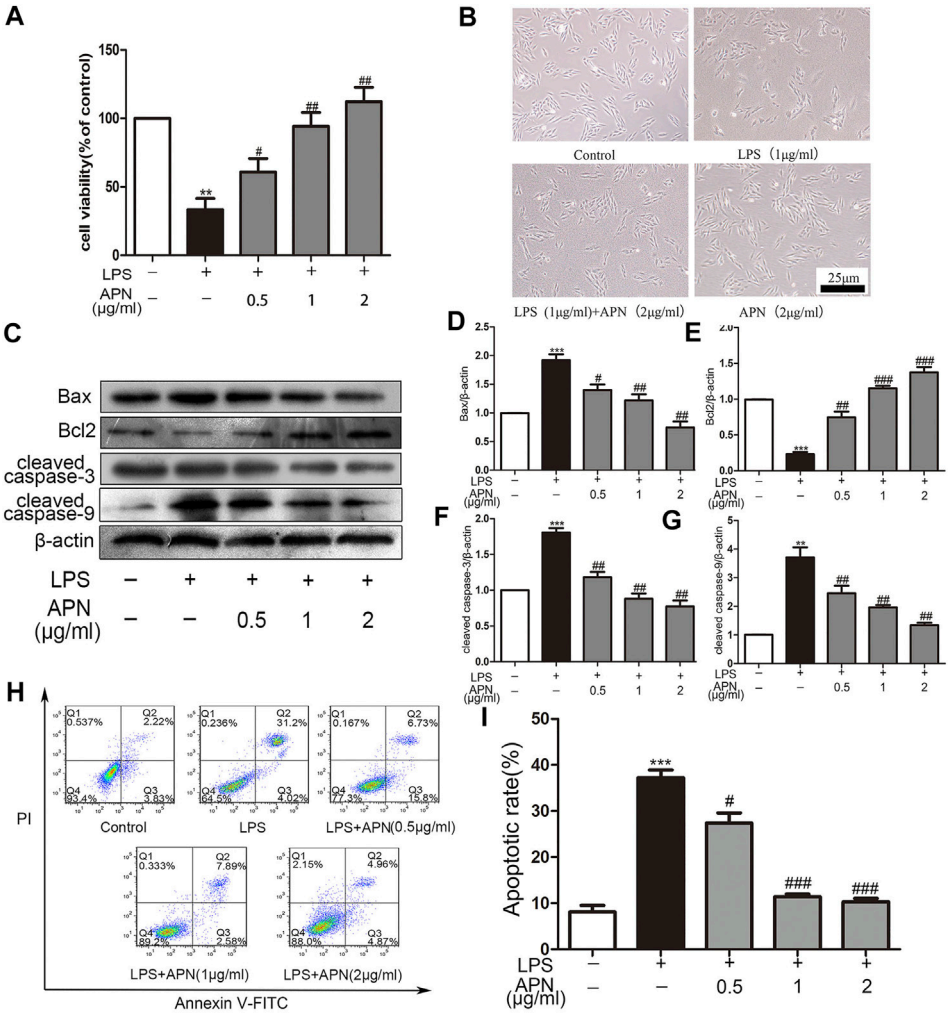

FIGURE 1 | The effects of APN on LPS-induced H9c2 cytotoxicity; cardiomyocyte apoptosis; and Bcl2, Bax, cleaved caspase-3 and cleaved caspase-9 expression in H9c2 cells. **(A)** APN can reduce LPS-induced cytotoxicity. The cells were pre-treated with three concentrations of APN (0.5, 1 and 2 μg/ml) for two hours to assess the preservation function of APN on H9c2 cytotoxicity induced by LPS. **(B)** Cell morphology was observed under an inverted microscope (magnification, ×40). The CCK-8 assay was used to determine cell viability. **(C)** LPS downregulated Bcl2 and upregulated Bax, cleaved caspase-3 and cleaved caspase-9 in H9c2 cells, but these effects were attenuated by APN. **(D–G)** Quantification of Bax, Bcl2, cleaved caspase-3 and cleaved caspase-9 expression. **(H)** The apoptosis rate after treatment with APN and LPS. **(I)** Statistical analysis of the apoptosis rate (*$p < 0.05$, **$p < 0.01$, ***$p < 0.001$ vs. control; $^{\#}p < 0.05$, $^{\#\#}p < 0.01$, $^{\#\#\#}p < 0.001$ vs. the LPS group. The data are shown as the means ± SEs (n = 6)).

protective effects. However, 2 μg/ml APN alone did not affect cell viability (Supplementary the **Supplementary Figure S1**). In subsequent experiments, 1 μg/ml LPS for 24 h and 2 μg/ml APN for 2 h were used to study the signaling pathways involved in the protection of cardiomyocytes from LPS-induced injury. Cellular morphology was observed by microscopy. As shown in the **Figure 1B**, cells exposed to LPS for 24 h exhibited disordered cell alignment and extensive cell shrinkage; however, the state of the cells in the co-treatment group was significantly improved. These results suggest that APN attenuates the cytotoxicity of H9c2 cells induced by LPS. Compared with the control group, The LPS downregulated Bcl2 expression and upregulated cleaved caspase-3, Bax, and cleaved caspase-9 expression. The APN reversed these effects in a concentration-dependent manner (the **Figures 1C–G**). We then performed apoptosis analysis with Annexin V/PI to determine the apoptosis rate. The Q2 region shows late apoptosis, while the Q3 region shows early apoptosis. As presented in the **Figures 1H,I**, exposure to 1 μg/ml LPS significantly increased the apoptosis rate of H9c2 cells, which was reduced by APN pre-treatment.

APN Downregulated Cx43 Expression and Activated the PI3K/AKT Signaling Pathway in H9c2 Rat Cardiomyocytes

The **Figures 2A,B** shows that LPS upregulated the expression of Cx43, while APN reversed these effects. However, the group

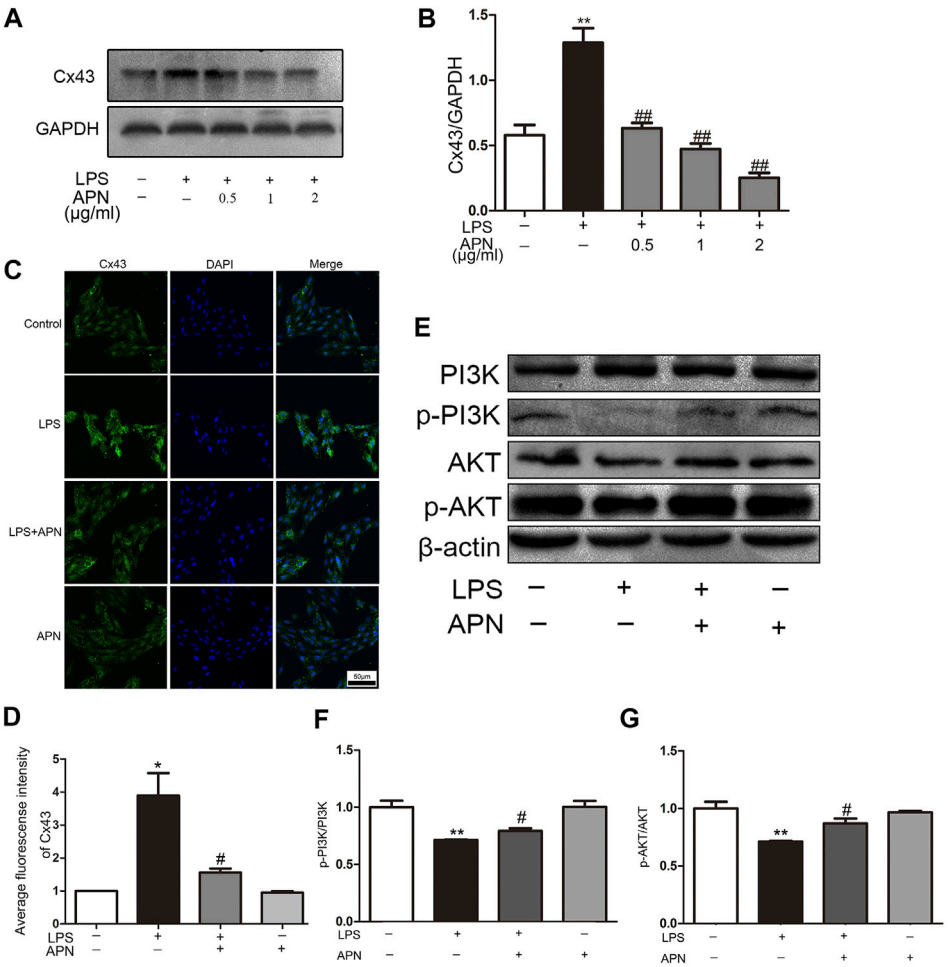

FIGURE 2 | APN downregulates Cx43 expression and activates the PI3K/AKT signaling pathway. **(A)** The effects of LPS and APN on Cx43. **(B)** Statistical analysis of Cx43. **(C)** Fluorescence intensity of Cx43 after treatment with LPS and APN. Scale bar: 50 μm **(D)** Quantitative analysis of the relative fluorescence intensity of Cx43. **(E)** The effects of LPS and APN on PI3K, p-PI3K, AKT, and p-AKT proteins. **(F–G)** Quantification of p-PI3K/PI3K and p-AKT/AKT levels (*P< 0.05, **P< 0.01 vs. control; $^{\#}p$ < 0.05, $^{\#\#}p$ < 0.01 vs. the LPS group. The data are shown as the means ± SEs (n = 6)).

treated with APN alone showed no difference in Cx43 expression (Supplementary the **Supplementary Figure S2**). The immunofluorescence results in the **Figures 2C,D** show that Cx43 was distributed in the cytoplasm and nucleus. The fluorescence intensity of Cx43 in the LPS group was higher than that in the APN pre-treatment group. This result was consistent with the Western blot analysis results. The **Figures 2E–G** shows that the p-PI3K and p-AKT protein levels were increased after treatment with 2 μg/ml APN. We previously showed that the PI3K/AKT pathway and Cx43 participate in the protective effect of APN against LPS-induced apoptosis in H9c2 cells.

Gap26 Reversed LPS-Induced Apoptosis and Activated the PI3K/AKT Signaling Pathway in H9c2 Rat Cardiomyocytes

The H9c2 cells were pre-treated with the Cx43 inhibitor Gap26 at 37°C for 30 min prior to 1 μg/ml LPS treatment for 24 h. The LPS downregulated Bcl2 and upregulated Bax, cleaved caspase-3 and cleaved caspase-9; however, the Gap26 reversed these effects (the **Figures 3A–E**). The flow cytometry results demonstrated that pre-treatment with Gap26 (0.5 μmol/L for 30 min) significantly changed the percentage of apoptotic H9c2 cells treated with LPS (the **Figures 3F,G**). The Gap26 alone did not reduce the number of apoptotic cells. Moreover, the Western blot analysis results showed that the p-PI3K and *p*-AKT protein levels were inhibited by LPS, these effects were attenuated by Gap26 (the **Figures 3H–J**).

PI3K/AKT Pathway Inhibition Altered the Effect of APN on LPS-Induced Apoptosis in H9c2 Rat Cardiomyocytes

We sought to determine whether LY294002 reverses the protective effect of APN against LPS-induced apoptosis. Pre-treatment with 10 μM LY294002 for 1 h significantly reversed the

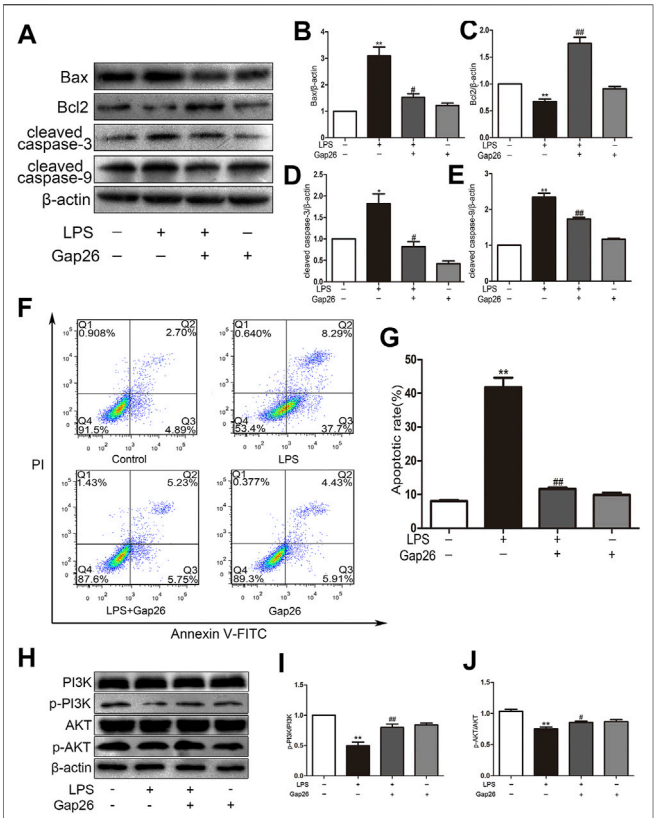

FIGURE 3 | Gap26 reverses LPS-induced apoptosis and activates the PI3K/AKT signalling pathway. **(A)** The effects of LPS and Gap26 on Bax, Bcl2, cleaved caspase-3 and cleaved caspase-9 protein levels. **(B–E)** Statistical analysis. **(F)** The rate of apoptosis after treatment with Gap26 and LPS. **(G)** Statistical analysis. **(H)** The effects of LPS and Gap26 on PI3K, p-PI3K, AKT, and p-AKT proteins. **(I–J)** Statistical analysis (*$p < 0.05$, **$p < 0.01$ vs. control, #$p < 0.05$, ##$p < 0.01$ vs. the LPS group. The data are shown as the means ± SEs (n = 6)).

protective effect of APN, as demonstrated by the downregulation of Bax, cleaved caspase-3 and cleaved caspase-9 and the upregulation of Bcl2 protein expression (the **Figures 4A–E**). In conclusion, the PI3K/AKT pathway can participate in the protective function of APN against H9c2 cell apoptosis.

APN Attenuated Sepsis Myocardial Injury and Downregulated Cx43 Expression in Septic Mice

We explored whether APN can protect against myocardial damage in septic mice. The haematoxylin and eosin staining was performed on myocardial tissue to observe differences in the four groups of myocardial tissues. The myocardial fibres were arranged neatly, the cytoplasm was rich and uniform, the intercellular space was normal, the boundary was clear, and there were no pathological changes in the sham group. In the LPS group, inflammatory cell infiltration was observed, accompanied by myocardial cell necrosis. In the LPS + APN group, myocardial cell necrosis was ameliorated, the number of myocardial fibres was increased, and myocardial damage and inflammatory cell infiltration were reduced. In addition, there were no significant changes in the APN group (the **Figure 5A**). In addition, Bax and cleaved caspase-3 were upregulated in the LPS group, and Bcl2 was downregulated in the LPS group; however, APN reversed these effects (the **Figures 5B–E**). Next, we further explored whether Cx43 is involved in the protective role of APN against myocardial damage in septic mice. Cx43 was upregulated in septic mice, while APN downregulated the expression of Cx43 (the **Figures 5F–H**).

DISCUSSION

Overall, our study indicates that APN protects against LPS-induced cardiomyocyte apoptosis. In addition, the data showed that APN activates the PI3K/AKT signaling pathway and downregulates the expression of Cx43. PI3K/AKT pathway inhibition altered the inhibitory effect of APN on LPS-induced apoptosis in H9c2 cells. The Cx43 selective inhibitor Gap26 reversed LPS-induced apoptosis and activated PI3K/AKT signaling pathway inhibited by LPS. In addition, in septic mice, APN protected the myocardium against sepsis-related damage by upregulating Cx43. Therefore, this study provides proof of concept that APN attenuates LPS-induced apoptosis by regulating the Cx43/PI3K/AKT pathway.

Sepsis has a rapid onset, abrupt development, and a high mortality rate. Accumulating evidence has shown that most patients with septic shock suffer from myocardial depression (Xu et al., 2020). LPS treatment mimics the pathological characteristics of myocardial infarction patients, such as myocardial morphology and function (Sánchez-Villamil et al., 2016; Shrestha et al., 2017). LPS is often used to induce myocardial injury. Some research has suggested that LPS can activate the apoptotic signaling pathway in cardiomyocytes (Wu et al., 2017; Xu et al., 2018; Zhang et al., 2020). Our study used an LPS-induced endotoxaemic heart injury model in H9c2 rat cardiomyocytes and C57BL/6J mice. Tan et al. found that LPS induced AC16 cell apoptosis (Tan et al., 2019). Herein, we showed that in H9c2 cells LPS (1 μg/ml) reduced cell viability; upregulated the levels of Bax, cleaved caspase-3 and cleaved caspase-9; and downregulated Bcl2 expression. In addition, the data showed that Bax and cleaved caspase-3 were upregulated and Bcl2 downregulated in septic mice.

APN, an endogenous bioactive polypeptide or protein secreted by adipocytes, is a high molecular weight (HMW) APN. Previous studies have shown that APN may have cardioprotective effects (Wang H. et al., 2020). In this study, pre-treatment with three concentrations of APN (0.5, 1, and 2 μg/ml) reversed the decrease in cell viability caused by LPS. Our results therefore show that APN protects against cardiotoxicity caused by LPS. Xiao et al. reported that APN reversed CoCl2-induced apoptosis in SMCs (Xiao et al., 2019). Thus, our results are consistent with those previously reported.

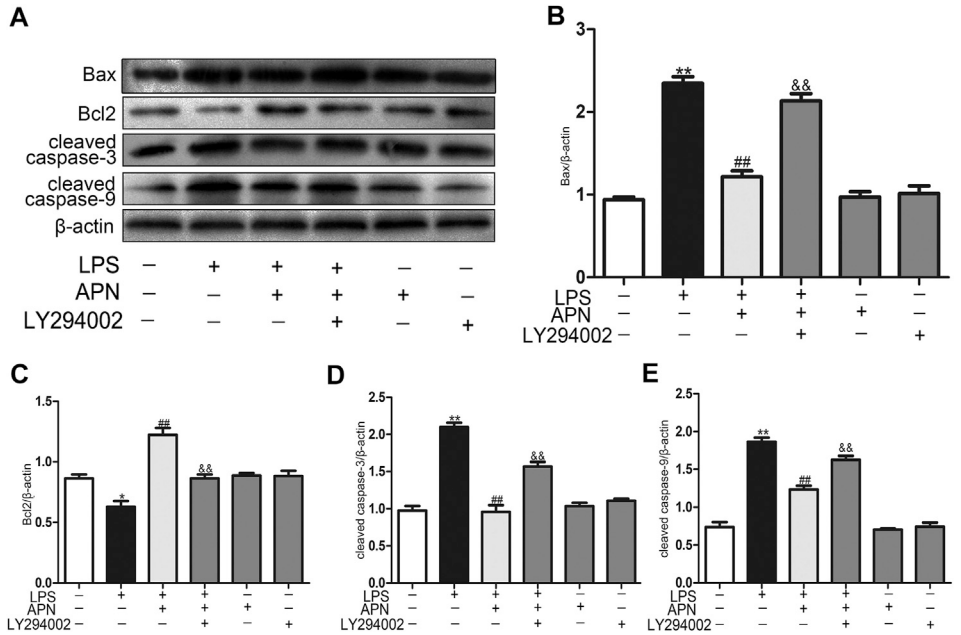

FIGURE 4 | PI3K/AKT pathway inhibition alters the effect of APN on LPS-induced apoptosis in H9c2 cells. **(A)** The effects of APN, LY294002 and LPS on Bax, Bcl2, cleaved caspase-3 and cleaved caspase-9 protein levels. **(B–E)** Statistical analysis. ($^{*}p < 0.05$, $^{**}p < 0.01$ vs. control; $^{\#}p < 0.05$, $^{\#\#}p < 0.01$ vs. the LPS group; $^{\&}p < 0.05$, $^{\&\&}p < 0.01$ vs. the LPS + APN group. The data are shown as the means ± SEs (n = 6)).

We also found that APN can protect against myocardial injury in septic mice.

Next, we explored the potential mechanism by which APN protects against myocardial injury induced by LPS. Apoptotic proteins are downstream effectors of Akt. Recently, data have shown that PI3K/AKT pathway activation inhibits cardiomyocyte apoptosis. Furthermore, PI3K/AKT signaling pathway activation may delay the progression of heart failure (Takatani et al., 2004). Shang X et al. found that resveratrol activated the PI3K/AKT signalling pathway and inhibited the NF-κB signaling pathway and related inflammatory factors in myocardial injury in septic rats (Shang et al., 2019). Chang JH et al. reported that PI3K/AKT signaling pathway activation protected against cardiomyocyte injury during ischemia-reperfusion in diabetic rats (Chang et al., 2020). We found that APN increased the levels of phosphorylated PI3K and AKT. Moreover, APN reversed the decrease in PI3K and AKT phosphorylation induced by LPS, which indicates that APN can activate the PI3K/AKT pathway in H9c2 cells. These findings are in accordance with the previous observation that APN upregulated the PI3K/AKT pathway in a myocardial post-ischaemic injury model (Wang et al., 2013). In addition, we used LY294002 to evaluate the effect of the PI3K/AKT pathway on the function of APN against LPS-induced apoptosis in H9c2 rat cardiomyocytes. The results showed that LY294002 reversed the protective effects of APN on LPS-induced apoptosis in H9c2 cells, as demonstrated by upregulation of Bax, cleaved caspase-3, and cleaved caspase-9 and downregulation of Bcl2. Wei et al. found that APN protects H9c2 cells against palmitic acid-induced apoptosis through the Akt signalling pathway (Dong et al., 2012). These data are consistent with our findings. Here, we examined whether the PI3K/AKT signaling pathway plays an important role in the APN-mediated protection of H9c2 cells.

Gap junctions are membrane channel structures that exist between adjacent cells, mediate the transmission of information between cells and have important biological functions (Pieperhoff and Franke, 2007). Cx43 is a major gap junction protein in mammalian ventricular myocytes. Allen et al. (Allen, 1992) found that in various heart diseases such as hypertrophic cardiomyopathy, heart failure and ischemic cardiomyopathy, the distribution and expression of Cx43 are altered. Cx43 plays a significant role in cell growth, proliferation and apoptosis. Recently, a study showed that Cx43 gene knockout or accelerated degradation protected astrocytes from apoptosis under ischemic stress (Wang X. et al., 2020). Ma JW et al. found that Cx43 inhibition attenuated oxidative stress and apoptosis in HUVECs (Ma et al., 2020). In our study, inhibiting Cx43 attenuated LPS-induced apoptosis. After treatment with LPS, the expression of Cx43 was reduced, and apoptosis gradually increased in H9c2 cells and septic mice. Different concentrations of APN downregulated Cx43 expression. Therefore, Cx43 also plays a key role in APN-mediated protection against myocardial injury in sepsis. Moreover, we found that Gap26 activated the PI3K/AKT signaling pathway. A recent study showed that disruption of Cx43 also enhanced the phosphorylation of Akt

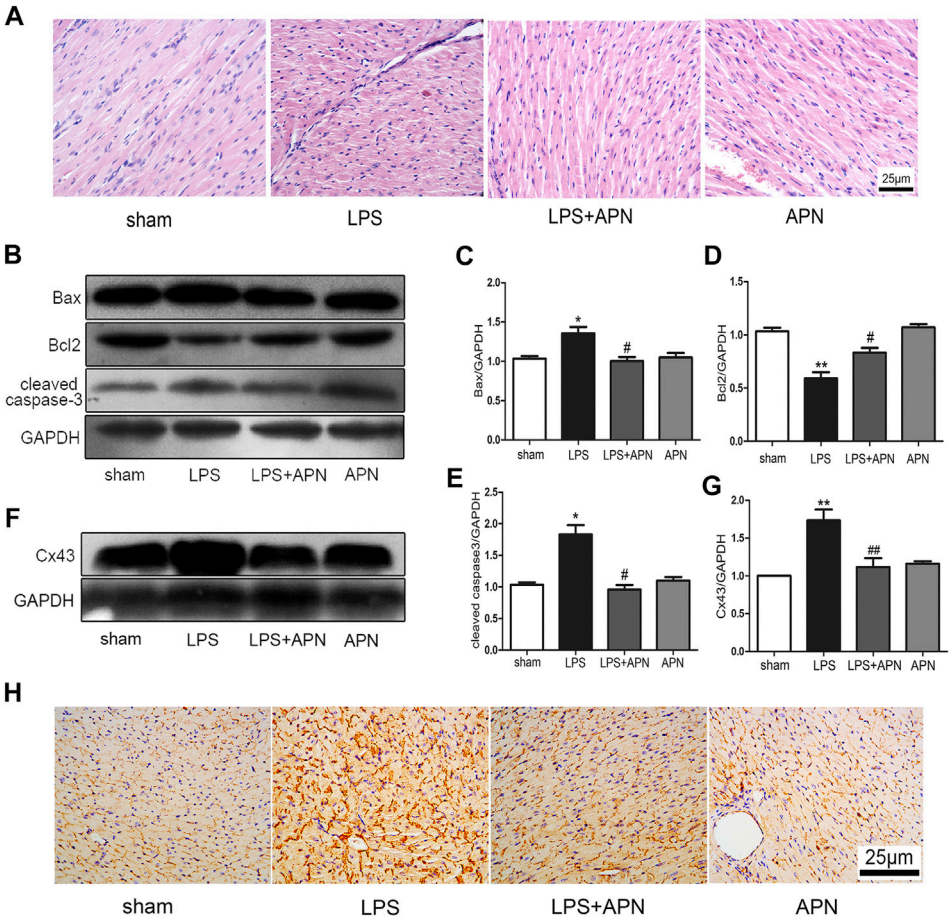

FIGURE 5 | The effects of APN on sepsis-induced myocardial injury. **(A)** HE staining of myocardial tissue at 400×. **(B)** Bcl2 was downregulated and Bax and cleaved caspase-3 were upregulated in myocardial tissues of septic mice, but these effects were attenuated by APN. **(C–E)** Quantification of Bax, Bcl2, and cleaved caspase-3 expression. **(F)** Cx43 was upregulated in myocardial tissue of septic mice, and this effect was changed by APN. **(G)** Quantification of Cx43 expression. **(H)** Immunohistochemical staining showed the expression of Cx43 in myocardial tissue. Scale bar: 25 μm. The brown immunostaining represents Cx43. (*$p < 0.05$, **$p < 0.01$ vs. control; $^{\#}p < 0.05$, $^{\#\#}p < 0.01$ vs. the LPS group. The data are shown as the means ± SEs (n = 6)).

(Wang Y. et al., 2020). This finding is consistent with our results. Our study showed that APN can protect against myocardial injury through the Cx43 and PI3K/AKT signaling pathways. Interestingly, a study found that treatment with a PI3K inhibitor (LY294002) reduced the expression of Cx43 in diabetes models (Bi et al., 2017). Therefore, our follow-up experiments will continue to explore whether changes in the PI3K/AKT signaling pathway related to APN-mediated protection against myocardial injury cause changes in Cx43 expression. In addition, we will continue to explore Cx43 phosphorylation in future research.

CONCLUSION

Our study demonstrates that APN protects against LPS-induced injury by regulating Cx43 expression and activating the PI3K/AKT signaling pathway. These results suggest that APN may be an effective treatment for cardiovascular disease.

DATA AVAILABILITY STATEMENT

The original contributions presented in the study are included in the article/**Supplementary Material**, further inquiries can be directed to the corresponding authors.

ETHICS STATEMENT

The animal study was reviewed and approved by shihezi university.

AUTHOR CONTRIBUTIONS

LuL, MY, XL and KM conceived and designed the experiments. LuL, RY, XQ and LC collected and statistically analyzed the data. LuL, LiL, JS interpreted the data. LuL, MY, KM and XL prepared

the manuscript. LuL, MY and JS performed the literature search. KM and XL received funding.

FUNDING

This work was supported by the National Natural Science Foundation of China (Nos. 81860085, 81860286), the Corps Science and Technology Cooperation Project of China (No. 2020BC004) and supported by the Non-profit Central Research Institute Fund of Chines Academy of Medical Sciences (2020-PT330-003).

ACKNOWLEDGMENTS

We thank the Key Laboratory of Xinjiang Endemic and Ethnic Diseases and the Department of Physiology and Pathophysiology of Shihezi University of Medicine for their support.

SUPPLEMENTARY MATERIAL

The Supplementary Material for this article can be found online at: https://www.frontiersin.org/articles/10.3389/fphar.2021.644225/full#supplementary-material

REFERENCES

Allen, A. (1992). The Cardiotoxicity of Chemotherapeutic Drugs. *Semin. Oncol.* 19 (5), 529–542.

Alvarez, S., Vico, T., and Vanasco, V. (2016). Cardiac Dysfunction, Mitochondrial Architecture, Energy Production, and Inflammatory Pathways: Interrelated Aspects in Endotoxemia and Sepsis. *Int. J. Biochem. Cel Biol.* 81, 307–314. doi:10.1016/j.biocel.2016.07.032

Bi, Y., Wang, G., Liu, X., Wei, M., and Zhang, Q. (2017). Low-after-high Glucose Down-Regulated Cx43 in H9c2 Cells by Autophagy Activation via Cross-Regulation by the PI3K/Akt/mTOR and MEK/ERK1/2 Signal Pathways. *Endocrine* 56 (2), 336–345. doi:10.1007/s12020-017-1251-3

Blanco, J., Muriel-Bombín, A., Sagredo, A. V., Taboada, F., Gandía, F., Tamayo, L., et al. (2008). Incidence, Organ Dysfunction and Mortality in Severe Sepsis: a Spanish Multicentre Study. *Crit. Care* 12, R158. doi:10.1186/cc7157

DeBosch, B., Sambandam, N., Weinheimer, C., Courtois, M., and Muslin, A. J. (2006). Akt2 Regulates Cardiac Metabolism and Cardiomyocyte Survival. *J. Biol. Chem.* 281, 32841–32851. doi:10.1074/jbc.M513087200

Chang, J.-H., Jin, M.-M., and Liu, J.-T. (2020). Dexmedetomidine Pretreatment Protects the Heart against Apoptosis in Ischemia/reperfusion Injury in Diabetic Rats by Activating PI3K/Akt Signaling In Vivo and In Vitro. *Biomed. Pharmacother.* 127, 110188. doi:10.1016/j.biopha.2020.110188

Dong, W.C., Yan, L., and Yun, Z. H. (2012). Globular Adiponectin Protects H9c2 Cells from Palmitate-Induced Apoptosis via Akt and ERK1/2 Signaling Pathways. *Lipids Health Dis.* 11, 135. doi:10.1186/1476-511X-11-135

Essick, E. E., Ouchi, N., Wilson, R. M., Ohashi, K., Ghobrial, J., Shibata, R., et al. (2011). Adiponectin Mediates Cardioprotection in Oxidative Stress-Induced Cardiac Myocyte Remodeling. *Am. J. Physiology-Heart Circulatory Physiol.* 301, H984–H993. doi:10.1152/ajpheart.00428.2011

Essick Eric, E., Wilson Richard, M., Pimentel David, R., et al. (2013). Adiponectin Modulates Oxidative Stress-Induced Autophagy in Cardiomyocytes. *[J] .PLoS One* 8, e68697. doi:10.1371/journal.pone.0068697

Fallach, R., Shainberg, A., Avlas, O., Fainblut, M., Chepurko, Y., Porat, E., et al. (2010). Cardiomyocyte Toll-like Receptor 4 Is Involved in Heart Dysfunction Following Septic Shock or Myocardial Ischemia. *J. Mol. Cell Cardiol.* 48, 1236–1244. doi:10.1016/j.yjmcc.2010.02.020

Ghantous, C. M., Azrak, Z., Hanache, S., et al. (2015). Differential Role of Leptin and Adiponectin in Cardiovascular System. *[J]. Int. J. Endocrinol.* 2015, 534320. doi:10.1155/2015/534320

Hamzehzadeh, L., Atkin, S. L., Majeed, M., Butler, A. E., and Sahebkar, A. (2018). The Versatile Role of Curcumin in Cancer Prevention and Treatment: a Focus on PI3K/AKT Pathway. *J. Cel. Physiol.* 233, 6530–6537. doi:10.1002/jcp.26620

Han, Fang., and Judd Robert, L. (2018). Adiponectin Regulation and Function. *Compr. Physiol.* 8, 1031–1063. doi:10.1002/cphy.c170046

Luo, M., Yan, D., Sun, Q., Tao, J., Xu, L., Sun, H., et al. (2020). Ginsenoside Rg1 Attenuates Cardiomyocyte Apoptosis and Inflammation via the TLR4/NF-kB/NLRP3 Pathway. *J. Cel Biochem* 121, 2994–3004. doi:10.1002/jcb.29556

Ma, J. W., Ji, D. D., Li, Q. Q., Zhang, T., and Luo, L. (2020). Inhibition of Connexin 43 Attenuates Oxidative Stress and Apoptosis in Human Umbilical Vein Endothelial Cells[J]. *BMC Pulm. Med.* 20 (1). doi:10.1186/s12890-019-1036-y

Matsui, T., Li, L., Wu, J. C., Cook, S. A., Nagoshi, T., Picard, M. H., et al. (2002). Phenotypic Spectrum Caused by Transgenic Overexpression of Activated Akt in the Heart. *J. Biol. Chem.* 277, 22896–22901. doi:10.1074/jbc.m200347200

Matsui, T., Tao, J., del Monte, F., Lee, K.-H., Li, L., Picard, M., et al. (2001). Akt Activation Preserves Cardiac Function and Prevents Injury after Transient Cardiac Ischemia In Vivo. *Circulation* 104, 330–335. doi:10.1161/01.cir.104.3.330

Merx, M. W., and Weber, C. (2007). Sepsis and the Heart. *Circulation* 116, 793–802. doi:10.1161/circulationaha.106.678359

Ostrakhovitch, E. A., and Tabibzadeh, S. (2019). Homocysteine and Age-Associated Disorders. *Ageing Res. Rev.* 49, 144–164. doi:10.1016/j.arr.2018.10.010

Pieperhoff, S., and Franke, W. W. (2007). The Area Composita of Adhering Junctions Connecting Heart Muscle Cells of Vertebrates - IV: Coalescence and Amalgamation of Desmosomal and Adhaerens Junction Components - Late Processes in Mammalian Heart Development. *Eur. J. Cel Biol.* 86 (7), 377–391. doi:10.1016/j.ejcb.2007.04.001

Poveda-Jaramillo, R. (2021). Heart Dysfunction in Sepsis. *J. Cardiothorac. Vasc. Anesth.* 35, 298–309. doi:10.1053/j.jvca.2020.07.026

Roberts, D. J., Tan-Sah, V. P., Smith, J. M., and Miyamoto, S. (2013). Akt Phosphorylates HK-II at Thr-473 and Increases Mitochondrial HK-II Association to Protect Cardiomyocytes. *J. Biol. Chem.* 288, 23798–23806. doi:10.1074/jbc.m113.482026

Sammon, J. D., Klett, D. E., Sood, A., Olugbade, K., Schmid, M., Kim, S. P., et al. (2015). Sepsis after Major Cancer Surgery. *J. Surg. Res.* 193, 788–794. doi:10.1016/j.jss.2014.07.046

Sánchez-Villamil, J. P., D'Annunzio, V., Holod, P. S., Rebagliati, I., Pérez, H., Peralta, J. G., et al. (2016). Cardiac-specific Overexpression of Thioredoxin 1 Attenuates Mitochondrial and Myocardial Dysfunction in Septic Mice. *Int. J. Biochem. Cel Biol.* 81, 323–334. doi:10.1016/j.biocel.2016.08.045

Shibata, R., Sato, K., Pimentel, D. R., Takemura, Y., Kihara, S., Ohashi, K., et al. (2005). Adiponectin Protects against Myocardial Ischemia-Reperfusion Injury through AMPK- and COX-2-dependent Mechanisms. *Nat. Med.* 11, 1096–1103. doi:10.1038/nm1295

Shrestha, G. S., Kwizera, A., Baelani, G. J. I., Azevedo, L. C. P., Pattnaik, R., Haniffa, R., et al. (2017). International Surviving Sepsis Campaign Guidelines 2016: the Perspective from Low-Income and Middle-Income Countries. *Lancet Infect. Dis.* 17, 893–895. doi:10.1016/s1473-3099(17)30453-x

Takatani, T., Takahashi, K., Uozumi, Y., Matsuda, T., Ito, T., Schaffer, S. W., et al. (2004). Taurine Prevents the Ischemia-Induced Apoptosis in Cultured Neonatal Rat Cardiomyocytes through Akt/caspase-9 Pathway. *Biochem. Biophysical Res. Commun.* 316 (2), 484–489. doi:10.1016/j.bbrc.2004.02.066

Tan, J., Sun, T., Shen, J., Zhu, H., Gong, Y., Zhu, H., et al. (2019). FAM46C Inhibits Lipopolysaccharides-Induced Myocardial Dysfunction via Downregulating Cellular Adhesion Molecules and Inhibiting Apoptosis. *Life Sci.* 229, 1–12. doi:10.1016/j.lfs.2019.03.048

Wang, H., Gao, Y.-X., Wu, Y.-N., Li, C., and Duan, J. (2020). Association between Plasma Adiponectin Levels and Left Ventricular Systolic Dysfunction in Sepsis Patients. *J. Crit. Care* 60, 195–201. doi:10.1016/j.jcrc.2020.06.020

Wang, T., Mao, X., Li, H., Qiao, S., Xu, A., Wang, J., et al. (2013). N-acetylcysteine and Allopurinol Up-Regulated the Jak/STAT3 and PI3K/Akt Pathways via

Adiponectin and Attenuated Myocardial Postischemic Injury in Diabetes. *Free Radic. Biol. Med.* 63 (14), 291–303. doi:10.1016/j.freeradbiomed.2013.05.043

Wang, X., Feng, L., Xin, M., Hao, Y., Wang, X., Shang, P., et al. (2020). Mechanisms Underlying Astrocytic Connexin-43 Autophagy Degradation during Cerebral Ischemia Injury and the Effect on Neuroinflammation and Cell Apoptosis. *Biomed. Pharmacother.* 127, 110125. doi:10.1016/j.biopha.2020.110125

Wang, Y., Wang, W., Wu, X., Li, C., Huang, Y., Zhou, H., et al. (2020). Resveratrol Sensitizes Colorectal *Cancer* Cells to Cetuximab by Connexin 43 Upregulation-Induced Akt Inhibition[J]. *Front. Oncol.* 10, 383. doi:10.3389/fonc.2020.00383

Wu, B., Ni, H., Zhuang, J. X., Zhang, J., Qi, Z., Chen, Q., et al. (2017). The Impact of Circulating Mitochondrial DNA on Cardiomyocyte Apoptosis and Myocardial Injury after TLR4 Activation in Experimental Autoimmune Myocarditis. *Cell Physiol Biochem* 42, 713–728. doi:10.1159/000477889

Xiao, J., Yang, R., Qin, X., Zhang, Z., Li, X., Li, L., et al. (2019). A Role of AMPK and Connexin 43 in the Suppression of CoCl2-Induced Apoptosis of Spiral Modiolar Artery Smooth Muscle Cells by Adiponectin. *Life Sci.* 238, 116876. doi:10.1016/j.lfs.2019.116876

Shang, X., Lin, K., Yu, R., Zhu, P., Zhang, Y., Wang, L., et al. (2019). Resveratrol Protects the Myocardium in Sepsis by Activating the Phosphatidylinositol 3-Kinases (PI3K)/AKT/Mammalian Target of Rapamycin (mTOR) Pathway and Inhibiting the Nuclear Factor-Kb (NF-Kb) Signaling Pathway. *Med. Sci. Monit.* 25, 9290–9298. doi:10.12659/MSM.918369

Xu, J., Lin, C., Wang, T., Zhang, P., Liu, Z., and Lu, C. (2018). Ergosterol Attenuates LPS-Induced Myocardial Injury by Modulating Oxidative Stress and Apoptosis in Rats. *Cel Physiol Biochem* 48, 583–592. doi:10.1159/000491887

Xu, Q., Xiong, H., Zhu, W., Liu, Y., and Du, Y. (2020). Small Molecule Inhibition of Cyclic GMP-AMP Synthase Ameliorates Sepsis-Induced Cardiac Dysfunction in Mice. *Life Sci.* 260, 118315. doi:10.1016/j.lfs.2020.118315

Yang, Y., Yan, X., Xue, J., Zheng, Y., Chen, M., Sun, Z., et al. (2019). Connexin43 Dephosphorylation at Serine 282 Is Associated with Connexin43-Mediated Cardiomyocyte Apoptosis. *Cell Death Differ* 26, 1332–1345. doi:10.1038/s41418-019-0277-x

Yu, T., Liu, D., Gao, M., Yang, P., Zhang, M., Song, F., et al. (2019). Dexmedetomidine Prevents Septic Myocardial Dysfunction in Rats via Activation of α7nAChR and PI3K/Akt- Mediated Autophagy. *Biomed. Pharmacother.* 120, 109231. doi:10.1016/j.biopha.2019.109231

Zhang, T., Liu, C.-F., Zhang, T.-N., Wen, R., and Song, W.-L. (2020). Overexpression of Peroxisome Proliferator-Activated Receptor γ Coactivator 1-α Protects Cardiomyocytes from Lipopolysaccharide-Induced Mitochondrial Damage and Apoptosis. *Inflammation* 43, 1806–1820. doi:10.1007/s10753-020-01255-4

Zhang, Z., Zhao, L., Zhou, Y., Lu, X., Wang, Z., Wang, J., et al. (2017). Taurine Ameliorated Homocysteine-Induced H9C2 Cardiomyocyte Apoptosis by Modulating Endoplasmic Reticulum Stress. *Apoptosis* 22, 647–661. doi:10.1007/s10495-017-1351-9

Conflict of Interest: The authors declare that the research was conducted in the absence of any commercial or financial relationships that could be construed as a potential conflict of interest.

frontiers in Pharmacology

BRIEF RESEARCH REPORT
published: 28 May 2021
doi: 10.3389/fphar.2021.679005

Apelin Does Not Impair Coronary Artery Relaxation Mediated by Nitric Oxide-Induced Activation of BK_{Ca} Channels

Amreen Mughal[†], *Chengwen Sun and Stephen T. O'Rourke* *

Department of Pharmaceutical Sciences, North Dakota State University, Fargo, ND, United States

Apelin-APJ receptor signaling regulates vascular tone in cerebral and peripheral arteries. We recently reported that apelin inhibits BK_{Ca} channel function in cerebral arteries, resulting in impaired endothelium-dependent relaxations. In contrast, apelin causes endothelium-dependent relaxation of coronary arteries. However, the effects of apelin on BK_{Ca} channel function in coronary arterial myocytes have not yet been explored. We hypothesized that apelin-APJ receptor signaling does not have an inhibitory effect on coronary arterial BK_{Ca} channels and hence does not alter nitric oxide (NO)-dependent relaxation of coronary arteries. Patch clamp recording was used to measure whole cell K^+ currents in freshly isolated coronary smooth muscle cells. Apelin had no effect on the increases in current density in response to membrane depolarization or to NS1619 (a BK_{Ca} channel opener). Moreover, apelin did not inhibit NO/cGMP-dependent relaxations that required activation of BK_{Ca} channels in isolated coronary arteries. Apelin-APJ receptor signaling caused a marked increase in intracellular Ca^{2+} levels in coronary arterial smooth muscle cells, but failed to activate PI3-kinase to increase phosphorylation of Akt protein. Collectively, these data provide mechanistic evidence that apelin has no inhibitory effects on BK_{Ca} channel function in coronary arteries. The lack of inhibitory effect on BK_{Ca} channels makes it unlikely that activation of APJ receptors in coronary arteries would adversely affect coronary flow by creating a vasoconstrictive environment. It can be expected that apelin or other APJ receptor agonists in development will not interfere with the vasodilator effects of endogenous BK_{Ca} channel openers.

Keywords: apelin, coronary artery, nitric oxide, vasorelaxation, BKCa channels

OPEN ACCESS

Edited by:
Ana Paula Davel,
State University of Campinas, Brazil

Reviewed by:
Roger Lyrio Santos,
Federal University of Espirito Santo, Brazil
Andrew P. Braun,
University of Calgary, Canada

***Correspondence:**
Stephen T. O'Rourke
stephen.orourke@ndsu.edu

[†]***Present address:***
Amreen Mughal, Department of Pharmacology, University of Vermont, Burlington, United States

Specialty section:
This article was submitted to Cardiovascular and Smooth Muscle Pharmacology, a section of the journal Frontiers in Pharmacology

Received: *10 March 2021*
Accepted: *18 May 2021*
Published: *28 May 2021*

Citation:
Mughal A, Sun C and O'Rourke ST (2021) Apelin Does Not Impair Coronary Artery Relaxation Mediated by Nitric Oxide-Induced Activation of BK_{Ca} Channels. Front. Pharmacol. 12:679005. doi: 10.3389/fphar.2021.679005

INTRODUCTION

Apelin is a vasoactive peptide found in many organs and tissues including, for example, adipose tissue (Boucher et al., 2005), atria (Földes et al., 2003), blood vessels (Kleinz and Davenport, 2004), lungs, kidneys, brain (Folino et al., 2015; Yan et al., 2020). Apelin acts via binding to G-protein-coupled-receptors known as APJ receptors, which are widely expressed throughout the cardiovascular system (Katugampola et al., 2001; Kleinz et al., 2005; Pitkin et al., 2010; Luo et al., 2018). An increasing body of evidence indicates that the apelin-APJ receptor signaling system regulates vascular function in mammalian arteries and veins (Gurzu et al., 2006; Jia et al., 2007; Salcedo et al., 2007; Wang et al., 2016; Nagano et al., 2019), including those from humans (Katugampola et al., 2001; Kleinz and Davenport, 2004; Maguire et al., 2009; Schinzari et al., 2017).

Based on their generally favorable hemodynamic properties, apelin and apelin-based mimetics are currently in development for the treatment of several cardiovascular disorders, including heart failure, pulmonary hypertension, and ischemia/reperfusion injury (Wang et al., 2013; Brame et al., 2015; Gerbier et al., 2017; Mughal and O'Rourke, 2018).

BK_{Ca} channels play a central role in maintaining membrane potential and excitability in vascular smooth muscle cells (Tykocki et al., 2017; Dopico et al., 2018). Opening of BK_{Ca} channels leads to efflux of potassium ions, cell membrane hyperpolarization, and smooth muscle relaxation (Brayden and Nelson, 1992; Nelson and Quayle, 1995). Several endogenous vasodilator molecules, including NO and certain hyperpolarizing factors released from endothelial cells, exert their smooth muscle relaxant effects by targeting BK_{Ca} channels (Bolotina et al., 1994; Campbell et al., 1996; Mistry and Garland, 1998; Earley et al., 2005; Zhang et al., 2012). Similarly, pharmacologic agents that increase BK_{Ca} channel opening cause vascular smooth muscle relaxation and vasodilation (Ghatta et al., 2006; Jackson, 2017). By contrast, substances that interfere with BK_{Ca} channel opening create an environment that favors vasoconstriction (Tang et al., 2017; Dogan et al., 2019). Thus, modulation of BK_{Ca} channel activity is a critical mechanism for regulating blood vessel diameter and flow.

It is widely recognized that the effects of vasoactive agents may vary depending on the anatomic location of the blood vessel under investigation and/or the experimental conditions. Previous work from our laboratory demonstrates that APJ receptors are expressed in coronary and cerebral arteries (Mughal et al., 2018a; Mughal et al., 2018b). In coronary arteries, apelin acts on endothelial APJ receptors to cause nitric oxide (NO) release and endothelium-dependent relaxation (Mughal et al., 2018a). By contrast, apelin causes neither vasoconstriction nor vasorelaxation in cerebral arteries, despite the presence of APJ receptors on both endothelial cells and myocytes (Mughal et al., 2018b). However, activation of cerebral arterial smooth muscle APJ receptors by apelin inhibits BK_{Ca} channel function, thereby impairing arterial relaxation induced by NO and an endothelium-dependent hyperpolarization (EDH) pathway (Mughal et al., 2018b; Mughal et al., 2020).

Direct effects of apelin on BK_{Ca} channels in coronary arterial smooth muscle cells, and on the functional response to endogenous mediators that act via BK_{Ca} channel activation, are presently unknown. Thus, the present study was designed to increase our understanding of the apelin-APJ receptor signaling pathway in coronary arteries. Here, we tested the hypothesis that apelin-APJ receptor signaling does not have an inhibitory effect on coronary arterial BK_{Ca} channels and hence does not alter nitric oxide (NO)-dependent relaxation of coronary arteries.

MATERIALS AND METHODS

Animals and Tissue Preparation

Twelve-week-old male Sprague-Dawley rats were used for all experiments (Envigo RMS, Indianapolis, IN, United States). Rats were housed at 22 ± 2°C (32% humidity) on a 12–12 h light-dark cycle and provided with food and water ad libitum. All animal protocols were approved by the North Dakota State University Institutional Animal Care and Use Committee. Rat hearts were isolated from animals anesthetized with isoflurane and placed into ice-cold physiological salt solution (PSS). Both left and right epicardial coronary arteries and associated branches were dissected and cleaned of surrounding tissues.

Smooth Muscle Cell Isolation

Smooth muscle cells were isolated by enzymatic digestion as described previously (Mughal et al., 2018b). Briefly, cell isolation was performed in isolation solution of the following composition (in mM): 60 NaCl, 80 Na-glutamate, 5 KCl, 2 $MgCl_2$, 10 glucose, and 10 HEPES (pH 7.2). Arterial segments were first incubated in 1.2 mg/ml papain (Worthington, Lakewood, NJ, United States) and 2.0 mg/ml dithioerythritol (Sigma Aldrich, St. Louis, MO, United States) for 17 min at 37°C, and then in 0.8 mg/ml type II collagenase (Worthington) for 12 min at 37°C. After digestion, the segments were washed with ice-cold isolation solution and triturated with a glass pipette to liberate single smooth muscle cells. Isolated cells were kept on ice and were used within 6–8 h following isolation for electrophysiology.

Electrophysiological Recording

Freshly isolated arterial myocytes were placed into a recording chamber (Warner Instruments, Hamden, CT, United States) and whole cell current recordings were performed using our previously described protocol (Mughal et al., 2018a). Briefly, cells were perfused with a bath solution containing (in mM) 145 NaCl, 5.4 KCl, 1.8 $CaCl_2$, 1 $MgCl_2$, 5 HEPES, 10 glucose; pH 7.4 (NaOH). The internal pipette solution contained (in mM) 145 KCl, 5 NaCl, 0.37 $CaCl_2$ (estimated free Ca^{2+} = 172 nM), 2 $MgCl_2$, 10 HEPES, 1 EGTA, 7.5 glucose; pH 7.2 (KOH). Whole cell K^+ currents were recorded at the room temperature (25°C) by stepping in 10 mV increments from a holding potential of −60 to +80 mV using an AxoPatch 200B amplifier equipped with an Axon CV 203BU headstage (Molecular Devices). The patch electrodes (3–4 MΩ) were pulled from 1.5 mm borosilicate glass capillaries. Voltage-activated currents were filtered at 2 kHz and digitized at 10 kHz, and capacitative and leakage currents were subtracted digitally. Series resistance and total cell capacitance were calculated from uncompensated capacitive transients in response to 10 ms hyperpolarizing step pulses (5 mV) or obtained by adjusting series resistance and whole-cell capacitance using the Axopatch 200B amplifier control system. All drugs were diluted in fresh bath solution and perfused into the experimental chamber. Data were collected and analyzed with pCLAMP 10.0 software (Molecular Devices, Sunnyvale, CA, United States). All currents were expressed as current density (current at the end of each voltage step divided by cell membrane capacitance).

Vascular Function Studies

Coronary arterial segments (120–150 μm; 1.2 mm in length) were suspended in wire myograph chambers (DMT, Aarhus, Denmark) for isometric tension recording, as described

previously (Mughal et al., 2018a). Briefly, the tissues were bathed in physiologic salt solution (PSS) of the following composition [(in mM): 119 NaCl, 15 $NaHCO_3$, 4.6 KCl, 1.2 $MgCl_2$, 1.2 NaH_2PO_4, 1.5 $CaCl_2$ and 5.5 glucose] at 37°C. Vessel reactivity was confirmed using KCl (60 mM) and presence of endothelium was tested using the endothelium-dependent vasodilator, acetylcholine (ACh; 10^{-6} M). Vessels that showed >90% relaxation to ACh were considered endothelium-intact vessels. Responses to the vasodilators used in this study were obtained in arterial rings contracted with 5-hydroxytryptamine (5-HT; 10^{-7} M) to a sub-maximal level [~30% of maximum contraction induced by KCl (60 mM)]. Paired experiments with inhibitors were performed in control rings isolated from the same animals.

Intracellular Ca^{2+} Imaging

Smooth muscle cells were plated in eight-well borosilicate cover glass chambers (ThermoFisher Scientific, Waltham, MA, United States) and allowed to adhere to the glass surface (at 37°C) in endothelial growth media with 5% FBS (Promocells, Heidelberg, Germany) for 60 min. After incubation, cells were thoroughly washed with Hanks' balanced salt solution and incubated for 60 min with fluo-4 AM (5 μM). At the end of incubation, cells were washed again and perfused with Hanks' balanced salt solution. Real-time Ca^{2+} imaging was performed using a Zeiss confocal laser-scanning microscope (Carl Zeiss, Germany) equipped with a 40× numerical aperture oil immersion lens (with excitation at 488 nm and emission at 515 nm). All experiments were carried out at room temperature in Hanks' balanced salt solution within 6–8 h following isolation. The effect of apelin (10^{-7} M) on intracellular Ca^{2+} levels, in the absence and presence of the APJ receptor antagonist (Lee et al., 2005), F13A (10^{-7} M × 5 min), was determined in paired experiments. Smooth muscle cells were freshly isolated from three animals (each animal on different day) and three to four cells were analyzed for each treatment from each animal.

Western Immunoblotting

Protein expression was performed according to our previously published method for coronary arteries with minor modification (Mughal et al., 2018a). Briefly, isolated coronary arteries were treated with apelin (10^{-7} M) for different durations (5, 10, 15 and 30 min) at 37°C. Then arterial segments were snap frozen and protein was isolated. Protein estimation was performed using a Pierce BCA protein estimation kit (ThermoFisher Scientific, Waltham, MA, United States). Aliquots of supernatant containing equal amounts of protein (40 μg) were separated on 7.5–10% polyacrylamide gel by SDS-PAGE, and electroblotted onto a PVDF membrane (Bio-Rad Laboratories, Hercules, CA, United States). Blots were blocked with 5% nonfat dry milk in Tris-buffered saline (TBS, pH 7.4) and incubated with primary antibodies, followed by secondary antibody linked to horseradish peroxidase (1:100; Cell Signaling). The blots were first probed with Akt antibody (1:500 dilution; Cell Signaling, Denver, MA, United States), followed by chemical stripping and reprobing with phospho-Akt (p-Akt) antibody (1:500 dilution; Cell Signaling, Denver, MA, United States). To ensure equal loading, the blots were probed for β-actin using an anti-actin antibody (1:500; Santa Cruz Biotechnology Inc.). Immunodetection was performed using an enhanced chemiluminescence light detection kit (ThermoFisher Scientific).

Drugs

The following drugs were used: acetylcholine (ACh), diethylamine NONOate (DEA NONOate), 5-HT, and NS1619 (Sigma Chemical, St. Louis, MO, United States); iberiotoxin (IBTx) and eight-Bromo-cGMP (8-Br-cGMP) (Tocris, Ellisville, MO); apelin-13 and F13A (H-Gln-Arg-Pro-Arg-Leu-Ser-His-Lys-Gly-Pro-Met-Pro-Ala-OH trifluoroacetate salt) (Bachem, Torrance, CA, United States). Drug solutions were prepared fresh daily, kept on ice, and protected from light until used. All drugs were dissolved initially in double-distilled water. Drugs were added to the myograph chambers in volumes not greater than 0.02 ml. Drug concentrations are reported as final molar concentrations in the myograph chamber.

Data Analysis

Relaxation responses are expressed as a percent of the initial tension induced by 5-HT (10^{-7} M). EC_{50} values (drug concentration that produced 50% of its own maximal response) were determined, converted to their negative logarithm, and expressed as -log molar EC_{50} (pD_2). For Ca^{2+} imaging studies, the amplitude of Fluo-4 AM fluorescence was calculated by peak fluorescence intensity (F) divided by baseline intensity (F0). Results are expressed as means ± SEM, and n refers to the number of animals from which blood vessels and/or smooth muscle cells were taken, unless otherwise stated. All data sets were tested for normal distribution using the Shapiro–Wilk test. Values were compared by Student's t-test or one-way ANOVA using Tukey's test as post-hoc analysis for paired or unpaired parametric distributed observations, as appropriate, to determine significance between groups. Mann-Whitney test was applied for non-parametric distributed observations. Values were considered significantly different when $p < 0.05$.

RESULTS

Electrophysiology Studies (Whole Cell K^+ Currents)

Whole cell K^+ currents were recorded in freshly isolated smooth muscle cells from coronary arteries. Superfusion of apelin (10^{-7} M, 5 min) had no inhibitory effect on whole cell K^+ currents, but addition of the selective BK_{Ca} channel blocker, iberiotoxin (10^{-7} M, 5 min), significantly reduced the current density (**Figure 1**). Incubation of coronary myocytes with NS1619 (10^{-5} M, 3 min), a selective BK_{Ca} channel opener, caused a significant increase in the current density (**Figures 2A,D**). The NS1619-induced increase in current density was markedly attenuated by iberiotoxin (**Figures 2B,E**), whereas apelin had no inhibitory effect (**Figures 2C,F**).

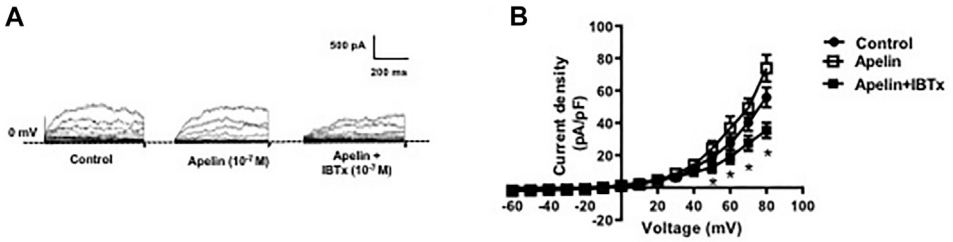

FIGURE 1 | Effect of apelin on whole cell K^+ currents in coronary arterial myocytes. Whole cell K^+ currents were recorded in freshly isolated myocytes in response to successive voltage pulses of 800 ms duration, increasing in 10 mV increments from −60 to +80 mV with or without apelin (10^{-7} M) or apelin plus IBTx (10^{-7} M). **(A)** Representative traces showing the current recordings from smooth muscle cell in the absence and presence of apelin alone or apelin plus IBTx. **(B)** Summary I–V curves of whole cell K^+ currents at baseline (control) and after treatment with apelin (10^{-7} M) alone or in the presence of IBTx (10^{-7} M). Dotted line represents zero current level (at 0 mV). Values are presented as the mean ± S. E. M. (n = 6). *p < 0.05 vs. control current density.

Vascular Relaxation Studies (NO/cGMP-Induced Relaxation)

In coronary arterial segments contracted with five-HT (10^{-7} M), the NO donor, DEA NONOate (DEA, 10^{-9} – 3×10^{-5} M), caused concentration-dependent relaxation (**Figure 3**). Iberiotoxin (10^{-7} M) caused a significant rightward shift in the DEA concentration-response curve (**Figure 3A**); however, DEA-induced relaxations were unaffected in the presence of apelin (10^{-7} M) [pD_2 = 6.38 ± 0.20 vs. 6.15 ± 0.28 in the absence and presence of apelin, respectively; p > 0.05 (n = 5)] (**Figure 3B**). Similarly, relaxations induced by acetylcholine (10^{-9} – 3×10^{-6} M), an endothelium-dependent vasodilator that acts via NO release from endothelial cells, were significantly inhibited by iberiotoxin (**Figure 3C**), but not by apelin [pD_2 = 7.16 ± 0.17 vs. 7.38 ± 0.30 in the absence and presence of apelin, respectively; p > 0.05 (n = 6)] (**Figure 3D**). The stable cGMP analog, 8-Bromo-cGMP [8-Br-cGMP (10^{-9} – 10^{-4} M)], also caused concentration-dependent relaxation of isolated coronary arteries. The response to 8-Br-cGMP was significantly attenuated in the presence of iberiotoxin (**Figure 3E**), but not apelin [pD_2 = 5.25 ± 0.16 vs. 5.41 ± 0.44 in the absence and presence of apelin, respectively; p > 0.05 (n = 4)] (**Figure 3F**).

Intracellular Signaling Studies (Ca_i^{2+} and PI3 Kinase Activity)

The functional status of coronary smooth muscle APJ receptors was assessed using intracellular calcium imaging. Apelin (10^{-7} M) caused a robust increase in intracellular Ca^{2+} levels in freshly isolated smooth muscle cells (**Figures 4A–C**). The apelin-induced rise in intracellular Ca^{2+} was comparable to that observed by

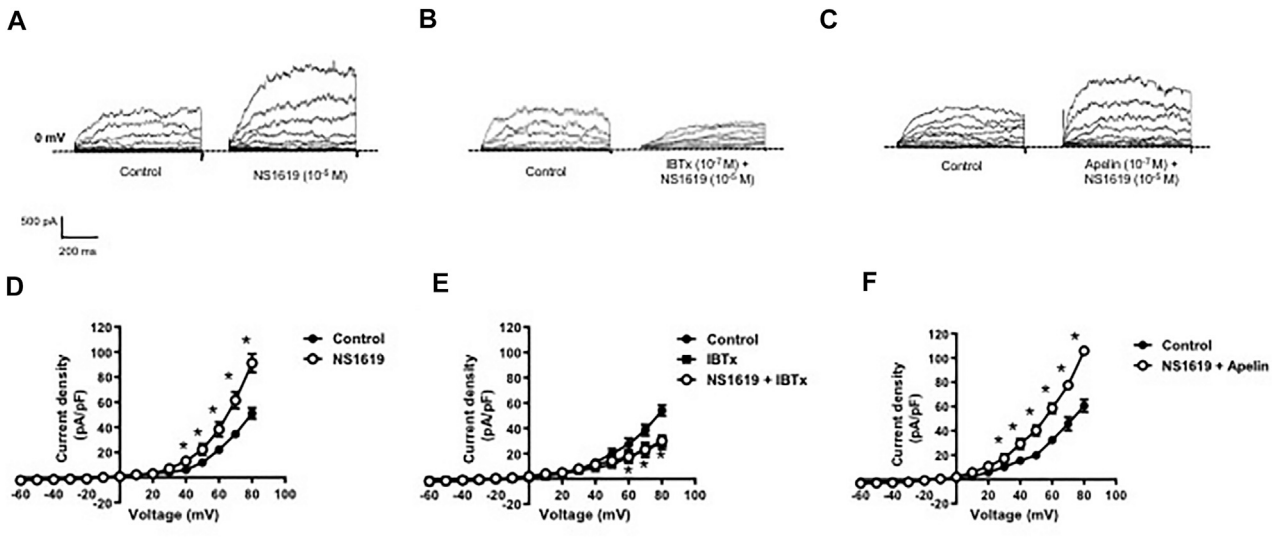

FIGURE 2 | Effect of apelin on NS1619-induced BK_{Ca} currents in coronary arterial myocytes. Whole cell BK_{Ca} currents induced in response to NS1619 (10^{-5} M) were recorded in freshly isolated coronary arterial myocytes. Representative traces showing the current recordings from smooth muscle cells after treatment with **(A)** NS1619 (10^{-5} M, 2 min) alone or **(B)** in the presence of IBTx (10^{-7} M, 5 min) or **(C)** apelin (10^{-7} M, 5 min). **(D–F)** Summary I–V curves of BK_{Ca} currents at baseline and after treatment with **(D)** NS1619 (10^{-5} M) alone or in the presence of **(E)** IBTx (10^{-7} M) or **(F)** apelin (10^{-7} M). Dotted line represents zero current level (at 0 mV). Values are presented as the mean ± S.E.M. (n = 6–7). *p < 0.05 vs. control current density.

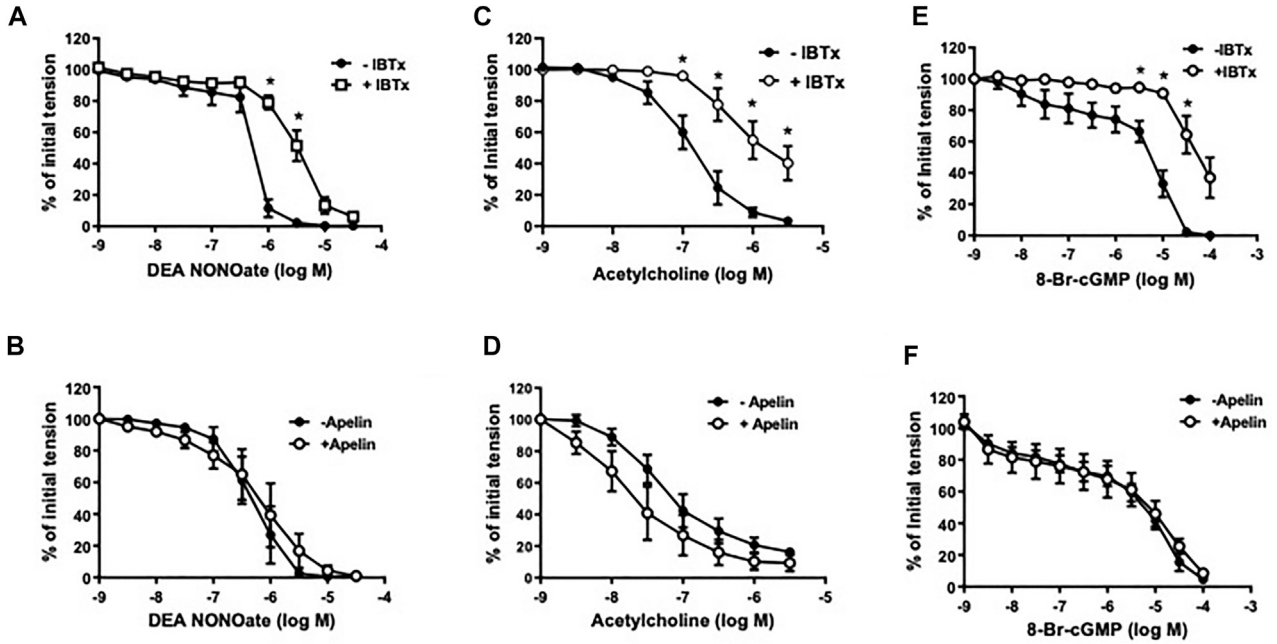

FIGURE 3 | Effect of apelin and iberiotoxin on NO-cGMP dependent vasorelaxation of coronary arteries. Log concentration-response curves in producing relaxation of coronary arteries for DEA NONOate **(A,B)**, acetylcholine **(C,D)** or 8-Bromo-cGMP **(E,F)** in the absence and presence of IBTx (10^{-7} M) **(A, C, E)** or apelin (10^{-7} M) **(B, D, F)**. Values are presented as the mean ± S.E.M. (n = 4–6). *p < 0.05 vs. control (in the absence of inhibitor).

depolarization with 60 mM K^+, which served as a positive control (**Figure 4C**). The APJ receptor antagonist, F13A (10^{-7} M, 5 min), abolished the apelin-induced response, thus confirming functional activation of smooth muscle APJ receptors in response to apelin in coronary arteries (**Figure 4C**).

Since apelin is known to increase PI3 kinase activity in cerebral arteries (Modgil et al., 2013), experiments were performed to evaluate the effect of apelin on PI3 kinase activity in coronary arteries. PI3-kinase activity was detected by measuring the ratio of phosphorylated Akt to total Akt, using immunoblot analysis. Apelin (10^{-7} M) treatment caused no significant change in PI3-kinase activity in coronary arteries, as indicated by unchanged P-Akt/total Akt ratio (**Figures 4D,E**).

DISCUSSION

The present study was designed to evaluate the effects of apelin on BK_{Ca} channels in coronary arterial smooth muscle cells. The key findings are: 1) apelin has no inhibitory effect on BK_{Ca} currents in coronary arterial smooth muscle cells; and 2) apelin does not inhibit NO/cGMP-induced relaxations, which are dependent on BK_{Ca} channels in coronary arteries (Darkow et al., 1997; Tunstall et al., 2011). These results are in striking contrast to our previous findings in cerebral arteries (Mughal et al., 2018b; Mughal et al., 2020), and clearly demonstrate that distinct molecular mechanisms underly the vasomotor effects of apelin in coronary and cerebral arteries.

BK_{Ca} channels are expressed in vascular smooth muscle cells from rat cerebral and coronary arteries (Modgil et al., 2013; Mughal et al., 2018a; Mughal et al., 2018b). In cerebral arteries, apelin inhibits smooth muscle BK_{Ca} channels and thereby impairs endothelium-dependent relaxations mediated by NO and an EDH pathway (Mughal et al., 2018b; Mughal et al., 2020). The results of the present study demonstrate that in coronary arterial myocytes apelin failed to inhibit increases in BK_{Ca} current density induced by membrane depolarization or by pharmacological activation with NS1619. Consistent with these electrophysiological findings, apelin was without effect on coronary arterial relaxation caused by endothelium-derived NO (i.e. acetylcholine), exogenously administered NO (i.e., DEA NONOate), and the stable, cell permeable cGMP analogue, 8-Br-cGMP. The absence of an inhibitory effect of apelin cannot be attributed to the lack of involvement of BK_{Ca} channels in NO/cGMP pathway-induced relaxation of rat coronary arteries since iberiotoxin, a potent and selective BK_{Ca} channel blocker (Kaczorowski and Garcia., 2016; Su et al., 2016), markedly impaired the responses to ACh, DEA, and 8-Br-cGMP. That apelin had no effect on these responses also cannot be explained by an absence of APJ receptors, which are indeed expressed in rat coronary arterial smooth muscle cells (Mughal et al., 2018a). Taken together, these data indicate that APJ receptors are not effectively coupled to BK_{Ca} channels in coronary arterial smooth muscle cells.

One possible explanation for the differential effect of apelin in cerebral vs coronary arterial smooth muscle cells could be related to the intracellular signaling pathways stimulated in response to apelin-APJ receptor activation. Binding of apelin to APJ receptors in cerebral arterial smooth muscle cells stimulates the PI3 kinase/Akt signaling pathway, which is required for apelin-induced

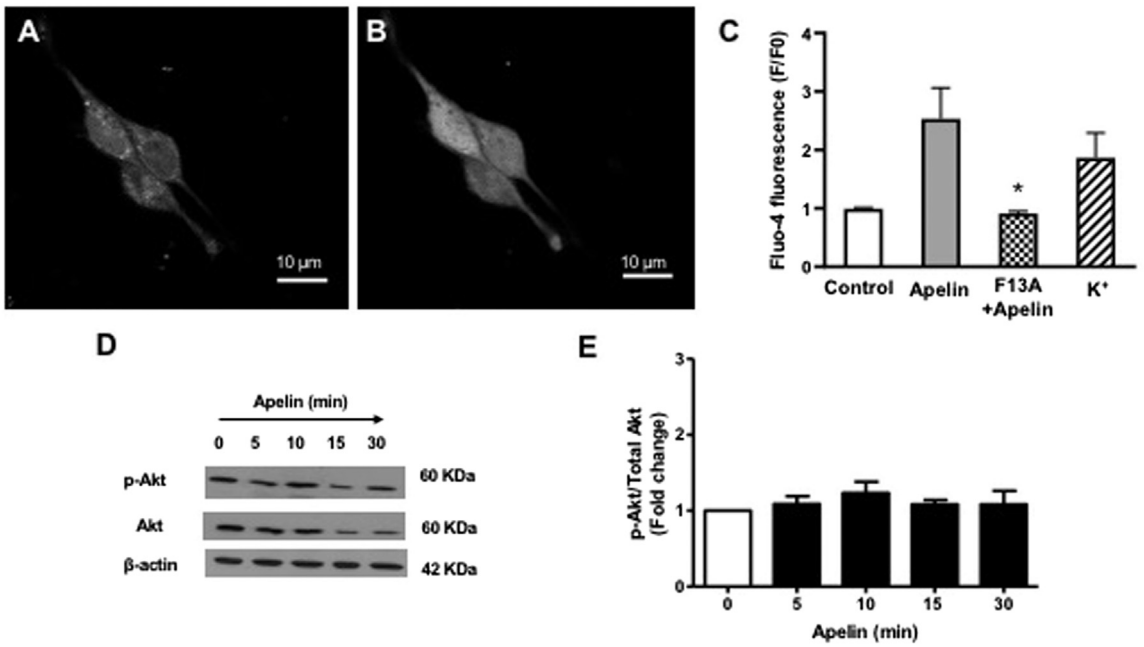

FIGURE 4 | Effect of apelin-APJ signaling on coronary intracellular Ca^{2+} levels and PI3-kinase activity. Representative images of freshly isolated coronary arterial smooth muscle cells loaded with Fluo-four AM (5 µM) **(A)** before and **(B)** after exposure to apelin (10^{-7} M). **(C)** Bar graph summarizing changes in fluorescence (F/F0) in response in apelin alone (10^{-7} M) or in the presence of F13A (10^{-7} M); 60 mM K^+ was used as a positive control for the experiments ($n = 3$). **(D)** Representative blots showing changes in phosphorylation of Akt (p-Akt) or Akt (total) protein expression in a time-dependent manner following treatment with apelin (10^{-7} M). **(E)** Summary data showing effect of apelin on PI3-kinase activity expressed as a ratio of p-Akt/Akt protein levels ($n = 3$). Values are presented as the mean ± S.E.M. *$p < 0.05$ vs. apelin alone; **$p < 0.05$ vs. control.

inhibition of BK_{Ca} channel function (Modgil et al., 2013). That apelin did not activate the PI3K/Akt-signaling pathway in coronary arterial smooth muscle cells provides a plausible mechanistic explanation as to why APJ receptors may not be efficiently linked to BK_{Ca} channels in coronary myocytes; however, the possibility that another intracellular signaling pathway plays a role in the lack of inhibitory effect of apelin on BK_{Ca} channel function cannot be ruled out. The absence of effect of apelin on BK_{Ca} channels and PI3 kinase/Akt signaling is not due to an inability to activate APJ receptor signaling in coronary arterial smooth muscle cells, since apelin caused a rapid and robust increase in intracellular Ca^{2+} levels. The apelin-induced rise in intracellular Ca^{2+} levels was attenuated by the APJ receptor antagonist, F13A, thus confirming that smooth muscle APJ receptors are indeed responsive to apelin in coronary arteries. It is also worth noting that although apelin caused an increase in intracellular Ca^{2+} levels in coronary smooth muscle cells, it does not cause contraction of isolated coronary arteries (Mughal et al., 2018a). This opens the possibility that apelin/APJ receptor signaling in coronary arterial smooth muscle cells may be involved in other cellular functions beyond the regulation of vascular tone.

The coronary circulation is controlled by multiple regulatory systems, including, for example, metabolic autoregulation, the sympathetic nervous system, circulating vasoactive molecules, and mediators produced by endothelial cells located within the blood vessel wall (Goodwill et al., 2017). The extent to which such systems play a role in regulating vasomotor tone varies between epicardial arteries (conductance vessels) and small arteries and arterioles (resistance vessels and microcirculation). For example, NO is a principal regulator of epicardial coronary vasomotor tone, whereas metabolic autoregulation and EDH pathways play a more prominent role in smaller resistance vessels and the microcirculation (Deussen et al., 2012; Ellinsworth et al., 2016; Goodwill et al., 2017). The present findings show a lack of inhibitory effect of apelin/APJ receptor signaling on the NO/cGMP/BK_{Ca} channel pathway in epicardial arteries, but whether or not this is true for other regions of the coronary circulation remains to be determined.

As with all biological studies, there are some limitations that should be considered. Although pre-constricted coronary arterial rings were used to investigate the effects of apelin on the vasodilators used in this study, it is possible that the vascular effects of apelin may differ in unstimulated arterial rings with intrinsic myogenic tone. In addition, our present findings are limited to arteries obtained from healthy adult male rats. It is well known that responses to vasoactive mediators may vary depending on the age and sex of the animals, as well as in pathological conditions. Thus, future studies with female rats, various age groups, and appropriate models of cardiovascular disease will be needed to further enhance our understanding of the vasomotor effects of apelin.

The results of the present study build on our knowledge of the actions of apelin in coronary arteries. The ability of apelin to cause endothelium-dependent relaxation (Mughal et al., 2018a), coupled with a lack of inhibitory effect on BK_{Ca} channels makes it unlikely that activation of APJ receptors in coronary arteries would adversely affect epicardial coronary flow by creating a vasoconstrictive environment. It could be expected that apelin or other APJ receptor agonists in development will not interfere with the vasodilator effects of endogenous BK_{Ca} channel openers, nor would these agents be likely to elicit coronary vasospasm, which has been hypothesized to be related to reduced K conductance in coronary artery smooth muscle cells (Dick and Tune, 2010).

DATA AVAILABILITY STATEMENT

The raw data supporting the conclusion of this article will be made available by the authors, without undue reservation.

ETHICS STATEMENT

The animal study was reviewed and approved by the North Dakota State University Animal Care and Use Committee.

AUTHOR CONTRIBUTIONS

Participated in research design: AM, CS, SO'R. Conducted experiments: AM. Performed data analysis: AM, CS, SO'R. Wrote or contributed to the writing of the manuscript: AM, SO'R .

FUNDING

This work was supported by the National Institutes of Health National Heart, Lung, and Blood Institute (Grant HL124338).

REFERENCES

Bolotina, V. M., Najibi, S., Palacino, J. J., Pagano, P. J., and Cohen, R. A. (1994). Nitric Oxide Directly Activates Calcium-dependent Potassium Channels in Vascular Smooth Muscle. *Nature* 368, 850–853. doi:10.1038/368850a0

Boucher, J., Masri, B., Daviaud, D., Gesta, S., Guigné, C., Mazzucotelli, A., et al. (2005). Apelin, a Newly Identified Adipokine Up-Regulated by Insulin and Obesity. *Endocrinology* 146, 1764–1771. doi:10.1210/en.2004-1427

Brame, A. L., Maguire, J. J., Yang, P., Dyson, A., Torella, R., Cheriyan, J., et al. (2015). Design, Characterization, and First-In-Human Study of the Vascular Actions of a Novel Biased Apelin Receptor Agonist. *Hypertension* 65, 834–840. doi:10.1161/hypertensionaha.114.05099

Brayden, J., and Nelson, M. (1992). Regulation of Arterial Tone by Activation of Calcium-dependent Potassium Channels. *Science* 256, 532–535. doi:10.1126/science.1373909

Campbell, W. B., Gebremedhin, D., Pratt, P. F., and Harder, D. R. (1996). Identification of Epoxyeicosatrienoic Acids as Endothelium-Derived Hyperpolarizing Factors. *Circ. Res.* 78, 415–423. doi:10.1161/01.res.78.3.415

Darkow, D. J., Lu, L., and White, R. E. (1997). Estrogen Relaxation of Coronary Artery Smooth Muscle Is Mediated by Nitric Oxide and cGMP. *Am. J. Physiology-Heart Circulatory Physiol.* 272, H2765–H2773. doi:10.1152/ajpheart.1997.272.6.h2765

Deussen, A., Ohanyan, V., Jannasch, A., Yin, L., and Chilian, W. (2012). Mechanisms of Metabolic Coronary Flow Regulation. *J. Mol. Cell Cardiol.* 52, 794–801. doi:10.1016/j.yjmcc.2011.10.001

Dick, G. M., and Tune, J. D. (2010). Role of Potassium Channels in Coronary Vasodilation. *Exp. Biol. Med. (Maywood)* 235, 10–22. doi:10.1258/ebm.2009.009201

Dogan, M. F., Yildiz, O., Arslan, S. O., and Ulusoy, K. G. (2019). Potassium Channels in Vascular Smooth Muscle: a Pathophysiological and Pharmacological Perspective. *Fundam. Clin. Pharmacol.* 33, 504–523. doi:10.1111/fcp.12493

Dopico, A. M., Bukiya, A. N., and Jaggar, J. H. (2018). Calcium- and Voltage-Gated BKchannels in Vascular Smooth Muscle. *Pflugers Arch.* 470, 1271–1289. doi:10.1007/s00424-018-2151-y

Earley, S., Heppner, T. J., Nelson, M. T., and Brayden, J. E. (2005). TRPV4 Forms a Novel Ca 2+ Signaling Complex with Ryanodine Receptors and BK Ca Channels. *Circ. Res.* 97, 1270–1279. doi:10.1161/01.res.0000194321.60300.d6

Ellinsworth, D. C., Sandow, S. L., Shukla, N., Liu, Y., Jeremy, J. Y., and Gutterman, D. D. (2016). Endothelium-derived Hyperpolarization and Coronary Vasodilation: Diverse and Integrated Roles of Epoxyeicosatrienoic Acids, Hydrogen Peroxide, and gap Junctions. *Microcirculation* 23, 15–32. doi:10.1111/micc.12255

Földes, G., Horkay, F., Szokodi, I., Vuolteenaho, O., Ilves, M., Lindstedt, K. A., et al. (2003). Circulating and Cardiac Levels of Apelin, the Novel Ligand of the Orphan Receptor APJ, in Patients with Heart Failure. *Biochem. Biophysical Res. Commun.* 308, 480–485. doi:10.1016/s0006-291x(03)01424-4

Folino, A., Montarolo, P. G., Samaja, M., and Rastaldo, R. (2015). Effects of Apelin on the Cardiovascular System. *Heart Fail. Rev.* 20, 505–518. doi:10.1007/s10741-015-9475-x

Gerbier, R., Alvear-Perez, R., Margathe, J. F., Flahault, A., Couvineau, P., Gao, J., et al. (2017). Development of Original Metabolically Stable Apelin-17 Analogs with Diuretic and Cardiovascular Effects. *FASEB J.* 31, 687–700. doi:10.1096/fj.201600784R

Ghatta, S., Nimmagadda, D., Xu, X., and O'Rourke, S. T. (2006). Large-conductance, Calcium-Activated Potassium Channels: Structural and Functional Implications. *Pharmacol. Ther.* 110, 103–116. doi:10.1016/j.pharmthera.2005.10.007

Goodwill, A. G., Dick, G. M., Kiel, A. M., and Tune, J. D. (2017). Regulation of Coronary Blood Flow. *Compr. Physiol.* 7, 321–382. doi:10.1002/cphy.c160016

Gurzu, B., Cristian Petrescu, B., Costuleanu, M., and Petrescu, G. (2006). Interactions between Apelin and Angiotensin II on Rat portal Vein. *J. Renin Angiotensin Aldosterone Syst.* 7, 212–216. doi:10.3317/jraas.2006.040

Jackson, W. F. (2017). Potassium Channels in Regulation of Vascular Smooth Musclecontraction and Growth. *Adv. Pharmacol.* 78, 89–144. doi:10.1016/bs.apha.2016.07.001

Jia, Y. X., Lu, Z. F., Zhang, J., Pan, C. S., Yang, J. H., Zhao, J., et al. (2007). Apelin Activates L-Arginine/nitric Oxide Synthase/nitric Oxide Pathway in Rat Aortas. *Peptides* 28, 2023–2029. doi:10.1016/j.peptides.2007.07.016

Kaczorowski, G. J., and Garcia, M. L. (2016). Developing Molecular Pharmacology of BK Channels for Therapeutic Benefit. *Int. Rev. Neurobiol.* 128, 439–475. doi:10.1016/bs.irn.2016.02.013

Katugampola, S. D., Maguire, J. J., Matthewson, S. R., and Davenport, A. P. (2001). [125 I]-(Pyr1)Apelin-13 Is a Novel Radioligand for Localizing the APJ Orphan Receptor in Human and Rat Tissues with Evidence for a Vasoconstrictor Role in Man. *Br. J. Pharmacol.* 132, 1255–1260. doi:10.1038/sj.bjp.0703939

Kleinz, M. J., and Davenport, A. P. (2004). Immunocytochemical Localization of the Endogenous Vasoactive Peptide Apelin to Human Vascular and Endocardial Endothelial Cells. *Regul. Peptides* 118, 119–125. doi:10.1016/j.regpep.2003.11.002

Kleinz, M. J., Skepper, J. N., and Davenport, A. P. (2005). Immunocytochemical Localisation of the Apelin Receptor, APJ, to Human Cardiomyocytes, Vascular Smooth Muscle and Endothelial Cells. *Regul. Peptides* 126, 233–240. doi:10.1016/j.regpep.2004.10.019

Lee, D. K., Saldivia, V. R., Nguyen, T., Cheng, R., George, S. R., and O'Dowd, B. F. (2005). Modification of the Terminal Residue of Apelin-13 Antagonizes

its Hypotensive Action. *Endocrinology* 146, 231–236. doi:10.1210/en.2004-0359

Luo, X., Liu, J., Zhou, H., and Chen, L. (2018). Apelin/APJ System: a Critical Regulator Ofvascular Smooth Muscle Cell. *J. Cel Physiol* 233, 5180–5188. doi:10.1002/jcp.26339

Maguire, J. J., Kleinz, M. J., Pitkin, S. L., and Davenport, A. P. (2009). [Pyr1]Apelin-13 Identified as the Predominant Apelin Isoform in the Human Heart. *Hypertension* 54, 598–604. doi:10.1161/hypertensionaha.109.134619

Mistry, D. K., and Garland, C. J. (1998). Nitric Oxide (NO)-induced Activation of Large Conductance Ca2+ -dependent K+ Channels (BKCa) in Smooth Muscle Cells Isolated from the Rat Mesenteric Artery. *Br. J. Pharmacol.* 124, 1131–1140. doi:10.1038/sj.bjp.0701940

Modgil, A., Guo, L., O'Rourke, S. T., and Sun, C. (2013). Apelin-13 Inhibits Large-Conductance Ca2+-Activated K+ Channels in Cerebral Artery Smooth Muscle Cells via a PI3-Kinase Dependent Mechanism. *PLoS One* 8, e83051. doi:10.1371/journal.pone.0083051

Mughal, A., Anto, S., Sun, C., and O'Rourke, S. T. (2020). Apelin Inhibits an Endothelium-Derived Hyperpolarizing Factor-like Pathway in Rat Cerebral Arteries. *Peptides* 132, 170350. doi:10.1016/j.peptides.2020.170350

Mughal, A., and O'Rourke, S. T. (2018). Vascular Effects of Apelin: Mechanisms and Therapeutic Potential. *Pharmacol. Ther.* 190, 139–147. doi:10.1016/j.pharmthera.2018.05.013

Mughal, A., Sun, C., and O'Rourke, S. T. (2018b). Apelin Reduces Nitric Oxide-Induced Relaxation of Cerebral Arteries by Inhibiting Activation of Large-Conductance, Calcium-Activated K Channels. *J. Cardiovasc. Pharmacol.* 71, 223–232. doi:10.1097/fjc.0000000000000563

Mughal, A., Sun, C., and O'Rourke, S. T. (2018a). Activation of Large Conductance, Calcium-Activated Potassium Channels by Nitric Oxide Mediates Apelin-Induced Relaxation of Isolated Rat Coronary Arteries. *J. Pharmacol. Exp. Ther.* 366, 265–273. doi:10.1124/jpet.118.248682

Nagano, K., Kwon, C., Ishida, J., Hashimoto, T., Kim, J.-D., Kishikawa, N., et al. (2019). Cooperative Action of APJ and α1A-adrenergic Receptor in Vascular Smooth Muscle Cells Induces Vasoconstriction. *J. Biochem.* 166, 383–392. doi:10.1093/jb/mvz071

Nelson, M. T., and Quayle, J. M. (1995). Physiological Roles and Properties of Potassium Channels in Arterial Smooth Muscle. *Am. J. Physiology-Cell Physiol.* 268, C799–C822. doi:10.1152/ajpcell.1995.268.4.c799

Pitkin, S. L., Maguire, J. J., Kuc, R. E., and Davenport, A. P. (2010). Modulation of the Apelin/APJ System in Heart Failure and Atherosclerosis in Man. *Br. J. Pharmacol.* 160, 1785–1795. doi:10.1111/j.1476-5381.2010.00821.x

Salcedo, A., Garijo, J., Monge, L., Fernández, N., Luis García-Villalón, A., Sánchez Turrión, V., et al. (2007). Apelin Effects in Human Splanchnic Arteries. Role of Nitric Oxide and Prostanoids. *Regul. Peptides* 144, 50–55. doi:10.1016/j.regpep.2007.06.005

Schinzari, F., Veneziani, A., Mores, N., Barini, A., Di Daniele, N., Cardillo, C., et al. (2017). Beneficial Effects of Apelin on Vascular Function in Patients with central Obesity. *Hypertension* 69, 942–949. doi:10.1161/hypertensionaha.116.08916

Su, Z., Brown, E. C., Wang, W., and MacKinnon, R. (2016). Novel Cell-free High-Throughput Screening Method for Pharmacological Tools Targeting K+ Channels. *Proc. Natl. Acad. Sci. USA* 113, 5748–5753. doi:10.1073/pnas.1602815113

Tang, X., Qian, L.-L., Wang, R.-X., Yao, Y., Dang, S.-P., Wu, Y., et al. (2017). Regulation of Coronary Arterial Large Conductance Ca2+-Activated K+ Channel Protein Expression and Function by N-3 Polyunsaturated Fatty Acids in Diabetic Rats. *J. Vasc. Res.* 54, 329–343. doi:10.1159/000479870

Tunstall, R. R., Shukla, P., Grazul-Bilska, A., Sun, C., and O'Rourke, S. T. (2011). MT2 Receptors Mediate the Inhibitory Effects of Melatonin on Nitric Oxide-Induced Relaxation of Porcine Isolated Coronary Arteries. *J. Pharmacol. Exp. Ther.* 336, 127–133. doi:10.1124/jpet.110.174482

Tykocki, N. R., Boerman, E. M., and Jackson, W. F. (2017). Smooth Muscle Ion Channelsand Regulation of Vascular Tone in Resistance Arteries and Arterioles. *Compr. Physiol.* 7, 485–581. doi:10.1002/cphy.c160011

Wang, W., McKinnie, S. M. K., Farhan, M., Paul, M., McDonald, T., McLean, B., et al. (2016). Angiotensin-Converting Enzyme 2 Metabolizes and Partially Inactivates Pyr-Apelin-13 and Apelin-17. *Hypertension* 68, 365–377. doi:10.1161/hypertensionaha.115.06892

Wang, W., McKinnie, S. M., Patel, V. B., Haddad, G., Wang, Z., Zhabyeyev, P., et al. (2013). Loss of Apelin Exacerbates Myocardial Infarction Adverse Remodeling and Ischemia-Reperfusion Injury: Therapeutic Potential of Synthetic Apelin Analogues. *J. Am. Heart Assoc.* 2, e000249. doi:10.1161/jaha.113.000249

Yan, J., Wang, A., Cao, J., and Chen, L. (2020). Apelin/APJ System: an Emerging Therapeutic Target for Respiratory Diseases. *Cell. Mol. Life Sci.* 77, 2919–2930. doi:10.1007/s00018-020-03461-7

Zhang, D. X., Borbouse, L., Gebremedhin, D., Mendoza, S. A., Zinkevich, N. S., Li, R., et al. (2012). H 2 O 2 -Induced Dilation in Human Coronary Arterioles: Role of Protein Kinase G Dimerization and Large-Conductance Ca 2+ -Activated K + Channel Activation. *Circ. Res.* 110, 471–480. doi:10.1161/circresaha.111.258871

Conflict of Interest: The authors declare that the research was conducted in the absence of any commercial or financial relationships that could be construed as a potential conflict of interest.

frontiers in Pharmacology

REVIEW
published: 22 June 2021
doi: 10.3389/fphar.2021.697720

Regional Heterogeneity of Perivascular Adipose Tissue: Morphology, Origin, and Secretome

Xinzhi Li[1]*, *Zhongyuan Ma*[2] *and Yi Zhun Zhu*[1]*

[1]School of Pharmacy and State Key Laboratory of Quality Research in Chinese Medicine, Macau University of Science and Technology, Macau, China, [2]Department of Cardiothoracic Surgery, Zhuhai People's Hospital, Jinan University Medical School, Guangzhou, China

Perivascular adipose tissue (PVAT) is a unique fat depot with local and systemic impacts. PVATs are anatomically, developmentally, and functionally different from classical adipose tissues and they are also different from each other. PVAT adipocytes originate from different progenitors and precursors. They can produce and secrete a wide range of autocrine and paracrine factors, many of which are vasoactive modulators. In the context of obesity-associated low-grade inflammation, these phenotypic and functional differences become more evident. In this review, we focus on the recent findings of PVAT's heterogeneity by comparing commonly studied adipose tissues around the thoracic aorta (tPVAT), abdominal aorta (aPVAT), and mesenteric artery (mPVAT). Distinct origins and developmental trajectory of PVAT adipocyte potentially contribute to regional heterogeneity. Regional differences also exist in ways how PVAT communicates with its neighboring vasculature by producing specific adipokines, vascular tone regulators, and extracellular vesicles in a given microenvironment. These insights may inspire new therapeutic strategies targeting the PVAT.

Keywords: adipocyte, preadipocyte, adipokine, cellular heterogeneity, obesity, vascular inflammation

OPEN ACCESS

Edited by:
Ana Paula Davel,
State University of Campinas, Brazil

Reviewed by:
InKyeom Kim,
Kyungpook National University, South Korea
Qiongxin Wang,
University of Alabama at Birmingham, United States

***Correspondence:**
Xinzhi Li
xizli@must.edu.mo
Yi Zhun Zhu
yzzhu@must.edu.mo

Specialty section:
This article was submitted to Cardiovascular and Smooth Muscle Pharmacology, a section of the journal Frontiers in Pharmacology

Received: *20 April 2021*
Accepted: *10 June 2021*
Published: *22 June 2021*

Citation:
Li X, Ma Z and Zhu YZ (2021) Regional Heterogeneity of Perivascular Adipose Tissue: Morphology, Origin, and Secretome. Front. Pharmacol. 12:697720. doi: 10.3389/fphar.2021.697720

INTRODUCTION

Obesity is becoming a substantial public health concern since it gives rise to a wide range of disorders (Olshansky et al., 2005). Obesity prevalence has tripled since 1975 and it is now one of the WHO's priorities to cease the quick rise in obesity (Jaacks et al., 2019). The burgeoning global epidemic of obesity, consequently leading to type 2 diabetes, dyslipidemias, cardiovascular disease, and even some cancers will soon be devastating if actions are not taken (Alberti et al., 2009; Grundy, 2012; Scheen and Van Gaal, 2014). Obesity occurs due to excess energy intake, dramatic fat mass accumulation caused by increased adipocyte size (hypertrophy), or increased adipocyte number (hyperplasia), or both. Given the systemic impacts, obesity cannot be seen simply as a fat accumulation, and it goes hand-in-hand with many metabolic complications. People often experienced obesity as a chronic affliction characterized by low-grade inflammation. Despite the absence of the four cardinal signs of typical inflammation, the unresolved inflammation, entwined with fibrosis and defected angiogenesis-induced hypoxia, is a common pathway in the development of various cardiometabolic diseases.

Excessive fat accumulation can happen in various adipose depots, including a kind of unique adipose tissue known as perivascular adipose tissue (PVAT). PVAT surrounds most blood vessels except capillaries, pulmonary and cerebral blood vessels. PVAT plays wide-ranging physiological

roles far beyond supporting connective tissue. It is now considered a metabolically active organ that regulates vascular function in both autocrine and paracrine fashions by producing various adipokines (Rajsheker et al., 2010; Van de Voorde et al., 2013). Over the decades, our understanding of PVAT biology has increased simultaneously with a rising prevalence of obesity and related metabolic complications. Not only does PVAT actively maintain vascular homeostasis, but it also markedly modulates various inflammation-related cardiovascular diseases. Due to the proximity of PVAT to the associated blood vessels, PAVT can be a unique target to improve arterial function in the setting of obesity.

PVATs are not only different from classical adipose tissues, they vary from location to location developmentally and functionally (Chang et al., 2020). Most intriguingly, PVAT's origin largely remains unknown, despite the development of cellular fate mapping and lineage tracing in other fat depots (Sanchez-Gurmaches et al., 2016; Guimaraes-Camboa et al., 2017; Schwalie et al., 2018; Merrick et al., 2019; Shao et al., 2019; Cattaneo et al., 2020). Numerous publications have presented us with a bulk of mixed information, given the fact that these publications always include more than one PVAT, which challenges readers outside of the field. The general information on the pathophysiological functions of PVAT has been the subject of many recent comprehensive reviews (Nosalski and Guzik, 2017; Hildebrand et al., 2018; Chang et al., 2020). In this review, we aim to form a conceptual picture of PVAT heterogeneity, mainly focusing on histology, developmental origin, and briefly on secretome.

DEPOT-SPECIFIC AND POLYCHROMATIC ADIPOSE TISSUE

Nomenclature of Perivascular Adipose Tissues

A PVAT is generally named after its adjacent vessel's name, such as pericoronary adipose tissue, referring to the fat tissue around the coronary artery. Over the years, various non-standard names were used for the same PVAT, which can be merely confusing or even misleading. For instance, "cardiac" PVAT surrounding the coronary artery or epicardial adipose tissue was abbreviated as either "C-PVAT" (Drosos et al., 2016), or "PVAT-CA" (Lu et al., 2017), or even "epi" for shorter (Mazurek et al., 2003). It is not uncommon that these names are mistakenly referred to, for example, in the case of pericardial and epicardial fat (Iacobellis, 2009). These facts reason the need to standardize nomenclature for PVATs. Some research articles have used a combined format to define these concepts (Tran et al., 2018; Ye et al., 2019). Throughout this review, we will use their traditional names according to their locations but with some specifications. In particular, we "standardized" these names by introducing a common name, "PVAT," following a lowercase letter, indicating where it is localized. For example, pericoronary adipose tissue is termed as "cPVAT," thoracic periaortic adipose tissue is abbreviated as "tPVAT," and abdominal periaortic adipose tissue as "aPVAT." Adipose tissue around the mesenteric artery is called "mPVAT." A comparison among the four most commonly studied PVATs is presented in **Table 1** and **Figure 1**.

Multicolored Adipose Tissue

Adipose tissues are empirically color-coded as white (WAT), brown (BAT), and beige/brown-in-white (brite) adipose tissues. The color explicitly reflects the main adipocyte population and the amount of iron-containing mitochondria in each adipocyte. The more mitochondria, the darker the color is. In addition to major depots, there are other location-specific adipose tissues, including mammary "pink" adipose tissue and bone marrow adipose tissue, which is primarily red in young individuals and turns yellow during aging. It would undoubtedly be oversimplified if we classify adipose tissues based solely on the appearing color and neglect their complexity and heterogeneity. Classical inter-scapular BAT has been previously assumed to contain a homogeneous population of brown adipocytes. A recent study has revealed a new brown adipocyte subpopulation with low thermogenic activity coexists with the classical high-thermogenic brown adipocytes (Song et al., 2020). More interestingly, these two brown adipocyte subpopulations may interconvert dynamically in response to the environmental temperature (Song et al., 2020). Using AdipoChaser mouse models, Wang et al. also demonstrated that "pink" mammary adipose tissue can undergo reversible dedifferentiation during lactation, where de-differentiated fibroblasts proliferate and re-differentiate into adipocytes upon weaning (Wang et al., 2018).

PVAT's color is not visually presented. Instead, it is determined by the subcellular composition and enrichment of specific genetic biomarkers. For example, tPVAT, characterized as brown adipose tissue, is labeled with highly expressed uncoupling protein-1 (UCP-1) and cell death activator CIDE-A (Cidea) (Tran et al., 2018). Conversely, aPVAT is seemingly white but contains a mixture of beige and white adipocytes (Padilla et al., 2013). Therefore, when we talk about the color of a PVAT, we mainly use generalized terminology to reflect their cellular characteristics and corresponding genetic profiles. Generally speaking, white PVAT adipocytes share a lot of similarities with their visceral counterparts, which are morphologically classified by the appearance of large unilocular lipid droplets, fewer mitochondria, and small cytoplasmic volumes. Brown PVAT adipocytes, on the other hand, are distinguished by multilocular lipid droplets and high density of mitochondria. In rodents, arteries including the mesenteric, carotid, and femoral are surrounded by WAT, while the thoracic aorta is encircled by BAT and the abdominal aorta by beige PVAT (a mixture of white and brown adipocytes) (Brown et al., 2014).

HISTOLOGICAL DISTINCTIONS OF PERIVASCULAR ADIPOSE TISSUES

Although the majority of adipose tissue, either by volume or by function, is adipocytes, white adipocytes comprise only one-third of the total cell number in WAT. The remaining 70% of cells are a heterogeneous collection of largely undefined stromal and immune

TABLE 1 | Reginal differences of perivascular adipose tissue.

	cPVAT	tPVAT	aPVAT	mPVAT
Anatomical location	Pericoronary, adjacent to the heart	Thoracic periaortic, from aortic arch at T4 to the T10–T11 vertebrae, above the diaphragm	Abdominal periaortic, from below the diaphragm to femoral bifurcation	Mesenteric arterial, around the resistance mesenteric arteries
Other name/ acronym	Epicardial adipose tissue (EAT), C-PVAT, PVAT-CA	Thoracic PVAT, Thor PVAT	Abd PVAT	Adipose tissue of mesenteric bed
Predominant adipocyte	Beige Sacks et al. (2013)	Brown	White, very few beige Police et al. (2009)	White
Morphology of adipocyte	Spotted multilocular, but mainly small unilocular adipocytes	Multilocular brown adipocytes, abundant mitochondria Fitzgibbons et al. (2011), Padilla et al. (2013)	Primarily unilocular, fewer mitochondria Police et al. (2009), Padilla et al. (2013)	Large unilocular Galvez et al. (2006), Gil-Ortega et al. (2010)
Highly expressed gene	UCP-1, PRDM16, PGC-1α, PPARγ, and the beige adipocyte-specific marker CD137 Sacks et al. (2009), Sacks et al. (2013)	UCP-1, PRDM16, PGC-1α Tran et al. (2018); Cidea, PPARγ Fitzgibbons et al. (2011); EBF2 Angueira et al. (2021)	Hoxc8, Nnat, Sncg, Mest Tran et al. (2018)	Hoxc8, Tcf21, Tbx1, Pat2, dermatopontin Walden et al. (2012), Friederich-Persson et al. (2017)
Developmental origin	Splanchnic mesoderm Sacks et al. (2013)	Multiple lineages including ectoderm-derived neural crest (periaoritic arch) and mesoderm Ye et al. (2019)	Mesoderm	Mesothelial lineage
Progenitor/stem cell marker	Unknown	Pparg-dependent Xiong et al. (2018); $Myf5^{+}/Myf5^{-}$ (Ye et al. (2019); $Pdgfra^{+}$	Pparg-dependent, $SM22\alpha^{+}$Chang et al. (2012)	CD34, CD44, and $Pdgfra^{+}$Contreras et al. (2016); $SM22\alpha^{+}$Chang et al. (2012)
Pro-/anti-inflammatory	Pro-inflammation and pro-atherosclerosis Numaguchi et al. (2019)	Anti-atherosclerosis and anti-inflammation in mouse; Fitzgibbons et al. (2011); proatherosclerosis in human Lehman et al. (2010), Britton et al. (2012)	Pro-inflammation and prone to aneurysm formation Police et al. (2009)	Pro-inflammation and Pro-atherosclerosis Sena et al. (2017)

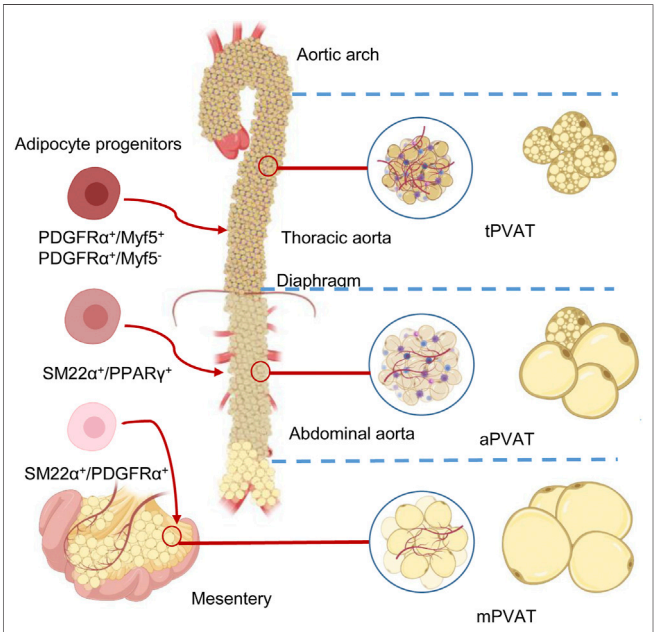

FIGURE 1 | Anatomical, morphological, and developmental differences of the perivascular adipose tissues (PVATs). The color differences reflect the different proportions of brown adipocytes in the adipose tissue. Adipose tissues around thoracic aorta (tPVAT), abdominal aorta (aPVAT), and mesenteric artery (mPVAT) have distinct fat cell populations that are derived from different adipocyte progenitors. These progenitors could be identified by highly expressed cell markers, such as platelet-derived growth factor receptor-α (PGDFRα), myogenic factor 5 (Myf5), smooth muscle protein 22-α (SM22α), and peroxisome proliferator-activated receptor-γ (PPARγ).

cells (Sarantopoulos et al., 2018). Understandably, PVAT is composed of adipocytes, nerves, and a stromal vascular fraction consisting of monocytes, endothelial cells, pericytes, macrophages, T cells, and mesenchymal stem cells (Chatterjee et al., 2009). Large vessels are separated from their PVATs by a layer of adventitia composed of elastic bundles, fibroblasts, nerves, and vasa vasorum. On the other hand, PVATs around small vessels and microvessels are seen as a seamless continuum from their associated blood vessels. Different PVATs are dominated by diverse adipocytes, indicating regional phenotypic heterogeneity in a given vasculature (Fitzgibbons et al., 2011).

Histology of Pericoronary Adipose Tissue

Broadly, cardiac fat depots include epicardial and pericardial adipose tissues. A big portion of epicardial fat surrounding the coronary arteries is called pericoronary adipose tissue (cPVAT) (Fernandez-Alfonso et al., 2017). Human cPVAT was firstly considered as a unique subtype of WAT since the cellular morphology and gene profile were more consistent with WAT than BAT (Chatterjee et al., 2009). Differentiated pericoronary adipocytes are irregularly shaped, smaller in size, and lower in lipid accumulation relative to subcutaneous and perirenal counterparts (Chatterjee et al., 2009). Meanwhile, human cPVAT exhibits an increased capacity to attract immune cells and induce angiogenesis, contributing to coronary atherosclerosis development (Chatterjee et al., 2009). Notably, these features were observed in differentiated preadipocytes *in vitro*, which might differ from *in vivo* physiological settings.

Evidence indeed showed cPVAT was composed of small unilocular adipocytes positively stained with brown fat marker

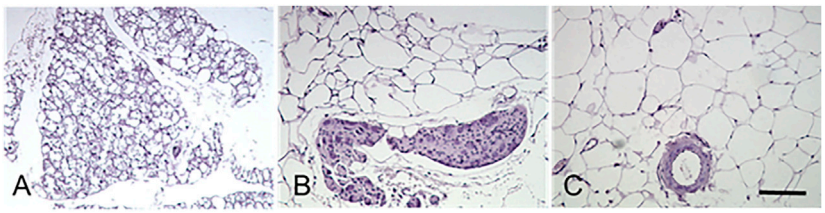

FIGURE 2 | Histological characteristics of the perivascular adipose tissues. Murine adipose tissues around thoracic aorta (tPVAT, panel **(A)**), abdominal aorta (aPVAT, panel **(B)**), and mesenteric artery (mPVAT, panel **(C)**) were stained by hematoxylin and eosin. Brown adipocytes in tPVAT are characterized by small-sized, multilocular lipid droplets, whereas white adipocytes in mPVAT are classified by the appearance of a larger unilocular lipid droplet and small cytoplasmic space. aPVAT has mixed adipocyte populations. Scale bar, 100 μm.

UCP-1 (Chatterjee et al., 2013; Sacks et al., 2013). Sacks et al. further proposed that it would be more reasonable that cPVAT might closely resemble beige adipocytes (Sacks et al., 2013; Sacks and Symonds, 2013). Consistent expression of UCP-1 in cPVAT has been repeatedly reported since then (Chechi et al., 2017), but less expression of adiponectin, an anti-inflammatory adipokine was also reported (Numaguchi et al., 2019). Thus cPVAT can be classified as beige adipose tissue, with a large proportion of white adipocytes, which may contribute to coronary atherosclerosis development.

Histology of Thoracic Periaortic Adipose Tissue

Thoracic periaortic PVAT (tPVAT) expands from the aortic arch at the T4 vertebra to the diaphragm's aortic hiatus at the T10–T11 vertebrae. The comparison of adipocyte size, inflammation, and macrophage polarization indicated that tPVAT was close to subcutaneous adipose tissue (Fitzgibbons et al., 2011). It is now widely accepted that tPVAT is morphologically and functionally like BAT (**Figure 2A**). Multilocular brown adipocytes and abundant mitochondria were observed under light or electron microscopy (Fitzgibbons et al., 2011; Padilla et al., 2013), which might contribute to the decreased atherosclerotic plaque burden (Fitzgibbons et al., 2011).

In tPVAT, the adipocyte phenotypic switching via specific signaling pathways is evident in both whitening and browning directions. In a diet-induced obesity mouse model, tPVAT adipocytes become "whiter", with a primarily unilocular appearance and larger lipid (Galvez-Prieto et al., 2008; Sacks and Symonds, 2013). Aging together with miR-146b-3p downregulation could decrease browning (Pan et al., 2018). Reduced brown adipogenic differentiation of resident stromal cells via loss of peroxisome proliferator-activated receptor-γ (PPARγ) coactivator-1 α (PGC-1α) was also observed in aged animals (Pan et al., 2019). Cold is a capable inducer for perivascular adipocyte to re-brown and to restore protective effects on metabolism and vascular function (Boa et al., 2017; Bussey et al., 2018). This relationship between tPVAT and adiposity, employed as a predictor for cardiovascular diseases, warrants further investigation in a clinical setting.

Histology of Abdominal Periaortic Adipose Tissue

Abdominal periaortic adipose tissue (aPVAT) is the adipose segments surrounding the abdominal aorta from below the diaphragm to the femoral bifurcation. As a continuum of thoracic aorta, the abdominal aorta is encircled by 4- to 10-fold more adipose tissue than the adipose tissue around the aortic arch in rats (Henrichot et al., 2005). aPVAT is more prone to accumulation when exposed to a high-fat diet and shows significant adipocyte hyperplasia and hypertrophy (Henrichot et al., 2005). A comparison with tPVAT demonstrates that aPVAT contains a mixture of cells, with a predominant proportion of unilocular white adipocytes and a small portion of brown adipocytes (Police et al., 2009). Moreover, the average aPVAT adipocyte size is much bigger than that of tPVAT (**Figure 2B**). Electron microscopy demonstrated that aPVAT was composed of white adipocytes with fewer mitochondria (Padilla et al., 2013). Upon a 4 month high-fat diet feeding, mouse aPVAT showed higher gene expression of inflammatory cytokines than tPVAT. Leptin coincided with the inflammatory cytokines in aPAVT, whereas UCP-1 was elevated in tPVAT but suppressed in aPVAT throughout diet-induced obesity (Police et al., 2009). Further studies provided evidence that only aPVAT-, but not tPVAT-conditioned medium could promote inflammatory cytokine MCP-1 generation and macrophage migration (Police et al., 2009). aPVAT was found to express a higher level of inflammatory receptors, including CD11c, IL-6R, and TNFR1/2 relative to tPVAT and inter-scapular brown adipose tissues (Padilla et al., 2013). These convincing pieces of evidence differentiate two segments of PVAT, although they wrap along the same artery. These intriguing features remain enigmatic due to the lack of solid advances in the developmental origin, transdifferentiation, and cellular fate mapping of PVAT.

Histology of Mesenteric Perivascular Adipose Tissue

In humans and mice, the fat tissue around the resistance mesenteric arteries forms mesenteric perivascular adipose tissue (mPVAT) (**Figure 2C**). Among adipose tissues collected from different locations, mPVAT was traditionally categorized as

visceral WAT (Walden et al., 2012) with slightly smaller adipocyte size than classical visceral adipocytes (Caesar et al., 2010). However, mPVAT adipocytes are four times larger than periaortic adipocytes, and mPVAT expresses much less brown adipocyte marker of UCP-1 and PR domaining containing 16 (PRDM16) compared with brown adipocytes (Galvez-Prieto et al., 2008; Walden et al., 2012). The enlarged cross-sectional area of mPVAT adipocytes during obesity could be reduced but not completely reversed after caloric restriction (Bussey et al., 2016).

mPVAT expressed WAT specific marker transcription factor 21 (Tcf21), beige specific marker T-box protein 1 (Tbx1), and transcription factor Pat2. Besides, treatment with a β3-agonist, CL-316,243, could increase beige markers in mPVAT (Friederich-Persson et al., 2017). Other brown adipocyte gene markers, including myosin regulatory light chain (Mylpf), lim homebox 8 (Lhx8), zinc fingers in the cerebellum1 (Zic1), and T-box 15 (Tbx15) are barely seen in mPVAT, whereas a series of white adipose genes such as homeobox C8 (Hoxc8), transcription factor 21 (Tcf21), and dermatopontin (Dpt) are highly expressed in mPVAT (Walden et al., 2012). These findings adequately help classify mPVAT as a WAT.

DIFFERENT ORIGIN OF PERIVASCULAR ADIPOSE TISSUES

Typical mature adipocytes originate from progenitor cells, which are committed preadipocytes derived from stem cells of multiple sources (Rodeheffer et al., 2008). The distinction between WAT and BAT reasonably leads to a simple classification of two precursor populations, giving rise to white and brown adipocytes, respectively. A commonly known classifier is *myf5*, which encodes myogenic factor 5 (Myf5) (Timmons et al., 2007), whereas PRDM16 may be a controller for brown adipocyte generation (Seale et al., 2008). However, using mTmG reporter, a study revealed that white adipocytes in the subcutaneous and retroperitoneal WAT also originate from Myf5-expressing precursors. This approach also demonstrated that Myf5 expression could not track many brown adipocytes (Sanchez-Gurmaches and Guertin, 2014a). The adipogenic capacity of vasculature-residing mural cells (e.g., pericytes) in the adipose tissue was well documented in many papers (Tang et al., 2008; Gupta et al., 2012; Tran et al., 2012; Berry and Rodeheffer, 2013). This statement is challenged by a study where pericytes do not contribute to adipocytes' generation, although they seem to act as progenitors *in vitro* (Guimaraes-Camboa et al., 2017). Merrick et al. further indicated that reticular interstitium rather than the vasculature is the residing site for interstitial progenitor cells, which give rise to the preadipocytes expressing intercellular adhesion molecule–1 and another group of cells expressing protein CD142 (Merrick et al., 2019). Most recent results further revealed that only fibroblasts, neither mural nor endothelial cells, are cells of the vascular wall with significant adipogenic potential *in vivo* in both WAT and BAT (Cattaneo et al., 2020). Thus developmental origins of adipose tissue and the mechanisms controlling its expansion are just beginning and more intriguing findings are expected to come soon. Adipocytes of different PVATs may originate from distinct precursors (Hepler et al., 2017; Tran et al., 2018). Despite the aforementioned development of cellular fate mapping and lineage tracing in other adipose depots, the origins of PVAT adipocytes, in general, are barely known. This session presents distinct adipocyte development in **Table 1** and **Figure 1**. A clear definition of adipocyte origin can reveal the determined precursors and the regulatory mechanisms.

Origin of Epicardial and Periaortic Arch Perivascular Adipose Tissue

Epicardial fat originates from the splanchnic mesoderm in human (Sacks et al., 2013) and in mouse (Walden et al., 2012). Periaortic adipose tissue is potentially derived from $Myf5^+$ progenitors (Sanchez-Gurmaches and Guertin, 2014a). A more recent study showed that periaortic adipocyte progenitors expressed smooth muscle protein 22-alpha (SM22α) during development. Besides, knockout of PPARγ in neural crest cells leads to developmental delay of the periaortic arch PVAT (Fu et al., 2019). This evidence indicates that periaortic arch PVAT adipocytes have multiple lineages, mainly from ectoderm-derived neural crest cells, rather than the mesoderm-derived $Myf5^+$ progenitors (Fu et al., 2019). A possible explanation is that ectoderm-derived neural crest cells have a broad differentiation potential and give rise to a diverse range of cell types. For example, neural crest cells were once identified as one of the progenitors of white adipocytes (Sanchez-Gurmaches and Guertin, 2014b). Another study revealed that neural crest-derived cells resided along the vessels within the subcutaneous adipose tissue. These results demonstrate that neural crest-derived adipocyte-committed progenitors contribute to adipogenesis (Sowa et al., 2013).

Origin of Thoracic Periaortic Adipose Tissue

Unlike periaortic arch PVAT, neural crest cells do not contribute to tPVAT development (Ye et al., 2019). Only about 10–30% of the brown adipocytes in tPVAT derive from $Myf5^+$ sources (Ye et al., 2019). A lineage-tracing study further elaborates that anterior tPVAT adipocytes can be traced to $SM22\alpha^+$ progenitors, whereas left lateral tPVAT presents both $SM22\alpha^+$ and $Myf5^+$ features (Ye et al., 2019). However, recent cell differentiation assays and genetic fate mapping studies show that fibroblastic progenitor cells but not vascular smooth muscle cells (VSMCs) are responsible for tPVAT adipogenesis (Angueira et al., 2021), which contradicts the previous findings (Chang et al., 2012; Ye et al., 2019). Progenitor cells for tPVAT are from a fibroblastic lineage, including ($Pdgfra^+$; $Ly6a^+$; $Pparg^-$) and preadipocytes ($Pdgfra^+$; $Ly6a^-$; $Pparg^+$). Bona fide VSMCs were not found to contribute to adipocyte formation in tPVAT (Angueira et al., 2021). Single-cell transcriptomic analyses both at embryonic (E18) and perinatal (P3, after birth) stages identified transcription factor early B cell factor-2 (EBF2) as a critical modulator of BAT (Angueira et al., 2020) and tPVAT development (Angueira et al., 2021).

Origin of Abdominal Periaortic Adipose Tissue

Abdominal PVAT preadipocytes demonstrate lower brown adipocyte developmental transcription factors relative to tPVAT (Tran et al., 2018). Abdominal PVAT lacks *Zic1* gene, encoding zinc finger proteins that are critical for early BAT development (Contreras et al., 2016). In the absence of the adipogenic transcription factor PPARγ in the VSMCs, failure of aPVAT development was observed (Chang et al., 2012). These findings demonstrate that aPVAT shares, at least to some extent, similar developmental origins with SM22α^+ and PPARγ^+ VSMCs.

Origin of Mesenteric Perivascular Adipose Tissue

Few studies have focused on the developmental origin of mPVAT, and some comparative data may provide limited clues. Given the proximity, mPVAT's developmental origins are thought to be similar to the visceral adipose tissue. Indeed, both mPVAT and perigonadal adipose tissue expressed comparable levels of white adipocyte signature gene *Tcf21* and the brite adipocyte-specific genes *Tbx1* and *Tmem26* (Contreras et al., 2016). Mesenteric and perigonadal adipose tissue are also found to share the same mesothelial origin in lineage tracing experiments, and preadipocytes of mPVAT have a transcriptional profile closer to that of subcutaneous, but not omental preadipocytes (Chau et al., 2014). Also, in this cell lineage analysis, 28% of mature mesenteric adipocytes were Wt1+ positive, suggesting the source of mesenchymal stem cells in mesenteric adipocytes is different from that of BAT, where Wt1 expression is undetectable (Chau et al., 2014). Chang et al. have suggested that mPVAT shares a developmental origin with VSMCs because the deletion of the PPAR γ in VSMCs resulted in a dramatic loss of mPVAT (Chang et al., 2012).

DIFFERENT SECRETOME OF PERIVASCULAR ADIPOSE TISSUES

Adipose tissue is capable to synthesize and secrete various substances just as endocrine cells do. In this sense, adipose tissue is the largest endocrine organ, and more than 600 hundred identified factors produced by adipocytes are collectively termed adipokines or adipocytokines (Halberg et al., 2008; Lehr et al., 2012). Paracrine crosstalk between PVAT and its neighboring artery, also known as "vasocrine" communication, actively regulates vascular inflammation and arterial remodeling (Yudkin et al., 2005). Anatomically distinct PVAT depots can release a quite different range of adipokines. Previous literatures have deeply explored and frequently revisited this topic (Omar et al., 2014; Owen et al., 2014; Akoumianakis et al., 2017; Nosalski and Guzik, 2017; Xia and Li, 2017; Oikonomou and Antoniades, 2019; Chang et al., 2020; Kim et al., 2020). We briefly summarized PVAT-derived adipokines, vascular tone regulators, and newly discovered exosomes/extracellular vesicles in this part. Unlike previous reviews, these factors are categorized by specific PVAT depots where detectable levels are reported (e.g. PCR, Western-blot, or immunostaining).

Pro- and Anti-Inflammatory Adipokines of Perivascular Adipose Tissues

Most PVAT-generated cytokines/chemokines such as tumor necrosis factor (TNF)-α, interleukin-6 (IL-6), plasminogen activator inhibitor-1 (PAI-1), and monocyte chemoattractant protein-1 (MCP-1), are pro-inflammatory and pro-atherosclerotic. Adiponectin is one of the few anti-inflammatory factors that possess multiple salutary effects for cardiovascular disease prevention (Xu and Vanhoutte, 2012). Phenotypic differences between tPVAT and aPVAT are evident that tPVAT generates much less pro-inflammatory cytokines, and is thus resistant to diet-induced inflammation (Police et al., 2009; Fitzgibbons et al., 2011). mPVAT and aPVAT are similarly prone to the expansion of adipocytes and diet-induced inflammation (Li et al., 2019). However, mPVAT is more sensitive to the high-fat diet challenge, where the adipose "browning" genes are dramatically down-regulated (Hou et al., 2016). Previous reviews in this field have elaborated on PVAT-derived adipokines and their interactions with other vascular cells (Brown et al., 2014; Gil-Ortega et al., 2015; Akoumianakis et al., 2017; Kim et al., 2019; Chang et al., 2020). The PVAT-generated representative pro- and anti-inflammatory factors are briefly updated in **Table 2**. Note that one type of adipokine can be generated from multiple sites and at the same time one PVAT can release a variety of adipokines. Members of the same adipokine family (i.e., pro-inflammatory or constricting) all share the same predicted vascular function.

Perivascular Adipose Tissue-Derived Vasodilators and Contracting Factors

Many PVAT-derived factors are also vascular tone regulators. Since the discovery of adipocyte-derived relaxing factor (ADRF) in 2002 (Lohn et al., 2002), understanding of the mechanisms by which PVAT maintains vascular homeostasis has been sought. A wide range of PVAT-derived relaxing factors have been proposed, such as adiponectin (Lynch et al., 2013), prostacyclin (Chang et al., 2012), gaseous molecules (e.g. NO and H_2S) (Szasz and Webb, 2012), methyl palmitate (Lee et al., 2011), angiotensin 1–7 (Lee et al., 2009), and omentin (Yamawaki et al., 2010). Potential contracting candidates include angiotensin II (Lu et al., 2010), endothelin-1 (Almabrouk et al., 2014; Tano et al., 2014), and resistin (Small et al., 2019) released by adipocytes. Depending on PVAT location and different circumstances, some factors including H_2S (Lucchesi et al., 2005), leptin, TNF-α, IL-6, and apelin may act as either vasorelaxant or constricting factors (Maenhaut and Van de Voorde, 2011). For example, leptin could induce vasodilation to modulate blood pressure homeostasis (Fruhbeck, 1999; Lembo et al., 2000); however, obesity-induced hyperleptinemia resulted in an increase of

TABLE 2 | PVAT-generated autocrine and paracrine factors.

	Anti-inflammatory factors	Pro-inflammatory factors
cPVAT	Adiponectin Iacobellis et al. (2005), Cheng et al. (2008), Chatterjee et al. (2009), Spiroglou et al. (2010) Omentin Gaborit et al. (2015) IL-10 Gruzdeva et al. (2019), Numaguchi et al. (2019)	MCP-1 (CCL2), IL-8, IL-6, Leptin, MIP-1α (CCL3) Chatterjee et al. (2009) TNF-α, IL-1β Mazurek et al. (2003) IL-13 Vianello et al. (2019) Visfatin, TNF-α Cheng et al. (2008) Chemerin, Vispin Spiroglou et al. (2010) Apelin Toczylowski et al. (2019) Plasminogen activator inhibitor-1, Resistin Langheim et al. (2010)
tPVAT	Adiponectin Chatterjee et al. (2009) IL-10, IL-4 Dobrian et al. (2015)	IL-6, TNF-α, RANTES (CCL5), MCP-1 (CCL2) Manka et al. (2014), Xiong et al. (2018) IL-17A Smith et al. (2010) IL12p40, CXCL10, CX3CL1, CCL2, CXCL16 Dobrian et al. (2015) Leptin Chatterjee et al. (2009) Resistin Jung et al. (2006) Visfatin Wang et al. (2009)
aPVAT	Adiponectin Kostopoulos et al. (2014), Horimatsu et al. (2018) IL-10 (Sakamoto et al. (2014)	IL-1, IL-6 Lohmann et al. (2009) MIP-1α (CCL3) Moos et al. (2005) RANTES Sakamoto et al. (2014) IL-8, MCP-1Henrichot et al. (2005) Leptin Police et al. (2009) Platelet-derived growth factor-D Zhang et al. (2018) Resistin and visfatin Spiroglou et al. (2010), Park et al. (2014) Chemerin Spiroglou et al. 2010)
White PVAT (mesenteric, femoral, common carotid)	Adiponectin Schmid et al. (2011), Weston et al. (2013) IL-10 Kassan et al. (2011)	IFN-γ, IL-17 Smith et al. (2010) MCP-1, TNF-α, IL-6, Plasminogen activator inhibitor-1 Takaoka et al. (2010) CCL2, CCL5 and CX3CL1, IL-1β, MIP-1α Lohmann et al. (2009)

CX3CL1, C-X3-C motif chemokine ligand 1; CXCL10, C-X-C motif chemokine ligand 10; CXCL16, C-X-C motif chemokine ligand 16; IFN-γ, Interferon-γ; IL, interleukin; MCP-1 (CCL2), monocyte chemoattractant protein-1 (C-C motif chemokine ligand 2); MIP-1α (CCL3), macrophage inflammatory protein-1α (C-C motif chemokine ligand 3); RANTES (CCL5), Regulated upon activation, normal T cell expressed and presumably secreted (C-C motif chemokine ligand 5); TNF-α, Tumor necrosis factor-α.

TABLE 3 | PVAT-derived relaxing and contracting factors.

	Relaxing factors	Contracting factors
cPVAT	Omentin Greulich et al. (2013) Adrenomedullin Iacobellis et al. (2009), Silaghi et al. (2007) Ang 1–7 Patel et al. (2016)	Angiotensinogen Calpastatin Owen et al. (2013)
tPVAT	NO Xia et al. (2016) Prostacyclin Awata et al. (2019) H_2O_2 Gao et al. (2007) Palmitic acid methyl ester Lee et al. (2011) H_2S Fang et al., 2009, Kohn et al. (2012) Leptin Fortuno et al. (2002), Lembo et al. (2000) C1q/tumor necrosis factor-related protein 9 (CTRP9)Han et al. (2018) Ang 1–7 Lee et al. (2009)	Angiotensinogen, chymase, Ang I Galvez-Prieto et al. (2008) Angiotensin II (Lee et al., 2011) Thromboxane A_2 Meyer et al. (2013)
aPVAT	Adiponectin, Apelin Kostopoulos et al. (2014) Prostacyclin Chang et al. (2012)	Angiotensinogen Yasue et al. (2010)
mPVAT	Adiponectin Lynch et al. (2013), Weston et al. (2013), Withers et al. (2014) NO Gil-Ortega et al. (2010), Kassan et al. (2011) H_2O_2 from browning mPVAT (Friederich-Persson et al., 2017) H_2S Schleifenbaum et al. (2010) Noradrenaline via activation of β3-adrenoceptors Saxton et al. (2018) Omentin Yamawaki et al. (2010) Chemerin Darios et al. (2016)	Ang II Lu et al. (2010) Superoxide anion Gao et al. (2006) Noradrenaline in α1 adrenoreceptor-dependent manner Ayala-Lopez et al. (2014) Resistin Small et al. (2019)

Ang, angiotensin; H_2O_2, Hydrogen peroxide; H_2S, hydrogen sulfide; NO, nitric oxide.

endothelin-1, which then leads to vasoconstriction (Quehenberger et al., 2002). Some reports have demonstrated that TNF-α causes vascular dilation mediated by NO (Maenhaut and Van de Voorde, 2011) or hydrogen peroxide (Cheranov and Jaggar, 2006) production. On the other hand, TNF-α can also constrict blood vessels by increasing endothelin-1 (Wort et al., 2009) and angiotensinogen levels (Brasier et al., 1996). Based on their principle functions and originating depots, these factors are summarized in **Table 3**.

Perivascular Adipose Tissue-Derived Extracellular Vesicle

Inter-cell and inter-organ signaling within PVAT remain a mystery. Recently, many studies, including our own, have delved deep to identify the messengers conveying the communication between a blood vessel and its surrounding PVAT (Li et al., 2019). Apart from the secretory cytokines and chemokines factors, adipocytes also secrete many types of extracellular vesicles (EVs) (Deng et al., 2009; Ogawa et al., 2010), typically including exosomes and microvesicles. EVs play important roles in intercellular communication by selective packaging of lipids, proteins, and microRNAs (miRNAs) (Valadi et al., 2007; van Niel et al., 2018). Adipose tissue was proved to constitute an essential source of circulating exosomal miRNAs, as a form of adipokine that acts locally or distantly (Thomou et al., 2017). In addition, these EVs could be taken up by neighboring or distant cells to modulate these recipient's functions (Bang et al., 2014; Sun et al., 2016). For instance, adipocyte-derived exosomal miRNAs enable the metabolic regulation of neighboring macrophages (Ogawa et al., 2010; Zhang et al., 2016). Vice versa, macrophages can secrete miRNA-containing exosomes to modulate local adipocyte function (Ying et al., 2017). Similarly, the endothelial-adipocyte interplay was the result of EV-mediated reciprocal trafficking of caveolin 1 (Crewe et al., 2018).

These observations led us to hypothesize that whether PVAT-adipocytes secrete exosomal miRNAs, if so, how they regulate vascular function in the context of obesity. Indeed, we have demonstrated that perivascular adipocytes produce and secrete miRNA-containing EVs, which can be taken up in neighboring VSMCs (Li et al., 2019). One of the most enriched miRNAs in PVAT and PVAT-derived EVs, miR-221-3p, is transported into adjacent VSMCs. The study further provided an EV-miR-221-3p-mediated mechanism by which PVAT triggers an early vascular remodeling in vascular inflammation (Li et al., 2019). In another study, increased miR-221/222 in the arteries promoted neointimal hyperplasia in the femoral artery following wire injury (Lightell et al., 2018).

CONCLUSION

Anatomically distinct PVATs vary in developmental origin, cellular composition, and secretome. The farther away a PVAT is from the heart, the more white-like the adipocytes are. This is true even in the same stem aorta but wrapped with distinct PVATs in the chest cage and the abdominal cavity. PVAT progenitor cells include but may not be limited to mural cells (pericyte or smooth muscle cells) and fibroblasts. These potential progenitors give rise to committed preadipocytes and contribute to adipogenesis. Adipogenesis and angiogenesis appear to co-exist, and preadipocytes and pericytes may co-develop as well, which should be further studied. The developmental trajectory of PVAT adipocytes is somehow still a "bloody mess" (Rosen and Spiegelman, 2014).

Adipocytes and their neighboring vascular cells constitute a perivascular microenvironment. In an inflammatory setting, a family of intercellular message-conveying machinery is involved in these cells' interplay. Perivascular adipocytes, partially via alteration of their secretome, modulate the nearby VSMCs (Miao and Li, 2012) and endothelial cells (Sena et al., 2017). For obesity, secretion of anti-inflammatory adiponectin is markedly reduced, whereas the generation of pro-inflammatory cytokines is dramatically elevated. Besides, the contiguity with adventitia makes it plausible that paracrine or vasocrine crosstalks between PVAT and the encircled blood vessel are reciprocal and bidirectional.

The continuing worldwide upsurge in obesity prompts us to unveil PVAT's significant role in vascular function. A better understanding of regional heterogeneity among PVATs is just a start. PVAT's function and dysfunction in vascular homeostasis and cardiovascular pathogeny remain our long-term tasks to pursue. Developmental fate mapping is an essential technique for answering some of these questions. Single-cell techniques have empowered this process by helping draw sophisticated cellular atlas. Some researchers have explored the heterogeneity of PVAT at a single-cell level and uncovered distinct clusters with specific signature markers and signaling pathways (Angueira et al., 2021). Creating a more precise map of such a complex tissue from single-cell sequencing data is, therefore, a challenging task, which on the other hand, opens an opportunity for us to dive into this unknown.

AUTHOR CONTRIBUTIONS

XL and YZ conceived the design and concepts. XL and YZ wrote the manuscript. ZM contributed key information for tables and figures. All authors contributed to the article and approved the submitted version.

FUNDING

This work was supported by the Macau FDCT grants (0123/2020/A to XL) and (0007/2019/AKP, 033/2017/AMJ, and 0067/2018/A2 to YZ).

REFERENCES

Akoumianakis, I., Tarun, A., and Antoniades, C. (2017). Perivascular Adipose Tissue as a Regulator of Vascular Disease Pathogenesis: Identifying Novel Therapeutic Targets. *Br. J. Pharmacol.* 174, 3411–3424. doi:10.1111/bph.13666

Alberti, K. G. M. M., Eckel, R. H., Grundy, S. M., Zimmet, P. Z., Cleeman, J. I., Donato, K. A., et al. (2009). Harmonizing the Metabolic Syndrome: A Joint Interim Statement of the International Diabetes Federation Task Force on Epidemiology and Prevention; National Heart, Lung, and Blood Institute; American Heart Association; World Heart Federation; International Atherosclerosis Society; and Interna. *Circulation* 120, 1640–1645. doi:10.1161/circulationaha.109.192644

Almabrouk, T. A. M., Ewart, M. A., Salt, I. P., and Kennedy, S. (2014). Perivascular Fat, AMP -Activated Protein Kinase and Vascular Diseases. *Br. J. Pharmacol.* 171, 595–617. doi:10.1111/bph.12479

Angueira, A. R., Sakers, A. P., Holman, C. D., Cheng, L., Arbocco, M. N., Shamsi, F., et al. (2021). Defining the Lineage of Thermogenic Perivascular Adipose Tissue. *Nat. Metab.* 3, 469–484. doi:10.1038/s42255-021-00380-0

Angueira, A. R., Shapira, S. N., Ishibashi, J., Sampat, S., Sostre-Colón, J., Emmett, M. J., et al. (2020). Early B Cell Factor Activity Controls Developmental and Adaptive Thermogenic Gene Programming in Adipocytes. *Cell Rep.* 30, 2869–2878. doi:10.1016/j.celrep.2020.02.023

Awata, W. M. C., Gonzaga, N. A., Borges, V. F., Silva, C. B. P., Tanus-Santos, J. E., Cunha, F. Q., et al. (2019). Perivascular Adipose Tissue Contributes to Lethal Sepsis-Induced Vasoplegia in Rats. *Eur. J. Pharmacol.* 863, 172706. doi:10.1016/j.ejphar.2019.172706

Ayala-Lopez, N., Martini, M., Jackson, W. F., Darios, E., Burnett, R., Seitz, B., et al. (2014). Perivascular Adipose Tissue Contains Functional Catecholamines. *Pharmacol. Res. Perspect.* 2, e00041. doi:10.1002/prp2.41

Bang, C., Batkai, S., Dangwal, S., Gupta, S. K., Foinquinos, A., Holzmann, A., et al. (2014). Cardiac Fibroblast-Derived microRNA Passenger Strand-Enriched Exosomes Mediate Cardiomyocyte Hypertrophy. *J. Clin. Invest.* 124, 2136–2146. doi:10.1172/jci70577

Berry, R., and Rodeheffer, M. S. (2013). Characterization of the Adipocyte Cellular Lineage *In Vivo*. *Nat. Cel Biol* 15, 302–308. doi:10.1038/ncb2696

Boa, B. C. S., Yudkin, J. S., van Hinsbergh, V. W. M., Bouskela, E., and Eringa, E. C. (2017). Exercise Effects on Perivascular Adipose Tissue: Endocrine and Paracrine Determinants of Vascular Function. *Br. J. Pharmacol.* 174, 3466–3481. doi:10.1111/bph.13732

Brasier, A. R., Li, J., and Wimbish, K. A. (1996). Tumor Necrosis Factor Activates Angiotensinogen Gene Expression by the Rel A Transactivator. *Hypertension* 27, 1009–1017. doi:10.1161/01.hyp.27.4.1009

Britton, K. A., Pedley, A., Massaro, J. M., Corsini, E. M., Murabito, J. M., Hoffmann, U., et al. (2012). Prevalence, Distribution, and Risk Factor Correlates of High Thoracic Periaortic Fat in the Framingham Heart Study. *J. Am. Heart Assoc.* 1, e004200. doi:10.1161/jaha.112.004200

Brown, N. K., Zhou, Z., Zhang, J., Zeng, R., Wu, J., Eitzman, D. T., et al. (2014). Perivascular Adipose Tissue in Vascular Function and Disease. *Arterioscler Thromb. Vasc. Biol.* 34, 1621–1630. doi:10.1161/atvbaha.114.303029

Bussey, C. E., Withers, S. B., Aldous, R. G., Edwards, G., and Heagerty, A. M. (2016). Obesity-Related Perivascular Adipose Tissue Damage is Reversed by Sustained Weight Loss in the Rat.*Arterioscler. Thromb. Vasc. Biol.* 36, 1377–1385. doi:10.1161/atvbaha.116.307210

Bussey, C. E., Withers, S. B., Saxton, S. N., Bodagh, N., Aldous, R. G., and Heagerty, A. M. (2018). β3 -Adrenoceptor Stimulation of Perivascular Adipocytes Leads to Increased Fat Cell-Derived NO and Vascular Relaxation in Small Arteries. *Br. J. Pharmacol.* 175, 3685–3698. doi:10.1111/bph.14433

Caesar, R., Manieri, M., Kelder, T., Boekschoten, M., Evelo, C., Müller, M., et al. (2010). A Combined Transcriptomics and Lipidomics Analysis of Subcutaneous, Epididymal and Mesenteric Adipose Tissue Reveals Marked Functional Differences. *PLoS One* 5, e11525. doi:10.1371/journal.pone.0011525

Cattaneo, P., Mukherjee, D., Spinozzi, S., Zhang, L., Larcher, V., Stallcup, W. B., et al. (2020). Parallel Lineage-Tracing Studies Establish Fibroblasts as the Prevailing *In Vivo* Adipocyte Progenitor. *Cell Rep.* 30, 571–582. doi:10.1016/j.celrep.2019.12.046

Chang, L., Garcia-Barrio, M. T., and Chen, Y. E. (2020). Perivascular Adipose Tissue Regulates Vascular Function by Targeting Vascular Smooth Muscle Cells. *Arterioscler. Thromb. Vasc. Biol.* 40, 1094–1109. doi:10.1161/atvbaha.120.312464

Chang, L., Villacorta, L., Li, R., Hamblin, M., Xu, W., Dou, C., et al. (2012). Loss of Perivascular Adipose Tissue on Peroxisome Proliferator-Activated Receptor-γ Deletion in Smooth Muscle Cells Impairs Intravascular Thermoregulation and Enhances Atherosclerosis. *Circulation* 126, 1067–1078. doi:10.1161/circulationaha.112.104489

Chatterjee, T. K., Aronow, B. J., Tong, W. S., Manka, D., Tang, Y., Bogdanov, V. Y., et al. (2013). Human Coronary Artery Perivascular Adipocytes Overexpress Genes Responsible for Regulating Vascular Morphology, Inflammation, and Hemostasis. *Physiol. Genomics* 45, 697–709. doi:10.1152/physiolgenomics.00042.2013

Chatterjee, T. K., Stoll, L. L., Denning, G. M., Harrelson, A., Blomkalns, A. L., Idelman, G., et al. (2009). Proinflammatory Phenotype of Perivascular Adipocytes. *Circ. Res.* 104, 541–549. doi:10.1161/circresaha.108.182998

Chau, Y.-Y., Bandiera, R., Serrels, A., Martínez-Estrada, O. M., Qing, W., Lee, M., et al. (2014). Visceral and Subcutaneous Fat Have Different Origins and Evidence Supports a Mesothelial Source. *Nat. Cell Biol.* 16, 367–375. doi:10.1038/ncb2922

Chechi, K., Voisine, P., Mathieu, P., Laplante, M., Bonnet, S., Picard, F., et al. (2017). Functional Characterization of the Ucp1-Associated Oxidative Phenotype of Human Epicardial Adipose Tissue. *Sci. Rep.* 7, 15566. doi:10.1038/s41598-017-15501-7

Cheng, K.-H., Chu, C.-S., Lee, K.-T., Lin, T.-H., Hsieh, C.-C., Chiu, C.-C., et al. (2008). Adipocytokines and Proinflammatory Mediators From Abdominal and Epicardial Adipose Tissue in Patients With Coronary Artery Disease. *Int. J. Obes.* 32, 268–274. doi:10.1038/sj.ijo.0803726

Cheranov, S. Y., and Jaggar, J. H. (2006). TNF-alpha Dilates Cerebral Arteries via NAD(P)H Oxidase-Dependent Ca2+ Spark Activation. *Am. J. Physiol. Cell Physiol.* 290, C964–C971. doi:10.1152/ajpcell.00499.2005

Contreras, G. A., Thelen, K., Ayala-Lopez, N., and Watts, S. W. (2016). The Distribution and Adipogenic Potential of Perivascular Adipose Tissue Adipocyte Progenitors is Dependent on Sexual Dimorphism and Vessel Location. *Physiol. Rep.* 4, e12993. doi:10.14814/phy2.12993

Crewe, C., Joffin, N., Rutkowski, J. M., Kim, M., Zhang, F., Towler, D. A., et al. (2018). An Endothelial-to-Adipocyte Extracellular Vesicle Axis Governed by Metabolic State. *Cell* 175, 695–708. doi:10.1016/j.cell.2018.09.005

Darios, E. S., Winner, B. M., Charvat, T., Krasinksi, A., Punna, S., and Watts, S. W. (2016). The Adipokine Chemerin Amplifies Electrical Field-Stimulated Contraction in the Isolated Rat superior Mesenteric Artery. *Am. J. Physiol. Heart Circ. Physiol.* 311, H498–H507. doi:10.1152/ajpheart.00998.2015

Deng, Z.-b., Poliakov, A., Hardy, R. W., Clements, R., Liu, C., Liu, Y., et al. (2009). Adipose Tissue Exosome-Like Vesicles Mediate Activation of Macrophage-Induced Insulin Resistance. *Diabetes* 58, 2498–2505. doi:10.2337/db09-0216

Dobrian, A. D., Hatcher, M. A., Brotman, J. J., Galkina, E. V., Taghavie-Moghadam, P., Pei, H., et al. (2015). STAT4 Contributes to Adipose Tissue Inflammation and Atherosclerosis. *J. Endocrinol.* 227, 13–24. doi:10.1530/joe-15-0098

Drosos, I., Chalikias, G., Pavlaki, M., Kareli, D., Epitropou, G., Bougioukas, G., et al. (2016). Differences Between Perivascular Adipose Tissue Surrounding the Heart and the Internal Mammary Artery: Possible Role for the Leptin-Inflammation-Fibrosis-Hypoxia axis. *Clin. Res. Cardiol.* 105, 887–900. doi:10.1007/s00392-016-0996-7

Fang, L., Zhao, J., Chen, Y., Ma, T., Xu, G., Tang, C., et al. (2009). Hydrogen Sulfide Derived From Periadventitial Adipose Tissue is a Vasodilator. *J. Hypertens.* 27, 2174–2185. doi:10.1097/hjh.0b013e328330a900

Fernández-Alfonso, M. S., Gil-Ortega, M., Aranguez, I., Souza, D., Dreifaldt, M., Somoza, B., et al. (2017). Role of PVAT in Coronary Atherosclerosis and Vein Graft Patency: Friend or Foe? *Br. J. Pharmacol.* 174, 3561–3572. doi:10.1111/bph.13734

Fitzgibbons, T. P., Kogan, S., Aouadi, M., Hendricks, G. M., Straubhaar, J., and Czech, M. P. (2011). Similarity of Mouse Perivascular and Brown Adipose Tissues and Their Resistance to Diet-Induced Inflammation. *Am. J. Physiol. Heart Circ. Physiol.* 301, H1425–H1437. doi:10.1152/ajpheart.00376.2011

Fortuño, A., Rodríguez, A., Gómez-Ambrosi, J., Muñiz, P., Salvador, J., Díez, J., et al. (2002). Leptin Inhibits Angiotensin II-Induced Intracellular Calcium Increase and Vasoconstriction in the Rat Aorta. *Endocrinology* 143, 3555–3560. doi:10.1210/en.2002-220075

Friederich-Persson, M., Nguyen Dinh Cat, A., Persson, P., Montezano, A. C., and Touyz, R. M. (2017). Brown Adipose Tissue Regulates Small Artery Function through NADPH Oxidase 4-Derived Hydrogen Peroxide and Redox-Sensitive Protein Kinase G-1α. *Arterioscler Thromb. Vasc. Biol.* 37, 455–465. doi:10.1161/atvbaha.116.308659

Fruhbeck, G. (1999). Pivotal Role of Nitric Oxide in the Control of Blood Pressure after Leptin Administration. *Diabetes* 48, 903–908. doi:10.2337/diabetes.48.4.903

Fu, M., Xu, L., Chen, X., Han, W., Ruan, C., Li, J., et al. (2019). Neural Crest Cells Differentiate into Brown Adipocytes and Contribute to Periaortic Arch Adipose Tissue Formation. *Arterioscler. Thromb. Vasc. Biol.* 39, 1629–1644. doi:10.1161/atvbaha.119.312838

Gaborit, B., Venteclef, N., Ancel, P., Pelloux, V., Gariboldi, V., Leprince, P., et al. (2015). Human Epicardial Adipose Tissue Has a Specific Transcriptomic Signature Depending on its Anatomical Peri-Atrial, Peri-Ventricular, or Peri-Coronary Location. *Cardiovasc. Res.* 108, 62–73. doi:10.1093/cvr/cvv208

Gálvez, B., de Castro, J., Herold, D., Dubrovska, G., Arribas, S., González, M. C., et al. (2006). Perivascular Adipose Tissue and Mesenteric Vascular Function in Spontaneously Hypertensive Rats. *Arterioscler Thromb. Vasc. Biol.* 26, 1297–1302. doi:10.1161/01.ATV.0000220381.40739.dd

Gálvez-Prieto, B., Bolbrinker, J., Stucchi, P., de Las Heras, A. I., Merino, B., Arribas, S., et al. (2008). Comparative Expression Analysis of the Renin-Angiotensin System Components Between White and Brown Perivascular Adipose Tissue. *J. Endocrinol.* 197, 55–64. doi:10.1677/joe-07-0284

Gao, Y.-J., Lu, C., Su, L.-Y., Sharma, A. M., and Lee, R. M. K. W. (2007). Modulation of Vascular Function by Perivascular Adipose Tissue: the Role of Endothelium and Hydrogen Peroxide. *Br. J. Pharmacol.* 151, 323–331. doi:10.1038/sj.bjp.0707228

Gao, Y., Takemori, K., Su, L., An, W., Lu, C., Sharma, A., et al. (2006). Perivascular Adipose Tissue Promotes Vasoconstriction: the Role of Superoxide Anion. *Cardiovasc. Res.* 71, 363–373. doi:10.1016/j.cardiores.2006.03.013

Gil-Ortega, M., Somoza, B., Huang, Y., Gollasch, M., and Fernández-Alfonso, M. S. (2015). Regional Differences in Perivascular Adipose Tissue Impacting Vascular Homeostasis. *Trends Endocrinol. Metab.* 26, 367–375. doi:10.1016/j.tem.2015.04.003

Gil-Ortega, M., Stucchi, P., Guzmán-Ruiz, R., Cano, V., Arribas, S., González, M. C., et al. (2010). Adaptative Nitric Oxide Overproduction in Perivascular Adipose Tissue During Early Diet-Induced Obesity. *Endocrinology* 151, 3299–3306. doi:10.1210/en.2009-1464

Greulich, S., Chen, W. J., Maxhera, B., Rijzewijk, L. J., van der Meer, R. W., Jonker, J. T., et al. (2013). Cardioprotective Properties of Omentin-1 in Type 2 Diabetes: Evidence from Clinical and *In Vitro* Studies. *PloS one* 8, e59697. doi:10.1371/journal.pone.0059697

Grundy, S. M. (2012). Pre-Diabetes, Metabolic Syndrome, and Cardiovascular Risk. *J. Am. Coll. Cardiol.* 59, 635–643. doi:10.1016/j.jacc.2011.08.080

Gruzdeva, O., Uchasova, E., Dyleva, Y., Borodkina, D., Akbasheva, O., Antonova, L., et al. (2019). Adipocytes Directly Affect Coronary Artery Disease Pathogenesis via Induction of Adipokine and Cytokine Imbalances. *Front. Immunol.* 10, 2163. doi:10.3389/fimmu.2019.02163

Guimarães-Camboa, N., Cattaneo, P., Sun, Y., Moore-Morris, T., Gu, Y., Dalton, N. D., et al. (2017). Pericytes of Multiple Organs do not Behave as Mesenchymal Stem Cells *In Vivo*. *Cell Stem Cell* 20, 345–359. doi:10.1016/j.stem.2016.12.006

Gupta, R. K., Mepani, R. J., Kleiner, S., Lo, J. C., Khandekar, M. J., Cohen, P., et al. (2012). Zfp423 Expression Identifies Committed Preadipocytes and Localizes to Adipose Endothelial and Perivascular Cells. *Cell Metab.* 15, 230–239. doi:10.1016/j.cmet.2012.01.010

Halberg, N., Wernstedt-Asterholm, I., and Scherer, P. E. (2008). The Adipocyte as an Endocrine Cell. *Endocrinol. Metab. Clin. North America* 37, 753–768. doi:10.1016/j.ecl.2008.07.002

Han, F., Zhang, Y., Shao, M., Mu, Q., Jiao, X., Hou, N., et al. (2018). C1q/TNF-related Protein 9 Improves the Anti-contractile Effects of Perivascular Adipose Tissue via the AMPK-eNOS Pathway in Diet-Induced Obese Mice. *Clin. Exp. Pharmacol. Physiol.* 45, 50–57. doi:10.1111/1440-1681.12851

Henrichot, E., Juge-Aubry, C. E., Pernin, A., Pache, J.-C., Velebit, V., Dayer, J.-M., et al. (2005). Production of Chemokines by Perivascular Adipose Tissue. *Arterioscler. Thromb. Vasc. Biol.* 25, 2594–2599. doi:10.1161/01.atv.0000188508.40052.35

Hepler, C., Vishvanath, L., and Gupta, R. K. (2017). Sorting Out Adipocyte Precursors and Their Role in Physiology and Disease. *Genes Dev.* 31, 127–140. doi:10.1101/gad.293704.116

Hildebrand, S., Stumer, J., and Pfeifer, A. (2018). PVAT and its Relation to Brown, Beige, and White Adipose Tissue in Development and Function. *Front. Physiol.* 9, 70. doi:10.3389/fphys.2018.00070

Horimatsu, T., Patel, A. S., Prasad, R., Reid, L. E., Benson, T. W., Zarzour, A., et al. (2018). Remote Effects of Transplanted Perivascular Adipose Tissue on Endothelial Function and Atherosclerosis. *Cardiovasc. Drugs Ther.* 32, 503–510. doi:10.1007/s10557-018-6821-y

Hou, N., Liu, Y., Han, F., Wang, D., Hou, X., Hou, S., et al. (2016). Irisin Improves Perivascular Adipose Tissue Dysfunction via Regulation of the Heme Oxygenase-1/Adiponectin Axis in Diet-Induced Obese Mice. *J. Mol. Cell. Cardiol.* 99, 188–196. doi:10.1016/j.yjmcc.2016.09.005

Iacobellis, G., Pistilli, D., Gucciardo, M., Leonetti, F., Miraldi, F., Brancaccio, G., et al. (2005). Adiponectin Expression in Human Epicardial Adipose Tissue *In Vivo* is Lower in Patients With Coronary Artery Disease. *Cytokine* 29, 251–255. doi:10.1016/j.cyto.2004.11.002

Iacobellis, G., di Gioia, C. R., Di Vito, M., Petramala, L., Cotesta, D., De Santis, V., et al. (2009). Epicardial Adipose Tissue and Intracoronary Adrenomedullin Levels in Coronary Artery Disease. *Horm. Metab. Res.* 41, 855–860. doi:10.1055/s-0029-1231081

Iacobellis, G. (2009). Epicardial and Pericardial Fat: Close, But Very Different. *Obesity (Silver Spring)* 17, 625. doi:10.1038/oby.2008.575

Jaacks, L. M., Vandevijvere, S., Pan, A., McGowan, C. J., Wallace, C., Imamura, F., et al. (2019). The Obesity Transition: Stages of the Global Epidemic. *Lancet Diabetes Endocrinol.* 7, 231–240. doi:10.1016/s2213-8587(19)30026-9

Jung, H., Park, K., Cho, Y., Chung, S., Cho, H., Cho, S., et al. (2006). Resistin is Secreted From Macrophages in Atheromas and Promotes Atherosclerosis. *Cardiovasc. Res.* 69, 76–85. doi:10.1016/j.cardiores.2005.09.015

Kassan, M., Galan, M., Partyka, M., Trebak, M., and Matrougui, K. (2011). Interleukin-10 Released by CD4 + CD25 + Natural Regulatory T Cells Improves Microvascular Endothelial Function Through Inhibition of NADPH Oxidase Activity in Hypertensive Mice. *Arterioscler Thromb. Vasc. Biol.* 31, 2534–2542. doi:10.1161/atvbaha.111.233262

Kim, H. W., Belin de Chantemèle, E. J., and Weintraub, N. L. (2019). Perivascular Adipocytes in Vascular Disease. *Arterioscler. Thromb. Vasc. Biol.* 39, 2220–2227. doi:10.1161/atvbaha.119.312304

Kim, H. W., Shi, H., Winkler, M. A., Lee, R., and Weintraub, N. L. (2020). Perivascular Adipose Tissue and Vascular Perturbation/Atherosclerosis. *Arterioscler. Thromb. Vasc. Biol.* 40, 2569–2576. doi:10.1161/atvbaha.120.312470

Kohn, C., Schleifenbaum, J., Szijarto, I. A., Marko, L., Dubrovska, G., Huang, Y., et al. (2012). Differential Effects of Cystathionine-Gamma-Lyase-Dependent Vasodilatory H2S in Periadventitial Vasoregulation of Rat and Mouse Aortas. *PLoS One* 7, e41951. doi:10.1371/journal.pone.0041951

Kostopoulos, C. G., Spiroglou, S. G., Varakis, J. N., Apostolakis, E., and Papadaki, H. H. (2014). Adiponectin/T-Cadherin and Apelin/APJ Expression in Human Arteries and Periadventitial Fat: Implication of Local Adipokine Signaling in Atherosclerosis? *Cardiovasc. Pathol.* 23, 131–138. doi:10.1016/j.carpath.2014.02.003

Langheim, S., Dreas, L., Veschini, L., Maisano, F., Foglieni, C., Ferrarello, S., et al. (2010). Increased Expression and Secretion of Resistin in Epicardial Adipose Tissue of Patients With Acute Coronary Syndrome. *Am. J. Physiol. Heart Circul. Physiol.* 298, H746–H753. doi:10.1152/ajpheart.00617.2009

Lee, R. M., Lu, C., Su, L.-Y., and Gao, Y.-J. (2009). Endothelium-Dependent Relaxation Factor Released by Perivascular Adipose Tissue. *J. Hypertens.* 27, 782–790. doi:10.1097/hjh.0b013e328324ed86

Lee, Y.-C., Chang, H.-H., Chiang, C.-L., Liu, C.-H., Yeh, J.-I., Chen, M.-F., et al. (2011). Role of Perivascular Adipose Tissue-Derived Methyl Palmitate in Vascular Tone Regulation and Pathogenesis of Hypertension. *Circulation* 124, 1160–1171. doi:10.1161/circulationaha.111.027375

Lehman, S. J., Massaro, J. M., Schlett, C. L., O'Donnell, C. J., Hoffmann, U., and Fox, C. S. (2010). Peri-aortic Fat, Cardiovascular Disease Risk Factors, and Aortic Calcification: the Framingham Heart Study. *Atherosclerosis* 210, 656–661. doi:10.1016/j.atherosclerosis.2010.01.007

Lehr, S., Hartwig, S., Lamers, D., Famulla, S., Müller, S., Hanisch, F.-G., et al. (2012). Identification and Validation of Novel Adipokines Released from

Primary Human Adipocytes. *Mol. Cell Proteomics* 11, 010504. doi:10.1074/mcp.m111.010504

Lembo, G., Vecchione, C., Fratta, L., Marino, G., Trimarco, V., d'Amati, G., et al. (2000). Leptin Induces Direct Vasodilation Through Distinct Endothelial Mechanisms. *Diabetes* 49, 293–297. doi:10.2337/diabetes.49.2.293

Li, X., Ballantyne, L. L., Yu, Y., and Funk, C. D. (2019). Perivascular Adipose Tissue-Derived Extracellular Vesicle miR-221-3p Mediates Vascular Remodeling. *FASEB J.* 33, 12704–12722. doi:10.1096/fj.201901548r

Lightell, D. J., Jr., Moss, S. C., and Woods, T. C. (2018). Upregulation of miR-221 and -222 in Response to Increased Extracellular Signal-Regulated Kinases 1/2 Activity Exacerbates Neointimal Hyperplasia in Diabetes Mellitus. *Atherosclerosis* 269, 71–78. doi:10.1016/j.atherosclerosis.2017.12.016

Lohmann, C., Schäfer, N., von Lukowicz, T., Sokrates Stein, M. A., Borén, J., Rütti, S., et al. (2009). Atherosclerotic Mice Exhibit Systemic Inflammation in Periadventitial and Visceral Adipose Tissue, Liver, and Pancreatic Islets. *Atherosclerosis* 207, 360–367. doi:10.1016/j.atherosclerosis.2009.05.004

Löhn, M., Dubrovska, G., Lauterbach, B., Luft, F. C., Gollasch, M., and Sharma, A. M. (2002). Periadventitial Fat Releases a Vascular Relaxing Factor. *FASEB J.* 16, 1057–1063. doi:10.1096/fj.02-0024com

Lu, C., Su, L.-Y., Lee, R. M. K. W., and Gao, Y.-J. (2010). Mechanisms for Perivascular Adipose Tissue-Mediated Potentiation of Vascular Contraction to Perivascular Neuronal Stimulation: the Role of Adipocyte-Derived Angiotensin II. *Eur. J. Pharmacol.* 634, 107–112. doi:10.1016/j.ejphar.2010.02.006

Lu, D., Wang, W., Xia, L., Xia, P., and Yan, Y. (2017). Gene Expression Profiling Reveals Heterogeneity of Perivascular Adipose Tissues Surrounding Coronary and Internal Thoracic Arteries. *Acta Biochim. Biophys. Sin (Shanghai)* 49, 1075–1082. doi:10.1093/abbs/gmx113

Lucchesi, P. A., Belmadani, S., and Matrougui, K. (2005). Hydrogen Peroxide Acts as Both Vasodilator and Vasoconstrictor in the Control of Perfused Mouse Mesenteric Resistance Arteries. *J. Hypertens.* 23, 571–579. doi:10.1097/01.hjh.0000160214.40855.79

Lynch, F. M., Withers, S. B., Yao, Z., Werner, M. E., Edwards, G., Weston, A. H., et al. (2013). Perivascular Adipose Tissue-Derived Adiponectin Activates BK(Ca) Channels to Induce Anticontractile Responses. *Am. J. Physiol. Heart Circ. Physiol.* 304, H786–H795. doi:10.1152/ajpheart.00697.2012

Maenhaut, N., and Van de Voorde, J. (2011). Regulation of Vascular Tone by Adipocytes. *BMC Med.* 9, 25. doi:10.1186/1741-7015-9-25

Manka, D., Chatterjee, T. K., Stoll, L. L., Basford, J. E., Konaniah, E. S., Srinivasan, R., et al. (2014). Transplanted Perivascular Adipose Tissue Accelerates Injury-Induced Neointimal Hyperplasia. *Arterioscler. Thromb. Vasc. Biol.* 34, 1723–1730. doi:10.1161/atvbaha.114.303983

Mazurek, T., Zhang, L., Zalewski, A., Mannion, J. D., Diehl, J. T., Arafat, H., et al. (2003). Human Epicardial Adipose Tissue is a Source of Inflammatory Mediators. *Circulation* 108, 2460–2466. doi:10.1161/01.cir.0000099542.57313.c5

Merrick, D., Sakers, A., Irgebay, Z., Okada, C., Calvert, C., Morley, M. P., et al. (2019). Identification of a Mesenchymal Progenitor Cell Hierarchy in Adipose Tissue. *Science* 364, eaav2501. doi:10.1126/science.aav2501

Meyer, M. R., Fredette, N. C., Barton, M., and Prossnitz, E. R. (2013). Regulation of Vascular Smooth Muscle Tone by Adipose-Derived Contracting Factor. *PLoS One* 8, e79245. doi:10.1371/journal.pone.0079245

Miao, C.-Y., and Li, Z.-Y. (2012). The Role of Perivascular Adipose Tissue in Vascular Smooth Muscle Cell Growth. *Br. J. Pharmacol.* 165, 643–658. doi:10.1111/j.1476-5381.2011.01404.x

Moos, M. P. W., John, N., Gräbner, R., Nossmann, S., Günther, B., Vollandt, R., et al. (2005). The Lamina Adventitia is the Major Site of Immune Cell Accumulation in Standard Chow-Fed Apolipoprotein E-Deficient Mice. *Arterioscler. Thromb. Vasc. Biol.* 25, 2386–2391. doi:10.1161/01.atv.0000187470.31662.fe

Nosalski, R., and Guzik, T. J. (2017). Perivascular Adipose Tissue Inflammation in Vascular Disease. *Br. J. Pharmacol.* 174, 3496–3513. doi:10.1111/bph.13705

Numaguchi, R., Furuhashi, M., Matsumoto, M., Sato, H., Yanase, Y., Kuroda, Y., et al. (2019). Differential Phenotypes in Perivascular Adipose Tissue Surrounding the Internal Thoracic Artery and Diseased Coronary Artery. *J. Am. Heart Assoc.* 8, e011147. doi:10.1161/jaha.118.011147

Ogawa, R., Tanaka, C., Sato, M., Nagasaki, H., Sugimura, K., Okumura, K., et al. (2010). Adipocyte-derived Microvesicles Contain RNA that Is Transported Into Macrophages and Might be Secreted into Blood Circulation. *Biochem. Biophys. Res. Commun.* 398, 723–729. doi:10.1016/j.bbrc.2010.07.008

Oikonomou, E. K., and Antoniades, C. (2019). The Role of Adipose Tissue in Cardiovascular Health and Disease. *Nat. Rev. Cardiol.* 16, 83–99. doi:10.1038/s41569-018-0097-6

Olshansky, S. J., Passaro, D. J., Hershow, R. C., Layden, J., Carnes, B. A., Brody, J., et al. (2005). A Potential Decline in Life Expectancy in the United States in the 21st Century. *N. Engl. J. Med.* 352, 1138–1145. doi:10.1056/nejmsr043743

Omar, A., Chatterjee, T. K., Tang, Y., Hui, D. Y., and Weintraub, N. L. (2014). Proinflammatory Phenotype of Perivascular Adipocytes. *Arterioscler. Thromb. Vasc. Biol.* 34, 1631–1636. doi:10.1161/atvbaha.114.303030

Owen, M. K., Noblet, J. N., Sassoon, D. J., Conteh, A. M., Goodwill, A. G., and Tune, J. D. (2014). Perivascular Adipose Tissue and Coronary Vascular Disease. *Arterioscler. Thromb. Vasc. Biol.* 34, 1643–1649. doi:10.1161/atvbaha.114.303033

Owen, M. K., Witzmann, F. A., McKenney, M. L., Lai, X., Berwick, Z. C., Moberly, S. P., et al. (2013). Perivascular Adipose Tissue Potentiates Contraction of Coronary Vascular Smooth Muscle. *Circulation* 128, 9–18. doi:10.1161/circulationaha.112.001238

Padilla, J., Jenkins, N. T., Vieira-Potter, V. J., and Laughlin, M. H. (2013). Divergent Phenotype of Rat Thoracic and Abdominal Perivascular Adipose Tissues. *Am. J. Physiol. Regul. Integr. Comp. Physiol.* 304, R543–R552. doi:10.1152/ajpregu.00567.2012

Pan, X. X., Cao, J.-M., Cai, F., Ruan, C. C., Wu, F., and Gao, P. J. (2018). Loss of miR-146b-3p Inhibits Perivascular Adipocyte Browning With Cold Exposure During Aging. *Cardiovasc. Drugs Ther.* 32, 511–518. doi:10.1007/s10557-018-6814-x

Pan, X. X., Ruan, C. C., Liu, X. Y., Kong, L. R., Ma, Y., Wu, Q. H., et al. (2019). Perivascular Adipose Tissue-Derived Stromal Cells Contribute to Vascular Remodeling during Aging. *Aging Cell* 18, e12969. doi:10.1111/acel.12969

Park, S. Y., Kim, K. H., Seo, K. W., Bae, J. U., Kim, Y. H., Lee, S. J., et al. (2014). Resistin Derived From Diabetic Perivascular Adipose Tissue Up-regulates Vascular Expression of Osteopontin via the AP -1 Signalling Pathway. *J. Pathol.* 232, 87–97. doi:10.1002/path.4286

Patel, V. B., Basu, R., and Oudit, G. Y. (2016). ACE2/Ang 1-7 Axis: A Critical Regulator of Epicardial Adipose Tissue Inflammation and Cardiac Dysfunction in Obesity. *Adipocyte* 5, 306–311. doi:10.1080/21623945.2015.1131881

Police, S. B., Thatcher, S. E., Charnigo, R., Daugherty, A., and Cassis, L. A. (2009). Obesity Promotes Inflammation in Periaortic Adipose Tissue and Angiotensin II-Induced Abdominal Aortic Aneurysm Formation. *Arterioscler. Thromb. Vasc Biol.* 29, 1458–1464. doi:10.1161/atvbaha.109.192658

Quehenberger, P., Exner, M., Sunder-Plassmann, R., Ruzicka, K., Bieglmayer, C., Endler, G., et al. (2002). Leptin Induces Endothelin-1 in Endothelial Cells *In Vitro*. *Circ. Res.* 90, 711–718. doi:10.1161/01.res.0000014226.74709.90

Rajsheker, S., Manka, D., Blomkalns, A. L., Chatterjee, T. K., Stoll, L. L., and Weintraub, N. L. (2010). Crosstalk Between Perivascular Adipose Tissue and Blood Vessels. *Curr. Opin. Pharmacol.* 10, 191–196. doi:10.1016/j.coph.2009.11.005

Rodeheffer, M. S., Birsoy, K., and Friedman, J. M. (2008). Identification of White Adipocyte Progenitor Cells *In Vivo*. *Cell* 135, 240–249. doi:10.1016/j.cell.2008.09.036

Rosen, E. D., and Spiegelman, B. M. (2014). What we Talk about When we Talk About Fat. *Cell* 156, 20–44. doi:10.1016/j.cell.2013.12.012

Sacks, H. S., Fain, J. N., Bahouth, S. W., Ojha, S., Frontini, A., Budge, H., et al. (2013). Adult Epicardial Fat Exhibits Beige Features. *J. Clin. Endocrinol. Metab.* 98, E1448–E1455. doi:10.1210/jc.2013-1265

Sacks, H. S., Fain, J. N., Holman, B., Cheema, P., Chary, A., Parks, F., et al. (2009). Uncoupling Protein-1 and Related Messenger Ribonucleic Acids in Human Epicardial and Other Adipose Tissues: Epicardial Fat Functioning as Brown Fat. *J. Clin. Endocrinol. Metab.* 94, 3611–3615. doi:10.1210/jc.2009-0571

Sacks, H., and Symonds, M. E. (2013). Anatomical Locations of Human Brown Adipose Tissue: Functional Relevance and Implications in Obesity and Type 2 Diabetes. *Diabetes* 62, 1783–1790. doi:10.2337/db12-1430

Sakamoto, S., Tsuruda, T., Hatakeyama, K., Imamura, T., Asada, Y., and Kitamura, K. (2014). Impact of Age-dependent Adventitia Inflammation on Structural Alteration of Abdominal Aorta in Hyperlipidemic Mice. *PLoS One* 9, e105739. doi:10.1371/journal.pone.0105739

Sanchez-Gurmaches, J., and Guertin, D. A. (2014a). Adipocyte Lineages: Tracing Back the Origins of Fat. *Biochim. Biophys. Acta* 1842, 340–351. doi:10.1016/j.bbadis.2013.05.027

Sanchez-Gurmaches, J., and Guertin, D. A. (2014b). Adipocytes Arise From Multiple Lineages That are Heterogeneously and Dynamically Distributed. *Nat. Commun.* 5, 4099. doi:10.1038/ncomms5099

Sanchez-Gurmaches, J., Hung, C.-M., and Guertin, D. A. (2016). Emerging Complexities in Adipocyte Origins and Identity. *Trends Cell Biol.* 26, 313–326. doi:10.1016/j.tcb.2016.01.004

Sarantopoulos, C. N., Banyard, D. A., Ziegler, M. E., Sun, B., Shaterian, A., and Widgerow, A. D. (2018). Elucidating the Preadipocyte and its Role in Adipocyte Formation: A Comprehensive Review. *Stem Cell Rev. Rep.* 14, 27–42. doi:10.1007/s12015-017-9774-9

Saxton, S. N., Ryding, K. E., Aldous, R. G., Withers, S. B., Ohanian, J., and Heagerty, A. M. (2018). Role of Sympathetic Nerves and Adipocyte Catecholamine Uptake in the Vasorelaxant Function of Perivascular Adipose Tissue. *Arterioscler. Thromb. Vasc. Biol.* 38, 880–891. doi:10.1161/atvbaha.118.310777

Scheen, A. J., and Van Gaal, L. F. (2014). Combating the Dual burden: Therapeutic Targeting of Common Pathways in Obesity and Type 2 Diabetes. *Lancet Diabetes Endocrinol.* 2, 911–922. doi:10.1016/s2213-8587(14)70004-x

Schleifenbaum, J., Köhn, C., Voblova, N., Dubrovska, G., Zavarirskaya, O., Gloe, T., et al. (2010). Systemic Peripheral Artery Relaxation by KCNQ Channel Openers and Hydrogen Sulfide. *J. Hypertens.* 28, 1875–1882. doi:10.1097/hjh.0b013e32833c20d5

Schmid, P. M., Resch, M., Steege, A., Fredersdorf-Hahn, S., Stoelcker, B., Birner, C., et al. (2011). Globular and Full-Length Adiponectin Induce NO-dependent Vasodilation in Resistance Arteries of Zucker Lean But Not Zucker Diabetic Fatty Rats. *Am. J. Hypertens.* 24, 270–277. doi:10.1038/ajh.2010.239

Schwalie, P. C., Dong, H., Zachara, M., Russeil, J., Alpern, D., Akchiche, N., et al. (2018). A Stromal Cell Population That Inhibits Adipogenesis in Mammalian Fat Depots. *Nature* 559, 103–108. doi:10.1038/s41586-018-0226-8

Seale, P., Bjork, B., Yang, W., Kajimura, S., Chin, S., Kuang, S., et al. (2008). PRDM16 Controls a Brown Fat/Skeletal Muscle Switch. *Nature* 454, 961–967. doi:10.1038/nature07182

Sena, C. M., Pereira, A., Fernandes, R., Letra, L., and Seiça, R. M. (2017). Adiponectin Improves Endothelial Function in Mesenteric Arteries of Rats Fed a High-Fat Diet: Role of Perivascular Adipose Tissue. *Br. J. Pharmacol.* 174, 3514–3526. doi:10.1111/bph.13756

Shao, M., Wang, Q. A., Song, A., Vishvanath, L., Busbuso, N. C., Scherer, P. E., et al. (2019). Cellular Origins of Beige Fat Cells Revisited. *Diabetes* 68, 1874–1885. doi:10.2337/db19-0308

Silaghi, A., Achard, V., Paulmyer-Lacroix, O., Scridon, T., Tassistro, V., Duncea, I., et al. (2007). Expression of Adrenomedullin in Human Epicardial Adipose Tissue: Role of Coronary Status. *Am. J. Physiol. Endocrinol. Metab.* 293, E1443–E1450. doi:10.1152/ajpendo.00273.2007

Small, H. Y., McNeilly, S., Mary, S., Sheikh, A. M., and Delles, C. (2019). Resistin Mediates Sex-Dependent Effects of Perivascular Adipose Tissue on Vascular Function in the Shrsp. *Sci. Rep.* 9, 6897. doi:10.1038/s41598-019-43326-z

Smith, E., Prasad, K.-M. R., Butcher, M., Dobrian, A., Kolls, J. K., Ley, K., et al. (2010). Blockade of Interleukin-17A Results in Reduced Atherosclerosis in Apolipoprotein E-Deficient Mice. *Circulation* 121, 1746–1755. doi:10.1161/circulationaha.109.924886

Song, A., Dai, W., Jang, M. J., Medrano, L., Li, Z., Zhao, H., et al. (2020). Low- and High-Thermogenic Brown Adipocyte Subpopulations Coexist in Murine Adipose Tissue. *J. Clin. Invest.* 130, 247–257. doi:10.1172/JCI129167

Sowa, Y., Imura, T., Numajiri, T., Takeda, K., Mabuchi, Y., Matsuzaki, Y., et al. (2013). Adipose Stromal Cells Contain Phenotypically Distinct Adipogenic Progenitors Derived From Neural Crest. *PLoS One* 8, e84206. doi:10.1371/journal.pone.0084206

Spiroglou, S. G., Kostopoulos, C. G., Varakis, J. N., and Papadaki, H. H. (2010). Adipokines in Periaortic and Epicardial Adipose Tissue: Differential Expression and Relation to Atherosclerosis. *J. Atheroscler. Thromb.* 17, 115–130. doi:10.5551/jat.1735

Sun, X., Lin, J., Zhang, Y., Kang, S., Belkin, N., Wara, A. K., et al. (2016). MicroRNA-181b Improves Glucose Homeostasis and Insulin Sensitivity by Regulating Endothelial Function in White Adipose Tissue. *Circ. Res.* 118, 810–821. doi:10.1161/circresaha.115.308166

Szasz, T., and Webb, R. C. (2012). Perivascular Adipose Tissue: More Than Just Structural Support. *Clin. Sci.* 122, 1–12. doi:10.1042/cs20110151

Takaoka, M., Suzuki, H., Shioda, S., Sekikawa, K., Saito, Y., Nagai, R., et al. (2010). Endovascular Injury Induces Rapid Phenotypic Changes in Perivascular Adipose Tissue. *Arterioscler Thromb. Vasc. Biol.* 30, 1576–1582. doi:10.1161/atvbaha.110.207175

Tang, W., Zeve, D., Suh, J. M., Bosnakovski, D., Kyba, M., Hammer, R. E., et al. (2008). White Fat Progenitor Cells Reside in the Adipose Vasculature. *Science* 322, 583–586. doi:10.1126/science.1156232

Tano, J.-Y., Schleifenbaum, J., and Gollasch, M. (2014). Perivascular Adipose Tissue, Potassium Channels, and Vascular Dysfunction. *Arterioscler. Thromb. Vasc. Biol.* 34, 1827–1830. doi:10.1161/atvbaha.114.303032

Thomou, T., Mori, M. A., Dreyfuss, J. M., Konishi, M., Sakaguchi, M., Wolfrum, C., et al. (2017). Adipose-Derived Circulating miRNAs Regulate Gene Expression in Other Tissues. *Nature* 542, 450–455. doi:10.1038/nature21365

Timmons, J. A., Wennmalm, K., Larsson, O., Walden, T. B., Lassmann, T., Petrovic, N., et al. (2007). Myogenic Gene Expression Signature Establishes that Brown and white Adipocytes Originate from Distinct Cell Lineages. *Proc. Natl. Acad. Sci.* 104, 4401–4406. doi:10.1073/pnas.0610615104

Toczylowski, K., Hirnle, T., Harasiuk, D., Zabielski, P., Lewczuk, A., Dmitruk, I., et al. (2019). Plasma Concentration and Expression of Adipokines in Epicardial and Subcutaneous Adipose Tissue are Associated With Impaired Left Ventricular Filling Pattern. *J. Transl. Med.* 17, 310. doi:10.1186/s12967-019-2060-7

Tran, K.-V., Fitzgibbons, T., Min, S. Y., DeSouza, T., and Corvera, S. (2018). Distinct Adipocyte Progenitor Cells Are Associated with Regional Phenotypes of Perivascular Aortic Fat in Mice. *Mol. Metab.* 9, 199–206. doi:10.1016/j.molmet.2017.12.014

Tran, K.-V., Gealekman, O., Frontini, A., Zingaretti, M. C., Morroni, M., Giordano, A., et al. (2012). The Vascular Endothelium of the Adipose Tissue Gives Rise to Both White and Brown Fat Cells. *Cell Metab.* 15, 222–229. doi:10.1016/j.cmet.2012.01.008

Valadi, H., Ekström, K., Bossios, A., Sjöstrand, M., Lee, J. J., and Lötvall, J. O. (2007). Exosome-Mediated Transfer of mRNAs and microRNAs is a Novel Mechanism of Genetic Exchange Between Cells. *Nat. Cell Biol.* 9, 654–659. doi:10.1038/ncb1596

Van de Voorde, J., Pauwels, B., Boydens, C., and Decaluwé, K. (2013). Adipocytokines in Relation to Cardiovascular Disease. *Metabolism* 62, 1513–1521. doi:10.1016/j.metabol.2013.06.004

van Niel, G., D'Angelo, G., and Raposo, G. (2018). Shedding Light on the Cell Biology of Extracellular Vesicles. *Nat. Rev. Mol. Cell Biol.* 19, 213–228. doi:10.1038/nrm.2017.125

Vianello, E., Marrocco-Trischitta Massimiliano, M., Dozio, E., Bandera, F., Tacchini, L., Canciani, E., et al. (2019). Correlational Study on Altered Epicardial Adipose Tissue as a Stratification Risk Factor for Valve Disease Progression through IL-13 Signaling. *J. Mol. Cell. Cardiol.* 132, 210–218. doi:10.1016/j.yjmcc.2019.05.012

Waldén, T. B., Hansen, I. R., Timmons, J. A., Cannon, B., and Nedergaard, J. (2012). Recruited vs. Nonrecruited Molecular Signatures of Brown, "brite," and white Adipose Tissues. *Am. J. Physiol. Endocrinol. Metab.* 302, E19–E31. doi:10.1152/ajpendo.00249.2011

Wang, P., Xu, T.-Y., Guan, Y.-F., Su, D.-F., Fan, G.-R., and Miao, C.-Y. (2009). Perivascular Adipose Tissue-Derived Visfatin Is a Vascular Smooth Muscle Cell Growth Factor: Role of Nicotinamide Mononucleotide. *Cardiovasc. Res.* 81, 370–380. doi:10.1093/cvr/cvn288

Wang, Q. A., Song, A., Chen, W., Schwalie, P. C., Zhang, F., Vishvanath, L., et al. (2018). Reversible De-Differentiation of Mature White Adipocytes Into Preadipocyte-Like Precursors During Lactation. *Cell Metab.* 28, 282–288. doi:10.1016/j.cmet.2018.05.022

Weston, A. H., Egner, I., Dong, Y., Porter, E. L., Heagerty, A. M., and Edwards, G. (2013). Stimulated Release of a Hyperpolarizing Factor (ADHF) From Mesenteric Artery Perivascular Adipose Tissue: Involvement of Myocyte BKCa Channels and Adiponectin. *Br. J. Pharmacol.* 169, 1500–1509. doi:10.1111/bph.12157

Withers, S. B., Simpson, L., Fattah, S., Werner, M. E., and Heagerty, A. M. (2014). cGMP-Dependent Protein Kinase (PKG) Mediates the Anticontractile Capacity of Perivascular Adipose Tissue. *Cardiovasc. Res.* 101, 130–137. doi:10.1093/cvr/cvt229

Wort, S. J., Ito, M., Chou, P.-C., Mc Master, S. K., Badiger, R., Jazrawi, E., et al. (2009). Synergistic Induction of Endothelin-1 by Tumor Necrosis Factor α and Interferon γ Is Due to Enhanced NF-κB Binding and Histone Acetylation at Specific κB Sites. *J. Biol. Chem.* 284, 24297–24305. doi:10.1074/jbc.m109.032524

Xia, N., Horke, S., Habermeier, A., Closs, E. I., Reifenberg, G., Gericke, A., et al. (2016). Uncoupling of Endothelial Nitric Oxide Synthase in Perivascular Adipose Tissue of Diet-Induced Obese Mice. *Arterioscler. Thromb. Vasc. Biol.* 36, 78–85. doi:10.1161/atvbaha.115.306263

Xia, N., and Li, H. (2017). The Role of Perivascular Adipose Tissue in Obesity-Induced Vascular Dysfunction. *Br. J. Pharmacol.* 174, 3425–3442. doi:10.1111/bph.13650

Xiong, W., Zhao, X., Villacorta, L., Rom, O., Garcia-Barrio, M. T., Guo, Y., et al. (2018). Brown Adipocyte-Specific PPARγ (Peroxisome Proliferator-Activated Receptor γ) Deletion Impairs Perivascular Adipose Tissue Development and Enhances Atherosclerosis in Mice. *Arterioscler. Thromb. Vasc. Biol.* 38, 1738–1747. doi:10.1161/atvbaha.118.311367

Xu, A., and Vanhoutte, P. M. (2012). Adiponectin and Adipocyte Fatty Acid Binding Protein in the Pathogenesis of Cardiovascular Disease. *Am. J. Physiol. Heart Circ. Physiol.* 302, H1231–H1240. doi:10.1152/ajpheart.00765.2011

Yamawaki, H., Tsubaki, N., Mukohda, M., Okada, M., and Hara, Y. (2010). Omentin, a Novel Adipokine, Induces Vasodilation in Rat Isolated Blood Vessels. *Biochem. Biophys. Res. Commun.* 393, 668–672. doi:10.1016/j.bbrc.2010.02.053

Yasue, S., Masuzaki, H., Okada, S., Ishii, T., Kozuka, C., Tanaka, T., et al. (2010). Adipose Tissue-Specific Regulation of Angiotensinogen in Obese Humans and Mice: Impact of Nutritional Status and Adipocyte Hypertrophy. *Am. J. Hypertens.* 23, 425–431. doi:10.1038/ajh.2009.263

Ye, M., Ruan, C.-C., Fu, M., Xu, L., Chen, D., Zhu, M., et al. (2019). Developmental and Functional Characteristics of the Thoracic Aorta Perivascular Adipocyte. *Cell. Mol. Life Sci.* 76, 777–789. doi:10.1007/s00018-018-2970-1

Ying, W., Riopel, M., Bandyopadhyay, G., Dong, Y., Birmingham, A., Seo, J. B., et al. (2017). Adipose Tissue Macrophage-Derived Exosomal miRNAs Can Modulate *In Vivo* and *In Vitro* Insulin Sensitivity. *Cell* 171, 372–384. doi:10.1016/j.cell.2017.08.035

Yudkin, J. S., Eringa, E., and Stehouwer, C. D. (2005). "Vasocrine" Signalling from Perivascular Fat: a Mechanism Linking Insulin Resistance to Vascular Disease. *Lancet* 365, 1817–1820. doi:10.1016/s0140-6736(05)66585-3

Zhang, Y., Mei, H., Chang, X., Chen, F., Zhu, Y., and Han, X. (2016). Adipocyte-Derived Microvesicles From Obese Mice Induce M1 Macrophage Phenotype through Secreted miR-155. *J. Mol. Cell Biol.* 8, 505–517. doi:10.1093/jmcb/mjw040

Zhang, Z.-B., Ruan, C.-C., Lin, J.-R., Xu, L., Chen, X.-H., Du, Y.-N., et al. (2018). Perivascular Adipose Tissue-Derived PDGF-D Contributes to Aortic Aneurysm Formation during Obesity. *Diabetes* 67, 1549–1560. doi:10.2337/db18-0098

Conflict of Interest: The authors declare that the research was conducted in the absence of any commercial or financial relationships that could be construed as a potential conflict of interest.

frontiers in Pharmacology

BRIEF RESEARCH REPORT
published: 10 September 2021
doi: 10.3389/fphar.2021.720224

Effects of High-Fat and High-Fat/High-Sucrose Diet-Induced Obesity on PVAT Modulation of Vascular Function in Male and Female Mice

Jamaira A. Victorio[1]*, *Daniele M. Guizoni*[1], *Israelle N. Freitas*[1], *Thiago R. Araujo*[2] and *Ana P. Davel*[1]*

[1]Department of Structural and Functional Biology, Laboratory of Vascular Biology, Institute of Biology, University of Campinas, Campinas, Brazil, [2]Department of Structural and Functional Biology, Obesity and Comorbidities Research Center-OCRC, Institute of Biology, University of Campinas, Campinas, Brazil

Increased adiposity in perivascular adipose tissue (PVAT) has been related to vascular dysfunction. High-fat (HF) diet-induced obesity models are often used to analyze the translational impact of obesity, but differences in sex and Western diet type complicate comparisons between studies. The role of PVAT was investigated in small mesenteric arteries (SMAs) of male and female mice fed a HF or a HF plus high-sucrose (HF + HS) diet for 3 or 5 months and compared them to age/sex-matched mice fed a chow diet. Vascular responses of SMAs without (PVAT-) or with PVAT (PVAT+) were evaluated. HF and HF + HS diets increased body weight, adiposity, and fasting glucose and insulin levels without affecting blood pressure and circulating adiponectin levels in both sexes. HF or HF + HS diet impaired PVAT anticontractile effects in SMAs from females but not males. PVAT-mediated endothelial dysfunction in SMAs from female mice after 3 months of a HF + HS diet, whereas in males, this effect was observed only after 5 months of HF + HS diet. However, PVAT did not impact acetylcholine-induced relaxation in SMAs from both sexes fed HF diet. The findings suggest that the addition of sucrose to a HF diet accelerates PVAT dysfunction in both sexes. PVAT dysfunction in response to both diets was observed early in females compared to age-matched males suggesting a susceptibility of the female sex to PVAT-mediated vascular complications in the setting of obesity. The data illustrate the importance of the duration and composition of obesogenic diets for investigating sex-specific treatments and pharmacological targets for obesity-induced vascular complications.

Keywords: obesity, perivascular adipose tissue, sex differences, resistance arteries, endothelial dysfunction

OPEN ACCESS

Edited by:
Mariarosaria Bucci,
University of Naples Federico II, Italy

Reviewed by:
Sophie Saxton,
University of Manchester, United Kingdom
Tim Murphy,
University of New South Wales, Australia

***Correspondence:**
Ana P. Davel
anadavel@unicamp.br
Jamaira A. Victorio
jamairavictorio@gmail.com

Specialty section:
This article was submitted to Cardiovascular and Smooth Muscle Pharmacology, a section of the journal Frontiers in Pharmacology

Received: *03 June 2021*
Accepted: *13 August 2021*
Published: *10 September 2021*

Citation:
Victorio JA, Guizoni DM, Freitas IN, Araujo TR and Davel AP (2021) Effects of High-Fat and High-Fat/High-Sucrose Diet-Induced Obesity on PVAT Modulation of Vascular Function in Male and Female Mice . Front. Pharmacol. 12:720224. doi: 10.3389/fphar.2021.720224

INTRODUCTION

Excessive body fat storage (i.e., increased intake energy with reduced energy expenditure) is a major feature of obesity. This condition results in chronic low-grade inflammation presenting a more complex resolution and represents a risk factor for the development and/or worsening of several chronic diseases, including cardiovascular diseases (CVDs) (Caballero et al., 2008; World Health Organization, 2019). Over time (1975–2016), the prevalence of obesity has increased in both sexes; however, women have shown a higher prevalence of obesity than men (Abarca-Gómez et al., 2017).

Conversely, men have a higher prevalence of increased blood pressure than women (Zhou et al., 2017). Despite the knowledge of sex-specific differences in the development of obesity and CVDs, few studies have covered obesity-related vascular (dys) function in males and females.

Adipose tissue is recognized as a secretory organ, and its anatomical location may predict modulation of adjacent tissues/organs during the development of obesity (Lim and Meigs, 2014; Vishvanath and Gupta, 2019). Perivascular adipose tissue (PVAT), a fat depot evolving almost all vessels, modulates vascular function, and thus, changes in morphology and vasoactive factors synthesized or secreted by PVAT may result in altered vascular function. Studies have demonstrated that obesity in humans is correlated with an increase in the volume of PVAT (Schlett et al., 2009; Wagner et al., 2012) and results in loss of the PVAT anticontractile effect (Greenstein et al., 2009). Using experimental models of male obesity, several studies have reported an impaired anticontractile effect of PVAT (da Costa et al., 2017; Gil-Ortega et al., 2014; Han et al., 2018; Ma et al., 2010; Withers et al., 2017; Xia et al., 2016; Xu et al., 2012), although an increased PVAT anticontractile effect has also been demonstrated in response to high-calorie diets (Gil-Ortega et al., 2010; Dos Reis Costa et al., 2021). In addition to the controversial data in male obesity experimental models, much less is known about PVAT function in females, especially in the setting of obesity (Victorio et al., 2020). Sexual dimorphism in PVAT immune cell content in response to a high-fat (HF) diet was recently demonstrated (Kumar et al., 2021), but it is still unclear whether obesogenic diets differentially impact PVAT anticontractile function in males and females over time.

Animal models are key tools for understanding and treating obesity comorbidities (Barrett et al., 2016). A HF diet with 45% or 60% of calories from fat is the most commonly used obesogenic diet in rodents. Although 60% fat diets induce a faster and more obese model, a 45% fat diet seems to be more relevant for human physiology (Speakman, 2019). In addition, a diet with 60% fat has less sucrose than a diet with 45% fat, and differences in total sugar and sugar sources may influence cardiovascular outcomes (Xi et al., 2015; Narain et al., 2016). Comparisons between sexes suggest that Western diets (high-fat and high-sucrose diets) eliminate the protective effect of female sex on endothelial function (Hunter et al., 2017; Davel et al., 2018b), but the impact on PVAT control of vascular tone is still unknown. The present study investigated whether two different HF obesogenic diets (60% HF versus 45% HF plus high sucrose) impact PVAT anticontractile function differentially in males and females over time.

METHODS

Animal Model

Male and female C57Bl6/J mice were purchased from the Multidisciplinary Center for Biological Investigation on Laboratory Animal Science of the University of Campinas. Animals were maintained in a room with controlled humidity and temperature (22 ± 2°C) under a 12 h:12 h light/dark cycle and received water and a chow diet (CD) ad libitum. At 2 months of age, the mice were divided to receive CD (3.86 kcal/g), a very HF (60% calories from fat; 5.55 kcal/g) diet, or a HF plus high-sucrose (HF + HS, 45% calories from fat and 30% from sucrose; 4.85 kcal/g) diet purchased from Quimtia© (Colombo, PR, Brazil) and PragSoluções© (Jaú, SP, Brazil), respectively, for a period of 3 or 5 months. Nutritional information for each diet is available in the supplementary material (**Supplementary Table S1**). Measurement of food consumption was performed weekly during the feeding protocol.

This study was approved by the Ethics Committee on Animal Use of the University of Campinas (protocol no. 4914-1/2018, 5474-1/2020) and carried out in accordance with the National Board of Animal Experimentation Control (CONCEA).

Blood Pressure Measurement

Systolic blood pressure (SBP) was assessed via tail-cuff plethysmography (LE5001 Pressure meter, Panlab, Harvard Apparatus, Barcelona, Spain) on the day before tissue collection and vascular function was assessed. Animals were restrained for 2 min before the first SBP measurement, which was considered successful when the mouse did not move, and a clear pulse was observed. Ten sequential measurements from each animal were registered. The SBP is expressed as the average of the ten measurements.

Body Parameters, Tissue Collection, and Biochemical Profile

Final body weight was obtained at each period. The day before tissue collection and vascular study performance and after SBP measurement, fasting glucose was measured in 4 h fasted mice by cutting the tail tip and using OneTouch Ultra® and reactive strips. At the end of each time point in the diet protocol, animals were anesthetized with a superdose of anesthesia (ketamine, 240 mg/kg; xylazine, 30 mg/kg). On the day we conducted the vascular study, blood samples were collected from fed animals by cardiac puncture and centrifuged to obtain serum samples, which were stored at −80°C until analyzing insulin and adiponectin levels. The peritoneal cavity was opened, and the mesenteric bed, perigonadal adipose tissue, and sex organs (testes/uterus) were removed. The fat pads and sex organs were weighed. The mesenteric bed was placed in ice-cold Krebs–Henseleit solution (KHS; in mM: NaCl 115; KCl 4.6; CaCl2·2H2O 2.5; KH2PO4 1.2; MgSO4·7H2O 12.4; NaHCO3 25; glucose 5.5) for vascular study.

Vascular Study

The second- and third-order mesenteric arteries (artery diameter ~130 μm) were dissected in ice-cold KHS. In some segments, adjacent PVAT was left intact (PVAT+), whereas, in others, PVAT was dissected out (PVAT-). Arteries were cut into 1–2 mm rings, mounted on a 20 μm diameter wire in a multichannel myograph (Model 610M, DMT A/S, Aarhus NA, Denmark), and left to equilibrate for at least 20 min before normalization using a standardized procedure (Mulvany and Halpern, 1977; Wenceslau et al., 2021). A normalization protocol that considers the inner circumference and wall tension was performed (Saxton et al., 2018). After normalization, the arteries were left for an additional 20 min equilibration period at 37°C and bubbled at 95% O_2/5% CO_2 to maintain a pH of 7.4. Next, arteries were contracted with 60 mM

KCl twice, first for 3 min following 15 min of equilibration and a second time for 10 min, to establish the maximum contractile response to KCl and confirm that the removal of PVAT did not damage the vascular smooth muscle. The maximum KCl response was similar in arteries with or without PVAT in males and females (**Supplementary Figure S1**). After a 30 min equilibration period, PVAT+ and PVAT- arteries were precontracted (50% of maximum KCl contraction) with phenylephrine (1 μM for PVAT- arteries and 10 μM for PVAT+ arteries); then, concentration-response curves to acetylcholine (0.1 nM–30 μM) were obtained to evaluate endothelium-dependent relaxation. To evaluate the anticontractile effect of PVAT, arteries were contracted with phenylephrine (1 nM–0.1 mM).

MATERIALS

Acetylcholine and phenylephrine were obtained from Sigma-Aldrich (Merck KGaA, Darmstadt, Germany). Salts for KHS were obtained from Labsynth (Diadema, Brazil). A mouse insulin ELISA was obtained from Merck (Merck KGaA; cat. #EZRMI-13K). A mouse adiponectin/Acrp30 DuoSet ELISA (DY1119) was obtained from R&D Systems (Minneapolis, United States).

Statistical Analysis

The results are expressed as the mean ± SEM and were analyzed via one-way or two-way ANOVA with a Bonferroni multiple comparison test for data that satisfied the Shapiro–Wilk normality test. When data did not pass the normality test, Mann–Whitney or Kruskal–Wallis tests were applied. p values <0.05 were considered to indicate a significant difference. The contractile response to phenylephrine is expressed in mN/mm. Relaxation responses are expressed as a percentage (%) of the precontraction with phenylephrine. The maximum response (Rmax) and potency (the negative logarithm to base 10 of the molar concentration of an agonist producing 50% of the maximal effect; pEC_{50}) were calculated in each concentration-response curve. In figures, PVAT- data are represented by white symbols and PVAT+ data by blue shapes for males and pink for females. Statistical analysis was performed with GraphPad Prism 8.4.3 software (GraphPad Software, San Diego, CA, United States).

RESULTS

HF and HF + HS Obesity Models in Males and Females

In both sexes, energy intake was similar between the HF and CD groups, while food consumption was lower in the HF group than that in the CD group (**Supplementary Table S2**). In contrast, compared to the CD group, males and females fed a HF + HS diet exhibited increased energy intake, while food consumption remained reduced in males and similar in females (**Supplementary Table S2**). In male and female mice fed with HF + HS diet, food consumption was higher than that in mice fed with HF diet (**Supplementary Table S2**), suggesting that adding sugar to a HF diet could result in a more palatable diet.

Feeding of a HF or HF + HS diet for 3 or 5 months increased body weight and perigonadal fat adiposity in males and females compared to those mice in the respective sex-matched CD group (**Supplementary Table S2**). The HF and HF + HS diets increased fasting glucose in both sexes at 3 and 5 months. The HF + HS diet induced a time-dependent increase in fasting glucose in males and females and in adiposity in females (**Supplementary Table S2**). Five months of HF diet feeding resulted in a significant threefold increase in insulin levels, and although the insulin levels doubled in the HF + HS group compared to the CD group, the difference did not reach significant values (male: CD = 0.92 ± 0.1; HF = 3.05 ± 0.2*; HF + HS = 1.96 ± 0.6 ng/ml; n = 3–4/group; *p < 0.05 vs. CD). Female obese mice showed doubled plasma insulin levels after 5 months of a HF or HF + HS diet compared to female CD-fed mice (female: CD = 0.57 ± 0.08; HF = 1.18 ± 0.01*; HF + HS = 1.23 ± 0.19* ng/ml; n = 3–4/group; *p < 0.05 vs. CD). Adiponectin levels were not changed by the diet protocol (male: CD = 366 ± 164; HF = 266 ± 69; HF + HS = 210 ± 23 pg/ml; female: CD = 212 ± 23; HF = 228 ± 31; HF + HS = 300 ± 90 pg/ml; n = 4/group; $p > 0.05$). SBP and testis and uterine weight did not differ between groups (**Supplementary Table S2**).

Anticontractile PVAT Function was Preserved in Males but Impaired in Females Following HF or HF + HS Diet Feeding

The anticontractile effect of PVAT was analyzed by comparing the contraction induced by phenylephrine in small mesenteric arteries with and without adjacent PVAT. In males fed a HF or HF + HS diet for 3 months, the anticontractile effect of PVAT was similar to that in CD sex-matched mice, as demonstrated by a similar $LogEC_{50}$ (pEC_{50}) and a reduced Rmax to phenylephrine in PVAT + arteries from the HF + HS groups compared to those from the CD group (**Figures 1A–D**; **Supplementary Table S3**). When male mice were fed a HF or HF + HS diets for 5 months, the anticontractile effect of PVAT was greater than that observed in CD mice (**Figures 1E–H**; **Supplementary Table S3**). In contrast, in females, the anticontractile effect of PVAT was impaired by both obesogenic diets, evidenced by a reduction in pEC_{50} to phenylephrine in PVAT + arteries of HF and HF + HS diet mice compared to the matched CD group at 3 and 5 months (**Figures 2A–H**). Rmax did not differ between female groups (**Supplementary Table S3**).

The HF + HS Diet Resulted in PVAT-Mediated Endothelial Dysfunction Faster in Females than in Males

Next, we evaluated PVAT modulation of acetylcholine-induced endothelium-dependent relaxation. The presence of PVAT did not impact the acetylcholine response in mesenteric arteries from CD or HF diet male mice (**Figures 3A–H**). Otherwise, following 5 months of a HF + HS diet, PVAT+ arteries exhibited impaired acetylcholine-induced relaxation compared to PVAT- arteries (**Figure 3G**), as demonstrated by the reduced pEC_{50} (**Figure 3H**) and Rmax to acetylcholine in PVAT+ arteries (Rmax in 5-month HF + HS males: PVAT- = 93.5 ± 1.5 vs. PVAT+ = 56.5 ± 7.1%, n = 3–4; $p < 0.05$).

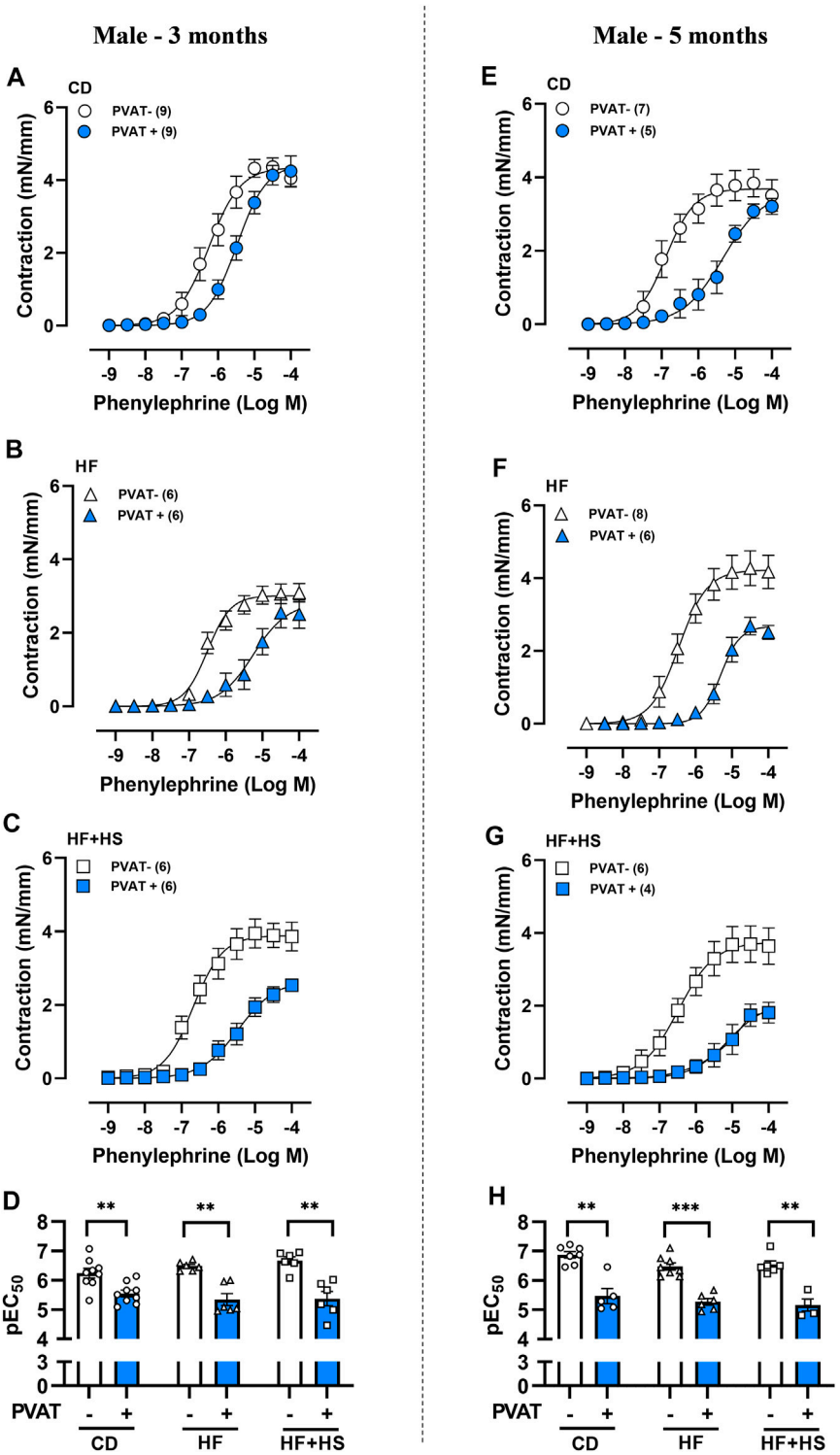

FIGURE 1 | Obesogenic diets did not impair the anticontractile effect of mesenteric PVAT in male mice. Concentration-response curves to phenylephrine in mesenteric arteries without PVAT (PVAT-; white symbols) or in the presence of adjacent PVAT (PVAT +; blue filled symbols) of male mice fed a chow diet (CD; **A,E;** circle symbols), high-fat diet (HF; **B,F;** triangle symbols) or HF plus high-sucrose diet (HF + HS; **C,G;** square symbols) for 3 (left panel) or 5 (right panel) months. Bar graphs show the potency of the response to phenylephrine (pEC_{50}) **(D,H)** in PVAT- (white bars) and PVAT+ (blue filled bars) arteries. The experimental number used is in parenthesis. $^{**}p < 0.01$; $^{***}p < 0.001$ vs. PVAT- arteries (Mann–Whitney *U* test).

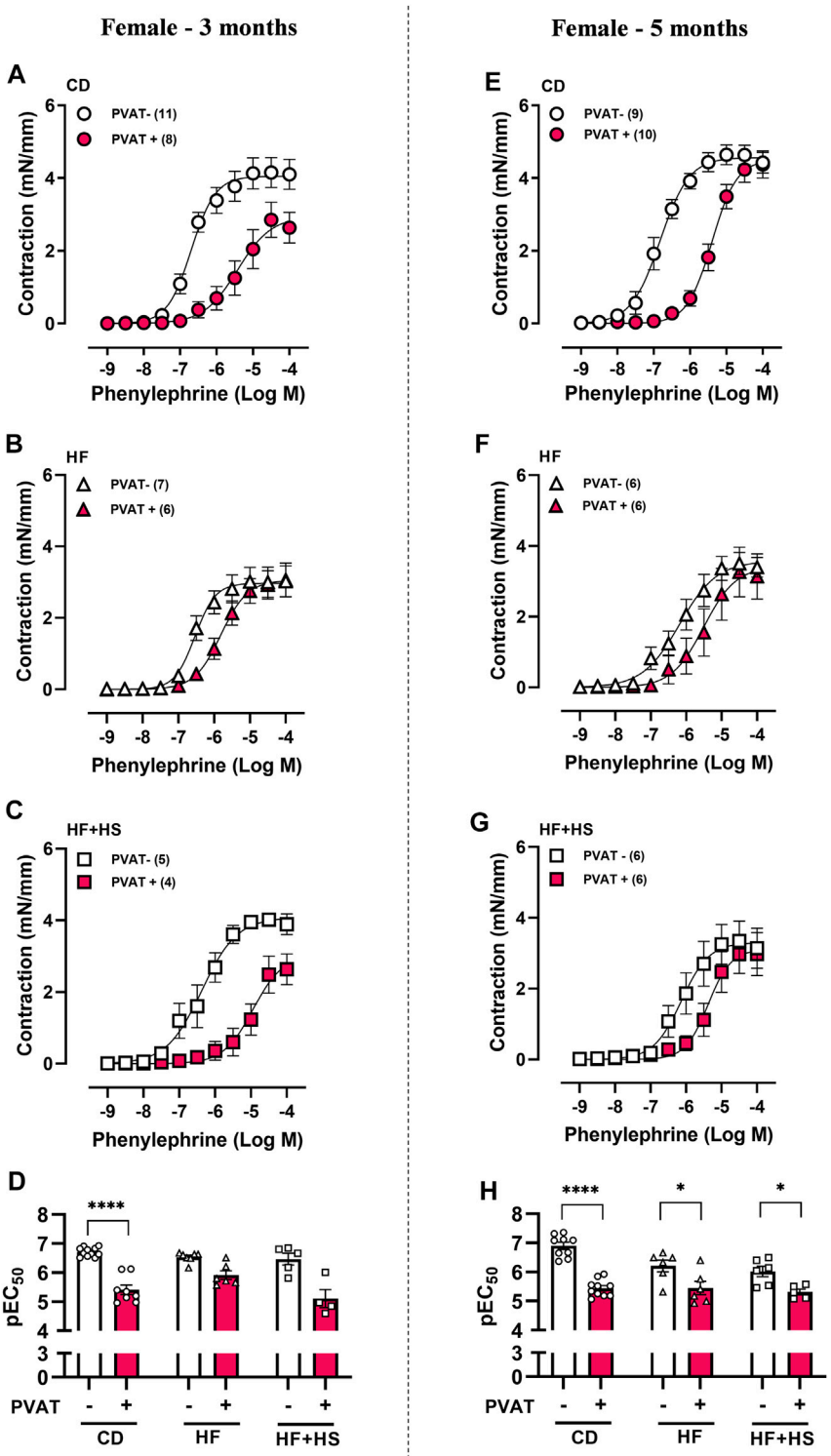

FIGURE 2 | The anticontractile effect of mesenteric PVAT is reduced by high-fat and high-fat plus high-sucrose diets in female mice. Concentration-response curves to phenylephrine in mesenteric arteries without PVAT (PVAT-; white symbols) or in the presence of adjacent PVAT (PVAT +; pink filled symbols) from female mice fed a chow diet (CD; **A,E;** circle symbols), high-fat diet (HF; **B,F;** triangle symbols), or HF plus high-sucrose diet (HF + HS; **C,G;** square symbols) for 3 (left panel) or 5 (right panel) months. Bar graphs show the potency of the response to phenylephrine (pEC_{50}) **(D,H)** in PVAT- (white bars) and PVAT+ (pink filled bars) arteries. The experimental number used is in parenthesis. ****$p < 0.0001$ vs. PVAT- (pEC_{50} 3 months) (Mann–Whitney *U* test). *$p < 0.05$, ****$p < 0.0001$ vs. PVAT- (pEC_{50} 5 months) (two-way ANOVA).

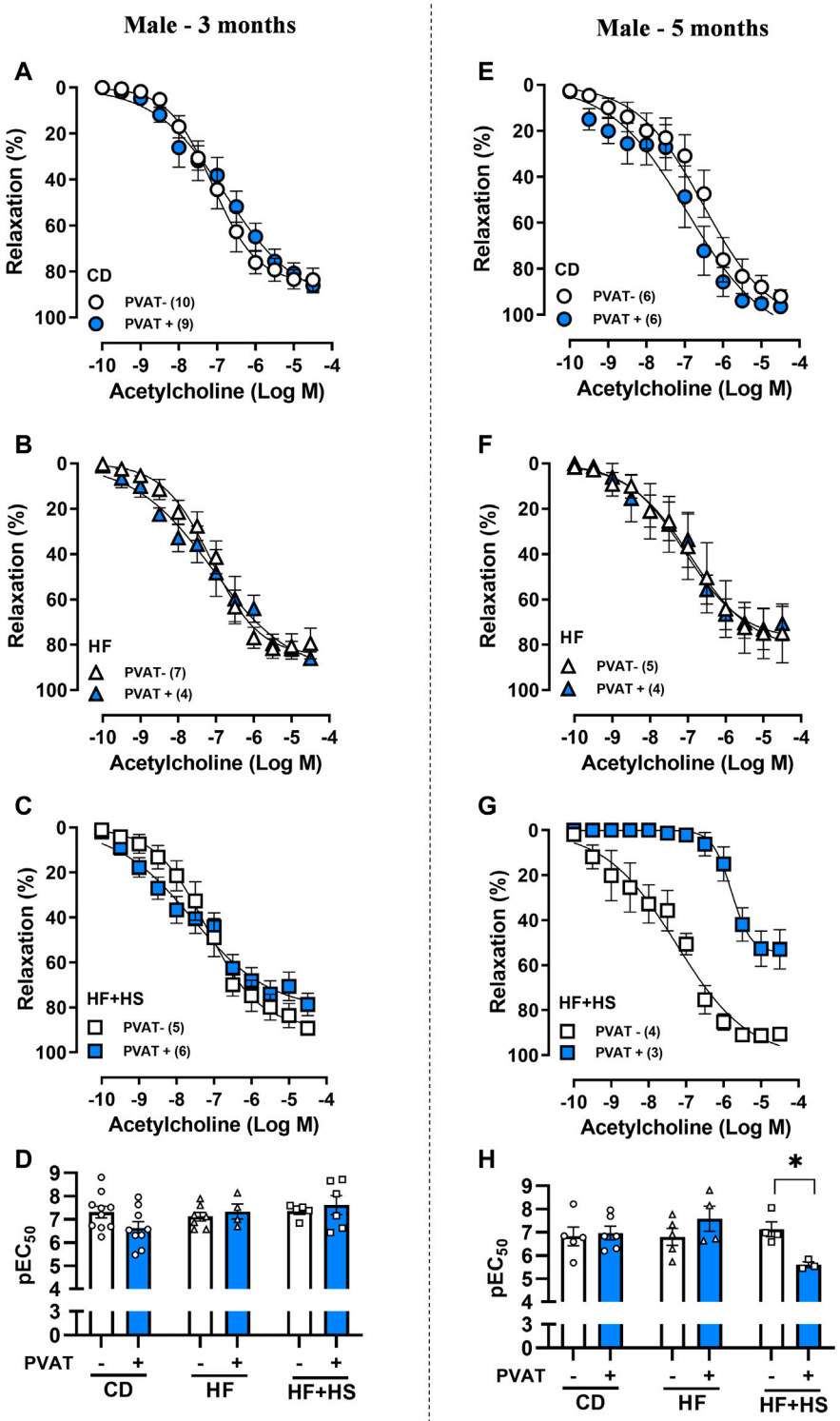

FIGURE 3 | Effect of adjacent PVAT on acetylcholine-induced relaxation of mesenteric arteries from male mice. Concentration-response curves to acetylcholine in mesenteric arteries without PVAT (PVAT-; white symbols) or in the presence of adjacent PVAT (PVAT +; blue filled symbols) from male mice fed a chow diet (CD; **A**,**E;** circle symbols), high-fat diet (HF; **B**,**F;** triangle symbols) and HF plus high-sucrose diet (HF + HS; **C**,**G;** square symbols) for 3 (left panel) or 5 (right panel) months. Bar graphs show the potency of the response to acetylcholine (pEC_{50}) **(D,H)** in PVAT- (white bars) and PVAT+ (blue filled bars) arteries. The experimental number used is in parenthesis. *$p < 0.05$ (two-way ANOVA).

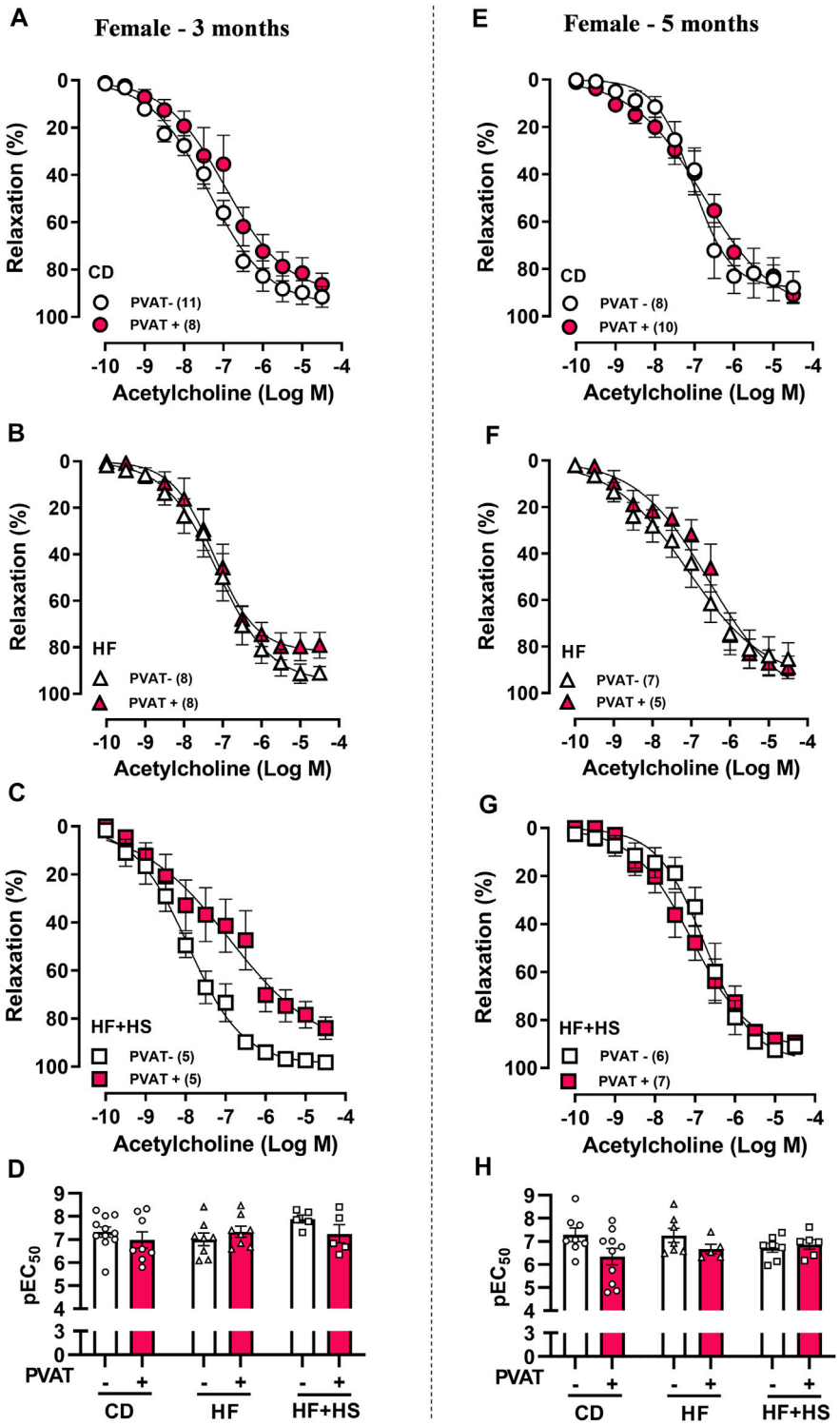

FIGURE 4 | Effect of adjacent PVAT on acetylcholine-induced relaxation of mesenteric arteries from female mice. Concentration-response curves to acetylcholine in mesenteric arteries without PVAT (PVAT-; white symbols) or in the presence of adjacent PVAT (PVAT +; pink filled symbols) from female mice fed a chow diet (CD; **A**,**D;** circle symbols), high-fat diet (HF; **B**,**E;** triangle symbols), and HF plus high-sucrose diet (HF + HS; **C**,**F**; square symbols) for 3 (left panel) or 5 (right panel) months. Bar graphs show the potency of the response to acetylcholine (pEC_{50}) **(D**,**H)** in PVAT- (white bars) and PVAT+ (pink filled bars). The experimental number used is in parenthesis. $p > 0.05$ (two-way ANOVA).

Similar to males, the presence of PVAT did not impact the acetylcholine response in mesenteric arteries from the CD or HF diet groups (**Figures 4A–H**). Nevertheless, the HF + HS diet impacted acetylcholine-induced relaxation earlier in females (**Figures 4A–C**); after 3 months of a HF + HS diet, PVAT+ arteries exhibited a reduced Rmax to acetylcholine compared to PVAT- arteries (Rmax in 3-month HF + HS females: PVAT- = 97.4 ± 0.6 vs. PVAT+ = 78.3 ± 5.3%, $n = 5$; $p < 0.05$) with no changes in pEC_{50} (**Figure 4D**). When the HF + HS diet was prolonged for up to 5 months, PVAT+ arteries presented the same acetylcholine response as PVAT- arteries with no changes in pEC_{50} or Rmax (**Figures 4G,H**). Notably, small mesenteric arteries in the female 5-month HF + HS diet group exhibited endothelial dysfunction independent of the presence of PVAT, since in this group, the acetylcholine-induced relaxation curve was shifted to the right in PVAT- arteries (pEC_{50} PVAT-: 3 months = 7.8 ± 0.1 vs. 5 months = 6.8 ± 0.2, $n = 5–6$; $p < 0.05$).

DISCUSSION

In this study, we evaluated the prolonged effects of two obesogenic HF diets (HF and HF + HS diets) on small mesenteric PVAT function in male and female mice. In males, 3 and 5 months of obesogenic diet feeding resulted in similar anticontractile effects of PVAT. In contrast to males, in females, we found that prolonged HF or HF + HS diet feeding resulted in an impaired anticontractile effect of PVAT. The HF + HS diet resulted in PVAT-mediated endothelial dysfunction as early as 3 months after obesogenic feeding in females but only after 5 months in males. The presence of PVAT did not impact acetylcholine-induced endothelial relaxation in mice fed a HF diet alone, suggesting that the addition of sucrose accelerates PVAT dysfunction in response to obesogenic diets. PVAT dysfunction in response to the HF and HF + HS diets was observed early in females compared to age-matched males, suggesting a susceptibility of the female sex to PVAT-mediated vascular complications in the setting of obesity. The data highlight the importance of an obesogenic diet and the duration of the feeding protocol for investigating treatments and pharmacological targets for obesity-induced vascular complications in males and females.

The anticontractile effect of PVAT was first described in rat thoracic aorta (Soltis and Cassis, 1991), followed by other vascular beds, including small mesenteric arteries (Aoqui et al., 2014; Gil-Ortega et al., 2014; Withers et al., 2017). It has been suggested that the presence of cardiometabolic risk factors, such as obesity, alters the secretory pattern of PVAT and might result in vascular dysfunction (Victorio and Davel, 2019). PVAT-dependent vascular dysfunction has been demonstrated in the aorta (da Costa et al., 2017; Ketonen et al., 2010) and mesenteric resistance arteries (Agabiti-Rosei et al., 2014; Gil-Ortega et al., 2014; Withers et al., 2017) in rat and mouse obese models. Several mechanisms have been described to be involved in PVAT dysfunction associated with obesity, which seems to depend on PVAT location and the duration of obesogenic diets and local/circulating adipokines (Victorio and Davel, 2019; Victorio et al., 2020). Adiponectin was demonstrated to act as a PVAT-derived anticontractile factor and could be a promising mediator of PVAT function in female mice. Here, we observed similar plasma adiponectin levels between the obese and control groups, independent of sex. Plasma adiponectin in male obesity has been demonstrated to be increased (Saxton et al., 2021), unchanged (Sousa et al., 2019), or reduced (Han et al., 2018). Adiponectin levels can differ with the time of induced obesity, with increased levels in early phases and reduced levels in prolonged phases (Victorio and Davel, 2019). Moreover, plasma adiponectin cannot represent what happens in local modulation of vascular function by PVAT, as demonstrated by Saxton and collaborators who have observed increased plasma adiponectin in obesity but reduced adiponectin content in PVAT (Saxton et al., 2021). Therefore, more studies are needed to evaluate the effects of different diets on PVAT adipokines, especially in females in the setting of obesity.

Time-dependent resistance of PVAT to dysfunction was observed in male obese mice. An increased anticontractile effect of PVAT associated with adaptative nitric oxide (NO) overproduction was found in the mesenteric arteries from male mice fed a high-fat diet (45% fat) for 8 weeks (Gil-Ortega et al., 2010) and in the aortas from mice fed a carbohydrate-enriched diet for 4 weeks (Dos Reis Costa et al., 2021). However, after 32 weeks of a 45% fat diet, altered redox status resulted in PVAT dysfunction in mesenteric arteries (Gil-Ortega et al., 2010; Gil-Ortega et al., 2014). In the present study, 3 or 5 months of a very HF diet (60% fat) did not impair either the anticontractile effect of PVAT in response to phenylephrine or the endothelium-dependent relaxation in response to acetylcholine. PVAT-dependent endothelial dysfunction was observed only after 5 months of the HF + HS diet in males. This suggests that the association of a HF and HS diet (i.e., Western diet) may accelerate PVAT and vascular dysfunction compared to a HF diet.

Since discovering the anticontractile effect of PVAT, it was expected that PVAT could increase acetylcholine-induced relaxation, but in our study, we did not observe an effect of PVAT in response to acetylcholine in male and female control mice. Similar to what was observed here, several studies have demonstrated that the presence of PVAT does not affect acetylcholine-induced relaxation in the aorta (Victorio et al., 2016; Hou et al., 2017; Simplicio et al., 2017; Sousa et al., 2019) or mesenteric arteries (Briones et al., 2012; Kagota et al., 2017). However, we cannot exclude the possibility that PVAT can act as a mechanical obstacle or diffusion limitation to agonists (Li et al., 2013; Mendizabal et al., 2013). In the setting of obesity, previous studies have demonstrated that PVAT-mediated impaired acetylcholine-induced relaxation in mice fed HF diet seems to be endothelium-dependent since relaxation to sodium nitroprusside was not altered (Sousa et al., 2019; Sousa et al., 2021). Both NO and endothelium-dependent hyperpolarization factor (EDH) seem to contribute to the endothelium-dependent relaxation in small mesenteric arteries from male and female mice (Hwa et al., 1994; Davel et al., 2018b). Nevertheless, NO has a greater contribution than EDH in males, while EDH contributes more than NO to endothelial relaxation induced by acetylcholine in females (Davel et al., 2018b). In the setting of HF-induced obesity, there is a reduction in endothelial NO contribution, which compensates for increased EDH participation; however, in females, an impaired EDH participation results in impaired acetylcholine-induced relaxation (Davel et al., 2018b).

Previous studies using HF or cafeteria diet have suggested that impaired aortic PVAT-derived NO is associated with a reduction in acetylcholine-induced relaxation in male mice (Xia et al., 2016; Lang et al., 2019). Further studies are needed to investigate the relative contribution of NO/EDH in the PVAT-mediated endothelial dysfunction in resistance arteries of males and females in response not only to obesity but also to other cardiovascular risk factors.

Reduced Rmax to phenylephrine in arteries with adjacent PVAT was observed following prolonged HF or HF + HS diet feeding in males. Silva and collaborators (Silva et al., 2016) have previously demonstrated that a high sugar diet, in addition to inducing endothelial dysfunction, upregulates the TNFα and iNOS pathways, decreasing vascular contractility in the aortas of obese male animals. Therefore, we cannot exclude a proinflammatory effect of a prolonged HF + HS diet on PVAT function. Lang and collaborators have demonstrated that a Western diet containing high sugar and dense foods accessible in Western societies impacted the aortic PVAT function more profoundly than a HF diet (45% fat) (Lang et al., 2019). Although a cafeteria diet has been demonstrated to be similar to a human diet and induced obesity, it can change feeding behavior (Martire et al., 2015); thus, it may be difficult to compare results in the literature because there is no standard protocol (Lang et al., 2019). Here, we used a chow diet as a standard diet, but a nonfat diet has been proposed for use as a control for fat-enriched diets (Lang et al., 2019), which may represent a limitation. However, as we meant to compare the effect of PVAT function after HF diet consumption to that a healthy/lean situation, we believe that the chow diet represented a better control.

Sugar consumption has been correlated with adverse effects on HDL and triglyceride levels, which can accelerate atherosclerosis (Howard and Wylie-Rosett, 2002). In addition, high sugar consumption may worsen diabetes control, and the combination of sugar with high fat promotes AGEs formation, which is involved in vascular complications associated with diabetes (Yonekura et al., 2005; Delbin et al., 2012). In women, a diet high in refined carbohydrates was associated with an increased risk of developing coronary heart disease (Liu et al., 2000). These previous studies have reinforced the importance of investigating the influence of high-calorie diets associated with high sugar content on the mechanisms that modulate vascular and PVAT function, especially in females.

In comparison to males, far less is known about functional PVAT changes in vascular tone in the setting of female obesity, which was a focus of the current study. A recent study revealed that sex-specific changes in the number of immune cells in mesenteric PVAT occurring with a HF diet (60% fat) became more prominent with the development and progression of obesity (Kumar et al., 2021). Here, we found that prolonged obesogenic diet feeding differentially impacted PVAT regulation of vascular responses in mesenteric arteries in males and females. HF and HF + HS diet feeding impaired the anticontractile effect of PVAT in females but not in males. In addition, 3 months of a HF + HS diet resulted in PVAT-mediated endothelial dysfunction in females, which was observed in males after 5 months of the same diet. Therefore, our data suggest that mesenteric PVAT in females is more susceptible to obesity-induced dysfunction than that in males. This is consistent with previous studies demonstrating that the female sex is more affected by endothelial dysfunction and vascular stiffness caused by obesity and type-2 diabetes (DeMarco et al., 2015; Jia et al., 2016; Davel et al., 2018a). Although we did not evaluate the levels of sex hormones, gonad weights (uterus and tests) were not significantly altered by either the HF or HF + HS diet, consistent with previous studies (Bruder-Nascimento et al., 2017; Faulkner et al., 2021). Loss of female sex hormones was not reported as a mechanistic switch for cardiovascular complications in obese female mice (Barris et al., 2021). A limitation of our study is that we did not investigate the mechanisms or anatomical differences underlying the sex differences in PVAT-mediated vascular complications in obesity, which need to be addressed in future investigations.

CONCLUSION

The results suggest that prolonged obesogenic diets impact mesenteric PVAT function more profoundly in females than in males, as after 3 and 5 months of HF or HF + HS feeding, impairment in the anticontractile PVAT effect was only observed in females. Our data also revealed that the combination of a HF diet with high sucrose accelerated PVAT dysfunction compared to a HF diet alone, resulting in PVAT-mediated endothelial dysfunction in males and females. PVAT-mediated endothelial dysfunction with a HF + HS diet occurs earlier in females than in males. Taken together, the data suggest a susceptibility of the female sex to PVAT-mediated vascular complications in the setting of obesity and highlight the importance of an obesogenic diet and the duration of the feeding protocol for investigating treatments and pharmacological targets for obesity-induced vascular complications in males and females.

DATA AVAILABILITY STATEMENT

The original contributions presented in the study are included in the article/**Supplementary Material**; further inquiries can be directed to the corresponding authors.

ETHICS STATEMENT

The animal study was reviewed and approved by the Ethics Committee on Animal Use of the University of Campinas (protocol no. 4914-1/2018, 5474-1/2020) and carried out in accordance with the National Board of Animal Experimentation Control (CONCEA).

AUTHOR CONTRIBUTIONS

JV and AD contributed to the conception and design of the study. JV, DG, IF, TA, and AD were responsible for acquisition and/or interpretation of data. JV and AD wrote the draft of the manuscript. All authors contributed to the manuscript revision and approved the submitted version.

FUNDING

This work was supported by Fundação de Amparo à Pesquisa do Estado de São Paulo (FAPESP grants 2018/00543-8, 2018/16505-8, and 2013/07607-8).

SUPPLEMENTARY MATERIAL

The Supplementary Material for this article can be found online at: https://www.frontiersin.org/articles/10.3389/fphar.2021.720224/full#supplementary-material

REFERENCES

Abarca-Gómez, L., Abdeen, Z. A., Hamid, Z. A., Abu-Rmeileh, N. M., Acosta-Cazares, B., and Acuin, C. E. A. (2017). Worldwide Trends in Body-Mass index, Underweight, Overweight, and Obesity from 1975 to 2016: a Pooled Analysis of 2416 Population-Based Measurement Studies in 128·9 Million Children, Adolescents, and Adults. *Lancet* 390, 2627–2642. doi:10.1016/S0140-6736(17)32129-3

Agabiti-Rosei, C., De Ciuceis, C., Rossini, C., Porteri, E., Rodella, L. F., Withers, S. B., et al. (2014). Anticontractile Activity of Perivascular Fat in Obese Mice and the Effect of Long-Term Treatment with Melatonin. *J. Hypertens.* 32, 1264–1274. doi:10.1097/hjh.0000000000000178

Aoqui, C., Chmielewski, S., Scherer, E., Eissler, R., Sollinger, D., Heid, I.., et al. (2014). Microvascular Dysfunction in the Course of Metabolic Syndrome Induced by High-Fat Diet. *Cardiovasc. Diabetol.* 13, 31. doi:10.1186/1475-2840-13-31

Barrett, P., Mercer, J. G., and Morgan, P. J. (2016). Preclinical Models for Obesity Research. *Dis. Model. Mech.* 9, 1245–1255. doi:10.1242/dmm.026443

Barris, C., Faulkner, J., and de Chantemele, E. B. (2021). Loss of Female Sex Hormones Does Not Induce a Mechanistic Switch for Development of Hypertension in Obese Female Mice - Barris - 2021. *Experimental Biology 2021 Meeting abstracts*. 35(S1), doi:10.1096/fasebj.2021.35.S1.04280

Briones, A. M., Nguyen Dinh Cat, A., Callera, G. E., Yogi, A., Burger, D., He, Y., et al. (2012). Adipocytes Produce Aldosterone through Calcineurin-dependent Signaling Pathways: Implications in Diabetes Mellitus-Associated Obesity and Vascular Dysfunction. *Hypertension* 59, 1069–1078. doi:10.1161/HYPERTENSIONAHA.111.190223

Bruder-Nascimento, T., Ekeledo, O. J., Anderson, R., Le, H. B., and Belin de Chantemele, E. J. (2017). Long Term High Fat Diet Treatment: An Appropriate Approach to Study the Sex-Specificity of the Autonomic and Cardiovascular Responses to Obesity in Mice. *Front. Physiol.* 8, 32. doi:10.3389/fphys.2017.00032

Caballero, A. E., Bousquet-Santos, K., Robles-Osorio, L., Montagnani, V., Soodini, G., Porramatikul, S., et al. (2008). Overweight Latino Children and Adolescents Have Marked Endothelial Dysfunction and Subclinical Vascular Inflammation in Association with Excess Body Fat and Insulin Resistance. *Diabetes care* 31, 576–582. doi:10.2337/dc07-1540

da Costa, R. M., Fais, R. S., Dechandt, C. R. P., Louzada-Junior, P., Alberici, L. C., Lobato, N. S., et al. (2017). Increased Mitochondrial ROS Generation Mediates the Loss of the Anti-contractile Effects of Perivascular Adipose Tissue in High-Fat Diet Obese Mice. *Br. J. Pharmacol.* 174, 3527–3541. doi:10.1111/bph.13687

Davel, A. P., Jaffe, I. Z., Tostes, R. C., Jaisser, F., and Belin de Chantemele, E. J. (2018a). New Roles of Aldosterone and Mineralocorticoid Receptors in Cardiovascular Disease: Translational and Sex-specific Effects. *Am. J. Physiol. Heart Circ. Physiol.* 315, H989–h999. doi:10.1152/ajpheart.00073.2018

Davel, A. P., Lu, Q., Moss, M. E., Rao, S., Anwar, I. J., DuPont, J. J., et al. (2018b). Sex-Specific Mechanisms of Resistance Vessel Endothelial Dysfunction Induced by Cardiometabolic Risk Factors. *J. Am. Heart Assoc.* 7 (4), e007675. doi:10.1161/jaha.117.007675

Delbin, M. A., Davel, A. P., Couto, G. K., de Araújo, G. G., Rossoni, L. V., Antunes, E., et al. (2012). Interaction between Advanced Glycation End Products Formation and Vascular Responses in Femoral and Coronary Arteries from Exercised Diabetic Rats. *PloS one* 7 (12), e53318. doi:10.1371/journal.pone.0053318

DeMarco, V. G., Habibi, J., Jia, G., Aroor, A. R., Ramirez-Perez, F. I., Martinez-Lemus, L. A., et al. (2015). Low-Dose Mineralocorticoid Receptor Blockade Prevents Western Diet-Induced Arterial Stiffening in Female Mice. *Hypertension* 66, 99–107. doi:10.1161/hypertensionaha.115.05674

Dos Reis Costa, D. E. F., Silveira, A. L. M., Campos, G. P., Nóbrega, N. R. C., de Araújo, N. F., de Figueiredo Borges, L., et al. (2021). High-Carbohydrate Diet Enhanced the Anticontractile Effect of Perivascular Adipose Tissue through Activation of Renin-Angiotensin System. *Front. Physiol.* 11, 628101. doi:10.3389/fphys.2020.628101

Faulkner, J. L., Harwood, D., Kennard, S., Antonova, G., Clere, N., and Belin de Chantemèle, E. J. (2021). Dietary Sodium Restriction Sex Specifically Impairs Endothelial Function via Mineralocorticoid Receptor-dependent Reduction in NO Bioavailability in Balb/C Mice. *Am. J. Physiol. Heart circulatory Physiol.* 320 (1), H211–H220. doi:10.1152/ajpheart.00413.2020

Gil-Ortega, M., Condezo-Hoyos, L., García-Prieto, C. F., Arribas, S. M., González, M. C., Aranguez, I., et al. (2014). Imbalance between Pro and Anti-oxidant Mechanisms in Perivascular Adipose Tissue Aggravates Long-Term High-Fat Diet-Derived Endothelial Dysfunction. *PLoS One* 9, e95312. doi:10.1371/journal.pone.0095312

Gil-Ortega, M., Stucchi, P., Guzmán-Ruiz, R., Cano, V., Arribas, S., González, M. C., et al. (2010). Adaptative Nitric Oxide Overproduction in Perivascular Adipose Tissue during Early Diet-Induced Obesity. *Endocrinology* 151, 3299–3306. doi:10.1210/en.2009-1464

Greenstein, A. S., Khavandi, K., Withers, S. B., Sonoyama, K., Clancy, O., Jeziorska, M., et al. (2009). Local Inflammation and Hypoxia Abolish the Protective Anticontractile Properties of Perivascular Fat in Obese Patients. *Circulation* 119, 1661–1670. doi:10.1161/CIRCULATIONAHA.108.821181

Han, F., Li, K., Pan, R., Xu, W., Han, X., Hou, N., et al. (2018). Calycosin Directly Improves Perivascular Adipose Tissue Dysfunction by Upregulating the adiponectin/AMPK/eNOS Pathway in Obese Mice. *Food Funct.* 9, 2409–2415. doi:10.1039/c8fo00328a

Hou, N., Du, G., Han, F., Zhang, J., Jiao, X., and Sun, X. (2017). Irisin Regulates Heme Oxygenase-1/Adiponectin Axis in Perivascular Adipose Tissue and Improves Endothelial Dysfunction in Diet-Induced Obese Mice. *Cell Physiol Biochem* 42, 603–614. doi:10.1159/000477864

Howard, B. V., and Wylie-Rosett, J. (2002). Sugar and Cardiovascular Disease: A Statement for Healthcare Professionals from the Committee on Nutrition of the Council on Nutrition, Physical Activity, and Metabolism of the American Heart Association. *Circulation* 106 (4), 523–527. doi:10.1161/01.cir.0000019552.77778.04

Hunter, I., Soler, A., Joseph, G., Hutcheson, B., Bradford, C., Zhang, F. F., et al. (2017). Cardiovascular Function in Male and Female JCR:LA-cp Rats: Effect of High-Fat/high-Sucrose Diet. *Am. J. Physiol. Heart circulatory Physiol.* 312 (4), H742–H751. doi:10.1152/ajpheart.00535.2016

Hwa, J. J., Ghibaudi, L., Williams, P., and Chatterjee, M. (1994). Comparison of Acetylcholine-dependent Relaxation in Large and Small Arteries of Rat Mesenteric Vascular Bed. *Am. J. Physiol.* 266 (3 Pt 2), H952–H958. doi:10.1152/ajpheart.1994.266.3.H952

Jia, G., Bender, S. B., and Sowers, J. R. (2016). Uncovering a Mineralocorticoid Receptor-dependent Adipose-Vascular Axis: Implications for Vascular Dysfunction in Obesity? *Diabetes* 65, 2127–2129. doi:10.2337/dbi16-0028

Kagota, S., Iwata, S., Maruyama, K., McGuire, J. J., and Shinozuka, K. (2017). Time-Dependent Differences in the Influence of Perivascular Adipose Tissue on Vasomotor Functions in Metabolic Syndrome. *Metab. Syndr. Relat. Disord.* 15 (5), 233–239. doi:10.1089/met.2016.0146

Ketonen, J., Shi, J., Martonen, E., and Mervaala, E. (2010). Periadventitial Adipose Tissue Promotes Endothelial Dysfunction via Oxidative Stress in Diet-Induced Obese C57Bl/6 Mice. *Circ. J.* 74, 1479–1487. doi:10.1253/circj.cj-09-0661

Kumar, R. K., Yang, Y., Contreras, A. G., Garver, H., Bhattacharya, S., Fink, G. D., et al. (2021). Phenotypic Changes in T Cell and Macrophage Subtypes in Perivascular Adipose Tissues Precede High-Fat Diet-Induced Hypertension. *Front. Physiol.* 12, 616055. doi:10.3389/fphys.2021.616055

Lang, P., Hasselwander, S., Li, H., and Xia, N. (2019). Effects of Different Diets Used in Diet-Induced Obesity Models on Insulin Resistance and Vascular

Dysfunction in C57BL/6 Mice. *Sci. Rep.* 9, 19556. doi:10.1038/s41598-019-55987-x

Li, R., Andersen, I., Aleke, J., Golubinskaya, V., Gustafsson, H., and Nilsson, H. (2013). Reduced Anti-contractile Effect of Perivascular Adipose Tissue on Mesenteric Small Arteries from Spontaneously Hypertensive Rats: Role of Kv7 Channels. *Eur. J. Pharmacol.* 698, 310–315. doi:10.1016/j.ejphar.2012.09.026

Lim, S., and Meigs, J. B. (2014). Links between Ectopic Fat and Vascular Disease in Humans. *Arteriosclerosis, Thromb. Vasc. Biol.* 34 (9), 1820–1826. doi:10.1161/ATVBAHA.114.303035

Liu, S., Willett, W. C., Stampfer, M. J., Hu, F. B., Franz, M., Sampson, L., et al. (2000). A Prospective Study of Dietary Glycemic Load, Carbohydrate Intake, and Risk of Coronary Heart Disease in US Women. *Am. J. Clin. Nutr.* 71 (6), 1455–1461. doi:10.1093/ajcn/71.6.1455

Ma, L., Ma, S., He, H., Yang, D., Chen, X., Luo, Z., et al. (2010). Perivascular Fat-Mediated Vascular Dysfunction and Remodeling through the AMPK/mTOR Pathway in High-Fat Diet-Induced Obese Rats. *Hypertens. Res.* 33, 446–453. doi:10.1038/hr.2010.11

Martire, S. I,, Westbrook, R. F., and Morris, M. J. (2015). Effects of Long-Term Cycling between Palatable Cafeteria Diet and Regular Chow on Intake, Eating Patterns, and Response to Saccharin and Sucrose. *Physiol. Behav.* 139, 80–88. doi:10.1016/j.physbeh.2014.11.006

Mendizabal, Y., Llorens, S., and Nava, E. (2013). Vasoactive Effects of Prostaglandins from the Perivascular Fat of Mesenteric Resistance Arteries in WKY and SHROB Rats. *Life Sci.* 93, 1023–1032. doi:10.1016/j.lfs.2013.10.021

Mulvany, M. J., and Halpern, W. (1977). Contractile Properties of Small Arterial Resistance Vessels in Spontaneously Hypertensive and Normotensive Rats. *Circ. Res.* 41 (1), 19–26. doi:10.1161/01.res.41.1.19

Narain, A., Kwok, C. S., and Mamas, M. A. (2016). Soft Drinks and Sweetened Beverages and the Risk of Cardiovascular Disease and Mortality: a Systematic Review and Meta-Analysis. *Int. J. Clin. Pract.* 70 (10), 791–805. doi:10.1111/ijcp.12841

Saxton, S. N., Ryding, K. E., Aldous, R. G., Withers, S. B., Ohanian, J., and Heagerty, A. M. (2018). Role of Sympathetic Nerves and Adipocyte Catecholamine Uptake in the Vasorelaxant Function of Perivascular Adipose Tissue. *Arterioscler Thromb. Vasc. Biol.* 38, 880–891. doi:10.1161/ATVBAHA.118.310777

Saxton, S. N., Toms, L. K., Aldous, R. G., Withers, S. B., Ohanian, J., and Heagerty, A. M. (2021). Restoring Perivascular Adipose Tissue Function in Obesity Using Exercise. *Cardiovasc. Drugs Ther.* doi:10.1007/s10557-020-07136-0

Schlett, C. L., Massaro, J. M., Lehman, S. J., Bamberg, F., O'Donnell, C. J., Fox, C. S., et al. (2009). Novel Measurements of Periaortic Adipose Tissue in Comparison to Anthropometric Measures of Obesity, and Abdominal Adipose Tissue. *Int. J. Obes. (Lond)* 33, 226–232. doi:10.1038/ijo.2008.267

Silva, J. F., Correa, I. C., Diniz, T. F., Lima, P. M., Santos, R. L., Cortes, S. F., et al. (2016). Obesity, Inflammation, and Exercise Training: Relative Contribution of iNOS and eNOS in the Modulation of Vascular Function in the Mouse Aorta. *Front. Physiol.* 7, 386. doi:10.3389/fphys.2016.00386

Simplicio, J. A., Gonzaga, N. A., Nakashima, M. A., De Martinis, B. S., Cunha, T. M., Tirapelli, L. F., et al. (2017). Tumor Necrosis Factor-α Receptor 1 Contributes to Ethanol-Induced Vascular Reactive Oxygen Species Generation and Hypertension. *J. Am. Soc. Hypertens.* 11, 684–696.e683. doi:10.1016/j.jash.2017.07.008

Soltis, E. E., and Cassis, L. A. (1991). Influence of Perivascular Adipose Tissue on Rat Aortic Smooth Muscle Responsiveness. *Clin. Exp. Hypertens. A.* 13, 277–296. doi:10.3109/10641969109042063

Sousa, A. S., Sponton, A. C. S., and Delbin, M. A. (2021). Perivascular Adipose Tissue and Microvascular Endothelial Dysfunction in Obese Mice: Beneficial Effects of Aerobic Exercise in Adiponectin Receptor (AdipoR1) and peNOS Ser1177. *Clin. Exp. Pharmacol. Physiol.* 1–11. doi:10.1111/1440-1681.13550

Sousa, A. S., Sponton, A. C. S., Trifone, C. B., and Delbin, M. A. (2019). Aerobic Exercise Training Prevents Perivascular Adipose Tissue-Induced Endothelial Dysfunction in Thoracic Aorta of Obese Mice. *Front. Physiol.* 10, 1009. doi:10.3389/fphys.2019.01009

Speakman, J. R. (2019). Use of High-Fat Diets to Study Rodent Obesity as a Model of Human Obesity. *Int. J. Obes.* 43 (8), 1491–1492. doi:10.1038/s41366-019-0363-7

Victorio, J. A., da Costa, R. M., Tostes, R. C., and Davel, A. P. (2020). Modulation of Vascular Function by Perivascular Adipose Tissue: Sex Differences. *Curr. Pharm. Des.* 26, 3768–3777. doi:10.2174/1381612826666200701211912

Victorio, J. A., and Davel, A. P. (2019). Perivascular Adipose Tissue Oxidative Stress on the Pathophysiology of Cardiometabolic Diseases. *Curr. Hypertens. Rev.* 10, 2174. doi:10.2174/1573402115666190410153634

Victorio, J. A., Fontes, M. T., Rossoni, L. V., and Davel, A. P. (2016). Different Anti-contractile Function and Nitric Oxide Production of Thoracic and Abdominal Perivascular Adipose Tissues. *Front. Physiol.* 7, 295. doi:10.3389/fphys.2016.00295

Vishvanath, L., and Gupta, R. K. (2019). Contribution of Adipogenesis to Healthy Adipose Tissue Expansion in Obesity. *J. Clin. Invest.* 129 (10), 4022–4031. doi:10.1172/JCI129191

Wagner, R., Machann, J., Lehmann, R., Rittig, K., Schick, F., Lenhart, J., et al. (2012). Exercise-induced Albuminuria Is Associated with Perivascular Renal Sinus Fat in Individuals at Increased Risk of Type 2 Diabetes. *Diabetologia* 55, 2054–2058. doi:10.1007/s00125-012-2551-z

Wenceslau, C. F., McCarthy, C. G., Earley, S., England, S. K., Filosa, J. A., Goulopoulou, S., et al. (2021). Guidelines for the Measurement of Vascular Function and Structure in Isolated Arteries and Veins. *Am. J. Physiol. Heart circulatory Physiol.* 321 (1), H77–H111. doi:10.1152/ajpheart.01021.2020

Withers, S. B., Forman, R., Meza-Perez, S., Sorobetea, D., Sitnik, K., Hopwood, T., et al. (2017). Eosinophils Are Key Regulators of Perivascular Adipose Tissue and Vascular Functionality. *Sci. Rep.* 7, 44571. doi:10.1038/srep44571

World Health Organization (2019). Obesity and Overweight. Available at: https://www.who.int/en/news-room/fact-sheets/detail/obesity-and-overweight.

Xi, B., Huang, Y., Reilly, K. H., Li, S., Zheng, R., Barrio-Lopez, M. T., et al. (2015). Sugar-sweetened Beverages and Risk of Hypertension and CVD: a Dose-Response Meta-Analysis. *Br. J. Nutr.* 113 (5), 709–717. doi:10.1017/S0007114514004383

Xia, N., Horke, S., Habermeier, A., Closs, E. I., Reifenberg, G., Gericke, A., et al. (2016). Uncoupling of Endothelial Nitric Oxide Synthase in Perivascular Adipose Tissue of Diet-Induced Obese Mice. *Arterioscler Thromb. Vasc. Biol.* 36, 78–85. doi:10.1161/ATVBAHA.115.306263

Xu, X., Liu, C., Xu, Z., Tzan, K., Wang, A., Rajagopalan, S., et al. (2012). Altered Adipocyte Progenitor Population and Adipose-Related Gene Profile in Adipose Tissue by Long-Term High-Fat Diet in Mice. *Life Sci.* 90, 1001–1009. doi:10.1016/j.lfs.2012.05.016

Yonekura, H., Yamamoto, Y., Sakurai, S., Watanabe, T., and Yamamoto, H. (2005). Roles of the Receptor for Advanced Glycation Endproducts in Diabetes-Induced Vascular Injury. *J. Pharmacol. Sci.* 97 (3), 305–311. doi:10.1254/jphs.cpj04005x

Zhou, B., Bentham, J., Di Cesare, M., Bixby, H., Danaei, G., and Cowan, M. J. E. A. (2017). Worldwide Trends in Blood Pressure from 1975 to 2015: a Pooled Analysis of 1479 Population-Based Measurement Studies with 19·1 Million Participants. *The Lancet* 389 (10064), 37–55. doi:10.1016/S0140-6736(16)31919-5

Conflict of Interest: The authors declare that the research was conducted in the absence of any commercial or financial relationships that could be construed as a potential conflict of interest.

Publisher's Note: All claims expressed in this article are solely those of the authors and do not necessarily represent those of their affiliated organizations, or those of the publisher, the editors and the reviewers. Any product that may be evaluated in this article, or claim that may be made by its manufacturer, is not guaranteed or endorsed by the publisher.

Advantages of publishing in Frontiers

OPEN ACCESS
Articles are free to read for greatest visibility and readership

FAST PUBLICATION
Around 90 days from submission to decision

HIGH QUALITY PEER-REVIEW
Rigorous, collaborative, and constructive peer-review

TRANSPARENT PEER-REVIEW
Editors and reviewers acknowledged by name on published articles

Frontiers
Avenue du Tribunal-Fédéral 34
1005 Lausanne | Switzerland

Visit us: www.frontiersin.org
Contact us: frontiersin.org/about/contact

REPRODUCIBILITY OF RESEARCH
Support open data and methods to enhance research reproducibility

DIGITAL PUBLISHING
Articles designed for optimal readership across devices

FOLLOW US
@frontiersin

IMPACT METRICS
Advanced article metrics track visibility across digital media

EXTENSIVE PROMOTION
Marketing and promotion of impactful research

LOOP RESEARCH NETWORK
Our network increases your article's readership